



ADVANCES IN VIRUS RESEARCH

VOLUME 63

KARL MARAMOROSCH
AARON J. SHATKIN

Advances in
VIRUS RESEARCH

VOLUME 63

ADVISORY BOARD

DAVID BALTIMORE

ROBERT M. CHANOCK

PETER C. DOHERTY

H. J. GROSS

B. D. HARRISON

PAUL KAESBERG

BERNARD MOSS

ERLING NORRBY

J. J. SKEHEL

R. H. SYMONS

M. H. V. VAN REGENMORTEL

Advances in VIRUS RESEARCH

Edited by

KARL MARAMOROSCH

Department of Entomology
Rutgers University
New Brunswick, New Jersey

AARON J. SHATKIN

Center for Advanced Biotechnology
and Medicine
Piscataway, New Jersey

VOLUME 63



ELSEVIER
ACADEMIC
PRESS

AMSTERDAM • BOSTON • HEIDELBERG • LONDON
NEW YORK • OXFORD • PARIS • SAN DIEGO
SAN FRANCISCO • SINGAPORE • SYDNEY • TOKYO

Elsevier Academic Press
525 B Street, Suite 1900, San Diego, California 92101-4495, USA
84 Theobald's Road, London WC1X 8RR, UK

This book is printed on acid-free paper. 

Copyright © 2004, Elsevier Inc. All Rights Reserved.

No part of this publication may be reproduced or transmitted in any form or by any means, electronic or mechanical, including photocopy, recording, or any information storage and retrieval system, without permission in writing from the Publisher.

The appearance of the code at the bottom of the first page of a chapter in this book indicates the Publisher's consent that copies of the chapter may be made for personal or internal use of specific clients. This consent is given on the condition, however, that the copier pay the stated per copy fee through the Copyright Clearance Center, Inc. (www.copyright.com), for copying beyond that permitted by Sections 107 or 108 of the U.S. Copyright Law. This consent does not extend to other kinds of copying, such as copying for general distribution, for advertising or promotional purposes, for creating new collective works, or for resale. Copy fees for pre-2004 chapters are as shown on the title pages. If no fee code appears on the title page, the copy fee is the same as for current chapters. 0065-3527/2004 \$35.00

Permissions may be sought directly from Elsevier's Science & Technology Rights Department in Oxford, UK: phone: (+44) 1865 843830, fax: (+44) 1865 853333, E-mail: permissions@elsevier.com.uk. You may also complete your request on-line via the Elsevier homepage (<http://elsevier.com>), by selecting "Customer Support" and then "Obtaining Permissions."

For all information on all Academic Press publications
visit our Web site at www.academicpress.com

ISBN: 0-12-039865-6

PRINTED IN THE UNITED STATES OF AMERICA
04 05 06 07 08 9 8 7 6 5 4 3 2 1

CONTENTS

Duck Hepatitis B Virus: An Invaluable Model System For HBV Infection

URSULA SCHULTZ, ELIZABETH GRGACIC, AND MICHAEL NASSAL

I.	Introduction	1
II.	Animal Models of HBV	3
III.	The Hepadnaviral Infectious Cycle: An Overview	7
IV.	DHBV Proteins and Their Basic Functions in Replication and Morphogenesis	12
V.	Experimental DHBV Infection	37
VI.	DHBV as a Model to Study Host Responses to and Control of HBV Infection	46
VII.	DHBV and the Development of Hepadnaviral Transduction Vectors	53
VIII.	Conclusions and Perspectives	54
	References	55

Novel Insights into Hepatitis C Virus Replication and Persistence

RALF BARTENSCHLAGER, MICHAEL FRESE, AND THOMAS PIETSCHMANN

I.	Introduction	72
II.	Genomic Organization	74
III.	Virus Structure	78
IV.	Experimental Systems	86
V.	Replication Cycle	93
VI.	Virus–Host Interaction	134
VII.	Antiviral Therapies	146
VIII.	Concluding Remarks	148
	References	149

The Regulation and Maturation of Antiviral Immune Responses

J. LINDSAY WHITTON, MARK K. SLIFKA, FEI LIU, ALEXANDER K. NUSSBAUM,
AND JASON K. WHITMIRE

I.	Overview of the Immune Response to Viral Infection	182
II.	B Lymphocytes and Their Role in Antiviral Immune Responses	184
III.	Antiviral T Cells: A Primer	192
IV.	CD8 ⁺ T Lymphocytes and Their Role in Antiviral Immune Responses	194
V.	CD4 ⁺ T Lymphocytes and Their Role in Antiviral Immune Responses	211
VI.	Immunopathology	221
VII.	Summary	222
	References.	223

Prospects for the Therapy and Prevention of Dengue Virus Infections

ELSA B. DAMONTE, CARLOS A. PUJOL, AND CELIA E. COTO

I.	Introduction	239
II.	The Agent	240
III.	The Human Disease	242
IV.	DENV as a Global Reemerging Agent	245
V.	Virus Structure and the Replicative Cycle: Possible Targets for Therapy	246
VI.	Viral Inhibitors	254
VII.	Strategies for Vaccine Development	268
VIII.	Concluding Remarks	272
	References.	273

Bacteriophage T4: Structure, Assembly, and Initiation Infection Studied in Three Dimensions

VADIM V. MESYANZHINOV

I.	Introduction	287
II.	Bacteriophage T4 Head Structure and Assembly	291
III.	The Tail	303
IV.	The Fibers	305
V.	The Baseplate Structure	311
VI.	Structure of the Star-Shaped Baseplate	337
VII.	The Mechanism of the Baseplate Conformational Transition and Initiation of the Infection	339

VIII.	Conclusion	341
	References	341

Genomic Organization, Biology, and Diagnosis of Taura Syndrome Virus and Yellowhead Virus of Penaeid Shrimp

ARUN K. DHAR, JEFF A. COWLEY, KENNETH W. HASSON,
AND PETER J. WALKER

I.	Introduction	353
II.	Taura Syndrome Disease	354
III.	Yellowhead Disease	383
IV.	Concluding Remarks	410
	References	411

Viruses of the Chestnut Blight Fungus, *Cryphonectria parasitica*

BRADLEY I. HILLMAN AND NOBUHIRO SUZUKI

I.	Introduction	424
II.	Fungi as Hosts for Virus Infection	425
III.	History of <i>C. parasitica</i> as a Virus Host	427
IV.	Viruses as the Cause of Hypovirulence and a Description of CHV1	427
V.	General Properties and Procedures for Studying <i>C. parasitica</i> Viruses	433
VI.	Structure and Characteristics of the CHV1 Genome	435
VII.	Host Genes and Signaling Pathways Affected by CHV1 Infection	444
VIII.	Other <i>Cryphonectria Hypoviruses</i>	447
IX.	Defective and Satellite RNAs of Hypoviruses	451
X.	Other Viruses of <i>C. parasitica</i>	453
XI.	Population Biology and Evolution of <i>Cryphonectria</i> Viruses	458
XII.	Conclusions	462
	References	462
	Index	473

DUCK HEPATITIS B VIRUS: AN INVALUABLE MODEL SYSTEM FOR HBV INFECTION

Ursula Schultz,^{*} Elizabeth Grgacic,[†] and Michael Nassal^{*}

^{*}University Hospital Freiburg, Department of Internal Medicine II/Molecular Biology
D-79106 Freiburg, Germany

[†]Macfarlane Burnet Institute for Medical Research and Public Health
Hepatitis Laboratory, Melbourne, Victoria 3004, Australia

- I. Introduction
 - II. Animal Models of HBV
 - A. Primate Orthohepadnaviruses
 - B. Non-Primate Orthohepadnaviruses
 - C. Bird HBVs (Avihepadnaviruses)
 - III. The Hepadnaviral Infectious Cycle: An Overview
 - IV. DHBV Proteins and Their Basic Functions in Replication and Morphogenesis
 - A. The Core Protein
 - B. The Reverse Transcriptase (P Protein)
 - C. Envelope Proteins
 - V. Experimental DHBV Infection
 - A. *In Vitro* Infection of Primary Duck Hepatocytes
 - B. Experimental *In Vivo* Infection
 - VI. DHBV as a Model to Study Host Responses to and Control of HBV Infection
 - A. Cytokines and Their Role in Controlling Hepadnaviral Infection
 - B. Chemotherapy and Vaccination
 - VII. DHBV and the Development of Hepadnaviral Transduction Vectors
 - VIII. Conclusions and Perspectives
- References

I. INTRODUCTION

Hepatitis B virus (HBV) is the causative agent of acute and chronic hepatitis B in humans. More than 350 million people worldwide are chronic virus carriers and face a significantly increased risk of developing liver cirrhosis and primary hepatocellular carcinoma (Blumberg, 1997). Effective prophylactic vaccines based on noninfectious empty envelopes (termed S particles or subviral particles), originally purified from the plasma of carriers and later produced in recombinant form in yeast or mammalian cell lines, have been available since the 1980s; for a comprehensive review on clinical aspects, including various vaccines, see Hollinger and Liang (2001). Nonetheless, for many developing countries, large-scale vaccination programs were hardly affordable.

This situation is improving, but an enormous number of chronic HBV carriers will be in need of better medication for decades to come. Current therapies are based on the systemic administration of high doses of interferon- α (IFN- α) or, more recently, on nucleoside analogs, such as 3-thiacytidine (lamivudine) and adefovir. However, both therapies have a sustained response rate of only about 30%, combinations exert no clear synergism, and lamivudine therapy leads to the rapid emergence of resistant virus variants (Pumpens *et al.*, 2002; Zoulim, 2001).

A full understanding of the molecular biology of HBV and its infectious cycle is hampered by experimental limitations: as of yet there is no feasible small animal infection model, and only a few aspects of its replication cycle are amenable to biochemical methods. The focus of this review is on one of two established animal virus models, namely duck hepatitis B virus (DHBV). Although humans and ducks are only distantly related hosts, HBV and DHBV, which are the type members of the orthohepadnaviruses and avihepadnaviruses (*hepatotropic DNA viruses*), share fundamental common features. In fact, many of the principles of hepadnavirus replication have been established using DHBV. Its major advantages are the ready availability of ducks, allowing experimental infections with wild-type and mutant viruses *in vivo* as well as in cultured primary hepatocytes, and the recent development of *in vitro* systems to study biochemically the intricate mechanism of hepadnaviral replication. Thus, unlike other hepadnaviruses DHBV offers the full range of experimental approaches, from the test tube to animal studies, to investigate fundamental as well as selected medical aspects of hepadnavirus biology.

The emphasis here is on the value of DHBV as a model for HBV, but the differences between the human and the duck viruses should not be neglected. DHBV can cause acute and chronic infections but is at variance with HBV and mammalian viruses in several aspects: (i) DHBV does not appear to be pathogenic for its host; (ii) DHBV probably lacks a regulatory protein comparable to the mammalian virus HBx gene product, a promiscuous transactivator that, by acting on the host cell, appears to be essential for establishment of infection and has been implicated in carcinogenesis; and (iii) a host-cell encoded glycoprotein, carboxypeptidase D (CPD), appears to be critical for DHBV infection, yet no evidence supports a similar role for its human homologue. This chapter will address these differences as well as peculiarities concerning the structure and function of individual viral proteins. Additional information on DHBV can be found in several recent reviews describing the general features of hepadnavirus biology (Ganem and Schneider, 2001; Nassal, 1999, 2000; Seeger and Mason,

2000) and describing DHBV-specific immunological aspects (Jilbert and Kotlarski, 2000).

II. ANIMAL MODELS OF HBV

Two salient features of hepadnaviruses are their pronounced liver tropism and their narrow host range. In general, therefore, the closer the hosts are related, the closer the respective viruses are related. Overall, however, the mammalian orthohepadnaviruses and the avian avihepadnaviruses share a very similar genome organization and replication characteristics (Section III); hence, numerous aspects of one type of hepadnavirus are also applicable to the other types.

A. Primate Orthohepadnaviruses

After the discovery of human HBV in 1970 (Dane *et al.*, 1970) and the discovery that chimpanzees are susceptible to infection with human HBV and cloned HBV DNA (Will *et al.*, 1982), HBV-like viruses were detected in hominoid primates, such as in all great apes. Their genome sequences are extremely close to the variants circulating in the human population. Therefore, it has long been disputed whether they are true animal viruses or have been contracted by contact with humans; recent data provide accumulating evidence that hominoid primates do represent a natural reservoir for HBV (Robertson and Margolis, 2002). Obviously, none of these primates, with the limited exception of chimpanzees, is a feasible experimental animal. A new HBV discovered in woolly monkeys (*Lagothrix lagotricha*), a New World primate, is clearly distinct from human HBV (Lanford *et al.*, 1998). Woolly monkeys are an endangered species and therefore are not suited as experimental animals. Successful transmission of woolly monkey HBV (WMHBV) to the related, nonendangered spider monkey (*Ateles geoffrey*) raised hopes for the establishment of a new, lower primate infection model. However, viral titers appear to be low (less than 10^5 virions per milliliter of serum), which is unpractical. Attempts to infect primary hepatocytes from marmosets (*Callithrix jacchus*), a close relative of woolly monkeys, remained negative (Köck, McNelly, and Nassal, unpublished data). In contrast, primary hepatocytes from tree shrews (*Tupaia belangeri*) can clearly be infected by HBV and WMHBV (Köck *et al.*, 2001) although the animals are not true primates, and their assumed phylogenetic closeness to primates remains controversial (Murphy *et al.*, 2001; Schmitz *et al.*,

2000). Moreover, transduction of HBV genomes into tree shrews using replication-defective adenovirus vectors as vehicles (Ren and Nassal, 2001) led to a long-lasting HBV viremia *in vivo*. It has not yet been proven, however, whether the circulating HBV was derived from a true HBV infection or solely from the AdHBV vector. Given that tree shrews are relatively easily bred in captivity, establishing a self-sustained HBV infection in these squirrel-sized animals would indeed represent a major advance; however, the full potential of the system remains to be explored.

In the absence of a practical HBV infection model, several surrogate systems have been established to study the human virus. The ability of certain human hepatoma cell lines, such as HepG2 and Huh7, to support HBV replication upon transfection of cloned wild-type, and mutant, HBV DNA is a highly valuable tool to investigate replication *per se*; most of our current knowledge is derived from this system. Because these cell lines cannot be infected, however, the early steps of the replication cycle, such as entry and genome uncoating, are difficult to study. This restriction may be overcome by the recent discovery of a new human hepatoma line that, under specialized conditions of culture and inoculation, appears to be susceptible to HBV infection although infectibility seems to be lost after a number of passages (Gripon *et al.*, 2002).

Another model that has been highly useful in particular for immunological studies uses HBV transgenic mice (reviewed in Chisari, 1996). The animals contain a chromosomally integrated and linear $1.3\times$ overlength HBV genome (the terminal duplication mimics the circular form of the natural virus genome; hence, transcription is controlled by the authentic regulatory elements). The mice produce substantial amounts of viral antigens and complete virions, but these cannot infect mouse hepatocytes; in addition, there is no clear-cut evidence that the central intracellular intermediate of the authentic infection, a covalently closed circular (ccc) DNA molecule that is maintained in an episomal state and serves as the natural template for transcription of the viral RNAs, is formed in the mice except, perhaps, in a very special genetic background (Raney *et al.*, 2001). Nonetheless, based on the advanced state of mouse genetics and on the availability of various knockout mice as well as cloned genes of and antibodies against all immunologically relevant gene products, fundamentally new insights into the immune response against HBV have been gained (Section VI). Most notably, T cells can suppress HBV replication in a noncytolytic fashion, mainly mediated by type I and type II interferons and TNF- α (Guidotti and Chisari, 1999). Alternatively, mice have been

xenotransplanted with hepatocytes from other species (Dandri *et al.*, 2001a), including humans (Dandri *et al.*, 2001b), and studies have shown that these mice can be infected with HBV. Though powerful for some applications, the chimeric animals are technically difficult to generate and, by necessity, the recipients have to be severely immunocompromised to avoid transplant rejection. This also limits the immunological conclusions that can be drawn.

Therefore, a combined approach integrating biochemical *in vitro* analysis, genetics and infection in cell culture, and *in vivo* biology is currently not available for HBV.

B. Non-Primate Orthohepadnaviruses

Shortly after the discovery of human HBV, several related viruses were found in a few nonprimate mammals: the North American woodchuck (Summers *et al.*, 1978), the Beechey ground squirrel (Marion *et al.*, 1980), and the arctic ground squirrel (Testut *et al.*, 1996). No HBV-like viruses were found in species that are commonly used as laboratory animals, such as mice and rats. Woodchuck hepatitis B virus (WHV) has therefore become the model of choice for mammalian HBVs, as reviewed in Roggendorf and Tolle (1995) and Tennant and Gerin (2001). Its sequence is about 60% similar to that of the human virus and, importantly, WHV causes chronic hepatitis and hepatocellular carcinoma, just as does HBV. WHV is therefore used for tracking fundamental pathogenetic and therapeutic aspects of hepadnaviral infection (Mason *et al.*, 1998; Yamamoto *et al.*, 2002; Zhou *et al.*, 2000); with cloning of several key factors of the innate and acquired immune response (Guo *et al.*, 2000; Lohrengel *et al.*, 1998; Salucci *et al.*, 2002; Yang *et al.*, 2000), immunological studies can now be conducted. Experiments in chronically WHV-infected woodchucks have revealed some unexpected differences to data obtained in HBV transgenic mice and in acutely infected humans and chimpanzees; for instance, conventional treatment or gene therapy with IFN- γ , a major player in suppressing HBV replication in mice and in clearing acute infection, had no significant impact on chronic WHV infection (Jacquard *et al.*, 2004; Lu *et al.*, 2002). The reasons are not clear but certainly worth being followed. The advantage of WHV's remarkable similarity to human HBV related disease is, however, partially offset by several practical limitations. Adult woodchucks weigh about 4 to 5 kg, and they are difficult to handle. They do not breed easily in captivity and, therefore, many experiments are performed with wild animals trapped in their natural habitat in the northeastern part of the United States. These animals are outbred, and many of them are

infested with other pathogens. In addition, woodchucks hibernate, during which time no experiments can be performed. Another fundamental limitation of the WHV system is the current lack of cell lines that efficiently support replication of cloned WHV DNA; hence, the power of reverse genetics cannot be applied to WHV.

C. Bird HBVs (*Avihepadnaviruses*)

In 1980, Mason *et al.*, discovered an HBV-related virus, duck HBV (DHBV), in Pekin ducks (*Anas platyrhynchos forma domestica*; derived from mallard ducks); since then, the virus has been detected in a substantial fraction of commercially bred flocks, with no signs of overt pathogenicity or progression of chronic infection into liver cancer, except possibly in the presence of carcinogens such as aflatoxin (Cova *et al.*, 1994). The presence of HBV in ducks is generally viewed as the result of a long-lasting coevolution between virus and host and is supported by the rapid replacement by noncytopathic viruses of an artificial, cytopathic DHBV variant (Lenhoff *et al.*, 1998).

Further avihepadnaviruses have been isolated from grey herons (*Ardea cinerea*) (Sprengel *et al.*, 1988), snow geese (*Anser caerulescens*) (Chang *et al.*, 1999), white storks (Pult *et al.*, 2001), and, most recently, cranes (several species of the genus *Grus*) (Prassolov *et al.*, 2003); the latter reference also contains comprehensive sequence comparisons as well as a phylogenetic tree of the host birds. In general, avihepadnaviruses have a narrow host range (Section V.A.4), similar to the mammalian viruses, such that DHBV does not infect chickens (a desirable host in view of the advanced genetic and immunological knowledge on this species) (Marion *et al.*, 1987) or even Muscovy ducks (*Cairina moschata*) (Pugh and Simmons, 1994), which belong to the same order as Pekin ducks (Anseriformes). In turn, the viruses from storks and herons (order Ciconiiformes) are not detectably infectious for ducks *in vivo*; however, primary duck hepatocytes can be infected with heron HBV (HHBV) (Ishikawa and Ganem, 1995) though with a low efficiency, as seen for DHBV infection of primary Muscovy duck hepatocytes. Unexpectedly, crane HBV (CHBV) appears to efficiently infect primary duck hepatocytes although its natural host is more closely related to storks and herons (Prassolov *et al.*, 2003); the genome sequence of CHBV, by contrast, is closer to that of DHBV and snow goose HBV (SGHBV). The evolutionary background of this disparity is unclear; hence, further investigations are certainly warranted.

In general practical terms, however, DHBV will remain the most important of the avihepadnaviruses. Protocols for the reproducible

preparation and *in vitro* infection of primary duck hepatocytes have been established (Section V.A). In addition, the chicken hepatoma cell line LMH fully supports DHBV replication after transfection with cloned DHBV DNA, yielding infectious virions, and such recombinant viruses can be analyzed for infectivity in duck hepatocytes and ducks. Finally, some biochemical aspects of replication can as of yet only be investigated with DHBV (Section IV.B). Hence, the DHBV–duck virus–host pair is at present the only practical system in which all facets of hepadnaviral replication and infection, from molecular interactions to virus fitness *in vivo*, can be addressed. Many fundamental discoveries have first been made with DHBV, such as hepadnaviruses replication by reverse transcription (Summers and Mason, 1982), the mechanisms of cccDNA formation (Tuttleman *et al.*, 1986a), and initiation of reverse transcription, including its cell-free reconstitution (Wang and Seeger, 1992). Host-range determinants (Ishikawa and Ganem, 1995) and putative receptors have also been defined (Breiner *et al.*, 1998; Ishikawa and Ganem, 1995; Kuroki *et al.*, 1995; Urban *et al.*, 1998). In addition, the link between viral persistence and cccDNA following antiviral treatment was detected, and the first demonstration of the *in vivo* efficacy of antisense approaches against a viral infection was made with DHBV (Offensperger *et al.*, 1993), recently shedding new light on the antisense mechanism as such (Thoma *et al.*, 2001). Finally, DHBV was crucial for the development of hepadnavirus-based liver-specific gene delivery systems (Protzer *et al.*, 1999).

III. THE HEPADNAVIRAL INFECTIOUS CYCLE: AN OVERVIEW

All hepadnaviruses are DNA viruses (i.e., infectious virions contain DNA). Summers and Mason were the first to demonstrate, using DHBV, that this DNA is generated by reverse transcription (Summers and Mason, 1982). Hence, hepadnaviruses are related to retroviruses although the latter, based on the genome form present in infectious virions, are RNA viruses. Retroviral RNA is reverse transcribed upon infection of a new cell (i.e., as an early event of the cycle), whereas in hepadnaviruses, reverse transcription occurs late in the originally infected cell. In addition, integration of proviral DNA into the host chromosome is an obligatory step in retroviral but not hepadnaviral replication. To account for these fundamental differences, hepadnaviruses, together with a few plant viruses that use a similar strategy such as cauliflower mosaic virus, have been termed pararetroviruses.

Foamy viruses may form an evolutionary link between the two groups since their virions probably contain mostly DNA, as in hepadnaviruses, but replication requires integration (Linial, 1999).

A schematic comparison of the DHBV virion and the DHBV genome with that of HBV is shown in Fig. 1; with small modifications, all avian hepadnaviruses are similar to DHBV, and all mammalian hepadnaviruses are similar to HBV. All hepadnavirions possess an outer envelope, that is, a host-derived lipid bilayer into which the large (L) proteins and a small (S) surface protein are embedded; the mammalian viruses have an additional middle (M) surface protein (Section IV.C). The envelope encloses the icosahedral nucleocapsid formed by the capsid, or core, protein. The viral genome is a partially duplex and circular (but not covalently closed) DNA (relaxed circular, or RC DNA) of about 3.0 kb (avian) or 3.2 kb (mammalian HBVs) in length. The (–)-strand DNA is at full length, and its 5'-terminal nucleotide is covalently linked to the terminal protein (TP) domain of the reverse transcriptase, called the P protein; the (+)-strand is incomplete to various extents. A typical feature of all hepadnavirus genomes is their compact organization. All nucleotides (nt) have coding capacity in one open reading frames (ORFs); many nt have this capacity in two ORFs. In addition, all regulatory elements such as promoters and enhancers, as well as various other *cis*-elements, overlap with coding information.

The three major ORFs, *C*, *P*, and *S*, encode the core protein, the P protein, and the small surface protein (S). *C* and *S* are preceded by the preC and preS (preS1 and preS2 in orthohepadnaviruses) regions that give rise to N-terminally extended proteins. The precore protein is a secreted nonassembling core protein variant that, after N- and C-terminal processing, is found in serum as HBeAg (or DHBeAg in DHBV). Its function might be to modulate the immune response to the core protein, but this is poorly understood (Section IV.A.3). Similarly, cotranslation of the preS region with *S* yields the L protein (which in HBV is the product of the complete *preS1/preS2/S* ORF; *preS2/S* gives the M protein). Three major internal promoters drive transcription of the *C*, *S*, and preS/S mRNAs, which all end after a common polyadenylation signal; the *C* and, in mammalian hepadnaviruses, the *S* transcripts have staggered 5'-ends bracketing the upstream preC and preS2 ATGs. The *C* mRNA encompasses the entire genome plus a terminal redundancy. The P protein is also translated from this transcript which, in addition, is packaged into nucleocapsids for reverse transcription; the transcript is therefore also termed RNA pregenome, or pregenomic RNA (pgRNA). One major difference between the avian and mammalian viruses is the presence, in the latter,

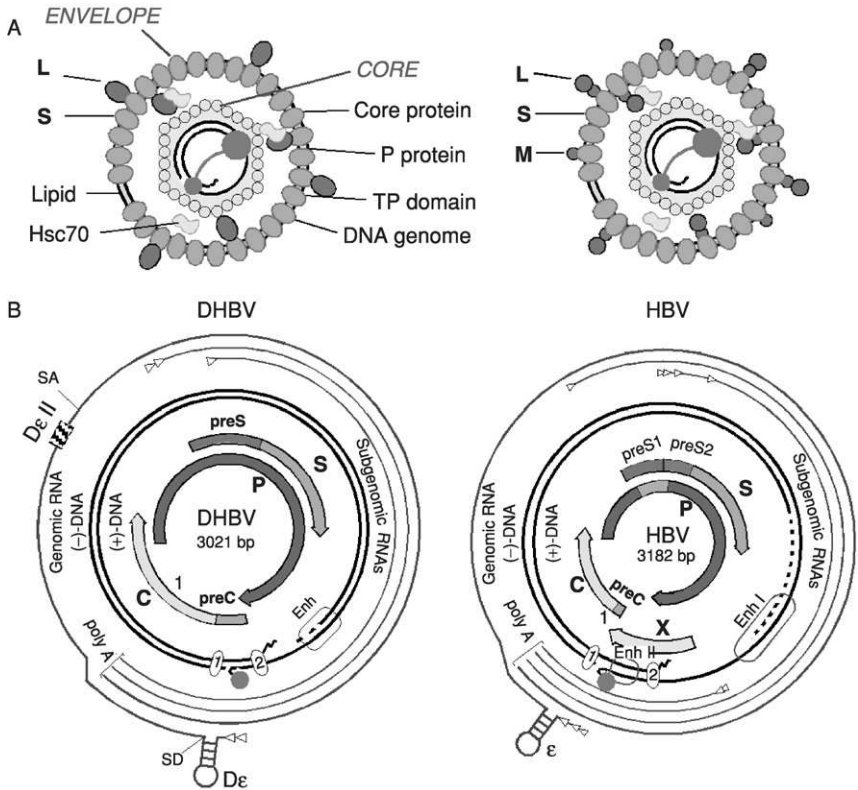


FIG 1. Comparison between DHBV and HBV. (A) Virion structure. The surface proteins (L and S in avihepadnaviruses; L, M, and S in orthohepadnaviruses) are embedded into the lipid envelope that enwraps the nucleocapsid formed by the core protein. Virions contain the cellular heat-shock protein Hsc70 and, possibly, other cellular factors. The genome inside the capsid is shown in its DNA form with one complete strand, with the covalently linked TP domain of P protein, and the incomplete second strand. (B) Genome organization. The different circles represent, from the periphery to the center, (i) the various transcripts with the arrowheads indicating start sites; (ii) the partially double-stranded DNA genome with the circles numbered 1 and 2 representing the direct repeat (DR) and Enh as the enhancer elements; and (iii) the open reading frames C, P, S, and X. The ϵ and D_{ϵ} denote the RNA stem-loops that act as encapsidation signals and replication origins for reverse transcription. The D_{ϵ} II is a second RNA element essential for encapsidation in avihepadnaviruses that has no known counterpart in the mammalian viruses. The SD and SA are the major splice donor and acceptor sites in DHBV. (See Color Insert.)

of an additional open reading frame called X. This frame encodes a regulatory protein whose exact function is still incompletely understood although a stimulatory effect on HBV replication has recently been reconstituted in transfected hepatoma cell lines (Bouchard *et al.*, 2001). Stimulation correlates with the ability of HBx to release Ca^{2+} from internal stores, which then leads to activation of kinases (Bouchard *et al.*, 2001; Nassal, 2002) that possibly target the capsid protein (Section IV.A). Avian hepadnaviruses apparently lack an X ORF although a “hidden” X-like ORF in DHBV has recently been shown to be present and expressed in cultured cells (Chang *et al.*, 2001). It is unclear, however, from what RNA the X-like product would be translated, and recent *in vivo* experiments in ducks did not provide evidence for a functional importance of the gene product in DHBV infection (Meier *et al.*, 2003). A second obvious difference is the size of the core protein, which consists of only about 180 amino acids (aa) in the mammalian hepadnaviruses but about 260 aa in the avian hepadnaviruses (Section IV.A).

A simplified view of the hepadnaviral infectious cycle is shown in Fig. 2. The individual steps are briefly outlined in the figure legend. Only those steps whose understanding has been greatly enhanced by using the DHBV system and those that are addressed in the following sections are listed. Enveloped virions bind, via exposed preS domains, to specific receptor(s) on the hepatocyte surface and are internalized (Section V.A.3). The nucleocapsid is released into the cytoplasm and transported to the nucleus by way of nuclear localization signals (NLSs) in the core protein (Section IV.A.1). The intact nucleocapsid can apparently traverse the nuclear pore whose functional diameter, with about 39 nm, appears to be significantly larger (Pante and Kann, 2002) than previously estimated (Dworetzky *et al.*, 1988). The disassembly of the capsid shell and release of the genomic RC DNA into the nucleoplasm are not well understood but, eventually, the RC DNA is converted into episomal cccDNA, which then acts as a transcriptional template for cellular RNA polymerase II. Nuclear export of the orthohepadnaviral transcripts is mediated by a posttranscriptional regulatory element (PRE) (Zang and Yen, 1999) whose counterpart, if any, in avihepadnaviruses has not been defined; notably, a major spliced transcript is produced from the pgRNA of avihepadnaviruses but not orthohepadnaviruses (Obert *et al.*, 1996).

Once in the cytoplasm, all viral RNAs are translated. The pgRNA packaging relies on a specific chaperone-mediated interaction between the P protein and an RNA stem-loop structure on the pgRNA called ϵ , which also acts as replication origin for RT (Section IV.B.2.1). The

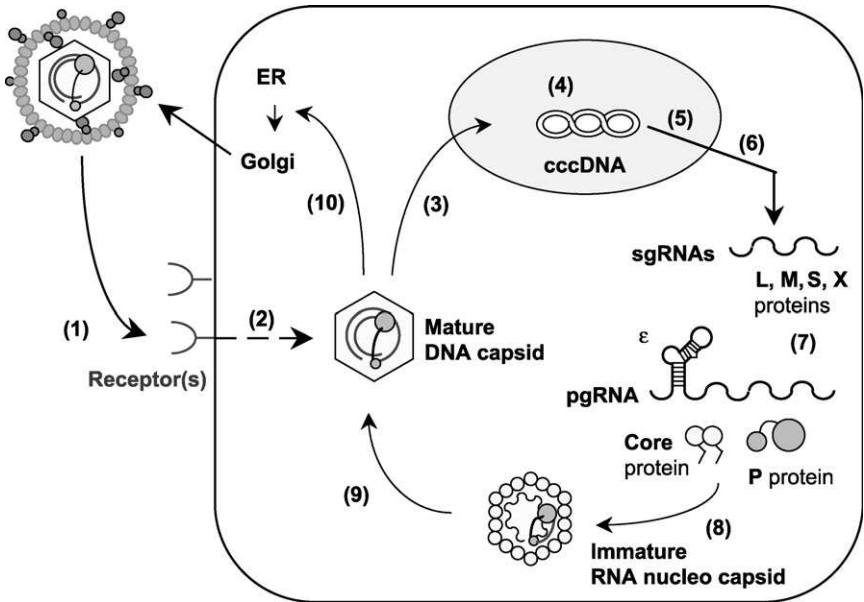


FIG 2. Simplified scheme of the hepadnaviral infectious cycle. Infectious enveloped virions containing the partially double-stranded circular DNA genome with the covalently linked P protein bind to cell surface receptor(s) (1), are internalized, and released the nucleocapsid into the cytoplasm (2). The nucleocapsid transports the genome to the nucleus (3) where it is converted into cccDNA (4). Transcription (5) yields subgenomic RNAs (sgRNAs) and pregenomic RNA (pgRNA) that are exported (6) and translated in the cytoplasm (7); sgRNAs give rise to the surface proteins L and S and, for orthohepadnaviruses only, the M and X proteins. The pgRNA is a bicistronic mRNA for core and P proteins. P protein binds to the ϵ RNA stem-loop, mediating pgRNA encapsidation (8). The precore precursor of HBeAg originates from a 5'-terminally extended pgRNA species (not shown) that is not encapsidated. Reverse transcription inside the immature RNA nucleocapsid leads to the mature DNA-containing nucleocapsid (9), which is either redirected to the nucleus for cccDNA amplification (3) or is exported via interaction with the surface proteins at the endoplasmic reticulum (ER) or a post-ER compartment (10). Some hepatoma cell lines support virion formation upon transfection or transduction of cloned hepadnaviral genomes but, with one recent exception (Gripon *et al.*, 2002), cannot be infected. (See Color Insert.)

complex of the P protein with pgRNA is then believed to act as a nucleation center for nucleocapsid assembly although the mechanism is poorly understood. The P protein binds predominantly but not exclusively to the pgRNA from which it has been translated, that is *in cis* (Bartenschlager *et al.*, 1990); however, there is also some evidence for a *cis*-preferential recruitment of the core protein, at least under certain

conditions (von Weizsäcker *et al.*, 2002). Whether initiation of reverse transcription precedes assembly of the capsid shell is not finally settled; however, the bulk of DNA synthesis occurs inside the specialized environment of the assembled nucleocapsid (Section IV.B.2.b). DNA synthesis seems to induce structural changes in the nucleocapsid (a “maturation signal”), enabling it to leave the cell via interaction with the preS domains of the L protein at the ER or a later pre-Golgi compartment. Notably, this requires preS to be on the opposite side of the membrane than is required for interaction with cellular receptors (Section IV.C.2.). Alternatively, the progeny nucleocapsids may be re-directed to the nucleus, giving rise to some 10 to 100 copies of cccDNA (Tuttleman *et al.*, 1986a). For DHBV, there is strong evidence that secretion versus nuclear transport is regulated by the availability of the L protein (Summers *et al.*, 1990).

IV. DHBV PROTEINS AND THEIR BASIC FUNCTIONS IN REPLICATION AND MORPHOGENESIS

All hepadnaviruses produce three types of particles (reviewed in Nassal, 1996): complete enveloped virions (diameter about 42 nm); nucleocapsids which, *in vivo*, are found only intracellularly (core particles; diameter about 30 to 34 nm in cryo-electron micrographs but only about 27 nm upon negative staining); and empty envelopes (S particles, or subviral particles, SVPs) that are secreted in vast excess over virions. Orthohepadnaviruses produce two morphologically distinct forms: 22-nm diameter (negative staining) spheres and filaments with the same diameter but variable lengths. Avihepadnaviral S particles are pleiomorphic but, in general, are less distinct from complete virions.

A. *The Core Protein*

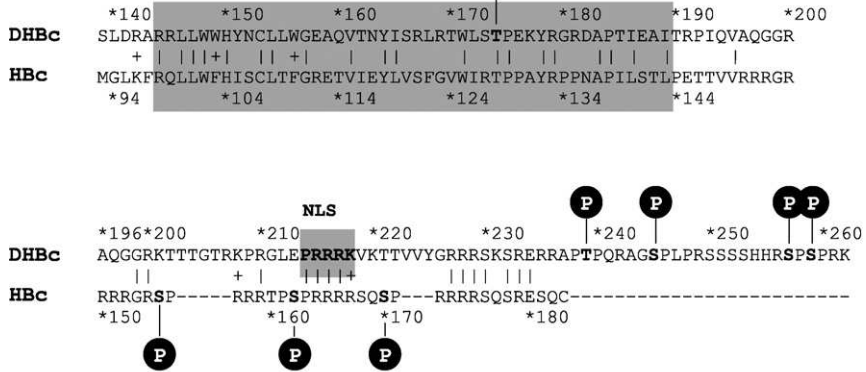
1. *Functions of the Core Protein*

All hepadnaviruses encode only a single core protein (Section IV.A.3 covers the secretory, nonassembling HBeAg). Its most obvious function is to form the viral nucleocapsid which, as with all viruses, serves as a protective container for the genome. The assembly capability resides in the larger N-terminal domain, and nucleic acid binding is provided by a C-terminal Arg-rich region. This two-domain structure is conserved between mammalian and avian hepadnavirus core proteins, but their

primary sequences differ substantially. The DHBV core protein consists of 262 aa, and its HBV counterpart has only 183 aa (185 aa in some subtypes); a comparison between parts of the two sequences is shown in Fig. 3. It should be noted that the similarity in the N-terminal part is rather low and that different algorithms yield different alignments; a BLASTP search of the SwissProt database using only the first 145 aa of the DHBV core protein (or DHBc) as a query does not detect the HBV core protein (or HBc). Apart from the basic C-terminal domain there is, however, one region of rather high similarity; it starts around aa 144 of DHBc (corresponding to aa 98 of HBc) and extends through what in the known HBc structure (Section IV.A.2) is the last central and the C-terminal helix as well as through a bent Pro-rich region involved in contacts between dimers (i.e., the multimerization sites required for assembly). Why the avian viruses with their even smaller genomes have a much larger core protein is enigmatic; evidently, the smaller mammalian virus protein is fully functional. The basic C terminus plays an important role in both proteins, not only in pgRNA packaging but also in facilitating reverse transcription.

A further core protein function is the transport of the genome to the nucleus where the RC DNA is converted into cccDNA. For the human virus, this is likely to occur by an importin α/β -dependent process mediated by one or more NLSs in the Arg-rich C-terminal region (Kann *et al.*, 1999). Intact capsids seem to traverse the nuclear pore into the nuclear basket; the pore itself is substantially larger than previously assumed (Pante and Kann, 2002). Under various circumstances, mammalian core protein and sometimes core particles have been found in the nucleoplasm, but their physiologic relevance is yet not clear. Nonassembled subunits are possibly imported and, after reaching a critical concentration, spontaneously assemble inside the nucleus. For the DHBV core protein, by contrast, no intranuclear accumulation has been reported. However, the basic motif PRRRRK (aa 214–218) is not only predicted but, using fusions of C-terminal DHBc segments with GFP, was also experimentally shown to act as an NLS (Mabit *et al.*, 2001); how exposure of this NLS is achieved on intact nucleocapsids is not clear. The simultaneous presence of a nuclear export signal (NES)-like activity might explain why there is no bulk accumulation of nucleocapsids in the nucleoplasm. Small amounts of nuclear core protein, however, have been detected (Summers, unpublished data, Mabit *et al.*, 2003) in distinct subnuclear bodies early in infection, a fraction of which colocalized with pgRNA; this raises the possibility that the core protein might somehow be involved in the synthesis and/or maturation of the RNA. Indeed, the

A



B

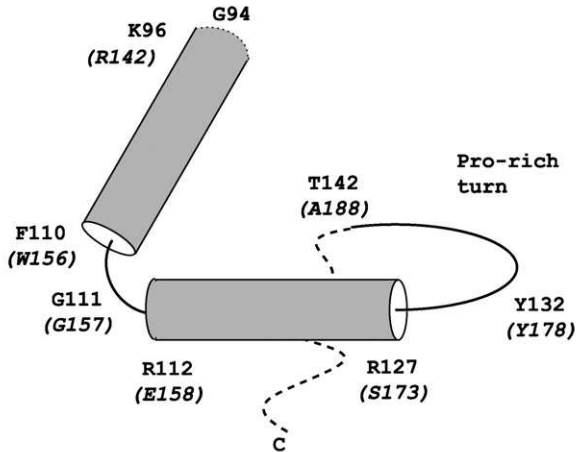


FIG 3. DHbc versus HBc. (A) The core proteins of DHBV and HBV. The proteins differ substantially in length (262 aa versus 183 aa) and sequence. The two regions with significant homology are shown in detail (| and +, identical and similar amino acids respectively). In the upper sequence, the homologous region is highlighted by shading. The lower alignment shows the C-terminal Arg-rich domains. NLS refers to the nuclear localization signal in DHbc; the encircled P indicates major phosphorylation sites. (B) The region that corresponds to the C-terminal end of the assembly domain (see also Fig. 4). This region's structure is shown in HBc and comprises about half of the penultimate helix plus the C-terminal helix as well as Pro-rich turn mediating interdimer contacts in the capsid. The positions of the HBc amino acids are indicated, and the corresponding DHbc amino acids are given in parentheses. The basic C-terminal domain (dotted line), whose structure is not known, is drawn pointing toward the capsid interior.

IFN- α resistance of a capsid protein deficient-mutant DHBV suggested that the core protein has a role in the establishment of viral transcript pools (Schultz *et al.*, 1999).

A hallmark of many functions involving viral capsid proteins is that they must be reversible to allow completion of the infectious cycle. Capsids must assemble and disintegrate; genomic nucleic acids must be bound and released; and nuclear import of the genome, if required for replication, must be followed by export to allow for release of progeny viruses. Apart from localization to different cellular compartments, two potential levels of regulation are the quaternary structure (assembled versus nonassembled) and chemical modification; obviously, each of them can influence the other. This discussion's understanding of these processes is limited for both mammalian and avian hepadnaviruses; however, phosphorylation seems to be an important regulatory mechanism. The major phosphorylation sites in DHBC and HBC are located in the Arg-rich C terminus; they involve Ser- and Thr-residues that are in a basic local environment and are followed by a Pro-residue (HBC: S155, S162, S170; DHBc: T139, S245, S257, S259) (Fig. 3). These motifs conform to consensus sites for different protein kinases, and various kinases including PKC (Kann *et al.*, 1993) and, recently, Ser-Arg-rich protein kinases (SRPK1 and 2) have been proposed to be responsible for HBC phosphorylation (Daub *et al.*, 2002); SRPK1 can also phosphorylate DHBC *in vitro* (Vogel and Nassal, unpublished data). In addition, a cdc2-kinase phosphorylation site may be present at Thr174 within the region that is most highly conserved between avi- and orthohepadnaviral core proteins (Barrasa *et al.*, 2001). Mutations supposed to affect phosphorylation can indeed profoundly influence particle assembly and function; however, direct structural consequences by the altered amino acid side chains are difficult to exclude. Intracellular DHBC is more highly phosphorylated than DHBC isolated from secreted virions (Mabit and Schaller, 2000; Pugh *et al.*, 1989), suggesting that phosphorylation and dephosphorylation are important during nucleocapsid assembly and maturation. For HBC, there is evidence that phosphorylation precedes, and is important for, pgRNA encapsidation (Gazina *et al.*, 2000), but for DHBC, the situation is less clear. Individual or combined, substitution of the four major phosphorylation sites by either Ala or Asp (supposed to mimic unphosphorylated and phosphorylated Ser and Thr, respectively) had no major effect on pgRNA encapsidation (Yu and Summers, 1994). The most prominent phenotype was an apparent defect of the S245A mutant in genome maturation. According to a recent reanalysis, however, the mutation may instead selectively decrease the

stability of nucleocapsids containing mature, complete RC DNA. Unexpectedly, introducing the likewise uncharged Asn instead of Ala led to stable capsids and enveloped virions, which were, however, noninfectious. This suggests that phosphorylation of Ser245 is not essential during RNA packaging and reverse transcription but that it may play a role after infection of a new cell, such as in destabilizing the capsid for genome uncoating (Köck *et al.*, 2003). At present, a coherent interpretation of these mutational data is difficult: it is not clear how well the substitutions mimic phosphorylated and nonphosphorylated serine or threonine because the structural details of charge distribution and hydrogen bonding patterns are not identical, the authentic phosphorylation reactions may proceed sequentially, and RNA/DNA binding as well as the overlapping NLS function of the Arg-rich region are certainly all influenced by the mutations.

Mutational analyses of the envelope proteins strongly suggest that nucleocapsid envelopment is due to specific interactions between the core particle and cytoplasmically exposed preS domains of the L protein (Section IV.C.3) (Bruss and Vieluf, 1995; Summers *et al.*, 1991). In an extensive mutational screen of the HBV core protein, most mutations affecting envelopment mapped to the canyons surrounding the tips of the capsid rather than the tip structures themselves (Ponsel and Bruss, 2003). Unfortunately, no similar high-resolution structural data are yet available for DHBc. However, also in the absence of the L protein, a fraction of DHBV nucleocapsids become membrane associated, and such capsids resemble those present in virions in that they are hypophosphorylated and contain mainly mature DNA genomes (Mabit and Schaller, 2000). This suggests that phosphorylation/dephosphorylation accompanies genome maturation, either as a cause, or as a consequence, and that these events could profoundly affect the capsid structure.

2. Capsid Structure and Assembly

Recombinantly expressed HBV core protein spontaneously assembles into capsid-like particles (CLPs). The isolated assembly domain (aa 1–149), lacking the Arg-rich C terminus, is particularly well expressed in bacteria (Birnbaum and Nassal, 1990). By cryo-electron microscopy and image processing (Baker *et al.*, 1999), electron density maps of such CLPs were determined at about 7.5 Å resolution. Integration of these and numerous biochemical data (reviewed in Nassal, 1996, 2000) allowed, for the first time ever, to directly predict the three-dimensional (3-D) fold of a protein from electron microscopy, as shown in Fig. 4 (Böttcher *et al.*, 1997; Conway *et al.*, 1997), and this

structural model was fully confirmed by X-ray crystallography (Wynne *et al.*, 1999). The capsid itself has icosahedral symmetry. There are two classes of capsids: a minor one consisting of 180 core protein subunits (triangulation number $T = 3$) and a major one consisting of 240 subunits ($T = 4$), which is probably the biologically relevant structure (Kenney *et al.*, 1995). Definitely solving this issue will require high-resolution analyses of authentic, genome-containing nucleocapsids. A characteristic feature, predicted by biochemical data (Nassal *et al.*, 1992; Zhou and Strandberg, 1992), is that two monomeric subunits form a very stable, symmetrical dimer; the overall dimer shape resembles the letter T, turned upside down, in which the dimer interface forms

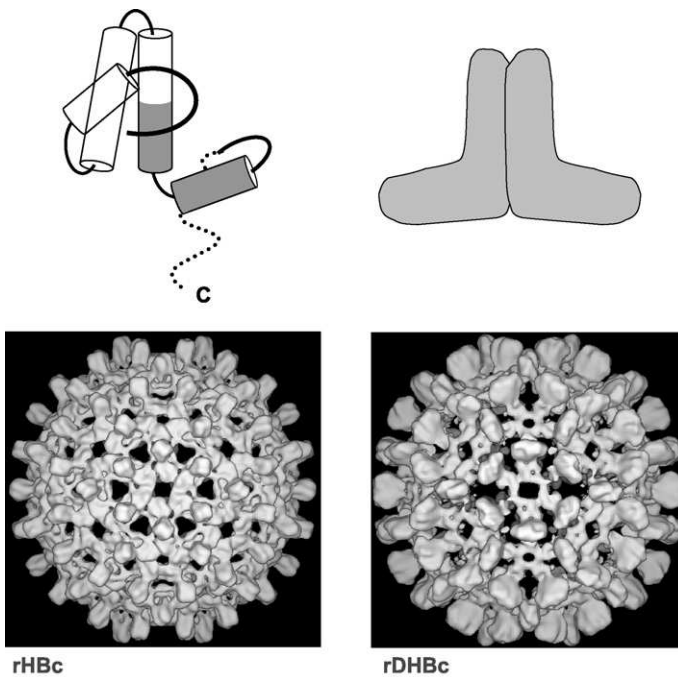


FIG 4. Structure of HBV and DHBV capsids. (Top left) The HBV core protein fold in one subunit. The shaded part corresponds to that shown in Fig. 3. (Top right) Interactions between the central two helices, two subunits that form a stable, four-helix-bundle dimer resembling an upside-down letter T. (Bottom left and right) The 3-D reconstructions, derived by cryo-electron microscopy of recombinant HBc and DHBc particles (Böttcher and Nassal, unpublished data). These images reveal a similar overall architecture but a much more elaborate structure in the DHBc spikes, indicating the presence of six helices per spike rather than the four in HBc.

the central stem, and each subunit contributes one half of the crossbar (Fig. 4). The crossbars, corresponding to the C-terminal part of the assembly domain's primary sequence, contain the interaction sites between individual dimers and are thus responsible for capsid assembly; the stems protrude from the capsid surface as prominent spikes that are readily visible by conventional negative staining electron microscopy.

Much fewer data are currently available for the DHBV core protein. One reason is that most investigators concentrated on the medically important human virus and, indeed, a new class of drugs targeting the capsid has very recently been described (Deres *et al.*, 2003). Another reason is that recombinant expression of DHBc was much less efficient. Transfection studies revealed that particles from a variant truncated after aa 226 were devoid of DNA (Schlicht *et al.*, 1989), while deleting fewer amino acids from the C terminus gradually affected (+)-strand DNA synthesis and RC DNA formation (Yu and Summers, 1991); alternatively, the lack of detectable RC DNA in variants lacking 16 or more amino acids might be explained by the selective destabilization of capsids containing full-length RC DNA (Köck *et al.*, 2003). Variants lacking just the last 12 aa appeared normal in RC DNA formation but were noninfectious (Schlicht *et al.*, 1989). Another study showed, by negative staining, that a recombinant derivative truncated at aa 229 still formed particles (Yang *et al.*, 1994). Earlier cryo-electron microscopy revealed that recombinant DHBV and HBV capsids have a similar architecture but that the spikes are much larger, consistent with the larger size of the DHBV core protein (Kenney *et al.*, 1995). Using a newly established and highly efficient bacterial expression system for DHBc, researchers are currently readdressing some of its fundamental biochemical properties. Various C-terminal deletions showed that the first 195 aa are still competent for particle formation; this corroborates the alignment shown in Fig. 3, according to which DHBc V195 is homologous to V149 in HBc. Different from HBc, such truncated DHBc molecules form increasingly polymorphic particles that are not suited for high-resolution structural studies. New data indicate that the region between aa 100 and 125 can be replaced by small foreign peptide sequences without abolishing particle formation. This segment is therefore probably part of the exposed surface spikes. Preliminary intermediate resolution 3-D reconstructions of DHBV capsids (Fig. 4) derived from the full-length protein strongly suggest that the protein forms similar T-shaped dimers as the human virus protein and that the interdimer contacts also rely on extensions protruding in opposite directions from the dimers; in addition, the

spikes appear to be formed by six rather than four helices (Böttcher and Nassal, unpublished data). The extra helices might be contributed by central regions, but the primary sequences of HBc and DHBc are too divergent for meaningful inferences, except that the high homology region following aa 145 (see Fig. 3) can be modeled into a similar structure as the corresponding sequence following aa 98 in HBc; this suggests that, in this region, DHBc has a similar structure and uses similar contacts for multimerization. An alternative, and intriguing, possibility is that the extra density at the spikes is caused by the C-terminal basic regions protruding out from the particles (see subsequent paragraphs). Additional data, however, such as structural analysis of internal deletion and insertion variants, are needed to directly trace the peptide chain.

As emphasized before, the nucleocapsid is not a static structure but rather a dynamic assembly that undergoes regulated structural transitions. Generation of progeny virions requires formation of stable nucleocapsids in the producer cell, whereas infection of a new cell requires disassembly, or at least opening, of this stable structure to allow release of the viral genome. In hepadnaviruses, yet another dimension is added by the fact that reverse transcription of the pgRNA takes place almost entirely inside the capsid. Hence, there are RNA-containing as well as DNA-containing nucleocapsids at various stages of maturation. At present, it is unclear, even with the high-resolution HBV capsid structures at hand, to which of those various forms of natural nucleocapsids they correspond. Given the experimental limitations with HBV, DHBV should offer a chance to obtain sufficient quantities of nucleocapsids halted at various maturation stages for high-resolution electron microscopy studies. There is little doubt, however, that the biochemical properties and, consequently, the structures of the nucleocapsid are indeed altered upon reverse transcription of the pgRNA. As was noted early on, enveloped virions contain almost exclusively mature RC DNA (Summers and Mason, 1982), suggesting that only nucleocapsids containing a replication-competent genome and a functional P protein gain the ability to be enveloped and be secreted; conceivably, formation of double-stranded DNA (dsDNA) inside the capsid lumen transmits a "maturation signal" (i.e., a structural change) to the capsid surface. Evidence supporting this model has been obtained for both HBV and DHBV (Gerelsaikhan *et al.*, 1996; Wei *et al.*, 1996); a possible experimental restriction is the release, by an unknown mechanism, of nonenveloped nucleocapsids from transfected cells that can obscure the analysis of the genome form present in secreted virions. However, it appears that even these released

nucleocapsids contain mainly mature RC DNA (Mabit and Schaller, 2000), and the selective envelopment of mature dsDNA-containing nucleocapsids has been corroborated after thorough separation of enveloped from nonenveloped DHBV particles (Perlman and Hu, 2003). Because phosphorylation patterns also change with maturation, and because the mapped phosphorylation sites reside in the Arg-rich C terminus (which, according to the EM data, is mostly if not entirely located inside the capsid lumen), it is tempting to speculate that the maturation signal consists of a rearrangement that leads to the exposure of this region on the capsid surface; such a mechanism could also make the NLSs accessible to the nuclear transport machinery. As of yet, however, there is no direct evidence to support this mechanism, and, as for phosphorylation *per se*, it is not clear how many of the 240 core protein subunits would have to undergo this switch to change the overall properties of the nucleocapsid.

3. *DHBeAg*

Translation of the joint preC/C ORF yields the precore protein, an N-terminally extended form of the core protein that, through the signal peptide function of the preC encoded amino acid, is directed into the cell's secretory pathway. During this passage, the HBV precore protein is processed such that the first 19 of the 29 additional N-terminal amino acids and the entire Arg-rich region are removed; the final product found in the serum of infected individuals is known as HBeAg. Likewise, all avihepadnaviruses contain an in-frame preC region that for DHBV comprises 43 aa, including four cysteines as in the mammalian viruses. In HBV, the one Cys residue remaining in mature HBeAg (at position -7 relative to the start of the core protein) is essential for the distinct structure and antigenicity of HBeAg: it forms an intramolecular disulfide bond with Cys61, which in HBeAg is located in the capsid spike, and an intermolecular disulfide bond to Cys61 in the second dimer subunit can form. Hence, the precore-specific intramolecular disulfide bond massively influences the protein's structure (Nassal and Rieger, 1993). The only cysteine in DHBeAg (position 153) clearly corresponds to Cys107 in HBcAg (see Fig. 3) and is highly unlikely to be available for disulfide bonding with any of the DHBV preC-encoded cysteines (Schlicht, 1991). Hence, the structural basis for DHBeAg as a distinct antigen from DHBeAg is unknown and so are the exact processing sites of the precore protein. The function of both the mammalian and the avian HBeAg and/or their precore precursors is still obscure; precore-deficient HBVs have frequently been found in patients (Carman *et al.*, 1989; Thomas, 1995).

Taking advantage of the DHBV system, Summers *et al.*, have begun to address this question by infecting ducks with mixtures of wild-type and precore-deficient DHBV variants (Zhang and Summers, 1999). Their data suggest that DHB_eAg, and by inference HB_eAg, may provide a selective advantage during some stages or conditions of infection but not others. DHBV provides a unique opportunity to follow up these promising results by quantitative analyses that are not possible with the human virus.

B. The Reverse Transcriptase (P Protein)

1. Structure of the P Protein

All hepadnaviral P proteins share a common principal structure (Fig. 5). With about 90 kDa, these proteins are substantially larger than retroviral RTs, mainly due to the presence of the additional N-terminal TP domain and a spacer region that connects TP to the polymerase and RNaseH domains typical of all RTs (Xiong and Eickbush, 1990). Although the P protein sequences are quite divergent even in these common domains, they contain several short signature boxes (Eickbush, 1994; Sousa, 1996) that occur in the corresponding domains of other polymerases. A recent molecular modeling study of the polymerase domain of the HBV P protein, using HIV pol as a template, predicts a high structural similarity to the corresponding domain of HIV-1 RT (Das *et al.*, 2001). Mutational studies on the box C motif containing the sequence Tyr-Met-Asp-Asp (YMDD) confirmed the importance of the two Asp residues (Chang *et al.*, 1990; Radziwill *et al.*, 1990), which in other RTs coordinate, together with a third acidic residue in box A, two essential metal ions (Steitz, 1999). The participation of box C residues in active site formation is further underlined by the natural occurrence of mutations during chemotherapy of chronic hepatitis B in humans with nucleoside analogues (Mutimer, 2001). These studies have been extended to phenylalanine 451 (F451) of the DHBV P protein because, based on alignments, this aromatic residue in the A-box could be equivalent to Y115 in the HIV-1 and F155 in the MoMLV RT; which are important parts of the dNTP binding pockets. Replacement of F451 by amino acids with smaller side chains, in particular Ala and Gly, enabled the protein to use rNTPs instead of dNTPs to initiate reverse transcription *in vitro* (see subsequent paragraphs). Hence, F451 is important for dNTP versus rNTP discrimination, indicating a similar architecture of the active site and the dNTP binding pocket in hepadnaviral and retroviral

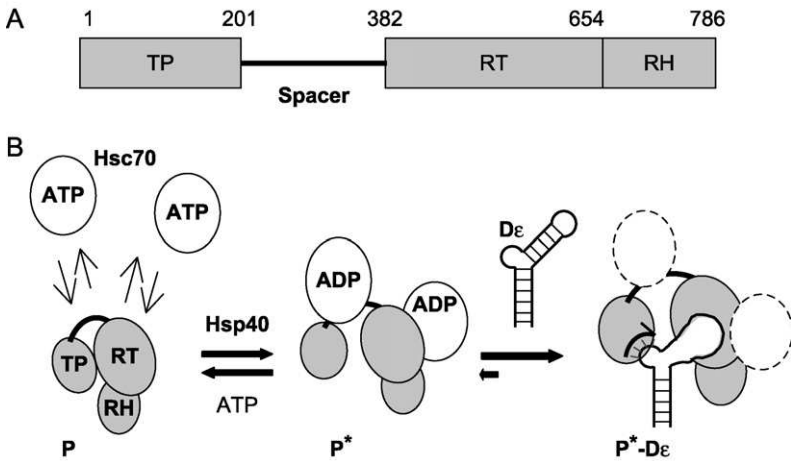


FIG 5. Structure and activation of DHBV reverse transcriptase. (A) Domain organization. The unique terminal protein (TP) at the N terminus is connected through a dispensable spacer to the reverse transcriptase (RT) and RNaseH (RH) domains found in all reverse transcriptases (B) Chaperone-mediated activation of DHBV P protein. The scheme is derived from a recently developed *in vitro* reconstitution system (Beck and Nassal, 2003). The P protein is in a closed conformation unable to bind ε RNA unless assisted by Hsc70 and Hsp40; in intact cells, additional factors might contribute to P activation. The weak initial interaction of Hsc70-ATP with P is stabilized through Hsp40, which stimulates the Hsc70 ATPase activity to form an activated P* complexed with probably two molecules of Hsc70-ADP. In the absence of $D\varepsilon$, an equilibrium concentration of P* is formed due to continuous decay and reformation; in its presence, a more stable P*- $D\varepsilon$ complex is formed. Through induced-fit structural alterations in the RNA and the protein, the complex becomes competent for initiating DNA synthesis of a short, $D\varepsilon$ -templated DNA primer whose 5'-end is covalently linked to a Tyr-residue in the TP domain. Whether the chaperones are still bound at this stage is not known. The DNA oligonucleotide is subsequently translocated to a direct repeat element close to the 3'-end of pgRNA to prime synthesis of a complete first-strand DNA molecule (not shown). (See Color Insert.)

reverse transcriptases. Further molecular modeling studies, including data already generated for the RNase domain (Chen *et al.*, 1994), may soon reveal a more detailed picture of the structure of P protein. However, the unique features of hepadnaviral replication including the priming role of TP, the template specificity for ε , and the strict dependence on cellular factors will not yield to this approach but rather require experiments directly addressing the underlying interactions.

2. Enzymatic Activities of the P Protein

a. Replication Initiation Many retroviral reverse transcriptases, even if recombinantly expressed in bacteria, can use any given RNA template when provided with a suitable primer and dNTPs (as is evident from their application to cDNA synthesis). For years, hepadnaviral P protein activity could be studied only by transfection, and most attempts to produce a recombinant P protein in a simple heterologous system, such as *Escherichia coli* had failed. A major advance was the demonstration, by Seeger and colleagues, that DHBV P protein (*in vitro*-translated in rabbit reticulocyte lysate (RL) and therefore under cell-free conditions) was able to perform the authentic template-specific initiation reaction (Wang and Seeger, 1992). The P mRNA used for *in vitro* translation contained, at its 3'-end, a copy of the RNA encapsidation signal (ϵ , or $D\epsilon$ for DHBV). This RNA stem-loop structure, present twice on the terminally redundant pgRNA, had been recognized as an essential cis-element for specific pgRNA packaging into nucleocapsids, mediated by P protein binding. Further experiments in the RL system soon suggested that the P- $D\epsilon$ interaction is also indispensable for initiation of DNA synthesis. This was confirmed genetically for both DHBV (Pollack and Ganem, 1994; Wang and Seeger, 1993) and HBV (Nassal and Rieger, 1996) although, in transfected cells and in the context of a complete virus genome, only the 5'-proximal ϵ copy is active (Rieger and Nassal, 1996). Hence, ϵ also acts as replication origin for first-strand DNA synthesis. A further useful feature of the RL system is that $D\epsilon$ provided as a separate, small RNA also fulfills this function.

Therefore, it became possible to investigate the influence of mutations in DHBV P protein (i.e., by using correspondingly altered *in vitro* transcripts as mRNAs) as well as in $D\epsilon$ RNA on the initiation reaction. Because of a limited size of about 60 nt, even completely synthetic $D\epsilon$ RNA variants could now be studied. Using chimeric RNA-DNA molecules, for instance, it was shown that five ribonucleotides in the $D\epsilon$ bulge region are necessary and sufficient to make a suitable template for the P protein; all other positions can also be occupied by deoxyribonucleotides (Schaaf *et al.*, 1999). Obviously, there are no restrictions concerning the exact composition of the bases and the sugar moieties that can be used for such studies. Once the secondary structures of wild-type $D\epsilon$ (wt $D\epsilon$) and various mutants had been established (Beck *et al.*, 1997), structural features could be correlated with the ability of a given RNA to bind to P protein and its suitability as a template for initiation of DNA synthesis (Beck and Nassal, 1997).

These two properties are not entirely equivalent: P protein binding is necessary but not sufficient for initiation. P binding usually requires that an RNA can adopt a wt-like secondary structure containing a few specific bases at defined positions; mutations causing formation of a stable non-wt-like structure prevent binding. Surprisingly, at first sight, some RNA mutants meeting the first criterion and binding to P failed to act as replication origin; another mutant bound despite a clearly different structure and supported DNA initiation just as did the wtRNA. This apparent paradox was explained by the finding that P protein binding is accompanied by a major structural change in the D ϵ RNA, in particular a loss of base pairing in the upper stem (Beck and Nassal, 1998). The mutant RNA that was inactive as a template could not undergo this structural alteration, whereas the mutant with a free-state structure different from wt adopted a wt-like structure when complexed with the P protein. This strongly suggests that the structural rearrangement is functionally important to properly juxtapose the priming Tyr-residue in the TP domain and the polymerase active site on the template region within D ϵ . This induced-fit mechanism also appears to affect the protein's structure because free P protein and P protein with bound D ϵ RNA differ in their susceptibility toward proteases (Tavis *et al.*, 1998). A thorough mechanistic understanding will, however, eventually require direct 3-D structural data.

This goal, until recently, seemed to be far out of reach, not only because of the difficulties in generating appreciable amounts of full-length recombinant P protein but also because the replication-competent P complexes generated in RL contained additional, functionally essential cellular components. RL contains abundant amounts of chaperones, many of which were originally identified as heat shock proteins (Hsps) because their expression is strongly induced by increased temperature or other stress conditions; however, most Hsps are also highly expressed under normal conditions because of their essential role in general protein folding (reviewed in Hartl and Hayer-Hartl, 2002). The most basic are Hsp70 (or Hsc70 when referring to the constitutively expressed form) and Hsp40; their bacterial homologues are DnaK and DnaJ. It is estimated that about 20% of all newly synthesized proteins in the eukaryotic cytosol are folded by the Hsp70/Hsp40 system. Another abundant eukaryotic chaperone is Hsp90. Besides Hsp90's general role in buffering the phenotypic consequences of mutations (Queitsch *et al.*, 2002), it is mostly recognized for its more specialized function in activating many key regulator proteins, such as nuclear hormone receptors and protein kinases. The best studied examples are

the steroid hormone receptors (Pratt and Toft, 2003). Upon binding of their cognate hormones, these receptors translocate into the nucleus to function as transcriptional transactivators. Free receptors are unable to bind hormone, probably because the hydrophobic steroid binding pocket is inaccessible. Opening of this pocket is only achieved when the receptors are complexed with Hsp90 and additional cofactors. Early immunoprecipitation studies suggested that, through sequential interactions with Hsp70, Hsp40, and the Hsp-organizing protein Hop, mature hormone binding competent complexes are assembled that contain Hsp90, a small acidic protein called p23, and a tetratricopeptide repeat (TPR) containing immunophilin such as cyclophilin 40 (protein kinase complexes appear to contain, instead, p50 whose yeast homologue is known as CDC37). Similar complexes were then reconstituted from the isolated receptors, stripped of their associated factors, by incubation in RL. Finally, hormone binding activity was reconstituted entirely from purified components. According to the current model, Hsp70 and Hsp90 are absolutely essential, while Hsp40, Hop, and p23 are not essential but increase the rate, or extent, of receptor complex formation.

Several lines of evidence suggested that the DHBV P protein is activated for D ϵ binding in an analogous manner. Depletion of RL from Hsp70 or Hsp90 by antibodies, or addition of geldanamycin, an antibiotic that inhibits the interaction of Hsp90 with p23, strongly reduced P protein activity (Hu and Seeger, 1996); p23 could be detected in DHBV nucleocapsids and, as inferred from its frequent association with Hsp90, it was proposed that the entire P protein chaperone complex is encapsidated (Hu *et al.*, 1997). A potential difficulty with these experiments is the tiny amount of P protein obtainable by *in vitro* translation and the very high abundance plus pleiotropic activity of most of the chaperones, both in intact cells and in RL. This warranted new efforts toward recombinant expression of P protein. Truncated versions of P protein fused to GST could indeed be generated in *E. coli*, though with limited yield (Hu and Anselmo, 2000); in a different approach, the TP and the reverse transcriptase/RNase H (RT/RH) domains of P protein were genetically separated and expressed as individual polypeptides (Beck and Nassal, 2001). Both preparations could be reconstituted into initiation-competent complexes in RL that retained the dependence on the authentic D ϵ template. Hu *et al.* (2002) reported the successful *in vitro* reconstitution of the GST fusion proteins with purified chaperones; reconstitution required Hsp70, Hsp40, Hsp90, and Hop; p23 accelerated activation but was not essential. This

is essentially the same set of factors that is also required for steroid hormone receptor activation.

In the meantime, improved bacterial expression constructs have been generated that allow for the efficient generation of soluble DHBV P protein derivatives in much larger quantities. An important feature is the fusion to a solubility-enhancing protein domain such as the bacterial NusA, or GrpE protein. Both fusion proteins could be reconstituted into priming-active complexes with purified chaperones; unexpectedly, however, Hsc70 and Hsp40 plus ATP were not only necessary but sufficient for activation (Beck and Nassal, 2003). Trivial explanations for this apparent contradiction, such as contamination with Hsp90, could be excluded; by improving the reaction conditions, the initially modest activation levels could be greatly increased such that they even exceeded those obtainable in RL. Kinetic analyses suggest that two molecules of Hsc70, mediated by stimulation of their ATPase activity by Hsp40, interact with P protein and generate a metastable activated state P^* that is able to bind $D\epsilon$ RNA. In the absence of $D\epsilon$, P^* decays with a half-life of several minutes while, in its presence, DNA synthesis-competent complexes accumulate with a constant rate over several hours (see Fig. 5B). The mechanism underlying P^* formation remains to be established. One option is that the C-terminal RNase H domain occludes the $D\epsilon$ RNA binding site, which must reside between the TP and RT domains to allow simultaneous access to the template region of the priming Tyr-residue in TP and the polymerase active site in RT; Hsc70 may prevent this occlusion by altering the relative juxtapositions of the individual domains. Whether Hsc70 remains bound to the P protein during $D\epsilon$ RNA binding and/or the subsequent initiation of DNA synthesis is not clear. However, such questions should now be experimentally addressable. With some optimism, the relatively simple composition of this two-chaperone reconstitution system may even provide a starting point for structural analyses of the hepadnaviral initiation complex.

These data indicate that, in contrast to steroid hormone receptors, there is no fundamental requirement for Hsp90 in *in vitro* P protein activation. Nonetheless, additional factors, including but not restricted to Hsp90, could be involved in more complex environments such as RL and particularly in intact cells. A growing number of factors modulating the chaperone activity of Hsc70 are known, such as Bag, Hip, and CHIP. The basic Hsc70 cochaperone Hsp40 comes, itself, in different forms. In addition, the Hsc70 interaction domain of Hsp40, called J-domain after the prototypic prokaryotic Hsp40 DnaJ, is present

in a large family of otherwise diverse proteins (Kelley, 1998). Several of them can recruit Hsc70 to specific targets; an example is hTid-1, a J-domain protein recently found associated with the HTLV-1 Tax protein (Cheng *et al.*, 2001) and the herpes simplex virus origin binding protein UL9 (Eom and Lehman, 2002). It would therefore not be too surprising if, *in vivo*, a specialized J-domain protein rather than normal Hsp40 were involved in P protein activation. Notably, apart from the chaperone dependence of telomerase (Forsythe *et al.*, 2001), Hsp40 has very recently also been implicated in Brome mosaic virus replication (Tomita *et al.*, 2003). Eventually, chaperone dependence may turn out to be an important aspect of viral replication in general.

As noted earlier, the HBV P protein as well as the DHBV protein can be *in vitro* translated, but the HBV P protein does not show any activity. The reasons are obscure. One speculation is that the rabbit chaperones in RL are not compatible with the human virus protein; this inactivity should now be addressable using the simple two-chaperone reconstitution system that would also allow the use of combinations of Hsc70 with different Hsp40s and possibly other J-domain proteins.

b. Genome Maturation While hepadnaviral replication initiation has now become amenable to biochemical studies, this has not yet been achieved for the subsequent steps of genome maturation because the various template switches proceed properly only within the specialized environment of the nucleocapsid. Core protein *in vitro* translated in RL can assemble into capsids; however, there is no clear evidence that, in the presence of cotranslated P protein and an ϵ -containing RNA, replication-competent nucleocapsids are formed; this may relate to the absence of the cap and polyA structures on the commonly used RNAs, but other explanations may be invoked as well. At any rate, analyses of genome maturation are currently restricted to genetic methods. Most of the new findings discussed next relate to the nucleic acid templates rather than P protein. In brief, the steps are as follows:

1. The short DNA oligonucleotide primer copied from ϵ and covalently attached to the TP domain of the P protein is translocated to a 3'-proximal direct repeat (DR1*) element (first template switch); sequence complementarity is important but, because of the short length of the ϵ -derived primer, cannot solely be responsible for the specificity of this template switch (Loeb *et al.*, 1996; Nassal and Rieger, 1996). Next, the DNA primer is extended all

- the way to the 5'-end of the pgRNA template, yielding a complete (-)-DNA strand with a short terminal redundancy.
2. Concomitantly with (-)-DNA synthesis, the RNA template is degraded by the RNase H activity of P protein, except for a 5'-terminal oligonucleotide whose 3'-end consists of the 5'-copy of DR1.
 3. For relaxed circular DNA formation, the RNA oligonucleotide is transferred to the third copy of the direct repeat, DR2, located shortly upstream of DR1*, where it serves as a conventional primer for (+)-strand DNA synthesis (second template switch), which then proceeds to the 5'-end of the (-)-DNA, generating a short terminal redundancy.
 4. In a final template switch, the 5'-end of the (-)-DNA template is exchanged for the identical sequence at the 3'-end, such that now the (+)-strand can further be elongated, yielding the relaxed circular genome. Transfer of the RNA oligonucleotide to DR2 is usually less than complete, and a fraction of (+)-strand DNAs are extended from the primer still bound to its original 5'-proximal position; this reaction, called *in situ* priming, gives rise to a linear double-stranded form of the genome; in DHBV, this side reaction is suppressed by a small hairpin that favors transfer of the RNA primer to DR2 (Habig and Loeb, 2002).

Again, sequence complementarity is essential for the specificity of these template switches, but it cannot explain how the proper copy of each of the repeat elements is selected during each step. The simultaneous requirement for the P protein at the 5'-proximal ε element and at the 3'-proximal DR1 prompted the early speculation of the pgRNA possibly adopting a circular structure (Nassal *et al.*, 1990); it is now well established that protein factors binding to an mRNA's 5'-cap and its 3'-poly(A) tail bring about such a circular structure, and evidence for a role of the cap in pgRNA encapsidation has been obtained (Jeong *et al.*, 2000). Similarly, proper juxtaposition of the critical elements on the (-)-DNA might explain the specificity of the template switches during (+)-strand DNA synthesis. Though attractive, this model also appeared difficult to prove experimentally. However, in a series of elegant genetic experiments, again using DHBV as a model, strong evidence has been provided that long-range base-pairing interactions between regions far apart in primary sequence are main contributors to the specificity of the template switches. The Loeb laboratory first showed that not only the directly involved donor and acceptor sites,

i.e., DR1 and DR2 and the short terminal redundancies are important for RNA primer translocation and circularization but so are previously unrecognized *cis*-elements called 3E, M, and 5E close to the two ends and in the center of the (–)-DNA (Havert *et al.*, 2002). The same group also succeeded in directly demonstrating that base-pairing between these elements is critical for their functions, likely because it brings the actual donor and acceptor sites into close proximity (Liu *et al.*, 2003; this reference also contains an illustrative scheme of the complex events during DNA synthesis). How the core protein and possibly other factors inside the nucleocapsid affect the dynamics of these rearrangements remains an intriguing mystery to be solved.

The importance of long-range nucleic acid interactions probably extends beyond reverse transcription. DHBV pgRNA contains splice sites, and a fraction of it is indeed spliced (Obert *et al.*, 1996); however, for core and P protein translation as well as for DHBV pgRNA's function as pregenome, the unspliced pgRNA is required. Because for intron-containing mRNAs splicing is the default pathway, the existence of a mechanism that suppresses pgRNA splicing is implied. Recently, strong evidence has been provided that this mechanism is based on splice site occlusion by base pairing with a remote part of the pgRNA (Loeb *et al.*, 2002).

A related aspect where DHBV appears to employ a more complicated mechanism than the mammalian hepadnaviruses is pgRNA encapsidation. The HBV ε RNA stem-loop is sufficient to mediate encapsidation of a foreign RNA; in DHBV, an additional RNA element, called region II is required and is more than 1 kb downstream of D ε (Calvert and Summers, 1994). In a recent quantitative study, region II was further narrowed down and shown to be as essential for encapsidation as the traditional D ε signal; basically, the same holds for HHBV (Ostrow and Loeb, 2002). This might suggest that an interaction between D ε and region II is required for efficient encapsidation.

C. Envelope Proteins

1. Primary Structures and Functions of the Envelope Proteins

The DHBV envelope proteins, encoded by a single ORF divided into the preS and the S domains (Fig. 6), are translated from two mRNAs (2.35 and 2.13 kb) acting as templates for the 36-kDa L protein and the major 17-kDa S protein (Büscher *et al.*, 1985). Both proteins (Fig. 6)

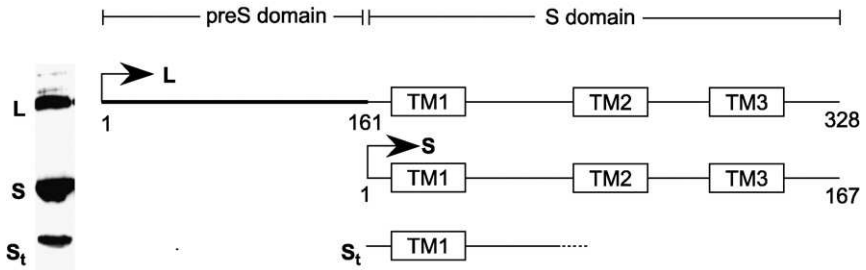


FIG 6. The major DHBV envelope proteins. (Left) The Western blot shows the major species of envelope proteins from DHBV subviral particles, with a (Right) schematic representation of their preS and S domain structures. The transmembrane domains are shown as numbered boxes, and the amino acid numbers indicate the sizes of preS, preS/S, and S. The Western blot was probed with a rabbit antiserum to the loop region between TM1 and TM2 in the S domain.

share an identical carboxy-terminal region of 167 aa, representing the S protein, with an additional 161 N-terminal aa forming the preS region (Pugh *et al.*, 1987). The preS region contains four potential in-frame start codons at nucleotides 801, 825, 882, and 957 (Mandart *et al.*, 1984). The full-length L protein is initiated from the AUG at position 801, yielding a protein with an N-terminal consensus sequence for myristylation (Persing *et al.*, 1987) and with an expected molecular weight of 35.7 kDa. The N-terminal myristoylation signal (Met-Gly) is conserved in the L protein of all the hepadnaviruses. The S protein, P17, is synthesised from the AUG at 1284 (Marion *et al.*, 1983). Western blots of liver or sera show two dominant L protein bands with sizes reported between 35 to 37 kDa (Fernholz *et al.*, 1993; Macrae *et al.*, 1991; Pugh *et al.*, 1987; Schlicht *et al.*, 1987). The slower migration of one of these two species is due to phosphorylation at serine 118 in preS (Grgacic and Anderson, 1994; Grgacic *et al.*, 1998; Rothmann *et al.*, 1998). The phosphorylated and nonphosphorylated forms of L are designated P35 and P36, respectively. A minor form of L, occasionally detected at approximately 37 kDa, may result from phosphorylation at additional Ser and Thr sites in preS. The other major L species consistently found in the liver is a protein of 28 kDa, shown to be a proteolytic product of the L protein rather than a product of internal initiation analogous to the middle (M) protein of mammalian hepadnaviruses (Fernholz *et al.*, 1993). Whether the other minor protein species occasionally detected to occur at 33 and 30 kDa (Fernholz *et al.*, 1993; Grgacic and Anderson, 1994) originate from translation

initiation at the other in-frame AUGs at 825, 882, and 957 is not clear. However, the sequential introduction of stop codons between successive AUGs in the preS/S ORF results in the synthesis of L polypeptides from the next available downstream start codon and at much higher levels than seen in the wild-type (Summers *et al.*, 1991).

A third envelope protein species (S_t), derived from the S protein, has been identified in serum particles and in endoplasmic reticulum (ER) fractions of infected primary hepatocyte cultures and transfected cells. This approximately 8-kDa species is a C-terminally truncated form of S and is a significant constituent of particles, existing in an approximate molar ratio of S_t :L:S of 1:4:8 (Grgacic, unpublished data). Whether S_t is generated by protease cleavage in the ER or perhaps through some translational defect remains unclear.

Unlike the HBV surface proteins, which exist in two forms, glycosylated and unglycosylated, the envelope proteins of DHBV are not glycosylated (Pugh *et al.*, 1987) although consensus glycosylation sites are present. This may be due to spatial constraints of the glycosylation site (being located two amino acids from the C terminus of TM2) or the normal proficiency of S folding. The partial S glycosylation resulting from point mutations in an important upstream structural region would suggest that glycosylation can occur but only in response to changes in S folding (Grgacic, 2002).

The hepatitis B surface proteins are multispansing transmembrane proteins, synthesized on the rough ER. The S and consequently the L proteins have three hydrophobic regions that are predicted to form α -helices. The location of the first two α -helices and the predicted β -turns are well conserved in all hepadnavirus surface sequences. The C-terminal region is more divergent, with incomplete alignment with the mammalian sequence (Stirk *et al.*, 1992). Thus, the predicted third α -helix of DHBV is in alignment with the fourth helix of the mammalian sequence. The topology of this C-terminal region has not been determined experimentally, but because of its hydrophobic nature, it may traverse the ER more than once.

The first and second hydrophobic regions of S are inserted into the ER cotranslationally and are able to cause translocation of N-terminal and C-terminal sequences respectively (Eble *et al.*, 1986, 1987, 1990). These two hydrophobic signal sequences, referred to as transmembrane regions 1 and 2 (TM1 and TM2), are not cleaved by a signal peptidase once translocated into the ER lumen. TM2, which serves as a signal sequence for translocation of the C-terminal region of the polyprotein into the ER lumen, also has a translocation stop signal between residues 80 and 99, which anchors the protein in the lipid bilayer. The

lengthy hydrophilic loop region between TM1 and TM2 has been shown to traverse the ER bilayer twice, thus forming a re-entrant loop region with the apex of this loop ultimately exposed to the mature particle's surface (Section IV.C.3) (Grgacic *et al.*, 2000).

The S protein is the major structural component of the particle: it determines envelope curvature and drives the budding and secretion of viral and subviral particles. While the roles of the various minor L species have not been determined, the L protein has crucial functions in assembly and entry that are based on the multiple membrane topologies it adopts.

2. Unusual Multiple Transmembrane Topologies of the L Protein

Until the seminal studies of Ostapchuk *et al.*, and Bruss *et al.*, in 1994 demonstrating that the entire preS domain of HBV L was initially located at the cytoplasmic side of the ER membrane, it was assumed that preS was translocated cotranslationally to the lumen of the ER for ultimate exposure to the particle surface. This new model of L protein topology (Fig. 7) brought about a fundamental change in the understanding of hepadnaviral assembly. In a process unique to the hepadnaviruses, the L protein is post-translationally translocated during morphogenesis and this is regulated, by an unknown mechanism, to 50% of L chains to achieve both the external receptor binding function and the internal capsid interaction function (Bruss and Thomssen, 1994; Bruss and Vieluf, 1995; Bruss *et al.*, 1994; Ostapchuk *et al.*, 1994) (Fig. 7). This mixed functional topology of L was later confirmed for DHBV (Guo and Pugh, 1997a; Swameye and Schaller, 1997) with the further insight that in addition to preS, TM1 was also post-translationally inserted into the ER (Swameye and Schaller, 1997).

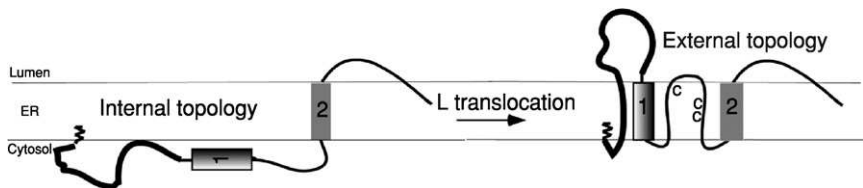


FIG 7. Dual topology of the L protein. (Left) The internal topology, present immediately after synthesis, is characterized by preS (heavy black line) and TM1 being cytosolically disposed. (Right) In the external topology, adopted post-translationally in about half the L molecules, the preS domain is translocated to the ER lumen and TM1, and the adjacent cysteine-containing loop is inserted in the ER membrane.

How such a dramatic topological shift, fundamental for production of infectious virions, is achieved is currently under investigation and surprisingly appears to differ between the mammalian and avian viruses. For DHBV, L translocation depends on the presence of the S protein (Grgacic *et al.*, 2000). In contrast, post-translational translocation of HBV L appears to be driven by the signal anchor (TM2) sequence via the host cell translocation machinery, independent of the S protein (Lambert and Prange, 2001). The role of DHBV S in translocation seems to be linked to particle assembly with L, since amino acid substitutions of two conserved charged residues in TM1 of S (K24 and E27) to Ala abrogate both particle assembly and L translocation (Grgacic *et al.*, 2000). Whether translocation occurs through assembly of envelope structures such as a hydrophilic translocation channel, as previously proposed (Stirk *et al.*, 1992), or through a chaperone-like role of S is unknown. What is intriguing is that DHBV and HBV have adopted different mechanisms of translocation, and this may be related to differing envelope protein folding pathways, as demonstrated by the inability of avi- and orthohepadnavirus virus envelope proteins to form pseudotypes between the two groups (Gerhardt and Bruss, 1995).

The envelope of DHBV contains a third topological form, intermediate to the internal/external L topologies (Guo and Pugh, 1997b) (Fig. 8). This latter form was identified, through analysis of protease digestion patterns, in exported subviral particles. It is assumed that this intermediate topology is in fact an intermediate of the post-translational translocation process and therefore exists as a topological form in the ER prior to particle formation. Circumstantial evidence supports this contention: (i) on exported particles, the phosphorylated site (S118) on phospho-L is not accessible to phosphatase digestion in the absence of detergent disruption despite its location between the receptor binding domain (aa 30–115) (Urban *et al.*, 1998) and an accessible V8 protease site at E139; (ii) the presence of the phosphorylated form of L in the 50% of L chains that are protected (i.e., translocated from protease attack in protease protection assays) suggests that the intermediate topology is formed in the ER.

3. Structure and Assembly of Subviral Particles and Virions

DHBV has a spherical structure with a uniform diameter of approximately 40 nm, similar to the 42 nm HBV Dane particle. The double-shelled structure seen by negative staining electron microscopy is formed by the inner core of 27 nm, which is covered by the envelope or surface proteins and a small amount of cellular membrane lipid. DHBV-infected ducks also produce large quantities of empty, subviral particles

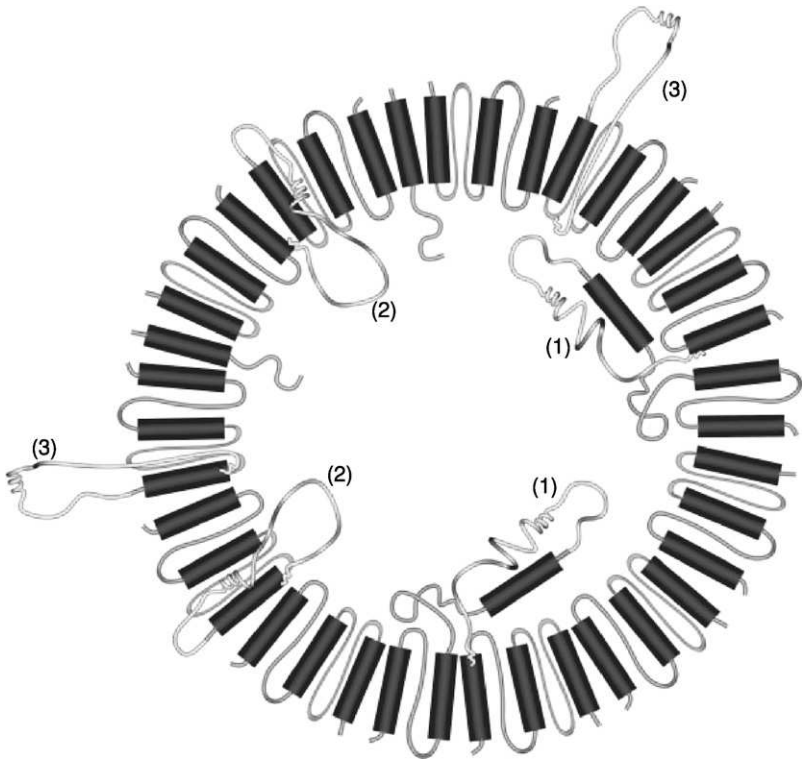


FIG 8. Model of the DHBV envelope. A cross-section view of the proposed envelope organization of S, L, and S_L proteins is shown. The predicted transmembrane domains (1–3) are indicated by the cylindrical segments, with the bulk being contributed by the S protein. The three topological forms of L are shown: (1) internal with TM1 and preS inside the particle, (2) intermediate with the TM1 and preS traversing the envelope/lipid shell, and (3) external with preS exposed to the particle surface. From Chojnacki, 2003.

(SVPs) of a pleomorphic but roughly spherical appearance with varying diameters (35–60 nm) (Mason *et al.*, 1980; McCaul *et al.*, 1985).

Unlike HBV where the spherical SVPs contain almost exclusively S protein, those of DHBV are composed of all the envelope proteins found in complete virions, including the mixed topologies of L; thus, they are a ready source of particles for assembly studies and examination of envelope topologies, which are pertinent to the infection process (Section IV.C.4).

The assembly of hepadnaviruses is little understood, but what is known is that mature virions are formed by the interaction of

performed cytoplasmic core particles with the preassembled surface proteins on the ER membrane. Following interaction with the appropriate proportions of surface proteins, the nucleocapsids bud into the lumen of the ER along with a 1000-fold excess of SVPs, and assembly is completed in an intermediate, pre-Golgi compartment (reviewed in Nassal, 1996). A unique feature of the hepadnaviruses in their status as enveloped viruses is that little or no cellular membrane proteins are present and the structural organization of the lipid bilayer may not be maintained in the mature particle (Gavilanes *et al.*, 1982; Satoh *et al.*, 2000), suggesting that the translocation, assembly along the ER membrane, and budding of the particle involves a more compact interaction between the envelope proteins. Increasingly, transmembrane domains are being identified as important structural elements in membrane protein assembly, and for many enveloped viruses, budding is dependent on the formation of an envelope lattice through lateral interactions of these domains (Garoff *et al.*, 1998). Studies on the HBV S protein have shown that TM1, while not essential for membrane insertion, plays a role in particle assembly (Bruss and Ganem, 1991; Prange *et al.*, 1992). Similarly, in DHBV, this TM domain was shown to be important for particle assembly with two charged residues, K24 and E27, identified as essential determinants for L translocation and particle assembly (Grgacic, 2002). It is not clear, however, if these residues are engaged in dimer formation through specific ionic interactions or contribute to assembly indirectly.

Assembly of the HBV envelope involves the accumulation of S monomers along the ER, where initial contacts may involve such lateral transmembrane interactions before they bud into the lumen and are stabilized by disulfide bonds into dimers, eventually forming higher order oligomers. Whereas the HBV S domain contains additional cysteine residues, with those in the second hydrophilic, surface-exposed loop involved in mixed dimer formation between L, S, and M (Wunderlich and Bruss, 1996), the DHBV envelope proteins only contain the three cysteines in the first hydrophilic loop that are strictly conserved in all hepadnaviruses. These cysteines have been shown to be essential for secretion of HBV subviral particles (Mangold and Streeck, 1993); however, they do not form intermolecular disulfide bonds upon secretion from the cell. For DHBV, the nature of the interactions involved in envelope assembly is still not defined; without any structural knowledge, a model of the particle based on envelope topologies, the ratio of the three major envelope proteins, and the known domains or determinants essential for assembly can only be assumed (Fig. 8).

4. Diverse Functional Roles of the L Protein

The L protein displays a more complex functional role than expected of a viral structural protein, and this is partly achieved by its mixed topology. The orientation of viral envelope proteins spanning the ER membrane is mirrored in the mature particle, so those domains located in the ER lumen are found on the ectodomain of the particle, and cytosolic domains remain internally disposed. Thus, the translocated form of L makes preS sequences available on the external surface of the mature virion for receptor binding (Klingmüller and Schaller, 1993; Le Seyec *et al.*, 1999), while maintenance of an internal preS domain enables the L protein to take on the suggested role of a matrix protein for interaction with the nucleocapsid (Bruss and Thomssen, 1994). Specific regions in preS and beyond (aa 117–137 and aa 157–167) are required for capsid envelopment (Lenhoff and Summers, 1994b) although other regions of the S domain of L, which are exposed to the cytosol, may also be involved. A defined region of preS (aa 30–115) acts as the minimum receptor-binding domain, binding to carboxypeptidase D (CPD; formerly known as gp180) with high affinity for attachment and internalization of the virus particle into the endosomal compartment (Breiner *et al.*, 1998; Köck *et al.*, 1996; Urban *et al.*, 1998, 2000). Factors that enable endosomal escape or fusion with the endosome membrane have not been defined although L chains that are in the intermediate topology and form a highly folded, spring-loaded structure, are strong candidates for a role in this process. Traversing the membrane six times, this metastable structure is able to undergo a major conformational change analogous to fusion activation. The conformational change induced experimentally in SVPs by low pH increases particle hydrophobicity and facilitates binding to synthetic and cell membranes through exposure of the previously hidden hydrophobic TM1 domain (Grgacic *et al.*, 2000). The latter in part encompasses the candidate fusion peptide, and peptides from this region of both HBV and DHBV display membrane destabilizing and fusogenic activity (Rodriguez-Crespo *et al.*, 1999, 2000).

The L protein also has a key regulatory role in replication through control of the pool size of cccDNA, as shown by comprehensive mutational analyses (Lenhoff and Summers, 1994a; Summers *et al.*, 1991). Most mutations in the preS region that interfered with nucleocapsid envelopment led to increased cccDNA levels (e.g., from the normal 20 copies to up to 600 copies per cell when the entire preS region was deleted), suggesting that sequestration by the L protein of core particles into the envelopment pathway competes with nuclear transport of

the nucleocapsid, thus stabilizing the number of cccDNA molecules. A few mutants, however, with deletions or substitutions of amino acid in the N-terminal part of the preS region were still competent for core particle envelopment and secretion, some even at accelerated rates compared to the wild-type, yet they produced abnormally high levels of cccDNA. This implies the existence of additional mechanisms controlling cccDNA levels that are not yet understood. In later studies, it was shown that a single amino acid substitution in the L protein (G133E) resulted in an infectious virus that elevated cccDNA levels, enhanced replication, and had cytopathic effects in hepatocytes and in the liver of ducklings (Lenhoff *et al.*, 1999). It is likely that the higher-than-normal replication contributes to the cytopathic effects, but the exact mechanism is unknown.

Other regulatory effects of L, which are not well characterized, relate to its phosphorylation and ability to act as a transactivator through ERK-type MAP kinase activation (Rothmann *et al.*, 1998). Although these studies showed that preS is phosphorylated in response to ER stress, indicating some host cell-virus cross talk, no essential role of L phosphorylation in virus replication was identified. However, ducklings infected with a mutant virus mimicking a constitutively phosphorylated L, through amino acid substitution with Asp, exhibited a pathogenic phenotype, which included weight loss and hepatic infiltration (Lin *et al.*, unpublished data; Rothmann *et al.*, 1998). Although cccDNA levels were not examined in these birds, these various studies point to the importance of a functional L protein in maintaining a nonpathogenic, persistent infection.

V. EXPERIMENTAL DHBV INFECTION

A. *In Vitro Infection of Primary Duck Hepatocytes*

The *in vitro* experimental infection of primary duck hepatocytes (Tuttleman *et al.*, 1986b) provided, for the first time, a manageable system for the study of the hepadnaviral infectious cycle. The system has been instrumental in the description of all the key steps of replication and has enabled the identification and characterization of the attachment receptor for virion internalization. This being said, it is not a system without limitations and inefficiencies. These largely stem from two factors: (i) the nonhomogeneous nature of primary cell cultures and (ii) the kinetics of experimental infection that are slow, asynchronous, and only partially productive. However, compared with

in vitro infection of primary human hepatocytes with HBV where less than 1% of cells become infected, *in vitro* infection of duck hepatocytes is at the least 20 times more successful and eventually results in multiple rounds of infection due to the greater longevity and better condition of cultured duck hepatocytes (Kürschner and Schaller, unpublished data).

1. Culture Conditions for Primary Duck Hepatocytes

The limited efficiency of *in vitro* infection is in stark contrast to the exceedingly efficient *in vivo* infection of neonatal ducklings where infection is rapid and most cells of the liver become infected within a short time. Clearly, the loss of liver architecture, specific cell-cell interactions, and the extracellular matrix reduce efficiency of *in vitro* infection. Coculture with epithelial cells and supplementation of the media with hormones, such as insulin and corticosteroids, have been variously adopted from studies in mammalian systems (Glebe *et al.*, 2001; Maher, 1988) and shown to promote survival and hepatocyte cell function (Fourel *et al.*, 1989). One agent that has been universally applied to the culture of duck hepatocytes is dimethyl sulphoxide (DMSO). At concentrations of between 1.5 to 2%, it maximizes the life span of primary hepatocytes, maintaining their differentiated state and the period of time they are susceptible to infection (Galle *et al.*, 1989; Pugh and Summers, 1989). The maintenance of susceptibility allows spread of progeny virus through multiple rounds of infection such that over a period of 2 weeks, most cells will eventually become infected.

Another important factor is the omission of fetal bovine serum from the culture medium, the presence of which causes hepatocytes to rapidly lose susceptibility to infection (Pugh and Summers, 1989; Tuttleman *et al.*, 1986b). It is assumed the loss of susceptibility is due to a general down modulation of cell surface receptors because in the presence of a serum supplement, the virus is unable to bind the hepatocyte surface (Pugh *et al.*, 1995).

2. Kinetics of Infection

Unlike HBV SVPs, those of DHBV mimic the virion in envelope protein composition and, when in vast excess of virions, are a confounding factor in the analysis of the kinetics of infection. In contrast to the competitive effect of SVPs when present in large excess, it has been observed that under conditions of very low MOI (MOI 0.01), which more closely resembles a natural infection, SVPs actually

enhance the outcome of infection (Bruns *et al.*, 1998). This effect is very much dependent on the ratio of virions to SVPs and appears to be mediated by the preS domain of L through cell-signaling events because specific preS sequences are essential, and enhancement can occur when SVPs are added up to 72 hr postinfection.

In studies simulating one-step growth kinetics, Qiao *et al.* (1999) used a virion-enriched inoculum through removal of up to 94% of SVPs for simultaneously adsorption to PDHs at 4 °C. After removal of a residual cell-bound virus by pH 2.2 treatment, it was determined that internalization and transport to the nuclear membrane required a period of approximately 4 hr. The subsequent step of uncoating/transfer to the nucleus, as measured by the appearance of the cccDNA, required 48 hr. It should be noted, however, that this study included 5% fetal bovine serum during plating and subsequently excluded DMSO from the culture medium, both factors which affect the susceptibility to infection (Section V.A.1.). In contrast, using a sensitive PCR assay selective for the detection of cccDNA derived from input viral DNA and not through replication, Köck and colleagues showed that transfer into the nucleus required only 20 hr (Köck and Schlicht, 1993; Köck *et al.*, 1996).

In the light of what is understood now of carboxypeptidase D (CPD), the receptor involved in entry and the *in vitro* culture conditions, there is a need for a renewed analysis of the kinetics of binding and uptake of virus. A survey of the literature and anecdotal information suggests that this process is very inefficient, often with more than half of the input virus not leading to productive infection. What is the fate then of these virions that do not result in productive infection? Binding to the cell surface per se is no indication of prospective internalization, and this may be due to the numerous ($> 10^5$) binding sites, nonspecific for infection, on hepatocytes (Klingmüller and Schaller, 1993), which perhaps contribute to the inability to achieve saturation of virus binding even with very high viral titres (Pugh *et al.*, 1995). Moreover, inocula removed after 24 hr can be used to further infect PDH cultures with only a two fold loss in infectivity, suggesting that nonspecific binding may also be slow (Kürschner and Schaller, unpublished data).

Many factors may contribute to the relative inefficiency of *in vitro* infection, including the presence of liver sinusoidal endothelial cells (LSEC) in hepatocyte cultures, which can take up DHBV particles via CPD attachment. Under these *in vitro* conditions, the normal liver architecture is abrogated, and particles may become trapped in LSECs from further cell-to-cell transport (Breiner *et al.*, 2001) (Section V.1.3). Because CPD is a Golgi-resident protein with little cell surface

exposure, virion entry may also be limited by receptor cycling and its asynchronous exposure on hepatocytes.

Clearly, the *in vitro* culture system is able to mimic some but not all the conditions conducive to efficient *in vivo* infection. Further studies, particularly of viral attachment and entry, may identify mechanisms that could be modulated to further enhance *in vitro* infection efficiency.

3. Early Steps of Infection

The participation of the preS domain of the large envelope protein in virus uptake has been clearly established, initially with studies showing that antibodies to the preS domain block binding and infection of hepatocytes (Cheung *et al.*, 1989, 1990; Neurath *et al.*, 1986) to the recent identification of CPD as the attachment receptor (Eng *et al.*, 1998; Tong *et al.*, 1995; Urban *et al.*, 1998). The entry of DHBV into the hepatocyte occurs via attachment of a defined sequence of preS (aa 30–115) to CPD (Urban *et al.*, 1998). That monoclonal antibodies to the S domain are also able to block infectivity (Pugh *et al.*, 1995) may occur through steric hindrance (there are proportionally more S domain sites than preS) and not through binding to a membrane attachment site per se. Therefore, it is not clear whether multivalent binding of DHBV via an additional and perhaps sequential membrane interaction occurs with S and/or the S domain of L.

CPD is a Golgi-resident protein that cycles to and from the plasma membrane via endosomes. DHBV SVPs are similarly endocytosed following attachment to CPD (Breiner and Schaller, 2000; Breiner *et al.*, 1998; Köck *et al.*, 1996). However, CPD does not confer host specificity because this protein is not restricted to DHBV-susceptible cell types. It rather appears to be involved in virus entry in conjunction with unidentified host factors. Increasingly, those engaged in the study of viral receptor binding have acknowledged the role of accessory factors (co-receptors and proteases) in viral entry. For viruses that infect via the bloodstream, an initial docking to a primary ligand may allow a subsequent stronger attachment to a secondary, less abundant high-affinity receptor, such as CPD. The enzymatic function of CPD, which entails removal of C-terminal basic residues, is not required for DHBV binding, entry, or infection (Breiner and Schaller, 2000; Eng *et al.*, 1998; Urban, unpublished data).

For hepatotropic viruses, entry to the liver via the bloodstream may initially be directed to the endothelium, which physically separates the blood from the underlying hepatocytes. Studies by Breiner *et al.* (2001) have shown that although nonpermissive for DHBV replication, liver sinusoidal endothelial cells preferentially take up DHBV SVPs *in vitro*

and *in vivo*, colocalizing with CPD in the vesicular compartment. Breiner *et al.* (2001) suggest that the virus is then further transported to the opposing plasma membrane and adjacent hepatocytes. Transport via a cell intermediary is not unprecedented and is a mechanism by which viruses, such as HIV-1, are able to traverse the mucosal epithelium (Bomsel, 1997; Kage *et al.*, 1998). Moreover, data (Lozach *et al.*, 2003; Pohlmann *et al.*, 2003) indicate that the envelope glycoprotein E2 of hepatitis C virus binds DC-SIGNR, a lectin present on the surface of LSEC, suggesting the possibility that HCV may also use LSEC to target the liver. Given that the structural arrangement of LSECs and hepatocytes is largely lost *in vitro*, this may be one explanation for the contrasting efficiency of *in vivo* infection.

Following internalization, DHBV is transported to the late endosome because Bafilomycin A₁, an inhibitor of vacuolar proton ATPases that blocks traffic from early to late endosomes, also blocks DHBV infection (Grgacic, unpublished data). Although Bafilomycin A₁ also raises endosomal pH, it has been demonstrated (using other agents that raise endosomal pH) that low pH is not a requirement for successful DHBV infection (Köck *et al.*, 1996; Rigg and Schaller, 1992). Moreover, the binding of preS to CPD is a high-affinity binding interaction (Urban *et al.*, 2000), which usually indicates entry via fusion at the plasma membrane. While these results have previously presented a dichotomy, it is becoming apparent that certain viruses can enter cells via endocytosis without a strict low pH requirement (Sieczkarski and Whittaker, 2002).

The location of the virus particle in the endosome exposes the viral envelope to proteases and low pH in a reducing environment, factors that have the potential to affect changes to the envelope for the fusion process. Studies on DHBV SVPs under conditions of low pH and/or reduction have indeed shown that drastic conformational changes occur in the L protein with no observable changes in the S protein. Increases in surface hydrophobicity and membrane binding are a prelude to viral fusion. In line with this phenomenon, the conformational change induced by low pH increased particle hydrophobicity, facilitating binding to membranes through exposure of a previously hidden hydrophobic domain encompassing the candidate fusion peptide (Grgacic *et al.*, 2000).

The candidate fusion peptide is a stretch of hydrophobic amino acids at the N terminus of TM1 (i.e., in S) identified through the similarity of the consensus sequence for fusion peptides with the HBV sequence (FLGPLLV) (Lu *et al.*, 1996) and the ability of synthetic peptides of this region from all the hepadnaviruses to induce membrane fusion

(Rodriguez-Crespo *et al.*, 1999, 2000). The fusion peptide could potentially act through either the L or the S protein. In either case, the fusion peptide would be an internal segment and therefore may (or may not) require prior protease cleavage for triggering insertion and fusion with the endosomal membrane.

Although raising the endosomal pH of the cell with lysosomotropic agents, such as NH_4Cl , does not inhibit DHBV infection (Köck *et al.*, 1996; Rigg and Schaller, 1992), this treatment is unlikely to raise the pH of the late endosome to neutrality (Yoshimori *et al.*, 1991). Together with a reducing environment, a pH of 6.5 can still affect a conformational change of the envelope because particles briefly treated this way also expose TM1 but are unable to bind membranes, because and virions remain infectious (Grgacic *et al.*, 2000). It is not clear whether such an intermediate conformational change in L is relevant to the fusion process, but given that a conformational change occurs even under these moderate pH-reducing conditions, it is possible that fusion could be fully triggered in the presence of a suitable protease. The observation that protease-pretreatment might enhance the ability of HBV to infect nonpermissive HepG2 cells by incubation at pH 5.5 for 12 hr (Lu *et al.*, 1996) adds some weight to this assumption; given the sequence homology of this region of the S domain, a similar fusion mechanism can be envisioned for all the hepadnaviruses.

4. Host-Range Studies

All hepadnaviruses exhibit a narrow host range, replicating almost exclusively in the liver of only related species. *In vivo*, DHBV infects only ducks of the *Anas* genus and some domestic geese (Marion, 1988). The preS domain is essential for infectivity, but its binding to the CPD attachment receptor for internalization cannot solely be responsible for the host range restriction: CPD is found on many other nonpermissive cell types, and recombinant CPD could not confer infectibility to cell lines capable of undergoing postentry replication steps (Breiner *et al.*, 1998). Moreover, the divergent HHBV preS binds to duck CPD with similar efficiency as DHBV preS (Breiner *et al.*, 1998; Urban *et al.*, 1998). This suggests the existence of a(n) additional receptor(s) or coreceptor(s) mediating host specificity, as was anticipated from the studies of Pugh *et al.* (1995) that showed reduced binding of DHBV to the weakly permissive Muscovy duck hepatocytes and no binding to nonpermissive chicken hepatocytes. Given the preS domain is the most variable region of the envelope sequence, preS was examined for such a determinant using HHBV, which infects primary duck hepatocytes with very low efficiency (Ishikawa and Ganem, 1995). Infectivity was

greatly enhanced by pseudotyping an env-minus HHBV genome with HHBV S and chimeric L proteins containing a DHBV preS region. Infectious virions were also obtained when only the preS aa 1–90 or 22–108, but not 43–161, were derived from DHBV, suggesting the sequence 22–90 contained an important host-range determinant. This determinant was further narrowed down to a minimal domain of 16 amino acids (aa 22–37) (Ishikawa, personal communication); at a similar N-proximal preS position, a host-range determinant has also been identified in HBV (Chouteau *et al.*, 2001). This region overlaps the stabilizing region of the CPD attachment receptor-binding domain by only seven amino acids, indicating that it could target an additional receptor, possibly as part of a receptor complex. Recent data, however, shed some doubt on such a simplified view: peptides consisting of preS aa 1–41 from both DHBV and HHBV inhibit DHBV infection of primary duck hepatocytes with similar efficiency (Urban and Gripon, 2002); crane HBV whose preS sequence in this part is more closely related to that of HHBV, including the presence of a 3-aa insertion absent from DHBV, is infectious for primary duck hepatocytes (Prassolov *et al.*, 2003) as is a chimeric DHBV carrying the supposed host-range determinant at aa 22–37 from HHBV (Dallmeier and Nassal, unpublished data). Hence, the question regarding the molecular determinants of the hepadnaviral host range is certainly not yet finally settled.

B. *Experimental In Vivo Infection*

The natural route of DHBV infection in the duck is from the dam to the egg via the bloodstream. The liver of such congenitally infected ducks remains persistently infected, with most hepatocytes showing evidence of DHBV replication. In contrast, experimental *in vivo* infection can result in three possible outcomes depending on the conditions of inoculation: persistent infection, transient infection, or no infection. The ability to control these different outcomes experimentally and the relative ease and efficiency of *in vivo* infection have provided a useful animal model to study both acute and chronic infection. Importantly, the pattern of acute and chronic infection in the duck model appears to mirror that of HBV infection.

1. *Age- and Dose-Dependence of Infection Outcome*

The development of persistent or transient infection is determined by the age posthatch at which a duck is experimentally infected. The infection of neonates, after inoculation with 10^8 to 10^9 genome equivalents, is rapid and efficient with the number of DHBV-positive cells

rising exponentially from 8 to 12% on day 3 to 100% on day 4 and resulting in persistent infection (Jilbert *et al.*, 1988). By 2 weeks of age, the chances of persistent infection have diminished, and by 4 weeks, a transient infection is typical (Fukuda *et al.*, 1987; Jilbert *et al.*, 1988, 1996; Vickery and Cossart, 1996). The two possible reasons that are believed to dictate these outcomes are (i) host-cell maturation and its capacity to support replication and (ii) the maturity of the host's immune system. The difference between a neonate liver and that of an adult bird is that as the duckling grows, hepatocytes rapidly divide, while the hepatocytes of the adult bird are largely quiescent. Partial hepatectomy of 50% or more of the liver of adult carrier ducks causes an average sixfold increase in viremia within 96 hr of surgery (Qiao *et al.*, 1992). Although this study showed that the dividing liver exported more virus, suggestive of an increase in viral replication and correlating with the kinetics of infection of congenitally or neonatally infected birds, it did not examine the permissiveness of DHBV-negative adult ducks to infection following partial hepatectomy. The latter experiment may explain to what degree the adult immune system controls the outcome of DHBV infection or whether an interplay of both immune and hepatocyte maturation occurs.

The ability to mount an immune response and clear infection is related to the age at the time of inoculation: the switch from persistent to transient infection appears to coincide with a loss in viremia and development of antibodies to viral S and core protein (Jilbert *et al.*, 1992, 1998). That anti-DHBs antibodies, generated during transient infection of adult ducks, are responsible for viral clearance was clearly demonstrated by the neutralization of infection in neonatal ducklings with serum from these adults ducks (Vickery *et al.*, 1989).

The outcome of DHBV infection is also affected by the dose of virus inoculated, with a higher dose generally increasing the age at which persistent infection ensues. For instance, with a low dose, persistence only occurs in 7-day-old or younger ducks, but with a higher dose, persistent infection can be achieved with 21-day-old ducks (Jilbert *et al.*, 1998). In this study, only adult ducks receiving the highest dose of 2×10^{11} DHBV genomes exhibited transient viremia and extensive signs of DHBV replication in the liver, while ducks receiving doses of between 10^3 and 10^9 genomes had no detectable viremia or replication after monitoring of liver biopsies for DHBV DNA or DHBsAg. Increases in the dose from lowest to highest shortened the time of appearance and levels of detectable antibodies. The study suggests that low doses induced a protective immune response, whereas high doses resulted in a nonprotective immune response and

moderately severe hepatitis, as evidenced by extensive mononuclear cell infiltration.

In contrast, as little as one viral particle is sufficient to infect neonatal ducklings such that virus spread is rapid, with infection remaining persistent (Jilbert *et al.*, 1996). This remarkable efficiency of *in vivo* experimental infection is in stark contrast to *in vitro* infection of hepatocyte cultures, adding support to the model for LSEC involvement in *in vivo* infection. Since particles have been shown to be preferentially taken up by these cells, it is unlikely that the virus is trapped and degraded here, but the virus is rather efficiently transported to the hepatocyte from this intermediary (Breiner *et al.*, 2001).

2. Fitness of DHBV Mutants

In chronically HBV-infected individuals, the presence of variants in addition to the wild-type virus is a common phenomenon (Pumpens *et al.*, 2002). Variants frequently encountered are those with a stop codon in the precore region, resulting in loss of HBeAg production, and/or mutations affecting HBsAg (termed vaccine escape mutants) or the polymerase gene as well as the overlapping S gene following lamivudine therapy. Some HBV variants have been associated with a more severe liver disease, but it is unclear whether the pathogenesis is directly due to the variant or whether the variant flourishes as a consequence of the selective pressure present in a particular host individual. Although a limited understanding can be gained of the replication of HBV variants in transfected cells, the answer to this question cannot be directly addressed with HBV. The duck, in contrast, is an ideal model in which to study the selection of such virus mutants in chronic infection: it provides an infection system where the input of viral variants can be controlled and in which chronic infection can develop under conditions of immune modulation. Despite the lack of liver disease as such in normal DHBV infection, the pathology of variants can be assessed, as in the case of certain cytopathic envelope mutants described by Lenhoff and colleagues (Lenhoff and Summers, 1994a; Lenhoff *et al.*, 1999). Regulation of cccDNA levels by the L protein is essential for the maintenance of a chronic infection. However, the cytopathic envelope mutant (G133E) caused increased replication and was unable to control cccDNA levels, resulting in direct hepatocyte cytotoxicity both *in vivo* and *in vitro* (Lenhoff and Summers, 1994a; Lenhoff *et al.*, 1999). Surprisingly, despite 100% of hepatocytes being infected in immature ducklings, this mutant proved not to be lethal, resulting in only a transient and mild hepatitis and reversion to a noncytopathic strain. These results would suggest that

the outcome of infection was largely determined by the growth of the variant: its rapid replication affected the number of spontaneous mutations, allowing reversion to noncytopathic strains, coupled with the death of cells infected with the G133E mutant. Thus, the rapid self-limiting growth of this variant was the only (major) determinant in the development of a noncytopathic, persistent infection outcome.

In contrast, studies using mixed infections of engineered precore stop mutants and wild-type DHBV (Zhang and Summers, 1999) revealed that the wild-type virus became predominant in some animals, whereas the precore-deficient virus, despite a generally lower replication competence, became predominant in other animals; interestingly, the latter birds had higher anticore antibody titers, compatible with an immune selection of the precore-deficient variant.

In a further assessment of viral competition in chronic DHBV infection using wild-type virus and a mutant with a partial replication defect (lowered cccDNA levels), it was observed that during the acute phase of infection (with a growing liver and ongoing cell division), the selection of the mutant versus the wild-type virus was determined by their relative growth rate; during the chronic phase of infection (when most cells are already infected and when the liver stops growing in the adult duck), the enrichment of the mutant versus wild-type virus was dependent on hepatocyte turnover or loss of cccDNA (Zhang and Summers, 2000).

In other words, hepatocyte injury, correlating with immune selection, in this case by increased anti-core antibody, resulted in the generation of new hepatocytes susceptible to infection but under conditions when any replication rate advantage of the wild-type virus over the mutant is no longer significant. These studies in ducks provide evidence that replication fitness is not the only parameter determining variant selection, and they show the value of this model for analyzing the phenotypes of HBV variants, including during antiviral therapy.

VI. DHBV AS A MODEL TO STUDY HOST RESPONSES TO AND CONTROL OF HBV INFECTION

A. Cytokines and Their Role in Controlling Hepadnaviral Infection

During infection with hepatitis B or C viruses, cytotoxic T lymphocytes (CTL) are thought to contribute to both liver cell injury and virus clearance (reviewed in Bertoletti and Maini, 2000; Rehermann, 2000). It is generally accepted that clearance of intracellular pathogens

requires the destruction of infected cells by major histocompatibility complex (MHC) class I-restricted CD8⁺ CTLs that kill their target cells via Perforin- or Fas-dependent mechanisms (Chisari and Ferrari, 1995). It has also been demonstrated that viral hepatitis in the course of an HBV infection relies on the production of proinflammatory cytokines such as IFN- γ by HBV-specific T cells in the liver (Bertoletti *et al.*, 1997; Ferrari *et al.*, 1987a,b). That these cytokines can potentially cure viral infections without killing the infected cell has only been appreciated in the last few years. Experimental approaches to study the influence of cytokines on HBV pathogenesis and clearance of the infection have been hampered because the host range of HBV is restricted to man and chimpanzees. In the latter animal model, it has been shown that viral replication is almost completely abolished in the liver of acutely infected chimpanzees largely before the onset of liver disease, concomitant with the intrahepatic appearance of IFN- γ (Guidotti *et al.*, 1999). Seminal studies with HBV transgenic mice that contain the entire viral genome and replicate the virus have shown that stimuli inducing the production IFN- γ and tumor necrosis factor alpha (TNF- α) in the liver are able to abolish virus replication and gene expression noncytopathically (Guidotti *et al.*, 1996b). Local induction of these cytokines can be triggered by adoptively transferred HBV-specific cytotoxic T lymphocytes (reviewed in Guidotti and Chisari, 1999). In the same animal model, similar IFN- γ -dependent antiviral mechanisms are observed following administration of IL-12, IL-18, α -galactosylceramide (specific activator of NKT cells), or anti-CD40 (an agonistic antibody activating antigen-presenting cells) (Cavanaugh *et al.*, 1997; Kakimi *et al.*, 2001; Kimura *et al.*, 2002a,b). Interference with HBV replication has also been observed following infection of HBV-transgenic mice with adenovirus, murine cytomegalovirus, and lymphocytic choriomeningitis virus (Cavanaugh *et al.*, 1998; Guidotti *et al.*, 1996a). At least for LCMV, it has been shown that IFN- α/β has a major contribution to this process since the effect was completely abrogated by antibodies against IFN- α/β . Furthermore, this effect was not detectable in mice genetically deficient for the type I IFN receptor (McClary *et al.*, 2000).

The relative sensitivity of viruses to cytokine-mediated purging might not only depend on the virus but also on the capability of the infected cell to react on the cytokines with the production of appropriate antiviral factors. Despite this enormous progress, the transgenic mouse model has its limits: (i) viral clearance cannot be studied because no cccDNA, the natural intracellular replication intermediate, is formed; (ii) early effects of cytokines cannot be studied because viral

gene expression is driven by the integrated transgene and, moreover, the animals are immunologically tolerant towards HBV. DHBV may therefore become important as a model, allowing one to define the dependence of the natural infection outcome on virus dose, inoculation route, and age of infection as well as the antiviral effects of various therapeutic and vaccination regimens. Studies of the immune response to DHBV infection, have been severely curbed by the poor knowledge on the cellular immune system of ducks however, and the lack of appropriate reagents. Recent advances in the characterization of several important cytokines and duck-specific cell surface markers will help overcome these limitations within the near future.

1. *Characterization of Duck Cytokines*

Until recently, only very few avian cytokines had been characterized, whereas a growing number of these molecules were already identified and functionally characterized in mammals. Classical approaches to identify cytokine genes in birds turned out to be difficult due to the lack of sequence conservation.

In ducks, an IFN-like activity was first demonstrated in supernatants of reovirus serotype 3-stimulated duck embryo fibroblasts. Partially purified duck IFN (DuIFN) was acid-stable and exhibited an antiviral activity against vesicular stomatitis virus and avian sarcoma virus in duck embryo fibroblasts (Ziegler and Joklik, 1981).

a. IFN- α It was only after the first chicken IFN had been cloned (Sick *et al.*, 1996) that cDNAs of type I IFNs from other birds were identified using homology screening approaches. This approach allowed the identification of a genomic duck DNA fragment that contained an intron-less gene for duck IFN (DuIFN). The fragment contained an ORF that coded for 191 aa, including a 30-residue signal peptide (Schultz *et al.*, 1995). As the precise relationship of this molecule to the various mammalian type I IFNs was not immediately clear and its sequence identity to ChIFN- α and ChIFN- β was virtually the same (50% and 53%), the precise classification of the DuIFN was not obvious. However, like ChIFN- α and mammalian IFN- α , DuIFN is strongly expressed in response to viral infection of embryo fibroblasts and in response to oral treatment of ducks with the imidazoquinoline S-28463 (Schultz *et al.*, 1995, 1999). Subsequent work revealed that *DuIFN* is a family member of approximately 10 closely related genes that form a cluster at the distal end of the long arm of the Z chromosome (Schultz, unpublished observations; Nanda *et al.*, 1998). These results led to the conclusion that DuIFN represents the functional

homologue of mammalian IFN- α (Lowenthal *et al.*, 2001) and thus belongs to the same subtype of IFNs that has been shown to be effective in the control of HBV replication in patients with chronic hepatitis. Recombinant DuIFN- α produced in either mammalian cells or in *E. coli* induces IFN-regulated genes and protects cells from destruction by cytolytic RNA viruses (Schultz *et al.*, 1995). In addition, DuIFN- α inhibits the replication of DHBV *in vitro* and *in vivo* (Heuss *et al.*, 1998; Schultz *et al.*, 1999).

b. IFN- γ When a ChIFN- γ cDNA (Weining *et al.*, 1996) was used as probe to screen a cDNA library generated from mRNA of phytohemagglutinin (PHA)-stimulated duck spleen cells, a DuIFN- γ cDNA clone was identified that coded for a polypeptide of 164 aa with a predicted signal peptide of 19 aa (Schultz and Chisari, 1999). This clone has a calculated molecular mass of 16.6 kDa and features three potential N-linked glycosylation sites. DuIFN- γ is 67% identical to ChIFN- γ and 21 to 34% identical to mammalian IFN- γ . Recombinant DuIFN- γ produced either in eukaryotic cells or in *E. coli* is biologically active (Schultz, unpublished observations; Schultz and Chisari, 1999). It potently induces the expression of genes known to be inducible by IFN- γ in mammals and chickens including IRF-1 and GBP (Jungwirth *et al.*, 1995; Schwemmle *et al.*, 1996), indicating that most components of the IFN system are well conserved among avian and mammalian species. In addition, DuIFN- γ exhibited an antiviral activity on chicken fibroblasts, albeit 16-fold less than on homologous cells (Schultz and Chisari, 1999), and it induced nitrite secretion in a chicken macrophage cell line (HD11) (Huang *et al.*, 2001). Despite these functional cross-reactivities, monoclonal antibodies raised against ChIFN- γ were not able to neutralize DuIFN- γ (Huang *et al.*, 2001).

c. IL-2 Very little is known about the biological activities of other duck cytokines. Nonetheless, recent database entries provide sequence information on IL-2 of ducks. IL-2 is known to play an important role in the differentiation and proliferation of NK, T, and B cells of mammals and chicken (Waldmann *et al.*, 1998). The four deposited sequences are from two different duck genus species *Anas platyrhynchos forma domestica* (Schmohl and Schultz, unpublished data; GenBank acc. no. AF294323, AF294322, and AY173028) and *Cairina moschata* (GenBank acc. no. AY193713). IL-2 from the latter species shows 96% sequence identity to the three IL-2 sequences from *A. platyrhynchos* that are identical. The cDNAs have been cloned independently by several research groups from mitogen-stimulated duck spleen cells.

Recombinant duck IL-2 might prove to be an appropriate growth factor to maintain duck T cell cultures and will allow the generation of antigen-specific T cell clones in the future.

d. IL-16 IL-16, originally described as lymphocyte attractant factor, is an immunomodulatory cytokine mainly secreted by activated T cells (Cruikshank *et al.*, 1998). The cDNAs for duck IL-16 have been identified in a cDNA library generated from mRNA of PHA-stimulated duck spleen cells (Schmohl and Schultz, unpublished data; GenBank acc. no. AF294320 and AF294321). IL-16 shows 90% amino acid sequence identity to chicken IL-16 and 67% identity to human IL-16.

e. IL-18 IL-18 was identified originally as IFN- γ -inducing factor and is produced during the acute immune response by macrophages and immature dendritic cells but can also be expressed in nonimmune cells (e.g., hepatocytes). An important function of IL-18 is the regulation of functionally distinct subsets of T-helper cells required for cell-mediated immune responses (Dinarello, 1999; Nakanishi *et al.*, 2001). In addition, IL-18 exerts antiviral properties against certain viruses. It protects mice challenged with encephalomyocarditis and vaccinia viruses, it improves survival rates of mice infected with herpes simplex virus, and it inhibits HBV replication in the livers of transgenic mice (Kimura *et al.*, 2002b; Pirhonen, 2001). A cDNA for duck IL-18 has been cloned from duck thymus mRNA that codes for a protein of 200 aa residues (Mannes and Schultz, unpublished data). The sequence shows 98% identity to the duck IL-18 sequence deposited in GenBank accession number AF336122 and 83% identity to the recently cloned chicken IL-18 (Schneider *et al.*, 2000). Because cytokine cDNAs have been deposited in the database only recently, recombinant duck cytokines are only beginning to be produced in laboratories (as of the publication date of this volume), but more information on their biological activity is expected to become available soon.

2. *Effect of Duck Cytokines on DHBV Infection*

Many cytokines are known to play pivotal roles in the control of viral infections. The induction of type I IFN (IFN- α/β) seems to be the most immediate and important direct antiviral host response. In addition, cytokines can contribute to the antiviral host response indirectly by modulating various aspects of the immune response. IFN- α/β inhibits the replication of many viruses *in vitro* and *in vivo*, including influenza viruses, retroviruses, picornaviruses, vesicular stomatitis virus (VSV), vaccinia virus, adenovirus, LCMV, HBV, and others (reviewed

in Vilcek and Sen, 1996). Therefore, IFN- α have been used for the treatment of a number of chronic virus infections in humans, including HBV and HCV (Hoofnagle, 1998). Since IFN treatment is effective in selected patients only, a systematic analysis of factors that might influence the clinical outcome of the IFN treatment is required. The mechanisms by which IFN- α inhibits virus replication has been the focus of many studies, but the transfection models did not allow the evaluation of the effect of IFN on early steps in infection or on virus spread (Davis and Jansen, 1994; Korba, 1996; Romero and Lavine, 1996; Tur-Kaspa *et al.*, 1990). The availability of recombinant DuIFN and the duck model of HBV offered the unique opportunity to identify all steps in the viral replication cycle that are sensitive to IFN. IFN- α -mediated inhibition of DHBV replication was observed to occur at two steps (see Fig. 9). The earliest effect of IFN was manifested as a decrease in total viral transcript levels produced early during infection when IFN was added before infection. This reduction was not due to a block in virus entry since initial cccDNA levels were not decreased compared to untreated DHBV-infected hepatocytes (Schultz *et al.*, 1999). Surprisingly, this effect was not detected in cells infected with a DHBV mutant virus defective in the synthesis of core protein, which

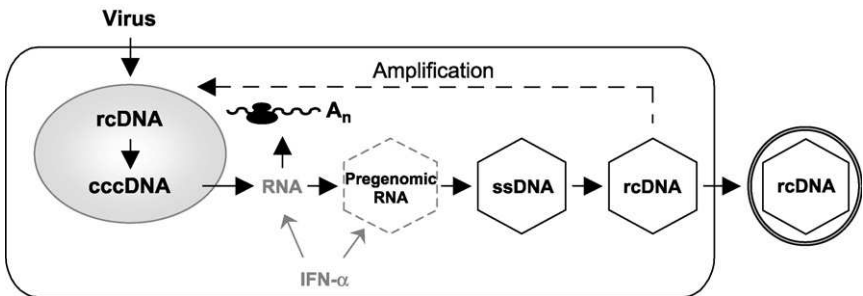


FIG 9. Steps of hepadnavirus replication potentially inhibited by IFN- α . The infection cycle shows conversion of the relaxed circular DNA (rcDNA) from the initially infecting virus into nuclear cccDNA, followed by transcription and packaging of pregenomic RNA (pgRNA) into capsids. Reverse transcription leads to single-strand DNA (ssDNA)- and rcDNA-containing nucleocapsids that either are secreted as virions or, intracellularly, amplify the cccDNA pool. While in different virus systems, IFN- α has been shown to interfere with various replication steps; the major effects observed on hepadnaviral replication are a reduced RNA accumulation and a selective inhibition of the synthesis and/or destabilization of immature pgRNA-containing nucleocapsids. DNA-containing nucleocapsids are not affected. In the absence of a core protein, RNA levels are lower *a priori* but are not further decreased by IFN- α ; hence, core protein enhances RNA accumulation, and this stimulating effect is counteracted by IFN- α .

suggested for the first time that a core protein might have an enhancing effect on viral transcript accumulation and that this novel function is the target of IFN- α . In addition, in IFN- α -treated hepatocytes, pregenomic RNA-containing capsids had vanished within 3 days, resulting in the successive depletion of replicative viral DNA intermediates from the infected hepatocyte (Schultz *et al.*, 1999). These results suggested that pregenome-containing capsids are depleted from IFN-treated cells by a novel mechanism that relies on the inhibition of formation and/or destabilization of immature DHBV capsids. Subsequently, it has been shown that a similar mechanism accounts for the inhibition of HBV replication by IFN- α/β in the liver of transgenic mice (Wieland *et al.*, 2000). Using a chicken hepatoma cell line that supports the replication of DHBV in an inducible and synchronized fashion, Seeger and colleagues could show that the half-life of RNA-containing capsids was reduced from 24 to 15 hr upon IFN treatment. In addition, they observed that IFN- α interfered with the accumulation of complete minus-strand DNA-containing capsids although there was no evidence that IFN- α affected DNA synthesis *in vitro*, suggesting that this effect might depend on cellular factors specific for this cell line (Guo *et al.*, 2003).

Previous studies in HBV-transgenic mice have shown that IFN- γ is able to suppress virus replication and gene expression. In primary duck hepatocytes, it has been observed that recombinant DuIFN- γ inhibits DHBV replication in a dose-dependent manner. Like IFN- α , IFN- γ does not inhibit initial cccDNA conversion from the relaxed circular viral DNA genome but rather abolishes the synthesis of progeny cccDNA by intracellular amplification. Accumulation of ssDNA and rcDNA was virtually abolished in IFN- γ treated cells, indicating that IFN- γ inhibits an early step in the viral replication cycle (Schultz and Chisari, 1999).

B. Chemotherapy and Vaccination

In contrast to all other mammalian hepadnaviruses, DHBV and its host offer the opportunity to study the effect of drugs biochemically in well-established *in vitro* systems as well as in primary hepatocyte cultures. Therefore, the DHBV system has been used by several investigators to study the mechanism by which certain drugs, in particular nucleoside analogues, interfere with the function of the reverse transcriptase (Seigner *et al.*, 2002; Zoulim *et al.*, 2002). Several of these drugs have been previously shown to inhibit DHBV replication in primary hepatocyte cultures and *in vivo* (Hafkemeyer *et al.*, 1996;

Offensperger *et al.*, 1996). In addition, the induction of protective immune responses in ducks has been the focus of several studies, and some reports have demonstrated that DNA-based vaccines are of protective and therapeutic effectiveness (Rollier *et al.*, 1999, 2000a,b); apparently, some animals even cleared nuclear cccDNA (Thermet *et al.*, 2003). When persistently DHBV infected ducks were treated with the nucleoside analogue adefovir and, in addition, were immunized with a plasmid expressing the DHBV L protein, they showed lower viremia than ducks from control groups, a stronger decrease in viral DNA in the liver, and a more sustained response (Le Guerhier *et al.*, 2003). These results obtained with DHBV suggest that a combination of antiviral drugs with immunotherapeutic approaches may be a promising approach for the treatment of chronic HBV.

VII. DHBV AND THE DEVELOPMENT OF HEPADNAVIRAL TRANSDUCTION VECTORS

It has been previously reported that hepatitis B virus (HBV) replication and gene expression are inhibited by the hepatic induction of certain proinflammatory cytokines (reviewed in Guidotti and Chisari, 1999). This implied that expression of cytokines in the liver of chronically HBV-infected patients might be of therapeutic value. The application of gene therapy, however, requires an appropriate gene-delivery system that allows for selectively targeting the liver and efficiently infecting quiescent hepatocytes. It has been shown that hepadnaviruses themselves can be converted into gene transfer vectors. Using DHBV as transfer-vector duck IFN- α could be transduced to primary hepatocytes and efficiently suppress the production of progeny virus (Protzer *et al.*, 1999). These results suggested that hepadnaviral vectors might be suitable to achieve a local expression of those cytokines that are relevant for the abolishment of hepadnavirus replication but would most likely have severe side effects when applied systemically (e.g., IFN- γ and TNF- α). To produce replication-deficient recombinant hepadnavirus, at least two plasmid constructs are required that allow the generation of wild-type virus to occur due to homologous recombination of the redundant sequences in the constructs. Because wild-type contamination could be disastrous for a viral vector to be used for therapeutic approaches, efforts have been made to eliminate the risk of wild-type virus being produced by using a construct devoid of redundant sequences and a packaging cell line (Klöcker *et al.*, 2003; Schultz and Nassal, unpublished data). Nonetheless, recombinant DHBV

might turn out to be a very valuable tool to evaluate the involvement of the recently cloned duck cytokines on the outcome of a hepadnavirus infection in the duck model system. Indeed, it could be shown that recombinant DHBV transducing IFN- γ leads to clearly detectable inhibition of wild-type DHBV (wtDHBV) replication and transcription, comparable to that observed with an IFN- α transducing recombinant virus. The antiviral effect of IFNs coincides with the induction of IFN-regulated genes. Recombinant DHBV transducing IL-2 has no effect on viral replication in hepatocyte cultures, as expected, since IL-2 responsive cells are most likely missing in hepatocyte cell cultures. In contrast, *in vivo* coinfection of ducklings with wtDHBV and either rDIFN- α , rDIFN- γ , or rDIL-2 inhibits the productive infection of the liver of these animals with wtDHBV (Schultz and Nassal, unpublished data).

VIII. CONCLUSIONS AND PERSPECTIVES

Despite substantial progress in the development of surrogate infection systems for HBV and a few other orthohepadnaviruses, none comes anywhere close to the experimental opportunities offered by DHBV. As outlined in this chapter, the unique potential of the DHBV system has, in the past, allowed the prototypical derivation of many mechanistic principles underlying hepadnaviral infection on the genetic level. At present, the DHBV system remains the only system allowing for a true biochemical analysis of key steps of viral replication. Even if human hepatocytes are available, they are extremely poorly infectable by HBV. This also holds true for the recently described HepaRG hepatoma cell line where infection of a small percentage of the cells requires an MOI of 200 and the additional presence of PEG, which may promote unorthodox viral entry with no evidence for viral spread. Compared to these systems, DHBV *in vitro* infection, though clearly inferior to *in vivo* infection, is rather efficient. Moreover, it remains the only system in which evolution of a hepadnavirus can be followed over more than one generation in a single culture, an important feature for studying antiviral resistance. Hence, DHBV will continue to be a most valuable model system and the first base for the study of therapeutic strategies. The apparent clearance of cccDNA in at least some chronically infected ducks following therapeutic DNA vaccination is a case in point.

ACKNOWLEDGMENTS

The authors thank many of their colleagues for providing unpublished data. They acknowledge support of their own research by grants from the Deutsche Forschungsgemeinschaft (DFG), the German Bundesministerium für Bildung und Forschung (BMBF), the Fonds der Chemischen Industrie (FCI), the Landesstiftung Baden-Württemberg, the National Health and Medical Research Council grant (ID 111710), and the research fund of the Burnet Institute.

REFERENCES

- Baker, T. S., Olson, N. H., and Fuller, S. D. (1999). Adding the third dimension to virus life cycles: Three-dimensional reconstruction of icosahedral viruses from cryo-electron micrographs. *Microbiol. Mol. Biol. Rev.* **63**:862–922.
- Barrasa, M. I., Guo, J. T., Saputelli, J., Mason, W. S., and Seeger, C. (2001). Does a cdc2 kinase-like recognition motif on the core protein of hepadnaviruses regulate assembly and disintegration of capsids? *J. Virol.* **75**:2024–2028.
- Bartenschlager, R., Junker-Niepmann, M., and Schaller, H. (1990). The P gene product of hepatitis B virus is required as a structural component for genomic RNA encapsidation. *J. Virol.* **64**:5324–5332.
- Beck, J., Bartos, H., and Nassal, M. (1997). Experimental confirmation of a hepatitis B virus (HBV) epsilon-like bulge-and-loop structure in avian HBV RNA encapsidation signals. *Virology* **227**:500–504.
- Beck, J., and Nassal, M. (1997). Sequence- and structure-specific determinants in the interaction between the RNA encapsidation signal and reverse transcriptase of avian hepatitis B viruses. *J. Virol.* **71**:4971–4980.
- Beck, J., and Nassal, M. (1998). Formation of a functional hepatitis B virus replication initiation complex involves a major structural alteration in the RNA template. *Mol. Cell. Biol.* **18**:6265–6272.
- Beck, J., and Nassal, M. (2001). Reconstitution of a functional duck hepatitis B virus replication initiation complex from separate reverse transcriptase domains expressed in *Escherichia coli*. *J. Virol.* **75**:7410–7419.
- Beck, J., and Nassal, M. (2003). Efficient Hsp90-independent *in vitro* activation by Hsc70 and Hsp40 of duck hepatitis B virus reverse transcriptase, an assumed Hsp90 client protein. *J. Biol. Chem.* **278**:36128–36138.
- Bertoletti, A., D'Elia, M. M., Boni, C., De Carli, M., Zignego, A. L., Durazzo, M., Missale, G., Penna, A., Fiaccadori, F., Del Prete, G., and Ferrari, C. (1997). Different cytokine profiles of intraphepatic T cells in chronic hepatitis B and hepatitis C virus infections. *Gastroenterology* **112**:193–199.
- Bertoletti, A., and Maini, M. K. (2000). Protection or damage: A dual role for the virus-specific cytotoxic T lymphocyte response in hepatitis B and C infection? *Curr. Opin. Microbiol.* **3**:387–392.
- Birnbaum, F., and Nassal, M. (1990). Hepatitis B virus nucleocapsid assembly: Primary structure requirements in the core protein. *J. Virol.* **64**:3319–3330.
- Blumberg, B. S. (1997). Hepatitis B virus the vaccine, and the control of primary cancer of the liver. *Proc. Natl. Acad. Sci. USA* **94**:7121–7125.
- Bomsel, M. (1997). Transcytosis of infectious human immunodeficiency virus across a tight human epithelial cell line barrier. *Nat. Med.* **3**:42–47.

- Böttcher, B., Wynne, S. A., and Crowther, R. A. (1997). Determination of the fold of the core protein of hepatitis B virus by electron cryomicroscopy. *Nature* **386**:88–91.
- Bouchard, M. J., Wang, L. H., and Schneider, R. J. (2001). Calcium signaling by HBx protein in hepatitis B virus DNA replication. *Science* **294**:2376–2378.
- Breiner, K. M., and Schaller, H. (2000). Cellular receptor traffic is essential for productive duck hepatitis B virus infection. *J. Virol.* **74**:2203–2209.
- Breiner, K. M., Schaller, H., and Knolle, P. A. (2001). Endothelial cell-mediated uptake of a hepatitis B virus: A new concept of liver targeting of hepatotropic microorganisms. *Hepatology* **34**:803–808.
- Breiner, K. M., Urban, S., and Schaller, H. (1998). Carboxypeptidase D (gp180), a Golgi-resident protein, functions in the attachment and entry of avian hepatitis B viruses. *J. Virol.* **72**:8098–8104.
- Bruns, M., Miska, S., Chassot, S., and Will, H. (1998). Enhancement of hepatitis B virus infection by noninfectious subviral particles. *J. Virol.* **72**:1462–1468.
- Bruss, V., and Ganem, D. (1991). Mutational analysis of hepatitis B surface antigen particle assembly and secretion. *J. Virol.* **65**:3813–3820.
- Bruss, V., Lu, X., Thomssen, R., and Gerlich, W. H. (1994). Post-translational alterations in transmembrane topology of the hepatitis B virus large envelope protein. *EMBO J.* **13**:2273–2279.
- Bruss, V., and Thomssen, R. (1994). Mapping a region of the large envelope protein required for hepatitis B virion maturation. *J. Virol.* **68**:1643–1650.
- Bruss, V., and Vieluf, K. (1995). Functions of the internal pre-S domain of the large surface protein in hepatitis B virus particle morphogenesis. *J. Virol.* **69**:6652–6657.
- Büscher, M., Reiser, W., Will, H., and Schaller, H. (1985). Transcripts and the putative RNA pregenome of duck hepatitis B virus: Implications for reverse transcription. *Cell* **40**:717–724.
- Calvert, J., and Summers, J. (1994). Two regions of an avian hepadnavirus RNA pregenome are required in cis for encapsidation. *J. Virol.* **68**:2084–2090.
- Carman, W. F., Jacyna, M. R., Hadziyannis, S., Karayiannis, P., McGarvey, M. J., Makris, A., and Thomas, H. C. (1989). Mutation preventing formation of hepatitis B e antigen in patients with chronic hepatitis B infection. *Lancet.* **2**:588–591.
- Cavanaugh, V. J., Guidotti, L. G., and Chisari, F. V. (1997). Interleukin-12 inhibits hepatitis B virus replication in transgenic mice. *J. Virol.* **71**:3236–3243.
- Cavanaugh, V. J., Guidotti, L. G., and Chisari, F. V. (1998). Inhibition of hepatitis B virus replication during adenovirus and cytomegalovirus infections in transgenic mice. *J. Virol.* **72**:2630–2637.
- Chang, L. J., Hirsch, R. C., Ganem, D., and Varmus, H. E. (1990). Effects of insertional and point mutations on the functions of the duck hepatitis B virus polymerase. *J. Virol.* **64**:5553–5558.
- Chang, S. F., Netter, H. J., Bruns, M., Schneider, R., Frolich, K., and Will, H. (1999). A new avian hepadnavirus infecting snow geese (*Anser caerulescens*) produces a significant fraction of virions containing single-stranded DNA. *Virology* **262**:39–54.
- Chang, S. F., Netter, H. J., Hildt, E., Schuster, R., Schaefer, S., Hsu, Y. C., Rang, A., and Will, H. (2001). Duck hepatitis B virus expresses a regulatory HBx-like protein from a hidden open reading frame. *J. Virol.* **75**:161–170.
- Chen, Y., Robinson, W. S., and Marion, P. L. (1994). Selected mutations of the duck hepatitis B virus P gene RNase H domain affect both RNA packaging and priming of minus-strand DNA synthesis. *J. Virol.* **68**:5232–5238.

- Cheng, H., Cenciarelli, C., Shao, Z., Vidal, M., Parks, W. P., Pagano, M., and Cheng-Mayer, C. (2001). Human T cell leukemia virus type 1 Tax associates with a molecular chaperone complex containing hTid-1 and Hsp70. *Curr. Biol.* **11**:1771–1775.
- Cheung, R. C., Robinson, W. S., Marion, P. L., and Greenberg, H. B. (1989). Epitope mapping of neutralizing monoclonal antibodies against duck hepatitis B virus. *J. Virol.* **63**:2445–2451.
- Cheung, R. C., Trujillo, D. E., Robinson, W. S., Greenberg, H. B., and Marion, P. L. (1990). Epitope-specific antibody response to the surface antigen of duck hepatitis B virus in infected ducks. *Virology* **176**:546–552.
- Chisari, F. V. (1996). Hepatitis B virus transgenic mice: Models of viral immunobiology and pathogenesis. *Curr. Top. Microbiol. Immunol.* **206**:149–173.
- Chisari, F. V., and Ferrari, C. (1995). Hepatitis B virus immunopathogenesis. *Annu. Rev. Immunol.* **13**:29–60.
- Chouteau, P., Le Seyec, J., Cannie, I., Nassal, M., Guguen-Guillouzo, C., and Gripon, P. (2001). A short N-proximal region in the large envelope protein harbors a determinant that contributes to the species specificity of human hepatitis B virus. *J. Virol.* **75**:11565–11572.
- Conway, J. F., Cheng, N., Zlotnick, A., Wingfield, P. T., Stahl, S. J., and Steven, A. C. (1997). Visualization of a 4-helix bundle in the hepatitis B virus capsid by cryo-electron microscopy. *Nature* **386**:91–94.
- Cova, L., Mehrotra, R., Wild, C. P., Chutimataewin, S., Cao, S. F., Dufloy, A., Prave, M., Yu, S. Z., Montesano, R., and Trepo, C. (1994). Duck hepatitis B virus infection, aflatoxin B1, and liver cancer in domestic Chinese ducks. *Br. J. Cancer.* **69**:104–109.
- Cruikshank, W. W., Kornfeld, H., and Center, D. M. (1998). Signaling and functional properties of interleukin-16. *Int. Rev. Immunol.* **6**:523–540.
- Dandri, M., Burda, M. R., Gocht, A., Torok, E., Pollok, J. M., Rogler, C. E., Will, H., and Petersen, J. (2001a). Woodchuck hepatocytes remain permissive for hepadnavirus infection and mouse liver repopulation after cryopreservation. *Hepatology* **34**:824–833.
- Dandri, M., Burda, M. R., Torok, E., Pollok, J. M., Iwanska, A., Sommer, G., Rogiers, X., Rogler, C. E., Gupta, S., Will, H., Greten, H., and Petersen, J. (2001b). Repopulation of mouse liver with human hepatocytes and *in vivo* infection with hepatitis B virus. *Hepatology* **33**:981–988.
- Dane, D. S., Cameron, C. H., and Briggs, M. (1970). Virus-like particles in serum of patients with Australia-antigen-associated hepatitis. *Lancet.* **1**:695–698.
- Das, K., Xiong, X., Yang, H., Westland, C. E., Gibbs, C. S., Sarafianos, S. G., and Arnold, E. (2001). Molecular modeling and biochemical characterization reveal the mechanism of hepatitis B virus polymerase resistance to lamivudine (3TC) and emtricitabine (FTC). *J. Virol.* **5**:4771–4779.
- Daub, H., Blencke, S., Habenberger, P., Kurtenbach, A., Dennenmoser, J., Wissing, J., Ullrich, A., and Cotten, M. (2002). Identification of SRPK1 and SRPK2 as the major cellular protein kinases phosphorylating hepatitis B virus core protein. *J. Virol.* **76**:8124–8137.
- Davis, M. G., and Jansen, R. W. (1994). Inhibition of hepatitis B virus in tissue culture by alpha interferon. *Antimicrob. Agents Chemother.* **38**:2921–2924.
- Deres, K., Schroder, C. H., Paessens, A., Goldmann, S., Hacker, H. J., Weber, O., Kramer, T., Niewohner, U., Pleiss, U., Stoltefuss, J., Graef, E., Koletzki, D., Masantschek, R. N., Reimann, A., Jaeger, R., Gross, R., Beckermann, B., Schlemmer, K. H., Haebich, D., and Rubsamen-Waigmann, H. (2003). Inhibition of hepatitis B virus replication by drug-induced depletion of nucleocapsids. *Science* **299**:893–896.

- Dinarelo, C. A. (1999). IL-18: A TH1-inducing, proinflammatory cytokine and new member of the IL-1 family. *J. Allergy Clin. Immunol.* **103**:11–24.
- Dworetzky, S. I., Lanford, R. E., and Feldherr, C. M. (1988). The effects of variations in the number and sequence of targeting signals on nuclear uptake. *J. Cell. Biol.* **107**:1279–1287.
- Eble, B. E., Lingappa, V. R., and Ganem, D. (1986). Hepatitis B surface antigen: An unusual secreted protein initially synthesized as a transmembrane polypeptide. *Mol. Cell. Biol.* **6**:1454–1463.
- Eble, B. E., Lingappa, V. R., and Ganem, D. (1990). The N-terminal (pre-S2) domain of a hepatitis B virus surface glycoprotein is translocated across membranes by downstream signal sequences. *J. Virol.* **64**:1414–1419.
- Eble, B. E., MacRae, D. R., Lingappa, V. R., and Ganem, D. (1987). Multiple topogenic sequences determine the transmembrane orientation of the hepatitis B surface antigen. *Mol. Cell. Biol.* **7**:3591–3601.
- Eickbush, T. H. (1994). Origin and evolutionary relationships of retroelements. In “The evolutionary biology of viruses” (S. S. Morse, ed.), Raven Press, New York.
- Eng, F. J., Novikova, E. G., Kuroki, K., Ganem, D., and Fricker, L. D. (1998). gp180, a protein that binds duck hepatitis B virus particles, has metalloprotease D-like enzymatic activity. *J. Biol. Chem.* **273**:8382–8388.
- Eom, C. Y., and Lehman, I. R. (2002). The human DnaJ protein, hTid-1, enhances binding of a multimer of the herpes simplex virus type 1 UL9 protein to oris, an origin of viral DNA replication. *Proc. Natl. Acad. Sci. USA* **99**:1894–1898.
- Fernholz, D., Wildner, G., and Will, H. (1993). Minor envelope proteins of duck hepatitis B virus are initiated at internal pre-S AUG codons but are not essential for infectivity. *Virology* **197**:64–73.
- Ferrari, C., Mondelli, M. U., Penna, A., Fiaccadori, F., and Chisari, F. V. (1987a). Functional characterization of cloned intrahepatic, hepatitis B virus nucleoprotein-specific helper T cell lines. *J. Immunol.* **139**:539–544.
- Ferrari, C., Penna, A., Giuberti, T., Tong, M. J., Ribera, E., Fiaccadori, F., and Chisari, F. V. (1987b). Intrahepatic, nucleocapsid antigen-specific T cells in chronic active hepatitis B. *J. Immunol.* **139**:2050–2058.
- Forsythe, H. L., Jarvis, J. L., Turner, J. W., Elmore, L. W., and Holt, S. E. (2001). Stable association of hsp90 and p23, but not hsp70, with active human telomerase. *J. Biol. Chem.* **276**:15571–15574.
- Fourel, I., Gripon, P., Hantz, O., Cova, L., Lambert, V., Jacquet, C., Watanabe, K., Fox, J., Guillouzo, C., and Trepo, C. (1989). Prolonged duck hepatitis B virus replication in duck hepatocytes cocultivated with rat epithelial cells: A useful system for antiviral testing. *Hepatology* **10**:186–191.
- Fukuda, R., Fukumoto, S., and Shimada, Y. (1987). A sequential study of viral DNA in serum in experimental transmission of duck hepatitis B virus. *J. Med. Virol.* **21**:311–320.
- Galle, P. R., Schlicht, H. J., Kuhn, C., and Schaller, H. (1989). Replication of duck hepatitis B virus in primary duck hepatocytes and its dependence on the state of differentiation of the host cell. *Hepatology* **10**:459–465.
- Ganem, D., and Schneider, R. (eds.) (2001). *Hepadnaviridae: The viruses and their replication*. In Fields Virology, 4th Edition, Lippincott Williams & Wilkins, Philadelphia.
- Garoff, H., Hewson, R., and Opstelten, D. J. (1998). Virus maturation by budding. *Microbiol. Mol. Biol. Rev.* **62**:1171–1190.
- Gavilanes, F., Gonzalez-Ros, J. M., and Peterson, D. L. (1982). Structure of hepatitis B surface antigen. Characterization of the lipid components and their association with the viral proteins. *J. Biol. Chem.* **257**:7770–7777.

- Gazina, E. V., Fielding, J. E., Lin, B., and Anderson, D. A. (2000). Core protein phosphorylation modulates pregenomic RNA encapsidation to different extents in human and duck hepatitis B viruses. *J. Virol.* **74**:4721–4728.
- Gerelsaikhan, T., Tavis, J. E., and Bruss, V. (1996). Hepatitis B virus nucleocapsid envelopment does not occur without genomic DNA synthesis. *J. Virol.* **70**:4269–4274.
- Gerhardt, E., and Bruss, V. (1995). Phenotypic mixing of rodent but not avian hepadnavirus surface proteins into human hepatitis B virus particles. *J. Virol.* **69**:1201–1208.
- Glebe, D., Berting, A., Broehl, S., Naumann, H., Schuster, R., Fiedler, N., Tolle, T. K., Nitsche, S., Seifer, M., Gerlich, W. H., and Schaefer, S. (2001). Optimised conditions for the production of hepatitis B virus from cell culture. *Intervirology* **44**:370–378.
- Grgacic, E. V. (2002). Identification of structural determinants of the first transmembrane domain of the small envelope protein of duck hepatitis B virus essential for particle morphogenesis. *J. Gen. Virol.* **83**:1635–1644.
- Grgacic, E. V., and Anderson, D. A. (1994). The large surface protein of duck hepatitis B virus is phosphorylated in the pre-S domain. *J. Virol.* **68**:7344–7350.
- Grgacic, E. V., Kuhn, C., and Schaller, H. (2000). Hepadnavirus envelope topology: Insertion of a loop region in the membrane and role of S in L protein translocation. *J. Virol.* **74**:2455–2458.
- Grgacic, E. V., Lin, B., Gazina, E. V., Snooks, M. J., and Anderson, D. A. (1998). Normal phosphorylation of duck hepatitis B virus L protein is dispensable for infectivity. *J. Gen. Virol.* **79**(Pt 11):2743–2751.
- Gripon, P., Rumin, S., Urban, S., Le Seyec, J., Glaise, D., Canine, I., Guyomard, C., Lucas, J., Trepo, C., and Guguen-Guillouzo, C. (2002). Infection of a human hepatoma cell line by hepatitis B virus. *Proc. Natl. Acad. Sci. USA* **99**:15655–15660.
- Guidotti, L. G., Borrow, P., Hobbs, M. V., Matzke, B., Gresser, I., Oldstone, M. B., and Chisari, F. V. (1996a). Viral cross talk: Intracellular inactivation of the hepatitis B virus during an unrelated viral infection of the liver. *Proc. Natl. Acad. Sci. USA* **93**:4589–4594.
- Guidotti, L. G., and Chisari, F. V. (1999). Cytokine-induced viral purging—role in viral pathogenesis. *Curr. Opin. Microbiol.* **2**:388–391.
- Guidotti, L. G., Ishikawa, T., Hobbs, M. V., Matzke, B., Schreiber, R., and Chisari, F. V. (1996b). Intracellular inactivation of the hepatitis B virus by cytotoxic T lymphocytes. *Immunity* **4**:25–36.
- Guidotti, L. G., Rochford, R., Chung, J., Shapiro, M., Purcell, R., and Chisari, F. V. (1999). Viral clearance without destruction of infected cells during acute HBV infection. *Science* **284**:825–829.
- Guo, J. T., and Pugh, J. C. (1997a). Topology of the large surface protein of duck hepatitis B virus suggests a mechanism for membrane translocation during particle morphogenesis. *J. Virol.* **71**:1107–1114.
- Guo, J. T., Pryce, M., Wang, X., Barrasa, M. I., Hu, J., and Seeger, C. (2003). Conditional replication of duck hepatitis B virus in hepatoma cells. *J. Virol.* **77**:1885–1893.
- Guo, J. T., and Pugh, J. C. (1997b). Topology of the large envelope protein of duck hepatitis B virus suggests a mechanism for membrane translocation during particle morphogenesis. *J. Virol.* **71**:1107–1114.
- Guo, J. T., Zhou, H., Liu, C., Aldrich, C., Saputelli, J., Whitaker, T., Barrasa, M. I., Mason, W. S., and Seeger, C. (2000). Apoptosis and regeneration of hepatocytes during recovery from transient hepadnavirus infections. *J. Virol.* **74**:1495–1505.
- Habig, J. W., and Loeb, D. D. (2002). Small DNA hairpin negatively regulates *in situ* priming during duck hepatitis B virus reverse transcription. *J. Virol.* **76**:980–989.

- Hafkemeyer, P., Keppler-Hafkemeyer, A., al Haya, M. A., von Janta-Lipinski, M., Matthes, E., Lehmann, C., Offensperger, W. B., Offensperger, S., Gerok, W., and Blum, H. E. (1996). Inhibition of duck hepatitis B virus replication by 2',3'-dideoxy-3'-fluoroguanosine *in vitro* and *in vivo*. *Antimicrob. Agents Chemother.* **40**:792–794.
- Hartl, F. U., and Hayer-Hartl, M. (2002). Molecular chaperones in the cytosol: From nascent chain to folded protein. *Science* **295**:1852–1858.
- Havert, M. B., Ji, L., and Loeb, D. D. (2002). Analysis of duck hepatitis B virus reverse transcription indicates a common mechanism for the two template switches during plus-strand DNA synthesis. *J. Virol.* **76**:2763–2769.
- Heuss, L. T., Heim, M. H., Schultz, U., Wissmann, D., Offensperger, W. B., Staeheli, P., and Blum, H. E. (1998). Biological efficacy and signal transduction through STAT proteins of recombinant duck interferon in duck hepatitis B virus infection. *J. Gen. Virol.* **79**:2007–2012.
- Hollinger, F. B., and Liang, T. J. (2001). Hepatitis B Virus. In “Fields virology,” 4th ed. Lippincott Williams & Wilkins, Philadelphia.
- Hoofnagle, J. H. (1998). Therapy of viral hepatitis. *Digestion* **59**:563–578.
- Hu, J., and Anselmo, D. (2000). *In vitro* reconstitution of a functional duck hepatitis B virus reverse transcriptase: Post-translational activation by Hsp90. *J. Virol.* **74**:11447–11455.
- Hu, J., and Seeger, C. (1996). Hsp90 is required for the activity of a hepatitis B virus reverse transcriptase. *Proc. Natl. Acad. Sci. USA* **93**:1060–1064.
- Hu, J., Toft, D., Anselmo, D., and Wang, X. (2002). *In vitro* reconstitution of functional hepadnavirus reverse transcriptase with cellular chaperone proteins. *J. Virol.* **76**:269–279.
- Hu, J., Toft, D. O., and Seeger, C. (1997). Hepadnavirus assembly and reverse transcription require a multicomponent chaperone complex which is incorporated into nucleocapsids. *EMBO J.* **16**:59–68.
- Huang, A., Scougall, C. A., Lowenthal, J. W., Jilbert, A. R., and Kotlarski, I. (2001). Structural and functional homology between duck and chicken interferon-gamma. *Dev. Comp. Immunol.* **25**:55–68.
- Ishikawa, T., and Ganem, D. (1995). The pre-S domain of the large viral envelope protein determines host range in avian hepatitis B viruses. *Proc. Natl. Acad. Sci. USA* **92**:6259–6263.
- Jacquard, A. C., Nassal, M., Pichoud, C., Ren, S., Schultz, U., Guerret, S., Chevallier, M., Werle, B., Peyrol, S., Jamard, C., Rimsky, L. T., Trepo, C., and Zoulim, F. (2004). Effect of a combination of clevudine and emtricitabine with adenovirus-mediated delivery of gamma interferon in the woodchuck model of hepatitis B virus infection. *Antimicrob. Agents Chemother.* **48**:2683–2692.
- Jeong, J. K., Yoon, G. S., and Ryu, W. S. (2000). Evidence that the 5'-end cap structure is essential for encapsidation of hepatitis B virus pregenomic RNA. *J. Virol.* **74**:5502–5508.
- Jilbert, A. R., Botten, J. A., Miller, D. S., Bertram, E. M., Hall, P. M., Kotlarski, J., and Burrell, C. J. (1998). Characterization of age- and dose-related outcomes of duck hepatitis B virus infection. *Virology* **244**:273–282.
- Jilbert, A. R., Freiman, J. S., Burrell, C. J., Holmes, M., Gowans, E. J., Rowland, R., Hall, P., and Cossart, Y. E. (1988). Virus-liver cell interactions in duck hepatitis B virus infection. A study of virus dissemination within the liver. *Gastroenterology* **95**:1375–1382.

- Jilbert, A. R., and Kotlarski, I. (2000). Immune responses to duck hepatitis B virus infection. *Dev. Comp. Immunol.* **24**:285–302.
- Jilbert, A. R., Miller, D. S., Scougall, C. A., Turnbull, H., and Burrell, C. J. (1996). Kinetics of duck hepatitis B virus infection following low-dose virus inoculation: One virus DNA genome is infectious in neonatal ducks. *Virology* **226**:338–345.
- Jilbert, A. R., Wu, T. T., England, J. M., Hall, P. M., Carp, N. Z., O'Connell, A. P., and Mason, W. S. (1992). Rapid resolution of duck hepatitis B virus infections occurs after massive hepatocellular involvement. *J. Virol.* **66**:1377–1388.
- Jungwirth, C., Rebbert, M., Ozato, K., Degen, H. J., Schultz, U., and Dawid, I. B. (1995). Chicken interferon consensus sequence-binding protein (ICSBP) and interferon regulatory factor (IRF) 1 genes reveal evolutionary conservation in the IRF gene family. *Proc. Natl. Acad. Sci. USA* **92**:3105–3109.
- Kage, A., Shoolian, E., Rokos, K., Ozel, M., Nuck, R., Reutter, W., Kottgen, E., and Pauli, G. (1998). Epithelial uptake and transport of cell-free human immunodeficiency virus type 1 and gp120-coated microparticles. *J. Virol.* **72**:4231–4236.
- Kakimi, K., Lane, T. E., Chisari, F. V., and Guidotti, L. G. (2001). Cutting edge: Inhibition of hepatitis B virus replication by activated NK T cells does not require inflammatory cell recruitment to the liver. *J. Immunol.* **167**:6701–6705.
- Kann, M., Sodeik, B., Vlachou, A., Gerlich, W. H., and Helenius, A. (1999). Phosphorylation-dependent binding of hepatitis B virus core particles to the nuclear pore complex. *J. Cell. Biol.* **145**:45–55.
- Kann, M., Thomssen, R., Kochel, H. G., and Gerlich, W. H. (1993). Characterization of the endogenous protein kinase activity of the hepatitis B virus. *Arch. Virol. Suppl.* **8**:53–62.
- Kelley, W. L. (1998). The J-domain family and the recruitment of chaperone power. *Trends Biochem. Sci.* **23**:222–227.
- Kenney, J. M., von Bonsdorff, C. H., Nassal, M., and Fuller, S. D. (1995). Evolutionary conservation in the hepatitis B virus core structure: Comparison of human and duck cores. *Structure* **3**:1009–1019.
- Kimura, K., Kakimi, K., Wieland, S., Guidotti, L. G., and Chisari, F. V. (2002a). Activated intrahepatic antigen-presenting cells inhibit hepatitis B virus replication in the liver of transgenic mice. *J. Immunol.* **169**:5188–5195.
- Kimura, K., Kakimi, K., Wieland, S., Guidotti, L. G., and Chisari, F. V. (2002b). Interleukin-18 inhibits hepatitis B virus replication in the livers of transgenic mice. *J. Virol.* **76**:10702–10707.
- Klingmüller, U., and Schaller, H. (1993). Hepadnavirus infection requires interaction between the viral pre-S domain and a specific hepatocellular receptor. *J. Virol.* **67**:7414–7422.
- Klöcker, U., Oberwinkler, H., Kurschner, T., and Protzer, U. (2003). Presence of replicating virus in recombinant hepadnavirus stocks results from recombination and can be eliminated by the use of a packaging cell line. *J. Virol.* **77**:2873–2881.
- Köck, J., Borst, E. M., and Schlicht, H. J. (1996). Uptake of duck hepatitis B virus into hepatocytes occurs by endocytosis but does not require passage of the virus through an acidic intracellular compartment. *J. Virol.* **70**:5827–5831.
- Köck, J., Kann, M., Putz, G., Blum, H. E., and Von Weizsäcker, F. (2003). Central role of a serine phosphorylation site within duck hepatitis B virus core protein for capsid trafficking and genome release. *J. Biol. Chem.* **278**:28123–28129.
- Köck, J., Nassal, M., MacNelly, S., Baumert, T. F., Blum, H. E., and von Weizsäcker, F. (2001). Efficient infection of primary *Tupaia* hepatocytes with purified human and woolly monkey hepatitis B virus. *J. Virol.* **75**:5084–5089.

- Köck, J., and Schlicht, H. J. (1993). Analysis of the earliest steps of hepadnavirus replication: Genome repair after infectious entry into hepatocytes does not depend on viral polymerase activity. *J. Virol.* **67**:4867–4874.
- Korba, B. E. (1996). *In vitro* evaluation of combination therapies against hepatitis B virus replication. *Antiviral Res.* **29**:49–51.
- Kuroki, K., Eng, F., Ishikawa, T., Turck, C., Harada, F., and Ganem, D. (1995). gp180, a host cell glycoprotein that binds duck hepatitis B virus particles, is encoded by a member of the carboxypeptidase gene family. *J. Biol. Chem.* **270**:15022–15028.
- Lambert, C., and Prange, R. (2001). Dual topology of the hepatitis B virus large envelope protein: Determinants influencing post-translational pre-S translocation. *J. Biol. Chem.* **276**:22265–22272.
- Lanford, R. E., Chavez, D., Brasky, K. M., Burns, R. B., III, and Rico-Hesse, R. (1998). Isolation of a hepadnavirus from the woolly monkey, a New World primate. *Proc. Natl. Acad. Sci. USA* **95**:5757–5761.
- Le Guerhier, F., Thermet, A., Guerret, S., Chevallier, M., Jamard, C., Gibbs, C. S., Treppe, C., Cova, L., and Zoulim, F. (2003). Antiviral effect of adefovir in combination with a DNA vaccine in the duck hepatitis B virus infection model. *J. Hepatol.* **38**:328–334.
- Le Seyec, J., Chouteau, P., Cannie, I., Guguen-Guillouzo, C., and Gripon, P. (1999). Infection process of the hepatitis B virus depends on the presence of a defined sequence in the pre-S1 domain. *J. Virol.* **73**:2052–2057.
- Lenhoff, R. J., Luscombe, C. A., and Summers, J. (1998). Competition *in vivo* between a cytopathic variant and a wild-type duck hepatitis B virus. *Virology* **251**:85–95.
- Lenhoff, R. J., Luscombe, C. A., and Summers, J. (1999). Acute liver injury following infection with a cytopathic strain of duck hepatitis B virus. *Hepatology* **29**:563–571.
- Lenhoff, R. J., and Summers, J. (1994a). Construction of avian hepadnavirus variants with enhanced replication and cytopathicity in primary hepatocytes. *J. Virol.* **68**:5706–5713.
- Lenhoff, R. J., and Summers, J. (1994b). Coordinate regulation of replication and virus assembly by the large envelope protein of an avian hepadnavirus. *J. Virol.* **68**:4565–4571.
- Linial, M. L. (1999). Foamy viruses are unconventional retroviruses. *J. Virol.* **73**:1747–1755.
- Liu, N., Tian, R., and Loeb, D. D. (2003). Base pairing among three cis-acting sequences contributes to template switching during hepadnavirus reverse transcription. *Proc. Natl. Acad. Sci. USA* **10**:10.
- Loeb, D. D., Mack, A. A., and Tian, R. (2002). A secondary structure that contains the 5'- and 3'-splice sites suppresses splicing of duck hepatitis B virus pregenomic RNA. *J. Virol.* **76**:10195–10202.
- Loeb, D. D., Tian, R., and Gulya, K. J. (1996). Mutations within DR2 independently reduce the amount of both minus- and plus-strand DNA synthesized during duck hepatitis B virus replication. *J. Virol.* **70**:8684–8690.
- Lohregel, B., Lu, M., and Roggendorf, M. (1998). Molecular cloning of the woodchuck cytokines: TNF-alpha, IFN-gamma, and IL-6. *Immunogenetics* **47**:332–335.
- Lowenthal, J. W., Staeheli, P., Schultz, U., Sekellick, M. J., and Marcus, P. J. (2001). Nomenclature of avian interferon proteins. *J. Interferon Cytokine Res.* **21**:547–549.
- Lozach, P. Y., Lortat-Jacob, H., De Lacroix De Lavalette, A., Staropoli, I., Foug, S., Amara, A., Houles, C., Fieschi, F., Schwartz, O., Virelizier, J. L., Arenzana-Seisdedos, F., and Altmeyer, R. (2003). DC-SIGN and L-SIGN are high-affinity binding receptors for hepatitis C virus glycoprotein E2. *J. Biol. Chem.* **278**:20358–20366.

- Lu, M., Lohrengel, B., Hilken, G., Kemper, T., and Roggendorf, M. (2002). Woodchuck gamma interferon upregulates major histocompatibility complex class I transcription but is unable to deplete woodchuck hepatitis virus replication intermediates and RNAs in persistently infected woodchuck primary hepatocytes. *J. Virol.* **76**:58–67.
- Lu, X., Block, T. M., and Gerlich, W. H. (1996). Protease-induced infectivity of hepatitis B virus for a human hepatoblastoma cell line. *J. Virol.* **70**:2277–2285.
- Mabit, H., Breiner, K. M., Knaust, A., Zachmann-Brand, B., and Schaller, H. (2001). Signals for bidirectional nucleocytoplasmic transport in the duck hepatitis B virus capsid protein. *J. Virol.* **75**:1968–1977.
- Mabit, H., Knaust, A., Breiner, K. M., and Schaller, H. (2003). Nuclear localization of the duck hepatitis B virus capsid protein: Detection and functional implications of distinct subnuclear bodies in a compartment associated with RNA synthesis and maturation. *J. Virol.* **77**:2157–2164.
- Mabit, H., and Schaller, H. (2000). Intracellular hepadnavirus nucleocapsids are selected for secretion by envelope protein-independent membrane binding. *J. Virol.* **4**:11472–11478.
- Macrae, D. R., Bruss, V., and Ganem, D. (1991). Myristylation of a duck hepatitis B virus envelope protein is essential for infectivity but not for virus assembly. *Virology* **181**:359–363.
- Maher, J. J. (1988). Primary hepatocyte culture: Is it home away from home? *Hepatology* **8**:1162–1166.
- Mandart, E., Kay, A., and Galibert, F. (1984). Nucleotide sequence of a cloned duck hepatitis B virus genome: Comparison with woodchuck and human hepatitis B virus sequences. *J. Virol.* **49**:782–792.
- Mangold, C. M., and Streeck, R. E. (1993). Mutational analysis of the cysteine residues in the hepatitis B virus small envelope protein. *J. Virol.* **67**:4588–4597.
- Marion, P. L. (1988). Use of animal models to study hepatitis B virus. *Prog. Med. Virol.* **35**:43–75.
- Marion, P. L., Cullen, J. M., Azcarraga, R. R., Van Davelaar, M. J., and Robinson, W. S. (1987). Experimental transmission of duck hepatitis B virus to Pekin ducks and to domestic geese. *Hepatology* **7**:724–731.
- Marion, P. L., Knight, S. S., Feitelson, M. A., Oshiro, L. S., and Robinson, W. S. (1983). Major polypeptide of duck hepatitis B surface antigen particles. *J. Virol.* **48**:534–541.
- Marion, P. L., Oshiro, L. S., Regnery, D. C., Scullard, G. H., and Robinson, W. S. (1980). A virus in Beechey ground squirrels that is related to hepatitis B virus of humans. *Proc. Natl. Acad. Sci. USA* **77**:2941–2945.
- Mason, W. S., Cullen, J., Moraleda, G., Saputelli, J., Aldrich, C. E., Miller, D. S., Tennant, B., Frick, L., Averett, D., Condreay, L. D., and Jilbert, A. R. (1998). Lamivudine therapy of WHV-infected woodchucks. *Virology* **245**:18–32.
- Mason, W. S., Seal, G., and Summers, J. (1980). Virus of Pekin ducks with structural and biological relatedness to human hepatitis B virus. *J. Virol.* **36**:829–836.
- McCaul, T. F., Tsiquaye, K. N., and Zuckerman, A. J. (1985). Studies by electron microscopy on the assembly of duck hepatitis B virus in the liver. *J. Med. Virol.* **16**:77–87.
- McClary, H., Koch, R., Chisari, F. V., and Guidotti, L. G. (2000). Relative sensitivity of hepatitis B virus and other hepatotropic viruses to the antiviral effects of cytokines. *J. Virol.* **74**:2255–2264.
- Meier, P., Scougall, C. A., Will, H., Burrell, C. J., and Jilbert, A. R. (2003). A duck hepatitis B virus strain with a knockout mutation in the putative X ORF shows similar infectivity and *in vivo* growth characteristics to wild-type virus. *Virology* **317**:291–298.

- Murphy, W. J., Eizirik, E., O'Brien, S. J., Madsen, O., Scally, M., Douady, C. J., Teeling, E., Ryder, O. A., Stanhope, M. J., de Jong, W. W., and Springer, M. S. (2001). Resolution of the early placental mammal radiation using Bayesian phylogenetics. *Science* **294**:2348–2351.
- Mutimer, D. (2001). Hepatitis B virus infection: Resistance to antiviral agents. *J. Clin. Virol.* **21**:239–242.
- Nakanishi, K., Yoshimoto, T., Tsutsui, H., and Okamura, H. (2001). Interleukin-18 regulates both Th1 and Th2 responses. *Annu. Rev. Immunol.* **19**:423–474.
- Nanda, I., Sick, C., Munster, U., Kaspers, B., Schartl, M., Staeheli, P., and Schmid, M. (1998). Sex chromosome linkage of chicken and duck type I interferon genes: Further evidence of evolutionary conservation of the Z chromosome in birds. *Chromosoma* **107**:204–210.
- Nassal, M. (1996). Hepatitis B virus morphogenesis. *Curr. Top. Microbiol. Immunol.* **214**:297–337.
- Nassal, M. (1999). Hepatitis B virus replication: Novel roles for virus–host interactions. *Intervirology* **42**:100–116.
- Nassal, M. (2000). Macromolecular interactions in hepatitis B virus replication and particle assembly. In “DNA virus replication” (A. J. Cann, ed.), Oxford University Press, Oxford.
- Nassal, M. (2002). Ca²⁺: The clue to hepatitis B virus X protein function? *Hepatology* **36**:755–757.
- Nassal, M., Junker-Niepmann, M., and Schaller, H. (1990). Translational inactivation of RNA function: Discrimination against a subset of genomic transcripts during HBV nucleocapsid assembly. *Cell* **63**:1357–1363.
- Nassal, M., and Rieger, A. (1993). An intramolecular disulfide bridge between Cys-7 and Cys61 determines the structure of the secretory core gene product (e antigen) of hepatitis B virus. *J. Virol.* **67**:4307–4315.
- Nassal, M., and Rieger, A. (1996). A bulged region of the hepatitis B virus RNA encapsidation signal contains the replication origin for discontinuous first-strand DNA synthesis. *J. Virol.* **70**:2764–2773.
- Nassal, M., Rieger, A., and Steinau, O. (1992). Topological analysis of the hepatitis B virus core particle by cysteine–cysteine cross-linking. *J. Mol. Biol.* **225**:1013–1025.
- Neurath, A. R., Kent, S. B., Strick, N., and Parker, K. (1986). Identification and chemical synthesis of a host-cell receptor binding site on hepatitis B virus. *Cell* **46**:429–436.
- Obert, S., Zachmann-Brand, B., Deindl, E., Tucker, W., Bartenschlager, R., and Schaller, H. (1996). A splice hepadnavirus RNA that is essential for virus replication. *EMBO J.* **15**:2565–2574.
- Offensperger, W. B., Offensperger, S., Keppler-Hafkemeyer, A., Hafkemeyer, P., and Blum, H. E. (1996). Antiviral activities of penciclovir and famciclovir on duck hepatitis B virus *in vitro* and *in vivo*. *Antivir. Ther.* **1**:141–146.
- Offensperger, W. B., Offensperger, S., Walter, E., Teubner, K., Igloi, G., Blum, H. E., and Gerok, W. (1993). *In vivo* inhibition of duck hepatitis B virus replication and gene expression by phosphorothioate modified antisense oligodeoxynucleotides. *EMBO J.* **12**:1257–1262.
- Ostapchuk, P., Hearing, P., and Ganem, D. (1994). A dramatic shift in the transmembrane topology of a viral envelope glycoprotein accompanies hepatitis B viral morphogenesis. *EMBO J.* **13**:1048–1057.
- Ostrow, K. M., and Loeb, D. D. (2002). Characterization of the cis-acting contributions to avian hepadnavirus RNA encapsidation. *J. Virol.* **76**:9087–9095.
- Pante, N., and Kann, M. (2002). Nuclear pore complex is able to transport macromolecules with diameters of about 39 nm. *Mol. Biol. Cell.* **13**:425–434.

- Perlman, D., and Hu, J. (2003). Duck hepatitis B virus virion secretion requires a double-stranded DNA genome. *J. Virol.* **77**:2287–2294.
- Persing, D. H., Varmus, H. E., and Ganem, D. (1987). The preS1 protein of hepatitis B virus is acylated at its amino terminus with myristic acid. *J. Virol.* **61**:1672–1677.
- Pirhonen, J. (2001). Regulation of IL-18 expression in virus infection. *Scand. J. Immunol.* **53**:533–539.
- Pohlmann, S., Zhang, J., Baribaud, F., Chen, Z., Leslie, G. J., Lin, G., Granelli-Piperno, A., Doms, R. W., Rice, C. M., and McKeating, J. A. (2003). Hepatitis C virus glycoproteins interact with DC-SIGN and DC-SIGNR. *J. Virol.* **7**:4070–4080.
- Pollack, J. R., and Ganem, D. (1994). Site-specific RNA binding by a hepatitis B virus reverse transcriptase initiates two distinct reactions: RNA packaging and DNA synthesis. *J. Virol.* **68**:5579–5587.
- Ponsel, D., and Bruss, V. (2003). Mapping of amino acid side chains on the surface of hepatitis B virus capsids required for envelopment and virion formation. *J. Virol.* **77**:416–422.
- Prange, R., Nagel, R., and Streeck, R. E. (1992). Deletions in the hepatitis B virus small envelope protein: Effect on assembly and secretion of surface antigen particles. *J. Virol.* **66**:5832–5841.
- Prassolov, A., Hohenberg, H., Kalinina, T., Schneider, C., Cova, L., Krone, O., Frolich, K., Will, H., and Sirma, H. (2003). New hepatitis B virus of cranes that has an unexpected broad host range. *J. Virol.* **77**:1964–1976.
- Pratt, W. B., and Toft, D. O. (2003). Regulation of signaling protein function and trafficking by the hsp90/hsp70-based chaperone machinery. *Exp. Biol. Med. (Maywood)* **228**:111–133.
- Protzer, U., Nassal, M., Chiang, P. W., Kirschfink, M., and Schaller, H. (1999). Interferon gene transfer by a hepatitis B virus vector efficiently suppresses wild-type virus infection. *Proc. Natl. Acad. Sci. USA* **96**:10818–10823.
- Pugh, J., Zweidler, A., and Summers, J. (1989). Characterization of the major duck hepatitis B virus core particle protein. *J. Virol.* **63**:1371–1376.
- Pugh, J. C., Di, Q., Mason, W. S., and Simmons, H. (1995). Susceptibility to duck hepatitis B virus infection is associated with the presence of cell surface receptor sites that efficiently bind viral particles. *J. Virol.* **69**:4814–4822.
- Pugh, J. C., and Simmons, H. (1994). Duck hepatitis B virus infection of Muscovy duck hepatocytes and nature of virus resistance *in vivo*. *J. Virol.* **68**:2487–2494.
- Pugh, J. C., Sninsky, J. J., Summers, J. W., and Schaeffer, E. (1987). Characterization of a pre-S polypeptide on the surfaces of infectious avian hepadnavirus particles. *J. Virol.* **61**:1384–1390.
- Pugh, J. C., and Summers, J. W. (1989). Infection and uptake of duck hepatitis B virus by duck hepatocytes maintained in the presence of dimethyl sulfoxide. *Virology* **172**:564–572.
- Pult, I., Netter, H. J., Bruns, M., Prassolov, A., Sirma, H., Hohenberg, H., Chang, S. F., Frolich, K., Krone, O., Kaleta, E. F., and Will, H. (2001). Identification and analysis of a new hepadnavirus in white storks. *Virology* **289**:114–128.
- Pumpens, P., Grens, E., and Nassal, M. (2002). Molecular epidemiology and immunology of hepatitis B virus infection. An update. *Intervirology* **45**:218–232.
- Qiao, M., Gowans, E. J., and Burrell, C. J. (1992). Intracellular factors, but not virus receptor levels, influence the age-related outcome of DHBV infection of ducks. *Virology* **186**:517–523.

- Qiao, M., Scougall, C. A., Duszynski, A., and Burrell, C. J. (1999). Kinetics of early molecular events in duck hepatitis B virus replication in primary duck hepatocytes. *J. Gen. Virol.* **80**:2127–2135.
- Queitsch, C., Sangster, T. A., and Lindquist, S. (2002). Hsp90 as a capacitor of phenotypic variation. *Nature* **417**:618–624.
- Radziwill, G., Tucker, W., and Schaller, H. (1990). Mutational analysis of the hepatitis B virus P gene product: Domain structure and RNase H activity. *J. Virol.* **64**:613–620.
- Raney, A. K., Eggers, C. M., Kline, E. F., Guidotti, L. G., Pontoglio, M., Yaniv, M., and McLachlan, A. (2001). Nuclear covalently closed circular viral genomic DNA in the liver of hepatocyte nuclear factor 1 alpha-null hepatitis B virus transgenic mice. *J. Virol.* **75**:2900–2911.
- Rehermann, B. (2000). Intrahepatic T cells in hepatitis B: Viral control versus liver cell injury. *J. Exp. Med.* **191**:1263–1268.
- Ren, S., and Nassal, M. (2001). Hepatitis B virus (HBV) virion and covalently closed circular DNA formation in primary *Tupaia* hepatocytes and human hepatoma cell lines upon HBV genome transduction with replication-defective adenovirus vectors. *J. Virol.* **75**:1104–1116.
- Rieger, A., and Nassal, M. (1996). Specific hepatitis B virus minus-strand DNA synthesis requires only the 5'-encapsidation signal and the 3'-proximal direct repeat DR1. *J. Virol.* **70**:585–589.
- Rigg, R. J., and Schaller, H. (1992). Duck hepatitis B virus infection of hepatocytes is not dependent on low pH. *J. Virol.* **66**:2829–2836.
- Robertson, B. H., and Margolis, H. S. (2002). Primate hepatitis B viruses—Genetic diversity, geography, and evolution. *Rev. Med. Virol.* **12**:133–141.
- Rodriguez-Crespo, I., Nunez, E., Yelamos, B., Gomez-Gutierrez, J., Albar, J. P., Peterson, D. L., and Gavilanes, F. (1999). Fusogenic activity of hepadnavirus peptides corresponding to sequences downstream of the putative cleavage site. *Virology* **261**:133–142.
- Rodriguez-Crespo, I., Yelamos, B., Albar, J. P., Peterson, D. L., and Gavilanes, F. (2000). Selective destabilization of acidic phospholipid bilayers performed by the hepatitis B virus fusion peptide. *Biochim. Biophys. Acta* **1463**:419–428.
- Roggendorf, M., and Tolle, T. K. (1995). The woodchuck: An animal model for hepatitis B virus infection in man. *Intervirology* **38**:100–112.
- Rollier, C., Charollos, C., Jamard, C., Trepo, C., and Cova, L. (2000a). Early life humoral response of ducks to DNA immunization against hepadnavirus large envelope protein. *Vaccine* **18**:3091–3096.
- Rollier, C., Charollos, C., Jamard, C., Trepo, C., and Cova, L. (2000b). Maternally transferred antibodies from DNA-immunized avians protect offspring against hepadnavirus infection. *J. Virol.* **74**:4908–4911.
- Rollier, C., Sunyach, C., Barraud, L., Madani, N., Jamard, C., Trepo, C., and Cova, L. (1999). Protective and therapeutic effect of DNA-based immunization against hepadnavirus large envelope protein. *Gastroenterology* **116**:658–665.
- Romero, R., and Lavine, J. E. (1996). Cytokine inhibition of the hepatitis B virus core promoter. *Hepatology* **23**:17–23.
- Rothmann, K., Schnoizer, M., Radziwill, G., Hildt, E., Moelling, K., and Schaller, H. (1998). Host cell-virus cross talk: Phosphorylation of a hepatitis B virus envelope protein mediates intracellular signaling. *J. Virol.* **72**:10138–10147.
- Salucci, V., Lu, M., Aurisicchio, L., La Monica, N., Roggendorf, M., and Palombo, F. (2002). Expression of a new woodchuck IFN-alpha gene by a helper-dependent adenoviral vector in woodchuck hepatitis virus-infected primary hepatocytes. *J. Interferon. Cytokine Res.* **22**:1027–1034.

- Satoh, O., Imai, H., Yoneyama, T., Miyamura, T., Utsumi, H., Inoue, K., and Umeda, M. (2000). Membrane structure of the hepatitis B virus surface antigen particle. *J. Biochem. (Tokyo)* **127**:543–550.
- Schaaf, S. G., Beck, J., and Nassal, M. (1999). A small 2'-OH-and base-dependent recognition element downstream of the initiation site in the RNA encapsidation signal is essential for hepatitis B virus replication initiation. *J. Biol. Chem.* **274**:37787–37794.
- Schlicht, H. J. (1991). Biosynthesis of the secretory core protein of duck hepatitis B virus: Intracellular transport, proteolytic processing, and membrane expression of the pre-core protein. *J. Virol.* **65**:3489–3495.
- Schlicht, H. J., Bartenschlager, R., and Schaller, H. (1989). The duck hepatitis B virus core protein contains a highly phosphorylated C terminus that is essential for replication but not for RNA packaging. *J. Virol.* **63**:2995–3000.
- Schlicht, H. J., Kuhn, C., Guhr, B., Mattaliano, R. J., and Schaller, H. (1987). Biochemical and immunological characterization of the duck hepatitis B virus envelope proteins. *J. Virol.* **61**:2280–2285.
- Schmitz, J., Ohme, M., and Zischler, H. (2000). The complete mitochondrial genome of *Tupaia belangeri* and the phylogenetic affiliation of scandentia to other eutherian orders. *Mol. Biol. Evol.* **17**:1334–1343.
- Schneider, K., Puehler, F., Baeuerle, D., Elvers, S., Staeheli, P., Kaspers, B., and Weining, K. C. (2000). cDNA cloning of biologically active chicken interleukin-18. *J. Interferon Cytokine Res.* **20**:879–883.
- Schultz, U., and Chisari, F. V. (1999). Recombinant duck interferon gamma inhibits duck hepatitis B virus replication in primary hepatocytes. *J. Virol.* **73**:3162–3168.
- Schultz, U., Köck, J., Schlicht, H. J., and Staeheli, P. (1995). Recombinant duck interferon: A new reagent for studying the mode of interferon action against hepatitis B virus. *Virology* **212**:641–649.
- Schultz, U., Summers, J., Staeheli, P., and Chisari, F. V. (1999). Elimination of duck hepatitis B virus RNA-containing capsids in duck interferon-alpha-treated hepatocytes. *J. Virol.* **73**:5459–5465.
- Schwemmler, M., Kaspers, B., Irion, A., Staeheli, P., and Schultz, U. (1996). Chicken guanylate-binding protein. Conservation of GTPase activity and induction by cytokines. *J. Biol. Chem.* **271**:10304–10308.
- Seeger, C., and Mason, W. S. (2000). Hepatitis B virus biology. *Microbiol. Mol. Biol. Rev.* **64**:51–68.
- Seigneres, B., Pichoud, C., Martin, P., Furman, P., Trepo, C., and Zoulim, F. (2002). Inhibitory activity of dioxolane purine analogs on wild-type and lamivudine-resistant mutants of hepadnaviruses. *Hepatology* **36**:710–722.
- Sick, C., Schultz, U., and Staeheli, P. (1996). A family of genes coding for two serologically distinct chicken interferons. *J. Biol. Chem.* **271**:7635–7639.
- Sieczkarski, S. B., and Whittaker, G. R. (2002). Dissecting virus entry via endocytosis. *J. Gen. Virol.* **83**:1535–1545.
- Sousa, R. (1996). Structural and mechanistic relationships between nucleic acid polymerases. *Trends Biochem. Sci.* **21**:186–190.
- Sprengel, R., Kaleta, E. F., and Will, H. (1988). Isolation and characterization of a hepatitis B virus endemic in herons. *J. Virol.* **62**:3832–3839.
- Steitz, T. A. (1999). DNA polymerases: Structural diversity and common mechanisms. *J. Biol. Chem.* **274**:17395–17398.
- Stirk, H. J., Thornton, J. M., and Howard, C. R. (1992). A topological model for hepatitis B surface antigen. *Intervirology* **33**:148–158.

- Summers, J., and Mason, W. S. (1982). Replication of the genome of a hepatitis B-like virus by reverse transcription of an RNA intermediate. *Cell* **29**:403–415.
- Summers, J., Smith, P. M., and Horwich, A. L. (1990). Hepadnavirus envelope proteins regulate covalently closed circular DNA amplification. *J. Virol.* **64**:2819–2824.
- Summers, J., Smith, P. M., Huang, M. J., and Yu, M. S. (1991). Morphogenetic and regulatory effects of mutations in the envelope proteins of an avian hepadnavirus. *J. Virol.* **65**:1310–1317.
- Summers, J., Smolec, J. M., and Snyder, R. (1978). A virus similar to human hepatitis B virus associated with hepatitis and hepatoma in woodchucks. *Proc. Natl. Acad. Sci. USA* **75**:4533–4537.
- Swameye, I., and Schaller, H. (1997). Dual topology of the large envelope protein of duck hepatitis B virus: Determinants preventing pre-S translocation and glycosylation. *J. Virol.* **71**:9434–9441.
- Tavis, J. E., Massey, B., and Gong, Y. (1998). The duck hepatitis B virus polymerase is activated by its RNA packaging signal, epsilon. *J. Virol.* **72**:5789–5796.
- Tennant, B. C., and Gerin, J. L. (2001). The woodchuck model of hepatitis B virus infection. *Ilar. J.* **42**:89–102.
- Testut, P., Renard, C. A., Terradillos, O., Vitvitski-Trepo, L., Tekaia, F., Degott, C., Blake, J., Boyer, B., and Buendia, M. A. (1996). A new hepadnavirus endemic in arctic ground squirrels in Alaska. *J. Virol.* **70**:4210–4219.
- Thermet, A., Rollier, C., Zoulim, F., Trepo, C., and Cova, L. (2003). Progress in DNA vaccine for prophylaxis and therapy of hepatitis B. *Vaccine* **21**:659–662.
- Thoma, C., Hasselblatt, P., Kock, J., Chang, S. F., Hockenjos, B., Will, H., Hentze, M. W., Blum, H. E., von Weizsacker, F., and Offensperger, W. B. (2001). Generation of stable mRNA fragments and translation of N-truncated proteins induced by antisense oligodeoxynucleotides. *Mol. Cell.* **8**:865–872.
- Thomas, H. C. (1995). The emergence of envelope and precore/core variants of hepatitis B virus: The potential role of antibody selection. *J. Hepatol.* **22**:1–8.
- Tomita, Y., Mizuno, T., Diez, J., Naito, S., Ahlquist, P., and Ishikawa, M. (2003). Mutation of host DnaJ homolog inhibits brome mosaic virus negative-strand RNA synthesis. *J. Virol.* **77**:2990–2997.
- Tong, S., Li, J., and Wands, J. R. (1995). Interaction between duck hepatitis B virus and a 170-kilodalton cellular protein is mediated through a neutralizing epitope of the pre-S region and occurs during viral infection. *J. Virol.* **69**:7106–7112.
- Tur-Kaspa, R., Teicher, L., Laub, O., Itin, A., Dagan, D., Bloom, B. R., and Shafritz, D. A. (1990). Alpha interferon suppresses hepatitis B virus enhancer activity and reduces viral gene transcription. *J. Virol.* **64**:1821–1824.
- Tuttleman, J. S., Pourcel, C., and Summers, J. (1986a). Formation of the pool of covalently closed circular viral DNA in hepadnavirus-infected cells. *Cell* **47**:451–460.
- Tuttleman, J. S., Pugh, J. C., and Summers, J. W. (1986b). *In vitro* experimental infection of primary duck hepatocyte cultures with duck hepatitis B virus. *J. Virol.* **58**:17–25.
- Urban, S., Breiner, K. M., Fehler, F., Klingmüller, U., and Schaller, H. (1998). Avian hepatitis B virus infection is initiated by the interaction of a distinct pre-S subdomain with the cellular receptor gp180. *J. Virol.* **72**:8089–8097.
- Urban, S., and Gripon, P. (2002). Inhibition of duck hepatitis B virus infection by a myristoylated pre-S peptide of the large viral surface protein. *J. Virol.* **76**:1986–1990.
- Urban, S., Schwarz, C., Marx, U. C., Zentgraf, H., Schaller, H., and Multhaup, G. (2000). Receptor recognition by a hepatitis B virus reveals a novel mode of high-affinity virus-receptor interaction. *EMBO J.* **19**:1217–1227.

- Vickery, K., and Cossart, Y. (1996). DHBV manipulation and prediction of the outcome of infection. *J. Hepatol.* **25**:504–509.
- Vickery, K., Freiman, J. S., Dixon, R. J., Kearney, R., Murray, S., and Cossart, Y. E. (1989). Immunity in Pekin ducks experimentally and naturally infected with duck hepatitis B virus. *J. Med. Virol.* **28**:231–236.
- Vilcek, J., and Sen, G. C. (1996). *Interferons and other cytokines*. In *Fields Virology*, 3rd Edition, Lippincott-Raven, Philadelphia.
- von Weizsäcker, F., Köck, J., Wieland, S., Beck, J., Nassal, M., and Blum, H. E. (2002). *Cis*-preferential recruitment of duck hepatitis B virus core protein to the RNA/polymerase preassembly complex. *Hepatology* **35**:209–216.
- Waldmann, T., Tagaya, Y., and Bamford, R. (1998). Interleukin-2, interleukin-15, and their receptors. *Int. Rev. Immunol.* **16**:205–226.
- Wang, G. H., and Seeger, C. (1992). The reverse transcriptase of hepatitis B virus acts as a protein primer for viral DNA synthesis. *Cell* **71**:663–670.
- Wang, G. H., and Seeger, C. (1993). Novel mechanism for reverse transcription in hepatitis B viruses. *J. Virol.* **67**:6507–6512.
- Wei, Y., Tavis, J. E., and Ganem, D. (1996). Relationship between viral DNA synthesis and virion envelopment in hepatitis B viruses. *J. Virol.* **70**:6455–6458.
- Weining, K. C., Schultz, U., Munster, U., Kaspers, B., and Staeheli, P. (1996). Biological properties of recombinant chicken interferon-gamma. *Eur. J. Immunol.* **26**:2440–2447.
- Wieland, S. F., Guidotti, L. G., and Chisari, F. V. (2000). Intrahepatic induction of alpha/beta interferon eliminates viral RNA-containing capsids in hepatitis B virus transgenic mice. *J. Virol.* **74**:4165–4173.
- Will, H., Cattaneo, R., Koch, H. G., Darai, G., Schaller, H., Schellekens, H., van Eerd, P. M., and Deinhardt, F. (1982). Cloned HBV DNA causes hepatitis in chimpanzees. *Nature* **299**:740–742.
- Wunderlich, G., and Bruss, V. (1996). Characterization of early hepatitis B virus surface protein oligomers. *Arch. Virol.* **141**:1191–1205.
- Wynne, S. A., Crowther, R. A., and Leslie, A. G. (1999). The crystal structure of the human hepatitis B virus capsid. *Mol. Cell.* **3**:771–780.
- Xiong, Y., and Eickbush, T. H. (1990). Origin and evolution of retroelements based upon their reverse transcriptase sequences. *EMBO J.* **9**:3353–3362.
- Yamamoto, T., Litwin, S., Zhou, T., Zhu, Y., Condreay, L., Furman, P., and Mason, W. S. (2002). Mutations of the woodchuck hepatitis virus polymerase gene that confer resistance to lamivudine and 2'-fluoro-5-methyl-beta-L-arabinofuranosyluracil. *J. Virol.* **76**:1213–1223.
- Yang, D. L., Lu, M., Hao, L. J., and Roggendorf, M. (2000). Molecular cloning and characterization of major histocompatibility complex class I cDNAs from woodchuck (*Marmota monax*). *Tissue Antigens* **55**:548–557.
- Yang, W., Guo, J., Ying, Z., Hua, S., Dong, W., and Chen, H. (1994). Capsid assembly and involved function analysis of twelve core protein mutants of duck hepatitis B virus. *J. Virol.* **68**:338–345.
- Yoshimori, T., Yamamoto, A., Moriyama, Y., Futai, M., and Tashiro, Y. (1991). Bafilomycin A₁, a specific inhibitor of vacuolar-type H(+)-ATPase, inhibits acidification and protein degradation in lysosomes of cultured cells. *J. Biol. Chem.* **266**:17707–17712.
- Yu, M., and Summers, J. (1991). A domain of the hepadnavirus capsid protein is specifically required for DNA maturation and virus assembly. *J. Virol.* **65**:2511–2517.
- Yu, M., and Summers, J. (1994). Multiple functions of capsid protein phosphorylation in duck hepatitis B virus replication. *J. Virol.* **68**:4341–4348.

- Zang, W. Q., and Yen, T. S. (1999). Distinct export pathway utilized by the hepatitis B virus post-transcriptional regulatory element. *Virology* **259**:299–304.
- Zhang, Y. Y., and Summers, J. (1999). Enrichment of a precore-minus mutant of duck hepatitis B virus in experimental mixed infections. *J. Virol.* **73**:3616–3622.
- Zhang, Y. Y., and Summers, J. (2000). Low dynamic state of viral competition in a chronic avian hepadnavirus infection. *J. Virol.* **74**:5257–5265.
- Zhou, S., and Strandberg, D. N. (1992). Hepatitis B virus capsid particles are assembled from core-protein dimer precursors. *Proc. Natl. Acad. Sci. USA* **89**:10046–10050.
- Zhou, T., Guo, J. T., Nunes, F. A., Molnar-Kimber, K. L., Wilson, J. M., Aldrich, C. E., Saputelli, J., Litwin, S., Condreay, L. D., Seeger, C., and Mason, W. S. (2000). Combination therapy with lamivudine and adenovirus causes transient suppression of chronic woodchuck hepatitis virus infections. *J. Virol.* **74**:11754–11763.
- Ziegler, R. E., and Joklik, W. K. (1981). Effect of interferon on multiplication of avian sarcoma virus B77 in duck embryo fibroblasts. *J. Interferon Res.* **1**:521–538.
- Zoulim, F. (2001). Detection of hepatitis B virus resistance to antivirals. *J. Clin. Virol.* **21**:243–253.
- Zoulim, F., Berthillon, P., Guerhier, F. L., Seigneres, B., Germon, S., Pichoud, C., Cheng, Y., and Trepo, C. (2002). Animal models for the study of HBV infection and the evaluation of new anti-HBV strategies. *J. Gastroenterol. Hepatol.* **17**:S460–S463.

NOVEL INSIGHTS INTO HEPATITIS C VIRUS REPLICATION AND PERSISTENCE

Ralf Bartenschlager, Michael Frese, and Thomas Pietschmann

Department of Molecular Virology, University of Heidelberg,
Im Neuenheimer Feld 345, 69120 Heidelberg, Germany

- I. Introduction
 - II. Genomic Organization
 - III. Virus Structure
 - A. Structural Proteins
 - B. Structure of Virus Particles
 - IV. Experimental Systems
 - A. *In Vivo* Models for HCV Infection and Replication
 - B. Cell Culture Systems
 - V. Replication Cycle
 - A. Receptor Candidates and Mechanism of Cell Entry
 - B. RNA Translation
 - C. Proteolytic Processing of Structural Proteins
 - D. Proteolytic Processing of Nonstructural Proteins
 - E. *Cis*-Acting RNA Sequences Required for Replication
 - F. Mechanism of RNA Replication
 - G. Membrane Topologies of Viral Proteins
 - H. Virus Assembly and Release
 - VI. Virus–Host Interaction
 - A. Cell Culture Adaptation and Host-Cell Permissiveness
 - B. Cytopathic Effects Exerted by HCV
 - C. HCV and the Host's Innate Immune Response
 - VII. Antiviral Therapies
 - A. Interferons and Ribavirin
 - B. Small Interfering RNAs
 - VIII. Concluding Remarks
- References

Hepatitis C virus (HCV) is a small enveloped RNA virus that belongs to the family *Flaviviridae*. A hallmark of HCV is its high propensity to establish a persistent infection that in many cases leads to chronic liver disease. Molecular studies of the virus became possible with the first successful cloning of its genome in 1989. Since then, the genomic organization has been delineated, and viral proteins have been studied in some detail. In 1999, an efficient cell culture system became available that recapitulates the intracellular part of the HCV life cycle, thereby allowing detailed molecular studies of various aspects of viral

RNA replication and persistence. This chapter attempts to summarize the current state of knowledge in these most actively worked on fields of HCV research.

I. INTRODUCTION

About 15 years ago, the genome of the *Hepatitis C virus* (HCV) was molecularly cloned from the serum of an experimentally infected chimpanzee (*Pan troglodytes*) by a blind immunoscreening approach (Choo *et al.*, 1989). Soon thereafter, diagnostic tests based on the use of recombinant antigens generated from this genome were implemented (Alter *et al.*, 1989; Kuo *et al.*, 1989). These tests demonstrated a clear association between antibodies against HCV antigens and a liver disease that was originally designated non-A, non-B hepatitis but that is now called hepatitis C. HCV is primarily transmitted by blood and blood products. This route of transmission, however, has virtually been eliminated by rigorous screening tests based on the detection of either HCV-specific antibodies by enzyme-linked immunosorbent assay (ELISA) or the viral genome by reverse transcriptase polymerase chain reaction (RT-PCR). An immunological test for the detection of the HCV nucleocapsid protein (core antigen) in patient serum has also been developed but so far is not used as routine application in diagnostic laboratories (Bouvier-Alias *et al.*, 2002; Laperche *et al.*, 2003). Because of these stringent control measures, new HCV infections are mostly restricted to transfusions of untested samples and to parenteral risk factors, most notably “needle sharing” among users of intravenous drugs (Yen *et al.*, 2003). In contrast, sexual transmission and intrauterine infections are rare.

Acute HCV infections are frequently asymptomatic or associated with rather mild symptoms. This property often disguises the medical problem that arises from the high propensity of HCV to establish a persistent infection in its host (Seeff, 2002). It has been estimated that about 80% of infected individuals are unable to eliminate the virus. These patients are at high risk for developing chronic liver disease. In about 10 to 20% of persistently infected individuals, the disease progresses to liver cirrhosis within 20 years after infection and eventually leads to hepatocellular carcinoma.

Although the liver is the primary organ for HCV replication and disease manifestation, persistent infections are often associated with extrahepatic symptoms, most notably lymphoproliferative disorders affecting B cells. For instance, 80% of patients with type II and

type III cryoglobulinemia are infected by HCV (Mayo, 2003). Moreover, about 40% of patients with HCV infection manifest symptoms of at least one extrahepatic disease, most often renal complications, neuropathy, lymphoma, Sjogren syndrome with or without cryoglobulinemia, porphyria cutanea, and diabetes. Development of these diseases appears to require a persistent HCV infection although manifestations most likely occur due to a compromised immune system. Thus, persistent HCV infection causes a multifaceted disease that involves the liver and nonhepatic organs.

For an infected individual, the overall rate of HCV replication is rather low, making a direct demonstration of viral proteins and RNA in infected tissues very difficult (Blight *et al.*, 1994; Chang *et al.*, 2003). Therefore, and because of technical problems encountered when working with liver biopsies, it is not yet clear which cells are infected *in vivo*. Apart from hepatocytes, the main target cells for HCV, infection of bile duct epithelial cells or sinusoidal endothelial cells has been proposed, but this observation is discussed controversially. Equally uncertain is the percentage of infected liver cells. Evidence suggests that about 5 to 10% of hepatocytes in infected tissue are HCV-positive although there appear to be significant interpatient differences (Wölk *et al.*, 2000). It was calculated that, on the average, the number of RNA molecules per productively infected hepatocyte ranges between 10 to 60 molecules (Chang *et al.*, 2003). A gradient distribution of genomes was found around virus-producing cells, suggesting an infection of neighboring hepatocytes as a mechanism of the virus spreading in the liver. Based on kinetic studies and mathematical modeling, it has been calculated that about 10^{12} virus particles are produced per day (Neumann *et al.*, 1998; Ramratnam *et al.*, 1999). Assuming that about 10% of all hepatocytes are infected and that the liver of an adult contains about 2×10^{11} hepatocytes, the virion production rate would be approximately 50 particles per cell a day on the average.

HCV has been classified as a member of the genus *Hepacivirus* that together with the genera *Pestivirus* and *Flavivirus* and the as of yet unassigned species *GB virus A* (GBV-A), *GB virus B* (GBV-B), and *GB virus C* (GBV-C) belongs to the family *Flaviviridae* (van Regenmortel *et al.*, 2000). Based on sequence analyses, HCV genomes can be grouped into at least six genotypes (also called clades) that differ in their nucleotide sequence by 31 to 34% (Pawlotsky, 2003; Robertson *et al.*, 1998; Simmonds *et al.*, 1993). Furthermore, within an HCV genotype, several subtypes can be defined that differ in their nucleotide sequence by 20 to 23%. In Western Europe and the United States, infections caused by genotype 1a [the American prototype that was

first cloned in 1989 (Choo *et al.*, 1989)] and genotype 1b [the Japanese prototype that was first described in 1990 (Kato *et al.*, 1990)] are the most frequent ones, followed by infections with the genotypes 2 and 3. The other genotypes are very rare in these countries and can only be found in distinct geographical regions like Egypt (genotype 4), South Africa (genotype 5), and Southeast Asia (genotype 6). The genomic variability of HCV is due to the high error rate of the viral RNA-dependent RNA polymerase (RdRp), which has been calculated to be in the range of about 10^{-4} (Lohmann *et al.*, 2000). Moreover, based on a comparative sequence analysis of HCV genomes isolated from patients or experimentally inoculated chimpanzees over intervals of 8 or 13 years, a mutation rate of 1.44×10^{-3} or 1.92×10^{-3} base substitutions per site per year was found (Ogata *et al.*, 1991; Okamoto *et al.*, 1992a).

The assumption that distinct HCV genotypes and subtypes are associated with a more severe course of disease is discussed controversially (Gervais *et al.*, 2001; Mondelli and Silini, 1999; Yamada *et al.*, 1994a). Several reports indicate an association between genotype 1b infections and the severity of liver disease (Nousbaum *et al.*, 1995; Silini *et al.*, 1995). The observation that this association is due to differences in age of patients and virus load rather than genotype, however, cannot be excluded because genotype 1b infections are more frequent among older patients and correlate with a higher virus titer in the serum. The distinction between different genotypes is, nevertheless, of importance for predicting the outcome of antiviral therapy in those infected with chronic hepatitis C. In the absence of selective antiviral drugs, patients are currently treated with a combination of polyethylene glycol (PEG)-conjugated interferon-alpha (IFN- α) and ribavirin (McHutchison and Fried, 2003). Whereas 80 to 90% of patients persistently infected with genotype 2 or genotype 3 viruses mount a sustained response and are able to eliminate the virus, only 50% of patients persistently infected with genotype 1 viruses can do so. Consequently, the determination of the infecting genotype has an important positive predictive value for the success of therapy.

II. GENOMIC ORGANIZATION

HCV possesses an RNA genome of positive polarity that is approximately 9.6 kb in length (Fig. 1). The genome encodes a large polyprotein of roughly 3000 amino acids that is flanked at the N and C termini by highly structured nontranslated regions (NTRs). An internal ribosome entry site (IRES) that is located in the 5'-NTR mediates the

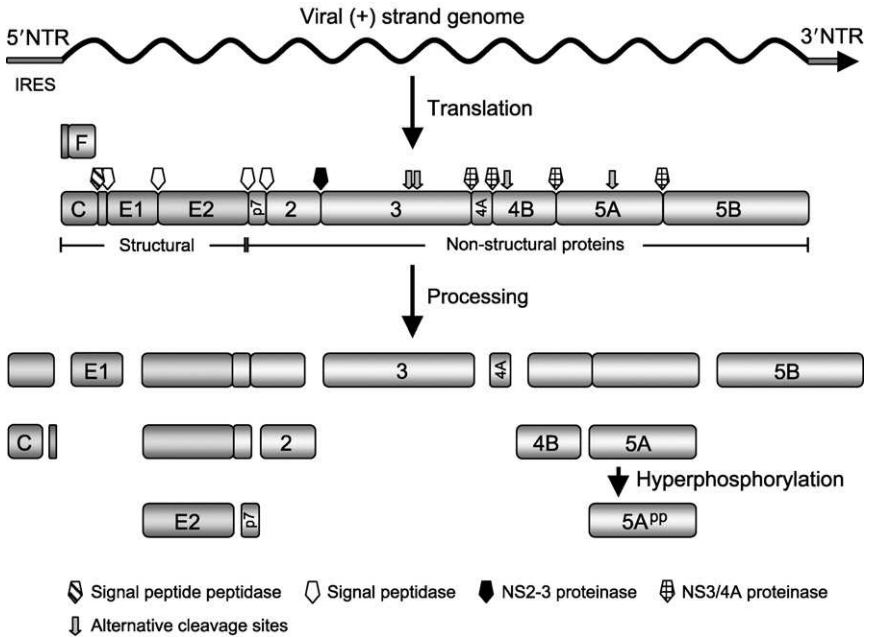


FIG. 1. Genomic organization of HCV and processing pathways of the polyprotein. A schematic representation of the HCV genome with the 5'- and 3'-NTRs is shown in the top, the translation products are given below. Proteinases involved in processing of the polyprotein are indicated by arrows that are specified at the bottom of the figure. The major cleavage pathways leading to distinct processing intermediates, most notably E2-p7-NS2 and NS4B-5A, are indicated. The hyperphosphorylation of NS5A probably occurs after full proteolytic cleavage. The F protein generated by ribosomal frameshifting is depicted above the polyprotein. For further details, see Section II.

expression of the polyprotein (Tsukiyama-Kohara *et al.*, 1992; Wang *et al.*, 1993a). In addition, most of the 5'-NTR as well as the 3'-NTR are required for RNA replication (Friebe *et al.*, 2001; Kim *et al.*, 2002b; Kolykhalov *et al.*, 1996; Tanaka *et al.*, 1995, 1996; Yamada *et al.*, 1996; Yi and Lemon, 2003a,b).

Besides the polyprotein, which is cotranslationally and posttranslationally processed by cellular and viral proteinases into at least ten different polypeptides, the expression of a novel HCV protein has been reported (Boulant *et al.*, 2003; Walewski *et al.*, 2001; Xu *et al.*, 2001). Translation of this additional viral gene product also initiates at the core gene AUG start codon, but ribosomes shift into an alternative reading frame in the vicinity of the eleventh codon. The resulting 17-kDa protein is therefore called the frameshift (F) or alternative

reading frame (ARF) protein (Varaklioti *et al.*, 2002; Xu *et al.*, 2001). It is important to note that patient sera were shown to react with this newly discovered protein, indicating its expression in natural infections (Walewski *et al.*, 2001; Xu *et al.*, 2001). Moreover, the F protein coding sequence is well conserved among different genotypes, suggesting that it plays a role in the HCV life cycle. The expression of recombinant, immunotagged versions of the F protein in cultured cells reveal that it is short-lived and ER-associated (Roussel *et al.*, 2003; Xu *et al.*, 2003). Because the F protein partly colocalizes with core and NS5A proteins in cotransfection experiments, it has been speculated that the F protein is part of the replication complex. HCV replicons, however, multiply in the absence of the F protein (Lohmann *et al.*, 1999a), demonstrating that its expression is not required for virus replication (Section IV,B). Thus, the role of the F protein remains to be defined.

As previously mentioned, the main translation product of the viral genome is a large polyprotein that contains the structural proteins in the N-terminal region and the nonstructural proteins in the C-terminal portion. The individual functional products are liberated by various cleavage events. The core to NS2 region is processed by the cellular enzymes signal peptidase and signal peptide peptidase (Fig. 1), the C terminus of NS2 is released from NS3 by the NS2-3 proteinase, and all other cleavages are mediated by the main viral proteinase complex composed of NS3 and NS4A.

For most viral proteins, defined functions have been ascribed. The core, E1, and E2 proteins are believed to be major constituents of the virus particle required for genome packaging (core), attachment of the virus to its target cell (E2), and the ensuing fusion process that delivers the genome into the cytoplasm (presumably E1). The hydrophobic p7 protein adopts a double membrane-spanning topology and has been proposed to be a member of a small protein family of viroporins (Carrere-Kremer *et al.*, 2002). These proteins are known to enhance membrane permeability and are believed to be required for late steps in virus assembly. Two groups independently showed that p7 forms an ion channel in artificial lipid bilayer systems, suggesting that it indeed may function as a viroporin (Griffin *et al.*, 2003; Pavlovic *et al.*, 2003). The NS3 protein is the key viral proteinase that, in conjunction with NS2, is required for cleavage at the NS2/3 site and, after association of the cofactor NS4A, performs the processing events at all downstream cleavage sites (Bartenschlager, 1999). In addition to its proteinase function, NS3 acts as an RNA helicase unwinding secondary structures, presumably during RNA replication. The replication process itself takes place at a specialized membrane compartment, the so-called membranous

web, which is primarily induced by the NS4B protein (Egger *et al.*, 2002; Gosert *et al.*, 2003) (Section V,F). The NS5A protein is a highly phosphorylated polypeptide that has been implicated in the resistance of HCV to IFNs (Enomoto *et al.*, 1995, 1996a; Gale *et al.*, 1997, 1998). Besides this observation, it is interesting to note that a large number of cell culture-adaptive mutations localize to the NS5A protein, suggesting that it may play a role in RNA replication (Section V,F). Finally, the NS5B protein, the most C-terminal cleavage product of the polyprotein, is the viral RNA-dependent RNA polymerase. This

TABLE I
HCV PROTEINS AND THEIR PRESUMED FUNCTIONS IN THE VIRAL LIFE CYCLE

HCV protein	Function	Apparent MW [kDa]	Posttranslational modification
F/ARF-protein	?	17	?
Core	RNA binding; nucleocapsid	23 (precursor), 21 (mature)	Proteolytic processing at C terminus by SPP
E1	Envelope protein; fusion domain?	31–35	Glycosylation
E2	Envelope protein; receptor binding	70	Glycosylation
p7	Viroporin (ion channel?)	7	?
NS2	Component of NS2-3 proteinase	21	?
NS3	Component of NS2-3 and NS3/4A proteinase (N-terminal domain); NTPase/helicase (C-terminal domain); interference with IRF-3	69	Methylation
NS4A	NS3/4A proteinase cofactor	6	–
NS4B	Induction of membranous vesicles	27	?
NS5A	IFN- α resistance?; RNA replication?	56 and 58 (basal and hyperphosphorylated form, respectively)	Phosphorylation
NS5B	RdRp	68	Phosphorylation?

enzyme most likely forms the catalytic center of a highly ordered replication complex composed of viral and cellular factors that interact on a membranous scaffold to multiply the HCV genome. The field's current understanding of the components and the configuration of this complex are described in greater detail in the following section. A brief summary of the individual protein products and their post-translational modifications and respective main function(s) is given in Table I.

III. VIRUS STRUCTURE

A. *Structural Proteins*

By definition, the structural proteins of a virus are polypeptides that are the main constituents of the virus particle. These proteins are required to carry the viral genome from one host cell to another. Besides the structural proteins, accessory viral and cellular proteins can also be packaged. In the case of HCV, little is known about the precise composition of the virus particle. Based on analogy to closely related flaviviruses, however, it can be assumed that the core protein and the glycoproteins E1 and E2 are the main structural components. It is unknown whether p7 is also a constituent of the virus particle. It is interesting to note, however, that for the closely related pestivirus *Bovine viral diarrhea virus* (BVDV), p7 does not seem to be a major component of the virus particle (Elbers *et al.*, 1996). Therefore, the discussion in this chapter focuses only on the core, E1, and E2 HCV proteins.

The core protein resides at the very N terminus of the polyprotein and is released from the precursor by cleavage at residue 191 that is mediated by the cellular signal peptidase (Hijikata *et al.*, 1991). This cleavage event liberates the N-terminal end of E1, whereas the core protein remains associated with the endoplasmic reticulum (ER) via the C-terminal E1 signal peptide. Data from several laboratories indicate that maturation of core requires a further cleavage performed by an ER-resident enzyme (Hussy *et al.*, 1996; Liu *et al.*, 1997; Moradpour *et al.*, 1996a; Santolini *et al.*, 1994). Evidence has been presented showing that further cleavage is most likely performed by signal peptide peptidase, resulting in a mature core protein of approximately 179 amino acids (McLauchlan *et al.*, 2002; Okamoto *et al.*, 2004). The apparent molecular weights of the individual forms of core on polyacrylamide gels are described as 23 and 21 kDa (Hope and McLauchlan, 2000; Moradpour *et al.*, 1996a; Yasui *et al.*, 1998) or 19

and 17 kDa (Hussy *et al.*, 1996; Lo *et al.*, 1994, 1995), respectively, which has led to some confusion regarding the nomenclature of the respective protein products. In one report, core protein from infected patients was shown to have a molecular weight of 21 kDa, suggesting that this is the mature form of core that makes up the viral capsid (Yasui *et al.*, 1998). Moreover, the p21 form is the predominant species found in several tissue culture expression systems including Huh-7 cells that contain autonomously replicating full-length HCV RNAs (Pietschmann *et al.*, 2002).

Various groups have described a complex intracellular localization of the core protein. It predominantly resides in the cytoplasm either in association with the ER or on the surface of lipid droplets (Barba *et al.*, 1997; Hope and McLauchlan 2000; Moradpour *et al.*, 1996a; Pietschmann *et al.*, 2002; Yasui *et al.*, 1998). Moreover, nuclear localization has been described (Liu *et al.*, 1997; Yasui *et al.*, 1998). Based on amino acid content and hydrophobicity profile, three different domains within the core protein can be distinguished (McLauchlan, 2000). These correspond to a hydrophilic domain with a high proportion of basic residues (23.4%) that is located at the N terminus of the protein (residues 1 to 122); a central, more hydrophobic region (residues 123 to 174) with reduced content of basic amino acids (5.8%); and a C-terminal domain with a yet higher hydrophobicity that serves as a signal sequence for E1 (residues 175 to 191) (McLauchlan, 2000). Several functions related to its role as a structural component of the virus particle have been described and were attributed to various regions of the polypeptide. For instance, the protein is known to bind nucleic acids (Fan *et al.*, 1999; Santolini *et al.*, 1994; Shimoike *et al.*, 1999), and the ability to do so has been localized to amino acids 1 to 75 (Santolini *et al.*, 1994). The protein has nucleic acid chaperone activity and facilitates the annealing of complementary DNA and RNA sequences, resulting in the formation of stable duplexes by a strand-exchange reaction (Cristofari *et al.*, 2004). Homo-oligomerization of the protein has been reported and appears to mainly involve sections of core contained in domain I, including residues 36 to 91 (Matsumoto *et al.*, 1996) and 82 to 102 (Nolandt *et al.*, 1997), although the central domain II may be involved as well (Yan *et al.*, 1998a). However, *in vitro* assembly studies with recombinant HCV core proteins demonstrated that the amino-terminal 124 residues of the protein are sufficient to direct the assembly of nucleocapsid-like structures, implying that this fragment contains all information essential for this process (Kunkel *et al.*, 2001). Interestingly, in this system, assembly requires the presence of structured RNA but not necessarily sequences derived

from the HCV genome (Kunkel *et al.*, 2001). This observation implies that the interaction of core with RNA is rather promiscuous, at least *in vitro*, suggesting that high (local) concentrations of the HCV genome are required to ensure its specific packaging. To date, not much is known about the interaction of the core protein with other viral proteins. Based on its presumed role in virus assembly, the core is assumed to contact the viral glycoproteins in the course of assembly. In line with this hypothesis, immunoprecipitation experiments revealed an association of core and E1 (Lo *et al.*, 1996). Interactions with other viral proteins have not been reported.

One intriguing peculiarity of the core protein is its interaction with lipid droplets that represent cellular storage compartments needed for membrane formation and used as energy source (Murphy and Vance, 1999). Because this association has been detected using varying expression systems employing different cell lines and also by using specimens obtained from infected chimpanzees (Barba *et al.*, 1997), the core protein most likely also interacts with lipid droplets in infected hepatocytes of patients with hepatitis C. It has been shown that the central domain of the core mediates this association (Hope and McLauchlan, 2000). Sequence comparisons have indicated that this region is also present in the putative core protein of GBV-B, the closest relative of HCV, but is missing in the homologous proteins of other flaviviruses (Hope *et al.*, 2002). It has also been speculated that the attachment of the core protein with lipid droplets may result in changes in lipid metabolism, which in turn may contribute to the development of steatosis frequently observed in HCV-infected livers (Barba *et al.*, 1997; McLauchlan, 2000). The observation that transgenic mice expressing HCV core develop steatosis and hepatocellular carcinoma has lent further support to this hypothesis (Lerat *et al.*, 2002; Moriya *et al.*, 1998). Besides the potential involvement of HCV core in lipid metabolism, the protein has been implicated in modulating a number of cellular processes, including apoptosis, transformation, and host-cell gene expression to name but a few. An adequate discussion of these diverse effects is beyond the scope of this chapter, and the interested reader is referred to a comprehensive review by McLauchlan (2000).

The E1 and E2 proteins are heavily glycosylated type I transmembrane proteins with an N-terminal ectodomain and a C-terminal hydrophobic membrane anchor (Dubuisson, 2000). As previously mentioned, proteolytic cleavages performed by the cellular signal peptidase produce the mature proteins. These extend from amino acid 192 to 383 (E1) and from residue 384 to 746 (E2) of the polyprotein, and they

exhibit an apparent molecular weight of approximately 30 to 35 kDa and 70 to 72 kDa, respectively (Grakoui *et al.*, 1993c; Ralston *et al.*, 1993). In the absence of efficient virus replication in cell culture, researchers have resorted to heterologous viral and nonviral expression systems to study the folding of these proteins. In the course of these analyses, a large body of data has been accumulated regarding the interaction and complex formation between E1 and E2 and the intracellular localization of these polypeptides. The biogenesis of E1 and E2 (reviewed in Op de Beeck *et al.*, 2001) is an intricate process involving various ER-resident chaperones, including calnexin, calreticulin, and BiP (Choukhi *et al.*, 1998; Dubuisson and Rice, 1996; Merola *et al.*, 2001). Although E2 protein folding is independent from other viral proteins, maturation of E1 is known to require coexpression of E2 (Michalak *et al.*, 1997). Merola *et al.* (2001) have demonstrated that the core protein also assists in the folding process of E1, emphasizing the importance of neighboring viral proteins in this process. It has been demonstrated that E1 and E2 are capable of forming noncovalently linked heterodimers (Deleersnyder *et al.*, 1997; Dubuisson *et al.*, 1994; Ralston *et al.*, 1993). These slowly maturing proteinase-resistant complexes, which are no longer associated with the ER chaperone calnexin, are selectively recognized by a conformation-dependent antibody and believed to represent the native prebudding form of the viral glycoproteins (Deleersnyder *et al.*, 1997). In addition, a nonproductive folding pathway exists, leading to the production of disulfide-linked glycoprotein aggregates (Dubuisson *et al.*, 1994; Grakoui *et al.*, 1993c). The propensity to form aggregates may represent an intrinsic property of the HCV glycoproteins (Op de Beeck *et al.*, 2001) and reflects their inefficient folding. Such aggregates, however, were not observed in cell lines persistently replicating selectable full-length HCV Con1 genomes (Pietschmann *et al.*, 2002). This implies that the tendency to aggregate may vary between different HCV isolates. Alternatively, the absence of aggregates in replicon cells may be related to a lower level of viral protein expression. Although comparative studies analyzing complex formation with different glycoprotein isolates and expression systems may resolve this issue, the biologic relevance of both glycoprotein complexes in the context of the viral life cycle awaits the development of an efficient cell culture system for HCV particle formation.

Several groups have attempted to map the sites of interaction between the two HCV glycoproteins. Initial data suggested that the ectodomains of both polypeptides carry the critical determinants required for association because E1 and E2 complexes were secreted upon coexpression of truncated forms of both proteins (Matsuura

et al., 1994). Moreover, Takikawa *et al.* (2000) reported cell surface-expressed oligomers of E1 and E2 upon coexpression of chimeric HCV E1 and E2 comprising the transmembrane (TM) domain of the vesicular stomatitis virus (VSV) G protein, again indicating that the ectodomains are sufficient for oligomerization. On the other hand, several groups observed that deletion of the TM domain of E2 or its replacement by a heterologous membrane anchor sequence abrogates heterodimerization (Cocquerel *et al.*, 1998; Michalak *et al.*, 1997; Patel *et al.*, 2001; Selby *et al.*, 1994), which clearly implies that this portion of the protein is essential for complex formation. In another study, an alanine scanning insertion mutagenesis performed on the TM domains of E1 and E2 defined distinct sections in these regions essential for heterodimerization, emphasizing the important role of the TM domains for glycoprotein assembly (Op de Beeck *et al.*, 2001). Taken together, interactions between the viral glycoproteins are likely to involve various regions of the proteins with interfaces located in both ectodomains and TM domains.

In the last few years, much attention has been devoted to the study of the TM regions of E1 and E2 and has led to the identification of the multifunctional nature of these protein domains. The regions are required for membrane anchorage and protein interactions, they harbor signal sequences essential for the insertion of the C-terminal polypeptide into the ER membrane, and they contain ER-retention signals responsible for their subcellular localization (Cocquerel *et al.*, 1998, 1999, 2000; Duvet *et al.*, 1998; Flint and McKeating, 1999). Highly conserved charged residues located in the middle of both TM domains were shown to play a major role in the observed retention (Cocquerel *et al.*, 2000). Interestingly, mutations affecting these residues did not only influence subcellular localization but also altered processing and disrupted heterodimerization (Cocquerel *et al.*, 2000). In two publications by Charloteaux *et al.* (2002) and Cocquerel *et al.* (2002), the exact topology of the TM regions has been investigated, and models have been proposed describing the regions' intramembrane architecture (Section V,G). From these studies, it became apparent that the TM domains exhibit a complex folding pattern, which is likely to be dynamic, allowing sufficient flexibility of the proteins to perform their different functions during the viral life cycle. Direct studies addressing these functions have been limited by the absence of a fully permissive cell culture system for HCV. Nevertheless, indirect evidence obtained from neutralization studies suggests that E2 is responsible for attachment to a receptor on host cells (Rosa *et al.*, 1996). Moreover, based on computational and sequence analyses, it was proposed that the E1

glycoprotein may function as fusion protein (Flint *et al.*, 1999b; Garry and Dash, 2003). The knowledge about the involvement of the HCV glycoproteins in virus attachment and entry is discussed in greater detail in the following section.

B. Structure of Virus Particles

Even though more than a decade has passed since the first HCV genome was cloned in 1989, not much knowledge has been acquired concerning the structure and composition of the virus particle. Progress in this area has been hampered mainly by two impediments. First, in patients with hepatitis C, various serum components associate intensively with virus particles, complicating their purification and obstructing direct morphological studies. Second, currently available cell culture systems do not allow sufficient production of virus particles. Consequently, models described thus far are based primarily on indirect measurements, analogies to closely related viruses, and structure predictions.

The basic biophysical properties of the HCV particle emerged from experiments on chimpanzees. Virus infectivity was destroyed by treatment with lipid solvents, which indicates that the particle contains an envelope (Feinstone *et al.*, 1983) (Fig. 2). A rough estimate of particle size was obtained by filtration studies. The experiments demonstrate that HCV is able to pass through filters with 50-nm pores (He *et al.*, 1987). Subsequent electron microscopy analyses established that HCV is a spherical enveloped particle with a size of approximately 40 to 70 nm in diameter (Kaito *et al.*, 1994; Li *et al.*, 1995; Shimizu *et al.*, 1996). By analogy to closely related flaviviruses, for which the structure of the virus particle is known [*Dengue virus* and *Tick-borne encephalitis virus* (TBEV)] (Ferlenghi *et al.*, 2001; Kuhn *et al.*, 2002), it can be assumed that the HCV envelope contains the viral glycoproteins E1 and E2. The envelope encloses a spherical nucleocapsid formed by multiple copies of the core protein, which in turn is associated with a single copy of the viral genome (Penin, 2003).

A structural model of the HCV glycoprotein E2 as deduced essentially from the X-ray crystal structure of the TBEV E protein has also been proposed (Yagnik *et al.*, 2000) (Fig. 2). According to this model, the E2 protein forms a head-to-tail homodimer that has an elongated, flat structure. The E1 protein may be located at each “end” of the E2 dimerization domain, resulting in a homodimeric pair of heterodimers (Fig. 2). Regions in E2 involved in CD81 binding (Section V,A) as well as the location of hypervariable region 1 and binding sites for

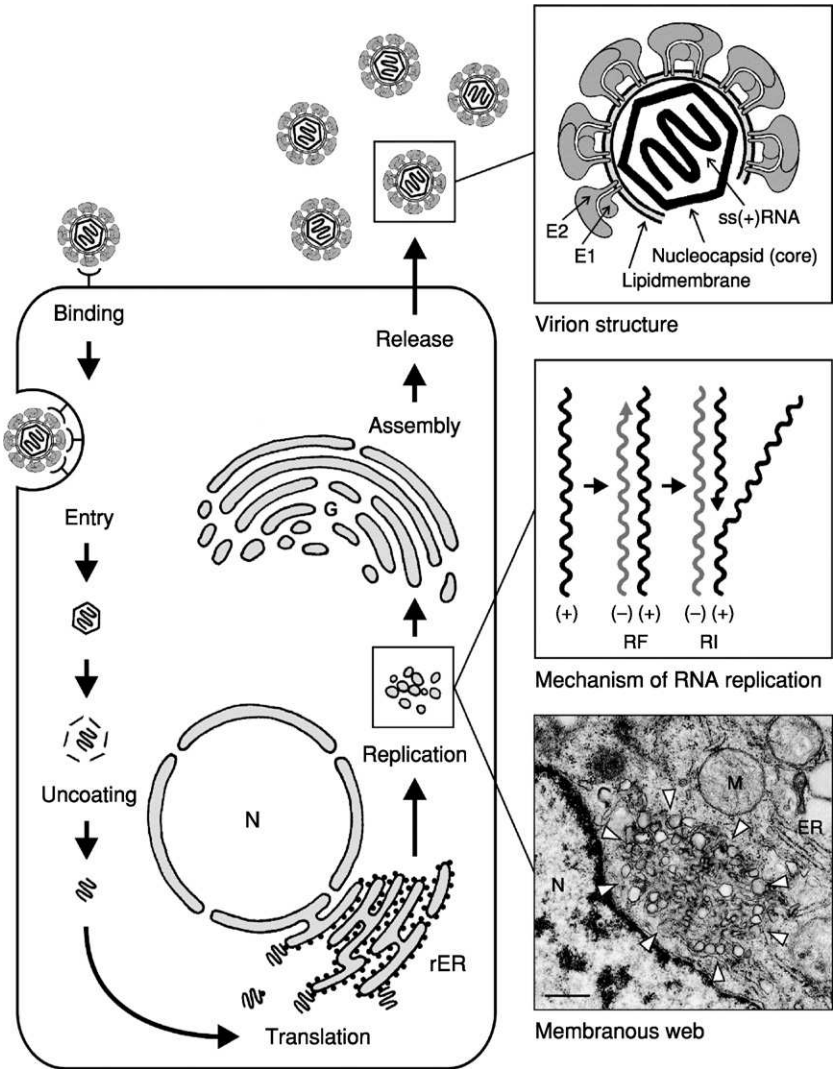


FIG 2. Hypothetical HCV replication cycle. HCV particles bind to the host cell via a specific interaction between the HCV envelope glycoproteins and a yet unknown cellular receptor. Bound particles are probably internalized by receptor-mediated endocytosis. After the viral genome is liberated from the nucleocapsid (uncoating) and translated at the rough ER, NS4B (perhaps in conjunction with other viral or cellular factors) induces the formation of membranous vesicles (referred to as the membranous web; electron micrograph in the lower right). These membranes are supposed to serve as scaffolds for the viral replication complex. After genome amplification and HCV protein expression, progeny virions are assembled. The site of virus particle formation has not yet been

neutralizing monoclonal antibodies were predicted in this structure. Although much of this model is speculative, it will provide a useful framework for future molecular studies of structure and function of HCV envelope glycoproteins.

As suggested in the latter paragraphs, HCV has the propensity to bind to different serum constituents, and, consequently, virus preparations are very heterogeneous. HCV RNA-containing particles associated with beta lipoproteins and with a very low buoyant density (≤ 1.08 g/ml) have been observed (Andre *et al.*, 2002; Miyamoto *et al.*, 1992; Prince *et al.*, 1996; Thomssen *et al.*, 1992). Moreover, an association with immunoglobulins has been reported, and these complexes exhibit an intermediate density of approximately 1.17 to 1.21 g/ml (Choo *et al.*, 1995; Hijikata *et al.*, 1993c; Thomssen *et al.*, 1993). In addition, patient plasma has been shown to contain nonenveloped nucleocapsids harboring HCV RNA and exhibiting yet higher density in the range of 1.32 to 1.34 g/ml (Maillard *et al.*, 2001). The infectious form of the HCV particle, however, appears to have a low density. This view is supported by two findings. First, following density gradient centrifugation, Bradley *et al.* (1991) recovered most of the infectivity of a chronic-phase chimpanzee plasma sample in a pool of gradient fractions encompassing buoyant densities between 1.09 to 1.11 g/ml. Second, in agreement with this finding, HCV RNA derived from a highly infectious plasma of a patient with HCV was exclusively found in fractions of very low density (≤ 1.09 g/ml), while RNA structures derived from a plasma sample with a lower infectivity were also found in fractions with higher density associated with antibodies (Hijikata *et al.*, 1993c). Because these data suggest that infectious virus particles may be associated with lipoproteins, it is tempting to speculate that



identified. It may take place at intracellular membranes derived from the ER or the Golgi compartment. Newly produced virus particles may leave the host cell by the constitutive secretory pathway. The upper right panel of the figure shows a schematic representation of an HCV particle. Note that the envelope proteins E1 and E2 are drawn according to the proposed structure and orientation of the TBEV envelope proteins M and E, respectively (Yagnik *et al.*, 2000). The middle panel shows a model for the synthesis of negative-stranded (-) and positive-stranded (+) progeny RNA via a double-stranded replicative form (RF) and a replicative intermediate (RI). The bottom panel shows an electron micrograph of a membranous web (arrow heads) in a Huh-7 cell containing subgenomic HCV replicons. The web is composed of small vesicles embedded in a membrane matrix. Note the close association of the membranous web with the rough ER. Bar: 500 nm; N: nucleus; ER: endoplasmic reticulum; M: mitochondria. The electron micrograph is adapted from Gosert *et al.* (2003), with permission from the American Society for Microbiology.

such an interaction is critical for infectivity. Accordingly, among other molecules, the low-density lipoprotein receptor (LDLr) has been postulated to mediate virus entry.

IV. EXPERIMENTAL SYSTEMS

A major hurdle in studying HCV replication has been, and still is, the lack of efficient and simple virus cultivation systems. Numerous attempts have been made to propagate HCV in small animals or cell culture. Until recently, these efforts have either failed or replication levels have been too low to allow reproducible studies (reviewed in Grakoui *et al.*, 2001; Pietschmann and Bartenschlager, 2003). Therefore, HCV-related viruses and surrogate systems have been used to study various aspects of the HCV life cycle. Most closely related are the BVDV and GBV-B viruses. The latter is a hepatotropic virus of unknown origin that has a genomic organization almost superimposable to the one of HCV (Beames *et al.*, 2000, 2001; Meyers and Thiel, 1996; Muerhoff *et al.*, 1995; Ohba *et al.*, 1996). Although GBV-B propagation in cell culture is rather inefficient (Xiang *et al.*, 2000), this virus is still a useful model because it readily infects tamarins (*Saguinus sp.*). Infected animals develop an acute, self-limiting hepatitis that resolves within 12 to 14 weeks (Beames *et al.*, 2000). Persistent infections have also been reported either in immunosuppressed animals or in animals who have been inoculated with an infectious molecular clone (Lanford and Bigger, 2002). Successful infections of owl monkeys (*Aotus trivirgatus*) and marmosets (*Callithrix jacchus*) have also been described (Bright *et al.*, 2004; Bukh *et al.*, 2001; Lanford *et al.*, 2003b). Marmosets are an especially attractive alternative because they are rather easy to breed in captivity and are frequently used for pharmacokinetic and toxicology studies. Moreover, treatment of GBV-B-infected animals with a drug that was originally developed for inhibition of the HCV NS3 proteinase resulted in a three-log drop in viral RNA serum levels within 4 days (Bright *et al.*, 2004). These results underscore the close relationship between HCV and GBV-B and suggest that GBV-B might be an interesting and valuable model system to gain information about HCV replication *in vivo*. In spite of the more distant relationship to HCV, BVDV has the advantage over GBV-B to replicate to high titers in many cell lines of bovine and even human origin. Infectious molecular clones are available, making this virus even more attractive for studying certain aspects of RNA replication *in vitro* that so far

cannot be addressed for HCV, such as virus assembly and release of infectious progeny (Agapov *et al.*, 2004).

Apart from the use of HCV-related viruses, several surrogate systems have been developed primarily for drug development and screening purposes (reviewed in Rosenberg, 2001). One example is a *Poliovirus* that expresses its polyprotein under control of the HCV IRES (Zhao *et al.*, 1999). Another example is a chimeric Sindbis virus (SinV) in which the HCV NS3/4A proteinase is fused to the N terminus of the SinV capsid protein (Filocamo *et al.*, 1997). Only after NS3/4A has accomplished its removal from the capsid protein, maturation of the SinV structural proteins occurs, making replication of this chimeric virus dependent on the activity of the HCV proteinase. Similarly, a chimeric BVDV carrying an engineered HCV NS3/4A proteinase has been constructed, and this virus only replicates after proteolytic removal of the HCV enzyme (Lai *et al.*, 2000). Although very useful for the development of NS3/4A-specific antiviral drugs, these systems do not allow detailed studies of HCV replication.

A. In Vivo Models for HCV Infection and Replication

Thus far, the only animal that can be infected reliably with HCV is the chimpanzee (*P. troglodytes*). In spite of ethical concerns and high costs, chimpanzee experiments have provided invaluable information. For instance, the first successful transmission of the non-A, non-B hepatitis agent from human serum to chimpanzees demonstrated the transmissible nature of this disease (Alter *et al.*, 1978; Hollinger *et al.*, 1978; Tabor *et al.*, 1978). Subsequently, chimpanzees were used to generate high-titered serum pools from which the first HCV genome was cloned (Choo *et al.*, 1989). In addition, the experimental inoculation of chimpanzees with an RNA version of a cloned consensus HCV genome not only demonstrated the functionality of this genome *in vivo* but also showed that HCV infection is sufficient to cause liver disease (Kolykhalov *et al.*, 1997; Yanagi *et al.*, 1997). Because the clinical course of disease in chimpanzees and humans is similar, studies of experimentally infected animals have shed light onto the role of the immune response in controlling virus infection (reviewed in Lanford and Bigger, 2002). Infected animals became viremic within a few days with peak titers in the range of 10^5 to 10^7 genome equivalents per milliliter. This initial viremia is seldom accompanied by elevated serum concentrations of liver enzymes, indicating that HCV replication does not cause liver cell damage *per se*. The animals mount a detectable

immune response that is characterized by seroconversion and the appearance of T cell immune reactivity. Comparable to the human situation, a significant proportion of infected animals is unable to clear the virus and contracts a persistent infection with fluctuating virus titers and eventual sporadic occurrence of liver inflammation. Although it is not yet clear how the virus escapes the immune response, an increasing body of evidence shows that a vigorous immune reaction correlates positively with virus elimination as well as liver cell damage. The latter observation is in keeping with the notion that HCV is not lytic per se.

Because of the inherent problems caused by working with chimpanzees, other primate species have also been inoculated with HCV. These experiments, however, have not been successful because the animals were either not susceptible to the infection or virus replication was too low to allow detailed analyses (reviewed in Grakoui *et al.*, 2001). Because of the possibility of successfully infecting tupaia (*Tupaia belangeri chinensis*) with the *Hepatitis B virus* (HBV), animals of this species were also inoculated with sera from patients with hepatitis C (Xie *et al.*, 1998). Infection, however, appears to be possible in only a small proportion of animals, that developed only transient or intermittent viremia with low titers.

The most convenient animal model in virus research is the laboratory mouse (*Mus musculus domesticus*). First, it is a well-established model that is extensively used throughout the world and is one for which numerous tools exist; second, the animals have a high reproduction rate and a rapid breeding cycle; third, mice are genetically and immunologically well characterized; and, fourth, transgenic animals provide a means to investigate the role of host-cell genes in disease development and virus replication. Unfortunately, owing to the narrow host range of HCV, the infection of mice is not possible. To overcome this block, xenotransplantation systems have been developed. In one setting, beige/nude/X-linked immunodeficient so-called Trimera mice (Ilan *et al.*, 2002) were totally body irradiated. After this hemoablation, the mice were rescued by transplantation of bone marrow cells derived from severe combined immunodeficient (SCID) mice, and human liver fragments infected *ex vivo* with HCV were transplanted under the kidney capsule of these animals. By using RT-PCR, it was shown that HCV RNA was present up to 50 days post-transplantation in up to 50% of animals that received HCV-infected human liver cells.

Although the results described in the latter paragraph are promising, the system is limited by the short half-life of the xenotransplant and the

low HCV RNA titers. A more efficient system has been described by Mercer *et al.* (2001). This model uses an immunocompromised mouse strain that carries a tandem array of four murine urokinase-type plasminogen activator (*uPA*) genes under control of the liver-specific albumin promoter. Postnatal expression of this transgene leads to overproduction of urokinase in the liver and results in the rapid death of hepatocytes. Survival of the mice is often due to deletions of the transgene in a few cells conferring a selective growth advantage and enabling these cells to repopulate the liver (Sandgren *et al.*, 1991). The survival rate can be enhanced by transplantation of primary hepatocytes early after birth. After xenotransplantation (e.g., of primary human hepatocytes), transferred cells migrate into the mouse liver, repopulate the organ, and form liver nodules that can build up to 50% of the total liver cell mass. The success of repopulation as determined by the size of the liver graft and its duration very much depends on homozygosity of the mouse strain for the *uPA* transgene, which is associated with high lethality. When mice with a chimeric liver that contains mouse and human hepatocytes were infected with HCV, however, persistent viremia was detected. About 75% of the inoculated animals developed virus titers in the range of 10^4 to more than 10^6 per milliliter, which is similar to what is observed in an infected patient (Mercer *et al.*, 2001). Immunohistochemistry confirmed that HCV replication was confined to human hepatocytes, corroborating that HCV does not infect mouse cells. Although these mice represent by far the most efficient small animal system for the propagation of HCV, some major drawbacks exist. Most serious is the high lethality of the *uPA* transgene in homozygous mice (greater than 30%). Furthermore, transplantation has to be performed within the first 5 to 14 days after birth, making the transplantation technically challenging. Finally, the quality of transplanted primary human cells is very crucial as is the constant support of these cells that so far cannot be cryopreserved without losing repopulation efficiency and susceptibility to HCV infection.

B. Cell Culture Systems

The efficient propagation of HCV in cell culture is a notoriously difficult task. Here, the discussion focuses on the development of the HCV replicon system. The reader who is interested in a broad overview of HCV cell culture systems is referred to publications by Bartenschlager and Lohmann (2001) as well as Kato and Shimotohno (2000).

Replication of HCV in infected cell lines of hepatic and nonhepatic origin as well as primary hepatocytes of humans and chimpanzees has been described by several groups. Moreover, the *in vitro* cultivation of primary cells isolated from tissues of persistently infected patients has been reported. The level of HCV replication, however, is rather low and, therefore, the detection of viral RNA by Northern blot or nuclease protection assays and the demonstration of HCV proteins by Western blot or immunofluorescence assays most often have not been possible. Instead, replication was determined by the qualitative detection of negative-stranded RNA by RT-PCR that, for technical reasons, is difficult to control (Gunji *et al.*, 1994; Lanford *et al.*, 1994; Takyar *et al.*, 2000). Additional criteria were the prolonged detection of positive-stranded RNA (up to 2 years), the existence of a genetic drift of HCV sequences during continued passage of infected cells, the transmission of HCV generated in these cell cultures to naive cells, and the inhibition of HCV replication by IFN- α or antisense oligonucleotides. Overall, these criteria document HCV replication in these systems, but the low efficiency prevents their use for detailed studies of virus replication.

Recently, a novel B cell line (designated SB) was established from spleen cells of an HCV-infected patient with type II-mixed cryoglobulinemia (Sung *et al.*, 2003). These cells continuously support replication of an HCV genome that belongs to the genotype 2b. Nuclease-resistant HCV RNA with a buoyant density of 1.13 to 1.15 g/ml was detected in the supernatant of these cells. Upon inoculation of primary human hepatocytes, or peripheral blood mononuclear cells (PBMCs) or the B cell line Raji with filtered supernatant from SB cells, HCV RNA was detected in inoculated cells, which indicates a productive infection. Based on nuclease protection assays, about 1 ng of HCV positive-stranded RNA was detected in 100 μ g of total cellular RNA, suggesting an average copy number of 10 molecules per cell, which is much higher compared to the infection systems described thus far for which copy numbers in the range of 0.01 to 0.1 copies per cell have been calculated. On the other hand, within a 96-h-incubation period, about 3×10^4 RNA copies were secreted into the supernatant of about 10^7 SB cells, indicating that only one RNA molecule is released from about 1,000 cells during the observation period. In spite of this limitation, the cell line might be useful to study certain aspects of the HCV life cycle, most notably the induction of apoptosis that was observed in a high percentage of HCV-infected SB cells (Sung *et al.*, 2003). Moreover, this study clearly shows that HCV can infect and productively replicate in B cells. However, whether B cells represent a potential reservoir for HCV *in vivo* remains to be seen.

Apart from the classical approach of infecting cell lines with well-defined HCV-containing patient samples, several investigators have tried to establish cell culture systems that are based on the transfection of cell lines or primary cell cultures with cloned full-length HCV genomes (reviewed in Bartenschlager and Lohmann, 2001). This approach has been successfully used for a number of other positive-stranded RNA viruses, but initial attempts with HCV was not successful. It was thought that this failure might be due to undesired mutations that were introduced during PCR-based amplification and cloning procedures, for instance. With the availability of cloned infectious HCV genomes (Kolykhalov *et al.*, 1997; Yanagi *et al.*, 1997, 1998), this hurdle appeared to be overcome, but even when using such genomes with proven functionality, researchers could not establish cell lines that support efficient HCV replication and particle production (Aizaki *et al.*, 2003). It has also been described that HCV replicates in CV-1 and HepG2 cells after transfection of a plasmid that carries a full-length genotype 1a genome. Transcription of the HCV sequence was under control of the bacteriophage T7 promoter, and T7 RNA polymerase was expressed in transfected cells after infection with a recombinant T7-pol vaccinia virus (Chung *et al.*, 2001). Replication of HCV was examined by a nuclease protection assay specific for negative-stranded RNA, resistance of HCV RNA replication against actinomycin D, generation of HCV quasi-species, and the inhibition of HCV RNA production by IFN- α . Moreover, an increase of mutations that clustered to certain regions of the HCV genome was observed when cells were treated with ribavirin, a drug that is supposed to act as an RNA virus mutagen (Contreras *et al.*, 2002) (Section VII). Although these results suggest that it is possible to establish a DNA-launched HCV replication system, the approach bears some technical limitations. For instance, it is difficult to differentiate between mutations that were introduced by T7 RNA polymerase and those generated by the HCV replicase. Most notably, vaccinia virus replication is cytopathic and, therefore, may cause pleiotropic effects both on the host cell metabolism and HCV replication. These effects may be avoided by using alternative T7 RNA polymerase delivery systems, which might also circumvent the problem that vaccinia virus replication is affected by IFN- α and ribavirin as well. Further studies are required to more rigorously test the applicability of this system for HCV replication in cell culture and to see whether the complete HCV life cycle can be studied with this approach.

The most efficient and robust cell culture model for HCV thus far is the replicon system. This system was initially based on the self-replication

of selectable subgenomic HCV RNAs in the human hepatoma cell line Huh-7 (Lohmann *et al.*, 1999a). These RNAs were derived from a cloned consensus genome of genotype 1b in which the coding sequence of the structural proteins or the coding sequence of the structural proteins plus the NS2 sequence was replaced by the selectable marker *neo*. A heterologous IRES element derived from the *Encephalomyocarditis virus* (EMCV) was inserted upstream of the NS2 or the NS3 coding region (Fig. 3). This insertion resulted in bicistronic constructs with the first cistron (*neo*) and the second cistron (the HCV replication factors NS3 to NS5B) being translated under control of the HCV and the EMCV IRES, respectively. Upon transfection of Huh-7 cells and subsequent selection with G418, a low number of cell clones was obtained that carried high amounts of HCV RNA (Fig. 3). Based on quantification by Northern blots, it has been calculated that about 10^8 HCV RNA copies per microgram of total RNA were detected, which corresponds to an average copy number of 1000 to 5000

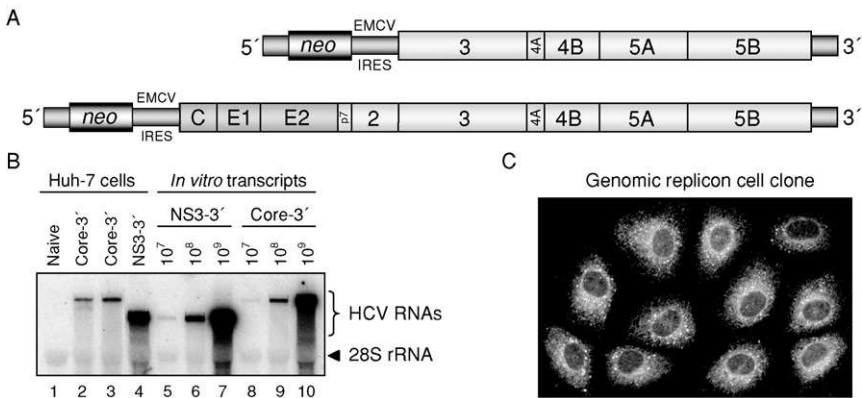


FIG 3. Structure of HCV replicons and demonstration of replicon RNA and viral proteins in Huh-7 cells. (A) Schematic representation of subgenomic and genomic HCV replicons. These RNAs are composed of the HCV 5'-NTR, the *neo* gene encoding the neomycin phosphotransferase that confers G418 resistance, the EMCV IRES, the HCV coding sequence from NS3 to NS5B or core to NS5B, and the HCV 3'-NTR. (B) Huh-7 cells transfected with replicon RNAs (depicted in panel A) and subsequently subjected to G418 selection. Single-cell clones were isolated, and total RNA was prepared and analyzed by HCV-specific Northern blot. RNA from two cell clones carrying a genomic replicon (lanes 2 and 3) and one cell clone carrying a subgenomic replicon (lane 4) are shown. Corresponding *in vitro*-transcribed HCV RNAs were used as size markers and for the estimation of replicon RNA copy numbers (lanes 5 to 10). Total RNA from naive Huh-7 cells served as negative control (lane 1). (C) Demonstration of NS5A expression in a cell clone carrying a selectable genomic HCV replicon by indirect immunofluorescence.

positive-stranded viral RNA molecules per cell. Most importantly, viral RNAs could be metabolically radiolabeled with [^3H] uridine in the presence of actinomycin D, demonstrating unequivocally the autonomous replication of these RNAs (Lohmann *et al.*, 1999a). When cells are passaged under continuous G418 selection, these RNAs can be kept under conditions promoting stable replication for many years (Pietschmann *et al.*, 2001). Furthermore, under appropriate conditions, the replicons can be detected in Huh-7 cells passaged in the absence of selective pressure, even after about 1 year, although there is a significant decline in the RNA copy number over time (Pietschmann *et al.*, 2001). With the identification of cell culture-adaptive mutations that tremendously enhance HCV RNA replication in Huh-7 cells (Section VI,A), it was possible to develop transient replication assays that no longer depend on cumbersome and time-consuming selection of cells and that permit rapid analyses of mutants (Blight *et al.*, 2000; Guo *et al.*, 2001; Krieger *et al.*, 2001; Lohmann *et al.*, 2001). Moreover, selectable cell culture-adapted full-length HCV genomes were constructed that stably or transiently replicate in Huh-7 cells to high levels (Blight *et al.*, 2002, 2003; Ikeda *et al.*, 2002; Pietschmann *et al.*, 2002) (Fig. 3). In spite of efficient RNA amplification and expression of all viral proteins, no clear evidence for the production of virus particles has been obtained in these systems.

V. REPLICATION CYCLE

The field's current understanding of HCV replication is largely hypothetical, but some details begin to emerge due to the availability of efficient *in vitro* systems. Of most importance are replicons that recapitulate the intracellular steps of RNA replication and HCV pseudo-particles that are instrumental for analyzing early events in the infectious process. The overall outline of the HCV replication cycle is depicted in Fig. 2, and the individual steps are discussed in detail in the following sections.

A. Receptor Candidates and Mechanism of Cell Entry

In general, virus entry into target cells is a complex multistep process involving diverse interactions between viral and cellular components that allow attachment of the virus particle and delivery of the viral genome into the host cell. To this end, viruses have evolved strategies to usurp normal cellular processes like endocytosis, membrane fusion, or nuclear transport for their own purposes. In the case of

enveloped viruses, subsequent to attachment, the internal structures of the particle are released into the target cell by means of an intricate fusion process between viral and cellular membranes. This fusion event is mediated by specialized viral proteins and takes place either directly at the plasma membrane or following internalization of the particle into endosomes. Theoretically, in the most simplistic model, interactions between a single viral envelope protein and a single cellular component present on the surface of the target cell may suffice to accomplish all entry processes. The situation, however, is often more complex because in many cases, viral attachment and fusion proteins are separate polypeptides that act coordinately and in a regulated manner to ensure proper timing in the initiation of membrane fusion. The *Human immunodeficiency virus* (HIV), for instance, requires two receptors, namely CD4 as primary receptor and members of the chemokine receptor family as coreceptors to enter its host cell (Clapham and McKnight, 2002). In addition, a high-affinity attachment receptor for HIV has been described (Geijtenbeek *et al.*, 2000). Although not essential for infection, this molecule increases the efficiency of infection of receptor-positive cells presumably by trapping virus particles on the plasma membrane (Lee *et al.*, 2001).

Owing to technical limitations, progress in understanding the early steps of the HCV life cycle has been rather slow. Therefore, much effort has been invested to develop appropriate surrogate systems that allow the search for candidate receptors and the analysis of HCV binding and entry into target cells. Besides HCV-containing plasma samples, virus-like particles produced by expression of HCV structural proteins in insect cells (Baumert *et al.*, 1998), liposomes containing E1/E2 heterodimers (Lambot *et al.*, 2002), and pseudo-types based on VSV or retroviruses have been developed (reviewed in Flint *et al.*, 2001). A major hurdle has been the propensity of the E proteins to aggregate and to be retained within the ER. Therefore, either truncated E1 and E2 proteins that lack the TM domain or chimeric molecules containing heterologous membrane anchors that allow a more efficient cell-surface expression were employed. For instance, Rosa *et al.* (1996) demonstrated high affinity binding of truncated E2 protein to human cells. Moreover, this binding could be neutralized by preincubation of E2 with sera obtained from chimpanzees that had been immunized with recombinant HCV glycoproteins. Interestingly, the titer of neutralization of these sera correlated with the protection of the respective chimpanzee in challenge experiments (Rosa *et al.*, 1996). This correlation supports the relevance of the *in vitro* binding assay used and suggests that the truncated E2 protein used in this study adopts a

conformation similar to the one of E2 naturally present on HCV particles. This is a critical prerequisite for studies aimed at dissecting virus receptor interactions.

By screening of a human cDNA expression library with a recombinant truncated E2-protein, CD81 was identified as a potential receptor candidate for HCV (Pileri *et al.*, 1998). CD81 belongs to the tetraspanin superfamily, is expressed in many tissues, and exhibits an apparent molecular weight of 25 kDa (Levy *et al.*, 1998). The protein contains four TM domains and two extracellular loops. The larger of these loops is sufficient for E2 binding that has been demonstrated to be species-specific since the homologous mouse protein does not bind to HCV E2 (Pileri *et al.*, 1998). Important to note is that soluble fusion proteins of the large extracellular loop (LEL) of CD81 were shown to bind HCV contained in infectious plasma (Pileri *et al.*, 1998). Binding could be blocked not only by soluble human LEL but also by antisera from successfully immunized chimpanzees vaccinated with E1 and E2. On the other hand, antisera from animals that were not protected from the challenge did not block the CD81/E2 binding, suggesting that neutralizing antibodies were responsible for the inhibition (Pileri *et al.*, 1998). These observations have been confirmed and extended by several other groups (Drummer *et al.*, 2002; Flint *et al.*, 1999a, 1999b, 2000; Higginbottom *et al.*, 2000; Meola *et al.*, 2000; Patel *et al.*, 2000; Petracca *et al.*, 2000). Among other findings, these studies identified the key residues involved in the interaction and demonstrated a requirement for the native conformation of E2 as judged by the reactivity with a panel of conformation-dependent antibodies (Flint *et al.*, 2000). Moreover, it was noted that the binding of E2 to CD81 does not explain the species restriction of HCV because CD81 derived from tamarins was shown to bind E2 with higher affinity than the human homologue even though these animals are not clearly susceptible to HCV infection (Meola *et al.*, 2000). Although it cannot be excluded that HCV replication is blocked at a step subsequent to virus entry, the almost ubiquitous expression of CD81 in human tissues contrasts the rather restricted tropism of the virus *in vivo*. This discrepancy suggests that additional coreceptor(s) may be required for productive infection.

Further receptor candidates have been identified. Scarselli *et al.* (2002) observed that HepG2 cells were able to efficiently bind a recombinant E2 protein in the absence of CD81. The cellular molecule responsible for E2 binding was identified as the human scavenger receptor class B type I (SR-BI). Interestingly, this protein is highly expressed in hepatocytes, which may account for the liver tropism of

HCV. Two groups independently reported that HCV E2 also binds to DC-SIGN and L-SIGN (Gardner *et al.*, 2003; Pohlmann *et al.*, 2003). DC-SIGN is a calcium-dependent lectin expressed as a homotetrameric type II membrane protein on some dendritic cell subsets and tissue macrophages (Soilleux *et al.*, 2002). This lectin is known to function as an attachment receptor for HIV and increases the efficiency of infection by trapping the virus on the cell surface for subsequent interaction with the receptor either on the same receptor cell or an adjacent receptor positive cell (Curtis *et al.*, 1992; Geijtenbeek *et al.*, 2000; Lee *et al.*, 2001). L-SIGN is a closely related lectin that is expressed on liver sinusoidal endothelial cells and that can also function as an HIV attachment receptor (Bashirova *et al.*, 2001; Pohlmann *et al.*, 2001). Accordingly, it was postulated that an interaction of HCV with these lectins may facilitate the infection process in a similar fashion.

As already mentioned, diverse assay systems have been employed to analyze virus receptor interactions. Based on the knowledge that serum-derived virus particles associate with lipoproteins (Prince *et al.*, 1996; Thomssen *et al.*, 1992, 1993), it has been postulated that HCV may enter target cells via the LDLr (Agnello *et al.*, 1999; Monazahian *et al.*, 1999; Wunschmann *et al.*, 2000). Using sera from infected individuals, Agnello *et al.* (1999) reported that endocytosis of HCV (quantified by *in situ* hybridization) correlated with LDLr activity on target cells (Agnello *et al.*, 1999). Moreover, internalization could be inhibited with antibodies directed against apolipoprotein A and E. Other groups obtained similar results by employing serum-derived virus particles for studies on virus entry. For instance, sucrose gradient-purified low and intermediate density particles (1.03 to 1.07 g/ml or 1.12 to 1.18 g/ml, respectively) bind to cells in an LDLr-dependent manner (Wunschmann *et al.*, 2000). Binding correlated with the extent of LDLr expression and was inhibited by LDL but not by soluble human CD81. On the other hand, binding of recombinant, truncated E2 was independent of LDLr expression and inhibited by human CD81 but not murine CD81 or LDL. Finally, the addition of low-density HCV particles to cells led to coentry of an indicator molecule, providing indirect evidence for virus entry (Wunschmann *et al.*, 2000). In summary, HCV particles associated with lipoproteins appear to enter cells via LDLr, but it is unclear whether this mode of entry leads to a productive infection.

Virus-like particles (VLPs) produced in heterologous expression systems have also been used to study the early steps of HCV infection. Upon baculovirus-directed expression of the HCV structural proteins in insect cells, Baumert *et al.* (1998) were the first to demonstrate

HCV-like enveloped particles. These VLPs had a diameter of approximately 40 to 60 nm and accumulated in large intracellular cisternae from which they were isolated and purified. They carry the E2 protein on their surface and exhibit biophysical properties comparable to virions isolated from HCV-infected humans (Baumert *et al.*, 1998). Insect-cell derived VLPs were evaluated as potential HCV vaccines (Lechmann *et al.*, 2001; Murata *et al.*, 2003) and used for cell binding studies (Wellnitz *et al.*, 2002). Dose-dependent and saturable binding to various human, but not mouse, cell lines could be demonstrated, and this interaction was blocked by several monoclonal antibodies directed against E2. Binding, however, appeared to be CD81-independent and did not correlate with LDLr expression on target cells (Wellnitz *et al.*, 2002). It is unknown whether the putative receptors already described play a role or whether alternative cellular molecule(s) mediate the specific interaction between human cells and VLPs. A different glycosylation pattern due to the VLP production in insect cells may account for the observed differences in binding requirements. Furthermore, it is not clear how faithfully these recombinant molecules mimic the authentic conformation of glycoproteins present on the natural HCV virion. Finally, without the opportunity to assess replication, it is difficult to determine whether the binding observed with VLPs is the one that leads to productive uptake and infection.

It is well known that certain viruses, in particular members of the families *Retroviridae* [e.g., HIV or *Murine leukemia virus* (MLV)] and *Rhabdoviridae* (e.g., VSV), can incorporate foreign viral glycoproteins into their lipid envelope during assembly (Briggs *et al.*, 2003). The resulting chimeric virus particles, the so-called pseudo-types or pseudo-particles, display foreign viral glycoproteins on their surface that mediate entry into new target cells. In the case of HCV, initially VSV-derived pseudo-types have been generated (Buonocore *et al.*, 2002; Lagging *et al.*, 1998; Matsuura *et al.*, 2001). To overcome the intracellular retention of HCV E1 and E2 and to support pseudo-typing of VSV, which buds at the plasma membrane, chimeric HCV proteins have been generated containing the E protein ectodomains fused to the TM and cytoplasmic domain of the VSV-G protein. Although this modification resulted in surface expression and incorporation of the chimeric proteins into VSV-based pseudo-types, conflicting data regarding their infectivity were obtained (Buonocore *et al.*, 2002; Lagging *et al.*, 1998; Matsuura *et al.*, 2001).

In addition, pseudo-types based on retroviral particles (MLV or HIV) that carry unmodified HCV E1 and E2 proteins have been generated (Bartosch *et al.*, 2003a; Hsu *et al.*, 2003). After transient transfection of

293T cells, both E1 and E2 were expressed to high levels in the cytoplasm. Surprisingly, a certain fraction was incorporated into the plasma membrane, suggesting that the generally observed ER retention of HCV glycoproteins can at least, to some extent, be overcome in this system. By using this approach, infectious E1- and E2-bearing HCV pseudo-types (HCVpp) could be generated that were able to infect various hepatoma cell lines as well as primary hepatocytes. Infection was determined by measuring the amount of a marker protein (e.g., green fluorescent protein) that was encoded in the retroviral vector (Bartosch *et al.*, 2003a). Titers of about 10^5 transducing units per milliliter were measured when using Huh-7 as target cells, indicating a high permissiveness of this particular cell line and highlighting the efficiency of pseudo-type formation in 293T cells. Important to note is that the infectivity of HCVpp required both E1 and E2 and could be neutralized by different monoclonal antibodies as well as sera from HCV-infected patients (Bartosch *et al.*, 2003a; Hsu *et al.*, 2003). Biochemical analyses revealed the presence of noncovalently associated E1–E2 hetero-oligomers with complex- or hybrid-type glycans on the surface of HCVpp (Op de Beeck *et al.*, 2004). In addition to the detection of native complexes, some viral glycoprotein aggregates were detected so that a potential role of these structures for the infectivity of HCVpp cannot be excluded. Although a preference for liver cell lines was found, HCVpp also infected other human and even animal cell lines, albeit with much lower efficiency. Pseudo-type entry was shown to occur in a pH-dependent fashion, and none of the currently proposed virus receptors alone, or in combination, was sufficient to confer permissiveness (Bartosch *et al.*, 2003a; Hsu *et al.*, 2003). The ability of anti-CD81 antibodies and soluble forms of human CD81 to specifically block HCVpp infection of target cells, however, suggests that CD81 is a component of the HCV receptor complex (Bartosch *et al.*, 2003a; Cormier *et al.*, 2004; Hsu *et al.*, 2003; Zhang *et al.*, 2004). Likewise, antibodies against SR-B1 prevented pseudo-type infectivity (Bartosch *et al.*, 2003b). With regard to the involvement of LDLr for HCVpp entry, Bartosch *et al.* (2003a) noted a weak neutralization activity of antiapolipoprotein E antibodies, but they did not note significant neutralization by LDL, VLDL, and antiapolipoprotein B antibodies. Whereas these data do not rule out an involvement of LDLr for the entry of lipoprotein-associated HCV particles, they indicate that LDLr is not a major receptor for HCVpp. In conclusion, these data suggest that CD81 and SR-B1 are involved in the infection process, but additional, hepatocyte-specific cofactors seem to be necessary for the infection of liver cells.

B. RNA Translation

Once HCV has entered the cell, which may occur by receptor-mediated endocytosis as depicted in Fig. 2 (Hsu *et al.*, 2003), the viral RNA is liberated into the cytoplasm and serves as an mRNA for synthesis of the viral proteins. As alluded to in the previous section, the HCV polyprotein is expressed under control of the IRES located in the 5'-NTR and mediating cap-independent RNA translation. Since HCV does not encode a methyl transferase and replicates in the cytoplasm where this enzyme is missing, the use of an IRES ensures translation of the noncapped viral RNA. Based on phylogenetic analyses and chemical and enzymatic probing, a structural model of the HCV IRES has been established (Fig. 4A) (Honda *et al.*, 1999; Wang *et al.*, 1994, 1995). The key element of the IRES is domain III that permits the direct binding of the 40S ribosomal subunit in the absence of additional translation factors in a way that the initiator AUG start codon is placed in the P-site of the ribosome (Pestova *et al.*, 1998). This property, which largely resembles a factor-independent, prokaryotic binding mode of mRNAs, is mainly achieved by the basal part of domain III, comprising subdomains IIIa, IIIc, IIId, and IIIe (Fig. 4A). Subdomain IIIb is required for binding of the translation initiation factor eIF-3 (Kieft *et al.*, 2001), which is essential for the association of the 60S subunit (Pestova *et al.*, 1998). The role of domain II has been established by cryo-electron microscopy studies and nuclear magnetic resonance (NMR) spectroscopy (Kim *et al.*, 2002a; Lukavsky *et al.*, 2003; Spahn *et al.*, 2001). Even though an IRES with or without domain II binds the 40S subunit with comparable efficiency (Otto *et al.*, 2002), structural changes in the 40S subunit have been observed only in the presence of domain II. By forming intensive interactions with the 40S subunit, domain II appears to induce or stabilize drastic conformational changes within the ribosomal subunit (Spahn *et al.*, 2001). Moreover, it was found that domain II forms an independent structure in the absence of the IRES context and folds in a way that markedly resembles the 40S subunit-bound form (Lukavsky *et al.*, 2003; Spahn *et al.*, 2001). These results suggest that domain II is not involved in long-range RNA:RNA interactions (Kim *et al.*, 2002a).

RNA mapping studies have defined the 5'-end of the HCV IRES between nucleotides 38 and 46 (Honda *et al.*, 1996b; Rijnbrand *et al.*, 1995; Yoo *et al.*, 1992). Therefore, domain I that can form a G:C-rich stem-loop (Fig. 4A) is not required for IRES function. When tested in the context of heterologous reporter constructs, deletion of this domain

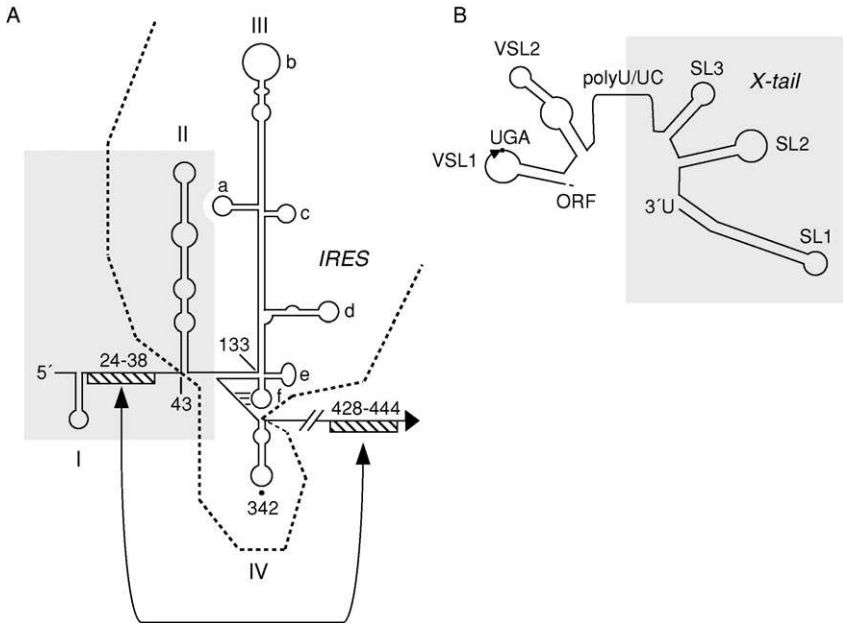


FIG 4. Structures of 5'- and 3'-NTRs. (A) Schematic presentation of the HCV 5'-NTR with domains I to IV (Honda *et al.*, 1999). The minimal regions required for RNA replication and IRES activity are indicated by a gray rectangle and a dashed line, respectively. The pseudo-knot structure that is generated by base pairing between the loop region of domain III_f and the intervening sequence connecting domains III_f and IV is highlighted with horizontal lines. Regions involved in a long-range RNA:RNA interaction are indicated with striped lines and a double-headed arrow. (B) Structure of the tripartite 3'-NTR composed of the variable region with stem-loops VSL1 and VSL2, the poly(U/UC)-tract, and the highly conserved X-tail sequence. Stem-loop structures are given according to the model of Blight and Rice (1997). Note that the stop codon of the polyprotein coding region resides in the loop of VSL1. The minimum region required for RNA replication *in vivo* and in cell culture is indicated by a gray rectangle.

stimulated translation (Yoo *et al.*, 1992), whereas its removal from a HCV replicon reduced protein expression by about threefold to fivefold and completely blocked RNA replication (Friebe *et al.*, 2001; Luo *et al.*, 2003). Thus, domain I is required for RNA replication and involved in translation (Friebe *et al.*, 2001; Kim *et al.*, 2002b; Luo *et al.*, 2003), suggesting that in a more authentic context, this domain plays an important role in regulating both processes. Domain IV consists of a small stem-loop containing the AUG initiator codon and forms a pseudo-knot via base pairing with a loop in domain III_f (Fig. 4A). It was found that mutagenesis or insertions of AUG codons in domain IV

upstream of the start codon of the open reading frame (ORF) have little or no effect on RNA translation, which suggests that the ribosome binds in close proximity of the initiator AUG with little or no scanning (Reynolds *et al.*, 1996; Rijnbrand *et al.*, 1996). Most studies indicate that sequences located immediately downstream of the start codon are required for RNA translation (Honda *et al.*, 1996a, 1996b; Lu and Wimmer, 1996; Reynolds *et al.*, 1995). Contradictory reports, however, exist concerning the role of the core coding sequence for HCV IRES activity. Although most evidence suggests that sequences of the core coding region and not the core protein itself are required for efficient RNA translation, it is unclear whether core sequences directly contribute to IRES function. Alternatively, they may be required to prevent unfavorable base pairings of the IRES with downstream sequences that would disturb the RNA structure or block binding sites for protein factors. In agreement with the latter assumption, it was found that expression of the reporter gene secretory alkaline phosphatase but not that of chloramphenicol acetyltransferase depends on downstream core coding sequences (Rijnbrand *et al.*, 2001). A mutational analysis of the core sequence demonstrated no requirement for a particular nucleotide or amino acid sequence. These results clearly favor the idea that IRES activity does not depend on core coding sequences but rather on the absence of stable stem-loop structures in the vicinity of the initiator AUG (Rijnbrand *et al.*, 2001). This hypothesis does not exclude the idea that the core protein may have a regulatory role in virus replication, such as modulating the switch from RNA translation to replication and/or packaging. In fact, Zhang *et al.* (2002) found that core protein causes an inhibition of translation from the HCV IRES, arguing for a regulatory function of this protein. Furthermore, convincing evidence has also been presented that sequences between nucleotides 24 to 38 in the IRES and 428 to 442 in the core coding sequence mediate a long-range RNA:RNA interaction that significantly suppresses translation efficiency (Kim *et al.*, 2003) (Fig. 4A). Mutational ablation of complementarity between these two sequences enhances RNA translation, which is repressed again by compensatory mutations that restore complementarity. This observation argues for a direct base pairing between these two sequences that may regulate RNA translation.

A number of proteins binding to the HCV IRES have been reported. Apart from multiple ribosomal proteins (Otto *et al.*, 2002), several noncanonical translation factors have been identified. These include the polypyrimidine tract binding protein (PTB) (Ali and Siddiqui, 1995), the La autoantigen (Ali and Siddiqui, 1997), the heterogeneous

nuclear ribonucleoprotein L (Hahm *et al.*, 1998), the poly(rC)-binding protein (PCBP-2) (Fukushi *et al.*, 2001), and several other proteins that so far have not yet been characterized (Yen *et al.*, 1995). The role these proteins may play in RNA translation has not been firmly established. For instance, Kaminski *et al.* (1995) found no effect on RNA translation in cell lysates after immunodepletion of PTB, suggesting that no amount or only very low amounts of PTB are required for translation. In case of the La protein, a stimulation of translation was observed when the purified protein was added to rabbit reticulocyte lysates (Ali and Siddiqui, 1997), and sequestration of La inhibited translation both *in vitro* and in cell culture (Ali *et al.*, 2000). Interestingly, La binds to the 5'-NTR in the context of the initiator AUG codon. Since the La protein has helicase activity, one of its function might be the melting of the stem structure of domain IV. In fact, it has been shown that mutational destabilization of this stem-loop structure increases translation efficiency (Honda *et al.*, 1996a). Another protein, PCBP-2 was shown to bind to a region that spans domains I and II of the 5'-NTR (Fukushi *et al.*, 2001). By comparing the translation efficiency of HCV RNAs carrying the complete 5'-NTR in rabbit reticulocyte lysates in the presence or absence of PCBP-2, it was found that this protein does not affect translation efficiency. It was therefore speculated that PCBP-2 might be required for the formation of a replication–initiation complex analogous to what has been described for the multiplication of polioviruses (Andino *et al.*, 1993; Parsley *et al.*, 1997).

Apart from canonical and noncanonical translation factors of the host cell HCV RNA sequences outside of the 5'-NTR may contribute to IRES activity, but this issue is controversially discussed. While Ito *et al.* (1998) reported a stimulation of RNA translation by sequences at the 3'-end of the HCV genome, others observed down-regulation (Murakami *et al.*, 2001) or no effect at all (Friebe and Bartenschlager, 2002; Imbert *et al.*, 2003). The reason for these discrepancies is not clear, but these may be due to differences in experimental systems. Further studies performed in a more natural context, such as using full-length HCV genomes, may help to clarify this issue.

In addition to directing translation of the polyprotein, the 5'-NTR also mediates expression of the F protein via a novel mode of ribosomal frameshifting (Boulant *et al.*, 2003; Choi *et al.*, 2003; Varaklioti *et al.*, 2002; Walewski *et al.*, 2001; Xu *et al.*, 2001). The ORF of the F protein resides in the $-2/+1$ reading frame relative to the ORF of the polyprotein and is generated probably by two consecutive -1 frameshifts. In agreement with this model, a 1.5-kDa protein has been identified

that is generated by translation of the -1 ORF and that might represent the product that arises from a single -1 frameshift (Choi *et al.*, 2003). Production of the F protein requires both an A-rich “slippery sequence” around nucleotide 380 and a putative double stem-loop structure immediately downstream of the frameshift sequence. Based on experiments with reporter gene constructs, the frameshift efficiency is in the range of 1 to 2%, a value similar to what has been described for ribosomal frameshifting with retroviruses. As alluded to in the previous paragraphs, however, the F protein apparently is not required for HCV RNA replication, at least not in cell culture, and it remains to be determined whether it plays a role *in vivo*.

C. Proteolytic Processing of Structural Proteins

During or after production of the HCV polyprotein, a series of proteolytic cleavage events take place that result in the formation of 10 different cleavage products and some distinct processing intermediates (Fig. 1). Several lines of evidence demonstrate that cleavage of the region spanning the N terminus of the core protein up to the N terminus of NS2 is mediated primarily by host-cell signal peptidase cleaving in the lumen of the ER after stretches of hydrophobic amino acids. First, cleavage at the core/E1, E1/E2, E2/p7, and p7/NS2 sites is membrane dependent (Hijikata *et al.*, 1991; Hussy *et al.*, 1996; Lin *et al.*, 1994a; Mizushima *et al.*, 1994a,b; Santolini *et al.*, 1994, 1995); second, the signal recognition particle is required for generation of the N terminus of core, E1, E2, NS2, and probably also p7 (Santolini *et al.*, 1994, 1995); third, hydrophobic signal peptides precede the N termini of these cleavage products (Hijikata *et al.*, 1991; Lin *et al.*, 1994a; Mizushima *et al.*, 1994a,b; Selby *et al.*, 1994); and fourth, arginine substitutions for alanine residues at the P1 positions of the E2/p7 and p7/NS2 junctions abolish cleavage at these sites (Mizushima *et al.*, 1994a,b). Several groups have observed a second cleavage at the C terminus of the core protein within the E1 signal sequence, but the exact position has not yet been defined (Hussy *et al.*, 1996; Liu *et al.*, 1997; Moradpour *et al.*, 1996b; Santolini *et al.*, 1994; Yasui *et al.*, 1998). Based on the apparent molecular weight of this 19-kDa product, however, the cleavage site most likely resides around residue 179 (Santolini *et al.*, 1994). The enzyme responsible for this cleavage has been identified as the host-cell signal peptide peptidase (SPP) (McLauchlan *et al.*, 2002). SPP is a presenillin-type aspartic proteinase that resides in the ER membrane. After cleavage in the intramembrane compartment, processed signal peptides are released into the

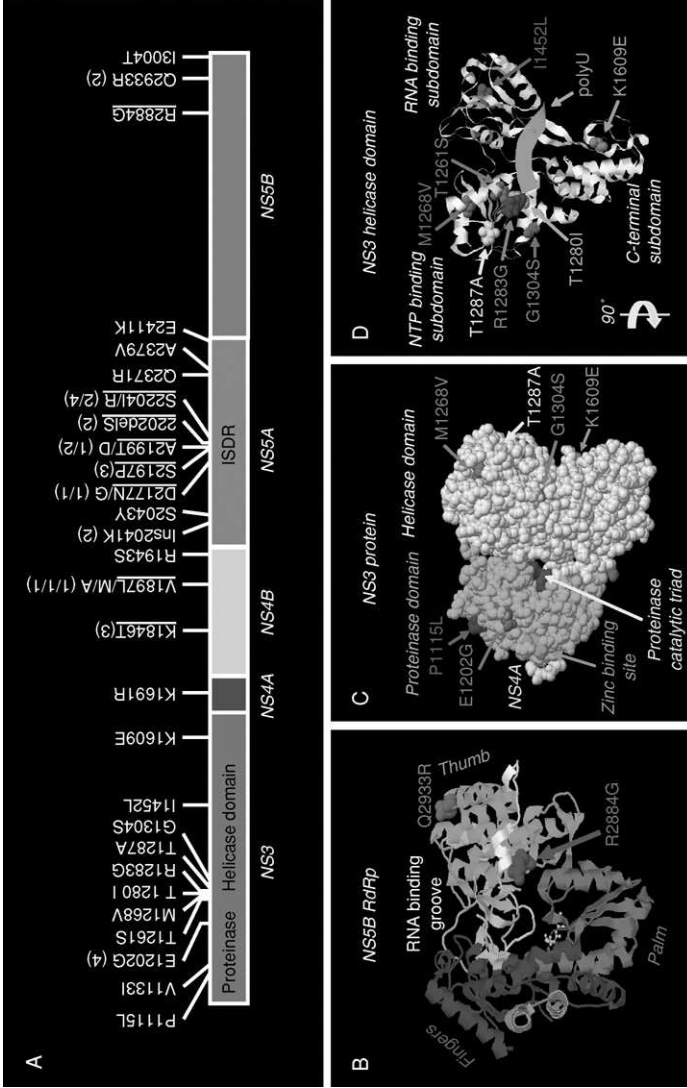
cytosol where they can promote post-targeting functions (Lemberg *et al.*, 2001). Interestingly, mutational inactivation of the E1 signal peptide in the C terminus of the core protein affected its intracellular distribution (McLauchlan *et al.*, 2002). Although wild-type core protein localized after cleavage to the surface of lipid droplets, this was no longer the case with the mutants. A model has been proposed according to which core protein is targeted to lipid droplets via an internal hydrophobic sequence designated domain 2 (Section V,G) that is thought to integrate into the cytosolic leaflet of the ER membrane. Intramembrane cleavage of the E1 signal sequence would mobilize the core protein and allow its transport to regions of the ER where triglycerides accumulate and pinch off as lipid droplets. In contrast, inhibition of the signal sequence cleavage would immobilize the core protein within the ER membrane and thereby prevent its transport to the sites of lipid droplet formation (McLauchlan *et al.*, 2002).

D. Proteolytic Processing of Nonstructural Proteins

Cleavage of the NS2 to NS5B region is achieved by two different viral enzymes: the NS2-3 proteinase that catalyzes cleavage between NS2 and NS3 and the NS3/4A proteinase complex that is responsible for processing of the remainder (Fig. 1).

1. The NS2-3 Proteinase

NS2 is liberated from NS3 by a rapid intramolecular cleavage for which the 117 C-terminal amino acids of NS2 and the first 180 residues of NS3 are required (Grakoui *et al.*, 1993a; Hijikata *et al.*, 1993a; Lin *et al.*, 1994b; Reed *et al.*, 1995; Santolini *et al.*, 1995; Tanji *et al.*, 1994a; Wilkinson, 1997). Alanine substitutions of His-952 and Cys-993 completely block processing between NS2 and NS3, suggesting that these residues are crucial for enzymatic activity. However, these mutations do not affect cleavage at NS3-dependent sites, demonstrating that in spite of a structural overlap of the NS2-3 and the NS3/4A proteinase, their activities are independent from each other (Grakoui *et al.*, 1993a; Hijikata *et al.*, 1993a). Based on the observations that zinc ions stimulated cleavage at this site by about threefold when using *in vitro* translation reactions and that the chelating agent EDTA exerted an inhibitory effect, it was postulated that NS2-3 might be a zinc-dependent metalloproteinase. As described in detail in the following paragraphs, zinc is a component of the NS3 proteinase domain (Fig. 5C), raising the question whether the observed stimulation by zinc ions is due to activation of the NS2-3 proteinase or to



structural integrity of the NS3 domain for which zinc is required. In agreement with the latter assumption, the active centers of metalloproteinases contain either a HEXXH or a HXXEH motif (where X is variable), which is not found in the NS2-3 proteinase (Jiang and Bond, 1992). Therefore, it has been proposed that this enzyme is a cysteine proteinase with His-952 and Cys-993 forming a catalytic dyad or, together with Glu-972, a catalytic triad (Gorbalenya and Snijder, 1998). Alternatively, the NS2-3 proteinase might be a metalloproteinase with zinc playing an essential role in catalysis (Ryan *et al.*, 1998; Wu *et al.*, 1998).



FIG 5. Location of cell culture-adaptive mutations in the HCV coding regions of subgenomic replicons and the positions of these mutations in the 3-D structures of NS5B RdRp, the full-length NS3, and the NS3 helicase. (A) Schematic presentation of the NS3 to NS5B coding region that is sufficient for autonomous replication of subgenomic replicons. Mutations that were conserved in a total of 26 independent replicon cell clones are given above (Lohmann *et al.*, 2003). Numbers in parenthesis indicate the frequency with which a given mutation was found in independent cell clones. The underlining is used to highlight those mutations that were found as single mutations in replicons, whereas all the other mutations were only found in certain combinations. (B) Location of adaptive mutations within the NS5B RdRp ectodomain. Ribbon diagram showing the front view of the NS5B 3-D structure. Fingers, thumb, and palm subdomains are colored in blue, green, and red, respectively. The other structural elements are colored as follows: cyan, two loops interconnecting the finger and thumb subdomains; gray, two antiparallel α -helices connecting the palm and finger subdomains; orange, the β -hairpin element; white, the C-terminal segment of the NS5B ectodomain. The catalytic site (GDD) motif is shown as a yellow ball and stick model. The putative RNA-binding groove is indicated. Cell culture-adaptive mutations depicted in panel A are highlighted as a space-filling model in different colors. Both residues are located at the surface of the thumb subdomain. Note that the protein used for crystallization lacks the C-terminal TM domain, and, therefore, I3004 is not present in this structure. The coordinates of this structure were retrieved from the PDB protein database under accession number 1C2P (Lesburg *et al.*, 1999). (C) Space-filling model of the 3-D structure of full-length NS3 complexed with an NS4A peptide showing the proteinase domain in cyan, the helicase domain in white, and NS4A in yellow. The locations of the zinc ion binding site (green), the active site of the proteinase (purple), and the location of cell culture-adaptive mutations are highlighted in different colors. Note that some of these mutations are buried in the molecule and, therefore, are not visible in the space-filling model (e.g., V1133I). (D) Ribbon diagram of the NS3 helicase showing the front view corresponding to a 90° clockwise rotation of the structure shown in panel B. The three different subdomains (NTP binding, RNA binding, and C-terminal subdomains) are labeled. Note that most mutations cluster in the NTP binding subdomain. Poly(U) complexed with this structure is shown as a green ribbon. The coordinates of these structures were retrieved from the PDB protein database under accession numbers 1CUI (Yao *et al.*, 1999) and 1A1V (Kim *et al.*, 1998) for the models shown in B and C, respectively. (See Color Insert.)

A clarification of this issue has been difficult because no robust trans-cleavage assay has been available. This is first due to NS2 being a highly hydrophobic protein that is very difficult to work with and, second, due to the autocatalytic nature of the cleavage reaction that occurs intramolecularly and very fast. To overcome these problems, *in vitro* translation reactions with NS2-encoding RNAs were performed in the absence of microsomal membranes. Under these conditions, no cleavage at the NS2/3 junction was observed, but the cleavage could be restored upon addition of detergent micelles mimicking membrane-mediated proteinase activation (Pieroni *et al.*, 1997). By using this system, it was found that cadmium could functionally substitute for zinc, suggesting that zinc plays a structural rather than a functional role for catalysis.

In two very elegant studies, minimal NS2-3 domains were expressed in *Escherichia coli* and purified from inclusion bodies to homogeneity (Pallaoro *et al.*, 2001; Thibeault *et al.*, 2001). After refolding and enzyme activation, the majority of NS2-3 underwent self-cleavage. This reaction occurred intramolecularly and appeared to require multimerization of the uncleaved protein. The fact that processing was independent from the nature of the added metal ion (zinc or cadmium) suggests that NS2-3 most likely is a cysteine proteinase with a catalytic dyad that requires zinc as a structural component (Pallaoro *et al.*, 2001). Although NS4A sequences inhibit self-cleavage of the NS2-3 enzyme (Darke *et al.*, 1999), the same sequences activate the proteinase activity of the NS3/4A complex (see the following chapter for more details). Moreover, inhibition was seen with peptides containing the NS2-3 cleavage site or an N-terminal peptidic cleavage product, indicating end-product inhibition of the proteinase (Thibeault *et al.*, 2001). Although under these experimental conditions, the enzyme can cleave in the absence of additional factors, this might not necessarily be the case in an infected cell. In fact, Waxman *et al.* (2001) presented evidence that the host-cell chaperone Hsp90 is required to activate the NS2-3 proteinase. This conclusion is based on the inhibition of cleavage *in vitro* and in cell culture by geldanamycin, herbimycin, and radicicol, three compounds that specifically block Hsp90 by binding to its ATP-binding site. Moreover, a physical interaction between the proteinase and the chaperone was found by coimmunoprecipitation. Based on these results, it can be speculated that unguided folding of NS2-3 is unfavorable for mediating cleavage, and proper folding depends on the assistance of Hsp90. It is interesting to note that in case of the closely related pestivirus BVDV, cleavage between NS2 and NS3 requires the interaction with a host-cell chaperone called Jiv, suggesting

that the interaction of distinct Flavivirus proteinases with cellular chaperones is an evolutionarily conserved trait (Rinck *et al.*, 2001).

2. The NS3/4A Proteinase Complex

Cleavage of the polyprotein by the NS3/4A proteinase complex has been studied in great detail and the three-dimensional (3-D) X-ray crystal structure as well as the NMR structure of this proteinase complex have been solved (Fig. 5C). It is beyond the scope of this review to describe all the details that have been published in this field and summarized in comprehensive reviews by Bartenschlager (1999) and de Francesco *et al.* (1998). This section therefore focuses only on the principal aspects.

NS3 is a chymotrypsin-like proteinase that requires the NS4A protein as a cofactor for full enzymatic activity. Sequence comparisons and mutation analyses demonstrated that His-1083, Asp-1107, and Ser-1165 in the N-terminal NS3 domain make up the catalytic triad of this serine proteinase (Bazan and Fletterick, 1989, 1990; Gorbalenya *et al.*, 1989a; Miller and Purcell, 1990). The enzyme is required for processing at the NS3/4A, NS4A/4B, NS4B/5A, and NS5A/5B junctions (Bartenschlager *et al.*, 1993; Eckart *et al.*, 1993; Grakoui *et al.*, 1993b; Hijikata *et al.*, 1993a; Manabe *et al.*, 1994; Tomei *et al.*, 1993) (Fig. 1). In addition, four further cleavages mediated by this proteinase have been identified with two being mapped in the NS3 helicase domain (Yang *et al.*, 2000), one close to the N terminus of NS4B (Kolykhalov *et al.*, 1994) and one in the middle of NS5A (Markland *et al.*, 1997). Thus far, their importance for RNA replication has not been studied, but it is interesting to mention that a similar cleavage in the NS3 helicase domain has been described for other flaviviruses like the *Yellow fever virus* (Arias *et al.*, 1993). Mutational inactivation of this cleavage site, however, did not affect replication and virus production, indicating that this processing event is dispensable for a productive Flavivirus replication cycle in cell culture.

As indicated in Fig. 1, the HCV polyprotein is cleaved in a preferential order (Bartenschlager *et al.*, 1994; Lin *et al.*, 1994b; Tanji *et al.*, 1994a). The first cleavage occurs cotranslationally and liberates NS3 from the remainder of the polyprotein (Bartenschlager *et al.*, 1994; Lin *et al.*, 1994b; Tanji *et al.*, 1994a; Tomei *et al.*, 1993). Subsequent cleavages can be mediated *in trans* with rapid processing at the NS5A/B junction, resulting in an NS4A-5A precursor that is cleaved with different kinetics (Bartenschlager *et al.*, 1994; Failla *et al.*, 1994; Lin *et al.*, 1994b; Tanji *et al.*, 1994a,b; Tomei *et al.*, 1993) The only protein for which a precursor:product relation could be established was a

rather stable NS4B-5A intermediate (Bartenschlager *et al.*, 1994; Failla *et al.*, 1994; Lin *et al.*, 1994b). This cleavage order was first observed in various heterologous expression systems but has been shown to occur in the same way in cells carrying stably replicating HCV replicons (Pietschmann *et al.*, 2001).

Although the enzymatic activity resides in the NS3 domain, heterodimerization with the NS4A cofactor is absolutely required for efficient polyprotein processing (Bartenschlager *et al.*, 1994, 1995b; Failla *et al.*, 1994; Lin *et al.*, 1994b; Steinkühler *et al.*, 1996a,b; Tanji *et al.*, 1995a) (Fig. 5C). Complex formation occurs via a tight interaction of the 22 N-terminal residues of NS3 with a 12-residue sequence in the center of NS4A (Bartenschlager *et al.*, 1995b; Failla *et al.*, 1995; Lin *et al.*, 1995; Satoh *et al.*, 1995; Tanji *et al.*, 1995a) that can be either coexpressed in a transfected cell or supplied as a synthetic peptide (Butkiewicz *et al.*, 1996; Steinkühler *et al.*, 1996a; Tomei *et al.*, 1996). The two proteins form a 1:1 complex that can cleave a minimal substrate with a length of 10 amino acid residues that correspond to a P6-P4' decamer peptide (Steinkühler *et al.*, 1996b,c). Interestingly, when using such peptide substrates, the order of cleavage efficiency at the trans-sites mirrored the one that was observed with the authentic polyprotein, which shows that the primary sequence around the scissile bond determines processing efficiency.

The mechanism by which NS4A activates the NS3 proteinase domain has for a long time been an enigma. It was assumed that NS4A induces conformational changes required for full proteolytic activity and, to a lesser extent, increases binding affinity to the substrate. This suggestion was partly supported by the determination of the X-ray crystal structure of the NS3 domain alone and the NS3/4A proteinase complex (Kim *et al.*, 1996; Love *et al.*, 1996; Yan *et al.*, 1998b). In the absence of NS4A, the 28 N-terminal residues of NS3 are flexible and extend away from the protein, whereas in the complex, they are folded into a β -strand and an α -helix. An additional β -strand is formed by NS4A that tightly intercalates into the N terminus of NS3 and forms an integral component of the enzyme (Love *et al.*, 1996; Yan *et al.*, 1998b). Another conformational change that is induced by NS4A leads to a repositioning of the catalytic triad that, after NS4A binding, closely resembles the one found with other serine-type proteinases, which explains the observed increase in catalytic efficiency. It was also found that in addition to NS4A, the substrate itself plays an important role for enzyme activation by stabilizing the correct geometry of the catalytic triad (Barbato *et al.*, 1999). This property is unique among chymotrypsin-like proteinases.

By using homology modeling studies, a zinc binding site in the NS3 domain was predicted (de Francesco *et al.*, 1996). In fact, the X-ray crystal structure revealed a tetrahedrally coordinated zinc ion that is complexed with three cysteine residues and, via a water molecule, with a histidine residue (Fig. 5C). The long distance between the zinc ion and the catalytic serine residue, the kind of coordination, and the possibility to replace zinc by cadmium or cobalt without losing activity strongly suggest that the zinc ion is not involved in catalysis but rather plays a structural role (de Francesco *et al.*, 1996; Stempniak *et al.*, 1997). In agreement with this assumption, mutations that affect the coordinating cysteine or histidine residues render the protein insoluble, and expression of wild-type NS3 in *E. coli* cultured in the presence of zinc markedly increases the amount of soluble protein.

Determination of the N termini of the cleavage products and sequence comparisons between a large number of HCV isolates revealed the substrate specificity of the NS3/4A proteinase complex (Grakoui *et al.*, 1993c; Leinbach *et al.*, 1994; Pizzi *et al.*, 1994). Crucial determinants are an acidic amino acid residue at the P6 position, a P1-cysteine at the *trans*-cleavage sites, a P1-threonine at the NS3/4A *cis*-cleavage site, and an amino acid with a small side-chain at the P1'-position (Grakoui *et al.*, 1993b). Because at least decameric peptides are required for efficient cleavage in various *in vitro* assays, a consensus cleavage sequence would read D/E-X-X-X-X-C/T↓S/A-X-X-X. Studies of altered protein and peptide substrates revealed that the P1-cysteine residue is the most important determinant for efficient *trans*-cleavage (Bartenschlager *et al.*, 1995a; Kolykhalov *et al.*, 1994; Komoda *et al.*, 1994; Leinbach *et al.*, 1994; Tanji *et al.*, 1994a). In contrast, processing between NS3 and NS4A is governed primarily by polyprotein folding that stabilizes the enzyme:substrate complex sufficiently to accommodate even unfavorable P1 amino acid residues.

For many positive-stranded RNA viruses, including all flaviviruses, proteinase activity and helicase activity reside in the same polypeptide (Fig. 5), indicating that a coupling of these two activities has an advantage for virus replication. In an attempt to identify potential mutual interactions, several groups studied the biochemical properties of full-length NS3 in respect to its proteinase and helicase activity. In part, conflicting results have been obtained (Gallinari *et al.*, 1998; Kanai *et al.*, 1995; Morgenstern *et al.*, 1997), but in most studies, an enhancement of the helicase activity was found in the bifunctional NS3 molecule. Moreover, direct binding of single-stranded RNA not only to the helicase but also to the proteinase domain was described and shown to result in an inhibition of the proteolytic activity (Gallinari

et al., 1998; Yao *et al.*, 1999). Finally, the X-ray crystal structure of the full-length NS3 molecule revealed that after cleavage, the C terminus of the helicase remains in the proteinase active site, leading to an autoinhibition that is released upon substrate binding (Yao *et al.*, 1999). This study also demonstrated that already within the uncleaved polyprotein, the individual proteins can fold substantially, including the N terminus of NS4A that forms the membrane spanning α -helix, which targets NS3 to intracellular membranes. In this case, the proteinase domain would, after cleavage at the NS3/4A site and subsequent membrane association, serve as a “spacer” that properly positions the helicase within the membrane-bound replication complex (Yao *et al.*, 1999).

E. Cis-Acting RNA Sequences Required for Replication

By analogy to other positive-stranded RNA viruses, it has been assumed that the 5'- and 3'-NTRs play major roles for RNA replication. Furthermore, as already indicated, the 5'-NTR harbors an IRES element, and, therefore, this region was studied most intensively, leading to the structure model shown in Fig. 4A. The role of 5'-terminal sequences in RNA replication have been studied in the replicon system. A series of replicons were generated in which various regions of the HCV 5' NTR were fused to the IRES sequence of *Poliovirus* or that of the *Classical swine fever virus*. By using these replicons, researchers were able to uncouple HCV replication and translation. This approach allowed the identification of the minimal RNA region required for replication, which was mapped to approximately the first 125 nucleotides of the HCV genome corresponding to stem-loops I and II (Friebe *et al.*, 2001; Kim *et al.*, 2002b; Reusken *et al.*, 2003) (Fig. 4A). Moreover, it was shown that the structure and not the primary sequence of stem-loop I plays an important role for RNA replication (Luo *et al.*, 2003). Since stem-loop II is also required for IRES activity, this result demonstrates a functional overlap of signals involved in RNA translation and replication. Based on this observation, it is tempting to speculate that domain II might be involved in regulating a switch from RNA translation to replication. For instance, it has been shown that poliovirus RNA replication is inhibited while translation is in progress (Gamarnik and Andino, 1998). This switch might be controlled by PCBP, a cellular protein involved in controlling the translation of numerous cellular and viral RNAs. Because translating ribosomes moving along the viral RNA into the 5'- to 3'-direction directly interfere with the replicase that copies the RNA in the 3'- to 5'-direction, a

mechanism may exist that down-regulates translation to allow RNA synthesis. It has been proposed that PCBP binding to the 5'-terminal cloverleaf structure of the poliovirus RNA enhances translation, while binding of the viral polymerase precursor 3CD to the cloverleaf represses translation and promotes the synthesis of negative-stranded RNA (Gamarnik and Andino, 1998). Interestingly, PCBP-2 was shown to interact with the HCV 5'-NTR, in particular stem-loop I, suggesting that this protein might also be involved in regulating a switch from translation to replication (Fukushi *et al.*, 2001; Spangberg and Schwarz, 1999). Moreover, removal of stem-loop I in HCV replicons leads to a reduction of viral RNA translation in cell culture, suggesting that either this RNA element per se or protein(s) binding to it regulate translation (Friebe *et al.*, 2001; Luo *et al.*, 2003). Although stem-loops I and II are sufficient to promote HCV RNA amplification, replication levels of replicons carrying only these elements at the 5'-end are rather low. This defect can be compensated when stem-loop III and the pseudo-knot structure are added to this minimal promoter element (Friebe *et al.*, 2001; Kim *et al.*, 2002b). Thus, the complete 5'-NTR of HCV is required for efficient RNA replication. So far, it is not clear whether the sequences needed in addition to the minimal promoter are required for the formation of its correct structure or directly participate in RNA replication (e.g. as binding sites for viral or cellular factors). Moreover, it is conceivable that the 3'-end of negative-stranded RNA serves as a recognition site for the viral replication machinery to initiate synthesis of positive-stranded RNA. Consequently, structures other than the ones that are formed by the 5'-NTR of positive-stranded RNA may be required. The analysis of this possibility requires adequate secondary structure models that were described in 2002 studies (Kashiwagi *et al.*, 2002; Schuster *et al.*, 2002; Smith *et al.*, 2002). It was shown that the 3'-end of negative-stranded RNA is not simply a mirror image of the 5'-NTR of the positive strand. Stem-loops I and IV as well as parts of stem-loop III (IIIa and IIIb) appear to be conserved in both orientations, whereas stem-loop II and the surrounding interdomain regions are reorganized into two large stem-loops. These models will guide future studies to dissect the roles these structures may play for the synthesis of positive- and negative-stranded RNA.

Initially, it was thought that the HCV genome would terminate with a poly(A) or poly(U) sequence (Han *et al.*, 1991; Hayashi *et al.*, 1993; Kato *et al.*, 1990; Okamoto *et al.*, 1991, 1992b, 1994; Takamizawa *et al.*, 1991; Taneka *et al.*, 1992; Wang *et al.*, 1993b; Yamada *et al.*, 1994b). Studies have showed, however, that other flaviviruses, like certain

strains of TBEV, carry downstream of a homoadenosine tract an approximately 350-nucleotide-long highly conserved RNA sequence at the very 3'-end of the genome that is essential for replication (Mandl *et al.*, 1991; Wallner *et al.*, 1995). This observation and the fact that HCV could not be propagated in cell culture after transfection of cloned full-length genomes terminating with poly(A) or poly(U) led to the assumption that the 3'-end of the originally cloned HCV genomes may lack some sequences that could not be cloned with conventional techniques. Therefore, alternative strategies were used to identify novel 3'-terminal sequences. One approach was based on primer extension by using a primer that hybridized to the 5'-end of the negative-stranded RNA. This cDNA was subjected to a 3'-tailing reaction with the newly created tail being used as a binding site for a primer that, together with the cDNA primer, allowed the amplification by PCR (Tanaka *et al.*, 1995). In another approach, an oligonucleotide was ligated to the 3'-end of the HCV positive-stranded genome by using a T4 RNA ligase, which allowed subsequent amplification by PCR (Kolykhalov *et al.*, 1996; Tanaka *et al.*, 1996; Yamada *et al.*, 1996). These attempts led to the identification of a novel 98-nucleotide-long sequence that is almost invariant between all HCV genomes known thus far (Fig. 4B). This sequence, designated the X-tail, has the potential to form a very long and stable 3'-terminal stem-loop structure that terminates with a G:U base pairing (Blight and Rice, 1997). Two additional stem-loops located upstream have also been predicted, but the structures of these are much less clear. A poly(U/UC) tract with an average length of 80 nucleotides separates the X-tail from the variable region residing downstream of the stop codon of the polyprotein ORF.

The importance of the 3'-NTR for RNA replication and infectivity *in vivo* was first tested by experimental inoculation of chimpanzees with cloned HCV genomes that carried various mutations. It was found that removal of a portion of the variable region did not impair infectivity, whereas deletion of the poly(U/UC) tract, the complete X-tail, or parts of it destroyed infectivity (Kolykhalov *et al.*, 2000; Yanagi *et al.*, 1999). These observations were confirmed and extended by analogous studies in the replicon system (Friebe and Bartenschlager, 2002; Yi and Lemon, 2003a,b). For instance, various deletions or nucleotide substitutions within the X-tail sequence severely reduced or completely blocked RNA replication. In contrast, a complete deletion of the variable region was viable but reduced the number of G418-resistant colonies about 100-fold when analyzed in the context of a subgenomic, selectable HCV replicon. Finally, small deletions in the

poly(U/UC) region were also tolerated, but a minimal length of 26 uridine residues was found to be indispensable for efficient RNA replication (Friebe and Bartenschlager, 2002). An HCV replicon carrying only six uridine residues gave rise to just a few G418-resistant colonies. Sequence analysis of HCV RNAs amplified from these cells revealed that these replicons corresponded to pseudo-revertants that had regained poly(U/UC) tracts with an average length of 45 to 50 nucleotides (Friebe and Bartenschlager, 2002). Taken together, these studies convincingly show that a minimal poly(U/UC) tract and the complete X-tail are essential for HCV replication. Furthermore, these results suggest that original data describing the replication of HCV genomes that lack these sequences should be taken with caution (Dash *et al.*, 1997; Yoo *et al.*, 1995).

Apart from sequences located in the 5'- and 3'-NTRs, RNA structures residing within the coding region may contribute to RNA replication. In the case of *Poliovirus*, a short RNA sequence that forms a stem-loop structure was found to be essential for RNA replication. This element, designated the *cis*-acting RNA element (CRE), serves as the priming site where the viral polymerase adds two uridine residues to the protein primer Vpg in a template-dependent manner (Paul *et al.*, 2000; Rieder *et al.*, 2000). Analogous RNA elements were identified in other picornaviruses, including *Foot-and-mouth disease virus* and *Human rhinovirus 14* (Mason *et al.*, 2002; McKnight and Lemon, 1998). Likewise, RNA elements residing in the coding sequence of HCV may contribute to replication. Several groups predicted a number of highly conserved RNA secondary structures within the HCV coding sequence that may serve such purposes (Friebe *et al.*, 2004; Hofacker *et al.*, 1998; Rijnbrand *et al.*, 2001; Smith and Simmonds, 1997; Tuplin *et al.*, 2002; You *et al.*, 2004). Among these RNA elements, one particular stem-loop structure that resides in the 3'-terminal coding region of NS5B was found to be indispensable for replication (Friebe *et al.*, 2004; You *et al.*, 2004). This element was designated as 5BSL3.2 and consists of an 8-bp lower and a 6-bp upper stem, an 8-nucleotide-long bulge, and a 12-nucleotide-long upper loop. Mutational disruption of the stem structure as well as multiple and even single nucleotide substitutions in the bulge or upper loop severely reduced or completely blocked RNA replication. Interestingly, in one study, replication of these mutants could be rescued when an intact copy of 5BSL3.2 was inserted into the variable region of the 3'-NTR, arguing that this RNA signal can act at least to some extent in a position-independent manner (Friebe *et al.*, 2004). Most important was the observation that the upper loop of 5BSL3.2 is engaged in a kissing-loop interaction with SL2 of the X-tail

sequence close to the 3'-end of the genome (Friebe *et al.*, 2004). The introduction of mismatches into the complementary sequences blocked replication that was rescued when full base pairing was restored, even though the primary sequences of the kissing loops had been largely randomized. These results clearly show that a long-range RNA:RNA interaction takes place at the 3'-end of the HCV genome and that formation of this pseudo-knot structure is essential for replication. The fact that this phenomenon was not observed in several previous biochemical assays using *in vitro* transcripts or synthetic RNA fragments indicates that viral and/or host-cell proteins are crucially involved in this RNA:RNA interaction.

It is interesting to note that in the upper loop of 5BSL3.2, a CACAGC sequence motif is found that is virtually invariant among HCV genotypes and that is also found in *cis*-acting RNA sequences of distantly related flaviviruses like *Kunjin virus*, *West Nile virus*, or *Dengue virus* (reviewed in Markoff, 2003). The 3'-terminal of about 100 nucleotides of these viruses forms a conserved RNA structure that carries in the upper loop the highly conserved pentanucleotide motif CACAG. This motif was shown to be crucial for RNA replication in the *Kunjin virus* (Khromykh *et al.*, 2003). Given the high genetic conservation in this particular region of the genome, one might speculate that ubiquitously expressed and evolutionary conserved host-cell proteins are involved in the formation of a replication complex that interacts with the 3'-end of the flavivirus genome.

F. Mechanism of RNA Replication

Detailed information about the mode of RNA replication is not available for HCV, but by analogy to other flaviviruses (Westaway *et al.*, 2002), a model as depicted in Fig. 2 can be proposed: Incoming positive-stranded RNA serves as a template for the synthesis of a single, negative-stranded RNA molecule that remains base paired with its template. The resulting double-stranded RNA, the so-called replicative form (RF), is then copied multiple times semiconservatively and asymmetrically into a single positive-stranded RNA via this replicative intermediate (RI). In this way, a positive-stranded RNA progeny is transcribed in fivefold to tenfold molar excess over negative-stranded RNA and may be used for translation, synthesis of new RF, or packaging into new virus particles.

As deduced from a mutation study with full-length genomes *in vivo*, four viral enzymes are required for replication and infectivity (Kolykhalov *et al.*, 2000). These are the NS2-3 and the NS3/4A

proteinases, the NS3 helicase, and the NS5B RdRp. Since subgenomic replicons expressing only NS3 to 5B are capable of RNA replication (Lohmann *et al.*, 1999a), the NS2-3 proteinase is not directly required for this process. The same might be true for the NS3/4A proteinase, a protein complex that cleaves other viral proteins but is probably not directly involved in RNA amplification. Thus, the main players of the membrane-associated replication complex most likely are the NS3 helicase and the NS5B RdRp.

1. *The NS3 Helicase*

Helicases catalyze the unwinding of duplex RNA or DNA molecules into single-stranded nucleic acids. This reaction requires energy that is generated by hydrolysis of nucleoside triphosphates (NTPs), which explains why all helicases identified thus far possess NTPase activity (reviewed in Kadare and Haenni, 1997; Lohman and Bjornson, 1996). Based on the existence of conserved amino acid sequence motifs, helicases have been classified into three different superfamilies. The HCV enzyme belongs to the superfamily 2 (Gorbalenya *et al.*, 1989b) that is characterized by the presence of seven conserved amino acid sequence motifs (Kadare and Haenni, 1997; Lohman and Bjornson, 1996). Motif I (also called Walker motif A) consists of a stretch of hydrophobic residues followed by the conserved sequence GXXXXGKS/T and is directly involved in binding of the β - and γ -phosphates of NTPs. Motif II (Walker motif B) is characterized by several hydrophobic residues followed by the signature sequence DEXH. This site chelates the Mg^{2+} ion of the Mg-NTP complex. Similar sequence motifs have been found in the C-terminal two-thirds of NS3, and it has been suggested that this region harbors helicase activity (Miller and Purcell, 1990). These predictions have been experimentally confirmed in several studies by demonstrating NTPase activity (Gallinari *et al.*, 1998; Gwack *et al.*, 1995; Preugschat *et al.*, 1996; Suzich *et al.*, 1993), duplex unwinding (Gallinari *et al.*, 1998; Gwack *et al.*, 1996; Jin and Peterson, 1995; Kanai *et al.*, 1995; Kim *et al.*, 1995; Preugschat *et al.*, 1996; Tai *et al.*, 1996), single-stranded polynucleotide binding (Gallinari *et al.*, 1998; Gwack *et al.*, 1996; Kanai *et al.*, 1995; Tai *et al.*, 1996), and the importance of the conserved amino acid motifs in NS3 for helicase activity (Chang *et al.*, 2000; Heilek and Peterson, 1997; Kim *et al.*, 1997; Preugschat *et al.*, 2000; Utama *et al.*, 2000; Wardell *et al.*, 1999). It was shown that the minimal functional domain required for both enzymatic activities is about 400 amino acids in length and maps between residues 1209 and 1608 of the HCV polyprotein. The protein binds to homopolymeric RNAs with the following order of affinity:

poly(U) \gg poly(A) $>$ poly(C) = poly(G) (Kanai *et al.*, 1995). Since the 3'-NTR of the positive-stranded RNA also contains a poly(U/UC) sequence (Fig. 4B), the *in vitro* data may indicate a preferential binding of NS3 to this region of the HCV genome. Moreover, some specificity of helicase binding to stem-loop I in the 3'-NTR (Fig. 4B) was observed (Paolini *et al.*, 2000a). This may explain why deletion of the X-tail also reduces RNA binding, suggesting that the poly(U/UC) tract is insufficient to confer binding specificity (Banerjee and Dasgupta, 2001). An even more stringent requirement for binding has been observed for the 3'-NTR of negative-stranded RNA (Banerjee and Dasgupta, 2001). Most important was the presence of a terminal stem-loop that corresponds to stem-loop I of the positive-stranded 5'-NTR (Fig. 4A). These results suggest that the NS3 helicase specifically binds to the putative HCV promoters for initiation of positive- and negative-stranded RNA synthesis.

Although ATP is the preferred nucleotide for the NTPase activity of NS3, the enzyme is rather nonselective and can hydrolyze all ribonucleotides and deoxyribonucleotides (Jin and Peterson, 1995; Morgenstern *et al.*, 1997; Preugschat *et al.*, 1996; Suzich *et al.*, 1993; Wardell *et al.*, 1999). NTPase activity is stimulated up to 25-fold by poly(U) or poly(dU), whereas the stimulation by poly(A) or poly(G) is much lower (Morgenstern *et al.*, 1997; Preugschat *et al.*, 1996; Suzich *et al.*, 1993). Stimulation very much depends on the length of the nucleic acid and appears to induce a conformational change in the NS3 helicase (Preugschat *et al.*, 1996). Whereas polynucleotides stimulate NTPase activity, they inhibit the helicase activity, suggesting that polynucleotides compete with overlapping binding sites (Morgenstern *et al.*, 1997; Preugschat *et al.*, 1996; Tai *et al.*, 1996). The helicase has been shown to bind to substrates that contain 3'- or 5'-single-stranded regions but not to blunt-ended RNAs. Nevertheless, the enzyme unwinds only substrates with 3'-overhangs (Gwack *et al.*, 1996). Similar to the helicases of other positive-stranded RNA viruses, the HCV enzyme is able to unwind RNA:RNA, RNA:DNA, and DNA:DNA duplexes in the 3'- to 5'-direction with respect to the template strand (Gwack *et al.*, 1996; Hong *et al.*, 1996; Tai *et al.*, 1996). This unwinding has an absolute requirement for a divalent metal ion that can be Mg^{2+} or Mn^{2+} and an NTP, preferably ATP, suggesting that helicase and NTPase activities are closely coupled (Preugschat *et al.*, 1996). Although the kinetic parameters of the isolated NS3 helicase domain are very similar to those of full-length NS3, some differences in biochemical properties of these two proteins exist. For instance, the pH optima of ATPase and RNA unwinding activities differ between an

NS3/4A protein complex and an isolated NS3 helicase domain (Gwack *et al.*, 1996; Hong *et al.*, 1996; Jin and Peterson, 1995; Kanai *et al.*, 1995; Morgenstern *et al.*, 1997; Preugschat *et al.*, 1996; Tai *et al.*, 1996). In addition, the ATPase activities of both proteins differ in their sensitivity toward polynucleotide-mediated stimulation, with a full-length NS3 having a lower apparent dissociation constant for poly(U) than the isolated helicase domain (Kanai *et al.*, 1995; Morgenstern *et al.*, 1997; Preugschat *et al.*, 1996; Suzich *et al.*, 1993).

A very surprising observation was made when NS3 helicase activity was studied under single-cycle conditions in which rebinding of the enzyme to the substrate was quenched by the addition of excess amounts of competing oligonucleotides (Pang *et al.*, 2002). It was found that full-length NS3 had a potent DNA but a very poor RNA helicase activity, which was primarily due to a weak binding of RNA duplex substrates. Upon the addition of the NS4A proteinase cofactor, however, RNA helicase activity was enhanced tremendously. This increase was achieved by enhancing RNA binding in a way that leads to more efficient unwinding. Thus, NS4A acts as an RNA loading factor and greatly enhances productive RNA binding (Pang *et al.*, 2002). These data may also explain why it is important for HCV (and perhaps for other positive-stranded RNA viruses) that proteinase and helicase reside on the same molecule.

Many of these observations have been corroborated and extended by the resolution of the X-ray crystal structure of the NS3 helicase either alone or complexed with a deoxyuridine octamer (Cho *et al.*, 1998; Kim *et al.*, 1998; Yao *et al.*, 1997) (Fig. 5D). According to these data, the helicase is a Y-shaped molecule that consists of three nearly equally sized domains. Domain 1 (the NTP binding subdomain) has a fold similar to that found in several other ATP transphosphorylases (Kim *et al.*, 1998). This domain contains the Walker motifs A and B that are both oriented toward the cleft between domains 1 and 2. At the bottom of the interdomain cleft resides a histidine residue that is essential for coupling the ATPase activity to polynucleotide binding. Mutations affecting this histidine residue abolish helicase activity without affecting ATPase activity (Heilek and Peterson, 1997). The interface between domains 1 and 2 is formed primarily by residues from the seven helicase motifs. Although the basic residues of motif VI were thought to be involved in substrate RNA binding, they rather appear to be required for ATP binding (Kim *et al.*, 1998). In the structure proposed by Kim *et al.* (1998), the bound single-stranded DNA oligonucleotide lies in a channel that separates domain 3 from domains 1 and 2 (Fig. 5D). Consistent with a rather nonspecific binding, the interactions

between the single-stranded DNA and the NS3 helicase are mostly confined to the DNA backbone. The side chains of two hydrophobic amino acids, tyrosine and valine, form a central binding cavity in the NS3 molecule. These residues were proposed to act as a pair of “book-ends” that limit the central cavity that can accommodate five nucleotides (Kim *et al.*, 1998). Based on these observations, a model was proposed according to which NS3 does not actively unwind the double-stranded substrate but rather functions by capturing the single-stranded regions that form due to “breathing” (spontaneous melting and hybridizing at the end of the double strand) (Kim *et al.*, 1998). The active process would therefore not be the unwinding itself but instead the translocation of the helicase along the single-stranded template. This process is mediated by ATP binding and hydrolysis that leads to a closing and opening of a large cleft between domains 2 and 1, respectively. This very attractive model, which has been supported by mutation studies (Lin and Kim, 1999; Paolini *et al.*, 2000b; Preugschat *et al.*, 2000; Rho *et al.*, 2001; Tai *et al.*, 2001; Wardell *et al.*, 1999), implies that NS3 can unwind double-stranded substrates as a monomer although an oligomeric state required for enzymatic activity has been suggested by other groups (Cho *et al.*, 1998; Khu *et al.*, 2001; Levin and Patel, 1999). Further studies are required to fully understand the helicase activity of NS3.

It is not known how the NS3 helicase contributes to virus replication. Therefore, attempts to assign a definite function of this enzyme to the viral life cycle are purely speculative. Nevertheless, this discussion will mention at least three possibilities. First, NS3 might be required for initiation of RNA translation, analogous to cellular elongation factor eIF-4A. This possibility, however, is not very likely because translation of HCV RNA occurs efficiently in the absence of viral proteins, and there is no evidence, apart from some controversial reports for the core protein (see previous paragraphs) that viral proteins affect RNA translation. Second, NS3 might be required for initiation of RNA replication by unwinding highly structured regions at the site where RNA synthesis is initiated (e.g. at the very stable stem-loop I at the 3'-end of the positive-stranded RNA) (Fig. 4B). Third, the helicase may participate in the elongation reaction and thereby increase the processing of the replication complex.

2. The NS5B RdRp

Although the role of the NS3 helicase in RNA replication is unclear, it is obvious that the NS5B RdRp forms the catalytic center of the HCV replication machinery. *In vitro*, the enzyme prefers a primer-dependent initiation of RNA synthesis that is achieved either

by elongation of primers hybridized to a template RNA strand or by self-priming due to intramolecular base pairing in which 3'-terminal sequences of the template are involved (Behrens *et al.*, 1996; Lohmann *et al.*, 1997; Yamashita *et al.*, 1998; Yuan *et al.*, 1997). The latter reaction results in the formation of approximately dimer-sized products (Behrens *et al.*, 1996; Lohmann *et al.*, 1997). In addition, NS5B can also initiate RNA synthesis *de novo*, and it is likely that this mechanism also operates *in vivo* (Luo *et al.*, 2000; Oh *et al.*, 1999; Zhong *et al.*, 2000). Interestingly, under conditions of high concentrations of GTP and ATP, the enzyme can synthesize RNA in a primer-independent manner from homopolymeric poly(C) or poly(U) templates, whereas RNA synthesis from poly(A) or poly(I) templates remains primer dependent irrespective of the NTP concentration (Luo *et al.*, 2000; Bartenschlager, R. and Lohmann, V., unpublished results). These results imply that NS5B can use only purine nucleotides for *de novo* initiation, with GTP being much more efficient than ATP, at least *in vitro* (Luo *et al.*, 2000; Zhong *et al.*, 2000). Interestingly, positive- and negative-stranded HCV genomes start with a guanosine and an adenine, respectively. The fact that positive-stranded RNA is synthesized in fivefold to tenfold excess over negative-stranded RNA (Lohmann *et al.*, 1999a) may be the consequence of more efficient *de novo* priming of positive-stranded RNA. A more favorable structure of the 3'-terminal region of the negative-stranded RNA may also contribute to this asymmetric replication (Reigadas *et al.*, 2001).

Linear sequence alignments between HCV NS5B and other viral and cellular polymerases have led to the identification of highly conserved amino acid sequence motifs crucial for enzymatic activity (Poch *et al.*, 1989). Initially, four such motifs have been identified in NS5B: motif A (DXXXXD) that is probably involved in NTP binding and catalysis, motif B (GXXXTXXXN) that has an invariant glycine involved in template and/or primer positioning, motif C (GDD) that represents the hallmark signature of most polymerases and is involved in NTP binding and catalysis, and motif D (AMTRY) that is probably also involved in NTP binding and catalysis. The importance of these sequence motifs was confirmed by intensive mutation studies. Most substitutions that affected highly conserved residues were deleterious with the notable exception of the arginine residue in motif D (Cheney *et al.*, 2002; Ishii *et al.*, 1999; Lohmann *et al.*, 1997; Qin *et al.*, 2001). Interestingly, all reverse transcriptases and nearly all viral RdRps carry a lysine residue at this position, whereas an invariant arginine is found with all HCV isolates. A very surprising observation was therefore that a lysine substitution for this arginine increased both

the RdRp activity of the purified protein *in vitro* and the RNA replication of a subgenomic HCV replicon into which this mutation was introduced (Cheney *et al.*, 2002; Lohmann *et al.*, 1997). This result indicates that some down-modulation of NS5B RdRp activity by this mutation in motif D is required for HCV replication.

For several viral replicases, copurification of host-encoded terminal nucleotidyl transferases (TNTases) or detection of a replicase inherent TNTase activity have been described (Andrews and Baltimore, 1986; Dasgupta 1983). In the case of HCV, a TNTase activity that added a single nucleotide to the 3'-end of the input RNA has initially been described (Behrens *et al.*, 1996). Because all mutations that blocked RdRp activity had no effect on this TNTase, it was concluded that the latter might be a cellular contaminant that was copurified in minute amounts with NS5B (Lohmann *et al.*, 1997). Several other groups supported this conclusion because they were unable to detect a TNTase in their NS5B preparations produced in different systems although the TNTase assays used were not sensitive (Oh *et al.*, 1999; Yamashita *et al.*, 1998). This result and the observation that NS5B can initiate RNA synthesis *de novo* argue against a role for a TNTase in HCV replication.

In most studies, NS5B was found to bind to and use virtually every RNA and even DNA templates, albeit with different efficiencies (Behrens *et al.*, 1996; Lohmann *et al.*, 1997; Yamashita *et al.*, 1998). Thus, it remains to be determined how template specificity is achieved. In one study, however, a preferential binding of NS5B to a sequence in the 3'-coding sequence of NS5B itself was found by means of electrophoretic mobility shift assays and competition experiments (Cheng *et al.*, 1999). Furthermore, two RNA binding domains in NS5B were mapped, one in the N-terminal region and one in the middle of the protein overlapping with motifs A and B (Cheng *et al.*, 1999). Although a specific binding of NS5B to a particular region in the 3'-region of the viral genome readily explains template specificity, the sequestration of the replication machinery into a rather compact membrane-associated replication complex may be sufficient to allow specific binding to and replication of the viral genome. In agreement with this assumption, crude replication complexes (CRCs) isolated from cell lines that carry an HCV replicon are unable to accept template RNAs added to the reaction (Ali *et al.*, 2002; Hardy *et al.*, 2003; Lai *et al.*, 2003). The only template used by these complexes is the endogenous replicon RNA that cofractionates with the CRCs. However, since these complexes preferentially or exclusively support elongation of primed RNA substrates but not, or to a much lesser extent, *de novo* synthesis, the

ability of the replication complex to accept exogenous template RNAs so far could not be rigorously tested.

Several groups determined the X-ray crystal structure of NS5B proteins lacking the hydrophobic C-terminal TM domain (Ago *et al.*, 1999; Bressanelli *et al.*, 1999, 2002; Lesburg *et al.*, 1999) (Section V,G and Fig. 5B). NS5B has a globular shape and, like other nucleic acid synthesizing enzymes, is composed of three subdomains designated as palm, finger, and thumb because of the similarity between the protein structure and the shape of a right hand. A peculiarity of the HCV enzyme is the tight interaction between the thumb and the finger subdomains, which results in a rather closed conformation with an encircled active site cavity (Fig. 5B). Given the extent of these inter-subdomain interactions, it is assumed that the global NS5B structure is rather inflexible and does not undergo the large-scale conformational changes observed with other polymerases (Jager *et al.*, 1994; Li *et al.*, 1998). In agreement with that assumption, NS5B is able to bind nucleotides at the active site in the absence of an RNA template, suggesting that the enzyme has a preformed active site (Bressanelli *et al.*, 2002). Interestingly, three distinct nucleotide binding sites have been found in the catalytic center of the enzyme that superimpose remarkably well to the ones described for the RNA polymerase of the bacteriophage phi6 (Butcher *et al.*, 2001) (see following paragraphs).

Another peculiarity of NS5B is the presence of a highly flexible β -hairpin loop in the thumb subdomain (Fig. 5B). This β -hairpin protrudes toward the active site that resides at the base of the palm subdomain and imposes a steric hindrance for the binding of double-stranded RNA substrates (Zhong *et al.*, 2000). This assumption is based on the observation that NS5B proteins that do not contain the β -loop are more active *in vitro*, are able to use double-stranded RNA substrates, and no longer initiate RNA synthesis at the very 3'-end of the template but rather internally (Cheney *et al.*, 2002; Hong *et al.*, 2001). Thus, the β -hairpin may generate a narrow "gate" that prevents the 3'-terminus of the template RNA from slipping through the active site, thereby ensuring the initiation of RNA synthesis from the 3'-end of the template strand. This is important for virus replication because only then is genetic information at the very termini preserved. Consequently, when a mutant lacking the β -hairpin was tested in the replicon system, replication was not detectable (Cheney *et al.*, 2002). Thus, although the β -loop is dispensable for *in vitro* RdRp activity, it is essential for RNA replication in cells. Interestingly, the poliovirus RdRp does not have such a β -loop, which may explain why this enzyme

is able to use double-stranded RNA substrates and has a different mode of initiating RNA synthesis (protein-dependent priming). In any case, once initiation has been accomplished, this β -hairpin probably moves away from the active site cavity, which can be achieved by minor structural changes (Lesburg *et al.*, 1999). It remains to be determined, however, whether the β -loop is the only determinant that helps to initiate RNA synthesis at the very 3'-end of the template.

An additional feature of HCV NS5B is the presence of a low-affinity GTP-specific binding site between the thumb and finger subdomains (Bressanelli *et al.*, 2002). This binding site is located about 30 Å away from the catalytic site and resides on the surface of the molecule. GTP binding to this site may therefore not directly contribute to catalysis but rather act as an allosteric regulator by which the interaction between the finger and the palm subdomains might be controlled. Alternatively, this binding site may be involved in NS5B oligomerization. It has been suggested that such an oligomerization may induce the correct conformation required to initiate RNA replication (Qin *et al.*, 2002; Wang *et al.*, 2002). In both cases, structural changes induced by GTP binding to the surface site would lead to a more efficient initiation of RNA synthesis. Indeed, in the presence of high GTP concentrations, NS5B RdRp was found to be much more active *in vitro* (Lohmann *et al.*, 1999b; Luo *et al.*, 2000).

A remarkable and unexpected similarity of the structural and biochemical properties of HCV NS5B and the RdRp of the double-stranded RNA bacteriophage phi6 was revealed by the determination of the X-ray crystal structure of the latter (Butcher *et al.*, 2001; Laurila *et al.*, 2002). In spite of the lack of sequence homology, the structures of both enzymes share considerable similarities and are almost superimposable. Both proteins have a rather closed conformation that arises due to intensive interactions between the finger and thumb subdomains, both initiate RNA synthesis *de novo*, and both are activated by high concentrations of GTP (Lohmann *et al.*, 1999b; Luo *et al.*, 2000). The X-ray cocrystal structure of phi6 RdRp with oligonucleotides and NTPs might therefore be useful to gain insight into the mechanism of HCV RNA replication. Based on these data, only single-stranded RNA templates fit into the template tunnel that is too narrow to accommodate double-stranded RNAs. A model has been proposed that in principle may also be valid for HCV. It is thought that a single-stranded RNA template binds to the template tunnel in a way that the template "overshoots" and locks into a specificity pocket that closes the template tunnel on the opposite side (Butcher *et al.*, 2000, 2001). Upon binding of NTPs that enter the active site via another

positively charged tunnel, the first nucleotide can form hydrogen bonds with the penultimate nucleotide. This would lead to a repositioning of the template and the release of the terminal base from the specificity pocket. In this way, the ultimate nucleotide becomes available for hydrogen bonding with a second nucleotide. The resulting initiation complex then allows formation of the first phosphodiester bond between the two complexed NTPs, which results in a displacement of the template tunnel lock. The next NTP then enters the active site and elongation proceeds. Most important for this *de novo* initiation is the C-terminal domain that has been referred to as the initiation platform (Butcher *et al.*, 2001). It serves two functions: first, it locks the template channel, thereby preventing binding of double-stranded RNA templates to the active site; second, it enables formation of stacking interactions with the initiation nucleotides, which facilitates the assembly of a functional initiation complex. In agreement with this assumption, it was shown that phi6 RdRp mutants that carry substitutions in the initiation platform prefer primer-dependent RNA synthesis over *de novo* initiation (Laurila *et al.*, 2002).

At least three lines of evidence suggest that similar mechanisms are operating with HCV RNA synthesis. First, shortening the β -hairpin in NS5B leads to enzymes that initiate from an internally annealed primer as compared to the unaltered enzyme that can only use short primers that are complementary to the 3'-end of the template (Hong *et al.*, 2001). Second, the β -hairpin contains a highly conserved tyrosine residue that may also form stacking interactions with initiating nucleotides. Third, HCV NS5B and the RdRp of phi6 share a high degree of structural homology.

3. Roles of NS4B, NS5A, and Host-Cell Factors for HCV RNA Replication

Apart from the NS3/4A complex and the NS5B RdRp, NS4B and NS5A are also required for RNA replication because, first, a high number of cell culture-adaptive mutations reside in these proteins (Blight *et al.*, 2000; Lohmann *et al.*, 2003) and, second, certain substitutions and deletions in these genes can reduce or block RNA replication (Krieger, N., and Bartenschlager, R. unpublished observations). How NS4B and NS5A contribute to RNA replication is not known. The transmembranous structure of NS4B (Fig. 6) and the absence of enzymatic activities suggest that this protein might play a noncatalytic role. Presumably, its main function is the induction of membranous vesicles or membrane invaginations that may serve as scaffolds for the assembly of the HCV replication complex (Egger *et al.*, 2002).

The contribution of NS5A to RNA replication is also poorly understood. By using a yeast two-hybrid screening, Tu *et al.* (1999) observed an interaction of NS5A and NS5B with the host-cell protein human vesicle-associated membrane protein-associated protein A (hVAP-A). This protein belongs to the class of target N-ethylmaleimide-sensitive factor attachment protein receptors (tSNAREs) that are involved in intracellular vesicle transport. The hVAP-A/NS5A and hVAP-A/NS5B interactions have been demonstrated both *in vitro* and in transfected cells. Moreover, expression of dominant-negative mutants of hVAP-A and RNAi-mediated knockdown of hVAP-A expression reduces the association of NS5B with detergent-resistant membranes (rafts) and leads to a reduction of HCV RNA replication, which argues that this cellular protein plays an important role in the formation of a functional replication complex (Gao *et al.*, 2004; Zhang *et al.*, 2004).

An additional study has described the interaction of NS5A with amphiphysin II, another membrane-associated protein implicated in SNARE-mediated vesicle traffic between the ER and Golgi compartment (Weir *et al.*, 2001; Zech *et al.*, 2003). Interestingly, this interaction was demonstrated both *in vitro* and with NS5A isolated from the replication complex in cells that carry subgenomic HCV replicons. The interaction sites were tentatively mapped to a proline-rich region in the C-terminal part of NS5A and the Src homology 3 domain of amphiphysin II. Mutations that reduced this interaction, however, did not affect replication of HCV replicons, indicating that formation of an amphiphysin II:NS5A complex is not important for HCV RNA replication in cell culture but might be of importance for other steps in the HCV life cycle (Zech *et al.*, 2003).

4. The HCV Replication Complex

In all cases studied thus far, the infection of a cell with a positive-stranded RNA virus leads to a rearrangement of intracellular membrane structures, a prerequisite for the formation of viral replication complexes. Morphologically, these membrane alterations often appear as an aggregation of vesicles derived from the ER (*Poliovirus*), Golgi (*Mouse hepatitis virus*), or lysosomal/endosomal compartments (*Semliki forest virus*). In the case of HCV, it was shown that NS4B is sufficient to induce membranous alterations that morphologically resemble the membranous web that was found in replicon cells and that represents the viral replication complex (Egger *et al.*, 2002; El-Hage *et al.*, 2003; Gosert *et al.*, 2003; Shi *et al.*, 2003). The mechanism underlying vesicle formation is not known, but at least two possibilities can be envisaged. First, NS4B recruits cellular proteins that are

involved in vesicle formation, or, second, NS4B is able to induce vesiculation on its own. The fact that NS4B has the ability to oligomerize favors the latter possibility (Dimitrova *et al.*, 2003). Membrane curvature may be induced via lateral interactions between NS4B molecules, a hypothesis that is in line with the formation of a membranous web in cells that inducibly express of NS4B and cells that contain HCV replicons (Egger *et al.*, 2002; Gosert *et al.*, 2003).

Three lines of evidence suggest that the membranous web in HCV-infected cells is derived from ER membranes. First, HCV RNA translation takes place at the rough ER; second, all nonstructural proteins are associated with ER membranes in cells carrying subgenomic replicons (Mottola *et al.*, 2002); third, the membranous web is often found in close proximity to ER membranes. It has been suggested that the membranes at which RNA replication occurs are lipid rafts recruited from intracellular sites (Gao *et al.*, 2004; Shi *et al.*, 2003). This conclusion is based on the resistance of these membranes to a treatment with 1% NP40 and their cofractionation with caveolin-2.

Crude replication complexes have been prepared from lysates of cells carrying HCV replicons. These complexes retain enzymatic activity by synthesizing viral RNA from the endogenous template for which both the NS3 helicase and the NS5B RdRp are required (Ali *et al.*, 2002; Hardy *et al.*, 2003; Lai *et al.*, 2003). Several findings suggest that the enzymatically active complex has a rather closed conformation. First of all, the replication complex is unable to use exogenously added RNA templates (Lai *et al.*, 2003). Furthermore, most of the viral RNA is nuclease resistant (Miyanari *et al.*, 2003) and with the exception of NS5A, *trans*-complementation of HCV proteins is not possible (Appel, N. and Bartenschlager, R., In Press). Interestingly, when these complexes are treated with proteinase K, more than 90% of the viral proteins are degraded without an effect on RNA synthesis activity (Miyanari *et al.*, 2003; Quinkert, D., Bartenschlager, R., and Lohmann, V., unpublished results). This result suggests that at a given time, only a minor fraction of HCV proteins is engaged in RNA synthesis, and this fraction is protected in the replication complex.

Once vesicles of the membranous web are formed, they may be transported to distinct cytoplasmic sites in a microtubule-dependent manner. This would explain the observation that drugs affecting the cytoskeleton (vinblastine, colchicine, or nocodazole) or the actin inhibitor cytochalasin D reduce replication of HCV replicons (Bost *et al.*, 2003). In this study, however, only replicon RNA levels were measured. Thus, it remains an open question whether these drugs indeed affect

the formation/architecture of the membranous web or some other replication step(s).

G. Membrane Topologies of Viral Proteins

As suggested in the previous sections, almost all HCV proteins are membrane associated, suggesting that their interactions with membranes are an important prerequisite for the formation of a functional replication complex. Several studies have addressed the membrane topologies of individual viral proteins. The main results described in these reports are presented in the following list. A schematic drawing of a model that summarizes these data is presented in Fig. 6.

1. The core protein carries two hydrophobic domains that interact with intracellular membranes: the transmembranous, C-terminal E1 signal sequence and domain 2 that appears to intercalate into the cytoplasmic leaflet of the ER membrane. The latter interaction is important for the association of core with lipid droplets, which depends on intramembrane cleavage of the C-terminal signal sequence by host-cell peptidase SPP (McLauchlan *et al.*, 2002).

2. E1 and E2 are both type I TM proteins that in the mature form span the lipid bilayer once. They form heterodimeric complexes via interactions between their TM domains. The majority of each protein resides on the luminal side of the ER (i.e., outside of the virus particle). The topologies adopted by the TM domains of E1 and E2 are unclear. However, the presence of a hydrophobic stretch of amino acid residues within the N terminus of both TM domains, followed by charged residues and the signal sequence of the downstream protein (E2 or p7), suggests two membrane-spanning segments with a charged residue facing the cytosol (Charloteaux *et al.*, 2002; Cocquerel *et al.*, 2000). On the other hand, it has been shown that after E1/E2 heterodimerization, the TM domains most likely exhibit a single membrane-spanning topology (Op de Beeck *et al.*, 2001). A model has been proposed in which prior to signalase cleavage, the TM domains form a transient hairpin structure in the translocon with both N termini and C termini oriented toward the ER lumen. After cleavage, a reorientation of the C-terminal hydrophobic stretch would occur, resulting in the formation of a single membrane-spanning TM domain that engages in heterodimerization (Fig. 6). According to an alternative model, the C-terminal domains of both glycoproteins should each form an amphipathic α -helix followed by two interacting transmembrane

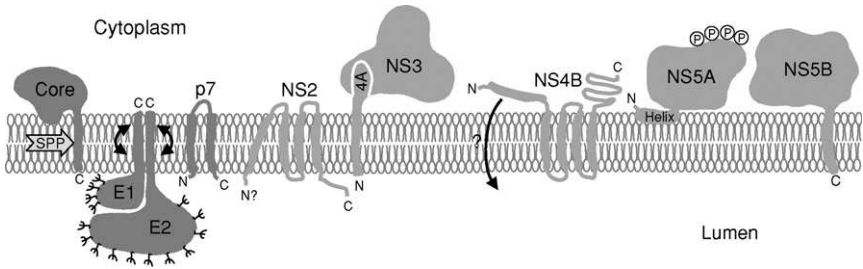


FIG 6. Membrane topology of HCV structural (red) and nonstructural proteins (orange) after polyprotein cleavage. The location of the N terminus and C terminus of the proteins relative to the ER lumen is given. The site of core protein cleavage by signal peptide peptidase (SPP) is indicated by the yellow arrow. The glycosylation sites in the envelope glycoproteins and the predicted reorientation of their TM domains after proteolytic cleavage are marked. The phosphorylation of NS5A and the amphipathic helix are indicated. Note that in the case of NS2, some molecules may also carry their N terminus on the cytosolic side. Further note that the N-terminal TM domain of NS4B may have a dual topology (Lundin *et al.*, 2003). (See Color Insert.)

β -strands (Charloteaux *et al.*, 2002). These β -strands would anchor the glycoproteins in the ER membrane, at least transiently, with anchoring being stabilized by the nearby amphipathic α -helix.

3. The small hydrophobic peptide p7 is an integral membrane protein carrying two TM domains that are interconnected by a short loop located on the cytoplasmic side of the membrane (Carrere-Kremer *et al.*, 2002). The signal sequence for p7 resides in the C terminus of E2, whereas the C-terminal TM domain of p7 functions as a signal sequence for NS2 (Lin *et al.*, 1994a; Mizushima *et al.*, 1994a). P7 can form hexameric complexes that may function as an ion channel (Griffin *et al.*, 2003; Pavlovic *et al.*, 2003). An *in vivo* study demonstrated that a functional p7 protein is critical for infectivity and revealed that the N- and/or C-terminal segment of p7 represent sequences with genotype-specific functions (Sakai *et al.*, 2003).

4. The topology of NS2 has also been studied. The C terminus or, perhaps in a fraction of the molecules, the N terminus resides on the luminal side of the ER (Santolini *et al.*, 1995; Yamaga and Ou, 2002) (Fig. 6). Membrane association of NS2 occurs cotranslationally and does not require p7 (Yamaga and Ou, 2002). By using deletion mapping and glycosylation site tagging, a tentative membrane topology model was proposed according to which NS2 has two internal signal sequences and four putative membrane spanning domains. The fact that an engineered glycosylation site in the N terminus of NS2 was used

independently of p7 suggests that the p7 signal sequence might be needed only for cleavage at the N terminus of NS2 but not for its membrane insertion.

5. NS3 expressed on its own localizes to the cytoplasm, in agreement with the absence of known membrane anchoring sequences (Wölk *et al.*, 2000). However, upon coexpression with NS4A, both proteins form a tight complex in which the NS3 molecule is targeted to intracellular membranes via a hydrophobic TM helix located in the 20 N-terminal residues of NS4A (Hijikata *et al.*, 1993b; Tanji *et al.*, 1995a; Wölk *et al.*, 2000; Yao *et al.*, 1999).

6. NS4B is a highly hydrophobic integral membrane protein with an apparent molecular weight of about 27 kDa (Hijikata *et al.*, 1993b; Hugle *et al.*, 2001). It is part of a multiprotein replication complex and induces the formation of intracellular membranous vesicles that partly colocalize with ER markers like calnexin and that contain detergent-resistant membranes (Egger *et al.*, 2002; Kim *et al.*, 1999b; Konan *et al.*, 2003; Mottola *et al.*, 2002; Shi *et al.*, 2003). Based on computer-aided topology modeling and glycosylation tagging, five putative TM domains were predicted with the C terminus of NS4B residing in the cytoplasm and the N terminus in the ER lumen (Lundin *et al.*, 2003). The latter observation is difficult to envisage because cleavage by the NS3/4A proteinase complex takes place on the cytoplasmic site. It has, therefore, been hypothesized that the N-terminal domain of NS4B is translocated posttranslationally across the membrane (Lundin *et al.*, 2003), reminiscent of the dual topology of the HBV large surface protein (Bruss *et al.*, 1994; Lambert and Prange, 2001). It is interesting to note that NS4B proteins of other flaviviruses are also membrane-associated with the N terminus located in the ER lumen (Cahour *et al.*, 1992; Lin *et al.*, 1993). In contrast to HCV, however, translocation in these cases is mediated by an N-terminal signal sequence that is not present in HCV NS4B.

7. Membrane association of NS5A is achieved by an amphipathic N-terminal α -helix that inserts parallel to the lipid bilayer into the cytoplasmic leaflet of the membrane, resulting in a monotopic orientation (Brass *et al.*, 2002; Penin *et al.*, 2004). The hydrophobic side of the helix is buried into the membrane, whereas the highly hydrophilic side of the helix is oriented toward the cytosol and could therefore serve as a potential binding site for viral and/or cellular proteins. The helix extends from amino acid residue 5 to 25. This sequence is sufficient to insert NS5A into the ER membrane in the absence of other HCV proteins and to target heterologous fusion proteins to the ER membrane (Brass *et al.*, 2002; Elazar *et al.*, 2003; Penin *et al.*, 2004).

Conversely, NS5A lacking this N-terminal region is transported to the nucleus because of the loss of membrane association and the activation of a cryptic nuclear localization signal (Ide *et al.*, 1996; Song *et al.*, 2000). Membrane association of NS5A via its N-terminal domain is essential for RNA replication because mutational ablation of membrane association blocks replication of HCV replicons in cell culture (Elazar *et al.*, 2003; Krieger, N., and Bartenschlager, R., unpublished observation). Interaction with the membrane occurs by a posttranslational mechanism with NS5A having the properties of an integral membrane protein (Brass *et al.*, 2002).

8. The NS5B RdRp carries a hydrophobic C-terminal sequence of 21 amino acids that anchors the protein into the ER membrane by a posttranslational mechanism (Ivashkina *et al.*, 2002; Schmidt-Mende *et al.*, 2001). This property and the location of the TM domain in the protein led to the conclusion that NS5B belongs to the group of tail-anchored proteins. NS5B is thus an integral membrane protein with a large ectodomain carrying the catalytic RdRp activity that resides on the cytoplasmic side. Interestingly, a replicon containing an artificial glycosylation site in the C terminus of NS5B was functional although the protein was glycosylated (Ivashkina *et al.*, 2002). This finding demonstrates that the C terminus of NS5B is indeed a single transmembrane-spanning region that tolerates certain insertions. Within the TM domain of NS5B, an invariant GVG-motif was identified. Although this motif was nonessential for membrane insertion, it may play a role in protein:protein interactions. In fact, glycine residues in α -helical TM domains create "holes" that might be filled in by bulky side chains of hydrophobic amino acid residues creating stable interactions within the membrane-spanning region of TM proteins (Ivashkina *et al.*, 2002; MacKenzie *et al.*, 1997). In agreement with such a model, amino acid substitutions affecting this motif completely abolish RNA replication (Moradpour *et al.*, 2004). Moreover, incubation of replicon cells with a membrane-permeable peptide that corresponds to the C-terminal membrane anchor reduced RNA replication about twofold (Lee *et al.*, 2004). Finally, coexpression of the C-terminal NS5B domain with a subgenomic replicon in a transient assay almost completely blocked RNA replication (Pietschmann, T., and Bartenschlager, R., unpublished results). These results underscore that the C-terminal NS5B domain in addition to membrane anchoring play some other role for RNA replication.

The model depicted in Fig. 6 does not take into account interactions between individual nonstructural proteins nor does it consider the

incorporation of host-cell proteins into the replication complex. In addition, viral RNA that must interact at least transiently with the NS3 helicase and the NS5B RdRp may also contribute to the structure of the replication complex. Numerous studies that deal with potential interactions between viral and cellular proteins have been described in the literature. Most of them have been summarized in a review by Tellinghuisen and Rice (2002); therefore, this section will discuss only those interactions that might be involved in RNA replication and virus particle production. The interaction of the core protein with lipid membranes as well as the E1/E2 heterodimerization have already been described in detail in the previous paragraphs. What has not yet been mentioned is the interaction of HCV core with tissue transglutaminase. It has been reported that the formation of core protein homodimers is enhanced in transfected cells under conditions that stimulate tissue transglutaminase activity (Lu *et al.*, 2001). Therefore, it has been suggested that core interaction with tissue transglutaminase plays an important role in virus assembly, but this hypothesis awaits experimental proof.

The best-studied interaction between two HCV proteins is the one between NS3 and NS4A that was described in detail in Section V,D. In addition, coimmunoprecipitation studies indicated interactions between NS4A and an NS4B/5A polyprotein substrate. This interaction probably plays a role in proteolytic processing (Lin *et al.*, 1997). Activation of the NS2-3 proteinase presumably via direct interaction with the Hsp90 chaperone has already been mentioned. An interaction between NS5A and NS5B has also been reported. It was shown that purified NS5A added to an *in vitro* RdRp reaction with a C-terminally truncated NS5B could modulate polymerase activity (Shirota *et al.*, 2002). As deduced from an extensive mutagenesis study performed on interaction sites in the context of the replicon system, the NS5A/5B interaction appears to be crucial for replication (Shimakami *et al.*, 2004). Both proteins were also shown to interact with the cellular SNARE-like protein hVAPA; it was postulated that via this interaction, the HCV proteins might be targeted to vesicle membranes and/or contribute to membrane rearrangements although the latter process can be mediated by NS4B alone (Egger *et al.*, 2002; Tu *et al.*, 1999). The interaction of NS5A with one or several host-cell kinases has been well established (Kim *et al.*, 1999a; Reed *et al.*, 1997; Tanji *et al.*, 1995b) and shown to be required for NS5A phosphorylation. It is not known which cellular kinase(s) is responsible for the phosphorylation of NS5A. By using a yeast two-hybrid screening process with a collection of 119 GST-tagged yeast kinases, *in vitro* kinase assays, and phosphopeptide

mapping studies, however, Coito *et al.* (2004) obtained evidence that p70S6 or kinases with similar specificity phosphorylate NS5A in mammalian cells. It will be interesting to see whether the expression of dominant-negative kinase mutants or RNAi-mediated knockdown of the kinase expression interferes with HCV RNA replication.

Another interaction that has been studied in some detail is the one between NS5A and PKR. This interaction is assumed to play an important role in counteracting the antiviral effects of IFN- α and it will therefore be discussed in detail in Section VI,C.

H. Virus Assembly and Release

As described in Section IV, efficient production of authentic HCV particles has not been achieved in cultured cells. Therefore, virus assembly could not be studied in detail. Although homotypic interaction of the core protein has been observed and interaction domains have been mapped by using various biochemical assays, assembly of particulate structures has not been possible for a long time (Matsumoto *et al.*, 1996; Nolandt *et al.*, 1997). Kunkel *et al.* (2001), however, have been able to develop a system that allows the formation of nucleocapsids *in vitro*. By using purified HCV core proteins, the group found that nucleocapsid-like particles (Nclps) form when structured RNAs are added to an *in vitro* assembly reaction. Nclp formation was observed with a C-terminally truncated core protein (residues 1 to 124) and structured RNAs with a length between 75 to 350 nucleotides. Particles obtained under these conditions were rather homogenous and spherical with an average diameter of about 60 nm. When a core protein was used that contains the C terminus up to residue 174, more heterogenous and irregularly shaped particles were found, suggesting that the C terminus affects the self-assembly properties of HCV core (Kunkel *et al.*, 2001). Moreover, a stabilizing effect of this protein region was found because core 1 to 124 was readily degraded by proteinases *in vitro*, whereas core 1 to 174 was rather stable (Kunkel and Watowich, 2002). When structured RNA was added to the shorter core fragment, however, the protein became resistant to proteinase digestion, which suggests that core proteins undergo substantial conformational changes upon binding to nucleic acids or assembly into Nclps. In summary, these data demonstrate that the core protein is able to self-assemble in the presence of structured RNA.

Formation of virus-like particles in mammalian cells has been achieved by using a chimeric semliki forest virus replicon that allows high-level expression of the HCV structural proteins in BHK-21 cells (Blanchard *et al.*, 2002). This cell line, however, contains a large

amount of intracisternal R-type particles that may complicate the unambiguous detection of HCV VLPs (Blanchard *et al.*, 2003a). Nevertheless, Blanchard *et al.* (2002) observed budding of VLPs with an average diameter of 50 nm toward the lumen of a dilated ER upon expression of HCV core, E1, and E2. Moreover, expression of full-length core protein (amino acid 1 to 191), but not that of a C-terminally truncated core protein lacking the E1 signal sequence (amino acid 174 to 191) or a core protein with an alanine substitution for the aspartic acid residue at position 111, resulted in the formation of VLPs (Blanchard *et al.*, 2003b). These results suggest that HCV budding is initiated by the core protein itself, arguing that the core constitutes the budding apparatus.

The way packaging specificity is achieved in HCV particle formation has not yet been elucidated. Although core proteins bind to RNA *in vitro* without specificity, a preferential binding of core to the 5'-half of the HCV genome and in particular to the 5'-NTR has been described in transfected cells (Shimoike *et al.*, 1999; Zhang *et al.*, 2002). Such a binding might reduce translation and regulate a switch from translation to packaging (Shimoike *et al.*, 1999). Envelopment of HCV nucleocapsids may be achieved by interaction between core protein and E1 (Lo *et al.*, 1996). The first hydrophobic domain of E1 has been implicated in such an interaction that is thought to occur at intracellular membranes via the C-terminal hydrophobic domain of core (Ma *et al.*, 2002). On the one hand, the envelope glycoproteins are retained in the ER, suggesting that virus assembly occurs at this site. On the other hand, all nonstructural proteins reside in the membranous web where RNA replication proceeds (Gosert *et al.*, 2003). This observation raises the question whether newly produced positive-stranded RNAs are transported to the ER or perhaps transported to a particular assembly compartment or whether the structural proteins are transported to or expressed in the membranous web. Wherever HCV nucleocapsid formation and envelopment occur, it is assumed that virus particles are released from the cell via the constitutive secretory pathway. In fact, structural proteins were detected in both the ER and *cis* Golgi compartment of infected cells, but the low efficiency of this system did not allow detailed studies (Serafino *et al.*, 2003). Moreover, complex N-linked glycans, indicative for Golgi transit, were found on the surface of virus particles partially purified from patient sera, but it is not clear whether these glycans are part of the viral envelope proteins or if they belong to cellular proteins that are tightly associated with the virus envelope (Sato *et al.*, 1993). Unfortunately, a clarification of these important questions is not possible with currently available cell culture systems for HCV.

VI. VIRUS–HOST INTERACTION

A. *Cell Culture Adaptation and Host-Cell Permissiveness*

Probably one of the most fascinating interplays between HCV RNA replication and the host cell relates to cell culture adaptation. As observed for many other viruses, especially those with a high mutation rate, passages in cell culture for prolonged times give rise to mutations that often improve virus replication *in vitro* but that frequently lead to an attenuation *in vivo*. Similarly, high-level HCV replication in Huh-7 cells is primarily due to cell culture-adaptive mutations that emerge in selectable replicons when cells are passaged under continuous selective pressure. When analyzing the nucleotide sequence of multiple replicons that were isolated from a given cell clone, at least one mutation was found that is conserved between all replicons in this cell clone, and this conserved mutation enhanced RNA replication (Blight *et al.*, 2000, 2003; Grobler *et al.*, 2003; Guo *et al.*, 2001; Kato *et al.*, 2003; Lohmann *et al.*, 2001). Cell culture-adaptive mutations were not observed in the 5'- and 3'-NTRs but were found in most nonstructural proteins with a clustering in certain regions (Blight *et al.*, 2000; Guo *et al.*, 2001; Ikeda *et al.*, 2002; Lohmann *et al.*, 2001, 2003) (Fig. 5A). Most mutations map to the center of NS5A and often affect serine residues required for hyperphosphorylation (Asabe *et al.*, 1997; Blight *et al.*, 2000; Kaneko *et al.*, 1994; Lohmann *et al.*, 2003; Tanji *et al.*, 1995b). A second cluster of adaptive mutations was found at a single position close to the carboxy terminus of the NS3 serine proteinase domain and at the N-terminal helicase domain (Blight *et al.*, 2003; Lohmann *et al.*, 2003). Interestingly, most of these mutations reside at one particular site of the solvent-accessible surface of helicase domain 1 (Blight *et al.*, 2003; Krieger *et al.*, 2001) (Fig. 5). The third cluster of adaptive mutations maps to two very distinct positions in NS4B (amino acids 1846 and 1897 of the HCV Con-1 polyprotein (Guo *et al.*, 2001; Kishine *et al.*, 2002; Lohmann *et al.*, 2003). According to the topology model of NS4B (Fig. 6), these two positions reside on the cytoplasmic loop connecting TM domains 2 and 3 and at the cytoplasmic C terminus of TM domain 4. The latter mutation at position 1897 has been found in replicons derived from two different HCV isolates of genotype 1b (Kishine *et al.*, 2002; Lohmann *et al.*, 2003). Moreover, introduction of the single adaptive mutation S2204I in NS5A that was identified with a genotype 1b replicon Con-1, into a genotype 1a replicon, was a crucial prerequisite for replication of this RNA, which indicates that at least some of the cell culture-adaptive mutations are operating with

different HCV isolates (Blight *et al.*, 2003; Windisch, M. P., Lohmann, V., and Bartenschlager, R., unpublished observations).

The demonstration of a replication enhancement exerted by such mutations was initially made by inserting them individually into the parental replicon construct and determining the number of G418-resistant cell colonies per microgram of transfected RNA. Later on, transient replication assays were developed that avoided the cumbersome and time-consuming selection of G418-resistant cell clones by a rapid and more direct analysis. In one version of this assay, a reporter gene or a transactivator was inserted instead of the selectable marker. With the introduction of a cell culture-adaptive mutation into the HCV coding region and transfection of Huh-7 cells, RNA replication was monitored by determining reporter gene activity or the level of transactivation (Krieger *et al.*, 2001; Yi *et al.*, 2002). Alternatively, self-amplification of adapted replicons was determined by quantitative RT-PCR (Blight *et al.*, 2000). By using these methods, the K1846T substitution in NS4B and the S2204I or S2204R substitutions in NS5A were found to enhance RNA replication most efficiently (at least in replicons derived from the HCV Con-1 isolate), whereas the weakest effect, if any, was achieved with mutations in NS3. However, when cell culture-adaptive mutations in NS3 were combined with those in NS4B, NS5A, or NS5B, RNA replication was increased cooperatively both in genotype 1b- and 1a-derived replicons (Blight *et al.*, 2003; Krieger *et al.*, 2001; Lohmann *et al.*, 2003; Yi *et al.*, 2002). In contrast, the combination of highly adaptive mutations in NS4B, NS5A, or NS5B with each other led to a decrease or even a complete block of replication (Lohmann *et al.*, 2003). These observations explain why the adaptive mutations in the NS4B to NS5B coding sequence were not found in combination with each other in a given HCV replicon (Fig. 5A). In contrast, mutations in NS3 were always found in association with one of the substitutions in the NS4B to NS5B region, indicating that the increase of RNA replication exerted by the NS3 mutations was not sufficient to establish persistent replication. Taken together, these results suggest that the mechanism of cell culture adaptation achieved by mutations in NS3 is different from the one exerted by substitutions in the NS4B to NS5B region.

It is not known how these mutations increase RNA replication in cell culture. It should be noted that these substitutions have not been found *in vivo* and almost invariably affect highly conserved amino acid residues. The only exception is the E1202G substitution that is present in about 5% of the HCV genomes reported in the DNA database (Lohmann *et al.*, 2003). Based on the X-ray crystal structure of NS5B

and full-length NS3 complexed with NS4A, the positions of several adaptive mutations were found to reside on the surface of the molecules and far away from the active sites of the enzymes (Fig. 5). It is, therefore, assumed that these mutations affect potential interaction sites between HCV proteins and cellular proteins. Alternatively, cell culture-adaptive mutations may influence the interaction between viral proteins or between viral proteins and RNA. In this case, adaptation should in principle be independent from a given cell line. One may therefore wonder why such mutations have not been observed *in vivo* because their emergence should increase RNA replication and lead to a selective growth advantage of the mutant. Several mechanisms, however, may operate that counterselect for high replicating mutants *in vivo*. First, high replication might stimulate a strong immune response, leading to the rapid elimination of these mutants; second, high-level HCV RNA replication may induce a selective stress response in the cell that leads to a down-regulation of HCV production or that can even induce apoptosis of the infected cell (Section VI,B); third, high-level RNA replication may interfere with virus particle formation. Translation, replication, and packaging are presumably tightly coupled reactions, requiring a mechanism that balances each of these steps. An “over-replication” might interfere with the encapsidation of positive-stranded RNA (e.g., by trapping viral RNA in replication complexes at the membranous web). If this assumption is true, one might expect that a wild-type HCV genome that does not contain adaptive mutations should allow particle production, which has not been observed with HCV genomes that carry adaptive mutations. In agreement with this assumption, the authors of this discussion found that adaptive mutations indeed prevent the release of HCV core protein into the culture supernatant of cells transfected with HCV genomes (Pietschmann, T., and Bartenschlager, R., unpublished results). Future experiments will determine whether these core-containing structures represent true infectious virus particles.

To determine whether cell culture-adaptive mutations affect infectivity *in vivo*, three such mutations (E1202G and T1280I in NS3 as well as S2197P in NS5A) were introduced into the infectious HCV Con-1 genome, and the RNA was inoculated intrahepatically into the liver of a chimpanzee. In several independent attempts, this genome failed to establish a productive infection (Bukh *et al.*, 2002). When genomes containing only the NS5A mutation were tested, the inoculated animal became viremic but only after a delay of about 1 week. Of note, all virus genomes recovered from the circulation corresponded to revertants. Thus, cell culture-adaptive mutations lead to an attenuation *in vivo*,

which might be the consequence of an inhibition of particle assembly, as has already been discussed. Although no intensive studies have been performed, an inverse correlation between the degree of cell culture adaptation and attenuation *in vivo* seems to exist. For instance, the HCV-N isolate has a very low infectivity *in vivo* (Beard *et al.*, 1999) but replicates efficiently in Huh-7 cells even in the absence of cell culture-adaptive mutations (Guo *et al.*, 2001; Ikeda *et al.*, 2002). A peculiarity of this genome is a four-amino-acid insertion in the center of NS5A that promotes replication in cell culture but is still tolerated sufficiently *in vivo*. In contrast, the H77 genotype 1a isolate that has a very high infectivity *in vivo* (Kolykhalov *et al.*, 1997) can only replicate in cell culture with the introduction of adaptive mutations (Blight *et al.*, 2003; Windisch, M. P., Lohmann, V., and Bartenschlager, R., unpublished results). The view of an apparent inverse correlation between RNA replication *in vivo* and *in vitro*, however, has been challenged. By using the HCV consensus genome of FH-1 that was derived from a patient with fulminant hepatitis, Kato *et al.* (2001) were able to establish a genotype 2a replicon that replicated with high efficiency in Huh-7 cells without cell culture-adaptive mutations (Kato *et al.*, 2003). In fact, the G418 transduction efficiency of selectable replicons derived from this isolate is about 50-fold higher compared to adapted replicons derived from the original HCV Con-1 isolate. Although this 2a genome has not been tested for its infectivity *in vivo*, this finding suggests that adaptive mutations may not always be necessary for replication in cell culture. A requirement for such mutations rather depends on the individual HCV isolate that is used for the construction of replicons.

Since 1999, cells of the human hepatoma cell line Huh-7 are frequently used as hosts for HCV replicons. Attempts to propagate HCV RNAs in other cell lines were not successful until Zhu *et al.* (2003a) first described the replication of subgenomic HCV RNAs in HeLa cells and the murine hepatoma cell line Hepa 1-6. Based on the assumption that replication in non-Huh-7 cells will require cell type-specific adaptive mutations, these authors used the total RNA of Huh-7 cells that stably replicated selectable HCV replicons. Owing to the high error rate of the NS5B RdRp, replicon RNAs in these cell clones have a much larger genetic heterogeneity compared to HCV RNAs synthesized by *in vitro* transcription of cloned DNA templates. In fact, a low number of G418-resistant colonies was obtained with HeLa and Hepa 1-6 cells but not with several other cell lines. Interestingly, in all cases, the major adaptive mutation in NS5A (S2204I) was preserved, but additional mutations were identified that were not present in the original

replicon used for transfection. Moreover, when total RNA of replicon-containing HeLa and Hepa 1–6 clones were passaged into naive cells, the number of G418-resistant colonies was consistently higher in comparison to *in vitro* transcripts carrying the same major adaptive mutations. This observation suggests that the additional mutations contribute to HCV RNA replication in these cell lines.

Ali *et al.* (2004) used a similar approach and established a human embryonic kidney 293 cell line containing HCV replicons. Initially, the group used coculturing of Huh-7 replicon cells with 293 cells. A low number of hybrids was obtained, one of which closely resembled naive 293 cells. Total RNA isolated from this cell clone was then transfected into naive 293 cells, giving rise to a number of stable replicon cell clones. Sequence analysis identified a large number of mutations that may confer adaptation specifically to 293 cells (Ali *et al.*, 2004).

Although the establishment of non-Huh-7 replicon cells has thus far not been possible with *in vitro* transcripts derived from genotype 1b replicons, the establishment of cells has been achieved with replicons derived from the genotype 2a replicon of FH-1 (Date *et al.*, 2004). Presumably owing to its exceptionally high replication capacity, transfection of two human liver cell lines (HepG2 and IMY-9) yielded viable replicon cell clones although efficiency of colony formation was reduced 100-fold to 1000-fold compared to Huh-7 cells. A cell culture-adaptive mutation in NS5B that was originally discovered in Huh-7 replicon cells increased the number of colonies with HepG2 and IMY-9 cells moderately. Several cell clones, however, contained replicons without mutations in the HCV coding region, demonstrating that this particular genotype 2a isolate can replicate in various cell lines in the absence of adaptive mutations. In summary, these results show that HCV replication does not depend on hepatocyte or primate-specific factors. The possibility to adapt HCV replicons to a murine cell line (Hepa 1–6) may open new avenues to develop a small animal model.

Since those observations, studies have demonstrated that in addition to cell culture-adaptive mutations, the host cell environment substantially affects the efficiency of HCV RNA replication (Blight *et al.*, 2002; Lohmann *et al.*, 2003; Murray *et al.*, 2003). Two independent lines of evidence support this conclusion. The first one stems from the observation that efficient HCV RNA replication can only be observed in a subpopulation of Huh-7 cells (Blight *et al.*, 2002; Murray *et al.*, 2003). This finding implies that at a given time, only a subset of cells is permissive and supports replication. Consequently, after transfection of selectable HCV replicons and subsequent selection, these

cells should be enriched, and removal of the replicon, in turn, should lead to a highly permissive cell population. This assumption has been confirmed. Cells that carry a stably replicating replicon were treated with IFN- α or a selective inhibitor (Blight *et al.*, 2002; Murray *et al.*, 2003). Both compounds led to an efficient block in HCV replication, and replicons were virtually eliminated after several weeks of treatment. Upon retransfection of these “cured” cells with selectable HCV replicons and selection, the number of cell clones was about fivefold higher compared to the number that was obtained with naive control cells. This result demonstrates that “cured” cells provide a more favorable environment for HCV RNA replication (Blight *et al.*, 2002; Murray *et al.*, 2003). The second line of evidence is based on the observation that different passages of Huh-7 cells may differ in their permissiveness by up to 100-fold in transient replication assays (Lohmann *et al.*, 2003). This difference was independent from the kind of adaptive mutation introduced into the replicon and also observed with nonadapted RNAs. The level of permissiveness, however, was difficult to control and subject to variations that could not be predicted. In a search for the underlying mechanism, variations in IRES-dependent HCV RNA translation and differences in RNA stability could be excluded (Lohmann *et al.*, 2003). Thus, one explanation is that the level of permissiveness is determined by host-cell factors required for RNA replication. In line with this assumption, it was found that replication efficiency decreased with increasing amounts of replicon RNA transfected into Huh-7 cells, which suggests that host-cell factors limit RNA amplification (Lohmann *et al.*, 2003).

B. Cytopathic Effects Exerted by HCV

The induction of membrane rearrangements and the synthesis of membrane-associated HCV proteins may have several consequences for the cell. One consequence involves interference with secretion as well as expression of cell surface proteins (Konan *et al.*, 2003; Tardiff *et al.*, 2003). Such effects were observed in cells that express an uncleaved NS4A-B protein as well as in Huh-7 cells that carry an HCV full-length genome, resulting in a reduced surface expression of several proteins, including MHC-I (Konan *et al.*, 2003). Morphologically, in NS4A-B expressing cells, two distinct membrane alterations were observed and designated as “swollen, partially vesiculated membranes” and “clustered aggregated membranes” with NS4A-B localizing only to the latter. These data suggest that HCV infection probably has a profound effect on host-cell homeostasis.

A second consequence involves membrane alterations induced by HCV proteins that may provoke an ER stress response. Usually, ER stress is induced by the loss of ER calcium homeostasis or the accumulation of misfolded, aggregated proteins (reviewed in Ma and Hendershot, 2001). ER stress induces an adaptive cellular response that leads, among other results, to the proteolytic cleavage and subsequent activation of the latent transcription factor ATF6. Another consequence is the activation of PKR-like ER kinase (PERK) that, via phosphorylation of the translation initiation factor eIF-2 α reduces RNA translation. Prolonged, high-level ER stress can even induce apoptosis by the activation of the ER-associated caspase 12. In fact, evidence suggests that in cells carrying HCV replicons, ATF6 is cleaved and transported to the nucleus (Tardif *et al.*, 2002). Although only one cell clone was analyzed in this study, it suggests that HCV replication and protein expression induce ER stress. Moreover, an inhibition of PERK by E2 was described (Pavio *et al.*, 2003). By using *in vitro* pull-down assays and transient transfection studies, an interaction between PERK and E2 was found. Protein synthesis was enhanced by E2, and E2 conferred a resistance toward ER stress inducers. These studies, however, were performed only with E2 expressed on its own, whereas *in vivo*, this protein is expressed in a heterodimeric complex with E1. Thus, the contribution of E2 to PERK inhibition in an infected cell remains to be determined.

C. HCV and the Host's Innate Immune Response

Boosting the innate immune system with recombinant IFN- α has likely saved the lives of many patients with hepatitis C and is still a key part of all approved therapies currently in use to treat these patients. Given the importance of IFN- α as a therapeutic agent, it is surprising how little is known about the complex interplay between HCV and the innate immune system. IFNs are a rather diverse class of cytokines with the ability to trigger the immune response (reviewed in Goodbourn *et al.*, 2000; Samuel, 2001). Two types of IFNs can be distinguished that have partially overlapping biologic functions. Type I IFNs comprise 13 closely related IFN- α subtypes and IFN- β as well as the more distantly related IFN- κ , IFN- ω , and IFN- ε . Furthermore, a novel cytokine family has been discovered that shares some sequence similarities with type I IFNs and the IL-10 family. Accordingly, the members of this family have been named IL-29, IL-28A, and IL-28B (Sheppard *et al.*, 2003) or IFN- λ_1 , IFN- λ_2 , and IFN- λ_3 , respectively (Kotenko *et al.*, 2003). The only type II IFN gene is IFN- γ for which

neither sequence nor structural similarities with type I IFNs have been found. Both types of IFNs exert their functions by binding to specific cell surface receptor complexes, which leads to phosphorylation, dimerization, and nuclear import of latent transcription factors known as signal transducers and activators of transcription (STATs). Type I IFNs induce the formation of the IFN-stimulated gene factor-3 (ISGF-3), a heterotrimer consisting of STAT1, STAT2, and the IFN-response factor-9 (IRF-9/p48). ISGF-3 binds to and activates genes containing a promoter with at least one IFN-stimulated response element (ISRE). In contrast, IFN- γ induces the formation of the gamma activation factor (GAF), a STAT1 homodimer that enhances gene expression by binding to the gamma activation site (GAS). Although both types of IFNs induce the expression of a partially overlapping set of proteins, experiments with genetically targeted mice in which either the type I or the type II IFN receptor function has been destroyed demonstrate that type I IFNs mediate most of the early immune response against virus infections (Müller *et al.*, 1994). In contrast, the contribution of IFN- γ is believed to be rather systemic, such as by enhancing the expression of proteins involved in antigen processing and presentation, including proteasome subunits and MHC molecules. In addition, IFN- γ induces chemokines that enhance and direct the adaptive immunity. Data, however, are accumulating that in certain virus infections, such as hepatitis B, IFN- γ efficiently inhibits viral replication by inducing effector proteins with antiviral activities.

Another difference between the two types of IFNs is their origin. Type I IFNs are released by almost all virus-infected cells, but, depending on the circumstances, amounts may vary dramatically. For example, it has been observed that hepatocytes are rather poor producers (Keskinen *et al.*, 1999), whereas certain blood leukocytes, termed natural IFN-producing cells (IPCs) produce large amounts of type I IFNs during virus infections (Cella *et al.*, 1999). In contrast to type I IFNs, the expression of IFN- γ is restricted to immune cells, such as activated T lymphocytes and natural killer (NK) cells.

With the development of HCV replicons, it became possible to analyze the role of individual cytokines in the innate immune response against HCV. Because most patients with HCV respond at least initially to a treatment with IFN- α , it was not unexpected to find that type I IFNs also blocks HCV RNA replication in cell Huh-7 cells (Blight *et al.*, 2000; Frese *et al.*, 2001; Guo *et al.*, 2001; Kato *et al.*, 2003), HuH6 cells (Windisch, M. P., and Bartenschlager, R., unpublished results), and cells of nonhepatic origin, such as HeLa cells (Guo *et al.*, 2003) and 293 cells (Ali *et al.*, 2004). Furthermore, it has been demonstrated that

IFN- γ is as potent as IFN- α in inhibiting HCV replicons (Frese *et al.*, 2002; Kato *et al.*, 2003; Lanford *et al.*, 2003a). These findings suggest that cytotoxic T cells and NK cells contribute to HCV clearance not only by killing cells but also by producing IFN- γ , thereby stimulating infected hepatocytes to inhibit viral replication. Liu *et al.* (2003) have substantiated this hypothesis by co-culturing activated, HCV-specific CD8⁺ T cells together with Huh-7 cells containing HCV replicons. Under these conditions, the group observed that T cells execute most of their antiviral activities in an IFN- γ -dependent, noncytolytic manner (Liu *et al.*, 2003). *In vivo*, IFN- γ might have an even greater importance for HCV clearance than type I IFNs. According to Thimme *et al.* (2002), HCV replication rapidly induces but is not controlled by the intrahepatic expression of type I IFN-regulated effector proteins in experimentally infected chimpanzees. Viral clearance rather follows the entry and accumulation of HCV-specific T cells in the liver and is accompanied by the production of IFN- γ , a process that is not necessarily accompanied by the destruction of infected cells (Thimme *et al.*, 2002).

A hallmark of all IFNs is their ability to enhance the expression of numerous genes, but only a few of them are known to encode effector proteins with antiviral activities (Samuel, 2001). Among these IFNs is the human MxA protein, a cytoplasmic GTPase that efficiently inhibits the replication of a broad variety of RNA viruses such as orthomyxoviruses, bunyaviruses, rhabdoviruses, and togaviruses (reviewed in Haller and Kochs, 2002). In healthy individuals, MxA expression is below the detection limit but increases dramatically during many viral infections and as a consequence of IFN- α treatment. Elevated MxA expression levels have also been found in the liver of patients with HCV, indicating an ongoing struggle between the innate immune system and HCV (MacQuillan *et al.*, 2002, 2003; Patzwahl *et al.*, 2001). It is unlikely, however, that the MxA protein is involved because constitutive expression of MxA does not inhibit subgenomic HCV replicons, and expression of dominant-negative mutants of MxA does not restore HCV replication during IFN- α treatment (Frese *et al.*, 2001).

Another IFN-induced effector protein that has been suspected to interfere with HCV replication is PKR, a constitutively expressed serine/threonine kinase with multiple functions in the control of host-cell transcription and translation (reviewed in Clemens and Elia, 1997). It has been noted that the binding of PKR to double-stranded RNAs generated during virus replication leads to the activation of the enzyme and the subsequent inhibition of protein translation. HCV researchers became interested in PKR because two viral proteins have been described to interact with this kinase, thereby enabling HCV to

escape the innate immune response. Based on the analysis of HCV sequences from hepatitis C patients treated with IFN- α , mutations within a discrete region of NS5A, the so-called IFN-sensitivity determining region (ISDR), were proposed to confer resistance to IFN- α (Enomoto *et al.*, 1995, 1996b). Although numerous subsequent studies were conducted to determine the predictive value of NS5A sequences in the outcome of IFN- α therapy, the existence of an ISDR is still controversially discussed (reviewed in Tan and Katze, 2001). Nevertheless, the description of the ISDR put NS5A in the focus of research. The finding that mutations in the ISDR affect the ability of NS5A to bind to and inhibit PKR (Gale *et al.*, 1998) led to the hypothesis that PKR blocks HCV replication, and NS5A is able to counteract antiviral activity of PKR. Experiments with HCV replicons, however, provided no further evidence for an involvement of NS5A in IFN resistance. On the contrary, point mutations in the ISDR or a deletion of 47 amino acids encompassing the entire ISDR enhanced viral replication without affecting IFN sensitivity of HCV replicons (Blight *et al.*, 2000; Guo *et al.*, 2001). These findings were extended in our (the authors of this chapter) laboratory by using two subgenomic genotype 1b replicons that differ only in their NS5A sequence. In one replicon, the ISDR was identical to that of IFN-susceptible strains, whereas the ISDR sequence of the other replicon contained mutations that have been suspected to confer IFN resistance and PKR binding (Gale *et al.*, 1998). Nevertheless, both replicons were equally sensitive to IFN- α (Kaul, A., and Bartenschlager, R., unpublished results). These results argue against a role of NS5A in directly blocking PKR. Alternatively, NS5A may counteract the IFN- α -induced antiviral state in a way that cannot be determined in the replicon system.

Of note, a second HCV protein has been reported to interact with PKR. It was found that E2 binds to PKR through its PKR-eIF-2 α homology domain (PePHD) (Pavio *et al.*, 2002; Taylor *et al.*, 1999). The significance of this observation has been challenged because an increasing number of clinical studies demonstrate that the PePHD is a highly conserved region with no conspicuous mutations accumulating during IFN- α therapy (reviewed in Tan and Katze, 2001). Furthermore, E2 expression does not seem to increase the resistance of HCV genotype 1b replicons toward IFNs. A genomic replicon that encodes an E2 protein with the PePHD sequence of a resistant HCV isolate had a similar degree of susceptibility as a subgenomic replicon lacking E2 (Frese *et al.*, 2002; Kaul, A., and Bartenschlager, R., unpublished results). The question whether PKR interferes with HCV RNA replication/translation was addressed in our laboratory by using small interfering

RNAs that target PKR mRNAs for degradation. We observed that a down-regulation of PKR expression levels did not restore HCV replication in the presence of IFN- α (Kaul, A., and Bartenschlager, R. unpublished results). Taken together, these data suggest that PKR is not the (major) effector protein involved in the IFN-induced inhibition of HCV.

Similar to PKR, 2'-5'oligoadenylate synthetases (OAS) are IFN-induced effector proteins that can trigger a general protein shut-off in virus-infected cells (reviewed in Samuel, 2001). The binding of OAS to dsRNA triggers its enzymatic activity and leads to the production of small oligoadenylates. These oligonucleotides bind to and activate the latent ribonuclease RNase L, which results in the degradation of both viral and cellular RNAs. In this context, it is interesting to note that an HCV protein has been implicated in the inhibition of OAS pathway. Taguchi *et al.* (2004) reported that the N-terminal portion of NS5A (amino acid 1 to 148) that lacks the ISDR and PKR-binding domain binds to OAS and is able to counteract the antiviral activity of IFN- α . It is, however, not yet known whether the OAS pathway indeed contributes to the IFN-induced inhibition of HCV replication. Only a few other IFN-induced effector proteins (e.g., the inducible nitric oxide synthetase and the indoleamine 2,3-dioxygenase) have been analyzed for their potential to inhibit HCV replicons, but none of them were found to interfere with HCV RNA replication (Frese *et al.*, 2002; Zhu *et al.*, 2003b). Thus, it is not known by which mechanism(s) IFNs inhibit HCV replication.

Several attempts have been made to systematically analyze the IFN-induced changes in the gene expression of HCV host cells. In two approaches, chimpanzees were experimentally infected with HCV, liver biopsy samples were taken, and the gene expression profile was monitored by using cDNA microarrays. The results revealed that the infection of the liver rapidly induces the up-regulation of numerous genes, including those encoding well-known IFN-induced effector proteins, such as the chimpanzee homologue of MxA (Bigger *et al.*, 2001; Su *et al.*, 2002). In both studies, the expression of MxA and that of other IFN- α -induced genes correlated well with the magnitude and duration of the infection, but transient and sustained viral clearance were rather associated with the induction of IFN- γ and the expression of IFN- γ -induced genes, suggesting a biphasic course of the innate immune response and a crucial role for IFN- γ in virus clearance. In another approach, cDNA microarrays were used to analyze IFN- α -induced changes in the gene expression profile of Huh-7 cells

containing HCV replicons (Zhu *et al.*, 2003b). Even if these studies did not directly lead to the identification of proteins inhibiting HCV replication, they will guide future investigations by providing lists of potential candidate genes.

Many, if not all, viruses have evolved mechanisms to counteract the innate immune response of their hosts. Viruses have been reported to prevent the induction of IFNs, intercept already secreted IFN molecules by soluble decoy receptors, block intracellular signaling pathways, down-regulate the expression of IFN-induced effector proteins, or inhibit IFN activities (reviewed in Basler and Garcia-Sastre, 2002; Goodbourn *et al.*, 2000). HCV has also been reported to interfere with several aspects of the innate immune response. As outlined and discussed earlier in this section, the binding of NS5A and/or E2 to PKR and OAS has been proposed to hinder the host cell from reducing viral protein translation. Furthermore, it has been demonstrated that the constitutive expression of NS5A enhances the expression of IL-8, thereby triggering signaling pathways that partly antagonize the effect of IFN- α (Girard *et al.*, 2002; Polyak *et al.*, 2001a,b). Such a mechanism might explain why the expression of the entire HCV polyprotein in osteosarcoma cells and in transgenic mice leads to an impaired Jak-STAT signaling and an increased susceptibility to virus infections (Blindenbacher *et al.*, 2003; Heim *et al.*, 1999). A microarray-based analysis of IFN-induced changes in the gene expression profile of Huh-7 cells with or without a subgenomic HCV replicon, however, revealed no further evidence that HCV nonstructural proteins such as NS5A generally affect the responsiveness to IFN- α (Geiss *et al.*, 2003).

An alternative way how HCV might escape the innate immune response has been reported by Foy *et al.* (2003), who demonstrated that the NS3/4A proteinase blocks the phosphorylation of the IFN regulatory factor-3, a transcription factor required for the activation of type I IFN genes. Furthermore, it has been noted by Keskinen *et al.* (1999) that hepatocytes are generally rather poor producers of type I IFNs. Taken together, these findings suggest that HCV-infected hepatocytes are not able to produce enough IFNs to trigger a strong intrahepatic innate immune response. This hypothesis is in line with findings made by Mihm *et al.* (2004) who did not detect increased levels of type I IFN mRNAs in most liver biopsy samples of chronic hepatitis C patients. The same specimens, however, often contained high numbers of IFN-induced mRNAs (e.g., MxA mRNAs). The finding that matching blood contained elevated mRNA levels of several type I IFNs (Mihm *et al.*, 2004) might explain the intrahepatic expression of type I

IFN-regulated genes in the absence of a detectable amount of intrahepatic type I IFN mRNAs.

The fact that most HCV-infected individuals do not spontaneously clear the virus but do so after a treatment with IFN- α suggests that the ability of HCV to control the innate immune system is an important prerequisite for a persistent infection. Thus, a better understanding of the underlying molecular mechanism by which the innate immune system inhibits HCV replication will certainly help develop new strategies to fight chronic hepatitis C.

VII. ANTIVIRAL THERAPIES

A. *Interferons and Ribavirin*

All therapies currently in use to treat patients with HCV rely on the antiviral activity of IFN- α that is given either alone or in combination with D-ribavirin. Due to space limitations, this section does not engage in the description of therapy regimens, side effects, and success rates but rather refers to other reviews that cover these issues (Alberti *et al.*, 2002; Jonas, 2002; McHutchison and Fried, 2003; Sulkowski and Thomas, 2003). In the following, the discussion will focus on observations that shed light onto a novel mechanism by which ribavirin may exert its antiviral effect (Crotty *et al.*, 2000, 2002). By using *Poliovirus* as a model system, it was shown that at high concentrations, ribavirin is accepted by the RdRp as a substrate and incorporated into newly synthesized RNAs. Because ribavirin can form base pairings both with cytidine and with uridine, incorporation of this drug leads to an increase of G-to-A and C-to-U transition mutations. Although the Kd of the polioviral RdRp for ribavirin is rather high, its incorporation may be enhanced by the inhibition of inosine monophosphate dehydrogenase that is caused by ribavirin as well and that leads to a depletion of intracellular GTP pools. These mechanisms increase the mutation rate to a level in which the majority of newly produced virus genomes carry lethal mutations (Crotty *et al.*, 2002).

It has been shown that ribavirin also increases the error rate of HCV NS5B RdRp. Treatment of cells with ribavirin leads to a reduction of infectivity of progeny virus that is released from infected primary hepatocytes and leads to an increase of the mutation rate of HCV replicons when high concentrations of this drug were used (Contreras *et al.*, 2002; Lanford *et al.*, 2003a). Although this mode of action

explains a block of productive virus replication, it is still unclear why ribavirin primarily reduces the number of relapse patients (i.e. patients treated with IFN- α monotherapy in which HCV rebounds after cessation of therapy), whereas in ribavirin monotherapy, virus titers are not reduced. It has been proposed that the antiviral effect of ribavirin cannot be measured by the determination of HCV RNA levels because ribavirin does not affect the overall RNA production but rather the infectivity of progeny HCV, which so far can also not be measured (Crotty *et al.*, 2002). In the long run, however, a reduction of infectious virus production should lead to a reduction in viremia that so far has not been observed in patients treated with ribavirin monotherapy. Moreover, if ribavirin is accepted as a substrate by RdRp, resistance mutations should emerge that have not yet been observed. Further studies will therefore be required to clarify this issue.

B. Small Interfering RNAs

In principle, every step in a viral life cycle represents a target for antiviral intervention. For reasons of selectivity, viral enzymes that are only expressed in infected cells provide the best targets for antiviral drugs. A summary of all recent developments in this area is provided in two reviews by de Francesco and Rice (2003) and Tan *et al.* (2002). This section, therefore, only describes a novel, yet more theoretical approach that is based on RNA interference (RNAi).

RNAi is a conserved cellular response to double-stranded RNA, in which small RNA duplexes, so-called small interfering RNAs (siRNAs), target homologous sequences for degradation (reviewed in Hannon, 2002). In plants, RNAi is an important antiviral defense mechanism (Waterhouse *et al.*, 2001). Whether mammalian viruses encounter RNAi-based defense mechanisms is not clear. Although mammalian cells express Dicer homologues, they normally do not produce siRNAs from exogenous double-stranded RNAs (reviewed in Caplen *et al.*, 2003). Nevertheless, RNAi can be used to inhibit virus replication in mammalian cells. It has been demonstrated that the transfection of chemically synthesized siRNAs efficiently inhibits the multiplication of HIV-1 (Jacque *et al.*, 2002) and that of several other viruses (reviewed in Caplen *et al.*, 2003). It has also been shown that HCV RNA replication is also sensitive to RNAi (Kapadia *et al.*, 2003; Krönke *et al.*, 2004; Randall *et al.*, 2003; Yokota *et al.*, 2003). The high degree of sequence diversity between different HCV genotypes and the rapid evolution of new quasi-species, however, is a problem for

the development of siRNA-based gene therapies because the antiviral activity of siRNAs depends very much on their complementarity to the target sequence. Thus, alternative strategies have been developed to overcome these obstacles. In one approach, HCV-specific siRNAs were prepared by digestion of *in vitro*-transcribed, double-stranded RNAs with RNase III from *E. coli*. These so-called esiRNAs simultaneously target multiple sites of the viral genome for degradation, a strategy that should prevent the evolution of escape mutants (Krönke *et al.*, 2004). In an alternative approach, siRNAs were designed to target highly conserved sequence motifs in the viral genome. The 5'-NTR or the early core coding region of the HCV genome has been mapped for sites that are both highly conserved between different HCV genotypes and sensitive for siRNAs (Krönke *et al.*, 2004; Yokota *et al.*, 2003). Interestingly, two sites were identified that can be used to target all known genotypes by universal siRNAs (Krönke *et al.*, 2004). Furthermore, a new method for the induction of RNAi has been explored. Brummelkamp *et al.* (2002) demonstrated that the constitutive expression of short hairpin RNAs (shRNAs) results in a persistent silencing of host gene expression and inspired virologists to construct plasmids and pseudo-typed retroviruses encoding HCV-specific shRNAs. Experiments with HCV replicons demonstrate that shRNAs can indeed be used to block HCV RNA replication in cultured cells (Krönke *et al.*, 2004; Yokota *et al.*, 2003). Moreover, transduced cells that stably express HCV-specific shRNAs were found to be largely resistant to a subsequent challenge with HCV replicons (Krönke *et al.*, 2004). These data suggest that a therapeutic induction of RNAi by shRNAs might be used in the future as an alternative approach to treat hepatitis C.

VIII. CONCLUDING REMARKS

The discovery of HCV about 15 years ago triggered worldwide efforts to analyze and devise methods to combat this pathogen. Important progress has been made in several areas, and the field's arsenal of experimental tools has grown considerably. Cell culture systems are now available that recapitulate most of the intracellular part of the HCV life cycle. These systems will undoubtedly help us to study various facets of HCV RNA replication and persistence in molecular details. More open than answered questions exist, but rapid progress can be expected in the next few years.

IX. NOTE

Recent experiments performed in the laboratory of Dr. Takaji Wakita (Department of Microbiology, Tokyo Metropolitan Institute for Neuroscience, Tokyo, Japan) and in our laboratory revealed that transfection of cultured cells with the JFH-1 genotype 2a consensus genome (Kato *et al.*, 2001) yields virus particles that are infectious in cell culture (Wakita *et al.*, 2004; Pietschmann *et al.*, 2004). These findings demonstrate that it is now possible to study the full multiplication cycle of HCV in cell culture.

ACKNOWLEDGMENTS

We are indebted to our colleagues Francois Penin for providing Fig. 5 and help in structural modeling, Rainer Gosert for providing the electron micrograph shown in Fig. 2, and Takaji Wakita for permission to cite his unpublished work. We thank Sandra Sparacio and Matthias Reiss for a careful reading of the manuscript and all past and present members of our laboratory for their contributions. Work in the authors' laboratory was supported by grants from the European Union (QLRT-PL 1999-00356 and QLRT-2001-01329), the Sonderforschungsbereich 638 (Teilprojekt A5), the Kompetenznetz Hepatitis (01 KI 0102 and TP 15.3), Axxima Pharmaceuticals, and the Bristol-Myers-Squibb Foundation.

REFERENCES

- Agapov, E. V., Murray, C. L., Frolov, I., Qu, L., Myers, T. M., and Rice, C. M. (2004). Uncleaved NS2-3 is required for production of infectious bovine viral diarrhea virus. *J. Virol.* **78**:2414–2425.
- Agnello, V., Abel, G., Elfahal, M., Knight, G. B., and Zhang, Q. X. (1999). Hepatitis C virus and other Flaviviridae viruses enter cells via low-density lipoprotein receptor. *Proc. Natl. Acad. Sci. USA* **96**:12766–12771.
- Ago, H., Adachi, T., Yoshida, A., Yamamoto, M., Habuka, N., Yatsunami, K., and Miyano, M. (1999). Crystal structure of the RNA-dependent RNA polymerase of hepatitis C virus. *Struc. Fold. Des.* **7**:1417–1426.
- Alberti, A., Boccatto, S., Vario, A., and Benvegna, L. (2002). Therapy of acute hepatitis C. *Hepatology* **36**:S195–S200.
- Ali, S., Pellerin, C., Lamarre, D., and Kukulj, G. (2004). Hepatitis C virus subgenomic replicons in the human embryonic kidney 293 cell line. *J. Virol.* **78**:491–501.
- Ali, N., Pruijn, G. J., Kenan, D. J., Keene, J. D., and Siddiqui, A. (2000). Human La antigen is required for the hepatitis C virus internal ribosome entry site-mediated translation. *J. Biol. Chem.* **275**:27531–27540.
- Ali, N., and Siddiqui, A. (1995). Interaction of polypyrimidine tract-binding protein with the 5'-noncoding region of the hepatitis C virus RNA genome and its functional requirement in internal initiation of translation. *J. Virol.* **69**:6367–6375.
- Ali, N., and Siddiqui, A. (1997). The La antigen binds 5'-noncoding region of the hepatitis C virus RNA in the context of the initiator AUG codon and stimulates

- internal ribosome entry site-mediated translation. *Proc. Natl. Acad. Sci. USA* **94**:2249–2254.
- Ali, N., Tardif, K. D., and Siddiqui, A. (2002). Cell-free replication of the hepatitis C virus subgenomic replicon. *J. Virol.* **76**:12001–12007.
- Alter, H. J., Purcell, R. H., Holland, P. V., and Popper, H. (1978). Transmissible agent in non-A, non-B hepatitis. *Lancet* **1**:459–463.
- Alter, H. J., Purcell, R. H., Shih, J. W., Melpolder, J. C., Houghton, M., Choo, Q. L., and Kuo, G. (1989). Detection of antibody to hepatitis C virus in prospectively followed transfusion recipients with acute and chronic non-A, non-B hepatitis. *N. Engl. J. Med.* **321**:1494–1500.
- Andino, R., Rieckhof, G. E., Achacoso, P. L., and Baltimore, D. (1993). Poliovirus RNA synthesis utilizes an RNP complex formed around the 5′-end of viral RNA. *EMBO J.* **12**:3587–3598.
- Andre, P., Komurian-Pradel, F., Deforges, S., Perret, M., Berland, J. L., Sodoyer, M., Pol, S., Brechot, C., Paranhos-Baccala, G., and Lotteau, V. (2002). Characterization of low- and very-low-density hepatitis C virus RNA-containing particles. *J. Virol.* **76**:6919–6928.
- Andrews, N. C., and Baltimore, D. (1986). Purification of a terminal uridylyltransferase that acts as host factor in the *in vitro* poliovirus replicase reaction. *Proc. Natl. Acad. Sci. USA* **83**:221–225.
- Arias, C. F., Preugschat, F., and Strauss, J. H. (1993). Dengue 2 virus NS2B and NS3 form a stable complex that can cleave NS3 within the helicase domain. *Virology* **193**:888–899.
- Asabe, S. I., Tanji, Y., Satoh, S., Kaneko, T., Kimura, K., and Shimotohno, K. (1997). The N-terminal region of hepatitis C virus-encoded NS5A is important for NS4A-dependent phosphorylation. *J. Virol.* **71**:790–796.
- Aizaki, H., Nagamori, S., Matsuda, M., Kawakami, H., Hashimoto, O., Ishiko, H., Kawada, M., Matsuura, T., Hasumura, S., Matsuura, Y., Suzuki, T., and Miyamura, T. (2003). Production and release of infectious hepatitis C virus from human liver cell cultures in the three-dimensional radial-flow bioreactor. *Virology* **314**:16–25.
- Banerjee, R., and Dasgupta, A. (2001). Specific interaction of hepatitis C virus protease/helicase NS3 with the 3′-terminal sequences of viral posi. *J. Virol.* **75**:1708–1721.
- Barba, G., Harper, F., Harada, T., Kohara, M., Goulinet, S., Matsuura, Y., Eder, G., Schaff, Z., Chapman, M. J., Miyamura, T., and Brechot, C. (1997). Hepatitis C virus core protein shows a cytoplasmic localization and associates to cellular lipid storage droplets. *Proc. Natl. Acad. Sci. USA* **94**:1200–1205.
- Barbato, G., Cicero, D. O., Nardi, M. C., Steinkühler, C., Cortese, R., De, F. R., and Bazzo, R. (1999). The solution structure of the N-terminal proteinase domain of the hepatitis C virus (HCV) NS3 protein provides new insights into its activation and catalytic mechanism. *J. Mol. Biol.* **289**:371–384.
- Bartenschlager, R. (1999). The NS3/4A proteinase of the hepatitis C virus: Unravelling structure and function of an unusual enzyme and a prime target for antiviral therapy. *J. Viral Hepat.* **10**:1–2.
- Bartenschlager, R., Ahlborn-Laake, L., Mous, J., and Jacobsen, H. (1993). Nonstructural protein 3 of the hepatitis C virus encodes a serine-type proteinase required for cleavage at the NS3/4 and NS4/5 junctions. *J. Virol.* **67**:3835–3844.
- Bartenschlager, R., Ahlborn-Laake, L., Mous, J., and Jacobsen, H. (1994). Kinetic and structural analyses of hepatitis C virus polyprotein processing. *J. Virol.* **68**:5045–5055.

- Bartenschlager, R., Ahlborn-Laake, L., Yasargil, K., Mous, J., and Jacobsen, H. (1995a). Substrate determinants for cleavage *in cis* and *in trans* by the hepatitis C virus NS3 proteinase. *J. Virol.* **69**:198–205.
- Bartenschlager, R., and Lohmann, V. (2001). Novel cell culture systems for the hepatitis C virus. *Antiviral Res.* **52**:1–17.
- Bartenschlager, R., Lohmann, V., Wilkinson, T., and Koch, J. O. (1995b). Complex formation between the NS3 serine-type proteinase of the hepatitis C virus and NS4A and its importance for polyprotein maturation. *J. Virol.* **69**:7519–7528.
- Bartosch, B., Dubuisson, J., and Cosset, F. L. (2003a). Infectious hepatitis C virus pseudo-particles containing functional E1–E2 envelope protein complexes. *J. Exp. Med.* **197**:633–642.
- Bartosch, B., Vitelli, A., Granier, C., Goujon, C., Dubuisson, J., Pascale, S., Scarselli, E., Cortese, R., Nicosia, A., and Cosset, F. L. (2003b). Cell entry of hepatitis C virus requires a set of coreceptors that include the CD81 tetraspanin and the SR-B1 scavenger receptor. *J. Biol. Chem.* **278**:41624–41630.
- Bashirova, A. A., Geijtenbeek, T. B., van Duijnhoven, G. C., Van Vliet, S. J., Eilering, J. B., Martin, M. P., Wu, L., Martin, T. D., Viebig, N., Knolle, P. A., Kewal-Ramani, V. N., van Kooyk, Y., and Carrington, M. (2001). A dendritic cell-specific intercellular adhesion molecule 3-grabbing nonintegrin (DC-SIGN)-related protein is highly expressed on human liver sinusoidal endothelial cells and promotes HIV-1 infection. *J. Exp. Med.* **193**:671–678.
- Basler, C. F., and Garcia-Sastre, A. (2002). Viruses and the type I interferon antiviral system: Induction and evasion. *Int. Rev. Immunol.* **21**:305–337.
- Baumert, T. F., Ito, S., Wong, D. T., and Liang, T. J. (1998). Hepatitis C virus structural proteins assemble into virus-like particles in insect cells. *J. Virol.* **72**:3827–3836.
- Bazan, J. F., and Fletterick, R. J. (1989). Detection of a trypsin-like serine protease domain in flaviviruses and pestiviruses. *Virology* **171**:637–639.
- Bazan, J. F., and Fletterick, R. J. (1990). Structural and catalytic models of trypsin-like viral proteases. *Semin. Virol.* **1**:311–322.
- Beames, B., Chavez, D., Guerra, B., Notvall, L., Brasky, K. M., and Lanford, R. E. (2000). Development of a primary tamarin hepatocyte culture system for GB virus-B: A surrogate model for hepatitis C virus. *J. Virol.* **74**:11764–11772.
- Beames, B., Chavez, D., and Lanford, R. E. (2001). GB virus B as a model for hepatitis C virus. *ILAR J.* **42**:152–160.
- Beard, M. R., Abell, G., Honda, M., Carroll, A., Gartland, M., Clarke, B., Suzuki, K., Lanford, R., Sangar, D. V., and Lemon, S. M. (1999). An infectious molecular clone of a Japanese genotype 1b hepatitis C virus. *Hepatology* **30**:316–324.
- Behrens, S. E., Tomei, L., and de Francesco, R. (1996). Identification and properties of the RNA-dependent RNA polymerase of hepatitis C virus. *EMBO J.* **15**:12–22.
- Bigger, C. B., Brasky, K. M., and Lanford, R. E. (2001). DNA microarray analysis of chimpanzee liver during acute resolving hepatitis C virus infection. *J. Virol.* **75**:7059–7066.
- Blanchard, E., Brand, D., Trassard, S., Goudeau, A., and Roingeard, P. (2002). Hepatitis C virus-like particle morphogenesis. *J. Virol.* **76**:4073–4079.
- Blanchard, E., Brand, D., and Roingeard, P. (2003a). Endogenous virus and hepatitis C virus-like particle budding in BHK-21 cells. *J. Virol.* **77**:3888–3889.
- Blanchard, E., Hourieux, C., Brand, D., Ait-Goughoulte, M., Moreau, A., Trassard, S., Sizaret, P.Y., Dubois, F., and Roingeard, P. (2003b). Hepatitis C virus-like particle budding: Role of the core protein and importance of its Asp111. *J. Virol.* **77**:10131–10138.

- Blight, K., Lesniewski, R. R., LaBrooy, J. T., and Gowans, E. J. (1994). Detection and distribution of hepatitis C-specific antigens in naturally infected liver. *Hepatology* **20**:553–557.
- Blight, K. J., Kolykhalov, A. A., and Rice, C. M. (2000). Efficient initiation of HCV RNA replication in cell culture. *Science* **290**:1972–1974.
- Blight, K. J., McKeating, J. A., Marcotrigiano, J., and Rice, C. M. (2003). Efficient replication of hepatitis C virus genotype 1a RNAs in cell culture. *J. Virol.* **77**:3181–3190.
- Blight, K. J., McKeating, J. A., and Rice, C. M. (2002). Highly permissive cell lines for subgenomic and genomic hepatitis C virus RNA replication. *J. Virol.* **76**:13001–13014.
- Blight, K. J., and Rice, C. M. (1997). Secondary structure determination of the conserved 98-base sequence at the 3'-terminus of hepatitis C virus genome RNA. *J. Virol.* **71**:7345–7352.
- Blindenbacher, A., Duong, F. H., Hunziker, L., Stutvoet, S. T., Wang, X., Terracciano, L., Moradpour, D., Blum, H. E., Alonzi, T., Tripodi, M., La Monica, N., and Heim, M. H. (2003). Expression of hepatitis c virus proteins inhibits interferon alpha signaling in the liver of transgenic mice. *Gastroenterology* **124**:1465–1475.
- Bost, A. G., Venable, D., Liu, L., and Heinz, B. A. (2003). Cytoskeletal requirements for hepatitis C virus (HCV) RNA synthesis in the HCV replicon cell culture system. *J. Virol.* **77**:4401–4408.
- Boulant, S., Becchi, M., Penin, F., and Lavergne, J.-P. (2003). Unusual multiple recoding events leading to alternative forms of hepatitis C virus core protein from genotype 1b. *J. Biol. Chem.* **278**:45785–45792.
- Bouvier-Alias, M., Patel, K., Dahari, H., Beaucourt, S., Larderie, P., Blatt, L., Hezode, C., Picchio, G., Dhumeaux, D., Neumann, A. U., McHutchison, J. G., and Pawlotsky, J. M. (2002). Clinical utility of total HCV core antigen quantification: A new indirect marker of HCV replication. *Hepatology* **36**:211–218.
- Bradley, D., McCaustland, K., Krawczynski, K., Spelbring, J., Humphrey, C., and Cook, E. H. (1991). Hepatitis C virus: Buoyant density of the factor VIII-derived isolate in sucrose. *J. Med. Virol.* **34**:206–208.
- Brass, V., Bieck, E., Montserret, R., Wölk, B., Hellings, J. A., Blum, H. E., Penin, F., and Moradpour, D. (2002). An amino-terminal amphipathic alpha-helix mediates membrane association of the hepatitis C virus nonstructural protein 5A. *J. Biol. Chem.* **277**:8130–8139.
- Bressanelli, S., Tomei, L., Rey, F. A., and de Francesco, R. (2002). Structural analysis of the hepatitis C virus RNA polymerase in complex with ribonucleotides. *J. Virol.* **76**:3482–3492.
- Bressanelli, S., Tomei, L., Roussel, A., Incitti, I., Vitale, R. L., Mathieu, M., de Francesco, R., and Rey, F. A. (1999). Crystal structure of the RNA-dependent RNA polymerase of hepatitis C virus. *Proc. Natl. Acad. Sci. USA* **96**:13034–13039.
- Briggs, J. A., Wilk, T., and Fuller, S. D. (2003). Do lipid rafts mediate virus assembly and pseudo-typing? *J. Gen. Virol.* **84**:757–768.
- Bright, H., Carroll, A. R., Watts, P. A., and Fenton, R. J. (2004). Development of a GB virus B marmoset model and its validation with a novel series of hepatitis C virus NS3 protease inhibitors. *J. Virol.* **78**:2062–2071.
- Bruss, V., Lu, X., Thomssen, R., and Gerlich, W. H. (1994). Posttranslational alterations in transmembrane topology of the hepatitis B virus large envelope protein. *EMBO J.* **13**:2273–2279.
- Brummelkamp, T. R., Bernards, R., and Agami, R. (2002). A system for stable expression of short interfering RNAs in mammalian cells. *Science* **296**:550–553.

- Bukh, J., Apgar, C. L., Govindarajan, S., and Purcell, R. H. (2001). Host-range studies of GB virus-B hepatitis agent, the closest relative of HCV, in New World monkeys and chimpanzees. *J. Med. Virol.* **65**:694–697.
- Bukh, J., Pietschmann, T., Lohmann, V., Krieger, N., Faulk, K., Engle, R. E., Govindarajan, S., Shapiro, M., St. Claire, M., and Bartenschlager, R. (2002). Mutations that permit efficient replication of hepatitis C virus RNA in Huh-7 cells prevent productive replication in chimpanzees. *Proc. Natl. Acad. Sci. USA* **99**:14416–14421.
- Buonocore, L., Blight, K. J., Rice, C. M., and Rose, J. K. (2002). Characterization of vesicular stomatitis virus recombinants that express and incorporate high levels of hepatitis C virus glycoproteins. *J. Virol.* **76**:6865–6872.
- Butcher, S. J., Grimes, J. M., Makeyev, E. V., Bamford, D. H., and Stuart, D. I. (2001). A mechanism for initiating RNA-dependent RNA polymerization. *Nature* **410**:235–240.
- Butcher, S. J., Makeyev, E. V., Grimes, J. M., Stuart, D. I., and Bamford, D. H. (2000). Crystallization and preliminary X-ray crystallographic studies on the bacteriophage phi6 RNA-dependent RNA polymerase. *Acta Crystallogr. D. Biol. Crystallogr.* **56**:1473–1475.
- Butkiewicz, N. J., Wendel, M., Zhang, R., Jubin, R., Pichardo, J., Smith, E. B., Hart, A. M., Ingram, R., Durkin, J., Mui, P. W., Murray, M. G., Ramanathan, L., and Dasmanapatra, B. (1996). Enhancement of hepatitis C virus NS3 proteinase activity by association with NS4A-specific synthetic peptides: Identification of sequence and critical residues of NS4A for the cofactor activity. *Virology* **225**:328–338.
- Cahour, A., Falgout, B., and Lai, C. J. (1992). Cleavage of the dengue virus polyprotein at the NS3/NS4A and NS4B/NS5 junctions is mediated by viral protease NS2B-NS3, whereas NS4A/NS4B may be processed by a cellular protease. *J. Virol.* **66**:1535–1542.
- Caplen, N. J. (2003). RNAi as a gene therapy approach. *Expert. Opin. Biol. Ther.* **3**:575–586.
- Carrere-Kremer, S., Montpellier-Pala, C., Cocquerel, L., Wychowski, C., Penin, F., and Dubuisson, J. (2002). Subcellular localization and topology of the p7 polypeptide of hepatitis C virus. *J. Virol.* **76**:3720–3730.
- Cella, M., Jarrossay, D., Faccetti, F., Alebardi, O., Nakajima, H., Lanzavecchia, A., and Colonna, M. (1999). Plasmacytoid monocytes migrate to inflamed lymph nodes and produce large amounts of type I interferon. *Nat. Med.* **5**:919–923.
- Chang, M., Williams, O., Mittler, J., Quintanilla, A., Carithers, R. L., Jr., Perkins, J., Corey, L., and Gretch, D. R. (2003). Dynamics of hepatitis C virus replication in human liver. *Am. J. Path.* **163**:433–444.
- Chang, S. C., Cheng, J. C., Kou, Y. H., Kao, C. H., Chiu, C. H., Wu, H. Y., and Chang, M. F. (2000). Roles of the AX(4)GKS and arginine-rich motifs of hepatitis C virus RNA helicase in ATP- and viral RNA-binding activity. *J. Virol.* **74**:9732–9737.
- Charloteaux, B., Lins, L., Moereels, H., and Brasseur, R. (2002). Analysis of the C-terminal membrane anchor domains of hepatitis C virus glycoproteins E1 and E2: Toward a topological model. *J. Virol.* **76**:1944–1958.
- Cheney, I. W., Naim, S., Lai, V. C., Dempsey, S., Bellows, D., Walker, M. P., Shim, J. H., Horscroft, N., Hong, Z., and Zhong, W. (2002). Mutations in NS5B polymerase of hepatitis C virus: Impacts on *in vitro* enzymatic activity and viral RNA replication in the subgenomic replicon cell culture. *Virology* **297**:298–306.
- Cheng, J.-U., Chang, M.-F., and Chang, S. C. (1999). Specific interaction between the hepatitis C virus NS5B RNA polymerase and the 3'-end of the viral RNA. *J. Virol.* **73**:7044–7049.

- Cho, H. S., Ha, N. C., Kang, L. W., Chung, K. M., Back, S. H., Jang, S. K., and Oh, B. H. (1998). Crystal structure of RNA helicase from genotype 1b hepatitis C virus: A feasible mechanism of unwinding duplex RNA. *J. Biol. Chem.* **273**:15045–15052.
- Choi, J., Xu, Z., and Ou, J. H. (2003). Triple decoding of hepatitis C virus RNA by programmed translational frameshifting. *Mol. Cell. Biol.* **23**:1489–1497.
- Choo, Q. L., Kuo, G., Weiner, A. J., Overby, L. R., Bradley, D. W., and Houghton, M. (1989). Isolation of a cDNA clone derived from a blood-borne non-A, non-B viral hepatitis genome. *Science* **244**:359–362.
- Choo, S. H., So, H. S., Cho, J. M., and Ryu, W. S. (1995). Association of hepatitis C virus particles with immunoglobulin: A mechanism for persistent infection. *J. Gen. Virol.* **76**:2337–2341.
- Choukhi, A., Ung, S., Wychowski, C., and Dubuisson, J. (1998). Involvement of endoplasmic reticulum chaperones in the folding of hepatitis C virus glycoproteins. *J. Virol.* **72**:3851–3858.
- Chung, R. T., He, W., Saquib, A., Contreras, A. M., Xavier, R. J., Chawla, A., Wang, T. C., and Schmidt, E. V. (2001). Hepatitis C virus replication is directly inhibited by IFN- α in a full-length binary expression system. *Proc. Natl. Acad. Sci. USA* **98**:9847–9852.
- Clapham, P. R., and McKnight, A. (2002). Cell surface receptors, virus entry, and tropism of primate lentiviruses. *J. Gen. Virol.* **83**:1809–1829.
- Clemens, M. J., and Elia, A. (1997). The double-stranded RNA-dependent protein kinase PKR: Structure and function. *J. Interferon Cytokine Res.* **17**:503–524.
- Cocquerel, L., Duvet, S., Meunier, J. C., Pillez, A., Cacan, R., Wychowski, C., and Dubuisson, J. (1999). The transmembrane domain of hepatitis C virus glycoprotein E1 is a signal for static retention in the endoplasmic reticulum. *J. Virol.* **73**:2641–2649.
- Cocquerel, L., Meunier, J. C., Pillez, A., Wychowski, C., and Dubuisson, J. (1998). A retention signal necessary and sufficient for endoplasmic reticulum localization maps to the transmembrane domain of hepatitis C virus glycoprotein E2. *J. Virol.* **72**:2183–2191.
- Cocquerel, L., Op, D. B., Lambot, M., Roussel, J., Delgrange, D., Pillez, A., Wychowski, C., Penin, F., and Dubuisson, J. (2002). Topological changes in the transmembrane domains of hepatitis C virus envelope glycoproteins. *EMBO J.* **21**:2893–2902.
- Cocquerel, L., Wychowski, C., Minner, F., Penin, F., and Dubuisson, J. (2000). Charged residues in the transmembrane domains of hepatitis C virus glycoproteins play a major role in the processing, subcellular localization, and assembly of these envelope proteins. *J. Virol.* **74**:3623–3633.
- Coito, C., Diamond, D. L., Neddermann, P., Korth, M. J., and Katze, M. G. (2004). High-throughput screening of the yeast kinome: Identification of human serine/threonine protein kinases that phosphorylate the hepatitis C virus NS5A protein. *J. Virol.* **78**:3502–3513.
- Contreras, A. M., Hiasa, Y., He, W., Terella, A., Schmidt, E. V., and Chung, R. T. (2002). Viral RNA mutations are region specific and increased by ribavirin in a full-length hepatitis C virus replication system. *J. Virol.* **76**:8505–8517.
- Cormier, E. G., Tsamis, F., Kajumo, F., Durso, R. J., Gardner, J. P., and Dragic, T. (2004). CD81 is an entry coreceptor for hepatitis C virus. *Proc. Natl. Acad. Sci. USA* **101**:7270–7274.
- Cristofari, G., Ivanyi-Nagy, R., Gabus, C., Boulant, S., Lavergne, J.-P., Penin, F., and Darlix, J.-L. (2004). The hepatitis C virus core protein, *ia*, a potent nucleic acid chaperone that directs dimerization of the viral (+) strand RNA *in vitro*. *Nucleic Acids Res.* **32**:2623–2631.

- Crotty, S., Cameron, C., and Andino, R. (2002). Ribavirin's antiviral mechanism of action: Lethal mutagenesis? *J. Mol. Med.* **80**:86–95.
- Crotty, S., Maag, D., Arnold, J. J., Zhong, W., Lau, J. Y., Hong, Z., Andino, R., and Cameron, C. E. (2000). The broad-spectrum antiviral ribonucleoside ribavirin is an RNA virus mutagen. *Nat. Med.* **6**:1375–1379.
- Curtis, B. M., Scharnrowske, S., and Watson, A. J. (1992). Sequence and expression of a membrane-associated C-type lectin that exhibits CD4-independent binding of human immunodeficiency virus envelope glycoprotein gp120. *Proc. Natl. Acad. Sci. USA* **89**:8356–8360.
- Darke, P.L., Jacobs, A.R., Waxman, L., and Kuo, L.C. (1999). Inhibition of hepatitis C virus NS2/3 processing by NS4A peptides. Implications for control of viral processing. *J. Biol. Chem.* **274**:34511–34514.
- Dasgupta, A. (1983). Purification of host factor required for *in vitro* transcription of poliovirus RNA. *Virology* **128**:245–251.
- Dash, S., Halim, A. B., Tsuji, H., Hiramatsu, N., and Gerber, M. A. (1997). Transfection of HepG2 cells with infectious hepatitis C virus genome. *Am. J. Pathol.* **151**:363–373.
- Date, T., Kato, T., Miyamoto, M., Zhao, Z., Yasui, K., Mizokami, M., and Wakita, T. (2004). Genotype 2a hepatitis C virus subgenomic replicon can replicate in HepG2 and IMY-N9 cells. *J. Biol. Chem.* **279**:22371–22376.
- de Francesco, R., and Rice, C. M. (2003). New therapies on the horizon for hepatitis C: Are we close? *Clin. Liver Dis.* **7**:211–242.
- de Francesco, R., Pessi, A., and Steinkühler, C. (1998). The hepatitis C virus NS3 proteinase: Structure and function of a zinc-containing serine proteinase. *Antivir. Ther.* **3**:99–109.
- de Francesco, R., Urbani, A., Nardi, M. C., Tomei, L., Steinkühler, C., and Tramontano, A. (1996). A zinc binding site in viral serine proteinases. *Biochemistry* **35**:13282–13287.
- Deleersnyder, V., Pillez, A., Wychowski, C., Blight, K., Xu, J., Hahn, Y. S., Rice, C. M., and Dubuisson, J. (1997). Formation of native hepatitis C virus glycoprotein complexes. *J. Virol.* **71**:697–704.
- Dimitrova, M., Imbert, I., Kieny, M. P., and Schuster, C. (2003). Protein:protein interactions between hepatitis C virus nonstructural proteins. *J. Virol.* **77**:5401–5414.
- Drummer, H. E., Wilson, K. A., and Pombourios, P. (2002). Identification of the hepatitis C virus E2 glycoprotein binding site on the large extracellular loop of CD81. *J. Virol.* **76**:11143–11147.
- Dubuisson, J. (2000). Folding, assembly, and subcellular localization of hepatitis C virus glycoproteins. *Curr. Top. Microbiol. Immunol.* **242**:135–148.
- Dubuisson, J., Hsu, H. H., Cheung, R. C., Greenberg, H. B., Russell, D. G., and Rice, C. M. (1994). Formation and intracellular localization of hepatitis C virus envelope glycoprotein complexes expressed by recombinant vaccinia and Sindbis viruses. *J. Virol.* **68**:6147–6160.
- Dubuisson, J., and Rice, C. M. (1996). Hepatitis C virus glycoprotein folding: Disulfide bond formation and association with calnexin. *J. Virol.* **70**:778–786.
- Duvet, S., Cocquerel, L., Pillez, A., Cacan, R., Verbert, A., Moradpour, D., Wychowski, C., and Dubuisson, J. (1998). Hepatitis C virus glycoprotein complex localization in the endoplasmic reticulum involves a determinant for retention and not retrieval. *J. Biol. Chem.* **273**:32088–32095.
- Eckart, M. R., Selby, M., Masiarz, F., Lee, C., Berger, K., Crawford, K., Kuo, C., Kuo, G., Houghton, M., and Choo, Q. L. (1993). The hepatitis C virus encodes a serine protease involved in processing of the putative nonstructural proteins from the viral polyprotein precursor. *Biochem. Biophys. Res. Commun.* **192**:399–406.

- Egger, D., Wölk, B., Gosert, R., Bianchi, L., Blum, H. E., Moradpour, D., and Bienz, K. (2002). Expression of hepatitis C virus proteins induces distinct membrane alterations including a candidate viral replication complex. *J. Virol.* **76**:5974–5984.
- Elazar, M., Cheong, K. H., Liu, P., Greenberg, H. B., Rice, C. M., and Glenn, J. S. (2003). Amphipathic helix-dependent localization of NS5A mediates hepatitis C virus RNA replication. *J. Virol.* **77**:6055–6061.
- El-Hage, N., and Luo, G. (2003). Replication of hepatitis C virus RNA occurs in a membrane-bound replication complex containing nonstructural viral proteins and RNA. *J. Gen. Virol.* **84**:2761–2769.
- Elbers, K., Tautz, N., Becher, P., Stoll, D., Rumenapf, T., and Thiel, H. J. (1996). Processing in the pestivirus E2-NS2 region: Identification of proteins p7 and E2p7. *J. Virol.* **70**:4131–4135.
- Enomoto, N., Sakuma, I., Asahina, Y., Kurosaki, M., Murakami, T., Yamamoto, C., Izumi, N., Marumo, F., and Sato, C. (1995). Comparison of full-length sequences of interferon-sensitive and resistant hepatitis C virus 1b. Sensitivity to interferon is conferred by amino acid substitutions in the NS5A region. *J. Clin. Invest.* **96**:224–230.
- Enomoto, N., Sakuma, I., Asahina, Y., Kurosaki, M., Murakami, T., Yamamoto, C., Ogura, Y., Izumi, N., Marumo, F., and Sato, C. (1996b). Mutations in the nonstructural protein 5A gene and response to interferon in patients with chronic hepatitis C virus 1b infection. *N. Engl. J. Med.* **334**:77–81.
- Enomoto, N., Sakuma, I., Asahina, Y., Kurosaki, M., Murakami, T., Yamamoto, C., Ogura, Y., Izumi, N., Marumo, F., and Sato, C. (1996a). Mutations in the nonstructural protein 5A gene and response to interferon in patients with chronic hepatitis C virus 1b infection. *N. Engl. J. Med.* **334**:77–81.
- Failla, C., Tomei, L., and de Francesco, R. (1994). Both NS3 and NS4A are required for proteolytic processing of hepatitis C virus nonstructural proteins. *J. Virol.* **68**:3753–3760.
- Failla, C., Tomei, L., and de Francesco, R. (1995). An amino-terminal domain of the hepatitis C virus NS3 protease is essential for interaction with NS4A. *J. Virol.* **69**:1769–1777.
- Fan, Z., Yang, Q. R., Twu, J. S., and Sherker, A. H. (1999). Specific *in vitro* association between the hepatitis C viral genome and core protein. *J. Med. Virol.* **59**:131–134.
- Feinstone, S. M., Mihalik, K. B., Kamimura, T., Alter, H. J., London, W. T., and Purcell, R. H. (1983). Inactivation of hepatitis B virus and non-A, non-B hepatitis by chloroform. *Infect. Immun.* **41**:816–821.
- Ferlenghi, I., Clarke, M., Ruttan, T., Allison, S. L., Schalich, J., Heinz, F. X., Harrison, S. C., Rey, F. A., and Fuller, S. D. (2001). Molecular organization of a recombinant subviral particle from tick-borne encephalitis virus. *Mol. Cell* **7**:593–602.
- Filocamo, G., Pacini, L., and Migliaccio, G. (1997). Chimeric Sindbis viruses dependent on the NS3 protease of hepatitis C virus. *J. Virol.* **71**:1417–1427.
- Flint, M., Dubuisson, J., Maidens, C. M., Harrop, R., Guile, G. R., Borrow, P., and McKeating, J. A. (2000). Functional characterization of intracellular and secreted forms of a truncated hepatitis C virus E2 glycoprotein. *J. Virol.* **74**:702–709.
- Flint, M., Maidens, C. M., Loomis, P. L., Shotton, C., Dubuisson, J., Monk, P., Higginbottom, A., Levy, S., and McKeating, J. A. (1999a). Characterization of hepatitis C virus E2 glycoprotein interaction with a putative cellular receptor, CD81. *J. Virol.* **73**:6235–6244.
- Flint, M., and McKeating, J. A. (1999). The C-terminal region of the hepatitis C virus E1 glycoprotein confers localization within the endoplasmic reticulum. *J. Gen. Virol.* **80**:1943–1947.

- Flint, M., Quinn, E. R., and Levy, S. (2001). In search of hepatitis C virus receptor(s). *Clin. Liver Dis.* **5**:873–893.
- Flint, M., Thomas, J., Maidens, C. M., Shotton, C., Levy, S., Barclay, W., and McKeating, J. A. (1999b). Functional analysis of cell surface-expressed hepatitis C virus E2 glycoprotein. *J. Virol.* **73**:6782–6790.
- Foy, E., Li, K., Wang, C., Sumpter, R., Jr., Ikeda, M., Lemon, S. M., and Gale, M., Jr. (2003). Regulation of interferon regulatory factor-3 by the hepatitis C virus serine protease. *Science* **300**:1145–1148.
- Frese, M., Pietschmann, T., Moradpour, D., Haller, O., and Bartenschlager, R. (2001). Interferon-alpha inhibits hepatitis C virus subgenomic RNA replication by an MxA-independent pathway. *J. Gen. Virol.* **82**:723–733.
- Frese, M., Schwärzle, V., Barth, K., Krieger, N., Lohmann, V., Mihm, S., Haller, O., and Bartenschlager, R. (2002). Interferon-gamma inhibits replication of subgenomic and genomic hepatitis C virus RNAs. *Hepatology* **35**:694–703.
- Friebe, P., and Bartenschlager, R. (2002). Genetic analysis of sequences in the 3'-nontranslated region of hepatitis C virus that are important for RNA replication. *J. Virol.* **76**:5326–5338.
- Friebe, P., Boudet, J., Simorre, J.-P., and Bartenschlager, R. (2004). A kissing loop interaction in the 3'-end of the hepatitis C virus genome essential for RNA replication. *J. Virol.* (In Press).
- Friebe, P., Lohmann, V., Krieger, N., and Bartenschlager, R. (2001). Sequences in the 5'-nontranslated region of hepatitis C virus required for RNA replication. *J. Virol.* **75**:12047–12057.
- Fukushi, S., Okada, M., Kageyama, T., Hoshino, F. B., Nagai, K., and Katayama, K. (2001). Interaction of poly(rC)-binding protein 2 with the 5'-terminal stem-loop of the hepatitis C-virus genome. *Virus Res.* **73**:67–79.
- Gale, M., Jr., Blakely, C. M., Kwieciszewski, B., Tan, S. L., Dossett, M., Tang, N. M., Korth, M. J., Polyak, S. J., Gretch, D. R., and Katze, M. G. (1998). Control of PKR protein kinase by hepatitis C virus nonstructural 5A protein: Molecular mechanisms of kinase regulation. *Mol. Cell. Biol.* **18**:5208–5218.
- Gale, M. J., Korth, M. J., Tang, N. M., Tan, S. L., Hopkins, D. A., Dever, T. E., Polyak, S. J., Gretch, D. R., and Katze, M. G. (1997). Evidence that hepatitis C virus resistance to interferon is mediated through repression of the PKR protein kinase by the nonstructural 5A protein. *Virology* **230**:217–227.
- Gallinari, P., Brennan, D., Nardi, C., Brunetti, M., Tomei, L., Steinkühler, C., and de Francesco, R. (1998). Multiple enzymatic activities associated with recombinant NS3 protein of hepatitis C virus. *J. Virol.* **72**:6758–6769.
- Gamarnik, A. V., and Andino, R. (1998). Switch from translation to RNA replication in a positive-stranded RNA virus. *Genes Dev.* **12**:2293–2304.
- Gao, L., Aizaki, H., He, J. W., and Lai, M. M. (2004). Interactions between viral non-structural proteins and host protein hVAP-33 mediate the formation of hepatitis C virus RNA replication complex on lipid raft. *J. Virol.* **78**:3480–3488.
- Gardner, J. P., Durso, R. J., Arrigale, R. R., Donovan, G. P., Maddon, P. J., Dragic, T., and Olson, W. C. (2003). L-SIGN (CD 209L) is a liver-specific capture receptor for hepatitis C virus. *Proc. Natl. Acad. Sci. USA* **100**:4498–4503.
- Garry, R. F., and Dash, S. (2003). Proteomics computational analyses suggest that hepatitis C virus E1 and pestivirus E2 envelope glycoproteins are truncated class II fusion proteins. *Virology* **307**:255–265.
- Geijtenbeek, T. B., Kwon, D. S., Torensma, R., van Vliet, S. J., van Duijnhoven, G. C., Middel, J., Cornelissen, I. L., Nottet, H. S., KewalRamani, V. N., Littman, D. R.,

- Figdor, C. G., and van Kooyk, Y. (2000). DC-SIGN, a dendritic cell-specific HIV-1-binding protein that enhances trans-infection of T cells. *Cell* **100**:587–597.
- Geiss, G. K., Carter, V. S., He, Y., Kwiciszewski, B. K., Holzman, T., Korth, M. J., Lazaro, C.A., Fausto, N., Bumgarner, R. E., and Katze, M. G. (2003). Gene expression profiling of the cellular transcriptional network regulated by alpha/beta interferon and its partial attenuation by the hepatitis C virus nonstructural 5A protein. *J. Virol.* **77**:6367–6375.
- Gervais, A., Martinot, M., Boyer, N., Auperin, A., Le Breton, W., Degott, C., Valla, D., and Marcellin, P. (2001). Quantitation of hepatic hepatitis C virus RNA in patients with chronic hepatitis C: Relationship with severity of disease, viral genotype, and response to treatment. *J. Hepatol.* **35**:399–405.
- Girard, S., Shalhoub, P., Lescure, P., Sabile, A., Misek, D. E., Hanash, S., Brechot, C., and Beretta, L. (2002). An altered cellular response to interferon and up-regulation of interleukin-8 induced by the hepatitis C viral protein NS5A uncovered by microarray analysis. *Virology* **295**:272–283.
- Goodbourn, S., Didcock, L., and Randall, R. E. (2000). Interferons: Cell signaling, immune modulation, antiviral response, and virus countermeasures. *J. Gen. Virol.* **81**:2341–2364.
- Gorbalenya, A. E., Donchenko, A. P., Koonin, E. V., and Blinov, V. M. (1989a). N-terminal domains of putative helicases of flavi- and pestiviruses may be serine proteases. *Nucleic Acids Res.* **17**:3889–3897.
- Gorbalenya, A. E., Koonin, E. V., Donchenko, A. P., and Blinov, V. M. (1989b). Two related superfamilies of putative helicases involved in replication, recombination, repair, and expression of DNA and RNA genomes. *Nucleic Acids Res.* **17**:4713–4730.
- Gorbalenya, A. E., and Snijder, E. J. (1998). Viral cysteine proteinases. *Perspect. Drug Discovery Design* **6**:64–86.
- Gosert, R., Egger, D., Lohmann, V., Bartenschlager, R., Blum, H. E., Bienz, K., and Moradpour, D. (2003). Identification of the hepatitis C virus RNA replication complex in Huh-7 cells harboring subgenomic replicons. *J. Virol.* **77**:5487–5492.
- Grakoui, A., Hanson, H. L., and Rice, C. M. (2001). Bad time for Bonzo? Experimental models of hepatitis C virus infection, replication, and pathogenesis. *Hepatology* **33**:489–495.
- Grakoui, A., McCourt, D. W., Wychowski, C., Feinstone, S. M., and Rice, C. M. (1993a). A second hepatitis C virus-encoded proteinase. *Proc. Natl. Acad. Sci. USA* **90**:10583–10587.
- Grakoui, A., McCourt, D. W., Wychowski, C., Feinstone, S. M., and Rice, C. M. (1993b). Characterization of the hepatitis C virus-encoded serine proteinase: Determination of proteinase-dependent polyprotein cleavage sites. *J. Virol.* **67**:2832–2843.
- Grakoui, A., Wychowski, C., Lin, C., Feinstone, S. M., and Rice, C. M. (1993c). Expression and identification of hepatitis C virus polyprotein cleavage products. *J. Virol.* **67**:1385–1395.
- Griffin, S. D., Beales, L. P., Clarke, D. S., Worsfold, O., Evans, S. D., Jaeger, J., Harris, M. P., and Rowlands, D. J. (2003). The p7 protein of hepatitis C virus forms an ion channel that is blocked by the antiviral drug, Amantadine. *FEBS Lett.* **535**:34–38.
- Grobler, J. A., Markel, E. J., Fay, J. F., Graham, D. J., Simcoe, A. L., Ludmerer, S. W., Murray, E. M., Migliaccio, G., and Flores, O. A. (2003). Identification of a key determinant of hepatitis C virus cell culture adaptation in domain II of NS3 helicase. *J. Biol. Chem.* **278**:16741–16746.
- Gunji, T., Kato, N., Hijikata, M., Hayashi, K., Saitoh, S., and Shimotohno, K. (1994). Specific detection of positive- and negative-stranded hepatitis C viral RNA using chemical RNA modification. *Arch. Virol.* **134**:293–302.

- Guo, J. T., Bichko, V. V., and Seeger, C. (2001). Effect of alpha interferon on the hepatitis C virus replicon. *J. Virol.* **75**:8516–8523.
- Guo, J. T., Zhu, Q., and Seeger, C. (2003). Cytopathic and noncytopathic interferon responses in cells expressing hepatitis C virus subgenomic replicons. *J. Virol.* **77**:10769–10779.
- Gwack, Y., Kim, D. W., Han, J. H., and Choe, J. (1995). NTPase activity of hepatitis C virus NS3 protein expressed in insect cells. *Mol. Cells* **5**:171–175.
- Gwack, Y., Kim, D. W., Han, J. H., and Choe, J. (1996). Characterization of RNA binding activity and RNA helicase activity of the hepatitis C virus NS3 protein. *Biochem. Biophys. Res. Commun.* **225**:654–659.
- Hahn, B., Kim, Y. K., Kim, J. H., Kim, T. Y., and Jang, S. K. (1998). Heterogeneous nuclear ribonucleoprotein L interacts with the 3'-border of the internal ribosomal entry site of hepatitis C virus. *J. Virol.* **72**:8782–8788.
- Haller, O., and Kochs, G. (2002). Interferon-induced Mx proteins: Dynammin-like GTPases with antiviral activity. *Traffic* **3**:710–717.
- Han, J. H., Shyamala, V., Richman, K. H., Brauer, M. J., Irvine, B., Urdea, M. S., Tekamp, O. P., Kuo, G., Choo, Q. L., and Houghton, M. (1991). Characterization of the terminal regions of hepatitis C viral RNA: Identification of conserved sequences in the 5'-untranslated region and poly(A) tails at the 3'-end. *Proc. Natl. Acad. Sci. USA* **88**:1711–1715.
- Hannon, G. J. (2002). RNA interference. *Nature* **418**:244–251.
- Hardy, R. W., Marcotrigiano, J., Blight, K. J., Majors, J. E., and Rice, C. M. (2003). Hepatitis C virus RNA synthesis in a cell-free system isolated from replicon-containing hepatoma cells. *J. Virol.* **77**:2029–2037.
- Hayashi, N., Higashi, H., Kaminaka, K., Sugimoto, H., Esumi, M., Komatsu, K., Hayashi, K., Sugitani, M., Suzuki, K., Tadao, O., Nozaki, C., Mizuno, K., and Shikata, T. (1993). Molecular cloning and heterogeneity of the human hepatitis C virus (HCV) genome. *J. Hepatol* **17**(Suppl 3):S94–S107.
- He, L. F., Alling, D., Popkin, T., Shapiro, M., Alter, H. J., and Purcell, R. H. (1987). Determining the size of non-A, non-B hepatitis virus by filtration. *J. Infect. Dis.* **156**:636–640.
- Heilek, G. M., and Peterson, M. G. (1997). A point mutation abolishes the helicase but not the nucleoside triphosphatase activity of hepatitis C virus NS3 protein. *J. Virol.* **71**:6264–6266.
- Heim, M. H., Moradpour, D., and Blum, H. E. (1999). Expression of hepatitis C virus proteins inhibits signal transduction through the Jak-STAT pathway. *J. Virol.* **73**:8469–8475.
- Higinbottom, A., Quinn, E. R., Kuo, C. C., Flint, M., Wilson, L. H., Bianchi, E., Nicosia, A., Monk, P. N., McKeating, J. A., and Levy, S. (2000). Identification of amino acid residues in CD81 critical for interaction with hepatitis C virus envelope glycoprotein E2. *J. Virol.* **74**:3642–3649.
- Hijikata, M., Kato, N., Ootsuyama, Y., Nakagawa, M., and Shimotohno, K. (1991). Gene mapping of the putative structural region of the hepatitis C virus genome by *in vitro* processing analysis. *Proc. Natl. Acad. Sci. USA* **88**:5547–5551.
- Hijikata, M., Mizushima, H., Akagi, T., Mori, S., Kakiuchi, N., Kato, N., Tanaka, T., Kimura, K., and Shimotohno, K. (1993a). Two distinct proteinase activities required for the processing of a putative nonstructural precursor protein of hepatitis C virus. *J. Virol.* **67**:4665–4675.
- Hijikata, M., Mizushima, H., Tanji, Y., Komoda, Y., Hirowatari, Y., Akagi, T., Kato, N., Kimura, K., and Shimotohno, K. (1993b). Proteolytic processing and membrane

- association of putative nonstructural proteins of hepatitis C virus. *Proc. Natl. Acad. Sci. USA* **90**:10773–10777.
- Hijikata, M., Shimizu, Y. K., Kato, H., Iwamoto, A., Shih, J. W., Alter, H. J., Purcell, R. H., and Yoshikura, H. (1993c). Equilibrium centrifugation studies of hepatitis C virus: Evidence for circulating immune complexes. *J. Virol.* **67**:1953–1958.
- Hofacker, I. L., Fekete, M., Flamm, C., Huynen, M. A., Rauscher, S., Stolorz, P. E., and Stadler, P. F. (1998). Automatic detection of conserved RNA structure elements in complete RNA virus genomes. *Nucleic Acids Res.* **26**:3825–3836.
- Hollinger, F. B., Gitnick, G. L., Aach, R. D., Szmunes, W., Mosley, J. W., Stevens, C. E., Peters, R. L., Weiner, J. M., Werch, J. B., and Lander, J. J. (1978). Non-A, non-B hepatitis transmission in chimpanzees: A project of the transfusion-transmitted viruses study group. *Intervirology* **10**:60–68.
- Honda, M., Beard, M. R., Ping, L. H., and Lemon, S. M. (1999). A phylogenetically conserved stem-loop structure at the 5'-border of the internal ribosome entry site of hepatitis C virus is required for cap-independent viral translation. *J. Virol.* **73**:1165–1174.
- Honda, M., Brown, E. A., and Lemon, S. M. (1996a). Stability of a stem-loop involving the initiator AUG controls the efficiency of internal initiation of translation on hepatitis C virus RNA. *RNA* **2**:955–968.
- Honda, M., Ping, L. H., Rijnbrand, R. A., Amphlett, E., Clarke, B., Rowlands, D., and Lemon, S. M. (1996b). Structural requirements for initiation of translation by internal ribosome entry within genome-length hepatitis C virus RNA. *Virology* **222**:31–42.
- Hong, Z., Cameron, C. E., Walker, M. P., Castro, C., Yao, N., Lau, J. Y., and Zhong, W. (2001). A novel mechanism to ensure terminal initiation by hepatitis C virus NS5B polymerase. *Virology* **285**:6–11.
- Hong, Z., Ferrari, E., Wright-Minogue, J., Chase, R., Risano, C., Seelig, G., Lee, C. G., and Kwong, A. D. (1996). Enzymatic characterization of hepatitis C virus NS3/4A complexes expressed in mammalian cells by using the herpes simplex virus amplicon system. *J. Virol.* **70**:4261–4268.
- Hope, R. G., and McLauchlan, J. (2000). Sequence motifs required for lipid droplet association and protein stability are unique to the hepatitis C virus core protein. *J. Gen. Virol.* **81**:1913–1925.
- Hope, R. G., Murphy, D. J., and McLauchlan, J. (2002). The domains required to direct core proteins of hepatitis C virus and GB virus-B to lipid droplets share common features with plant oleosin proteins. *J. Biol. Chem.* **277**:4261–4270.
- Hsu, M., Zhang, J., Flint, M., Logvinoff, C., Cheng-Mayer, C., Rice, C. M., and McKeating, J. A. (2003). Hepatitis C virus glycoproteins mediate pH-dependent cell entry of pseudotyped retroviral particles. *Proc. Natl. Acad. Sci. USA* **100**:7271–7276.
- Hugle, T., Fehrmann, F., Bieck, E., Kohara, M., Kräusslich, H. G., Rice, C. M., Blum, H. E., and Moradpour, D. (2001). The hepatitis C virus nonstructural protein 4B is an integral endoplasmic reticulum membrane protein. *Virology* **284**:70–81.
- Hussy, P., Langen, H., Mous, J., and Jacobsen, H. (1996). Hepatitis C virus core protein: Carboxy-terminal boundaries of two processed species suggest cleavage by a signal peptide peptidase. *Virology* **224**:93–104.
- Ide, Y., Zhang, L., Chen, M., Inchauspe, G., Bahl, C., Sasaguri, Y., and Padmanabhan, R. (1996). Characterization of the nuclear localization signal and subcellular distribution of hepatitis C virus nonstructural protein NS5A. *Gene* **182**:203–211.
- Ikeda, M., Yi, M., Li, K., and Lemon, S. M. (2002). Selectable subgenomic and genome-length dicistronic RNAs derived from an infectious molecular clone of the HCV-N

- strain of hepatitis C virus replicate efficiently in cultured Huh-7 cells. *J. Virol.* **76**:2997–3006.
- Ilan, E., Arazi, J., Nussbaum, O., Zauberman, A., Eren, R., Lubin, I., Neville, L., Ben Moshe, O., Kischitzky, A., Litchi, A., Margalit, I., Gopher, J., Mounir, S., Cai, W., Daudi, N., Eid, A., Jurim, O., Czerniak, A., Galun, E., and Dagan, S. (2002). The hepatitis C virus (HCV)-Trimer mouse: A model for evaluation of agents against HCV. *J. Infect. Dis.* **185**:153–161.
- Imbert, I., Dimitrova, M., Kien, F., Kieny, M. P., and Schuster, C. (2003). Hepatitis C virus IRES efficiency is unaffected by the genomic RNA 3'-NTR even in the presence of viral structural or nonstructural proteins. *J. Gen. Virol.* **84**:1549–1557.
- Ishii, K., Tanaka, Y., Yap, C. C., Aizaki, H., Matsuura, Y., and Miyamura, T. (1999). Expression of hepatitis C virus NS5B protein: Characterization of its RNA polymerase activity and RNA binding. *Hepatology* **29**:1227–1235.
- Ito, T., Tahara, S. M., and Lai, M. C. (1998). The 3'-untranslated region of hepatitis C virus RNA enhances translation from an internal ribosomal entry site. *J. Virol.* **72**:8789–8796.
- Ivashkina, N., Wölk, B., Lohmann, V., Bartenschlager, R., Blum, H. E., Penin, F., and Moradpour, D. (2002). The hepatitis C virus RNA-dependent RNA polymerase membrane insertion sequence is a transmembrane segment. *J. Virol.* **76**:13088–13093.
- Jacque, J. M., Triques, K., and Stevenson, M. (2002). Modulation of HIV-1 replication by RNA interference. *Nature* **418**:435–438.
- Jager, J., Smerdon, S. J., Wang, J., Boisvert, D. C., and Steitz, T. A. (1994). Comparison of three different crystal forms shows HIV-1 reverse transcriptase displays an internal swivel motion. *Structure* **2**:869–876.
- Jiang, W., and Bond, J. S. (1992). Families of metalloendopeptidases and their relationships. *FEBS Lett.* **312**:110–114.
- Jin, L., and Peterson, D. L. (1995). Expression, isolation, and characterization of the hepatitis C virus ATPase/RNA helicase. *Arch. Biochem. Biophys.* **323**:47–53.
- Jonas, M. M. (2002). Children with hepatitis C. *Hepatology* **36**:S173–S178.
- Kadare, G., and Haenni, A. L. (1997). Virus-encoded RNA helicases. *J. Virol.* **71**:2583–2590.
- Kaito, M., Watanabe, S., Tsukiyama, K. K., Yamaguchi, K., Kobayashi, Y., Konishi, M., Yokoi, M., Ishida, S., Suzuki, S., and Kohara, M. (1994). Hepatitis C virus particle detected by immunoelectron microscopic study. *J. Gen. Virol.* **75**:1755–1760.
- Kaminski, A., Hunt, S. L., Patton, J. G., and Jackson, R. J. (1995). Direct evidence that polypyrimidine tract binding protein (PTB) is essential for internal initiation of translation of encephalomyocarditis virus RNA. *RNA* **1**:924–938.
- Kanai, A., Tanabe, K., and Kohara, M. (1995). Poly(U) binding activity of hepatitis C virus NS3 protein, a putative RNA helicase. *FEBS Lett.* **376**:221–224.
- Kaneko, T., Tanji, Y., Satoh, S., Hijikata, M., Asabe, S., Kimura, K., and Shimotohno, K. (1994). Production of two phosphoproteins from the NS5A region of the hepatitis C viral genome. *Biochem. Biophys. Res. Commun.* **205**:320–326.
- Kapadia, S. B., Brideau-Andersen, A., and Chisari, F. V. (2003). Interference of hepatitis C virus RNA replication by short interfering RNAs. *Proc. Natl. Acad. Sci. USA* **100**:2014–2018.
- Kashiwagi, T., Hara, K., Kohara, M., Iwahashi, J., Hamada, N., Honda-Yoshino, H., and Toyoda, T. (2002). Promoter/origin structure of the complementary strand of hepatitis C virus genome. *J. Biol. Chem.* **277**:28700–28705.
- Kato, N., Hijikata, M., Ootsuyama, Y., Nakagawa, M., Ohkoshi, S., Sugimura, T., and Shimotohno, K. (1990). Molecular cloning of the human hepatitis C virus genome

- from Japanese patients with non-A, non-B hepatitis. *Proc. Natl. Acad. Sci. USA* **87**:9524–9528.
- Kato, N., and Shimotohno, K. (2000). Systems to culture hepatitis C virus. *Curr. Top. Microbiol. Immunol.* **242**:261–278.
- Kato, N., Sugiyama, K., Namba, K., Dansako, H., Nakamura, T., Takami, M., Naka, K., Nozaki, A., and Shimotohno, K. (2003). Establishment of a hepatitis C virus subgenomic replicon derived from human hepatocytes infected *in vitro.* *Biochem. Biophys. Res. Commun.* **306**:756–766.
- Kato, T., Date, T., Miyamoto, M., Furusaka, A., Tokushige, K., Mizokami, M., and Wakita, T. (2003). Efficient replication of the genotype 2a hepatitis C virus subgenomic replicon. *Gastroenterology* **125**:1808–1817.
- Kato, T., Furusaka, A., Miyamoto, M., Date, T., Yasui, K., Hiramoto, J., Nagayama, K., Tanaka, T., and Wakita, T. (2001). Sequence analysis of hepatitis C virus isolated from a fulminant hepatitis patient. *J. Med. Virol.* **64**:334–339.
- Keskinen, P., Nyqvist, M., Sareneva, T., Pirhonen, J., Melén, K., and Julkunen, I. (1999). Impaired antiviral response in human hepatoma cells. *Virology* **263**:364–375.
- Khromykh, A. A., Kondratieva, N., Sgro, J. Y., Palmenberg, A., and Westaway, E. G. (2003). Significance in replication of the terminal nucleotides of the *Flavivirus* genome. *J. Virol* **77**:10623–10629.
- Khu, Y. L., Koh, E., Lim, S. P., Tan, Y. H., Brenner, S., Lim, S. G., Hong, W. J., and Goh, P. Y. (2001). Mutations that affect dimer formation and helicase activity of the hepatitis C virus helicase. *J. Virol.* **75**:205–214.
- Kieft, J. S., Zhou, K., Jubin, R., and Doudna, J. A. (2001). Mechanism of ribosome recruitment by hepatitis C IRES RNA. *RNA* **7**:194–206.
- Kim, D. W., Gwack, Y., Han, J. H., and Choe, J. (1995). C-terminal domain of the hepatitis C virus NS3 protein contains an RNA helicase activity. *Biochem. Biophys. Res. Commun.* **215**:160–166.
- Kim, D. W., Kim, J., Gwack, Y., Han, J. H., and Choe, J. (1997). Mutational analysis of the hepatitis C virus RNA helicase. *J. Virol.* **71**:9400–9409.
- Kim, I., Lukavsky, P. J., and Puglisi, J. D. (2002a). NMR study of 100-kDa HCV IRES RNA using segmental isotope labeling. *J. Am. Chem. Soc.* **124**:9338–9339.
- Kim, J., Lee, D., and Choe, J. (1999a). Hepatitis C virus NS5A protein is phosphorylated by casein kinase II. *Biochem. Biophys. Res. Commun.* **257**:777–781.
- Kim, J. E., Song, W. K., Chung, K. M., Back, S. H., and Jang, S. K. (1999b). Subcellular localization of hepatitis C viral proteins in mammalian cells. *Arch. Virol.* **144**:329–343.
- Kim, J. L., Morgenstern, K. A., Griffith, J. P., Dwyer, M. D., Thomson, J. A., Murcko, M. A., Lin, C., and Caron, P. R. (1998). Hepatitis C virus NS3 RNA helicase domain with a bound oligonucleotide: The crystal structure provides insights into the mode of unwinding. *Structure* **6**:89–100.
- Kim, J. L., Morgenstern, K. A., Lin, C., Fox, T., Dwyer, M. D., Landro, J. A., Chambers, S. P., Markland, W., Lepre, C. A., O'Malley, E. T., Harbeson, S. L., Rice, C. M., Murcko, M. A., Caron, P. R., and Thomson, J. A. (1996). Crystal structure of the hepatitis C virus NS3 protease domain complexed with a synthetic NS4A cofactor peptide. *Cell* **87**:343–355.
- Kim, Y. K., Lee, S. H., Kim, C. S., Seol, S. K., and Jang, S. K. (2003). Long-range RNA:RNA interaction between the 5'-nontranslated region and the core coding sequences of hepatitis C virus modulates the IRES-dependent translation. *RNA* **9**:599–606.
- Kim, Y. K., Kim, C. S., Lee, S. H., and Jang, S. K. (2002b). Domains I and II in the 5'-nontranslated region of the HCV genome are required for RNA replication. *Biochem. Biophys. Res. Commun.* **290**:105–112.

- Kishine, H., Sugiyama, K., Hijikata, M., Kato, N., Takahashi, H., Noshi, T., Nio, Y., Hosaka, M., Miyanari, Y., and Shimotohno, K. (2002). Subgenomic replicon derived from a cell line infected with the hepatitis C virus. *Biochem. Biophys. Res. Commun.* **293**:993–999.
- Kolykhalov, A. A., Agapov, E. V., Blight, K. J., Mihalik, K., Feinstone, S. M., and Rice, C. M. (1997). Transmission of hepatitis C by intrahepatic inoculation with transcribed RNA. *Science* **277**:570–574.
- Kolykhalov, A. A., Agapov, E. V., and Rice, C. M. (1994). Specificity of the hepatitis C virus NS3 serine protease: Effects of substitutions at the 3/4A, 4A/4B, 4B/5A, and 5A/5B cleavage sites on polyprotein processing. *J. Virol.* **68**:7525–7533.
- Kolykhalov, A. A., Feinstone, S. M., and Rice, C. M. (1996). Identification of a highly conserved sequence element at the 3'-terminus of hepatitis C virus genome RNA. *J. Virol.* **70**:3363–3371.
- Kolykhalov, A. A., Mihalik, K., Feinstone, S. M., and Rice, C. M. (2000). Hepatitis C virus-encoded enzymatic activities and conserved RNA elements in the 3'-nontranslated region are essential for virus replication *in vivo*. *J. Virol.* **74**:2046–2051.
- Komoda, Y., Hijikata, M., Sato, S., Asabe, S., Kimura, K., and Shimotohno, K. (1994). Substrate requirements of hepatitis C virus serine proteinase for intermolecular polypeptide cleavage in *Escherichia coli*. *J. Virol.* **68**:7351–7357.
- Konan, K. V., Giddings, T. H., Jr., Ikeda, M., Li, K., Lemon, S. M., and Kirkegaard, K. (2003). Nonstructural protein precursor NS4A/B from hepatitis C virus alters function and ultrastructure of host secretory apparatus. *J. Virol.* **77**:7843–7855.
- Kotenko, S. V., Gallagher, G., Baurin, V. V., Lewis-Antes, A., Shen, M., Shah, N. K., Langer, J. A., Sheikh, F., Dickensheets, H., and Donnelly, R. P. (2003). IFN-lambdas mediate antiviral protection through a distinct class II cytokine receptor complex. *Nat. Immunol.* **4**:69–77.
- Krieger, N., Lohmann, V., and Bartenschlager, R. (2001). Enhancement of hepatitis C virus RNA replication by cell culture-adaptive mutations. *J. Virol.* **75**:4614–4624.
- Kronke, J., Kittler, R., Buchholz, F., Windisch, M. P., Pietschmann, T., Bartenschlager, R., and Frese, M. (2004). Alternative approaches for efficient inhibition of hepatitis C virus RNA replication by small interfering RNAs. *J. Virol.* **78**:3436–3646.
- Kuhn, R. J., Zhang, W., Rossmann, M. G., Pletnev, S. V., Corver, J., Lenches, E., Jones, C. T., Mukhopadhyay, S., Chipman, P. R., Strauss, E. G., Baker, T. S., and Strauss, J. H. (2002). Structure of dengue virus: Implications for *Flavivirus* organization, maturation, and fusion. *Cell* **108**:717–725.
- Kunkel, M., Lorinczi, M., Rijnbrand, R., Lemon, S. M., and Watowich, S. J. (2001). Self-assembly of nucleocapsid-like particles from recombinant hepatitis C virus core protein. *J. Virol.* **75**:2119–2129.
- Kunkel, M., and Watowich, S. J. (2002). Conformational changes accompanying self-assembly of the hepatitis C virus core protein. *Virology* **294**:239–245.
- Kuo, G., Choo, Q. L., Alter, H. J., Gitnick, G. L., Redeker, A. G., Purcell, R. H., Miyamura, T., Dienstag, J. L., Alter, M. J., and Stevens, C. E. (1989). An assay for circulating antibodies to a major etiologic virus of human non-A, non-B hepatitis. *Science* **244**:362–364.
- Lagging, L. M., Meyer, K., Owens, R. J., and Ray, R. (1998). Functional role of hepatitis C virus chimeric glycoproteins in the infectivity of pseudo-typed virus. *J. Virol.* **72**:3539–3546.
- Lai, V. C., Dempsey, S., Lau, J. Y., Hong, Z., and Zhong, W. (2003). *In vitro* RNA replication directed by replicase complexes isolated from the subgenomic replicon cells of hepatitis C virus. *J. Virol.* **77**:2295–2300.

- Lai, V. C., Zhong, W., Skelton, A., Ingravallo, P., Vassilev, V., Donis, R. O., Hong, Z., and Lau, J. Y. (2000). Generation and characterization of a hepatitis C virus NS3 protease-dependent bovine viral diarrhea virus. *J. Virol.* **74**:6339–6347.
- Lambert, C., and Prange, R. (2001). Dual topology of the hepatitis B virus large envelope protein: Determinants influencing posttranslational pre-S translocation. *J. Biol. Chem.* **276**:22265–22272.
- Lambot, M., Fretier, S., Op, D. B., Quatannens, B., Lestavel, S., Clavey, V., and Dubuisson, J. (2002). Reconstitution of hepatitis C virus envelope glycoproteins into liposomes as a surrogate model to study virus attachment. *J. Biol. Chem.* **277**:20625–20630.
- Lanford, R. E., and Bigger, C. (2002). Advances in model systems for hepatitis C virus research. *Virology* **293**:1–9.
- Lanford, R. E., Chavez, D., Notvall, L., and Brasky, K. M. (2003b). Comparison of tamarins and marmosets as hosts for GBV-B infections and the effect of immunosuppression on duration of viremia. *Virology* **311**:72–80.
- Lanford, R. E., Guerra, B., Lee, H., Averett, D. R., Pfeiffer, B., Chavez, D., Notvall, L., and Bigger, C. (2003a). Antiviral effect and virus-host interactions in response to alpha-interferon, gamma-interferon, poly(I)-poly(C), tumor necrosis factor-alpha, and ribavirin in hepatitis C virus subgenomic replicons. *J. Virol.* **77**:1092–1104.
- Lanford, R. E., Sureau, C., Jacob, J. R., White, R., and Fuerst, T. R. (1994). Demonstration of *in vitro* infection of chimpanzee hepatocytes with hepatitis C virus using strand-specific RT/PCR. *Virology* **202**:606–614.
- Laperche, S., Marrec, N. L., Simon, N., Bouchardeau, F., Defer, C., Maniez-Montreuil, M., Levayer, T., Zappitelli, J. P., and Lefrere, J. J. (2003). A new HCV core antigen assay based on disassociation of immune complexes: An alternative to molecular biology in the diagnosis of early HCV infection. *Transfusion* **43**:958–962.
- Laurila, M. R., Makeyev, E. V., and Bamford, D. H. (2002). Bacteriophage phi 6 RNA-dependent RNA polymerase: Molecular details of initiating nucleic acid synthesis without primer. *J. Biol. Chem.* **277**:17117–17124.
- Lechmann, M., Murata, K., Satoi, J., Vergalla, J., Baumert, T. F., and Liang, T. J. (2001). Hepatitis C virus-like particles induce virus-specific humoral and cellular immune responses in mice. *Hepatology* **34**:417–423.
- Lee, K. J., Choi, J., Ou, J. H., and Lai, M. M. (2004). The C-terminal transmembrane domain of hepatitis C virus (HCV) RNA polymerase is essential for HCV replication *in vivo*. *J. Virol.* **78**:3797–3802.
- Lee, B., Leslie, G., Soilleux, E., O'Doherty, U., Baik, S., Levroney, E., Flummerfelt, K., Swiggard, W., Coleman, N., Malim, M., and Doms, R. W. (2001). *Cis* expression of DC-SIGN allows for more efficient entry of human and simian immunodeficiency viruses via CD4 and a coreceptor. *J. Virol.* **75**:12028–12038.
- Leinbach, S. S., Bhat, R. A., Xia, S. M., Hum, W. T., Stauffer, B., Davis, A. R., Hung, P. P., and Mizutani, S. (1994). Substrate specificity of the NS3 serine proteinase of hepatitis C virus as determined by mutagenesis at the NS3/NS4A junction. *Virology* **204**:163–169.
- Lemberg, M. K., Bland, F. A., Weihofen, A., Braud, V. M., and Martoglio, B. (2001). Intramembrane proteolysis of signal peptides: An essential step in the generation of HLA-E epitopes. *J. Immunol.* **167**:6441–6446.
- Lesburg, C. A., Cable, M. B., Ferrari, E., Hong, Z., Mannarino, A. F., and Weber, P. C. (1999). Crystal structure of the RNA-dependent RNA polymerase from hepatitis C virus reveals a fully encircled active site. *Nat. Struct. Biol.* **6**:937–943.

- Lerat, H., Honda, M., Beard, M. R., Loesch, K., Sun, J., Yang, Y., Okuda, M., Gosert, R., Xiao, S. Y., Weinman, S. A., and Lemon, S. M. (2002). Steatosis and liver cancer in transgenic mice expressing the structural and nonstructural proteins of hepatitis C virus. *Gastroenterology* **122**:352–365.
- Levin, M. K., and Patel, S. S. (1999). The helicase from hepatitis C virus is active as an oligomer. *J. Biol. Chem.* **274**:31839–31846.
- Levy, S., Todd, S. C., and Maecker, H. T. (1998). CD81 (TAPA-1): A molecule involved in signal transduction and cell adhesion in the immune system. *Annu. Rev. Immunol.* **16**:89–109.
- Li, X., Jeffers, L. J., Shao, L., Reddy, K. R., DeMedina, M., Scheffel, J., Moore, B., and Schiff, E. R. (1995). Identification of hepatitis C virus by immunoelectron microscopy. *J. Viral Hepat.* **2**:227–234.
- Li, Y., Korolev, S., and Waksman, G. (1998). Crystal structures of open and closed forms of binary and ternary complexes of the large fragment of *Thermus aquaticus* DNA polymerase I: Structural basis for nucleotide incorporation. *EMBO J.* **17**:7514–7525.
- Lin, C., Amberg, S. M., Chambers, T. J., and Rice, C. M. (1993). Cleavage at a novel site in the NS4A region by the yellow fever virus NS2B-3 proteinase is a prerequisite for processing at the downstream 4A/4B signalase site. *J. Virol.* **67**:2327–2335.
- Lin, C., and Kim, J. L. (1999). Structure-based mutagenesis study of hepatitis C virus NS3 helicase. *J. Virol.* **73**:8798–8807.
- Lin, C., Lindenbach, B. D., Pragai, B. M., McCourt, D. W., and Rice, C. M. (1994a). Processing in the hepatitis C virus E2–NS2 region: Identification of p7 and two distinct E2-specific products with different C termini. *J. Virol.* **68**:5063–5073.
- Lin, C., Pragai, B. M., Grakoui, A., Xu, J., and Rice, C. M. (1994b). Hepatitis C virus NS3 serine proteinase: Trans-cleavage requirements and processing kinetics. *J. Virol.* **68**:8147–8157.
- Lin, C., Thomson, J. A., and Rice, C. M. (1995). A central region in the hepatitis C virus NS4A protein allows formation of an active NS3/NS4A serine proteinase complex *in vivo* and *in vitro*. *J. Virol.* **69**:4373–4380.
- Lin, C., Wu, J. W., Hsiao, K., and Su, M. S. (1997). The hepatitis C virus NS4A protein: Interactions with the NS4B and NS5A proteins. *J. Virol.* **71**:6465–6471.
- Liu, C., Zhu, H., Tu, Z., Xu, Y. L., and Nelson, D. R. (2003). CD8+ T-cell interaction with HCV replicon cells: Evidence for both cytokine- and cell-mediated antiviral activity. *Hepatology* **37**:1335–1342.
- Liu, Q. Y., Tackney, C., Bhat, R. A., Prince, A. M., and Zhang, P. (1997). Regulated processing of hepatitis C virus core protein is linked to subcellular localization. *J. Virol.* **71**:657–662.
- Lo, S. Y., Masiarz, F., Hwang, S. B., Lai, M. M., and Ou, J. H. (1995). Differential subcellular localization of hepatitis C virus core gene products. *Virology* **213**:455–461.
- Lo, S. Y., Selby, M., Tong, M., and Ou, J. H. (1994). Comparative studies of the core gene products of two different hepatitis C virus isolates: Two alternative forms determined by a single amino acid substitution. *Virology* **199**:124–131.
- Lo, S. Y., Selby, M. J., and Ou, J. H. (1996). Interaction between hepatitis C virus core protein and E1 envelope protein. *J. Virol.* **70**:5177–5182.
- Lohman, T. M., and Bjornson, K. P. (1996). Mechanisms of helicase-catalyzed DNA unwinding. *Annu. Rev. Biochem.* **65**:169–214.
- Lohmann, V., Hoffmann, S., Herian, U., Penin, F., and Bartenschlager, R. (2003). Viral and cellular determinants of hepatitis C virus RNA replication in cell culture. *J. Virol.* **77**:3007–3019.

- Lohmann, V., Körner, F., Dobierzewska, A., and Bartenschlager, R. (2001). Mutations in hepatitis C virus RNAs conferring cell culture adaptation. *J. Virol.* **75**:1437–1449.
- Lohmann, V., Körner, F., Herian, U., and Bartenschlager, R. (1997). Biochemical properties of hepatitis C virus NS5B RNA-dependent RNA polymerase and identification of amino acid sequence motifs essential for enzymatic activity. *J. Virol.* **71**:8416–8428.
- Lohmann, V., Körner, F., Koch, J. O., Herian, U., Theilmann, L., and Bartenschlager, R. (1999a). Replication of subgenomic hepatitis C virus RNAs in a hepatoma cell line. *Science* **285**:110–113.
- Lohmann, V., Overton, H., and Bartenschlager, R. (1999b). Selective stimulation of hepatitis C virus and pestivirus NS5B RNA polymerase activity by GTP. *J. Biol. Chem.* **274**:10807–10815.
- Lohmann, V., Roos, A., Körner, F., Koch, J. O., and Bartenschlager, R. (2000). Biochemical and structural analysis of the NS5B RNA-dependent RNA polymerase of the hepatitis C virus. *J. Viral Hepat.* **7**:167–174.
- Love, R. A., Parge, H. E., Wickersham, J. A., Hostomsky, Z., Habuka, N., Moomaw, E. W., Adachi, T., and Hostomska, Z. (1996). The crystal structure of hepatitis C virus NS3 proteinase reveals a trypsin-like fold and a structural zinc binding site. *Cell* **87**:331–342.
- Lu, H. H., and Wimmer, E. (1996). Poliovirus chimeras replicating under the translational control of genetic elements of hepatitis C virus reveal unusual properties of the internal ribosomal entry site of hepatitis C virus. *Proc. Natl. Acad. Sci. USA* **93**:1412–1417.
- Lu, W., Strohecker, A., and Ou Jh, J. H. (2001). Posttranslational modification of the hepatitis C virus core protein by tissue transglutaminase. *J. Biol. Chem.* **276**:47993–47999.
- Lukavsky, P. J., Kim, I., Otto, G. A., and Puglisi, J. D. (2003). Structure of HCV IRES domain II determined by NMR. *Nat. Struct. Biol.* **10**:1033–1038.
- Lundin, M., Monne, M., Widell, A., Von Heijne, G., and Persson, M. A. (2003). Topology of the membrane-associated hepatitis C virus protein NS4B. *J. Virol.* **77**:5428–5438.
- Luo, G., Hamatake, R. K., Mathis, D. M., Racela, J., Rigat, K. L., Lemm, J., and Colonno, R. J. (2000). *De novo* initiation of RNA synthesis by the RNA-dependent RNA polymerase (NS5B) of hepatitis C virus. *J. Virol.* **74**:851–863.
- Luo, G., Xin, S., and Cai, Z. (2003). Role of the 5'-proximal stem-loop structure of the 5'-untranslated region in replication and translation of hepatitis C virus RNA. *J. Virol.* **77**:3312–3318.
- Ma, H. C., Ke, C. H., Hsieh, T. Y., and Lo, S. Y. (2002). The first hydrophobic domain of the hepatitis C virus E1 protein is important for interaction with the capsid protein. *J. Gen. Virol.* **83**:3085–3092.
- Ma, Y., and Hendershot, L. M. (2001). The unfolding tale of the unfolded protein response. *Cell* **107**:827–830.
- MacKenzie, K. R., Prestegard, J. H., and Engelman, D. M. (1997). A transmembrane helix dimer: Structure and implications. *Science* **276**:131–133.
- MacQuillan, G. C., de Boer, W. B., Platten, M. A., McCaul, K. A., Reed, W. D., Jeffrey, G. P., and Allan, J. E. (2002). Intrahepatic MxA and PKR protein expression in chronic hepatitis C virus infection. *J. Med. Virol.* **68**:197–205.
- MacQuillan, G. C., Mamotte, C., Reed, W. D., Jeffrey, G. P., and Allan, J. E. (2003). Up-regulation of endogenous intrahepatic interferon-stimulated genes during chronic hepatitis C virus infection. *J. Med. Virol.* **70**:219–227.

- Maillard, P., Krawczynski, K., Nitkiewicz, J., Bronnert, C., Sidorkiewicz, M., Gounon, P., Dubuisson, J., Faure, G., Crainic, R., and Budkowska, A. (2001). Nonenveloped nucleocapsids of hepatitis C virus in the serum of infected patients. *J. Virol.* **75**:8240–8250.
- Manabe, S., Fuke, I., Tanishita, O., Kaji, C., Gomi, Y., Yoshida, S., Mori, C., Takamizawa, A., Yosida, I., and Okayama, H. (1994). Production of nonstructural proteins of hepatitis C virus requires a putative viral protease encoded by NS3. *Virology* **198**:636–644.
- Mandl, C. W., Kunz, C., and Heinz, F. X. (1991). Presence of poly(A) in a flavivirus: Significant differences between the 3′-noncoding regions of the genomic RNAs of tick-borne encephalitis virus strains. *J. Virol.* **65**:4070–4077.
- Markland, W., Petrillo, R. A., Fitzgibbon, M., Fox, T., McCarrick, R., McQuaid, T., Fulghum, J. R., Chen, W. Y., Fleming, M. A., Thomson, J. A., and Chambers, S. P. (1997). Purification and characterization of the NS3 serine protease domain of hepatitis C virus expressed in *Saccharomyces cerevisiae*. *J. Gen. Virol.* **78**:39–43.
- Markoff, L. (2003). 5′- and 3′-noncoding regions in flavivirus RNA. *Adv. Virus Res.* **59**:177–228.
- Mason, P. W., Bezborodova, S. V., and Henry, T. M. (2002). Identification and characterization of a *cis*-acting replication element (cre) adjacent to the internal ribosome entry site of foot-and-mouth disease virus. *J. Virol.* **76**:9686–9694.
- Matsumoto, M., Hwang, S. B., Jeng, K. S., Zhu, N., and Lai, M. M. (1996). Homotypic interaction and multimerization of hepatitis C virus core protein. *Virology* **218**:43–51.
- Matsuura, Y., Suzuki, T., Suzuki, R., Sato, M., Aizaki, H., Saito, I., and Miyamura, T. (1994). Processing of E1 and E2 glycoproteins of hepatitis C virus expressed in mammalian and insect cells. *Virology* **205**:141–150.
- Matsuura, Y., Tani, H., Suzuki, K., Kimura-Someya, T., Suzuki, R., Aizaki, H., Ishii, K., Moriishi, K., Robison, C. S., Whitt, M. A., and Miyamura, T. (2001). Characterization of pseudo-type VSV possessing HCV envelope proteins. *Virology* **286**:263–275.
- Mayo, M. J. (2003). Extrahepatic manifestations of hepatitis C infection. *Am. J. Med. Sci.* **325**:135–148.
- McHutchison, J. G., and Fried, M. W. (2003). Current therapy for hepatitis C: Pegylated interferon and ribavirin. *Clin. Liver Dis.* **7**:149–161.
- McKnight, K. L., and Lemon, S. M. (1998). The rhinovirus type 14 genome contains an internally located RNA structure that is required for viral replication. *RNA* **4**:1569–1584.
- McLauchlan, J. (2000). Properties of the hepatitis C virus core protein: A structural protein that modulates cellular processes. *J. Viral Hepat.* **7**:2–14.
- McLauchlan, J., Lemberg, M. K., Hope, G., and Martoglio, B. (2002). Intramembrane proteolysis promotes trafficking of hepatitis C virus core protein to lipid droplets. *EMBO J.* **21**:3980–3988.
- Meola, A., Sbardellati, A., Bruni, E. B., Cerretani, M., Pezzanera, M., Ceccacci, A., Vitelli, A., Levy, S., Nicosia, A., Traboni, C., McKeating, J., and Scarselli, E. (2000). Binding of hepatitis C virus E2 glycoprotein to CD81 does not correlate with species permissiveness to infection. *J. Virol.* **74**:5933–5938.
- Mercer, D. F., Schiller, D. E., Elliott, J. F., Douglas, D. N., Hao, C., Rinfret, A., Addison, W. R., Fischer, K. P., Churchill, T. A., Lakey, J. R., Tyrrell, D. L., and Kneteman, N. M. (2001). Hepatitis C virus replication in mice with chimeric human livers. *Nat. Med.* **7**:927–933.
- Merola, M., Brazzoli, M., Cocchiarella, F., Heile, J. M., Helenius, A., Weiner, A. J., Houghton, M., and Abrignani, S. (2001). Folding of hepatitis C virus E1 glycoprotein in a cell-free system. *J. Virol.* **75**:11205–11217.

- Meyers, G., and Thiel, H. J. (1996). Molecular characterization of pestiviruses. *Adv. Virus Res.* **47**:53–118.
- Michalak, J. P., Wychowski, C., Choukhi, A., Meunier, J. C., Ung, S., Rice, C. M., and Dubuisson, J. (1997). Characterization of truncated forms of hepatitis C virus glycoproteins. *J. Gen. Virol.* **78**:2299–2306.
- Mihm, S., Frese, M., Meier, V., Wietzke-Braun, P., Scharf, J.-G., Bartenschlager, R., and Ramadori, G. (2004). Interferon type I gene expression in chronic hepatitis C. *Lab. Invest.* **84**:1148–1159.
- Miller, R. H., and Purcell, R. H. (1990). Hepatitis C virus shares amino acid sequence similarity with pestiviruses and flaviviruses as well as members of two plant virus supergroups. *Proc. Natl. Acad. Sci. USA* **87**:2057–2061.
- Miyamoto, H., Okamoto, H., Sato, K., Tanaka, T., and Mishiro, S. (1992). Extraordinarily low density of hepatitis C virus estimated by sucrose density gradient centrifugation and the polymerase chain reaction. *J. Gen. Virol.* **73**:715–718.
- Miyanari, Y., Hijikata, M., Yamaji, M., Hosaka, M., Takahashi, H., and Shimotohno, K. (2003). Hepatitis C virus nonstructural proteins in the probable membranous compartment function in viral genome replication. *J. Biol. Chem.* **278**:50301–50308.
- Mizushima, H., Hijikata, M., Asabe, S., Hirota, M., Kimura, K., and Shimotohno, K. (1994a). Two hepatitis C virus glycoprotein E2 products with different C termini. *J. Virol.* **68**:6215–6222.
- Mizushima, H., Hijikata, M., Tanji, Y., Kimura, K., and Shimotohno, K. (1994b). Analysis of N-terminal processing of hepatitis C virus nonstructural protein 2. *J. Virol.* **68**:2731–2734.
- Monazahian, M., Bohme, I., Bonk, S., Koch, A., Scholz, C., Grethe, S., and Thomssen, R. (1999). Low-density lipoprotein receptor as a candidate receptor for hepatitis C virus. *J. Med. Virol.* **57**:223–229.
- Mondelli, M. U., and Silini, E. (1999). Clinical significance of hepatitis C virus genotypes. *J. Hepatol.* **31**:65–70.
- Moradpour, D., Brass, V., Bieck, E., Friebe, P., Gosert, R., Blum, H. E., Bartenschlager, R., Penin, F., and Lohmann, V. (2004). Membrane association of the RNA-dependent RNA polymerase is essential for hepatitis C virus RNA replication. *J. Virol.* (In press).
- Moradpour, D., Englert, C., Wakita, T., and Wands, J. R. (1996a). Characterization of cell lines allowing tightly regulated expression of hepatitis C virus core protein. *Virology* **222**:51–63.
- Moradpour, D., Wakita, T., Tokushige, K., Carlson, R. I., Krawczynski, K., and Wands, J. R. (1996b). Characterization of three novel monoclonal antibodies against hepatitis C virus core protein. *J. Med. Virol.* **48**:234–241.
- Morgenstern, K. A., Landro, J. A., Hsiao, K., Lin, C., Gu, Y., Su, M. S., and Thomson, J. A. (1997). Polynucleotide modulation of the protease, nucleoside triphosphatase, and helicase activities of a hepatitis C virus NS3/NS4A complex isolated from transfected COS cells. *J. Virol.* **71**:3767–3775.
- Moriya, K., Fujie, H., Shintani, Y., Yotsuyanagi, H., Tsutsumi, T., Ishibashi, K., Matsuura, Y., Kimura, S., Miyamura, T., and Koike, K. (1998). The core protein of hepatitis C virus induces hepatocellular carcinoma in transgenic mice. *Nat. Med.* **4**:1065–1067.
- Mottola, G., Cardinali, G., Ceccacci, A., Trozzi, C., Bartholomew, L., Torrisi, M. R., Pedrazzini, E., Bonatti, S., and Migliaccio, G. (2002). Hepatitis C virus nonstructural proteins are localized in a modified endoplasmic reticulum of cells expressing viral subgenomic replicons. *Virology* **293**:31–43.

- Muerhoff, A. S., Leary, T. P., Simons, J. N., Pilot, M. T., Dawson, G. J., Erker, J. C., Chalmers, M. L., Schlauder, G. G., Desai, S. M., and Mushahwar, I. K. (1995). Genomic organization of GB viruses A and B: Two new members of the Flaviviridae associated with GB agent hepatitis. *J. Virol.* **69**:5621–5630.
- Müller, U., Steinhoff, U., Reis, L. F. L., Hemmi, S., Pavlovic, J., Zinkernagel, R. M., and Aguet, M. (1994). Functional role of type I and type II interferons in antiviral defense. *Science* **264**:1918–1921.
- Murakami, K., Abe, M., Kageyama, T., Kamoshita, N., and Nomoto, A. (2001). Down-regulation of translation driven by hepatitis C virus internal ribosomal entry site by the 3'-untranslated region of RNA. *Arch. Virol.* **146**:729–741.
- Murata, K., Lechmann, M., Qiao, M., Gunji, T., Alter, H. J., and Liang, T. J. (2003). Immunization with hepatitis C virus-like particles protects mice from recombinant hepatitis C virus-vaccinia infection. *Proc. Natl. Acad. Sci. USA* **100**:6753–6758.
- Murphy, D. J., and Vance, J. (1999). Mechanisms of lipid-body formation. *Trends Biochem. Sci.* **24**:109–115.
- Murray, E. M., Grobler, J. A., Markel, E. J., Pagnoni, M. F., Paonessa, G., Simon, A. J., and Flores, O. A. (2003). Persistent replication of hepatitis C virus replicons expressing the beta-lactamase reporter in subpopulations of highly permissive Huh-7 cells. *J. Virol.* **77**:2928–2935.
- Neumann, A. U., Lam, N. P., Dahari, H., Gretch, D. R., Wiley, T. E., Layden, T. J., and Perelson, A. S. (1998). Hepatitis C viral dynamics *in vivo* and the antiviral efficacy of interferon-alpha therapy. *Science* **282**:103–107.
- Nolandt, O., Kern, V., Muller, H., Pfaff, E., Theilmann, L., Welker, R., and Kräusslich, H. G. (1997). Analysis of hepatitis C virus core protein interaction domains. *J. Gen. Virol.* **78**:1331–1340.
- Nousbaum, J. B., Pol, S., Nalpas, B., Landais, P., Berthelot, P., Brechot, C., Gigou, M., Feray, C., Thiers, V., Okamoto, H., Mishiro, S., Poussin, K., Paterlini, P., Rumi, M., and Colombo, M. (1995). Hepatitis C virus type 1b (II) infection in France and Italy. *Ann. Intern. Med.* **122**:161.
- Ogata, N., Alter, H. J., Miller, R. H., and Purcell, R. H. (1991). Nucleotide sequence and mutation rate of the H strain of hepatitis C virus. *Proc. Natl. Acad. Sci. USA* **88**:3392–3396.
- Oh, J. W., Ito, T., and Lai, M. C. (1999). A recombinant hepatitis C virus RNA-dependent RNA polymerase capable of copying the full-length viral RNA. *J. Virol.* **73**:7694–7702.
- Ohba, K., Mizokami, M., Lau, J. Y., Orito, E., Ikeo, K., and Gojobori, T. (1996). Evolutionary relationship of hepatitis C, pesti-, flavi-, plantviruses, and newly discovered GB hepatitis agents. *FEBS Lett.* **378**:232–234.
- Okamoto, H., Kojima, M., Sakamoto, M., Iizuka, H., Hadiwandowo, S., Suwignyo, S., Miyakawa, Y., and Mayumi, M. (1994). The entire nucleotide sequence and classification of a hepatitis C virus isolate of a novel genotype from an Indonesian patient with chronic liver disease. *J. Gen. Virol.* **75**:629–635.
- Okamoto, H., Kojima, M., Okada, S., Yoshizawa, H., Iizuka, H., Tanaka, T., Muchmore, E. E., Peterson, D. A., Ito, Y., and Mishiro, S. (1992a). Genetic drift of hepatitis C virus during an 8.2-year infection in a chimpanzee: Variability and stability. *Virology* **190**:894–899.
- Okamoto, H., Kurai, K., Okada, S., Yamamoto, K., Iizuka, H., Tanaka, T., Fukuda, S., Tsuda, F., and Mishiro, S. (1992b). Full-length sequence of a hepatitis C virus genome having poor homology to reported isolates: Comparative study of four distinct genotypes. *Virology* **188**:331–341.
- Okamoto, H., Okada, S., Sugiyama, Y., Kurai, K., Iizuka, H., Machida, A., Miyakawa, Y., and Mayumi, M. (1991). Nucleotide sequence of the genomic RNA of hepatitis C virus

- isolated from a human carrier: Comparison with reported isolates for conserved and divergent regions. *J. Gen. Virol.* **72**:2697–2704.
- Okamoto, K., Moriishi, K., Miyamura, T., and Matsuura, Y. (2004). Intramembrane proteolysis and endoplasmic reticulum retention of hepatitis C virus core protein. *J. Virol.* **78**:6370–6380.
- Op de Beeck, A., Cocquerel, L., and Dubuisson, J. (2001). Biogenesis of hepatitis C virus envelope glycoproteins. *J. Gen. Virol.* **82**:2589–2595.
- Op de Beeck, A., Voisset, C., Bartosch, B., Ciczora, Y., Cocquerel, L., Keck, Z., Fong, S., Cosset, F. L., and Dubuisson, J. (2004). Characterization of functional hepatitis C virus envelope glycoproteins. *J. Virol.* **78**:2994–3002.
- Otto, G. A., Lukavsky, P. J., Lancaster, A. M., Sarnow, P., and Puglisi, J. D. (2002). Ribosomal proteins mediate the hepatitis C virus IRES-HeLa 40S interaction. *RNA* **8**:913–923.
- Pallaoro, M., Lahm, A., Biasiol, G., Brunetti, M., Nardella, C., Orsatti, L., Bonelli, F., Orru, S., Narjes, F., and Steinkühler, C. (2001). Characterization of the hepatitis C virus NS2/3 processing reaction by using a purified precursor protein. *J. Virol.* **75**:9939–9946.
- Pang, P. S., Jankowsky, E., Planet, P. J., and Pyle, A. M. (2002). The hepatitis C viral NS3 protein is a processive DNA helicase with cofactor enhanced RNA unwinding. *EMBO J.* **21**:1168–1176.
- Paolini, C., de Francesco, R., and Gallinari, P. (2000a). Enzymatic properties of hepatitis C virus NS3-associated helicase. *J. Gen. Virol.* **81**:1335–1345.
- Paolini, C., Lahm, A., de Francesco, R., and Gallinari, P. (2000b). Mutational analysis of hepatitis C virus NS3-associated helicase. *J. Gen. Virol.* **81**:1649–1658.
- Parsley, T. B., Towner, J. S., Blyn, L. B., Ehrenfeld, E., and Semler, B. L. (1997). Poly (rC) binding protein 2 forms a ternary complex with the 5′-terminal sequences of poliovirus RNA and the viral 3CD proteinase. *RNA* **3**:1124–1134.
- Patel, A. H., Wood, J., Penin, F., Dubuisson, J., and McKeating, J. A. (2000). Construction and characterization of chimeric hepatitis C virus E2 glycoproteins: Analysis of regions critical for glycoprotein aggregation and CD81 binding. *J. Gen. Virol.* **81**:2873–2883.
- Patel, J., Patel, A. H., and McLauchlan, J. (2001). The transmembrane domain of the hepatitis C virus E2 glycoprotein is required for correct folding of the E1 glycoprotein and native complex formation. *Virology* **279**:58–68.
- Patzwahl, R., Meier, V., Ramadori, G., and Mihm, S. (2001). Enhanced expression of interferon-regulated genes in the liver of patients with chronic hepatitis C virus infection: Detection by suppression-subtractive hybridization. *J. Virol.* **75**:1332–1338.
- Paul, A. V., Rieder, E., Kim, D. W., van Boom, J. H., and Wimmer, E. (2000). Identification of an RNA hairpin in poliovirus RNA that serves as the primary template in the *in vitro* uridylation of VPg. *J. Virol.* **74**:10359–10370.
- Pavio, N., Romano, P. R., Graczyk, T. M., Feinstone, S. M., and Taylor, D. R. (2003). Protein synthesis and endoplasmic reticulum stress can be modulated by the hepatitis C virus envelope protein E2 through the eukaryotic initiation factor-2alpha kinase PERK. *J. Virol.* **77**:3578–3585.
- Pavio, N., Taylor, D. R., and Lai, M. M. (2002). Detection of a novel unglycosylated form of hepatitis C virus E2 envelope protein that is located in the cytosol and interacts with PKR. *J. Virol.* **76**:1265–1272.
- Pavlovic, D., Neville, D. C., Argaud, O., Blumberg, B., Dwek, R. A., Fischer, W. B., and Zitzmann, N. (2003). The hepatitis C virus p7 protein forms an ion channel that is

- inhibited by long-alkyl-chain iminosugar derivatives. *Proc. Natl. Acad. Sci. USA* **100**:6104–6108.
- Pawlotsky, J. M. (2003). Hepatitis C virus genetic variability: Pathogenic and clinical implications. *Clin. Liver Dis.* **7**:45–66.
- Penin, F. (2003). Structural biology of hepatitis C virus. *Clin. Liver Dis.* **7**:1–21, vii.
- Pestova, T. V., Shatsky, I. N., Fletcher, S. P., Jackson, R. J., and Hellen, C. U. (1998). A prokaryotic-like mode of cytoplasmic eukaryotic ribosome binding to the initiation codon during internal translation initiation of hepatitis C and classical swine fever virus RNAs. *Genes Dev.* **12**:67–83.
- Penin, F., Dubuisson, J., Rey, F. A., Moradpour, D., and Pawlotsky, J. M. (2004). Structural biology of hepatitis C virus. *Hepatology* **39**:5–19.
- Petracca, R., Falugi, F., Galli, G., Norais, N., Rosa, D., Campagnoli, S., Burgio, V., di Stasio, E., Giardina, B., Houghton, M., Abrignani, S., and Grandi, G. (2000). Structure–function analysis of hepatitis C virus envelope-CD81 binding. *J. Virol.* **74**:4824–4830.
- Pieroni, L., Santolini, E., Fipaldini, C., Pacini, L., Migliaccio, G., and La, M. N. (1997). *In vitro* study of the NS2-3 protease of hepatitis C virus. *J. Virol.* **71**:6373–6380.
- Pietschmann, T., and Bartenschlager, R. (2003). Tissue culture and animal models for hepatitis C virus. *Clin. Liver Dis.* **7**:23–43.
- Pietschmann, T., Lohmann, V., Kaul, A., Krieger, N., Rinck, G., Rutter, G., Strand, D., and Bartenschlager, R. (2002). Persistent and transient replication of full-length hepatitis C virus genomes in cell culture. *J. Virol.* **76**:4008–4021.
- Pietschmann, T., Lohmann, V., Rutter, G., Kurpanek, K., and Bartenschlager, R. (2001). Characterization of cell lines carrying self-replicating hepatitis C virus RNAs. *J. Virol.* **75**:1252–1264.
- Pietschmann, T., Koutsoudakis, G., Kallis, S., Kato, T., Fong, S., Wakita, T., and Bartenschlager, R. (2004). Chimeric Hepatitis C Virus Infectious in Cell Culture. Submitted for Publication.
- Pileri, P., Uematsu, Y., Campagnoli, S., Galli, G., Falugi, F., Petracca, R., Weiner, A. J., Houghton, M., Rosa, D., Grandi, G., and Abrignani, S. (1998). Binding of hepatitis C virus to CD81. *Science* **282**:938–941.
- Pizzi, E., Tramontano, A., Tomei, L., La, M. N., Failla, C., Sardana, M., Wood, T., and De, F. R. (1994). Molecular model of the specificity pocket of the hepatitis C virus protease: Implications for substrate recognition. *Proc. Natl. Acad. Sci. USA* **91**:888–892.
- Poch, O., Sauvaget, I., Delarue, M., and Tordo, N. (1989). Identification of four conserved motifs among the RNA-dependent polymerase encoding elements. *EMBO J.* **8**:3867–3874.
- Pohlmann, S., Soilleux, E. J., Baribaud, F., Leslie, G. J., Morris, L. S., Trowsdale, J., Lee, B., Coleman, N., and Doms, R. W. (2001). DC-SIGNR, a DC-SIGN homologue expressed in endothelial cells, binds to human and simian immunodeficiency viruses and activates infection *in trans*. *Proc. Natl. Acad. Sci. USA* **98**:2670–2675.
- Pohlmann, S., Zhang, J., Baribaud, F., Chen, Z., Leslie, G. J., Lin, G., Granelli-Piperno, A., Doms, R. W., Rice, C. M., and McKeating, J. A. (2003). Hepatitis C virus glycoproteins interact with DC-SIGN and DC-SIGNR. *J. Virol.* **77**:4070–4080.
- Polyak, S. J., Khabar, K. S., Paschal, D. M., Ezelle, H. J., Duverlie, G., Barber, G. N., Levy, D. E., Mukaida, N., and Gretch, D. R. (2001a). Hepatitis C virus nonstructural 5A protein induces interleukin-8, leading to partial inhibition of the interferon-induced antiviral response. *J. Virol.* **75**:6095–6106.
- Polyak, S. J., Khabar, K. S., Rezeiq, M., and Gretch, D. R. (2001b). Elevated levels of interleukin-8 in serum are associated with hepatitis C virus infection and resistance to interferon therapy. *J. Virol.* **75**:6209–6211.

- Preugschat, F., Averett, D. R., Clarke, B. E., and Porter, D. T. (1996). A steady-state and pre-steady-state kinetic analysis of the NTPase activity associated with the hepatitis C virus NS3 helicase domain. *J. Biol. Chem.* **271**:24449–24457.
- Preugschat, F., Danger, D. P., Carter, L. H., III, Davis, R. G., and Porter, D. J. (2000). Kinetic analysis of the effects of mutagenesis of W501 and V432 of the hepatitis C virus NS3 helicase domain on ATPase and strand-separating activity. *Biochemistry* **39**:5174–5183.
- Prince, A. M., Huima-Byron, T., Parker, T. S., and Levine, D. M. (1996). Visualization of hepatitis C virions and putative defective interfering particles isolated from low-density lipoproteins. *J. Viral Hepat.* **3**:11–17.
- Qin, W., Luo, H., Nomura, T., Hayashi, N., Yamashita, T., and Murakami, S. (2002). Oligomeric interaction of hepatitis C virus NS5B is critical for catalytic activity of RNA-dependent RNA polymerase. *J. Biol. Chem.* **277**:2132–2137.
- Qin, W., Yamashita, T., Shirota, Y., Lin, Y., Wei, W., and Murakami, S. (2001). Mutational analysis of the structure and functions of hepatitis C virus RNA-dependent RNA polymerase. *Hepatology* **33**:728–737.
- Ralston, R., Thudium, K., Berger, K., Kuo, C., Gervase, B., Hall, J., Selby, M., Kuo, G., Houghton, M., and Choo, Q. L. (1993). Characterization of hepatitis C virus envelope glycoprotein complexes expressed by recombinant vaccinia viruses. *J. Virol.* **67**:6753–6761.
- Ramratnam, B., Bonhoeffer, S., Binley, J., Hurley, A., Zhang, L. Q., Mittler, J. E., Markowitz, M., Moore, J. P., Perelson, A. S., and Ho, D. D. (1999). Rapid production and clearance of HIV-1 and hepatitis C virus assessed by large volume plasma apheresis. *Lancet* **354**:1782–1785.
- Randall, G., Grakoui, A., and Rice, C. M. (2003). Clearance of replicating hepatitis C virus replicon RNAs in cell culture by small interfering RNAs. *Proc. Natl. Acad. Sci. USA* **100**:235–240.
- Reed, K. E., Grakoui, A., and Rice, C. M. (1995). Hepatitis C virus-encoded NS2-3 protease: Cleavage-site mutagenesis and requirements for bimolecular cleavage. *J. Virol.* **69**:4127–4136.
- Reed, K. E., Xu, J., and Rice, C. M. (1997). Phosphorylation of the hepatitis C virus NS5A protein *in vitro* and *in vivo*: Properties of the NS5A-associated kinase. *J. Virol.* **71**:7187–7197.
- Reigadas, S., Ventura, M., Sarih-Cottin, L., Castroviejo, M., Litvak, S., and Astier-Gin, T. (2001). HCV RNA-dependent RNA polymerase replicates *in vitro* the 3'-terminal region of the minus-strand viral RNA more efficiently than the 3'-terminal region of the plus RNA. *Eur. J. Biochem.* **268**:5857–5867.
- Reusken, C. B., Dalebout, T. J., Eerligh, P., Bredenbeek, P. J., and Spaan, W. J. (2003). Analysis of hepatitis C virus/classical swine fever virus chimeric 5'-NTRs: Sequences within the hepatitis C virus IRES are required for viral RNA replication. *J. Gen. Virol.* **84**:1761–1769.
- Reynolds, J. E., Kaminski, A., Carroll, A. R., Clarke, B. E., Rowlands, D. J., and Jackson, R. J. (1996). Internal initiation of translation of hepatitis C virus RNA: The ribosome entry site is at the authentic initiation codon. *RNA* **2**:867–878.
- Reynolds, J. E., Kaminski, A., Kettinen, H. J., Grace, K., Clarke, B. E., Carroll, A. R., Rowlands, D. J., and Jackson, R. J. (1995). Unique features of internal initiation of hepatitis C virus RNA translation. *EMBO J.* **14**:6010–6020.
- Rho, J., Choi, S., Seong, Y. R., Choi, J., and Im, D. S. (2001). The arginine-1493 residue in QRRGRTGR1493G motif IV of the hepatitis C virus NS3 helicase domain is essential

- for NS3 protein methylation by the protein arginine methyltransferase 1. *J. Virol.* **75**:8031–8044.
- Rieder, E., Paul, A. V., Kim, D. W., van Boom, J. H., and Wimmer, E. (2000). Genetic and biochemical studies of poliovirus *cis*-acting replication element cre in relation to VPg uridylylation. *J. Virol.* **74**:10371–10380.
- Rijnbrand, R., Bredenbeek, P., van der, Straaten, T., Whetter, L., Inchauspe, G., Lemon, S., and Spaan, W. (1995). Almost the entire 5'-nontranslated region of hepatitis C virus is required for cap-independent translation. *FEBS Lett.* **365**:115–119.
- Rijnbrand, R., Bredenbeek, P. J., Haasnoot, P. C., Kieft, J. S., Spaan, W. J., and Lemon, S. M. (2001). The influence of downstream protein-coding sequence on internal ribosome entry on hepatitis C virus and other flavivirus RNAs. *RNA* **7**:585–597.
- Rijnbrand, R. C., Abbink, T. E., Haasnoot, P. C., Spaan, W. J., and Bredenbeek, P. J. (1996). The influence of AUG codons in the hepatitis C virus 5'-nontranslated region on translation and mapping of the translation initiation window. *Virology* **226**:47–56.
- Rinck, G., Birghan, C., Harada, T., Meyers, G., Thiel, H. J., and Tautz, N. (2001). A cellular J-domain protein modulates polyprotein processing and cytopathogenicity of a pestivirus. *J. Virol.* **75**:9470–9482.
- Robertson, B., Myers, G., Howard, C., Brettin, T., Bukh, J., Gaschen, B., Gojbori, T., Maertens, G., Mizokami, M., Nainan, O., Netesov, S., Nishioka, K., Shin, I. T., Simmonds, P., Smith, D., Stuyver, L., and Weiner, A. (1998). Classification, nomenclature, and database development for hepatitis C virus (HCV) and related viruses: Proposals for standardization. International Committee on Virus Taxonomy. *Arch. Virol.* **143**:2493–2503.
- Rosa, D., Campagnoli, S., Moretto, C., Guenzi, E., Cousens, L., Chin, M., Dong, C., Weiner, A. J., Lau, J. Y., Choo, Q. L., Chien, D., Pileri, P., Houghton, M., and Abrignani, S. (1996). A quantitative test to estimate neutralizing antibodies to the hepatitis C virus: Cytofluorimetric assessment of envelope glycoprotein 2 binding to target cells. *Proc. Natl. Acad. Sci. USA* **93**:1759–1763.
- Rosenberg, S. (2001). Recent advances in the molecular biology of hepatitis C virus. *J. Mol. Biol.* **313**:451–464.
- Roussel, J., Pillez, A., Montpellier, C., Duverlie, G., Cahour, A., Dubuisson, J., and Wychowski, C. (2003). Characterization of the expression of the hepatitis C virus F protein. *J. Gen. Virol.* **84**:1751–1759.
- Ryan, M. D., Monaghan, S., and Flint, M. (1998). Virus-encoded proteinases of the Flaviviridae. *J. Gen. Virol.* **79**:947–959.
- Sakai, A., Claire, M. S., Faulk, K., Govindarajan, S., Emerson, S. U., Purcell, R. H., and Bukh, J. (2003). The p7 polypeptide of hepatitis C virus is critical for infectivity and contains functionally important genotype-specific sequences. *Proc. Natl. Acad. Sci. USA* **100**:11646–11651.
- Samuel, C. E. (2001). Antiviral actions of interferons. *Clin. Microbiol. Rev.* **14**:778–809.
- Sandgren, E. P., Palmiter, R. D., Heckel, J. L., Daugherty, C. C., Brinster, R. L., and Degen, J. L. (1991). Complete hepatic regeneration after somatic deletion of an albumin-plasminogen activator transgene. *Cell* **66**:245–256.
- Santolini, E., Migliaccio, G., and La, M. N. (1994). Biosynthesis and biochemical properties of the hepatitis C virus core protein. *J. Virol.* **68**:3631–3641.
- Santolini, E., Pacini, L., Fipaldini, C., Migliaccio, G., and LaMonica, N. (1995). The NS2 protein of hepatitis C virus is a transmembrane polypeptide. *J. Virol.* **69**:7461–7471.
- Sato, K., Okamoto, H., Aihara, S., Hoshi, Y., Tanaka, T., and Mishiro, S. (1993). Demonstration of sugar moiety on the surface of hepatitis C virions recovered from the circulation of infected humans. *Virology* **196**:354–357.

- Satoh, S., Tanji, Y., Hijikata, M., Kimura, K., and Shimotohno, K. (1995). The N-terminal region of hepatitis C virus nonstructural protein 3 (NS3) is essential for stable complex formation with NS4A. *J. Virol.* **69**:4255–4260.
- Scarselli, E., Ansuini, H., Cerino, R., Roccasecca, R. M., Acali, S., Filocamo, G., Traboni, C., Nicosia, A., Cortese, R., and Vitelli, A. (2002). The human scavenger receptor class B type I is a novel candidate receptor for the hepatitis C virus. *EMBO J.* **21**:5017–5025.
- Schmidt-Mende, J., Bieck, E., Hugle, T., Penin, F., Rice, C. M., Blum, H. E., and Moradpour, D. (2001). Determinants for membrane association of the hepatitis C virus RNA-dependent RNA polymerase. *J. Biol. Chem.* **276**:44052–44063.
- Schuster, C., Isel, C., Imbert, I., Ehresmann, C., Marquet, R., and Kieny, M. P. (2002). Secondary structure of the 3'-terminus of hepatitis C virus minus-strand RNA. *J. Virol.* **76**:8058–8068.
- Seeff, L. B. (2002). Natural history of chronic hepatitis C. *Hepatology* **36**:S35–S46.
- Selby, M. J., Glazer, E., Masiarz, F., and Houghton, M. (1994). Complex processing and protein:protein interactions in the E2:NS2 region of HCV. *Virology* **204**:114–122.
- Serafino, A., Valli, M. B., Andreola, F., Crema, A., Ravagnan, G., Bertolini, L., and Carloni, G. (2003). Suggested role of the Golgi apparatus and endoplasmic reticulum for crucial sites of hepatitis C virus replication in human lymphoblastoid cells infected *in vitro*. *J. Med. Virol.* **70**:31–41.
- Sheppard, P., Kindsvogel, W., Xu, W., Henderson, K., Schlutsmeyer, S., Whitmore, T. E., Kuestner, R., Garrigues, U., Birks, C., Roraback, J., Ostrander, C., Dong, D., Shin, J., Presnell, S., Fox, B., Haldeman, B., Cooper, E., Taft, D., Gilbert, T., Grant, F. J., Tackett, M., Krivan, W., McKnight, G., Clegg, C., Foster, D., and Klucher, K. M. (2003). IL-28, IL-29 and their class II cytokine receptor IL-28R. *Nat. Immunol.* **4**:63–68.
- Shi, S. T., Lee, K. J., Aizaki, H., Hwang, S. B., and Lai, M. M. (2003). Hepatitis C virus RNA replication occurs on a detergent-resistant membrane that cofractionates with caveolin-2. *J. Virol.* **77**:4160–4168.
- Shimakami, T., Hijikata, M., Luo, H., Ma, Y. Y., Kaneko, S., Shimotohno, K., and Murakami, S. (2004). Effect of interaction between hepatitis C virus NS5A and NS5B on hepatitis C virus RNA replication with the hepatitis C virus replicon. *J. Virol.* **78**:2738–2748.
- Shimizu, Y. K., Feinstone, S. M., Kohara, M., Purcell, R. H., and Yoshikura, H. (1996). Hepatitis C virus: Detection of intracellular virus particles by electron microscopy. *Hepatology* **23**:205–209.
- Shimoike, T., Mimori, S., Tani, H., Matsuura, Y., and Miyamura, T. (1999). Interaction of hepatitis C virus core protein with viral sense RNA and suppression of its translation. *J. Virol.* **73**:9718–9725.
- Shirota, Y., Luo, H., Qin, W., Kaneko, S., Yamashita, T., Kobayashi, K., and Murakami, S. (2002). Hepatitis C virus (HCV) NS5A binds RNA-dependent RNA polymerase (RdRP) NS5B and modulates RNA-dependent RNA polymerase activity. *J. Biol. Chem.* **277**:11149–11155.
- Silini, E., Bono, F., Cividini, A., Cerino, A., Bruno, S., Rossi, S., Belloni, G., Brugnetti, B., Civardi, E., Salvaneschi, L., and Mondelli, M. U. (1995). Differential distribution of hepatitis C virus genotypes in patients with and without liver function abnormalities. *Hepatology* **21**:285–290.
- Simmonds, P., Holmes, E. C., Cha, T. A., Chan, S. W., McOmish, F., Irvine, B., Beall, E., Yap, P. L., Kolberg, J., and Urdea, M. S. (1993). Classification of hepatitis C virus into six major genotypes and a series of subtypes by phylogenetic analysis of the NS-5 region. *J. Gen. Virol.* **74**:2391–2399.

- Smith, D. B., and Simmonds, P. (1997). Characteristics of nucleotide substitution in the hepatitis C virus genome: Constraints on sequence change in coding regions at both ends of the genome. *J. Mol. Evol.* **45**:238–246.
- Smith, R. M., Walton, C. M., Wu, C. H., and Wu, G. Y. (2002). Secondary structure and hybridization accessibility of hepatitis C virus 3'-terminal sequences. *J. Virol.* **76**:9563–9574.
- Soilleux, E. J., Morris, L. S., Leslie, G., Chehimi, J., Luo, Q., Levroney, E., Trowsdale, J., Montaner, L. J., Doms, R. W., Weissman, D., Coleman, N., and Lee, B. (2002). Constitutive and induced expression of DC-SIGN on dendritic cell and macrophage subpopulations *in situ* and *in vitro*. *J. Leukoc. Biol.* **71**:445–457.
- Song, J., Nagano-Fujii, M., Wang, F., Florese, R., Fujita, T., Ishido, S., and Hotta, H. (2000). Nuclear localization and intramolecular cleavage of N-terminally deleted NS5A protein of hepatitis C virus. *Virus Res.* **69**:109–117.
- Spahn, C. M., Kieft, J. S., Grassucci, R. A., Penczek, P. A., Zhou, K., Doudna, J. A., and Frank, J. (2001). Hepatitis C virus IRES RNA-induced changes in the conformation of the 40s ribosomal subunit. *Science* **291**:1959–1962.
- Spangberg, K., and Schwarz, S. (1999). Poly(C) binding protein interacts with the hepatitis C virus 5'-untranslated region. *J. Gen. Virol.* **80**:1371–1376.
- Steinkühler, C., Tomei, L., and de Francesco, R. (1996a). *In vitro* activity of hepatitis C virus protease NS3 purified from recombinant baculovirus-infected Sf9 cells. *J. Biol. Chem.* **271**:6367–6373.
- Steinkühler, C., Urbani, A., Tomei, L., Biasiol, G., Sardana, M., Bianchi, E., Pessi, A., and de Francesco, R. (1996b). Activity of purified hepatitis C virus protease NS3 on peptide substrates. *J. Virol.* **70**:6694–6700.
- Steinkühler, C., Urbani, A., Tomei, L., Biasiol, G., Sardana, M., Bianchi, E., Pessi, A., and de Francesco, R. (1996c). Activity of purified hepatitis C virus protease NS3 on peptide substrates. *J. Virol.* **70**:6694–6700.
- Stempniak, M., Hostomska, Z., Nodes, B. R., and Hostomsky, Z. (1997). The NS3 proteinase domain of hepatitis C virus is a zinc-containing enzyme. *J. Virol.* **71**:2881–2886.
- Su, A. I., Pezacki, J. P., Wodicka, L., Brideau, A. D., Supekova, L., Thimme, R., Wieland, S., Bukh, J., Purcell, R. H., Schultz, P. G., and Chisari, F. V. (2002). Genomic analysis of the host response to hepatitis C virus infection. *Proc. Natl. Acad. Sci. USA* **99**:15669–15674.
- Sulkowski, M. S., and Thomas, D. L. (2003). Hepatitis C in the HIV-infected patient. *Clin. Liver Dis.* **7**:179–194.
- Sung, V. M., Shimodaira, S., Doughty, A. L., Picchio, G. R., Can, H., Yen, T. S., Lindsay, K. L., Levine, A. M., and Lai, M. M. (2003). Establishment of B cell lymphoma cell lines persistently infected with hepatitis C virus *in vivo* and *in vitro*: The apoptotic effects of virus infection. *J. Virol.* **77**:2134–2146.
- Suzich, J. A., Tamura, J. K., Palmer, H. F., Warrener, P., Grakoui, A., Rice, C. M., Feinstone, S. M., and Collett, M. S. (1993). Hepatitis C virus NS3 protein polynucleotide-stimulated nucleoside triphosphatase and comparison with the related pestivirus and flavivirus enzymes. *J. Virol.* **67**:6152–6158.
- Tabor, E., Gerety, R. J., Drucker, J. A., Seeff, L. B., Hoofnagle, J. H., Jackson, D. R., April, M., Barker, L. F., and Pineda-Tamondong, G. (1978). Transmission of non-A, non-B hepatitis from man to chimpanzee. *Lancet* **1**:463–466.
- Taguchi, T., Nagano-Fujii, M., Akutsu, M., Kadoya, H., Ohgimoto, S., Ishido, S., and Hotta, H. (2004). Hepatitis C virus NS5A protein interacts with 2',5'-oligoadenylate synthetase and inhibits antiviral activity of IFN in an IFN sensitivity-determining region-independent manner. *J. Gen. Virol.* **85**:959–969.

- Tai, C. L., Chi, W. K., Chen, D. S., and Hwang, L. H. (1996). The helicase activity associated with hepatitis C virus nonstructural protein 3 (NS3). *J. Virol.* **70**:8477–8484.
- Tai, C. L., Pan, W. C., Liaw, S. H., Yang, U. C., Hwang, L. H., and Chen, D. S. (2001). Structure-based mutational analysis of the hepatitis C virus NS3 helicase. *J. Virol.* **75**:8289–8297.
- Takamizawa, A., Mori, C., Fuke, I., Manabe, S., Murakami, S., Fujita, J., Onishi, E., Andoh, T., Yoshida, I., and Okayama, H. (1991). Structure and organization of the hepatitis C virus genome isolated from human carriers. *J. Virol.* **65**:1105–1113.
- Takikawa, S., Ishii, K., Aizaki, H., Suzuki, T., Asakura, H., Matsuura, Y., and Miyamura, T. (2000). Cell fusion activity of hepatitis C virus envelope proteins. *J. Virol.* **74**:5066–5074.
- Takyar, S. T., Li, D., Wang, Y., Trowbridge, R., and Gowans, E. J. (2000). Specific detection of minus-strand hepatitis C virus RNA by reverse-transcription polymerase chain reaction on poly(A)(+)-purified RNA. *Hepatology* **32**:382–387.
- Tan, S. L., Pause, A., Shi, Y., and Sonenberg, N. (2002). Hepatitis C therapeutics: Current status and emerging strategies. *Nat. Rev. Drug Discov.* **1**:867–881.
- Tan, S.-L., and Katze, M. G. (2001). How hepatitis C virus counteracts the interferon response: The jury is still out on NS5A. *Virology* **284**:1–12.
- Tanaka, T., Kato, N., Cho, M. J., and Shimotohno, K. (1995). A novel sequence found at the 3'-terminus of hepatitis C virus genome. *Biochem. Biophys. Res. Commun.* **215**:744–749.
- Tanaka, T., Kato, N., Cho, M. J., Sugiyama, K., and Shimotohno, K. (1996). Structure of the 3'-terminus of the hepatitis C virus genome. *J. Virol.* **70**:3307–3312.
- Tanaka, T., Kato, N., Nakagawa, M., Ootsuyama, Y., Cho, M. J., Nakazawa, T., Hijikata, M., Ishimura, Y., and Shimotohno, K. (1992). Molecular cloning of hepatitis C virus genome from a single Japanese carrier: Sequence variation within the same individual and among infected individuals. *Virus Res.* **23**:39–53.
- Tanji, Y., Hijikata, M., Hirowatari, Y., and Shimotohno, K. (1994a). Hepatitis C virus polyprotein processing: Kinetics and mutagenic analysis of serine proteinase-dependent cleavage. *J. Virol.* **68**:8418–8422.
- Tanji, Y., Hijikata, M., Hirowatari, Y., and Shimotohno, K. (1994b). Identification of the domain required for trans-cleavage activity of hepatitis C viral serine proteinase. *Gene* **145**:215–219.
- Tanji, Y., Hijikata, M., Satoh, S., Kaneko, T., and Shimotohno, K. (1995a). Hepatitis C virus-encoded nonstructural protein NS4A has versatile functions in viral protein processing. *J. Virol.* **69**:1575–1581.
- Tanji, Y., Kaneko, T., Satoh, S., and Shimotohno, K. (1995b). Phosphorylation of hepatitis C virus-encoded nonstructural protein NS5A. *J. Virol.* **69**:3980–3986.
- Tardif, K. D., Mori, K., and Siddiqui, A. (2002). Hepatitis C virus subgenomic replicons induce endoplasmic reticulum stress activating an intracellular signaling pathway. *J. Virol.* **76**:7453–7459.
- Tardif, K. D., and Siddiqui, A. (2003). Cell surface expression of major histocompatibility complex class I molecules is reduced in hepatitis C virus subgenomic replicon-expressing cells. *J. Virol.* **77**:11644–11650.
- Taylor, D. R., Shi, S. T., Romano, P. R., Barber, G. N., and Lai, M. C. (1999). Inhibition of the interferon-inducible protein kinase PKR by HCV E2 protein. *Science* **285**:107–110.
- Tellinghuisen, T. L., and Rice, C. M. (2002). Interaction between hepatitis C virus proteins and host-cell factors. *Curr. Opin. Microbiol.* **5**:419–427.

- Thibeault, D., Maurice, R., Pilote, L., Lamarre, D., and Pause, A. (2001). *In vitro* characterization of a purified NS2/3 protease variant of hepatitis C virus. *J. Biol. Chem.* **276**:46678–46684.
- Thimme, R., Bukh, J., Spangenberg, H. C., Wieland, S., Pemberton, J., Steiger, C., Govindarajan, S., Purcell, R. H., and Chisari, F. V. (2002). Viral and immunological determinants of hepatitis C virus clearance, persistence, and disease. *Proc. Natl. Acad. Sci. USA* **99**:15661–15668.
- Thomssen, R., Bonk, S., Propfe, C., Heermann, K. H., Kochel, H. G., and Uy, A. (1992). Association of hepatitis C virus in human sera with beta-lipoprotein. *Med. Microbiol. Immunol.* **181**:293–300.
- Thomssen, R., Bonk, S., and Thiele, A. (1993). Density heterogeneities of hepatitis C virus in human sera due to the binding of beta-lipoproteins and immunoglobulins. *Med. Microbiol. Immunol.* **182**:329–334.
- Tomei, L., Failla, C., Santolini, E., De Francesco, R., and LaMonica, N. (1993). NS3 is a serine protease required for processing of hepatitis C virus polyprotein. *J. Virol.* **67**:4017–4026.
- Tomei, L., Failla, C., Vitale, R. L., Bianchi, E., and de Francesco, R. (1996). A central hydrophobic domain of the hepatitis C virus NS4A protein is necessary and sufficient for the activation of the NS3 protease. *J. Gen. Virol.* **77**:1065–1070.
- Tsukiyama-Kohara, K., Iizuka, N., Kohara, M., and Nomoto, A. (1992). Internal ribosome entry site within hepatitis C virus RNA. *J. Virol.* **66**:1476–1483.
- Tu, H., Gao, L., Shi, S. T., Taylor, D. R., Yang, T., Mircheff, A. K., Wen, Y. M., Gorbalenya, A. E., Hwang, S. B., and Lai, M. C. (1999). Hepatitis C virus RNA polymerase and NS5A complex with a SNARE-like protein. *Virology* **263**:30–41.
- Tuplin, A., Wood, J., Evans, D. J., Patel, A. H., and Simmonds, P. (2002). Thermodynamic and phylogenetic prediction of RNA secondary structures in the coding region of hepatitis C virus. *RNA* **8**:824–841.
- Utama, A., Shimizu, H., Hasebe, F., Morita, K., Igarashi, A., Shoji, I., Matsuura, Y., Hatsu, M., Takamizawa, K., Hagiwara, A., and Miyamura, T. (2000). Role of the DEXH motif of the Japanese encephalitis virus and hepatitis C virus NS3 proteins in the ATPase and RNA helicase activities. *Virology* **273**:316–324.
- van Regenmortel, M. H. V., Fauquet, C. M., Bishop, D. H. L., Carstens, E. B., Estes, M. K., Lemon, S. M., Maniloff, J., Mayo, M. A., McGeoch, D. J., Pringle, C. R., and Wickner, R. B. (2000). Virus taxonomy. In “The Eighth Report of the International Committee on Taxonomy of Viruses”. Academic Press, San Diego.
- Varaklioti, A., Vassilaki, N., Georgopoulou, U., and Mavromara, P. (2002). Alternate translation occurs within the core coding region of the hepatitis C viral genome. *J. Biol. Chem.* **277**:17713–17721.
- Wakita, T., Kato, T., Date, T., Miyamoto, M., Zhao, Z., and Mizokami, M. (2004). Hepatitis C Virus Produced from Viral RNA Replicating Cells Infectious for a Hepatoma Cell Line. Submitted for Publication.
- Walewski, J. L., Keller, T. R., Stump, D. D., and Branch, A. D. (2001). Evidence for a new hepatitis C virus antigen encoded in an overlapping reading frame. *RNA* **7**:710–721.
- Wallner, G., Mandl, C. W., Kunz, C., and Heinz, F. X. (1995). The flavivirus 3′-noncoding region: Extensive size heterogeneity independent of evolutionary relationships among strains of tick-borne encephalitis virus. *Virology* **213**:169–178.
- Wang, C., Sarnow, P., and Siddiqui, A. (1993a). Translation of human hepatitis C virus RNA in cultured cells is mediated by an internal ribosome-binding mechanism. *J. Virol.* **67**:3338–3344.

- Wang, C., Sarnow, P., and Siddiqui, A. (1994). A conserved helical element is essential for internal initiation of translation of hepatitis C virus RNA. *J. Virol.* **68**:7301–7307.
- Wang, C. Y., Le, S. Y., Ali, N., and Siddiqui, A. (1995). An RNA pseudo-knot is an essential structural element of the internal ribosome entry site located within the hepatitis C virus 5'-noncoding region. *RNA* **1**:526–537.
- Wang, Q. M., Hockman, M. A., Staschke, K., Johnson, R. B., Case, K. A., Lu, J., Parsons, S., Zhang, F., Rathnachalam, R., Kirkegaard, K., and Colacino, J. M. (2002). Oligomerization and cooperative RNA synthesis activity of hepatitis C virus RNA-dependent RNA polymerase. *J. Virol.* **76**:3865–3872.
- Wang, Y., Okamoto, H., Tsuda, F., Nagayama, R., Tao, Q. M., and Mishiro, S. (1993b). Prevalence, genotypes, and an isolate (HC-C2) of hepatitis C virus in Chinese patients with liver disease. *J. Med. Virol.* **40**:254–260.
- Wardell, A. D., Errington, W., Ciaramella, G., Merson, J., and McGarvey, M. J. (1999). Characterization and mutational analysis of the helicase and NTPase activities of hepatitis C virus full-length NS3 protein. *J. Gen. Virol.* **80**:701–709.
- Waterhouse, P. M., Wang, M. B., and Lough, T. (2001). Gene silencing as an adaptive defence against viruses. *Nature* **411**:834–842.
- Waxman, L., Whitney, M., Pollok, B. A., Kuo, L. C., and Darke, P. L. (2001). Host-cell factor requirement for hepatitis C virus enzyme maturation. *Proc. Natl. Acad. Sci. USA* **98**:13931–13935.
- Weir, M. L., Xie, H., Klip, A., and Trimble, W. S. (2001). VAP-A binds promiscuously to both v- and tSNAREs. *Biochem. Biophys. Res. Commun.* **286**:616–621.
- Wellnitz, S., Klumpp, B., Barth, H., Ito, S., Depla, E., Dubuisson, J., Blum, H. E., and Baumert, T. F. (2002). Binding of hepatitis C virus-like particles derived from infectious clone H77C to defined human cell lines. *J. Virol.* **76**:1181–1193.
- Westaway, E. G., Mackenzie, J. M., and Khromykh, A. A. (2002). Replication and gene function in Kunjin virus. *Curr. Top. Microbiol. Immunol.* **267**:323–351.
- Wilkinson, C. S. (1997). Hepatitis C virus NS2-3 proteinase. *Biochem. Soc. Trans.* **25**:S611.
- Wölk, B., Sansonno, D., Kräusslich, H. G., Dammacco, F., Rice, C. M., Blum, H. E., and Moradpour, D. (2000). Subcellular localization, stability, and trans-cleavage competence of the hepatitis C virus NS3/NS4A complex expressed in tetracycline-regulated cell lines. *J. Virol.* **74**:2293–2304.
- Wu, Z., Yao, N., Le, H. V., and Weber, P. C. (1998). Mechanism of autoproteolysis at the NS2/NS3 junction of the hepatitis C virus polyprotein. *Trends. Biochem. Sci.* **23**:92–94.
- Wunschmann, S., Medh, J. D., Klinzmann, D., Schmidt, W. N., and Stapleton, J. T. (2000). Characterization of hepatitis C virus (HCV) and HCV E2 interactions with CD81 and the low-density lipoprotein receptor. *J. Virol.* **74**:10055–10062.
- Xiang, J., Wunschmann, S., Schmidt, W., Shao, J., and Stapleton, J. T. (2000). Full-length GB virus C (Hepatitis G virus) RNA transcripts are infectious in primary CD4-positive T cells. *J. Virol.* **74**:9125–9133.
- Xie, Z. C., Riezu, B. J., Lasarte, J. J., Guillen, J., Su, J. H., Civeira, M. P., and Prieto, J. (1998). Transmission of hepatitis C virus infection to tree shrews. *Virology* **244**:513–520.
- Xu, Z., Choi, J., Yen, T. S., Lu, W., Strohecker, A., Govindarajan, S., Chien, D., Selby, M. J., and Ou, J. (2001). Synthesis of a novel hepatitis C virus protein by ribosomal frameshift. *EMBO J.* **20**:3840–3848.
- Xu, Z., Choi, J., Lu, W., and Ou, J. (2003). Hepatitis C virus f protein is a short-lived protein associated with the endoplasmatic reticulum. *J. Virol.* **77**:1578–1583.

- Yagnik, A. T., Lahm, A., Meola, A., Roccasecca, R. M., Ercole, B. B., Nicosia, A., and Tramontano, A. (2000). A model for the hepatitis C virus envelope glycoprotein E2. *Proteins* **40**:355–366.
- Yamada, M., Kakumu, S., Yoshioka, K., Higashi, Y., Tanaka, K., Ishikawa, T., and Takayanagi, M. (1994a). Hepatitis C virus genotypes are not responsible for development of serious liver disease. *Dig. Dis. Sci.* **39**:234–239.
- Yamada, N., Tanihara, K., Mizokami, M., Ohba, K., Takada, A., Tsutsumi, M., and Date, T. (1994b). Full-length sequence of the genome of hepatitis C virus type 3a: Comparative study with different genotypes. *J. Gen. Virol.* **75**:3279–3284.
- Yamada, N., Tanihara, K., Takada, A., Yoriyuzi, T., Tsutsumi, M., Shimomura, H., Tsuji, T., and Date, T. (1996). Genetic organization and diversity of the 3′-noncoding region of the hepatitis C virus genome. *Virology* **223**:255–261.
- Yamaga, A. K., and Ou, J. H. (2002). Membrane topology of the hepatitis C virus NS2 protein. *J. Biol. Chem.* **277**:33228–33234.
- Yamashita, T., Kaneko, S., Shirota, Y., Qin, W., Nomura, T., Kobayashi, K., and Murakami, S. (1998). RNA-dependent RNA polymerase activity of the soluble recombinant hepatitis C virus NS5B protein truncated at the C-terminal region. *J. Biol. Chem.* **273**:15479–15486.
- Yan, B. S., Tam, M. H., and Syu, W. J. (1998a). Self-association of the C-terminal domain of the hepatitis-C virus core protein. *Eur. J. Biochem.* **258**:100–106.
- Yan, Y. W., Li, Y., Munshi, S., Sardana, V., Cole, J. L., Sardana, M., Steinkuehler, C., Tomei, L., de Francesco, R., Kuo, L. C., and Chen, Z. G. (1998b). Complex of NS3 protease and NS4A peptide of BK strain hepatitis C virus: A 2.2-angstrom resolution structure in a hexagonal crystal form. *Protein Science* **7**:837–847.
- Yanagi, M., Purcell, R. H., Emerson, S. U., and Bukh, J. (1997). Transcripts from a single full-length cDNA clone of hepatitis C virus are infectious when directly transfected into the liver of a chimpanzee. *Proc. Natl. Acad. Sci. USA* **94**:8738–8743.
- Yanagi, M., St, Shapiro, M., Emerson, S. U., Purcell, R. H., and Bukh, J. (1998). Transcripts of a chimeric cDNA clone of hepatitis C virus genotype 1b are infectious *in vivo*. *Virology* **244**:161–172.
- Yanagi, M., St, C. M., Emerson, S. U., Purcell, R. H., and Bukh, J. (1999). *In vivo* analysis of the 3′-untranslated region of the hepatitis C virus after *in vitro* mutagenesis of an infectious cDNA clone. *Proc. Natl. Acad. Sci. USA* **96**:2291–2295.
- Yang, S. H., Lee, C. G., Song, M. K., and Sung, Y. C. (2000). Internal cleavage of hepatitis C virus NS3 protein is dependent on the activity of NS34A protease. *Virology* **268**:132–140.
- Yao, N., Hesson, T., Cable, M., Hong, Z., Kwong, A. D., Le, H. V., and Weber, P. C. (1997). Structure of the hepatitis C virus RNA helicase domain. *Nat. Struct. Biol.* **4**:463–467.
- Yao, N. H., Reichert, P., Taremi, S. S., Prosser, W. W., and Weber, P. C. (1999). Molecular views of viral polyprotein processing revealed by the crystal structure of the hepatitis C virus bifunctional protease-helicase. *Structure Fold. Des.* **7**:1353–1363.
- Yasui, K., Wakita, T., Tsukiyama, K. K., Funahashi, S. I., Ichikawa, M., Kajita, T., Moradpour, D., Wands, J. R., and Kohara, M. (1998). The native form and maturation process of hepatitis C virus core protein. *J. Virol.* **72**:6048–6055.
- Yen, J. H., Chang, S. C., Hu, C. R., Chu, S. C., Lin, S. S., Hsieh, Y. S., and Chang, M. F. (1995). Cellular proteins specifically bind to the 5′-noncoding region of hepatitis C virus RNA. *Virology* **208**:723–732.
- Yen, T., Keeffe, E. B., and Ahmed, A. (2003). The epidemiology of hepatitis C virus infection. *J. Clin. Gastroenterol.* **36**:47–53.

- Yi, M., Bodola, F., and Lemon, S. M. (2002). Subgenomic hepatitis C virus replicons inducing expression of a secreted enzymatic reporter protein. *Virology* **304**:197–210.
- Yi, M., and Lemon, S. M. (2003a). 3'-nontranslated RNA signals required for replication of hepatitis C virus RNA. *J. Virol.* **77**:3557–3568.
- Yi, M., and Lemon, S. M. (2003b). Structure–function analysis of the 3'-stem-loop of hepatitis C virus genomic RNA and its role in viral RNA replication. *RNA* **9**:331–345.
- Yokota, T., Sakamoto, N., Enomoto, N., Tanabe, Y., Miyagishi, M., Maekawa, S., Yi, L., Kurosaki, M., Taira, K., Watanabe, M., and Mizusawa, H. (2003). Inhibition of intra-cellular hepatitis C virus replication by synthetic- and vector-derived small interfering RNAs. *EMBO Rep.* **4**:602–608.
- Yoo, B. J., Selby, M. J., Choe, J., Suh, B. S., Choi, S. H., Joh, J. S., Nuovo, G. J., Lee, H. S., Houghton, M., and Han, J. H. (1995). Transfection of a differentiated human hepatoma cell line (Huh-7) with *in vitro*-transcribed hepatitis C virus (HCV) RNA and establishment of a long-term culture persistently infected with HCV. *J. Virol.* **69**:32–38.
- Yoo, B. J., Spaete, R. R., Geballe, A. P., Selby, M., Houghton, M., and Han, J. H. (1992). 5'-end-dependent translation initiation of hepatitis C viral RNA and the presence of putative positive and negative translational control elements within the 5'-untranslated region. *Virology* **191**:889–899.
- You, S., Stump, D. D., Branch, A. D., and Rice, C. M. (2004). A *cis*-acting replication element in the sequence encoding the NS5B RNA-dependent RNA polymerase is required for hepatitis C virus RNA replication. *J. Virol.* **78**:1352–1366.
- Yuan, Z. H., Kumar, U., Thomas, H. C., Wen, Y. M., and Monjardino, J. (1997). Expression, purification, and partial characterization of HCV RNA polymerase. *Biochem. Biophys. Res. Commun.* **232**:231–235.
- Zech, B., Kurtenbach, A., Krieger, N., Strand, D., Blencke, S., Morbitzer, M., Salassidis, K., Cotten, M., Wissing, J., Obert, S., Bartenschlager, R., Herget, T., and Daub, H. (2003). Identification and characterization of amphiphysin II as a novel cellular interaction partner of the hepatitis C virus NS5A protein. *J. Gen. Virol.* **84**:555–560.
- Zhang, J., Randall, G., Higginbottom, A., Monk, P., Rice, C. M., and McKeating, J. A. (2004). CD81 is required for hepatitis C virus glycoprotein-mediated viral infection. *J. Virol.* **78**:1448–1455.
- Zhang, J., Yamada, O., Sakamoto, T., Yoshida, H., Iwai, T., Matsushita, Y., Shimamura, H., Araki, H., and Shimotohno, K. (2004). Down-regulation of viral replication by adenoviral-mediated expression of siRNA against cellular cofactors for hepatitis C virus. *Virology* **320**:135–143.
- Zhang, J., Yamada, O., Yoshida, H., Iwai, T., and Araki, H. (2002). Autogenous translational inhibition of core protein: Implication for switch from translation to RNA replication in hepatitis C virus. *Virology* **293**:141–150.
- Zhao, W. D., Wimmer, E., and Lahser, F. C. (1999). Poliovirus/hepatitis C virus (internal ribosomal entry site-core) chimeric viruses: Improved growth properties through modification of a proteolytic cleavage site and requirement for core RNA sequences but not for core-related polypeptides. *J. Virol.* **73**:1546–1554.
- Zhong, W., Uss, A. S., Ferrari, E., Lau, J. Y., and Hong, Z. (2000). *De novo* initiation of RNA synthesis by hepatitis C virus nonstructural protein 5B polymerase. *J. Virol.* **74**:2017–2022.
- Zhu, Q., Guo, J. T., and Seeger, C. (2003a). Replication of hepatitis C virus subgenomes in nonhepatic epithelial and mouse hepatoma cells. *J. Virol.* **77**:9204–9210.

THE REGULATION AND MATURATION OF ANTIVIRAL IMMUNE RESPONSES

J. Lindsay Whitton,^{*} Mark K. Slifka,[†] Fei Liu,[†]
Alexander K. Nussbaum,[†] and Jason K. Whitmire[†]

^{*}Department of Neuropharmacology, CVN-9, The Scripps Research Institute
La Jolla, California 92037

[†]Oregon Health Sciences University, Vaccine and Gene Therapy Institute
Beaverton, Oregon 97006

- I. Overview of the Immune Response to Viral Infection
- II. B Lymphocytes and Their Role in Antiviral Immune Responses
 - A. How Antibodies Combat Viral Infections
 - B. Memory B Cells Acting as Antigen Presenting Cells
 - C. The Cells That Serve as the Source of Long-Term Antibody Production
 - D. How B Cell (Antibody) Functions Mature Over the Course of Infection
- III. Antiviral T Cells: A Primer
- IV. CD8⁺ T Lymphocytes and Their Role in Antiviral Immune Responses
 - A. The Kinetics of the Antiviral CD8⁺ T Cell Response
 - B. The Antiviral Functions of CD8⁺ T Cells
 - C. CD8⁺ T Cell Effector Functions Maturing Over the Course of Infection
- V. CD4⁺ T Lymphocytes and Their Role in Antiviral Immune Responses
 - A. The kinetics of the antiviral CD4⁺ T cell response
 - B. Two Subsets of CD4⁺ T Cells
 - C. The Antiviral Functions of CD4⁺ T Cells
 - D. Maturation of the CD4⁺ T Cell Response
- VI. Immunopathology
- VII. Summary
- References

In this chapter, we review how the immune response to viral infection is regulated, and how the effector arms of the response mature over the course of infection and beyond. The complexity of the antiviral immune response is great, and requires that we be selective in the topics that we discuss. Consequently, we focus almost entirely on the adaptive (antigen-specific) immune response, and refer only briefly to innate immunity; our discussion of adaptive immunity, although covering both antibodies and T cells, favors T cells. Our overall intent is to describe the adaptive immune response, focusing on both quantitative and qualitative changes that occur over the course of a viral infection.

I. OVERVIEW OF THE IMMUNE RESPONSE TO VIRAL INFECTION

Over the past several thousand years, the urbanization of human society has permitted viral infections to wreak havoc on human health. Led by smallpox, viruses have killed or incapacitated hundreds of millions of people throughout past centuries, but the advent of widespread antiviral vaccination has had dramatic effects: not only has it permitted the eradication of the smallpox virus, and the approaching extirpation of poliovirus, but it also has come close to consigning diseases such as measles, mumps, and rubella to the pages of history. Despite this progress, viruses continue to exact a heavy toll in human suffering. Human immunodeficiency virus (HIV) is thought to infect almost one in four Africans (Gregson *et al.*, 2002); previously unidentified viruses have emerged to cause substantial harm—most recently exemplified by the novel coronavirus that causes severe acute respiratory syndrome (SARS) (Fouchier *et al.*, 2003; Kuiken *et al.*, 2003); and old adversaries, such as influenza virus, give sporadic reminders of the threats that they pose (Shortridge *et al.*, 1998).

The main bulwark protecting the population from microbial onslaught is the immune system. The efficacy of the antiviral immune response is well established: (i) the majority of infections, even by viruses considered highly pathogenic, are resolved by an immunocompetent host; (ii) this requires an intact immune system, because even normally innocuous virus infections can be fatal in immunosuppressed individuals; and (iii) the enormous benefits of antiviral vaccination rely on the adaptive immune response. The importance of vaccination is well demonstrated by the current reemergence of measles as an important human pathogen. Irrational parental fears of measles vaccine side effects have led to reduced vaccine uptake in some countries, with potentially catastrophic consequences. There have been sporadic outbreaks of measles in areas of the United States with low vaccine uptake (Robbins, 1993), and in the United Kingdom, parental acceptance of the MMR vaccine has dropped to a level that may eventually permit the measles virus to become endemic once again (Jansen *et al.*, 2003). Perhaps most striking is that low vaccine coverage has resulted in an explosion of measles in Japan—an estimated 30,000 to 200,000 cases annually (Nakayama *et al.*, 2003)—and deaths have numbered in the hundreds. Thus, to address current and future viral challenges, and to further improve the safety and efficacy of available antiviral vaccines, it is imperative that the immune responses to viral infection be fully understood.

The immune response can be classified in several ways, but we consider classification most logical by *antigen specificity*. Thus, immune responses may be termed *nonantigen-specific* or *antigen-specific*. As the name indicates, nonantigen-specific responses do not rely on recognition of specific antigenic motifs; these responses are broad-based and include phagocytes, natural killer cells, type I interferons, and “barrier” defenses, such as skin, lysozyme, and gastric acid. Their actions are exerted very early in the course of combating an infection, and they do not require any form of antigenic “instruction”; consequently, they are termed *innate* immune responses. In contrast, the antigen-specific immune system can learn from experience and thus is termed *adaptive* immunity. Upon first encounter with any given antigen, the antigen-specific responses will be somewhat slow to develop, usually becoming detectable only after the innate responses have approached their peak; however—and in contrast to the innate responses—upon second exposure to the same agent, the antigen-specific responses are greatly improved, both in quantity and quality. These enhanced antigen-specific secondary immune responses—termed *anamnestic* (from the Greek word for *recall*)—originate from memory cells that are specific for the antigens previously encountered and that are the cornerstone of all antiviral vaccines. Both the innate and adaptive immune responses play key roles in controlling a viral infection, and it is becoming increasingly clear that these responses are not, as previously supposed, separate and are instead inextricably linked; however, our goal in this chapter is to cover the adaptive response, and we shall provide no further description of the innate immune system herein.

Adaptive immunity relies on lymphocytes, of which there are two classes: T-lymphocytes (derived from the thymus) and B lymphocytes (named for the avian organ, the bursa of Fabricius). B lymphocytes give rise to antibody-producing plasma cells. Antibodies act mainly to diminish the infectivity of free virus, whereas T cells recognize (and often kill) infected cells. Thus, antibodies and T lymphocytes act in a complementary manner. Antibodies neutralize viruses in the fluid phase (e.g., blood, lymph, interstitial spaces), thereby reducing the number of infected cells and easing the T lymphocytes’ workload. T lymphocytes kill infected cells before virus maturation has occurred, minimizing the release of an infectious virus and thus easing the load on antibodies. In the following pages, we shall review the biology of B and T lymphocyte responses to virus infection and vaccination.

II. B LYMPHOCYTES AND THEIR ROLE IN ANTIVIRAL IMMUNE RESPONSES

Preexisting antibody provides the first line of defense against infection. The potential of serum transfer in the prevention and treatment of infectious disease was first appreciated more than 100 years ago, and serum- or plasma-derived antibody preparations were the only therapeutic resources available prior to the advent of antibiotics or antiviral drugs, and the development of pathogen-specific vaccines. Although highly effective vaccines now play the predominant role in protection against many viral and bacterial pathogens, in recent years the development of safer "humanized" monoclonal antibodies, together with a better understanding of the antimicrobial roles of humoral immunity, have led to a resurgence in the study of antibody-mediated protection against disease. Herein, we describe the antiviral functions of antibody molecules and the role of humoral immunity in a variety of acute and chronic viral infections.

B lymphocytes recognize microbial antigens via the B cell receptor [BcR, more commonly termed immunoglobulin (Ig) or antibody (Ab)], a cell-surface molecule which, as the B cell matures into a plasma cell, is synthesized in secretable form. There are several different classes (isotypes) of Ig (see following paragraphs), and we shall use the most abundant class, IgG, as the basis for our description of structure of antibodies and of the genes that encode them. An IgG molecule comprises four chains, two "heavy" (H) and two "light" (L). The H chain is composed of an N-terminal variable region, followed by three constant domains that are almost identical within any one antibody class (e.g., IgG or IgM) and that define the effector functions of that antibody class. The L chain contains one variable and one constant region. Each L chain is noncovalently paired with one H chain, and the contiguous H and L variable regions together form one antigen recognition site, thereby defining the antigen specificity of the antibody. Two identical H/L chain pairs are themselves noncovalently linked to form the canonical Y-shaped IgG molecule, which has two antigen recognition sites. This Y-shaped structure is common to all antibody classes (Section, II.A.1). The DNA sequences encoding the constant and variable regions are physically separate in the germ line, but undergo rearrangement to form the gene that encodes an H or L chain. Furthermore, the variable regions themselves are generated by the rearrangement of small genetic segments: the variable region of a heavy chain results from the rearrangement of three segments, termed V_H , D_H , and J_H , and the variable region of an L chain is formed by the fusion of a V_L segment and a J_L segment. A variety of V, D, and

J segments are present in the genome, and this combinatorial aspect of antibody gene formation allows a relatively small number of V, D, and J segments to generate a large number of different variable regions, estimated (in humans) at around 300 for L chains and 11,000 for heavy H chains. If H and L chains associate randomly, this provides $\sim 3.3 \times 10^6$ possible combinations (and, thus, antigen specificities) of H/L pairs. In addition, during the process of V-(D)-J rearrangement, small numbers of nucleotides can be added or lost, and this “junctional diversity” increases the number of different H/L specificities to around 10^{11} . Antibody diversity can be further increased by the process of somatic hypermutation, described later.

A. *How Antibodies Combat Viral Infections*

Antibodies can exert their antimicrobial effects by a variety of different mechanisms (Burton, 2002). For instance, a virus can be “neutralized” prior to infection of its target cell. This can occur by the antibody’s binding to the surface of the virus and, by steric hindrance, blocking its ability to bind to its target. Alternatively, some antibodies can be directly virucidal, or they may activate the complement cascade (reviewed in Spear *et al.*, 2001), leading to disruption of the viral membrane. In addition to these mechanisms of direct antibody-mediated killing of the invading pathogen, many types of phagocytic cell express antibody Fc-receptors; antibodies can bind to these receptors, coating the phagocyte and allowing it to recognize, engulf, and destroy microbial pathogens. Although most antibody functions are exerted on free virus particles, in some cases a virus remains vulnerable to antibody-mediated destruction even after it has entered a host cell; if virus proteins are presented on the cell surface and are recognized by the ensuing antiviral antibody response, then destruction of the infected target cell may occur by means of complement-dependent cytotoxicity or by destruction by antibody-dependent cell-cytotoxicity mediated by NK cells or other cell types expressing the appropriate Fc-receptors. For example, when researchers examined the direct *ex vivo* cytolytic response of volunteers immunized with vaccinia, they could not detect a direct *ex vivo* T-cell-mediated lytic response but instead found that direct *ex vivo* lytic activity required NK cells and vaccinia-specific antibodies (Perrin *et al.*, 1977). Interestingly, antibodies do not necessarily need to destroy the infected cell to stop or slow the spread of infection. Some antibodies have been shown to block virus release from infected cells (Gerhard, 2001; Vanderplasschen *et al.*, 1997), interrupt cell-to-cell spread (Burioni *et al.*, 1994; Pantaleo

et al., 1995; Vanderplasschen *et al.*, 1997) or, in the case of some neurotropic viruses such as measles (Fujinami and Oldstone, 1979) or Sindbis virus (Levine *et al.*, 1991), antiviral antibodies may block viral replication without directly resulting in destruction of the infected cell. Together, these studies demonstrate that humoral immunity can result from a multitude of independent and interrelated mechanisms of antiviral activity.

1. *Different Antibody Classes and Their Attributes*

Antibody is produced in five different classes: IgG, IgM, IgA, IgD, and IgE. These antibody molecules differ in their molecular composition as well as in their biologic functions (Padlan, 1994).

- IgG is the most abundant class of immunoglobulin in the serum (mean adult serum level is ~ 12 mg/mL) and, in humans, can be organized into four subclasses, IgG1, IgG2, IgG3, and IgG4, which respectively constitute approximately 70%, 15%, 10%, and 5% of total serum IgG. The main effector function shared by all four IgG subclasses is neutralization, although human IgG3 also very effectively activates the complement system. IgG1 is especially effective in opsonization, a process in which the pathogen becomes coated with antibody and the multiple exposed IgG constant domains facilitate internalization by phagocytes expressing Fc receptors. Opsonization is generally more important in countering bacterial, rather than viral, infection.

- IgM is structurally similar to an IgG molecule, but its H chains carry a fourth constant region. It is the first immunoglobulin expressed at the surface of a developing B cell, and as the cell matures, the antibody is secreted into the plasma in the form of a star-shaped multimeric array of five antibodies; plasma IgM molecules therefore contain 10 antigen recognition sites. The multiplicity of antigen-binding sites would seem to make IgM well-suited for neutralization and it is, perhaps, surprising that its main biological role appears to be complement activation.

- IgA is similar in appearance to IgG, but forms a dimer that has the capacity to be actively transferred across epithelial surfaces, allowing its entry into luminal spaces; as a result, dimeric IgA is a key factor in providing barrier mucosal immunity.

- IgE structure is similar to that of a single IgM molecule (with four constant regions in the H chain), but it does not form multimers. Its serum level is orders of magnitude lower than that of other classes, and it is instead found on the surface of mast cells, where it plays a role in allergies (and, perhaps, in immunity to parasites).

• IgD is superficially similar to IgG, but its function remains unknown (although it can substitute for IgM, if genetic defects prevent the synthesis of that antibody class; Lutz *et al.*, 1998). The biological features of the three classes most important for controlling virus infection—IgM, IgG, and IgA—are summarized in Table I.

2. *The Efficacy of Antibodies in Controlling a Variety of Human Viral Diseases*

There are several possible outcomes of virus infection: some virus families cause acute (i.e., short-lived) infections, whereas others can persist in the host for months or years. It is, therefore, important to understand the role played by antibodies in preventing infection, or disease progression, under these widely disparate circumstances. One school of thought is that antibodies play a key role in controlling acute infections, but not persistent infections (Kagi and Hengartner, 1996). The authors noted that during acute infections, infected cells are rapidly destroyed by the virus, and therefore cellular immunity (which exerts its effect by acting on infected cells) may be of minimal importance; under these circumstances, the host must rely on antiviral antibodies. In contrast, cellular immunity may be more important than antibodies during persistent infection, when the host's goal is to eradicate virus that is "hiding" inside cells. Does this proposal fit the data? The prophylactic and therapeutic efficacy of antibodies against a number of human viruses is summarized in Table II. In support of the hypothesis, there are many instances of lytic viral infections (most notably poxviruses and flaviviruses) that are highly susceptible to antibody-dependent immunity. However, there are several exceptions,

TABLE I

SUMMARY OF THE BIOLOGIC FEATURES OF THE THREE IG CLASSES THAT COMBAT VIRUS INFECTIONS

	IgM	IgG	IgA
Appearance time	Early	Later	Later
Location of abundance	Serum	Serum and interstitial spaces	Serum and mucosal secretions
Placenta crossing	No	Yes	No
Antigen recognition sites	10	2	4
Neutralization	+	++	++
Complement activation	+++	++	+

TABLE II
SUMMARY OF ANTIBODY EFFICACY IN THE PREVENTION AND TREATMENT OF A
VARIETY OF HUMAN VIRAL DISEASES

Virus family	Pathogen	Antibody-mediated protection?	
		Prevention	Treatment
Arenaviridae	Junin virus	—	Yes ¹⁷
	Lassa fever virus	—	Yes ¹⁸ Possible ¹⁹ No ²⁰
Filoviridae	Ebola virus	Yes ¹	Yes ²¹
Flaviviridae	Yellow fever virus	Yes ²	No ²²
	West Nile virus	Yes ³	Yes ²³
	Tick-borne encephalitis virus	Yes ⁴	Possible ²⁴
Hepadnaviridae	Hepatitis B virus	Yes ⁵	No ²⁵
Herpesviridae	Cytomegalovirus	Yes ⁶	Possible ²⁶
	Varicella-zoster virus	Yes ⁷	Yes ²⁷
Paramyxoviridae	Measles virus	Yes ⁸	Yes ²⁸
	Respiratory syncytial virus	Yes ⁹	—
Picornaviridae	Polio virus	Yes ¹⁰	—
	Hepatitis A virus	Yes ¹¹	—
Poxviridae	Vaccinia virus	Yes ¹²	Yes ²⁹
	Smallpox virus	Yes ¹³	Possible ³⁰
Retroviridae	Simian human immunodeficiency virus	Yes ¹⁴	—
Rhabdoviridae	Rabies virus	Yes ¹⁵	—
Togaviridae	Chikungunya virus	Yes ¹⁶	No ³¹

¹ Gupta *et al.*, 2001; Parren *et al.*, 2002; ² Monath and Cetron, 2002; Sawyer, 1931; ³ Ben-Nathan *et al.*, 2003; ⁴ Kreil and Eibl, 1997; ⁵ Anonymous, 2003; ⁶ Wittes *et al.*, 1996; ⁷ Balfour, Jr. *et al.*, 1977; Fisher and Edwards, 1998; ⁸ Stiehm, 1979; ⁹ Romero, 2003; ¹⁰ Hammon *et al.*, 1953; ¹¹ Ward and Krugman, 1962; ¹² Kempe, 1960; ¹³ Kempe *et al.*, 1961; ¹⁴ Nishimura *et al.*, 2002; Parren *et al.*, 2001; ¹⁵ Prosnjak *et al.*, 2003; ¹⁶ Igarashi *et al.*, 1971; ¹⁷ Enria and Barrera Oro, 2002; ¹⁸ Frame, 1989; ¹⁹ McCormick, 1986; ²⁰ White, 1972; ²¹ Mupapa *et al.*, 1999; ²² Monath, 2003; ²³ Ben-Nathan *et al.*, 2003; ²⁴ Kreil and Eibl, 1997; ²⁵ Keller and Stiehm, 2000; ²⁶ Keller and Stiehm, 2000; ²⁷ Ogilvie, 1998; ²⁸ Stiehm, 1979; ²⁹ Kempe, 1960; ³⁰ Peirce *et al.*, 1958; ³¹ Igarashi *et al.*, 1971.

in which a preexisting antibody response to a typically nonlytic (persistent) virus appears to afford partial and, in some cases, complete protection against infection. For example, some arenaviruses can persist for the lifetime of the host, but it is well established that administration of convalescent serum or plasma results in a significant level of protection against lethal Junin virus infection (Enria and Barrera Oro, 2002), although the results for protection against Lassa fever virus, another member of the Arenavirus family, have been mixed (Clayton, 1977; McCormick, 1986). The prototypic arenavirus, LCMV, can establish lifelong persistence in mice, and immunity against this agent is mediated largely by CD8⁺ T cells, consistent with the hypothesis. Monoclonal LCMV-specific antibodies, however, can ameliorate disease (Wright and Buchmeier, 1991), and a vaccine that appeared to induce antibodies in the absence of protective levels of CD8⁺ T cells also could confer protection (Di Simone and Buchmeier, 1995), again indicating that the hypothesis may be an oversimplification.

The results outlined in Table II illustrate an important point; antibodies are generally more effective prophylactically than therapeutically. Preexisting antibody (from acquired immunity or by passive transfer) often can prevent, or at least ameliorate, disease caused by a subsequent virus infection, but the same antibody is less effective when administered after severe, disease symptoms have appeared. This may be due to overwhelming levels of virus that cannot be adequately controlled by a finite amount of transferred antibody. Conversely, there may be very little virus remaining at a time when symptoms are most severe, because many symptoms of viral diseases reflect the immunopathology that occurs during virus clearance (Slifka and Whitton, 2000b) (see Section VI). Nevertheless, antibody-mediated therapies are beginning to gain wider acceptance, especially now that humanized monoclonal antibodies are more easily obtained and can be used in place of convalescent sera. For example, Palivizumab is the first humanized monoclonal antibody licensed for the prevention of respiratory syncytial virus (RSV) infections and, since its introduction in 1998, it has had a significant impact on the number and duration of RSV-associated hospitalizations in susceptible infant populations (Romero, 2003). Other monoclonal antibody formulations are also showing promise; in animal models, a combination of monoclonal antibodies has been shown to be effective in postexposure prophylaxis against rabies virus (Prosniak *et al.*, 2003), and a vaginally applied monoclonal antibody directed against the HIV-1 gp120 molecule protects against mucosal virus transmission (Veazey *et al.*, 2003). Monoclonal antibody therapy has at least two major advantages over

convalescent serum, including (i) low lot-to-lot variation in neutralizing titer, giving a guaranteed standard of therapeutic efficacy and (ii) a significantly decreased risk of contamination with human viruses or other clinically relevant pathogens, a common risk factor encountered when administering convalescent serum or plasma.

B. Memory B Cells Acting as Antigen-Presenting Cells

In addition to producing antibodies to directly combat microbial infections, some B cells—most prominently memory B cells—also help to regulate the immune response by acting as antigen-presenting cells. Memory B cells are detectable in lymphoid organs and the bloodstream within 1 to 2 weeks after acute viral infection, and are maintained at steady-state levels thereafter. These cells do not secrete antibody, and instead maintain cell-surface expression of their immunoglobulin receptors so that they can recognize their specific antigen. Once bound, the antigen is internalized and processed, and the viral epitopes are presented at the cell surface by major histocompatibility complex (MHC) class II molecules; these complexes on the surface of memory B cells are extremely effective triggers of antigen-specific CD4⁺ T cells responses (Lanzavecchia, 1985), the importance of which is described below. Highly activated memory B cells can also proliferate and differentiate into antibody-secreting plasma cells, the main cell type involved with maintaining antibody levels after vaccination or infection. There appears to be a clear division of labor between these related cell types, in that memory B cells are mainly involved with antigen processing, presentation, and mounting anamnestic immune responses, whereas plasma cells are unlikely to be involved with antigen uptake or presentation, because they are largely deficient in surface immunoglobulin and show little or no MHC class II expression (Abney *et al.*, 1978; Halper *et al.*, 1978; Slifka *et al.*, 1998). Plasma cells instead devote most of their energy to the production and secretion of antibody.

C. The Cells That Serve as the Source of Long-Term Antibody Production

Many viruses, and many vaccines (both live and inert), induce antibody responses that remain detectable for years after antigen exposure and, since the half-life of an antibody molecule is measured in weeks, the longevity of the response must be explained by ongoing antibody synthesis. There is general agreement that long-term antibody levels

are maintained by the combined efforts of two largely distinct cell types, memory B cells and plasma cells, but there is substantial controversy regarding the role(s) played by each. Plasma cells secrete up to 10,000 molecules of antibody per second (Helmreich *et al.*, 2003; Hibi and Dosch, 1986), and typically are measured by the ELISPOT technique, which detects spontaneous antibody production by individual cells. Plasma cells accumulate in the spleen or in draining lymph nodes during the early stages of an acute viral infection, but then as the infection is resolved and the local immune response subsides, the majority of virus-specific plasma cells are typically found in the bone marrow compartment (Bachmann *et al.*, 1994; Hyland *et al.*, 1994; Slifka *et al.*, 1995; Youngman *et al.*, 2002). For many years, it was believed that plasma cells were very short-lived (a half-life of less than 3 days), thus requiring continuous replenishment by proliferating memory B cells if long-lived antibody responses were to be maintained (Slifka and Ahmed, 1996). As noted above, memory B cells undoubtedly can differentiate into plasma cells, and it was thought that they must do so at a very high frequency to replace the short-lived plasma cells. However, this notion has recently been challenged by studies demonstrating that individual plasma cells can survive for months to years in the absence of proliferation (Manz *et al.*, 1997), and without their being reconstituted by resident memory B cells (Slifka *et al.*, 1998). In mice, virus-specific plasma cells could be observed more than 500 days after memory B cell depletion, indicating that at least a subpopulation of plasma cells could survive for the life of this host. The life span of plasma cells in humans is currently unknown, and it will be interesting to learn whether plasma cells in larger, more long-lived mammals have a maximal life span of only 1 to 2 years (as found in mice) or whether the life span is extended commensurate with host longevity.

D. How B Cell (Antibody) Functions Mature Over the Course of Infection

B cell responses mature in at least three ways over the course of a viral infection.

- First, B cells produce secreted Ig molecules (antibodies). Naive B cells express IgM, restricted to their cell surfaces. Following an appropriate encounter with cognate antigen, the cells are activated, begin to divide, and produce the secreted, multimeric, form of IgM, which facilitates activation of the complement cascade.

- Second, B cells undergo class switching, alluded to previously. In this process, the variable regions (and, hence, the antigen specificity) of the antibody remain unchanged, but the H chain constant domains are rearranged. For example, the IgM constant domains may be replaced with IgG constant domains. The IgM-secreting B cell will now instead secrete IgG, with identical antigen specificity but with different structure (divalent instead of decavalent) and new effector functions (e.g., enters interstitial spaces, better neutralizing activity) (see Table I).

- Third, during the process of expansion that results from antigen contact, multiple mutations are introduced into the variable regions of the antigen-specific B cells in a process termed *somatic hypermutation*. Somatic hypermutation has (at least) two consequences. One consequence is that many of the changes may reduce or abolish recognition of the triggering antigen, but the resulting B cells and antibodies may now recognize a different antigenic moiety; thus, the process further increases the diversity of the antibody response (to as high as 10^{14} – 10^{16} specificities). Another consequence is that some of the mutations will increase the antibody's affinity for the original antigen, and those B cells that express the improved Ig molecules are preferentially expanded by continued antigen contact. As a result, as long as antigen is present to drive the response, the overall affinity of the antigen-specific antibody population will increase and antibodies can reach extremely high affinities (the range of K^d for antibodies begins at about 10^{-7} M and extends as high as about 10^{-12} M). High-affinity antibodies are more specific for their cognate antigen (diminishing the risk of side effects), and the stronger binding enhances their effector functions (e.g., neutralization, complement fixation, etc.). The strong binding between an individual antibody and its antigen may be effectively irreversible; therefore, antibodies should be considered disposable effector molecules. As will be described next, these features distinguish the maturation of antibody responses from the changes in T cell responses that take place during infection.

III. ANTIVIRAL T CELLS: A PRIMER

In contrast to antibodies, which generally recognize antigenic moieties on intact molecules, most T lymphocytes recognize short (9–24 amino acid) fragments (epitopes) of foreign proteins that are presented

on the cell surface by host glycoproteins encoded in the MHC. Antigen recognition by a T cell relies on the T cell receptor (TcR), a cell surface molecule present in multiple identical copies, each of which is structurally reminiscent of one arm of the Y in an antibody molecule. The TcR is a heterodimer, with each chain comprising one constant region (common to all T cells) and one variable region (which varies among different T cells). There are two categories of TcR: $\alpha\beta$, and $\gamma\delta$. The function of cells bearing the $\gamma\delta$ heterodimer remains largely unknown, and will not be discussed in this review. The great majority of $CD8^+$ T cells responding to viral infection express $\alpha\beta$ TcR heterodimers, and it is this population that has been intensively studied over the past decade. The paired variable regions in an $\alpha\beta$ TcR determine its antigen specificity and, therefore, the specificity of the T cell itself. $\alpha\beta$ T cells are subdivided into two major classes distinguished by their expression of cell surface proteins termed CD8 and CD4. There are two major types of MHC molecule: class I and class II. In general, $CD8^+$ T cells recognize peptide epitopes presented at the cell surface by MHC class I, and $CD4^+$ T cells recognize peptides presented by MHC class II. During the recognition process, broadly speaking, the TcR recognizes the specific combination of peptide epitope and MHC molecule, thus conferring antigen specificity upon the cell; and the CD4 or CD8 molecules interact directly with conserved areas of their respective MHC molecules (Konig *et al.*, 1992; Salter *et al.*, 1990), increasing the avidity of the interaction and helping to assemble the signal transduction apparatus.

There are (at least) two key differences between the MHC class I and class II molecules, and these define the biologic roles of $CD4^+$ and $CD8^+$ T cells. They are summarized in Table III. First, the molecules differ in their distribution: class I molecules are almost ubiquitous, whereas class II molecules are expressed by a relatively limited number of cells, most of which are specialized antigen presenting cells (APCs) important in the induction of an immune response. Second, the molecules differ in the source of viral peptides that they present. MHC class I molecules present epitopes from proteins made within the cell, thus ensuring that, in general, $CD8^+$ T cells will recognize only cells actively infected with a virus. In contrast, MHC class II molecules present peptides that come from proteins taken up from the extracellular milieu; thus, specialized APCs can be recognized by $CD4^+$ T cells even if they are not actively infected. These differences in MHC distribution and function have profound implications for the biological activities of T lymphocytes. $CD8^+$ T cells can, in principle, recognize (and exert their effects on) almost any somatic cell that is unfortunate

TABLE III
MHC DISTRIBUTION AND FUNCTION DEFINE THE BIOLOGIC ROLES OF
THE TWO TYPES OF T LYMPHOCYTE

	CD8 ⁺ T cells	CD4 ⁺ T cells
Recognize epitopes presented by:	MHC class I	MHC class II
Source of antigen presented by MHC and recognized by T cell usually as an:	Endogenous antigen, so CD8 ⁺ T cells recognize infected cells	Exogenous antigen, so cells recognized by CD4 ⁺ T cells need not be infected
Distribution of MHC class I/II expression allows the related T cells to recognize:	Almost all nucleated cells, with the possible exception of neurons	Specialized antigen-presenting cells (class II negative somatic cells invisible to CD4 ⁺ T cells)
T cell functions can:	Usually can kill infected cells and release cytokine, also an important function	Provide "help" to B cells (thereby aiding antibody production) help maintain CD8 ⁺ T cell memory, and directly inhibit virus production

enough to become infected; thus, CD8⁺ T cells can be effective front line combatants against virus infection. In contrast, CD4⁺ T cells are unable to recognize the majority of infected cells, and therefore are less plausible candidates for the direct control of infection (although they may have some direct effects) (Section V.C.3); however, their interactions with specialized APCs ensure that CD4⁺ T cells play important roles in marshalling the immune response. As might be expected from their different roles in countering virus infection, the two T cell types differ somewhat in the ways in which they respond to infection. Therefore, we shall consider them separately, beginning with the better-understood CD8⁺ T cell responses; and in both cases, we shall consider how, over the course of infection, the T cells vary in quantity and in quality.

IV. CD8⁺ T LYMPHOCYTES AND THEIR ROLE IN ANTIVIRAL IMMUNE RESPONSES

Virus-specific CD8⁺ T cells develop when naive cells carrying an appropriate TcR encounter a specialized APC that is presenting the appropriate peptide via its MHC class I molecules. Elegant work

has shown that, in many cases, the APC itself must first be activated through the CD40/CD40L pathway to provide appropriate stimulation to the naive CD8⁺ T cells (Bennett *et al.*, 1998; Ridge *et al.*, 1998; Schoenberger *et al.*, 1998).

A. *The Kinetics of the Antiviral CD8⁺ T Cell Response*

The kinetics of antiviral CD8⁺ T cell responses have been extensively studied in a number of animal model systems and, more recently, in humans. Careful quantitation has provided a relatively detailed picture of the numbers of virus-specific (and/or epitope-specific) CD8⁺ T cells present at all phases of infection. Lymphocytic choriomeningitis virus (LCMV) infection of mice has been widely used in studying many aspects of antiviral immunity, and a quantitative overview of the LCMV-specific CD8⁺ T cell response is presented in Fig. 1. The response is traditionally considered as having three phases: expansion, contraction, and memory. Although shown in the figure as entirely separate, there is some temporal overlap between the phases.

1. *CD8⁺ T Cells: The Expansion Phase*

The expansion phase begins when a naive antigen-specific CD8⁺ T cell encounters its cognate antigen, which results in triggering of a program that leads to the cell's division and differentiation. A study in mice indicated that there may be approximately 100 to 200 naive cells specific for a given antigen, and, since a mouse has $\sim 2 \times 10^7$ CD8⁺ T cells in total, the frequency of naive CD8⁺ T cells of a given antigen specificity would be about 1 in 10^5 (Blattman *et al.*, 2002). If, indeed, a mouse contains CD8⁺ T cells of only approximately 10^5 different specificities, this is far below the number of antibody specificities that are available to the animal, and may have implications for either the number of epitopes that can be recognized or for the fidelity of TcR-antigen recognition.

Triggering of a naive CD8⁺ T cell requires that it receives at least two signals: (i) contact with cognate epitope, delivered via the TcR and (ii) costimulatory signals, which come from a variety of receptor-ligand interactions. The widespread expression of MHC class I molecules ensures that most somatic cells can present viral antigen to CD8⁺ T cells, but only a few cell types—in particular, activated dendritic cells and memory B cells—express the appropriate costimulatory molecules. Consequently, only those cells—located in lymphoid tissues such as the lymph nodes—can trigger naive CD8⁺ T cells to enter the activation pathway. The interaction between a naive CD8⁺ T cell and

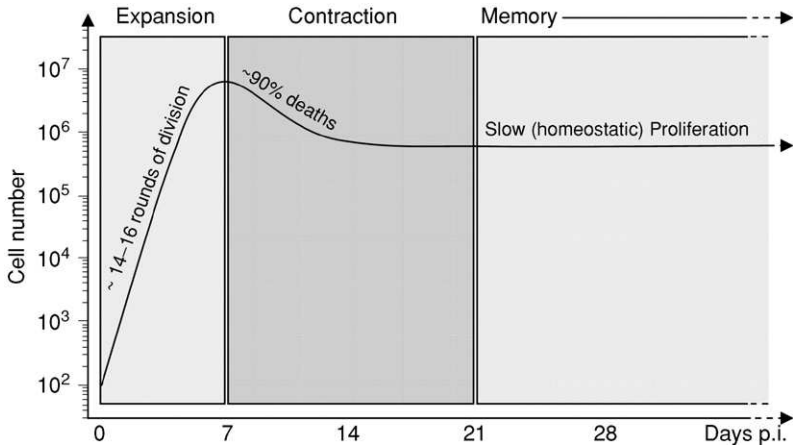


FIG 1. A quantitative overview of the CD8⁺ T cell response to a viral epitope. This graph represents the changes that occur in response to LCMV infection in a population of naive CD8⁺ T cells identical viral epitope specificity. Prior to infection, the size of this pool of identical precursor cells is assumed to be about 100 cells (in accordance with the data of Blattman *et al.*, 2002). The expansion, contraction, and memory phases are indicated by shading. As noted in Section IV.A, the transitions between the post infection (p.i.) phases are not abrupt, and it is likely that there is substantial temporal overlap between successive phases. This graph should be considered a representative graph only; the kinetics of the CD8⁺ T cell response will differ depending on the nature of the infection (e.g., virus; acute vs persistent infection).

an activated APC expressing its cognate antigen may be rather brief; recent studies from several laboratories indicate that only a few hours of antigen exposure are required to cause a CD8⁺ T cell and its progeny to proceed through the expansion, contraction, and memory phases and to express appropriate effector functions (Kaech and Ahmed, 2001; Mercado *et al.*, 2000; van Stipdonk *et al.*, 2001). Following antigen triggering, CD8⁺ T cells divide and continue to do so rather rapidly. The T cell responses shown in Fig. 1 are intended to demonstrate the quantitative changes that may take place in a single population of about 100 naive cells, all of which are specific for the same epitope. In the first 7 days of a viral infection, a naive cell may undergo approximately 14 to 16 rounds of division, permitting a single cell to generate between 16,000 to 65,000 progeny (Blattman *et al.*, 2002). The graph in Fig. 1 assumes that all of the naive cells receive the appropriate antigenic signal, but this may not occur *in vivo*. For example, under some circumstances, increasing the antigen (epitope) expression increases the overall epitope-specific CD8⁺ T cell response (Wherry *et al.*,

1999), consistent with the possibility that the lower expression may have recruited only a proportion of the epitope-specific naive cells into the responding population. It is also possible that all naive cells were activated at both levels of epitope expression, but that the higher level led to increased proliferation (e.g., more rapid, or more prolonged, cell division). Regardless of the mechanism, it is likely that the quantity of antigen available during the early phases of an infection can play a key role in determining the intensity of the CD8⁺ T cell response. Does the duration of antigen availability have a marked effect? The effect of persistent antigen is unclear; it has been suggested that persistent antigen may cause the related T cells to undergo more rounds of cell division (Kaech *et al.*, 2002), but others have noted that the duration of antigen exposure has a minimal effect on the CD8⁺ T cell response (Badovinac *et al.*, 2002).

In summary, naive CD8⁺ T cells are preprogrammed and, after brief antigen contact, they expand, express their effector functions, contract, and enter the memory phase. This reliance on an easily triggered program may have advantages and disadvantages. Viruses have developed many strategies to evade the immune system, including the rapid down-regulation of APC function. If CD8⁺ T cells were to require prolonged or repeated contact with antigen-charged APCs, there would be a significant risk that viruses could undermine the developing CD8⁺ T cell response by limiting APC function. Because only brief antigen contact is needed to initiate the program, the host has a better chance of being able to mount a meaningful response. An additional advantage of programming is that it may permit the activated cell to quickly exit the lymphoid tissues (where the initial triggering occurs) and, presumably, to continue its rapid division in peripheral sites, even in the absence of ongoing antigen contact. In this way, the antiviral functions of the expanding cell population are more rapidly deployed than they would be if the cells had to remain in the lymphoid tissues to receive repeated antigenic signals. A possible disadvantage of programming is that the cells may continue to expand long after the virus (and the antigen) has been eradicated; this is potentially harmful, because autoaggressive CD8⁺ T cells may play a role in virus-induced autoimmune disease (von Herrath *et al.*, 2003).

Upon activation, CD8⁺ T cells up-regulate the expression of several "activation markers," such as CD11a, CD25 (IL-2 receptor- α), CD44, and CD69; they also down-regulate other molecules, including CD62L (L-selectin) and CC-chemokine receptor 7 (CCR7). The understanding of these proteins' functions is incomplete, but several of the proteins appear to play an important part in regulating the anatomical

distribution of the T cells. It has been known for many years that T lymphocyte recirculation is not random, with some cells being retained in lymph nodes and others preferring peripheral tissues (Cahill *et al.*, 1977). Naive CD8⁺ T cells appear to remain in lymphoid tissues because they express on their cell surface high levels of proteins such as CD62L (Gallatin *et al.*, 1983) and CCR7, which can mediate adhesion to lymph node venules (Baekkevold *et al.*, 2001). T cell activation results in the rapid down-regulation of these proteins, and this (along with other factors) allows the cell to exit the node. Once released from the nodes, T cells patrol the peripheral tissues, and settle preferentially in tissues that express particular ligands and/or chemokines, which interact with proteins on the T cell membrane (for example, with CD11a and CD44). There is increasing evidence that T cells home to specific organs, although it remains uncertain whether this behavior is imprinted on the individual T cell by the APC during priming or whether the behavior results from positive selection of activated T cells carrying the appropriate cell-surface molecules. In any event, it appears that during viral infections and other inflammatory processes, T cell trafficking is tightly controlled (reviewed in Weninger *et al.*, 2002).

2. CD8⁺ T Cells: The Contraction Phase

Over the past decade, the expansion and memory phases of the T cell response have been exhaustively studied, but the intervening contraction (death) phase has received much less attention. Although this situation is changing, the understanding of the contraction phase is, at best, elementary. This results in some terminological confusion in the literature, which will, no doubt, be resolved as a clear picture of the contraction phase emerges over the coming years.

As already noted, about 90% of T cells die during the contraction phase, which is relatively brief, and is complete by approximately 15 to 21 days postinfection (Badovinac and Harty, 2002; Badovinac *et al.*, 2002; Kaech *et al.*, 2002; Sprent and Surh, 2002). Although the expansion and contraction phases usually are considered as temporally distinct, this is probably an oversimplification; T cell death begins even as T cell numbers continue to rise. Thus, between approximately 6 to 10 days postinfection, the expansion and contraction phases overlap. Conceptually, one can propose at least four general mechanisms that might precipitate T cell contraction; these mechanisms are not necessarily mutually exclusive. First, activated T cells may be destined to die, regardless of the milieu in which they find themselves; for example, it has been proposed that when a naive T cell first encounters its cognate antigen, a program may be triggered that leads to the death

of progeny cells after a certain number of divisions. This is an intriguing hypothesis, and there is experimental evidence consistent with an early programming event (Badovinac *et al.*, 2002). However, if such early programming takes place, it is unlikely to be sole regulator of contraction, because the fate of activated T cells can be altered by their environment; some of these environmental factors contribute to the remaining three mechanisms. Second, T cell numbers appear to decline in parallel with viral clearance; perhaps the cells die because they can no longer find their cognate antigen. Originally popular, this idea has fallen from favor. Third, T cells may reach a stage where antigen contact becomes lethal, rather than stimulatory [activation-induced cell death (AICD)]. Fourth, as the infection is resolved, there is a general reduction in the proinflammatory cytokine status, and activated T cells could die because of cytokine withdrawal [activated T cell autonomous death (ACAD)].

In addition to identifying the factor(s) that precipitate T cell death, it is important also to ask a related question: by what molecular mechanism do the cells die? Are they killed, or do they commit suicide? If the latter is true, are the cells intrinsically suicidal, or do they act upon instructions? Most studies suggest that the reduction in T cell numbers relies largely on programmed cell death (PCD), a process of cell suicide that is central to many aspects of cell regulation and tissue development. During PCD, the cell dismantles itself in an ordered manner; this contrasts with necrosis, a process of passive cellular disintegration. PCD is important for various aspects of immune regulation. It plays crucial roles in thymic T cell selection, in the killing of virus-infected cells by T cells, and, most relevant to this chapter, in the regulation of virus-specific T cell numbers following infection. Many papers on T cell contraction state that death occurs through apoptosis, and the terms PCD and apoptosis often are used interchangeably. However, the two are not synonymous; in several cell types, including T cells, PCD also can be mediated by triggering of nonapoptotic pathways, and some studies suggest that T cell contraction may be largely nonapoptotic (Holler *et al.*, 2000a). Three types of PCD have been proposed (reviewed in Jaattela and Tschopp, 2003), which can be categorized depending on the morphology of the dying cell, and the part played by caspases (aspartate-specific cysteine proteases that activate the effector phase of cell suicide; Cohen, 1997; Thornberry and Lazebnik, 1998).

1. Classic apoptosis, in which the chromatin of the dying cell condenses at the nuclear margins, and which is caspase-dependent

2. Apoptosis-like PCD, which also shows chromatin condensation, but may be caspase-independent
3. Necrosis-like PCD, in which chromatin condensation is absent, and which can be distinguished from regular necrosis because the former is driven by active cellular processes (Denecker *et al.*, 2001; Vercammen *et al.*, 1998)

We shall discuss the two main mechanisms thought to be responsible for PCD of virus-specific T cells: (i) activation-induced cell death (AICD), also called antigen-driven apoptosis, and (ii) activated T cell autonomous death (ACAD), also called growth factor deprivation-induced apoptosis (Hildeman *et al.*, 2002a; Janssen *et al.*, 2000; Lenardo *et al.*, 1999; Welsh and McNally, 1999).

a. AICD Activated T cells express the FasL molecule, permitting them to induce apoptosis of virus-infected cells that express the death receptor Fas. The Fas–FasL interaction can initiate a caspase cascade, beginning with the cleavage of procaspase-8, and culminating in apoptotic T cell death (reviewed in Budd, 2001). A role for the Fas pathway in T cell homeostasis *in vivo* is strongly supported by observations in mice lacking Fas (*lpr* mice) or FasL (*gld* mice), both of which develop uncontrolled lymphoproliferation (Nagata and Suda, 1995). However, inhibition of the caspase pathway, using either drugs (Hildeman *et al.*, 1999; Holler *et al.*, 2000a) or genetic manipulation (Smith *et al.*, 1996) usually does not result in lymphoproliferation, suggesting the existence of an alternative, caspase-independent pathway that may mediate T cell death. What is the evidence that the Fas pathway and/or the caspase cascade may play a role in AICD during the immune response to virus infection? The Fas pathway is thought to be central to AICD; antigen-driven overstimulation of the T cell receptor induces Fas expression, rendering the T cell susceptible to FasL-driven apoptosis (Brunner *et al.*, 1995). Since AICD is antigen-driven, it is thought to play its part relatively early in infection when the antigen load is high. Furthermore, T cells are rendered more sensitive to Fas-triggered apoptosis when they are actively dividing, and when IL-2 levels are high (Refaeli *et al.*, 1998); these are precisely the conditions present during the later part of the expansion phase. Thus, AICD may drive much of the T cell death that occurs toward the end of the expansion phase. Furthermore, AICD is thought to be crucial for the down-regulation of antiviral T cell responses in persistent virus infection (i.e., when antigen remains in the organism for an extended period of time) (Zhou *et al.*, 2002). However, the fact that the *in vitro* induction of AICD often requires repetitive stimulation through the TCR has led

to some doubt about its contribution to the contraction phase of an antiviral immune response *in vivo* (Hildeman *et al.*, 2002a), and this, together with the observations of caspase-independent death pathways, has led to the search for alternative mechanisms of T cell death.

b. ACAD ACAD is thought to be responsible for the bulk of virus-specific CD8⁺ T cell death that occurs after the virus has been eradicated (i.e., later in the contraction phase). Unlike AICD, ACAD does not depend on the ligation of death receptors (i.e., it is Fas-independent), and it is instead controlled by molecular regulators within the T cell, with the bcl-2 protein family playing a key role (Strasser *et al.*, 1995; van Parijs *et al.*, 1998). The bcl-2 family comprises at least three subgroups of proteins, arrayed in opposing factions. The first subgroup contains antiapoptotic proteins, such as Bcl-2 and Bcl-x_L, and the second is populated by proapoptotic proteins, such as Bax and Bak. Members of the third subgroup, termed BH3-only proteins, favor apoptosis by inhibiting their antiapoptotic relatives or enhancing the activity of the proapoptotic molecules. One BH3-only protein, Bim, has been proposed as the key molecular regulator of ACAD (Hildeman *et al.*, 2002a,b). ACAD can be inhibited by the expression of high levels of Bcl-2, and IL-2 selectively induces the antiapoptotic members of the bcl-2 family, thereby preventing ACAD (Akbar *et al.*, 1996). Furthermore, elevated levels of Bcl-2 protein have been reported in memory T cells (Grayson *et al.*, 2001). The bcl-2 protein family controls mitochondrial outer membrane permeability, and the proapoptotic family members act by disregulating the membrane potential of these vital organelles; this lethal effect appears to be a final common pathway employed by various inducers of caspase-independent cell death. One consequence of the disregulation is the intracellular release of cytochrome c, which in turn activates procaspase-9 and triggers the caspase cascade. Thus, caspase activation occurs in both AICD and ACAD, but its significance differs greatly between the two pathways. In AICD, caspase activation is required for cell death. In contrast, caspase activation is a secondary feature of ACAD, being required for the DNA fragmentation characteristic of apoptosis, but cell death occurs even in the absence of caspases (Ferraro-Peyret *et al.*, 2002).

In summary, there are at least two independent but partially overlapping pathways that may induce T cell death. The likelihood that one or both pathways will be activated in any one cell depends on a variety of factors, which may include the history of antigen contact, the number of cell divisions, and the extracellular microenvironment. At the

peak of the infection, the rapid cell division and high IL-2 levels will tend to favor AICD but, as the inflammatory milieu dissipates, the decline in IL-2 will cause the balance of power within the warring factions of the bcl-2 family to shift, leading to changes in mitochondrial membrane potential, and caspase-independent cell death (ACAD). A recent study in which IL-2 was delivered *in vivo* at various times over the course of an antiviral immune response has confirmed that the timing of IL-2 administration is critical; IL-2 reduced T cell numbers when administered relatively soon after infection, during the expansion phase (consistent with IL-2 inducing AICD), but increased T cell survival when administered during the contraction phase (consistent with IL-2 preventing ACAD) (Blattman *et al.*, 2003).

3. CD8⁺ T Cells: The Memory Phase

CD8⁺ memory T cells play a critical role in protecting against many viral infections, and there is ample evidence that vaccines which induce only CD8⁺ memory T cells can confer good protection against subsequent viral challenge (del Val *et al.*, 1991; Klavinskis *et al.*, 1989; Whitton *et al.*, 1993). The induction of virus-specific CD8⁺ memory T cells is, therefore, a central goal of antiviral vaccine design. The number of CD8⁺ T cells that enter the memory phase is related to the extent of the primary response (Hou *et al.*, 1994; Marshall *et al.*, 2001), but the ontogeny of CD8⁺ memory T cells remains controversial. Some studies suggest that they arise directly from effector cells that escape the contraction phase (Jacob and Baltimore, 1999; Opferman *et al.*, 1999), and that passage into the memory phase may be a stochastic process (Sourdive *et al.*, 1998). Other data indicate that memory cells may represent a separate lineage that can be generated without expressing their effector functions (Lauvau *et al.*, 2001; Manjunath *et al.*, 2001). Regardless of precisely how these cells are generated, it is clear that, in immunocompetent animals, the resting level of memory cells remains relatively stable for a prolonged period (months or years) after infection or vaccination. The establishment of this stable CD8⁺ T cell memory population requires CD4⁺ T cells; in mice lacking CD4⁺ T cells, where the primary CD8⁺ T cell response (i.e., the expansion phase) can be relatively normal, the number of memory cells, and the extent of antiviral protection, decrease with each passing month (von Herrath *et al.*, 1996). The activity of CD4⁺ T cells that stabilizes CD8⁺ T cell memory may be exerted very early, perhaps when the naive CD8⁺ T cells are being programmed (Janssen *et al.*, 2003; Shedlock and Shen, 2003; Sun and Bevan, 2003).

In normal mice, the maintenance of a stable level of CD8⁺ memory T cells requires that the cells continue to divide in a homeostatic manner. This homeostatic division is regulated by cytokines, in particular by IL-7 and IL-15 (Becker *et al.*, 2002; Schluns *et al.*, 2000, 2002; Tan *et al.*, 2002), and occurs in the absence of cognate antigen (Lau *et al.*, 1994; Murali-Krishna *et al.*, 1999). It has been suggested (Sallusto *et al.*, 1999) that there may be two types of memory T cell, termed *effector memory* (cells that are cytolytic and produce cytokines immediately upon antigen encounter) and *central memory* (“effectorless” cells that do not express IFN- γ or perforin immediately upon antigen contact); evaluation of CCR7 expression suggested that CCR7⁺ cells were central memory and CCR7⁻ cells were effector memory. As proposed, this central/memory hypothesis had three distinguishing tenets: (i) effector memory cells are both constitutively lytic and cytokine competent, (ii) central memory cells express neither cytokines nor perforin upon antigen contact; and (iii) the effector and central memory populations can be distinguished on the basis of CCR7 expression. Emerging data are challenging all tenets of the hypothesis. First, several labs have shown that long after virus clearance, virus-specific memory cells can quickly produce IFN- γ in response to antigen contact, but most of them are nonlytic and thus would be excluded from the Sallusto/Lanzavecchia definition of effector memory cells. Second, in our own laboratory, we have found that almost all virus-specific CD8⁺ memory T cells (identified using a tetramer) are also cytokine competent cells (data not shown), suggesting that virus-specific “effectorless” (i.e., central memory) cells, if they exist, are a very minor component of the response; similar findings have been reported in other models of infection (Masopust *et al.*, 2001). Third, with regard to CCR7 expression, Pircher and colleagues (Unsoeld *et al.*, 2002) used a new reagent to detect mouse CCR7 in LCMV TcR transgenic mice and found that, a few days after LCMV infection, virus-specific TcR transgenic CD8⁺ T cells that were lytic and cytokine competent showed no clear pattern in their level of CCR7 expression (Unsoeld *et al.*, 2002). To determine the relationship (if any) between CCR7 expression and effector function in normal (not TcR transgenic) T cells, we infected mice with LCMV, and, several months later, the effector functions of their virus-specific CD8⁺ memory T cells were evaluated directly *ex vivo* by intracellular cytokine staining (ICCS) using the dominant NP_{118–126} peptide as stimulator. Cells were stained to detect CD8 and CCR7, and we included CD62L for comparative purposes. In addition, to determine the effects of antigen re-exposure,

some long-term LCMV-immune mice were reinfected with LCMV and sacrificed 4 days later; their splenocytes were analyzed as already described. Representative results are shown in Fig. 2; all cells shown are CD8⁺ T cells and the axes represent IFN- γ /CD62L (Fig. 2A) or IFN- γ /CCR7 (Fig. 2B). Prior to secondary infection (left columns in Figs. 2A and 2B), peptide-responsive (i.e., IFN- γ ⁺) CD8⁺ memory T cells in the spleen were almost all CD62L⁻ and CCR7⁺; this identification of CCR7⁺ cells that respond immediately to antigen contact is not consistent with the central/effector memory hypothesis. Four days after virus infection (post-2^o; right column in Fig. 2A and 2B), the cytokine competent cells had expanded and were still CD62L⁻, but their CCR7 status had markedly changed, with the majority of the responding cells being CCR7⁻. Thus, our data show that, in normal CD8⁺ memory T cells, CCR7 expression does not correlate with the absence of immediate effector function. Rather, we suggest that it may correlate with the infection status, because CCR7 expression decreases markedly in the 4 days following secondary virus infection. CCR7 is thought to mediate attachment to endothelial cells (Campbell *et al.*, 1998; Gunn *et al.*, 1998) and alters the distribution of cells within the spleen (Potsch *et al.*, 1999); presumably (like CD62L) CCR7 is down-regulated during infection to permit efficient extravasation of effector T cells. Similar findings have recently been reported by others (Ravkov *et al.*, 2003). Furthermore, *in vivo* analyses have shown that both of these proposed classes of CD8⁺ memory cell can confer protective immunity, and they might be better considered as parts of a continuum in which “effector memory” cells serve as the origin for “central memory” cells, which are distinguished more by their anatomical locations than by their effector functions (Wherry *et al.*, 2003). In summary, although there is no doubt that CD8⁺ memory T cells may be somewhat heterogenous in their function and distribution, there is little to support the original classification into two discrete populations based on marker expression and effector activity.

The great majority of published work on memory cells has focused on tissues in which T cells are abundant, usually in the spleen and lymph nodes. The information derived is interesting and relevant, but it represents an incomplete snapshot of antiviral CD8⁺ T cell responses *in vivo* because many of their biologic effects must be exerted in non-lymphoid tissues. Although it has been known for many years that memory T cells can be found in nonlymphoid tissues (Mackay *et al.*, 1992; Sprent, 1976), their detailed analysis is a new area of research, and the emerging data are rather inconclusive. One study showed that CD8⁺ memory T cells in lung and liver were immediately cytolytic

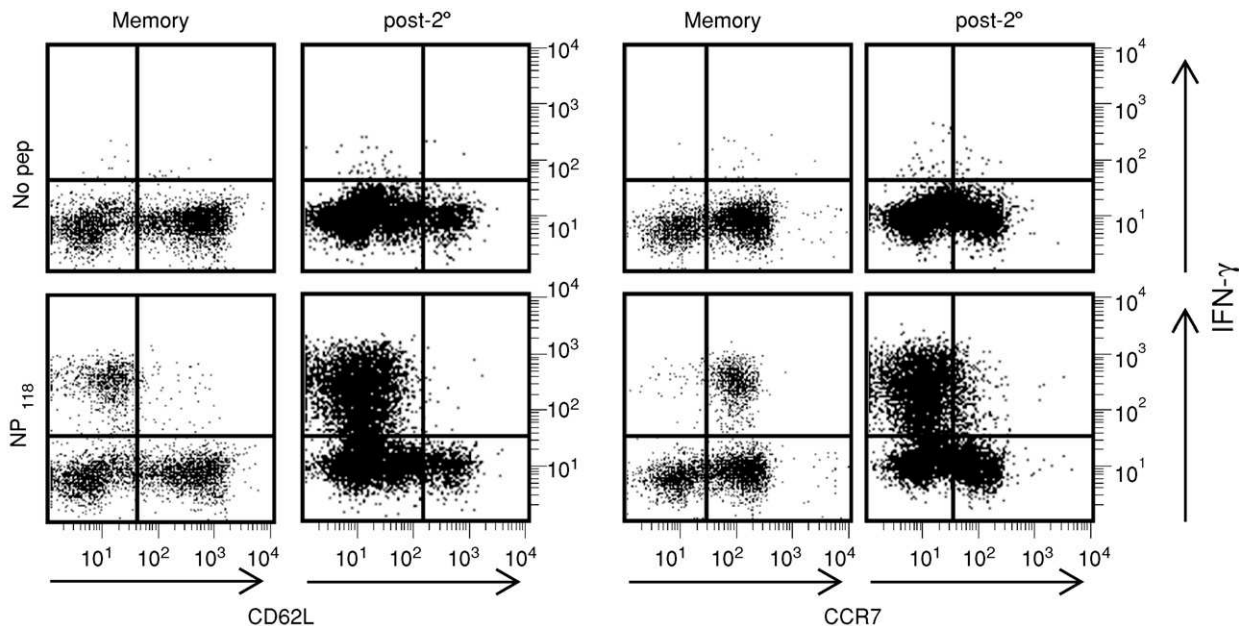


FIG 2. CCR7⁺ cells express effector functions. Mice were infected with LCMV (Armstrong strain) and allowed to clear the virus. Some of these long-term immune mice were reinfected with LCMV 6 months later and they were sacrificed 4 days after reinfection (post-2°). The remaining mice were sacrificed without having been reinfected (memory). For both the memory and post-2° populations, the cell-surface phenotype (CD62L, left panel; CCR7, right panel) and antigen-responsiveness of splenic CD8⁺ T cells were analyzed as described in Section V.A.3.

(Masopust *et al.*, 2001), but others have investigated the effector functions of CD8⁺ memory T cells in the lung parenchyma and airways and have found that virus-specific cells are not immediately cytolytic (Hogan *et al.*, 2001a; Ostler *et al.*, 2001). Furthermore, even in an exhaustively studied organ, the spleen, controversy remains. Selin and Welsh (1997) showed that a small proportion of LCMV-specific memory cells in the spleen were cytolytic. Oehen and Brduscha-Riem (1998) extended this observation in an LCMV transgenic TcR model, demonstrating that some of the transgenic LCMV-specific CD8⁺ memory T cells in the spleens were cytolytic in a short-term (6 h) assay. However, the Lefrancois laboratory showed that, in contrast to Oehen's findings, CD8⁺ memory cells in the spleen were not cytolytic (Masopust *et al.*, 2001). Our own observations suggest that, soon after the virus is cleared, lytic activity is rapidly lost by the great majority of LCMV-specific cells in the spleen (Rodriguez *et al.*, 2001). The regulation and expression of T cell effector functions in peripheral tissues will be the focus of much study in the coming years, as will the quantity of T cells that are resident at these sites. It is known that the number of virus-specific CD8⁺ memory T cells in peripheral tissues, such as lung tissue, remains relatively stable for many months, but it remains uncertain whether this outcome is achieved by homeostatic division of lung-resident cells or whether the population is continually replenished by the immigration of new memory cells from lymphoid tissues; the available data favor the second mechanism (Ely *et al.*, 2003; Hogan *et al.*, 2002).

B. The Antiviral Functions of CD8⁺ T Cells

Virus-specific CD8⁺ T lymphocytes control microbial infections in two general ways: by secreting cytokines, such as IFN- γ and TNF, and by lysing infected cells. It has long been assumed that for controlling viral infections, the cytolytic function of CD8⁺ T cells far outweighs the contribution made by their release of cytokines. There are at least two mechanisms by which CD8⁺ T cells can cause lysis of infected target cells: first, by the insertion of a pore-forming protein, perforin, into the target cell membrane, thus facilitating the entry of toxic molecules such as granzymes and, second, by triggering "death pathways," as exemplified by the Fas/FasL pathway. In this pathway an interaction between the Fas molecule (on the target cell) and its ligand, FasL (on the T cell), results in apoptotic death of the infected cell. Many (probably most) CD8⁺ T cells develop cytolytic capability within hours of antigen contact, but epitope-specific CD8⁺ T cells can

differ in their cytolytic capacities, and virus-specific CD8⁺ T cells very rapidly lose their lytic activity after virus clearance, although they remain cytokine competent—that is, capable of producing cytokines immediately upon antigen contact (Rodriguez *et al.*, 2001). The role of the Fas/FasL pathway in direct antiviral defense is unclear; Fas/FasL interactions have been implicated in regulating virus infection of hepatocytes (Kafrouni *et al.*, 2001) and neurons (Medana *et al.*, 2000), but, in the absence of perforin, this pathway appears incapable of controlling LCMV infection (Walsh *et al.*, 1994). There is no doubt that perforin is important in the clearance of several virus infections, such as LCMV (Kagi *et al.*, 1994; Walsh *et al.*, 1994), but cytolytic activity, long considered the crown jewel in the CD8⁺ T cell armamentarium, is in some cases dispensable; perforin plays little role in controlling infections caused by vaccinia, Semliki Forest virus, vesicular stomatitis virus (Kagi *et al.*, 1995), rotaviruses (Franco *et al.*, 1997b), and coxsackie viruses (Gebhard *et al.*, 1998). Furthermore, exposure to cytokines can directly reduce viral replication, and cytokines alone are able to “cure” some infected cells by inactivating viral replication in the absence of cell death (Estcourt *et al.*, 1998; Guidotti and Chisari, 1996; Levy *et al.*, 1996; Walker *et al.*, 1991). Thus, both cytokines and cytotoxicity contribute to the antiviral activity of CD8⁺ T cells.

C. CD8⁺ T Cell Effector Functions Maturing Over the Course of Infection

Over the past decade, the majority of analyses of CD8⁺ T cell responses to infection have been quantitative rather than qualitative. However, as indicated by the “central memory/effector memory” controversy, the focus is beginning to change. As already described, antibody responses mature over the course of infection and upon reexposure to cognate antigen, and it is reasonable to propose that the host might benefit if virus-specific CD8⁺ T cells also were to improve with time. Our laboratory has investigated this possibility, and has shown that changes in antigen responsiveness do, indeed, take place. We have identified three distinct changes, at least two of which may enhance the ability of CD8⁺ T cells to control virus infection. Each of these changes occurs at different times over the course of infection: the first is complete by about 8 days postinfection, the second is complete by about 21 days, and the third is complete after the cells have entered the memory phase. This chronology is reflected by the order of presentation in the following subsections.

1. *Early in Infection, CD8⁺ T Cells Improve Their Ability to be Triggered by Very Low Levels of Antigen*

One way in which T cells could enhance their biological efficacy would be by optimizing their sensitivity to antigen contact; this could, in principle, be achieved by increasing the affinity of the TcR for the relevant epitope/MHC complex. Others have reported that, between 8 days postinfection and the memory phase, T cell populations carrying TcR of higher affinity are selectively expanded (Busch and Pamer, 1999; Savage *et al.*, 1999); however, this leads to only a very small (about twofold to fourfold) increase in the antigen-responsiveness of the T cell population and, for several reasons, it appears that TcR affinity can contribute nothing more to the maturing CD8⁺ T cell response. Most importantly, and in contrast to antibodies (whose affinities for cognate antigen range from 10^{-7} to 10^{-12} M), the affinities of TcRs for peptide–MHC are very low *in vivo*, ranging from 10^{-4} to 10^{-7} M (Eisen *et al.*, 1996; Valitutti and Lanzavecchia, 1997). This low affinity is unlikely to result from structural constraints because *in vitro* mutagenesis of a TcR can generate a receptor with very high affinity for cognate antigen (Holler *et al.*, 2000b). Thus, the low affinity of TcR *in vivo* appears to result from selective pressures that favor cells bearing low-affinity receptors and/or oppose cells expressing high-affinity molecules. Consistent with the idea that high-affinity TcRs are not evolutionarily desirable, these receptors appear incapable of somatic hypermutation; the sequence of a TcR in a naive cell remains unaltered following activation and expansion. Several proposals have been advanced to explain this *in vivo* “affinity ceiling” for TcR–MHC interactions: (i) high-affinity TcR may be deleted during thymic selection; (ii) T cells bearing high-affinity TcR that escape thymic deletion may become dysfunctional, or be actively eliminated, by prolonged TcR contact with cognate antigen in the host periphery (Valitutti and Lanzavecchia, 1997); and (iii) cells carrying TcR with affinities of approximately 10^{-7} M can be triggered by very low levels of cognate antigen, so the host has no need to produce cells with higher affinity receptors (Salzmann and Bachmann, 1998; Sykulev *et al.*, 1995).

Does this mean that CD8⁺ T cells improve their antigen responsiveness only about twofold to fourfold during viral infection? Prior studies compared cells at the peak of the immune response with cells in the memory phase; these time points were selected because cells were sufficiently numerous to be readily detectable by then-current methods. However, technological advances allowed us to investigate the antigen-responsiveness of virus-specific T cells from much earlier

times postinfection, when cells are few in number. We found that between approximately 4 and 8 days postinfection, the quantity of peptide antigen needed to trigger cytokine production by virus-specific CD8⁺ T cells diminished by about 70-fold, and remained stable thereafter, essentially for the lifetime of the animal (Slifka and Whitton, 2001). By optimizing their ability to be triggered by very low levels of antigen, CD8⁺ T cells ensure that they can recognize cells very early (minutes/hours) after they have become infected, thus maximizing the chance that the T cells' effector functions (e.g., cytokine production, cytolytic activity) will be exerted before the virus has had the opportunity to complete its cycle of replication, maturation, and egress. This occurs without a demonstrable selection of cells bearing high-affinity TcR. We proposed that this optimization is mediated by "hard-wiring" of the signal transduction apparatus, a suggestion confirmed by another study (Kersh *et al.*, 2003). In this light, we proposed an additional explanation for the *in vivo* affinity ceiling of TcRs. T cells are serial killers, and their biological function relies on their being able to rapidly disengage from one target cell and move to another; this antiviral activity might be fatally compromised if T cells were irrevocably linked to a target cell by high-affinity TcR. This explanation is consistent with an elegant study that showed there is an optimal "dwell time" in the interaction between an epitope/class I complex and the TcR of a CD8⁺ T cell. If this interaction is too weak, or too strong, the T cell does not proliferate; only those CD8⁺ T cells bearing TcR that are "just right" are rapidly expanded, and thus are included in the antiviral immune response (Kalergis *et al.*, 2001).

2. *The Speed with Which CD8⁺ T Cells Initiate IFN- γ Production Increases Until ~ 21 Days Post-Infection*

We have explained that T cells increase their antigen-responsiveness *in vivo* by becoming able to respond to lower levels of antigen. Recent studies suggest that as few as 10 peptide/MHC complexes are sufficient to stimulate coordinated signaling via the TcR (Irvine *et al.*, 2002), in which case the antigen-sensitivity of activated T cells approaches the lowest possible limit of antigen concentration on the cell surface. How else might the cells improve their effector response? We reasoned that they might do so by increasing the speed with which they begin cytokine production after being triggered by antigen contact. To determine how quickly an epitope-specific population of CD8⁺ T cells could initiate IFN- γ synthesis in response to antigen contact (their "on-rate"), the proportion of cells synthesizing IFN- γ was evaluated after 1, 2, 3, 4, and 6 hr of peptide exposure. The response at 6 hr

was defined as 100%, the prior responses were plotted as a fraction of that maximum response, and the time taken for 50% of cells to respond to antigen (the half-maximal on-rate; OR1/2) was identified for each population. Representative results are shown in Fig. 3. The OR1/2 of cells harvested at 8 days postinfection was approximately 3.75 h, but the OR1/2 decreased markedly between day 8 and day 15 and, by 21 days postinfection, the cell populations had become maximally responsive to antigen contact (OR1/2 \sim 1 h); this rapid response was retained in long-term immune animals (day 30+). Reinfection of long-term immune mice did not appreciably accelerate the response (day 4 post-2^o), indicating that an OR1/2 of approximately 1 h may represent the fastest possible response by a CD8⁺ T cell population (data not shown). It is important to ask whether this acceleration in response—from about 4 to 1 h—is likely to be biologically significant. Although this improvement may, at first blush, appear modest, one must remember that for most viruses, a single round of propagation (from infection, through replication, to release of infectious progeny) takes place over a short time period (usually about 6–24 h); consequently, even a small increase in the rapidity with which a triggered CD8⁺ T cell can express an antiviral function might substantially decrease the ability of a virus to complete its replication cycle in an infected cell.

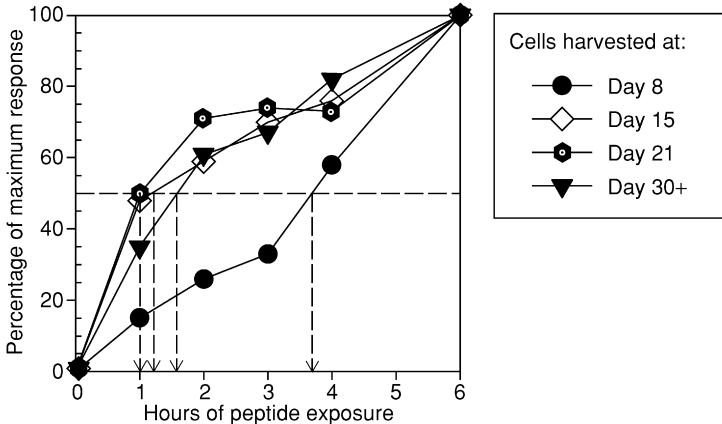


FIG. 3. Onset of IFN- γ synthesis becomes more rapid as CD8⁺ T cells mature. The C57BL/6 mice were infected with LCMV, and the maturation of effector function was followed by determining the OR1/2 of cells harvested over the course of infection. The OR1/2 values for one epitope-specific CD8⁺ T cell population at 8, 15, 21, and 30+ days after primary virus infection are shown by drop-arrows.

3. $CD8^+$ Memory T Cells Produce Both IFN^- and TNF Immediately Following In Vitro Antigen Contact

We have shown that cytokine production by $CD8^+$ T cells is very tightly regulated; $IFN-\gamma$ and tumor necrosis factor (TNF) are produced only when the T cell is in contact with cognate antigen (Slifka *et al.*, 1999). However, as shown in Fig. 4, the pattern of cytokines produced by virus-specific cells changes as the immune response to infection proceeds (Slifka and Whitton, 2000a). When cells are harvested from LCMV-infected BALB/c mice during the expansion phase of the primary response (up to 7 to 8 days postinfection, for many viruses) and are exposed to antigen *in vitro*, two broad populations can be distinguished: one produces only $IFN-\gamma$, while the other produces both $IFN-\gamma$ and TNF. As the response contracts (day 15), the ratio of these two populations changes, and double-positive cells outnumber single-positive cells by approximately 5:1; this process continues into the memory phase (day 60), at which time almost all cells respond to antigen contact by immediately producing $IFN-\gamma$ and TNF. This maturational shift in cytokine profiles also was observed following LCMV infection of C57BL/6 mice, and during recombinant vaccinia virus infection (not shown). A similar change in phenotype occurs during the response to secondary infection (not shown); the cells are initially double-positive (i.e., they are memory phenotype), but, soon after infection, single-positive cells appear. After infection is cleared, the population reverts to the double-positive memory phenotype. These observations have been confirmed in both the influenza model (Belz *et al.*, 2001) and the murine gamma herpesvirus model (Liu *et al.*, 2002). The physiologic significance of this change has not been determined.

V. $CD4^+$ T LYMPHOCYTES AND THEIR ROLE IN ANTIVIRAL IMMUNE RESPONSES

$CD4^+$ T cell responses can be detected after many infections in humans and in mice and, in many situations, are indispensable for effective immunity. These cells display pleiotropic functions in the immune response to microbial infections. They are at the center of events, and orchestrate actions and movements by other subsets of cells including B cells, $CD8^+$ T cells, dendritic cells, and macrophages. In some cases, they also may combat infection directly, as described next.

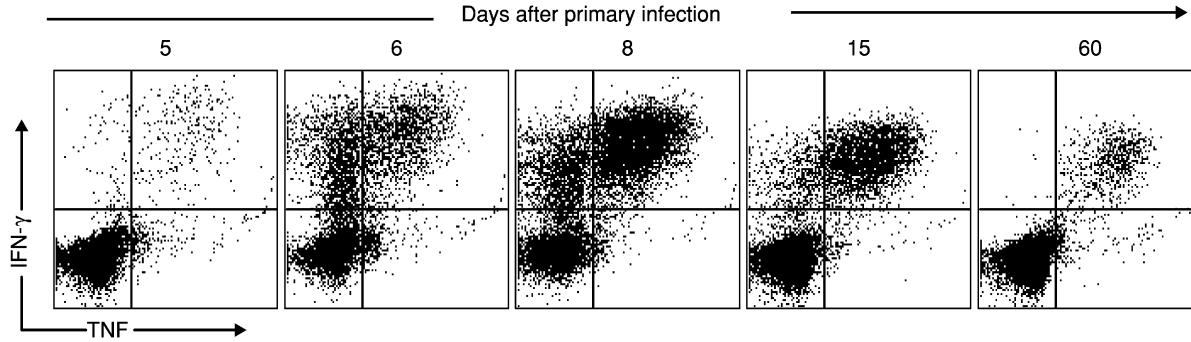


FIG 4. The cytokines produced upon antigen contact changes as the CD8⁺ T cell response matures. Mice were infected with LCMV and, at the indicated time points postinfection, were sacrificed, and their spleens were harvested to determine the pattern of cytokine production by CD8⁺ T cells over the course of a primary virus infection. Splenic CD8⁺ T cell responses were determined using the intracellular cytokine staining procedure, and the acquired data were analyzed using CellQuest software. All cells shown are CD8⁺ T cells and, as indicated, the x- and y-axes represent TNF and IFN-, respectively.

A. *The Kinetics of the Antiviral CD4⁺ T Cell Response*

Technological developments have permitted accurate quantitation of virus-specific CD4⁺ T cell responses without *in vitro* expansion. Using flow-cytometry-based assays, including intracellular staining for IFN- γ or TNF, CD4 responses have been followed in a number of infections. Like the CD8 response, the CD4 response shows three phases: expansion, contraction, and long-term memory. Differences between the two cell types, however, have been reported for all three phases.

1. *CD4⁺ T Cells: The Expansion Phase*

Like the CD8 response, transient exposure to antigen induces a program of CD4 proliferation (Lee *et al.*, 2002), and the great majority of CD4⁺ T cells activated during infection are antigen-specific (i.e., few cells are driven by nonspecific bystander activation) (Homann *et al.*, 2001; Whitmire *et al.*, 1998). However, CD4⁺ T cell responses are typically much lower in magnitude than the concurrent CD8⁺ T cell responses (Maini *et al.*, 1998, 2000; Whitmire *et al.*, 1998, 2000). This difference correlates with a lower proliferation rate, as revealed by BrdU incorporation or CFSE labeling; it has been estimated that, in the week following LCMV infection, a virus-specific CD4⁺ T cell undergoes only about nine cell divisions (Homann *et al.*, 2001). The survival of the proliferating cells is improved with prolonged antigen stimulation (Lee *et al.*, 2002). The CD4 expansion phase also is regulated by several costimulatory interactions, including CD40L–CD40 (Whitmire *et al.*, 1999), CD28–B7 (Suresh *et al.*, 2001), OX40–OX40L (Kopf *et al.*, 1999), and ICOS (Kopf *et al.*, 2000) although these interactions are not required for T-help-independent CD8⁺ T cell responses. CD4⁺ T cells may be regulated more tightly than CD8⁺ T cells via expression of CTLA4 or DR6 or other molecules that inhibit proliferation (Bird *et al.*, 1998; Doyle *et al.*, 2001). There is also evidence that there are intrinsic differences in the proliferative potential of CD4⁺ T cells and CD8⁺ T cells (Foulds *et al.*, 2002). Perhaps CD4⁺ T cells differentiation requires prolonged/repeated antigen contact, whereas CD8⁺ T cells commit to full differentiation after only brief stimulation (Kaech and Ahmed, 2001; van Stipdonk *et al.*, 2001).

2. *CD4⁺ T Cells: The Contraction Phase*

Contraction of the CD4⁺ T cell response is quantitatively similar to that of CD8⁺ T cells, in that about 90% of the cells die; however, in contrast to the abrupt contraction of CD8⁺ T cells, which is usually

complete within 1 week of the peak response, CD4⁺ T cell contraction lingers over the course of several weeks (Homann *et al.*, 2001; Kamperschroer and Quinn, 1999). IL-2 treatment can increase both proliferation and survival of CD4⁺ T cells (Blattman *et al.*, 2003), suggesting that cytokine withdrawal may play an important part in CD4⁺ T cell contraction.

3. CD4⁺ T Cells: The Memory Phase

A number of reports have shown that CD4⁺ T cell responses to LCMV, Sendai virus, and influenza virus in mice can be readily detected long after the infection has been cleared (Topham and Doherty, 1998; Topham *et al.*, 1996a; Varga and Welsh, 1998; Whitmire *et al.*, 1998), and this CD4⁺ T cell memory is maintained in the absence of antigen and MHC class II (Swain *et al.*, 1999). Some studies suggest that CD4 memory is even more stable than CD8 memory (Chang *et al.*, 2001; Varga *et al.*, 2001), but this is somewhat controversial; one study reported a decline in CD4 memory cell number over a prolonged period, in contrast to CD8⁺ memory T cells, which remained stable in the same mice (Homann *et al.*, 2001). The changes correlated with levels of the antiapoptotic molecule Bcl2, which were lower in CD4⁺ memory T cells than in CD8⁺ memory T cells. Despite the conflicting conclusions from these studies, it is clear that CD4⁺ T cell memory is regulated differently from CD8⁺ T cell memory. For example, it appears that the survival of CD4 memory cells is not dependent on IL-15 or IL-7 (Tan *et al.*, 2002), and cells lacking a common cytokine receptor chain survive, indicating that IL-2, -4, -7, -9, and -15 may not be required (Lantz *et al.*, 2000). However—as evidence that the understanding of this process is far from complete—a recent paper reported that the homeostasis of CD4⁺ memory T cells was regulated by IL-7 signaling (Seddon *et al.*, 2003). CD4⁺ memory T cells show improved responsiveness to antigen, and can respond very quickly to antigen reencounter by producing cytokines (Homann *et al.*, 2001; Rogers *et al.*, 2000).

B. Two Subsets of CD4⁺ T Cells

For the most part, CD8⁺ T cells are at the front line; their biological effects are exerted directly upon infected cells. The functions of CD4⁺ T cells are more disparate and usually serve to assist, or otherwise regulate, the responses of B cells and CD8⁺ T cells. Because their main function is to provide help to other lymphocytes, CD4⁺ T cells often are termed “T helper” (T_h) cells, and (at least) two different subsets of T_h can be defined according to their pattern of cytokine production. T_h1

cells produce IL-2, IFN- γ , lymphotoxin, and TNF, whereas T_h2 cells produce IL-4, IL-5, and IL-10. T_h1 cells are associated with the induction of the IgG2a subclass of IgG antibody, and T_h2 cells direct the production of IgG1. Both T_h1 and T_h2 cells can be induced following many viral infections, including CMV (Kallas *et al.*, 1998; Tsai *et al.*, 1997), HIV (Imami *et al.*, 2002), EBV (Steigerwald-Mullen *et al.*, 2000; Wilson *et al.*, 2001), RSV (Bendelja *et al.*, 2000; Tripp *et al.*, 2002), HBV (Diepolder *et al.*, 2001), HCV (Godkin *et al.*, 2002; Rosen *et al.*, 2002; Tsai *et al.*, 1997), and measles virus (Ovsyannikova *et al.*, 2003; Ward and Griffin, 1993) in humans. The cells can also be induced following LCMV (Su *et al.*, 1998; Whitmire *et al.*, 1998), influenza (Graham *et al.*, 1994), Sendai (Mo *et al.*, 1995), coxsackievirus B3 (Huber and Pfaeffle, 1994), RSV (Srikiatkachorn *et al.*, 1999; Tripp *et al.*, 2001), and others in mice. The ratio of T_h1 to T_h2 cells induced by infection can vary markedly, depending on the infectious agent and host genetic background. Both cell types can be specific for the same epitopes (Varga *et al.*, 2000; Whitmire *et al.*, 1998), and there is evidence arguing that antigen dose alone does not dictate the type of T_h cell induced. There are some correlations between the T_h1/T_h2 ratio induced by virus infection and the clinical outcome (Imami *et al.*, 2002; Tsai *et al.*, 1997; Wang *et al.*, 2003), although this is a controversial issue (Bergamini *et al.*, 2001). For example, clearance of acute HCV infection is associated with a strong T_h1 cell response, whereas individuals who developed chronic HCV infection had predominantly T_h2 responses (Tsai *et al.*, 1997).

Some viruses, such as measles virus, HCMV, and MCMV, are found to induce a generalized T_h1 to T_h2 shift, and cause immune suppression. Studies of chronic LCMV infection have indicated that primary T_h1 T cell responses are reduced in magnitude (Ciurea *et al.*, 2001) compared to acute LCMV infection, with IL-2⁺ cells being most affected (Fuller and Zajac, 2003), and the virus-specific CD4⁺ T cells that are initially induced disappear over time (Fuller and Zajac, 2003; Oxenius *et al.*, 1998). In contrast, in mice infected with gamma-herpesvirus, which persists at low levels, virus-specific IL-2⁺ CD4 T cell responses can be detected long after initial infection (Flano *et al.*, 2001). In terms of activation requirements, fewer T_h1 and T_h2 CD4⁺ T cells are induced by virus infection in the absence of intact CD40–CD40L or B7–CD28 costimulation pathways (Whitmire *et al.*, 1999); however, other model systems have provided evidence that T_h2 cells have a lower reliance on costimulation. While the definition of the T_h1 and T_h2 subsets is clear—and there is evidence in cell lines for chromosomal restructuring, suggesting irrevocable differentiation—is it possible

that, during an *in vivo* infection, some cells at times make cytokines of both classes? There is a precedent for this in humans infected with CMV (Kallas *et al.*, 1998), but because IL-4 is best detected by ELISA or ELISPOT assays, proof of this in mice must await improved intracellular staining techniques that allow costaining for both IFN- γ and IL-4.

C. The Antiviral Functions of CD4⁺ T Cells

1. CD4⁺ T Cells Helping B Cells

A long recognized function of CD4⁺ T cells is their ability to induce B cell differentiation; they are involved in class switching, and in the transition of virus-specific memory B cells into antibody-secreting plasma cells. Because preexisting antibody is a first line of defense against reinfection, these CD4⁺ T cell functions are crucial for protection. CD4⁺ T cells drive B cell differentiation and proliferation by acting through the CD40L-CD40 pathway, and they modify antibody class-switching by stimulating B cells with IFN- γ or IL-4. These differentiation events occur primarily in germinal centers where activated CD4⁺ T cells associate with antigen-reactive B cells (Garside *et al.*, 1998; Pape *et al.*, 2003). CD4⁺ T cells deliver their help to B cells in an antigen-specific manner. Memory B cells can internalize viral antigen via their surface-bound antibodies; these antigens are processed within the B cell, and epitope peptides are presented at the cell surface in association with MHC class II molecules (Section II.B). Only those CD4⁺ T cells that are specific for the epitopes will, therefore, be triggered, ensuring that during a virus infection, only virus-specific CD4⁺ T cells will be triggered to respond, and their signals will be delivered only to the virus-specific memory B cells. Recent studies have identified a protein named SAP that plays a key role in the differentiation of CD4⁺ T cells (Wu *et al.*, 2001). SAP-deficient mice mount antigen-specific CD4⁺ T cell responses to infection, but these cells cannot support the development of long-lived plasma cells (Crotty *et al.*, 2003). The reason that SAP^{-/-} CD4⁺ T cells are unable to provide this particular type of help remains unknown; the cells make normal amounts of IFN- γ , IL-2, and IL-4, and they express CD40L.

2. CD4⁺ T Cell Importance in the Induction and/or Maintenance of CD8⁺ T Cell Responses

Many viruses (e.g., LCMV, Sendai, vaccinia, influenza, ectromelia, gamma-herpesvirus-68, and Theiler's virus) induce strong primary CD8⁺ T cell responses even in the absence of CD4⁺ T cells (Ahmed

et al., 1988; Belz *et al.*, 2002, 2003; Buller *et al.*, 1987; Hou *et al.*, 1995; Johnson *et al.*, 1999; Mo *et al.*, 1997). These infections often are systemic, and may directly activate innate defenses and APC costimulatory molecule expression by infecting APCs (Olson *et al.*, 2001; Wu and Liu, 1994); these infections may instead express peptides of high avidity for MHC class I and TcR (Franco *et al.*, 2000; Heath *et al.*, 1993), thus triggering the program of CD8⁺ T cell differentiation without the need for accessory molecule expression. In contrast, viruses that replicate to a lower extent or are localized to peripheral sites, often induce a detectable primary CD8⁺ T cell response only when CD4⁺ T cells are present. Examples of such T-help-dependent antiviral CD8⁺ T cell responses in mice are those induced by Rauscher leukemia virus, Japanese encephalitis virus, herpes simplex virus, and mouse hepatitis virus (Edelmann and Wilson, 2001; Hom *et al.*, 1991; Jennings *et al.*, 1991; Murali-Krishna *et al.*, 1996; Stohlman *et al.*, 1998).

CD4⁺ T cells can provide help to CD8⁺ T cells in at least two ways. The first, described previously, involves APC licensing via the CD40-pathway; this enhances the costimulatory signals that are delivered to naive CD8⁺ T cells, and triggers their program of proliferation and differentiation. A second means by which CD4⁺ T cells can enhance primary CD8 responses is by secreting IL-2. The effects of IL-2 on CD8⁺ T cells are manifold: this cytokine induces FasL expression on CD8⁺ T cells, thus increasing those cells' cytotoxic potential (Esser *et al.*, 1997), and IL-2 also may increase IFN- γ production by those cells (Cousens *et al.*, 1995). IL-2 thus augments the proliferation of CD8⁺ T cells (Cousens *et al.*, 1995) and prolongs their survival (Akbar *et al.*, 1996; Blattman *et al.*, 2003; Kelly *et al.*, 2002; Krummel *et al.*, 1999) so that effector cells can pursue virus-infected cells for longer periods of time. For example, during coronavirus infection of the CNS, high numbers of CD4⁺ T cells and CD8⁺ T cells can be found in the brain parenchyma (Haring *et al.*, 2001). If CD4⁺ T cells are absent, coronavirus-specific CD8⁺ T cells still migrate to sites of infection in the CNS, but they are much more likely to undergo apoptosis (Stohlman *et al.*, 1998); this is consistent with their having an *in vivo* requirement for CD4⁺-produced IL-2. Finally, there is strong evidence suggesting that CD8⁺ memory T cell numbers are influenced by IL-2 (Blattman *et al.*, 2003). However, IL-2 can also have deleterious effects on CD8⁺ T cells, including increasing apoptosis of activated cells, depending on when and how much it is produced and to what extent the CD8⁺ T cells are stimulated (Van Parijs *et al.*, 1999). Given the possible opposing effects of IL-2, it will be interesting to learn how CD4⁺ T cell production of this cytokine is regulated. It is conceivable that different

amounts of the cytokine are produced at different times depending on what effect is needed.

In addition to possible effects on the primary CD8⁺ T cell response, CD4⁺ T cells also may regulate the quality and quantity of CD8⁺ T cell memory; primary CD8 responses to LCMV and influenza virus are relatively normal in CD4^{-/-} mice, but memory responses measured by limiting dilution assay, or after secondary infection, are much reduced (Belz *et al.*, 2002; von Herrath *et al.*, 1996). Recent publications suggest that CD4⁺ T cells may deliver a signal during the early programming of naive CD8⁺ T cells, which facilitates their survival and ensures that they can respond appropriately to secondary antigen challenge (Section IV.A.3) CD4⁺ T cells also may play a key role in sustaining CD8⁺ T cells during persistent virus infections. During persistent infection, in the absence of CD4⁺ T cells, CD8⁺ T cells are quickly deleted or are rendered nonresponsive (Battegay *et al.*, 1994; Hunziker *et al.*, 2002; Matloubian *et al.*, 1994; Zajac *et al.*, 1998).

3. *Direct and/or Bystander Antiviral Functions of CD4⁺ T Cells*

CD4⁺ T cells orchestrate many aspects of the antiviral immune response, and these cells can, therefore, be said to have many distinct antiviral functions. For example, as already described, their provision of help to B cells can be considered an antiviral function because, in its absence, the antiviral antibody response is compromised, and the virus thereby gains an advantage. These effects—which result from the well-established helper activities of CD4⁺ T cells—have been extensively catalogued and appear to constitute the great majority of antiviral effects of CD4⁺ T cells (Doherty *et al.*, 1997). However, these effects are indirect, being mediated through other effector cells (e.g., CD8⁺ T cells or B cells, described previously, or macrophages, not discussed further herein) or molecules produced by other cells (e.g., antibodies). In addition to these indirect effects, one can conceive of at least two other ways in which CD4⁺ T cells might exert antiviral effects. First, the cells might act directly on virus-infected target cells that express viral epitopes in association with MHC class II; this would be analogous to the front line activities of CD8⁺ T cells. Second, one could envision that a CD4⁺ T cell might encounter an antigen-expressing (but uninfected) APC and be triggered to produce cytokines that directly inhibited the replication of viruses in adjacent infected (and probably MHC class II negative) cells; herein, we shall term this a “bystander” antiviral effect. Thus, we suggest that CD4⁺ T cells may exert their antiviral effects in three ways: in a direct manner, in an indirect manner, or as bystanders. The indirect effects

were discussed previously. What is the evidence for the remaining two mechanisms?

a. Possible Direct Antiviral Effects of CD4⁺ T Cells CD4⁺ T cells may mediate direct purging of MHC class II-expressing cells, such as B cells (which can be infected by, for example, EBV or murine gamma herpesvirus), macrophages, and dendritic cells (which can be infected by several viruses), or microglia (targets of several CNS infections, including Theiler's virus or mouse hepatitis virus). However, the restricted anatomical distribution of MHC class II molecules means that CD4⁺ T cells may be unable to recognize or act directly upon the great majority of cells that become infected following virus challenge, and this presents an obvious obstacle to the concept that CD4⁺ T cells commonly exert direct antiviral effects (Section III). Nevertheless, it is clear that several cell types (e.g., epithelial cells) can up-regulate MHC class II expression during viral infection, rendering them potentially recognizable to CD4⁺ T cells. Furthermore, the existence of cytolytic CD4⁺ T cells is not in doubt, and one might infer that such cell—whose cytolytic effects rely on direct contact with an antigen-expressing target cell—are unlikely to exist without good reason. Cytolytic CD4⁺ T cells were first identified *in vivo* (as distinct from CD4⁺ T cell lines or clones) in LCMV-infected β 2-microglobulin-deficient mice (Muller *et al.*, 1992), and subsequent careful analyses suggested that these virus-specific CD4⁺ T cells could exert profound effects in the absence of CD8⁺ T cells (Quinn *et al.*, 1993). Indeed, some β 2-microglobulin-deficient mice cleared LCMV infection despite the lack of CD8⁺ T cells (Muller *et al.*, 1992), suggesting (but not proving) that the CD4⁺ T cells might have a direct antiviral effect. This interpretation is strengthened by the observations (Zajac *et al.*, 1996) that (i) the cytotoxic effect of the CD4⁺ T cells is Fas-mediated, and (ii) the *in vivo* effects are Fas-dependent; Fas-dependence strongly suggests that the effects require a direct cell/cell interaction between a FasL⁺ CD4⁺ T cell and a Fas-expressing target cell. However, the model of β 2-microglobulin-deficient mice is fraught with difficulties (reviewed in Frelinger and Serody, 1998), and direct cytolytic effects of CD4⁺ T cells on infected cells *in vivo* remain to be demonstrated. Cytolytic CD4⁺ T cells also have been identified following Epstein-Barr virus infection (Khanolkar *et al.*, 2001), and perforin⁺ CD4⁺ T cells have been reported in HIV infected individuals (Appay *et al.*, 2002). The mere existence of such cells, however, cannot be considered proof of their having a direct (or indeed, any) antiviral effect.

Perhaps the best evidence for direct CD4⁺ T cell-mediated control of infection is in the murine gamma-herpesvirus model, in which it

appears likely (although not certain) that the CD4⁺ T cells exert their effects, via IFN- γ production, directly on virus-infected MHC class II-positive target cells (Christensen *et al.*, 1999). There is other circumstantial evidence consistent with the idea that CD4⁺ T cells may exert some direct effector functions. CD4⁺ T cells are generally thought of as functioning in the spleen or lymph nodes, but there is increasing evidence that CD4⁺ memory T cells can reside in peripheral, nonlymphoid sites (Hogan *et al.*, 2001b; Marzo *et al.*, 2002; McSorley *et al.*, 2002; Reinhardt *et al.*, 2001). These cells show a highly activated phenotype with elevated levels of CD25 and CD44, and decreased levels of CD45RB and CD11a, making them distinct from splenic memory CD4⁺ T cells (Cauley *et al.*, 2002; Hogan *et al.*, 2001b). CD4⁺ T cells in the periphery tend to make IFN- γ , (arguably, consistent with a direct effector function) while those that reside preferentially in lymphoid organs make more IL-2 (consistent with an immunoregulatory activity). However, these arguments are very much conjectural, and exceptions exist; as noted, CD4⁺ T cells in the coronavirus-infected brain produce survival factors—possibly IL-2—to rescue CD8⁺ T cells.

b. Possible Bystander Antiviral Effects of CD4⁺T Cells Many situations exist in which transfer of virus-specific CD4⁺ T cells has a profound effect on the outcome of virus infection and/or disease. For example, transfer of poliovirus-specific CD4⁺ T cells into human-poliovirus-receptor transgenic mice protects the recipients from lethal poliovirus infection (Mahon *et al.*, 1995). Infection of neurons is required for a lethal outcome, and these cells do not usually express MHC class II molecules; therefore, this effect is unlikely to be direct. Similarly, transfer of HBV-specific effector CD4⁺ T cells reduces viral load in mice transgenic for HBV (Franco *et al.*, 1997a), and CD4⁺ T cells can mediate protection against Sendai infection independently of antibody or CD8⁺ T cells (Zhong *et al.*, 2001). To evaluate possible bystander effects mediated by CD4⁺ T cells, chimeric mice have been produced that express MHC class II molecules on some cells but not on others. Using this approach, it has been shown that influenza virus-specific CD4⁺ T cells can clear infection from MHC class II-negative cells, consistent with bystander effects; however, indirect (antibody-mediated) effects were not excluded (Topham *et al.*, 1996b).

D. Maturation of the CD4⁺T Cell Response

The cytokine profiles of CD4⁺ T cells change over time. At the peak of the response to LCMV, most of the CD4⁺ T cell response is T_h1 in phenotype, and there is a mixture of virus-specific CD4⁺ T cells that

make IFN- γ ; IFN- γ and IL-2; IFN- γ and TNF; or all three cytokines. The majority of these CD4⁺ T cells make only IFN- γ in response to antigen contact although approximately 30% also make IL-2 (Harrington *et al.*, 2002; Varga and Welsh, 2000), and a few synthesize TNF (Harrington *et al.*, 2002; Homann *et al.*, 2001; Varga and Welsh, 2000). In contrast, during the memory phase, very few single-positive cells can be identified, and essentially all of the cells are double-positive (IFN- γ ⁺ TNF⁺ or IFN- γ ⁺ IL-2⁺; Harrington *et al.*, 2002; Homann *et al.*, 2001). These patterns are reminiscent of the changes reported for CD8⁺ T cells (Slifka and Whitton, 2000a) (Fig. 4). The significance of these changes is unclear. Could the cytokine double-positive cells have differentiated further than the single-positive cells? Are the single-positive cells a distinct lineage that terminally-differentiate into short-lived effector cells? Like CD8⁺ T cells, CD4⁺ T cells have been categorized into central memory cells (defined as CD62L^{hi}, CCR7⁺) and effector memory cells (CD62L^{lo}, CCR7⁻). The expression of CD62L and CCR7 affects the localization of T cells, with the central memory cells preferentially localized in the secondary lymphoid organs and the effector memory cells traveling through peripheral sites; however, as for CD8⁺ T cells, there is no clear relationship between CD4⁺ T cell effector function, and the expression of these marker proteins.

VI. IMMUNOPATHOLOGY

Immune responses are not invariably successful in controlling infection, and infections remain a major (and increasing) cause of human morbidity and mortality. It is easy to forgive the occasional failure on the part of the immune system, especially when one considers the innumerable strategies developed by microbes to evade its unwelcome attentions. However; it is important to realize that successful immune responses themselves are delivered at a cost because, in eradicating infection, the immune system also can damage the host. This phenomenon is termed *immunopathology*, and it is an extremely common feature of virus infection. Many of the symptoms of common viral infections—for example, the chills, muscle aches, and fever of influenza as well as the characteristic rash of measles—are not caused directly by the virus but instead result from the immune response to the virus. A detailed review of this topic would far exceed the scope of this chapter. Suffice it to say that the very nature of the CD8⁺ T cell

response—which often involves lysis of infected cells or the release of highly toxic cytokines—means that immunopathology is an almost inevitable consequence of viral infection. We have argued that the need to minimize immunopathology has provided a strong selective pressure that ensures that the effector functions of CD8⁺ T cells are held in an extraordinarily tight rein (Slifka and Whitton, 2000b; Slifka *et al.*, 1999). Moreover, antibodies should *not* be considered innocent parties. Antibody–antigen complexes may be deposited at various anatomical interfaces (e.g., in the basement membrane of the kidney) and can lead to complement activation and severe inflammatory damage. One key question, which has been approached only infrequently, is to ask if we can uncouple the harmful and the beneficial effects of the immune response. Coxsackie virus infection of humans or mice often results in severe myocarditis, and survivors have extensive myocardial scarring (often causing dilated cardiomyopathy, which is treatable only by transplantation). There is no approved treatment for coxsackie virus myocarditis. Using the mouse model, we have found that myocarditis and subsequent scarring are much reduced in perforin-deficient mice, but these animals clear the virus infection with kinetics indistinguishable from those observed in normal mice (Gebhard *et al.*, 1998). Thus, we suggest that the development of a reagent capable of specifically blocking perforin activity might permit the treatment of coxsackie virus myocarditis, without compromising the host's ability to recover from the infection.

VII. SUMMARY

Evolutionary pressures imposed by an unremitting onslaught of infectious agents have shaped the mammalian immune system, and our very existence stands as proof of the potency of the antimicrobial immune response. The cooperative nature of the antibody and T cell arms of the adaptive immune system has long been recognized, but our understanding of the immune response to infection remains far from complete. Recent studies have begun to reveal previously unappreciated subtleties in the T cell response, which are tailored to most effectively detect a viral challenge and to provide a rapid and effective reply. If safer and more effective vaccines are to be designed, and if the harmful effects of the immune response are to be diminished while retaining beneficial components, we must not rest on our laurels; many important questions remain to be answered.

ACKNOWLEDGMENTS

We are grateful to Annette Lord for excellent secretarial support. This work was supported by NIH grants AI 27028 and AI 52351 (JLW) and AI-051346 (MKS), by ONPRC grant RR00163 (MKS), and by a Long-Term Fellowship (LT00410/2001-M) from the Human Frontier Science Program (AKN). This is manuscript number 16000-NP from the Scripps Research Institute.

REFERENCES

- Anonymous (2003). Postexposure prophylaxis of hepatitis B. *Morb. Mortal. Wkly. Rep.* **33**:285–290.
- Abney, E. R., Cooper, M. D., Kearney, J. F., Lawton, A. R., and Parkhouse, R. M. (1978). Sequential expression of immunoglobulin on developing mouse B lymphocytes: A systematic survey that suggests a model for the generation of immunoglobulin isotype diversity. *J. Immunol.* **120**:2041–2049.
- Ahmed, R., Butler, L. D., and Bhatti, L. (1988). T4⁺ T helper cell function *in vivo*: Differential requirement for induction of antiviral cytotoxic T cell and antibody responses. *J. Virol.* **62**:2102–2106.
- Akbar, A. N., Borthwick, N. J., Wickremasinghe, R. G., Panayiotidis, P., Pilling, D., Bofill, M., Krajewski, S., Reed, J. C., and Salmon, M. (1996). Interleukin-2 receptor common gamma-chain signaling cytokines regulate activated T cell apoptosis in response to growth factor withdrawal: Selective induction of anti-apoptotic (bcl-2, bcl-xL) but not proapoptotic (bax, bcl-xS) gene expression. *Eur. J. Immunol.* **26**:294–299.
- Appay, V., Zaunders, J. J., Papagno, L., Sutton, J., Jaramillo, A., Waters, A., Easterbrook, P., Grey, P., Smith, D., McMichael, A. J., Cooper, D. A., Rowland-Jones, S. L., and Kelleher, A. D. (2002). Characterization of CD4⁺ CTLs *ex vivo*. *J. Immunol.* **168**:5954–5958.
- Bachmann, M. F., Kundig, T. M., Odermatt, B., Hengartner, H., and Zinkernagel, R. M. (1994). Free recirculation of memory B cells versus antigen-dependent differentiation to antibody-forming cells. *J. Immunol.* **153**:3386–3397.
- Badovinac, V. P., and Harty, J. T. (2002). CD8⁺ T cell homeostasis after infection: Setting the “curve” *Microbes. Infect.* **4**:441–447.
- Badovinac, V. P., Porter, B. B., and Harty, J. T. (2002). Programmed contraction of CD8⁺ T cells after infection. *Nat. Immunol.* **3**:619–626.
- Baekkevold, E. S., Yamanaka, T., Palframan, R. T., Carlsen, H. S., Reinholt, F. P., von Andrian, U. H., Brandtzaeg, P., and Haraldsen, G. (2001). The CCR7 ligand *elc* (CCL19) is transcytosed in high endothelial venules and mediates T cell recruitment. *J. Exp. Med.* **193**:1105–1112.
- Balfour, H. H., Jr., Groth, K. E., McCullough, J., Kalis, J. M., Marker, S. C., Nesbit, M. E., Simmons, R. L., and Najarian, J. S. (1977). Prevention or modification of varicella using zoster immune plasma. *Am. J. Dis. Child* **131**:693–696.
- Battegay, M., Moskophidis, D., Rahemtulla, A., Hengartner, H., Mak, T. W., and Zinkernagel, R. M. (1994). Enhanced establishment of a virus carrier state in adult CD4⁺ T cell-deficient mice. *J. Virol.* **68**:4700–4704.
- Becker, T. C., Wherry, E. J., Boone, D., Murali-Krishna, K., Antia, R., Ma, A., and Ahmed, R. (2002). Interleukin 15 is required for proliferative renewal of virus-specific memory CD8⁺ T cells. *J. Exp. Med.* **195**:1541–1548.

- Belz, G. T., Liu, H., Andreansky, S., Doherty, P. C., and Stevenson, P. G. (2003). Absence of a functional defect in CD8⁺ T cells during primary murine gamma-herpesvirus-68 infection of I-A^{b-/-} mice. *J. Gen. Virol.* **84**:337–341.
- Belz, G. T., Wodarz, D., Diaz, G., Nowak, M. A., and Doherty, P. C. (2002). Compromised influenza virus-specific CD8⁺ T cell memory in CD4⁺ T cell-deficient mice. *J. Virol.* **76**:12388–12393.
- Belz, G. T., Xie, W., and Doherty, P. C. (2001). Diversity of epitope and cytokine profiles for primary and secondary influenza a virus-specific CD8⁺ T cell responses. *J. Immunol.* **166**:4627–4633.
- Ben-Nathan, D., Lustig, S., Tam, G., Robinzon, S., Segal, S., and Rager-Zisman, B. (2003). Prophylactic and therapeutic efficacy of human intravenous immunoglobulin in treating West Nile virus infection in mice. *J. Infect. Dis.* **188**:5–12.
- Bendelja, K., Gagro, A., Bace, A., Lokar-Kolbas, R., Krsulovic-Hresic, V., Drazenovic, V., Mlinaric-Galinovic, G., and Rabatic, S. (2000). Predominant type-2 response in infants with respiratory syncytial virus (RSV) infection demonstrated by cytokine flow cytometry. *Clin. Exp. Immunol.* **121**:332–338.
- Bennett, S. R., Carbone, F. R., Karamalis, F., Flavell, R. A., Miller, J. F., and Heath, W. R. (1998). Help for cytotoxic-T-cell responses is mediated by CD40 signalling. *Nature* **393**:478–480.
- Bergamini, A., Bolacchi, F., Cerasari, G., Carvelli, C., Faggioli, E., Cepparulo, M., Demin, F., Uccella, I., Bongiovanni, B., Niuitta, P., Capozzi, M., Lupi, M., Piscitelli, E., Rocchi, G., and Angelico, M. (2001). Lack of evidence for the Th2 predominance in patients with chronic hepatitis C. *Clin. Exp. Immunol.* **123**:451–458.
- Bird, J. J., Brown, D. R., Mullen, A. C., Moskowitz, N. H., Mahowald, M. A., Sider, J. R., Gajewski, T. F., Wang, C. R., and Reiner, S. L. (1998). Helper T cell differentiation is controlled by the cell cycle. *Immunity* **9**:229–237.
- Blattman, J. N., Antia, R., Sourdive, D. J., Wang, X., Kaech, S. M., Murali-Krishna, K., Altman, J. D., and Ahmed, R. (2002). Estimating the precursor frequency of naive antigen-specific CD8⁺ T cells. *J. Exp. Med.* **195**:657–664.
- Blattman, J. N., Grayson, J. M., Wherry, E. J., Kaech, S. M., Smith, K. A., and Ahmed, R. (2003). Therapeutic use of IL-2 to enhance antiviral T cell responses *in vivo*. *Nat. Med.* **9**:540–547.
- Brunner, T., Mogil, R. J., LaFace, D., Yoo, N. J., Mahboubi, A., Echeverri, F., Martin, S. J., Force, W. R., Lynch, D. H., and Ware, C. F. (1995). Cell-autonomous Fas (CD95)/Fas-ligand interaction mediates activation-induced apoptosis in T cell hybridomas. *Nature* **373**:441–444.
- Budd, R. C. (2001). Activation-induced cell death. *Curr. Opin. Immunol.* **13**:356–362.
- Buller, R. M. L., Holmes, K. L., Hugin, A., Frederickson, T. N., and Morse, H. C., III. (1987). Induction of cytotoxic T cell responses *in vivo* in the absence of CD4 helper cells. *Nature* **328**:77–79.
- Burioni, R., Williamson, R. A., Sanna, P. P., Bloom, F. E., and Burton, D. R. (1994). Recombinant human Fab to glycoprotein D neutralizes infectivity and prevents cell-to-cell transmission of herpes simplex viruses 1 and 2 *in vitro*. *Proc. Natl. Acad. Sci. USA* **91**:355–359.
- Burton, D. R. (2002). Antibodies, viruses, and vaccines. *Nat. Rev. Immunol.* **2**:706–713.
- Busch, D. H., and Pamer, E. G. (1999). T cell affinity maturation by selective expansion during infection. *J. Exp. Med.* **189**:701–710.
- Cahill, R. N., Poskitt, D. C., Frost, D. C., and Trnka, Z. (1977). Two distinct pools of recirculating T lymphocytes: Migratory characteristics of nodal and intestinal T lymphocytes. *J. Exp. Med.* **145**:420–428.

- Campbell, J. J., Bowman, E. P., Murphy, K., Youngman, K. R., Siani, M. A., Thompson, D. A., Wu, L., Zlotnik, A., and Butcher, E. C. (1998). 6-C-kine (SLC), a lymphocyte adhesion-triggering chemokine expressed by high endothelium, is an agonist for the MIP-3beta receptor CCR7. *J. Cell Biol.* **141**:1053–1059.
- Cauley, L. S., Cookenham, T., Miller, T. B., Adams, P. S., Vignali, K. M., Vignali, D. A., and Woodland, D. L. (2002). Cutting edge: Virus-specific CD4⁺ memory T cells in nonlymphoid tissues express a highly activated phenotype. *J. Immunol.* **169**:6655–6658.
- Chang, K. M., Thimme, R., Melpolder, J. J., Oldach, D., Pemberton, J., Moorhead-Loudis, J., McHutchison, J. G., Alter, H. J., and Chisari, F. V. (2001). Differential CD4⁺ and CD8⁺ T cell responsiveness in hepatitis C virus infection. *Hepatology* **33**:267–276.
- Christensen, J. P., Cardin, R. D., Branum, K. C., and Doherty, P. C. (1999). CD4⁺ T cell-mediated control of a gamma-herpesvirus in B cell-deficient mice is mediated by IFN- γ . *Proc. Natl. Acad. Sci. USA* **96**:5135–5140.
- Ciurea, A., Hunziker, L., Klenerman, P., Hengartner, H., and Zinkernagel, R. M. (2001). Impairment of CD4⁺ T cell responses during chronic virus infection prevents neutralizing antibody responses against virus escape mutants. *J. Exp. Med.* **193**:297–305.
- Clayton, A. J. (1977). Lassa immune serum. *Bull. WHO* **55**:435–439.
- Cohen, G. M. (1997). Caspases: The executioners of apoptosis. *Biochem. J.* **326**:1–16.
- Cousens, L. P., Orange, J. S., and Biron, C. A. (1995). Endogenous IL-2 contributes to T cell expansion and IFN- γ production during lymphocytic choriomeningitis virus infection. *J. Immunol.* **155**:5690–5699.
- Crotty, S., Kersh, E. N., Cannons, J., Schwartzberg, P. L., and Ahmed, R. (2003). SAP is required for generating long-term humoral immunity. *Nature* **421**:282–287.
- del Val, M., Schlicht, H. J., Volkmer, H., Messerle, M., Reddehase, M. J., and Koszinowski, U. H. (1991). Protection against lethal cytomegalovirus infection by a recombinant vaccine containing a single nonameric T cell epitope. *J. Virol.* **65**:3641–3646.
- Denecker, G., Vercammen, D., Declercq, W., and Vandenaabeele, P. (2001). Apoptotic and necrotic cell death induced by death domain receptors. *Cell Mol. Life Sci.* **58**:356–370.
- di Simone, C., and Buchmeier, M. J. (1995). Protection of mice from lethal LCMV infection by a reconstituted glycoprotein vaccine. In "Vaccines 95" (R. M. Chanock, F. Brown, H. S. Ginsberg, and E. Norrby, eds.). Cold Spring Harbor Laboratory, Plainview, NY.
- Diepolder, H. M., Gruener, N. H., Gerlach, J. T., Jung, M. C., Wierenga, E. A., and Pape, G. R. (2001). Different levels of T cell receptor triggering induce distinct functions in hepatitis B and hepatitis C virus-specific human CD4⁺ T cell clones. *J. Virol.* **75**:7803–7810.
- Doherty, P. C., Topham, D. J., Tripp, R. A., Cardin, R. D., Brooks, J. W., and Stevenson, P. G. (1997). Effector CD4⁺ and CD8⁺ T cell mechanisms in the control of respiratory virus infections. *Immunol. Rev.* **159**:105–117.
- Doyle, A. M., Mullen, A. C., Villarino, A. V., Hutchins, A. S., High, F. A., Lee, H. W., Thompson, C. B., and Reiner, S. L. (2001). Induction of cytotoxic T lymphocyte antigen 4 (CTLA-4) restricts clonal expansion of helper T cells. *J. Exp. Med.* **194**:893–902.
- Edelmann, K. H., and Wilson, C. B. (2001). Role of CD28/CD80-86 and CD40/CD154 costimulatory interactions in host defense to primary herpes simplex virus infection. *J. Virol.* **75**:612–621.
- Eisen, H. N., Sykulev, Y., and Tsomides, T. J. (1996). Antigen-specific T cell receptors and their reactions with complexes formed by peptides with major histocompatibility complex proteins. *Adv. Protein Chem.* **49**:1–56.

- Ely, K. H., Roberts, A. D., and Woodland, D. L. (2003). Cutting edge: Effector memory CD8⁺ T cells in the lung airways retain the potential to mediate recall responses. *J. Immunol.* **171**:3338–3342.
- Enria, D. A., and Barrera Oro, J. G. (2002). Junin virus vaccines. *Curr. Top. Microbiol. Immunol.* **263**:239–261.
- Esser, M. T., Dinglasan, R. D., Krishnamurthy, B., Gullo, C. A., Graham, M. B., and Braciale, V. L. (1997). IL-2 induces Fas ligand/Fas (CD95L/CD95) cytotoxicity in CD8⁺ and CD4⁺ T lymphocyte clones. *J. Immunol.* **158**:5612–5618.
- Estcourt, M. J., Ramshaw, I. A., and Ramsay, A. J. (1998). Cytokine responses in virus infections: Effects on pathogenesis, recovery, and persistence. *Curr. Opin. Microbiol.* **1**:411–418.
- Ferraro-Peyret, C., Quemeneur, L., Flacher, M., Revillard, J. P., and Genestier, L. (2002). Caspase-independent phosphatidylserine exposure during apoptosis of primary T lymphocytes. *J. Immunol.* **169**:4805–4810.
- Fisher, R. G., and Edwards, K. M. (1998). Varicella-zoster. *Pediatr. Rev.* **19**:62–66.
- Flano, E., Woodland, D. L., Blackman, M. A., and Doherty, P. C. (2001). Analysis of virus-specific CD4⁺ T cells during long-term gamma-herpesvirus infection. *J. Virol.* **75**:7744–7748.
- Fouchier, R. A., Kuiken, T., Schutten, M., van Amerongen, G., van Doornum, G. J., van den Hoogen, B. G., Peiris, M., Lim, W., Stohr, K., and Osterhaus, A. D. (2003). Aetiology: Koch's postulates fulfilled for SARS virus. *Nature* **423**:240.
- Foulds, K. E., Zenewicz, L. A., Shedlock, D. J., Jiang, J., Troy, A. E., and Shen, H. (2002). Cutting edge: CD4⁺ and CD8⁺ T cells are intrinsically different in their proliferative responses. *J. Immunol.* **168**:1528–1532.
- Frame, J. D. (1989). Clinical features of Lassa fever in Liberia. *Rev. Infect. Dis.* **11**:S783–S789.
- Franco, A., Guidotti, L. G., Hobbs, M. V., Paschetto, V., and Chisari, F. V. (1997a). Pathogenetic effector function of CD4-positive T helper 1 cells in hepatitis B virus transgenic mice. *J. Immunol.* **159**:2001–2008.
- Franco, A., Tilly, D. A., Gramaglia, I., Croft, M., Cipolla, L., Meldal, M., and Grey, H. M. (2000). Epitope affinity for MHC class I determines helper requirement for CTL priming. *Nat. Immunol.* **1**:145–150.
- Franco, M. A., Tin, C., Rott, L. S., van Cott, J. L., McGhee, J. R., and Greenberg, H. B. (1997b). Evidence for CD8⁺ T cell immunity to murine rotavirus in the absence of perforin, fas, and γ interferon. *J. Virol.* **71**:479–486.
- Frelinger, J. A., and Serody, J. (1998). Immune response of β 2-microglobulin-deficient mice to pathogens. *Curr. Top. Microbiol. Immunol.* **232**:99–114.
- Fujinami, R. S., and Oldstone, M. B. A. (1979). Antiviral antibody reacting on the plasma membrane alters measles virus expression inside the cell. *Nature* **279**:529–530.
- Fuller, M. J., and Zajac, A. J. (2003). Ablation of CD8⁺ and CD4⁺ T cell responses by high viral loads. *J. Immunol.* **170**:477–486.
- Gallatin, W. M., Weissman, I. L., and Butcher, E. C. (1983). A cell-surface molecule involved in organ-specific homing of lymphocytes. *Nature* **304**:30–34.
- Garside, P., Ingulli, E., Merica, R. R., Johnson, J. G., Noelle, R. J., and Jenkins, M. K. (1998). Visualization of specific B and T lymphocyte interactions in the lymph node. *Science* **281**:96–99.
- Gebrand, J. R., Perry, C. M., Harkins, S., Lane, T., Mena, I., Asensio, V. C., Campbell, I. L., and Whitton, J. L. (1998). Coxsackie virus B3-induced myocarditis: Perforin exacerbates disease but plays no detectable role in virus clearance. *Am. J. Pathol.* **153**:417–428.

- Gerhard, W. (2001). The role of the antibody response in influenza virus infection. *Curr. Top. Microbiol. Immunol.* **260**:171–190.
- Godkin, A. J., Thomas, H. C., and Openshaw, P. J. (2002). Evolution of epitope-specific memory CD4⁺ T cells after clearance of hepatitis C virus. *J. Immunol.* **169**:2210–2214.
- Graham, M. B., Braciale, V. L., and Braciale, T. J. (1994). Influenza virus-specific CD4⁺ T helper type 2 T lymphocytes do not promote recovery from experimental virus infection. *J. Exp. Med.* **180**:1273–1282.
- Grayson, J. M., Murali-Krishna, K., Altman, J. D., and Ahmed, R. (2001). Gene expression in antigen-specific CD8⁺ T cells during viral infection. *J. Immunol.* **166**:795–799.
- Gregson, S., Terceira, N., Kakowa, M., Mason, P. R., Anderson, R. M., Chandiwana, S. K., and Carael, M. (2002). Study of bias in antenatal clinic HIV-1 surveillance data in a high contraceptive prevalence population in sub-Saharan Africa. *AIDS* **16**:643–652.
- Guidotti, L. G., and Chisari, F. V. (1996). To kill or to cure: Options in host defense against viral infection. *Curr. Opin. Immunol.* **8**:478–483.
- Gunn, M. D., Tangemann, K., Tam, C., Cyster, J. G., Rosen, S. D., and Williams, L. T. (1998). A chemokine expressed in lymphoid high endothelial venules promotes the adhesion and chemotaxis of naive T lymphocytes. *Proc. Natl. Acad. Sci. USA* **95**:258–263.
- Gupta, M., Mahanty, S., Bray, M., Ahmed, R., and Rollin, P. E. (2001). Passive transfer of antibodies protects immunocompetent and immunodeficient mice against lethal Ebola virus infection without complete inhibition of viral replication. *J. Virol.* **75**:4649–4654.
- Halper, J., Fu, S. M., Wang, C. Y., Winchester, R., and Kunkel, H. G. (1978). Patterns of expression of human “Ia-like” antigens during the terminal stages of B cell development. *J. Immunol.* **120**:1480–1484.
- Hammon, W. M., Coriell, L. L., Wehrle, P. F., and Stokes, J. (1953). Evaluation of Red Cross gamma globulin as a prophylactic agent for poliomyelitis 4. Final report of results based on clinical diagnoses. *JAMA* **151**:1272–1285.
- Haring, J. S., Pewe, L. L., and Perlman, S. (2001). High-magnitude, virus-specific CD4⁺ T cell response in the central nervous system of coronavirus-infected mice. *J. Virol.* **75**:3043–3047.
- Harrington, L. E., van der Most, R. G., Whitton, J. L., and Ahmed, R. (2002). Recombinant vaccinia virus induced T cell immunity: Quantitation of the response to the virus vector and the foreign epitope. *J. Virol.* **76**:3329–3337.
- Heath, W. R., Kjer-Nielsen, L., and Hoffmann, M. W. (1993). Avidity for antigen can influence the helper dependence of CD8⁺ T lymphocytes. *J. Immunol.* **151**:5993–6001.
- Helmreich, E., Kern, M., and Eisen, H. N. (2003). The secretion of antibody by isolated lymph node cells. *J. Biol. Chem.* **236**:464–473.
- Hibi, T., and Dosch, H. M. (1986). Limiting dilution analysis of the B cell compartment in human bone marrow. *Eur. J. Immunol.* **16**:139–145.
- Hildeman, D. A., Mitchell, T., Teague, T. K., Henson, P., Day, B. J., Kappler, J., and Marrack, P. C. (1999). Reactive oxygen species regulate activation-induced T cell apoptosis. *Immunity* **10**:735–744.
- Hildeman, D. A., Zhu, Y., Mitchell, T., Kappler, J., and Marrack, P. (2002a). Molecular mechanisms of activated T cell death *in vivo*. *Curr. Opin. Immunol.* **14**:354–359.
- Hildeman, D. A., Zhu, Y., Mitchell, T. C., Bouillet, P., Strasser, A., Kappler, J., and Marrack, P. (2002b). Activated T cell death *in vivo* mediated by proapoptotic bcl-2 family member bim. *Immunity* **16**:759–769.
- Hogan, R. J., Cauley, L. S., Ely, K. H., Cookenham, T., Roberts, A. D., Brennan, J. W., Monard, S., and Woodland, D. L. (2002). Long-term maintenance of virus-specific

- effector memory CD8⁺ T cells in the lung airways depends on proliferation. *J. Immunol.* **169**:4976–4981.
- Hogan, R. J., Usherwood, E. J., Zhong, W., Roberts, A. A., Dutton, R. W., Harmsen, A. G., and Woodland, D. L. (2001a). Activated antigen-specific CD8⁺ T cells persist in the lungs following recovery from respiratory virus infections. *J. Immunol.* **166**:1813–1822.
- Hogan, R. J., Zhong, W., Usherwood, E. J., Cookenham, T., Roberts, A. D., and Woodland, D. L. (2001b). Protection from respiratory virus infections can be mediated by antigen-specific CD4⁺ T cells that persist in the lungs. *J. Exp. Med.* **193**:981–986.
- Holler, N., Zaru, R., Micheau, O., Thome, M., Attinger, A., Valitutti, S., Bodmer, J. L., Schneider, P., Seed, B., and Tschopp, J. (2000a). Fas triggers an alternative caspase-8-independent cell death pathway using the kinase RIP as effector molecule. *Nat. Immunol.* **1**:489–495.
- Holler, P. D., Holman, P. O., Shusta, E. V., O'Herrin, S., Wittrup, K. D., and Kranz, D. M. (2000b). *In vitro* evolution of a T cell receptor with high affinity for peptide/MHC. *Proc. Natl. Acad. Sci. USA* **97**:5387–5392.
- Hom, R. C., Finberg, R. W., Mullaney, S., and Ruprecht, R. M. (1991). Protective cellular retroviral immunity requires both CD4⁺ and CD8⁺ immune T cells. *J. Virol.* **65**:220–224.
- Homann, D., Teyton, L., and Oldstone, M. B. A. (2001). Differential regulation of antiviral T cell immunity results in stable CD8⁺ but declining CD4⁺ T cell memory. *Nat. Med.* **7**:913–919.
- Hou, S., Hyland, L., Ryan, K. W., Portner, A., and Doherty, P. C. (1994). Virus-specific CD8⁺ T cell memory determined by clonal burst size. *Nature* **369**:652–654.
- Hou, S., Mo, X. Y., Hyland, L., and Doherty, P. C. (1995). Host response to Sendai virus in mice lacking class II major histocompatibility complex glycoproteins. *J. Virol.* **69**:1429–1434.
- Huber, S. A., and Pfaeffle, B. (1994). Differential Th1 and Th2 cell responses in male and female BALB/c mice infected with coxsackie virus group B type 3. *J. Virol.* **68**:5126–5132.
- Hunziker, L., Klenerman, P., Zinkernagel, R. M., and Ehl, S. (2002). Exhaustion of cytotoxic T cells during adoptive immunotherapy of virus carrier mice can be prevented by B cells or CD4⁺ T cells. *Eur. J. Immunol.* **32**:374–382.
- Hyland, L., Sangster, M., Sealy, R., and Coleclough, C. (1994). Respiratory virus infection of mice provokes a permanent humoral immune response. *J. Virol.* **68**:6083–6086.
- Igarashi, A., Fukuoka, T., and Fukai, K. (1971). Passive immunization of mice with rabbit antisera against Chikungunya virus and its components. *Biken. J.* **14**:353–355.
- Imami, N., Pires, A., Hardy, G., Wilson, J., Gazzard, B., and Gotch, F. (2002). A balanced type 1/type 2 response is associated with long-term nonprogressive human immunodeficiency virus type 1 infection. *J. Virol.* **76**:9011–9023.
- Irvine, D. J., Purbhoo, M. A., Krogsaard, M., and Davis, M. M. (2002). Direct observation of ligand recognition by T cells. *Nature* **419**:845–849.
- Jaattela, M., and Tschopp, J. (2003). Caspase-independent cell death in T lymphocytes. *Nat. Immunol.* **4**:416–423.
- Jacob, J., and Baltimore, D. (1999). Modelling T cell memory by genetic marking of memory T cells *in vivo*. *Nature* **399**:593–597.
- Jansen, V. A. A., Stollenwerk, N., Jensen, H. J., Ramsay, M. E., Edmunds, W. J., and Rhodes, C. J. (2003). Measles outbreaks in a population with declining vaccine uptake. *Science* **301**:804.

- Janssen, E. M., Lemmens, E. E., Wolfe, T., Christen, U., von Herrath, M. G., and Schoenberger, S. P. (2003). CD4⁺ T cells are required for secondary expansion and memory in CD8⁺ T lymphocytes. *Nature* **421**:852–856.
- Janssen, O., Sanzenbacher, R., and Kabelitz, D. (2000). Regulation of activation-induced cell death of mature T-lymphocyte populations. *Cell Tissue Res.* **301**:85–99.
- Jennings, S. R., Bonneau, R. H., Smith, P. M., Wolcott, R. M., and Chervenak, R. (1991). CD4⁺ T lymphocytes are required for the generation of the primary but not the secondary CD8⁺ cytolytic T lymphocyte response to herpes simplex virus in C57BL/6 mice. *Cell Immunol.* **133**:234–252.
- Johnson, A. J., Njenga, M. K., Hansen, M. J., Kuhns, S. T., Chen, L., Rodriguez, M., and Pease, L. R. (1999). Prevalent class I-restricted T-cell response to the Theiler's virus epitope Db:VP2121-130 in the absence of endogenous CD4 help, tumor necrosis factor alpha, gamma interferon, perforin, or costimulation through CD28. *J. Virol.* **73**:3702–3708.
- Kaech, S. M., and Ahmed, R. (2001). Memory CD8⁺ T cell differentiation: Initial antigen encounter triggers a developmental program in naive cells. *Nat. Immunol.* **2**:415–422.
- Kaech, S. M., Wherry, E. J., and Ahmed, R. (2002). Effector and memory T cell differentiation: Implications for vaccine development. *Nat. Rev. Immunol.* **2**:251–262.
- Kafrouni, M. I., Brown, G. R., and Thiele, D. L. (2001). Virally infected hepatocytes are resistant to perforin-dependent CTL effector mechanisms. *J. Immunol.* **167**:1566–1574.
- Kagi, D., and Hengartner, H. (1996). Different roles for cytotoxic T cells in the control of infections with cytopathic versus noncytopathic viruses. *Curr. Opin. Immunol.* **8**:472–477.
- Kagi, D., Ledermann, B., Burki, K., Seiler, P., Odermatt, B., Olsen, K. J., Podack, E. R., Zinkernagel, R. M., and Hengartner, H. (1994). Cytotoxicity mediated by T cells and natural killer cells is greatly impaired in perforin-deficient mice. *Nature* **369**:31–37.
- Kagi, D., Seiler, P., Pavlovic, J., Ledermann, B., Burki, K., Zinkernagel, R. M., and Hengartner, H. (1995). The roles of perforin- and Fas-dependent cytotoxicity in protection against cytopathic and noncytopathic viruses. *Eur. J. Immunol.* **25**:3256–3262.
- Kalergis, A. M., Boucheron, N., Doucey, M. A., Palmieri, E., Goyarts, E. C., Vegh, Z., Luescher, I. F., and Nathenson, S. G. (2001). Efficient T cell activation requires an optimal dwell-time of interaction between the TCR and the pMHC complex. *Nat. Immunol.* **2**:229–234.
- Kallas, E. G., Reynolds, K., Andrews, J., Fitzgerald, T., Kasper, M., Menegus, M., and Evans, T. G. (1998). Cytomegalovirus-specific IFN- γ and IL-4 are produced by antigen expanded human blood lymphocytes from seropositive volunteers. *Immunol. Lett.* **64**:63–69.
- Kamperschroer, C., and Quinn, D. G. (1999). Quantification of epitope-specific MHC class II-restricted T cells following lymphocytic choriomeningitis virus infection. *Cell Immunol.* **193**:134–146.
- Keller, M. A., and Stiehm, E. R. (2000). Passive immunity in prevention and treatment of infectious diseases. *Clin. Microbiol. Rev.* **13**:602–614.
- Kelly, E., Won, A., Refaeli, Y., and van Parijs, L. (2002). IL-2 and related cytokines can promote T cell survival by activating AKT. *J. Immunol.* **168**:597–603.
- Kempe, C. H. (1960). Studies on smallpox and complications of smallpox vaccination. *Pediatrics* **25**:176–189.
- Kempe, C. H., Bowles, C., Meiklejohn, G., Berge, T. O., St. Vincent, L., Babu, B. V. S., Govindarajan, S., Ratnakannan, N. R., Downie, A. W., and Murthy, V. R. (1961). The

- use of vaccinia hyperimmune gammaglobulin in the prophylaxis of smallpox. *Bull. WHO* **25**:41–48.
- Kersh, E. N., Kaeck, S. M., Onami, T. M., Moran, M., Wherry, E. J., Miceli, M. C., and Ahmed, R. (2003). TCR signal transduction in antigen-specific memory CD8⁺ T cells. *J. Immunol.* **170**:5455–5463.
- Khanolkar, A., Yagita, H., and Cannon, M. J. (2001). Preferential utilization of the perforin/granzyme pathway for lysis of Epstein-Barr virus-transformed lymphoblastoid cells by virus-specific CD4⁺ T cells. *Virology* **287**:79–88.
- Klavinskis, L. S., Oldstone, M. B. A., and Whitton, J. L. (1989). Designing vaccines to induce cytotoxic T lymphocytes: Protection from lethal viral infection. In "Vaccines 89. Modern approaches to new vaccines including prevention of AIDS" (F. Brown, R. Chanock, H. Ginsberg, and R. Lerner, eds.). Cold Spring Harbor Laboratory, Cold Spring Harbor.
- Konig, R., Huang, L. Y., and Germain, R. N. (1992). MHC class II interaction with CD4 mediated by a region analogous to the MHC class I binding site for CD8. *Nature* **356**:796–798.
- Kopf, M., Coyle, A. J., Schmitz, N., Barner, M., Oxenius, A., Gallimore, A., Gutierrez-Ramos, J. C., and Bachmann, M. F. (2000). Inducible costimulator protein (ICOS) controls T helper cell subset polarization after virus and parasite infection. *J. Exp. Med.* **192**:53–61.
- Kopf, M., Ruedl, C., Schmitz, N., Gallimore, A., Lefrang, K., Ecabert, B., Odermatt, B., and Bachmann, M. F. (1999). OX40-deficient mice are defective in Th cell proliferation but are competent in generating B cell and CTL responses after virus infection. *Immunity* **11**:699–708.
- Kreil, T. R., and Eibl, M. M. (1997). Pre- and postexposure protection by passive immunoglobulin but no enhancement of infection with a *Flavivirus* in a mouse model. *J. Virol.* **71**:2921–2927.
- Krummel, M. F., Heath, W. R., and Allison, J. (1999). Differential coupling of second signals for cytotoxicity and proliferation in CD8⁺ T cell effectors: Amplification of the lytic potential by B7. *J. Immunol.* **163**:2999–3006.
- Kuiken, T., Fouchier, R. A., Schutten, M., Rimmelzwaan, G. F., van Amerongen, G., van Riel, D., Laman, J. D., de Jong, T., van Doornum, G., Lim, W., Ling, A. E., Chan, P. K., Tam, J. S., Zambon, M. C., Gopal, R., Drosten, C., van der, W. S., Escriou, N., Manuguerra, J. C., Stohr, K., Peiris, J. S., and Osterhaus, A. D. (2003). Newly discovered coronavirus as the primary cause of severe acute respiratory syndrome. *Lancet* **362**:263–270.
- Lantz, O., Grandjean, I., Matzinger, P., and di Santo, J. P. (2000). Gamma chain required for naive CD4⁺ T cell survival but not for antigen proliferation. *Nat. Immunol.* **1**:54–58.
- Lanzavecchia, A. (1985). Antigen-specific interaction between T and B cells. *Nature* **314**:537–539.
- Lau, L. L., Jamieson, B. D., Somasundaram, T., and Ahmed, R. (1994). Cytotoxic T cell memory without antigen. *Nature* **369**:648–652.
- Lauvau, G., Vijn, S., Kong, P., Horng, T., Kerkusiek, K., Serbina, N., Tuma, R. A., and Pamer, E. G. (2001). Priming of memory but not effector CD8⁺ T cells by a killed bacterial vaccine. *Science* **294**:1735–1739.
- Lee, W. T., Pasos, G., Cecchini, L., and Mittler, J. N. (2002). Continued antigen stimulation is not required during CD4⁺ T cell clonal expansion. *J. Immunol.* **168**:1682–1689.
- Lenardo, M., Chan, K. M., Hornung, F., McFarland, H., Siegel, R., Wang, J., and Zheng, L. (1999). Mature T lymphocyte apoptosis—Immune regulation in a dynamic and unpredictable antigenic environment. *Annu. Rev. Immunol.* **17**:221–253.

- Levine, B., Hardwick, J. M., Trapp, B. D., Crawford, T. O., Bollinger, R. C., and Griffin, D. E. (1991). Antibody-mediated clearance of alphavirus infection from neurons. *Science* **254**:856–860.
- Levy, J. A., Mackewicz, C. E., and Barker, E. (1996). Controlling HIV pathogenesis: The role of the noncytotoxic anti-HIV response of CD8⁺ T cells. *Immunol. Today* **17**:217–224.
- Liu, H., Andreansky, S., Diaz, G., Hogg, T., and Doherty, P. C. (2002). Reduced functional capacity of CD8⁺ T cells expanded by postexposure vaccination of gamma-herpesvirus-infected CD4-deficient mice. *J. Immunol.* **168**:3477–3483.
- Lutz, C., Ledermann, B., Kosco-Vilbois, M. H., Ochsenbein, A. F., Zinkernagel, R. M., Kohler, G., and Brombacher, F. (1998). IgD can largely substitute for loss of IgM function in B cells. *Nature* **393**:797–801.
- Mackay, C. R., Marston, W. L., Dudler, L., Spertini, O., Tedder, T. F., and Hein, W. R. (1992). Tissue-specific migration pathways by phenotypically distinct subpopulations of memory T cells. *Eur. J. Immunol.* **22**:887–895.
- Mahon, B. P., Katrak, K., Nomoto, A., Macadam, A. J., Minor, P. D., and Mills, K. H. (1995). Poliovirus-specific CD4⁺ Th1 clones with both cytotoxic and helper activity mediate protective humoral immunity against a lethal poliovirus infection in transgenic mice expressing the human poliovirus receptor. *J. Exp. Med.* **181**:1285–1292.
- Maini, M. K., Gudgeon, N., Wedderburn, L. R., Rickinson, A. B., and Beverley, P. C. (2000). Clonal expansions in acute EBV infection are detectable in the CD8 and not the CD4 subset and persist with a variable CD45 phenotype. *J. Immunol.* **165**:5729–5737.
- Maini, M. K., Wedderburn, L. R., Hall, F. C., Wack, A., Casorati, G., and Beverley, P. C. (1998). A comparison of two techniques for the molecular tracking of specific T cell responses: CD4⁺ human T cell clones persist in a stable hierarchy but at a lower frequency than clones in the CD8⁺ population. *Immunology* **94**:529–535.
- Manjunath, N., Shankar, P., Wan, J., Weninger, W., Crowley, M. A., Hieshima, K., Springer, T. A., Fan, X., Shen, H., Lieberman, J., and von Andrian, U. H. (2001). Effector differentiation is not prerequisite for generation of memory cytotoxic T lymphocytes. *J. Clin. Invest.* **108**:871–878.
- Manz, R. A., Thiel, A., and Radbruch, A. (1997). Lifetime of plasma cells in the bone marrow. *Nature* **388**:133–134.
- Marshall, D. R., Turner, S. J., Belz, G. T., Wingo, S., Andreansky, S., Sangster, M. Y., Riberdy, J. M., Liu, T., Tan, M., and Doherty, P. C. (2001). Measuring the diaspora for virus-specific CD8⁺ T cells. *Proc. Natl. Acad. Sci. USA* **98**:6313–6318.
- Marzo, A. L., Vezys, V., Williams, K., Tough, D. F., and Lefrancois, L. (2002). Tissue-level regulation of Th1 and Th2 primary and memory CD4⁺ T cells in response to *Listeria* infection. *J. Immunol.* **168**:4504–4510.
- Masopust, D., Vezys, V., Marzo, A. L., and Lefrancois, L. (2001). Preferential localization of effector memory cells in nonlymphoid tissue. *Science* **291**:2413–2417.
- Matloubian, M., Concepcion, R. J., and Ahmed, R. (1994). CD4⁺ T cells are required to sustain CD8⁺ cytotoxic T cell responses during chronic viral infection. *J. Virol.* **68**:8056–8063.
- McCormick, J. B. (1986). Clinical epidemiologic and therapeutic aspects of Lassa fever. *Med. Microbiol. Immunol.* **175**:153–155.
- McSorley, S. J., Asch, S., Costalonga, M., Reinhardt, R. L., and Jenkins, M. K. (2002). Tracking *Salmonella*-specific CD4⁺ T cells *in vivo* reveals a local mucosal response to a disseminated infection. *Immunity* **16**:365–377.

- Medana, I. M., Gallimore, A., Oxenius, A., Martinic, M. M., Wekerle, H., and Neumann, H. (2000). MHC class I-restricted killing of neurons by virus-specific CD8⁺ T lymphocytes is effected through the Fas/FasL but not the perforin pathway. *Eur. J. Immunol.* **30**:3623–3633.
- Mercado, R., Vijh, S., Allen, S. E., Kerksiek, K., Pilip, I. M., and Pamer, E. G. (2000). Early programming of T cell populations responding to bacterial infection. *J. Immunol.* **165**:6833–6839.
- Mo, X. Y., Sarawar, S. R., and Doherty, P. C. (1995). Induction of cytokines in mice with parainfluenza pneumonia. *J. Virol.* **69**:1288–1291.
- Mo, X. Y., Tripp, R. A., Sangster, M. Y., and Doherty, P. C. (1997). The cytotoxic T-lymphocyte response to Sendai virus is unimpaired in the absence of γ interferon. *J. Virol.* **71**:1906–1910.
- Monath, T. P. (2003). Yellow fever. In “Vaccines” (S. A. Plotkin and W. A. Orenstein, eds.). 4th ed. W. B. Saunders, Philadelphia.
- Monath, T. P., and Cetron, M. S. (2002). Prevention of yellow fever in persons traveling to the tropics. *Clin. Infect. Dis.* **34**:1369–1378.
- Muller, D., Koller, B. H., Whitton, J. L., LaPan, K., Brigman, K. K., Frelinger, J. A., and LaPan, K. E. (1992). LCMV-specific, class II-restricted cytotoxic T cells in β 2-microglobulin-deficient mice. *Science* **255**:1576–1578.
- Mupapa, K., Massamba, M., Kibadi, K., Kuvula, K., Bwaka, A., Kipasa, M., Colebunders, R., and Muyembe-Tamfum, J. J. (1999). Treatment of Ebola hemorrhagic fever with blood transfusions from convalescent patients. International Scientific and Technical Committee. *J. Infect. Dis.* **179**(Suppl. 1):S18–S23.
- Murali-Krishna, K., Lau, L. L., Sambhara, S., Lemonnier, F., Altman, J. D., and Ahmed, R. (1999). Persistence of memory CD8⁺ T cells in MHC class I-deficient mice. *Science* **286**:1377–1381.
- Murali-Krishna, K., Ravi, V., and Manjunath, R. (1996). Protection of adult but not newborn mice against lethal intracerebral challenge with Japanese encephalitis virus by adoptively transferred virus-specific cytotoxic T lymphocytes: Requirement for L3T4⁺ T cells. *J. Gen. Virol.* **77**:705–714.
- Nagata, S., and Suda, T. (1995). Fas and Fas ligand: lpr and gld mutations. *Immunol. Today* **16**:39–43.
- Nakayama, T., Zhou, J., and Fujino, M. (2003). Current status of measles in Japan. *J. Infect. Chemother.* **9**:1–7.
- Nishimura, Y., Igarashi, T., Haigwood, N., Sadjadpour, R., Plishka, R. J., Buckler-White, A., Shibata, R., and Martin, M. A. (2002). Determination of a statistically valid neutralization titer in plasma that confers protection against simian-human immunodeficiency virus challenge following passive transfer of high-titered neutralizing antibodies. *J. Virol.* **76**:2123–2130.
- Oehen, S., and Brduscha-Riem, K. (1998). Differentiation of naive CTL to effector and memory CTL: Correlation of effector function with phenotype and cell division. *J. Immunol.* **161**:5338–5346.
- Ogilvie, M. M. (1998). Antiviral prophylaxis and treatment in chickenpox. A review prepared for the UK Advisory Group on Chickenpox on behalf of the British Society for the Study of Infection. *J. Infect* **36**(Suppl. 1):31–38.
- Olson, J. K., Girvin, A. M., and Miller, S. D. (2001). Direct activation of innate and antigen-presenting functions of microglia following infection with Theiler's virus. *J. Virol.* **75**:9780–9789.
- Opferman, J. T., Ober, B. T., and Ashton-Rickardt, P. G. (1999). Linear differentiation of cytotoxic effectors into memory T lymphocytes. *Science* **283**:1745–1748.

- Ostler, T., Hussell, T., Surh, C. D., Openshaw, P., and Ehl, S. (2001). Long-term persistence and reactivation of T cell memory in the lung of mice infected with respiratory syncytial virus. *Eur. J. Immunol.* **31**:2574–2582.
- Ovsyannikova, I. G., Dhiman, N., Jacobson, R. M., Vierkant, R. A., and Poland, G. A. (2003). Frequency of measles virus-specific CD4⁺ and CD8⁺ T cells in subjects seronegative or highly seropositive for measles vaccine. *Clin. Diagn. Lab Immunol.* **10**:411–416.
- Oxenius, A., Zinkernagel, R. M., and Hengartner, H. (1998). Comparison of activation versus induction of unresponsiveness of virus-specific CD4⁺ and CD8⁺ T cells upon acute versus persistent viral infection. *Immunity* **9**:449–457.
- Padlan, E. A. (1994). Anatomy of the antibody molecule. *Mol. Immunol.* **31**:169–217.
- Pantaleo, G., Demarest, J. F., Vaccarezza, M., Graziosi, C., Bansal, G. P., Koenig, S., and Fauci, A. S. (1995). Effect of anti-V3 antibodies on cell-free and cell-to-cell human immunodeficiency virus transmission. *Eur. J. Immunol.* **25**:226–231.
- Pape, K. A., Kouskoff, V., Nemazee, D., Tang, H. L., Cyster, J. G., Tze, L. E., Hippen, K. L., Behrens, T. W., and Jenkins, M. K. (2003). Visualization of the genesis and fate of isotype-switched B cells during a primary immune response. *J. Exp. Med.* **197**:1677–1687.
- Parren, P. W., Geisbert, T. W., Maruyama, T., Jahrling, P. B., and Burton, D. R. (2002). Pre- and postexposure prophylaxis of Ebola virus infection in an animal model by passive transfer of a neutralizing human antibody. *J. Virol.* **76**:6408–6412.
- Parren, P. W., Marx, P. A., Hessel, A. J., Luckay, A., Harouse, J., Cheng-Mayer, C., Moore, J. P., and Burton, D. R. (2001). Antibody protects macaques against vaginal challenge with a pathogenic R5 simian/human immunodeficiency virus at serum levels giving complete neutralization *in vitro*. *J. Virol.* **75**:8340–8347.
- Peirce, E. R., Melville, F. S., Downie, A. W., and Duckworth, M. J. (1958). Antivaccinal gamma-globulin in smallpox prophylaxis. *Lancet* **2**:635–638.
- Perrin, L. H., Zinkernagel, R. M., and Oldstone, M. B. (1977). Immune response in humans after vaccination with vaccinia virus: Generation of a virus-specific cytotoxic activity by human peripheral lymphocytes. *J. Exp. Med.* **146**:949–969.
- Potsch, C., Vohringer, D., and Pircher, H. (1999). Distinct migration patterns of naive and effector CD8⁺ T cells in the spleen: Correlation with CCR7 receptor expression and chemokine reactivity. *Eur. J. Immunol.* **29**:3562–3570.
- Prośniak, M., Faber, M., Hanlon, C. A., Rupprecht, C. E., Hooper, D. C., and Dietzschold, B. (2003). Development of a cocktail of recombinant-expressed human rabies virus-neutralizing monoclonal antibodies for postexposure prophylaxis of rabies. *J. Infect. Dis.* **188**:53–56.
- Quinn, D. G., Zajac, A. J., Frelinger, J. A., and Muller, D. (1993). Transfer of lymphocytic choriomeningitis disease in β 2-microglobulin-deficient mice by CD4⁺ T cells. *Int. Immunol.* **5**:1193–1198.
- Ravkov, E. V., Myrick, C. M., and Altman, J. D. (2003). Immediate early effector functions of virus-specific CD8⁺CCR7⁺ memory cells in humans defined by HLA and CC chemokine ligand 19 tetramers. *J. Immunol.* **170**:2461–2468.
- Refaeli, Y., van Paris, L., London, C. A., Tschopp, J., and Abbas, A. K. (1998). Biochemical mechanisms of IL-2-regulated Fas-mediated T cell apoptosis. *Immunity* **8**:615–623.
- Reinhardt, R. L., Khoruts, A., Merica, R., Zell, T., and Jenkins, M. K. (2001). Visualizing the generation of memory CD4⁺ T cells in the whole body. *Nature* **410**:101–105.
- Ridge, J. P., di Rosa, F., and Matzinger, P. (1998). A conditioned dendritic cell can be a temporal bridge between a CD4⁺ T-helper and a T-killer cell. *Nature* **393**:474–477.

- Robbins, A. S. (1993). Controversies in measles immunization recommendations. *West. J. Med.* **158**:36–39.
- Rodriguez, F., Slifka, M. K., Harkins, S., and Whitton, J. L. (2001). Two overlapping subdominant epitopes identified by DNA immunization induce protective CD8⁺ T cell populations with differing cytolytic activities. *J. Virol.* **75**:7399–7409.
- Rogers, P. R., Dubey, C., and Swain, S. L. (2000). Qualitative changes accompany memory T cell generation: Faster, more effective responses at lower doses of antigen. *J. Immunol.* **164**:2338–2346.
- Romero, J. R. (2003). Palivizumab prophylaxis of respiratory syncytial virus disease from 1998 to 2002: Results from four years of Palivizumab usage. *Pediatr. Infect. Dis. J.* **22**:S46–S54.
- Rosen, H. R., Miner, C., Sasaki, A. W., Lewinsohn, D. M., Conrad, A. J., Bakke, A., Bouwer, H. G., and Hinrichs, D. J. (2002). Frequencies of HCV-specific effector CD4⁺ T cells by flow cytometry: Correlation with clinical disease stages. *Hepatology* **35**:190–198.
- Sallusto, F., Lenig, D., Forster, R., Lipp, M., and Lanzavecchia, A. (1999). Two subsets of memory T lymphocytes with distinct homing potentials and effector functions. *Nature* **401**:708–712.
- Salter, R. D., Benjamin, R. J., Wesley, P. K., Buxton, S. E., Garrett, T. P. J., Clayberger, C., Krensky, A. M., Norment, A. M., Littman, D. R., and Parham, P. (1990). A binding site for the T cell coreceptor CD8 on the $\alpha 3$ domain of HLA-A2. *Nature* **345**:41–46.
- Salzmann, M., and Bachmann, M. F. (1998). Estimation of maximal affinities between T cell receptors and MHC/peptide complexes. *Mol. Immunol.* **35**:65–71.
- Savage, P. A., Boniface, J. J., and Davis, M. M. (1999). A kinetic basis for T cell receptor repertoire selection during an immune response. *Immunity* **10**:485–492.
- Sawyer, W. A. (1931). Persistence of yellow fever immunity. *J. Prev. Med.* **5**:413–428.
- Schluns, K. S., Kieper, W. C., Jameson, S. C., and Lefrancois, L. (2000). Interleukin-7 mediates the homeostasis of naive and memory CD8⁺ T cells *in vivo*. *Nat. Immunol.* **1**:426–432.
- Schluns, K. S., Williams, K., Ma, A., Zheng, X. X., and Lefrancois, L. (2002). Cutting edge: Requirement for IL-15 in the generation of primary and memory antigen-specific CD8⁺ T cells. *J. Immunol.* **168**:4827–4831.
- Schoenberger, S. P., Toes, R. E., van der Voort, E. I., Offringa, R., and Melief, C. J. (1998). T cell help for cytotoxic T lymphocytes is mediated by CD40–CD40L interactions. *Nature* **393**:480–483.
- Seddon, B., Tomlinson, P., and Zamoyska, R. (2003). Interleukin 7 and T cell receptor signals regulate homeostasis of CD4 memory cells. *Nat. Immunol.* **4**:680–686.
- Selin, L. K., and Welsh, R. M. (1997). Cytolytically active memory CTL present in lymphocytic choriomeningitis virus-immune mice after clearance of virus infection. *J. Immunol.* **158**:5366–5373.
- Shedlock, D. J., and Shen, H. (2003). Requirement for CD4⁺ T cell help in generating functional CD8⁺ T cell memory. *Science* **300**:337–339.
- Shortridge, K. F., Zhou, N. N., Guan, Y., Gao, P., Ito, T., Kawaoka, Y., Kodihalli, S., Krauss, S., Markwell, D., Murti, K. G., Norwood, M., Senne, D., Sims, L., Takada, A., and Webster, R. G. (1998). Characterization of avian H5N1 influenza viruses from poultry in Hong Kong. *Virol.* **252**:331–342.
- Slifka, M. K., and Ahmed, R. (1996). Long-term humoral immunity against viruses: Revisiting the issue of plasma cell longevity. *Trends Microbiol.* **4**:394–400.
- Slifka, M. K., Antia, R., Whitmire, J. K., and Ahmed, R. (1998). Humoral immunity due to long-lived plasma cells. *Immunity* **8**:363–372.

- Slifka, M. K., Matloubian, M., and Ahmed, R. (1995). Bone marrow is a major site of long-term antibody production after acute viral infection. *J. Virol.* **69**:1895–1902.
- Slifka, M. K., Rodriguez, F., and Whitton, J. L. (1999). Rapid on/off cycling of cytokine production by virus-specific CD8⁺ T cells. *Nature* **401**:76–79.
- Slifka, M. K., and Whitton, J. L. (2000a). Activated and memory CD8⁺ T cells can be distinguished by their cytokine profiles and phenotypic markers. *J. Immunol.* **164**:208–216.
- Slifka, M. K., and Whitton, J. L. (2000b). Clinical implications of dysregulated cytokine production. *J. Mol. Med.* **78**:74–80.
- Slifka, M. K., and Whitton, J. L. (2001). Functional avidity maturation of CD8⁺ T cells without selection of higher affinity TCR. *Nat. Immunol.* **2**:711–717.
- Smith, K. G., Strasser, A., and Vaux, D. L. (1996). CrmA expression in T lymphocytes of transgenic mice inhibits CD95 (Fas/APO-1)-transduced apoptosis but does not cause lymphadenopathy or autoimmune disease. *EMBO J.* **15**:5167–5176.
- Sourdive, D. J., Murali-Krishna, K., Altman, J. D., Zajac, A. J., Whitmire, J. K., Pannetier, C., Kourilsky, P., Evavold, B., Sette, A., and Ahmed, R. (1998). Conserved T cell receptor repertoire in primary and memory CD8⁺ T cell responses to an acute viral infection. *J. Exp. Med.* **188**:71–82.
- Spear, G. T., Hart, M., Olinger, G. G., Hashemi, F. B., and Saifuddin, M. (2001). The role of the complement system in virus infections. *Curr. Top. Microbiol. Immunol.* **260**:229–245.
- Sprent, J. (1976). Fate of H2-activated T lymphocytes in syngeneic hosts. I. Fate in lymphoid tissues and intestines traced with 3H-thymidine, 125I-deoxyuridine, and 51 chromium. *Cell Immunol.* **21**:278–302.
- Sprent, J., and Surh, C. D. (2002). T cell memory. *Annu. Rev. Immunol.* **20**:551–579.
- Srikiatkachorn, A., Chang, W., and Braciale, T. J. (1999). Induction of Th1 and Th2 responses by respiratory syncytial virus attachment glycoprotein is epitope and major histocompatibility complex independent. *J. Virol.* **73**:6590–6597.
- Steigerwald-Mullen, P., Kurilla, M. G., and Braciale, T. J. (2000). Type 2 cytokines predominate in the human CD4⁺ T-lymphocyte response to Epstein-Barr virus nuclear antigen 1. *J. Virol.* **74**:6748–6759.
- Stiehm, E. R. (1979). Standard and special human immune serum globulins as therapeutic agents. *Pediatrics* **63**:301–319.
- Stohlman, S. A., Bergmann, C. C., Lin, M. T., Cua, D. J., and Hinton, D. R. (1998). CTL effector function within the central nervous system requires CD4⁺ T cells. *J. Immunol.* **160**:2896–2904.
- Strasser, A., Harris, A. W., Huang, D. C., Krammer, P. H., and Cory, S. (1995). Bcl-2 and Fas/APO-1 regulate distinct pathways to lymphocyte apoptosis. *EMBO J.* **14**:6136–6147.
- Su, H. C., Cousens, L. P., Fast, L. D., Slifka, M. K., Bungiro, R. D., Ahmed, R., and Biron, C. A. (1998). CD4⁺ and CD8⁺ T cell interactions in IFN- γ and IL-4 responses to viral infections: Requirements for IL-2. *J. Immunol.* **160**:5007–5017.
- Sun, J. C., and Bevan, M. J. (2003). Defective CD8⁺ T cell memory following acute infection without CD4⁺ T cell help. *Science* **300**:339–342.
- Suresh, M., Whitmire, J. K., Harrington, L. E., Larsen, C. P., Pearson, T. C., Altman, J. D., and Ahmed, R. (2001). Role of CD28–B7 interactions in generation and maintenance of CD8⁺ T cell memory. *J. Immunol.* **167**:5565–5573.
- Swain, S. L., Hu, H., and Huston, G. (1999). Class II independent generation of CD4⁺ memory T cells from effectors. *Science* **286**:1381–1383.
- Sykulev, Y., Cohen, R. J., and Eisen, H. N. (1995). The law of mass action governs antigen-stimulated cytolytic activity of CD8⁺ cytotoxic T lymphocytes. *Proc. Natl. Acad. Sci. USA* **92**:11990–11992.

- Tan, J. T., Ernst, B., Kieper, W. C., LeRoy, E., Sprent, J., and Surh, C. D. (2002). Interleukin (IL)-15 and IL-7 jointly regulate homeostatic proliferation of memory phenotype CD8⁺ cells but are not required for memory phenotype CD4⁺ cells. *J. Exp. Med.* **195**:1523–1532.
- Thornberry, N. A., and Lazebnik, Y. (1998). Caspases: Enemies within. *Science* **281**:1312–1316.
- Topham, D. J., and Doherty, P. C. (1998). Longitudinal analysis of the acute Sendai virus-specific CD4⁺ T cell response and memory. *J. Immunol.* **161**:4530–4535.
- Topham, D. J., Tripp, R. A., Hamilton-Easton, A. M., Sarawar, S. R., and Doherty, P. C. (1996a). Quantitative analysis of the influenza virus-specific CD4⁺ T cell memory in the absence of B cells and Ig. *J. Immunol.* **157**:2947–2952.
- Topham, D. J., Tripp, R. A., Sarawar, S. R., Sangster, M. Y., and Doherty, P. C. (1996b). Immune CD4⁺ T cells promote the clearance of influenza virus from major histocompatibility complex class II^{-/-} respiratory epithelium. *J. Virol.* **70**:1288–1291.
- Tripp, R. A., Hou, S., Etchart, N., Prinz, A., Moore, D., Winter, J., and Anderson, L. J. (2001). CD4⁺ T cell frequencies and T_H1/T_H2 cytokine patterns expressed in the acute and memory response to respiratory syncytial virus I-E(d)-restricted peptides. *Cell Immunol.* **207**:59–71.
- Tripp, R. A., Moore, D., Barskey, A. T., Jones, L., Moscattello, C., Keyserling, H., and Anderson, L. J. (2002). Peripheral blood mononuclear cells from infants hospitalized because of respiratory syncytial virus infection express T helper-1 and T helper-2 cytokines and CC chemokine messenger RNA. *J. Infect. Dis.* **185**:1388–1394.
- Tsai, S. L., Liaw, Y. F., Chen, M. H., Huang, C. Y., and Kuo, G. C. (1997). Detection of type 2-like T-helper cells in hepatitis C virus infection: Implications for hepatitis C virus chronicity. *Hepatology* **25**:449–458.
- Unsoeld, H., Krautwald, S., Voehringer, D., Kunzendorf, U., and Pircher, H. (2002). Cutting edge: CCR7⁺ and CCR7⁻ memory T cells do not differ in immediate effector cell function. *J. Immunol.* **169**:638–641.
- Valitutti, S., and Lanzavecchia, A. (1997). Serial triggering of TCRs: A basis for the sensitivity and specificity of antigen recognition. *Immunol. Today* **18**:299–304.
- van Parijs, L., Peterson, D. A., and Abbas, A. K. (1998). The Fas/Fas ligand pathway and Bcl-2 regulate T cell responses to model self and foreign antigens. *Immunity* **8**:265–274.
- van Parijs, L., Refaeli, Y., Lord, J. D., Nelson, B. H., Abbas, A. K., and Baltimore, D. (1999). Uncoupling IL-2 signals that regulate T cell proliferation, survival, and Fas-mediated activation-induced cell death. *Immunity* **11**:281–288.
- van Stipdonk, M. J., Lemmens, E. E., and Schoenberger, S. P. (2001). Naive CTLs require a single brief period of antigenic stimulation for clonal expansion and differentiation. *Nat. Immunol.* **2**:423–429.
- Vanderplasschen, A., Hollinshead, M., and Smith, G. L. (1997). Antibodies against vaccinia virus do not neutralize extracellular enveloped virus but prevent virus release from infected cells and comet formation. *J. Gen. Virol.* **78**:2041–2048(Pt 8).
- Varga, S. M., Selin, L. K., and Welsh, R. M. (2001). Independent regulation of lymphocytic choriomeningitis virus-specific T cell memory pools: Relative stability of CD4 memory under conditions of CD8 memory T cell loss. *J. Immunol.* **166**:1554–1561.
- Varga, S. M., and Welsh, R. M. (1998). Detection of a high frequency of virus-specific CD4⁺ T cells during acute infection with lymphocytic choriomeningitis virus. *J. Immunol.* **161**:3215–3218.
- Varga, S. M., and Welsh, R. M. (2000). High frequency of virus-specific interleukin-2-producing CD4⁺ T cells and Th1 dominance during lymphocytic choriomeningitis virus infection. *J. Virol.* **74**:4429–4432.

- Varga, S. M., Wissinger, E. L., and Braciale, T. J. (2000). The attachment (G) glycoprotein of respiratory syncytial virus contains a single immunodominant epitope that elicits both T_{h1} and T_{h2} $CD4^+$ T cell responses. *J. Immunol.* **165**:6487–6495.
- Veazey, R. S., Shattock, R. J., Pope, M., Kirijan, J. C., Jones, J., Hu, Q., Ketas, T., Marx, P. A., Klasse, P. J., Burton, D. R., and Moore, J. P. (2003). Prevention of virus transmission to macaque monkeys by a vaginally applied monoclonal antibody to HIV-1 gp120. *Nat. Med.* **9**:343–346.
- Vercammen, D., Brouckaert, G., Denecker, G., van de Craen, M., Declercq, W., Fiers, W., and Vandenabeele, P. (1998). Dual signaling of the Fas receptor: Initiation of both apoptotic and necrotic cell death pathways. *J. Exp. Med.* **188**:919–930.
- von Herrath, M. G., Fujinami, R. S., and Whitton, J. L. (2003). Microorganisms and autoimmunity—Making the barren field fertile? *Nature Reviews Microbiology* **1**:151–157.
- von Herrath, M. G., Yokoyama, M., Dockter, J., Oldstone, M. B. A., and Whitton, J. L. (1996). $CD4$ -deficient mice have reduced levels of memory cytotoxic T lymphocytes after immunization and show diminished resistance to subsequent virus challenge. *J. Virol.* **70**:1072–1079.
- Walker, C. M., Erickson, A. L., Hsueh, F. C., and Levy, J. A. (1991). Inhibition of human immunodeficiency virus replication in acutely infected $CD4^+$ cells by $CD8^+$ cells involves a noncytotoxic mechanism. *J. Virol.* **65**:5921–5927.
- Walsh, C. M., Matloubian, M., Liu, C. C., Ueda, R., Kurahara, C. G., Christensen, J. L., Huang, M. T., Young, J. D., Ahmed, R., and Clark, W. R. (1994). Immune function in mice lacking the perforin gene. *Proc. Natl. Acad. Sci. USA* **91**:10854–10858.
- Wang, J. H., Layden, T. J., and Eckels, D. D. (2003). Modulation of the peripheral T cell response by $CD4$ mutants of hepatitis C virus: Transition from a T_{h1} to a T_{h2} response. *Hum. Immunol.* **64**:662–673.
- Ward, B. J., and Griffin, D. E. (1993). Changes in cytokine production after measles virus vaccination: Predominant production of IL-4 suggests induction of a T_{h2} response. *Clin. Immunol. Immunopathol.* **67**:171–177.
- Ward, R., and Krugman, S. (1962). Etiology, epidemiology, and prevention of viral hepatitis. *Prog. Med. Virol.* **4**:87–118.
- Welsh, R. M., and McNally, J. M. (1999). Immune deficiency, immune silencing, and clonal exhaustion of T cell responses during viral infections. *Curr. Opin. Microbiol.* **2**:382–387.
- Weninger, W., Manjunath, N., and von Andrian, U. H. (2002). Migration and differentiation of $CD8^+$ T cells. *Immunol. Rev.* **186**:221–233.
- Wherry, E. J., Puorro, K. A., Porgador, A., and Eisenlohr, L. C. (1999). The induction of virus-specific CTL as a function of increasing epitope expression: Responses rise steadily until excessively high levels of epitope are attained. *J. Immunol.* **163**:3735–3745.
- Wherry, E. J., Teichgraber, V., Becker, T. C., Masopust, D., Kaech, S. M., Antia, R., von Andrian, U. H., and Ahmed, R. (2003). Lineage relationship and protective immunity of memory $CD8^+$ T cell subsets. *Nat. Immunol.* **4**:225–234.
- White, H. A. (1972). Lassa fever. A study of 23 hospital cases. *Trans. R. Soc. Trop. Med. Hyg.* **66**:390–401.
- Whitmire, J. K., Asano, M. S., Murali-Krishna, K., Suresh, M., and Ahmed, R. (1998). Long-term $CD4$ T_{h1} and T_{h2} memory following acute lymphocytic choriomeningitis virus infection. *J. Virol.* **72**:8281–8288.
- Whitmire, J. K., Flavell, R. A., Grewal, I. S., Larsen, C. P., Pearson, T. C., and Ahmed, R. (1999). $CD40$ – $CD40$ ligand costimulation is required for generating antiviral $CD4^+$

- T cell responses but is dispensable for CD8⁺ T cell responses. *J. Immunol.* **163**:3194–3201.
- Whitmire, J. K., Murali-Krishna, K., Altman, J. D., and Ahmed, R. (2000). Antiviral CD4⁺ and CD8⁺ T cell memory: Differences in the size of the response and activation requirements. *Philos. Trans. R. Soc. London B Biol. Sci.* **355**:373–379.
- Whitton, J. L., Sheng, N., Oldstone, M. B. A., and McKee, T. A. (1993). A “string-of-beads” vaccine, comprising linked minigenes, confers protection from lethal-dose virus challenge. *J. Virol.* **67**:348–352.
- Wilson, A. D., Hopkins, J. C., and Morgan, A. J. (2001). *In vitro* cytokine production and growth inhibition of lymphoblastoid cell lines by CD4⁺ T cells from Epstein-Barr virus (EBV) seropositive donors. *Clin. Exp. Immunol.* **126**:101–110.
- Wittes, J. T., Kelly, A., and Plante, K. M. (1996). Meta-analysis of CMVIG studies for the prevention and treatment of CMV infection in transplant patients. *Transplant. Proc.* **28**:17–24.
- Wright, K. E., and Buchmeier, M. J. (1991). Antiviral antibodies attenuate T cell-mediated immunopathology following acute lymphocytic choriomeningitis virus infection. *J. Virol.* **65**:3001–3006.
- Wu, C., Nguyen, K. B., Pien, G. C., Wang, N., Gullo, C., Howie, D., Sosa, M. R., Edwards, M. J., Borrow, P., Satoskar, A. R., Sharpe, A. H., Biron, C. A., and Terhorst, C. (2001). SAP controls T cell responses to virus and terminal differentiation of Th2 cells. *Nat. Immunol.* **2**:410–414.
- Wu, Y., and Liu, Y. (1994). Viral induction of costimulatory activity on antigen-presenting cells bypasses the need for CD4⁺ T cell help in CD8⁺ T cell responses. *Curr. Biol.* **4**:499–505.
- Youngman, K. R., Franco, M. A., Kuklin, N. A., Rott, L. S., Butcher, E. C., and Greenberg, H. B. (2002). Correlation of tissue distribution, developmental phenotype, and intestinal homing receptor expression of antigen-specific B cells during the murine antirotavirus immune response. *J. Immunol.* **168**:2173–2181.
- Zajac, A. J., Blattman, J. N., Murali-Krishna, K., Sourdive, D. D., Suresh, M., Altman, J. D., and Ahmed, R. (1998). Viral immune evasion due to persistence of activated T cells without effector function. *J. Exp. Med.* **188**:2205–2213.
- Zajac, A. J., Quinn, D. G., Cohen, P. L., and Frelinger, J. A. (1996). Fas-dependent CD4⁺ cytotoxic T-cell-mediated pathogenesis during virus infection. *Proc. Natl. Acad. Sci. USA* **93**:14730–14735.
- Zhong, W., Roberts, A. D., and Woodland, D. L. (2001). Antibody-independent antiviral function of memory CD4⁺ T cells *in vivo* requires regulatory signals from CD8⁺ effector T cells. *J. Immunol.* **167**:1379–1386.
- Zhou, S., Ou, R., Huang, L., and Moskophidis, D. (2002). Critical role for perforin-, Fas/FasL-, and TNFR1-mediated cytotoxic pathways in down-regulation of antigen-specific T cells during persistent viral infection. *J. Virol.* **76**:829–840.

PROSPECTS FOR THE THERAPY AND PREVENTION OF DENGUE VIRUS INFECTIONS

Elsa B. Damonte, Carlos A. Pujol, and Celia E. Coto

Laboratory of Virology, Department of Biological Chemistry
College of Exact and Natural Sciences, Ciudad Universitaria
University of Buenos Aires, 1428 Buenos Aires, Argentina

- I. Introduction
 - II. The Agent
 - A. Classification
 - B. Virus Life Cycle in Nature
 - III. The Human Disease
 - A. Clinical Features
 - B. Pathogenesis
 - C. Genetic Variation in DENV
 - IV. DENV as a Global Reemerging Agent
 - V. Virus Structure and the Replicative Cycle: Possible Targets for Therapy
 - A. The Virion
 - B. The Replicative Cycle
 - VI. Viral Inhibitors
 - A. *In Vitro* Studies
 - B. *In Vivo* Systems
 - VII. Strategies for Vaccine Development
 - VIII. Concluding Remarks
- References

I. INTRODUCTION

Dengue fever (DF) is a mosquito-borne infection that in recent years has become a major international public health concern. More than 100 million cases of DF occur yearly, and more than 2 billion people are at risk every year. Dengue virus (DENV) is found in tropical and subtropical regions around the world, predominantly in urban and semi-urban areas. However, due to the global growth of population, urbanization, and the spread of the main mosquito vector, *Aedes aegypti*, dengue diseases are not only a burden to the health of developing countries but a major emerging worldwide problem.

The etiological agents involved are viruses from four *Flavivirus* sister-species (Chevillon and Failloux, 2003), each defining a distinct serotype: DENV-1, DENV-2, DENV-3, and DENV-4, respectively, which cocirculate. Infection with DENV produces a spectrum of clinical illness ranging

from silent infection to either DF or the severe and fatal dengue hemorrhagic disease (DHF) and dengue shock syndrome (DSS).

Three strategies can be intended to control human DENV diseases: (i) the elimination of the mosquito vector, (ii) the development of safe vaccines to prevent infection, and (iii) the search of specific chemotherapeutic agents for treatment. This chapter is mainly focused on the last two approaches presenting a review of the current knowledge on stages of the DENV replication cycle to identify potential targets for antiviral drug discovery, the main antiviral inhibitors reported to have anti-DENV activity, and the strategies for DENV vaccine development.

II. THE AGENT

A. Classification

In 1906, Bancroft published the first evidence implicating the mosquito *A. aegypti* as vector of DENV, and 1 year later Ashburn and Craig demonstrated the presence of the filterable causative agent in the blood of patients (Clarke and Casals, 1965). Extensive studies of the disease in human volunteers were carried out in the Philippines since there were no animal models to reproduce the infection (Clarke and Casals, 1965). The original natural reservoir of DENV appeared to have been tropical African primates although the virus also seemed to establish reservoir status in monkeys of Southeast Asia.

DENV was originally classified as an arthropod-borne animal virus (arbovirus) based on a combination of laboratory and epidemiological determinants. The arboviruses comprise a huge collection of infectious agents that are biologically transmitted between susceptible hosts by hematophagous arthropods. Currently, arboviruses have been taxonomically classified in different virus families according to viral genes, virion structure, and the viral replication cycle. Most of them, however, can be maintained in an environment only if one or more efficient vectors and hosts have an intimate and frequent association. Thus, an efficient vector must have a preference for blood from a competent host, and a sufficient population of both components must be associated in time and place in an environment compatible with the virus completing extrinsic incubation.

DENV belongs to the genus *Flavivirus* of family Flaviviridae, which are members of the positive-stranded virus supergroup 2 (SF-2), bearing distant similarity in their RNA-dependent RNA polymerases to coliphages and several plant-infecting viruses (Lindenbach and Rice,

2001). The genus *Flavivirus* comprises over 70 viruses, many of which are important human pathogens causing a variety of diseases including fever, encephalitis, and hemorrhagic fever. Viruses within the genus are categorized into antigenic complexes and subcomplexes based on classical serological criteria (Calisher, 1988; Calisher *et al.*, 1989) or into clusters, clades, and species according to molecular phylogenetics (Kuno *et al.*, 1998). Clades established by phylogeny correlate significantly with existing antigenic complexes and, based on nucleotide sequence data, the four members of DENV serotype complex (DENV-1, DENV-2, DENV-3, and DENV-4) are considered four distinct species belonging to the mosquito-borne cluster clade IX of *Flavivirus* (Lindenbach and Rice, 2001). Although epidemiologically similar, infection with one serotype leads to lifelong protection against homologous reinfection, but only brief protection against heterologous challenge is observed (Kurane and Ennis, 1992). As stated by Chevillon and Failloux (2003), the four DENV serotypes define four sister-species of viruses because (i) the corresponding viruses are genetically tightly related to one another, (ii) recombination occurs within but not across serotypes, and (iii) any pair of viruses from the same serotype remains more closely related than any pair belonging to different serotypes. Like many RNA viruses, it was recently demonstrated that DENV-3 is present as quasi-species in plasma of infected persons (Wang *et al.*, 2002), directly implying the pathogenesis of the dengue virus.

B. Virus Life Cycle in Nature

The normal cycle of DENV infection is considered to be human–mosquito–human. From feeding on an infected and viremic human, the female mosquito is able to transmit the virus after an incubation period of 8 to 10 days wherein DENV infection, replication, and dissemination result in infection of the salivary glands. The virus is then injected into another person when the mosquito introduces anticoagulant substances present in the saliva to prevent blood clotting. The mosquito remains able to transmit DENV for its entire life. Two distinct transmission cycles occur: (i) endemic and epidemic dengue involving human hosts and transmission by *A. aegypti*, with *A. albopictus* and other *Aedes* mosquitoes serving as secondary vectors; and (ii) a zoonotic or sylvatic cycle in sylvatic habitats of Africa and Malaysia, involving nonhuman primate reservoir hosts and several different *Aedes* mosquitoes (Gubler and Trent, 1994; Wang *et al.*, 2000).

III. THE HUMAN DISEASE

A. *Clinical Features*

As mentioned previously the diseases caused by DENV have been classified into distinct categories: DF, DHF, and DSS (Henchal and Putnak, 1990; Kautner *et al.*, 1997). DF is usually mild and nonspecific in most children and is associated with pharyngitis, rhinitis, a mild cough, and a fever for several days to a week. Classic DF, most likely to occur in older children and adults, is a febrile viral syndrome of sudden onset, characterized by a fever for 2 to 5 days (often biphasic and rarely lasting more than 7 days), a severe headache, intense myalgias, arthralgias, retro-orbital pain, anorexia, and a rash. The initial fever begins abruptly with a frontal or retro-orbital headache and low back pain. Severe limb or "breakbone" pain develops in the first 1 or 2 days, often concurrent with an evanescent generalized erythroderma. Nausea and vomiting are common between days 2 and 5. Around day 5 or 6, the fever subsides and a diffuse morbilliform rash appears; the rash may be pruritic and heals with desquamation. After a 2-day absence, fever recurs. Minor bleeding phenomena, such as epistaxis, petechiae, and gingival bleeding, may occur at any time during the febrile phase. Major bleeding phenomena, such as menorrhagia and hemorrhage, can occur, signs of which have been associated with pathologic changes of peptic ulcer disease.

All DENV serotypes can cause DF, a generally self-limited disease, but a minority of patients (1–5%) may experience more complicated and severe diseases like DHF and DSS. DHF, also known as Philippine hemorrhagic fever, Thai hemorrhagic fever, or Singapore hemorrhagic fever, is a severe febrile disease characterized by abnormalities of haemostasis and increased vascular permeability, which in some instances results in DSS (Kalayanarooj *et al.*, 1997). DSS is a form of hypovolaemic shock that is associated clinically with haemoconcentration, and it can lead to death. DHF and DSS are recognized primarily in children; in tropical Asia, DSS is observed almost exclusively among indigenous children 15 years of age and younger. Illness is often biphasic, beginning abruptly with fever, malaise, headache, anorexia, nausea and vomiting, cough, and facial flushing. Severe bone and limb pain are often absent. Coincident with defervescence, the condition of the patient worsens, with profound weakness and prostration, diaphoresis, restlessness, facial pallor and circumoral cyanosis, cool and clammy extremities, rapid but therapy pulse, and a narrow pulse pressure. The liver may be enlarged in 10% of children. In this setting,

hemorrhagic phenomena are frequent, and elevated transaminase levels, hypoalbuminemia, and hyponatremia (especially in adults) are common features. In severe cases, pleural effusions and ascites correlate with hypoproteinemia and marked liver dysfunction.

B. Pathogenesis

As already stated, infections produced by DENV have been classified in categories from subclinical infection to sometimes fatal disease. However, as for other diseases, the various manifestations can be seen as a continuum from mild to severe reactions, which may be determined by factors like virus virulence; host age; nutritional, genetic, and immunological characteristics; and intercurrent infections (Bielefeldt-Ohmann, 1997; Kalayanarooj *et al.*, 1997). By epidemiological and clinical associations, it has been shown that both immunological and viral factors determine the severity of the disease (Halstead, 1988; Rosen, 1977). Infection with one DENV serotype does not provide protective immunity against the others, and sequential heterotypic infection has been shown to increase virus replication and thus the probability of developing DHF by a process known as antibody-dependent enhancement (ADE) (Halstead, 1988; Kliks *et al.*, 1989; Morens, 1994). For ADE to occur, two prerequisites must be fulfilled: (i) cross-reactive but nonseroneutralizing antibodies elicited during the first infection must bind to the second DENV strain; and (ii) unneutralized, infectious virus-antibody complexes must bind to Fc receptors of macrophages, one of the proposed main target cells for DENV. Cases of DHF and DSS in children younger than 1 year of age, and with no previous exposure to DENV, have been accommodated within this theory by invoking the effect of residual maternal DENV specific antibodies (Bielefeldt-Ohmann, 1997).

Several authors comment that, regardless of the role that DENV-antibody complexes may play in infection enhancement, they do play an undisputable role in inflammatory processes (Deo *et al.*, 1997; Walport and Taylor, 1997). Immune complexes contain two types of potential ligands and may trigger inflammatory responses in tissues. Other than the interaction of the Fc portion of antibodies with the Fc-receptor portion of leukocytes, complement components, either fixed to the complexes or released as soluble anaphylatoxins, provide a further series of triggering effector molecules (Bielefeldt-Ohmann, 1997). Complement consumption in concert with various cytokines and vasoactive factors secreted by serotype cross-reactive T cells and activated macrophages precipitate the profound vascular and hemorrhagic changes

leading to DHF and DSS (Kurane and Ennis, 1994; Morens, 1994). Rothman and Ennis (1999) proposed that the proximal cause of plasma leakage in secondary DENV infections is the synergistic effect of interferon γ , tumor necrosis factor α , and activated complement proteins on endothelial cells throughout the body. They also explained that the pathways leading to elevated levels of these vasoactive molecules are set in motion much earlier in infection (Rothman and Ennis, 1999). At the earliest stage of infection, preformed DENV-specific antibodies increase the number of virus infected monocytes, and as a result, the number of cells presenting DENV antigens to T lymphocytes is increased. In the middle stages of infection, the level of T lymphocyte activation is markedly increased, reflecting the enhanced antigen presentation, the high frequency of DENV specific T lymphocytes in secondary infection, and the more rapid activation and proliferation of memory T lymphocytes.

Despite the arguments in favor of host immunological reactions, there are still cases of DHF and DSS that cannot be adequately explained by ADE, particularly in confirmed cases of primary infection (Watts *et al.*, 1999). To explain the increasing number of severe forms of DENV infections in which viral factors are implicated, an alternative hypothesis comes from evolutionary studies of DENV revealing the genetic diversity and the cocirculation in nature of virus strains that differ in virulence. An important piece of evidence supporting this theory arises from molecular evolution studies.

C. Genetic Variation in DENV

Several investigations proved that, like most RNA viruses, DENV exhibits substantial genetic diversity, most notably in the existence of four distinct serotypes that are no more similar to each other than some different species of flaviviruses (Kuno *et al.*, 1998). Several causes of the genetic variation in DENV have been discussed (Holmes and Burch, 2000). The first factor involved is the intrinsic error per round of replication of the RNA-dependent RNA polymerase (Drake, 1993). Second, genetic diversity might also be generated by recombination, probably by a copy choice mechanism in which the RNA polymerase switches between the genomes of two viruses from a serotype that have infected the same cell and form a hybrid RNA molecule (Worobey *et al.*, 1999). A third way in which genetic variation can enter population is via migration (gene flow). There are plenty of data indicating that DENV is often transported a large distance by hosts and vectors; in fact, serotypes and genotypes have broad geographical distributions (Rico-Hesse, 1990). Several studies support the importance

of viral factors on the production of the severe forms of dengue (Leitmeyer *et al.*, 1999; Rico-Hesse, 1990; Rico-Hesse *et al.*, 1997, 1998). These investigations stated that despite cocirculation of several DENV serotypes in the Americas, it was not until the Cuban epidemic of 1981 that the first case of DHF occurred, and this coincided with the introduction of a higher pathogenic new genetic variant of DENV-2 from Southeast Asia.

IV. DENV AS A GLOBAL REEMERGING AGENT

Globalization is now a frequently mentioned term referring not only to political or economical issues but also to urgent health threats like those represented by emerging and reemerging virus infection diseases. A typical example of a global disease is provided by DENV infections.

The initial reported epidemics of DF occurred in 1779 to 1780 in Asia, Africa, and North America; the near simultaneous occurrence of outbreaks on three continents indicated that these viruses and their mosquito vector have had a worldwide distribution in the tropics for more than 200 years. During most of this time, DF was considered a benign, nonfatal disease of visitors to the tropics. Generally, there were long intervals (10–40 years) between major epidemics, mainly because the viruses and their vectors could only be transported between population centers by sailing vessels.

The global epidemiology and transmission dynamics of DENV changed dramatically in Southeast Asia during World War II (Gubler and Meltzer, 1999). The disruption and change in ecology caused by the war effort expanded the geographical distribution and increased the densities of *A. aegypti*, making many countries highly permissive for epidemic transmission. Troop movements accelerated the spread of viruses between population centers in the region and caused major epidemics. The consequence was a global pandemic of dengue beginning in Southeast Asia and extending to the Pacific region and the Americas (Gubler, 2002). Epidemics caused by multiple serotypes (hyperendemicity) have been more frequent since then, and the geographic distribution of DENV mosquito vectors has expanded. In Southeast Asia, epidemic DHF first appeared in the 1950s, but by 1975, DHF had become a leading cause of hospitalization and death among children in many countries in that area. Successive introduction and circulation of the four serotypes into the Caribbean as well as Central America and South America has occurred since 1977. A DHF

epidemic was first reported in the Caribbean in 1981, and since 1982, epidemics have occurred in 14 Central or South American countries (Gubler, 2002). Evolving transmission patterns are probably the result of a combination of changing human demographics and expanding vector population and not only due to alterations in viral virulence. DF can be found wherever *A. aegypti* is present and introduced, whether in rural or urban areas.

One hundred million cases of DF are reported yearly by the World Health Organization (WHO), making it one of the most important viral diseases in the world. Cases seen in the United States are imported from the Caribbean region, the others arriving from South America, Africa, or Asia. Transmission of DENV is often seasonal, with rates increasing during hot and humid months. The vector *A. aegypti* breeds in peridomestic fresh water, such as water that might be stored in natural and artificial containers in and around human dwellings (e.g., old tires, flowerpots, water storage containers). This day-biting species is most active in the early morning and late afternoon. Modern transportation facilitated and increased the movement of people and commodities within and between regions of the world, leading to increased movement of both the mosquitoes and the viruses. In the 1980s and 1990s, the vectors and the viruses continued their global expansion, causing increased frequency and magnitude of epidemic DF and the emergence of DHF. Further efforts are needed to increase the amount of molecular data as well as viral sampling in vectors and silently infected patients to improve knowledge of dengue disease dynamics (Chevillon and Failloux, 2003).

V. VIRUS STRUCTURE AND THE REPLICATIVE CYCLE: POSSIBLE TARGETS FOR THERAPY

The knowledge of the virion structure and the viral life cycle is essential to elucidate potential targets of antiviral therapy and, thus, to obtain key information for the rational design of antiviral drugs. The main characteristics of the virion and the current information about the different stages of the replicative cycle are presented in this section.

A. *The Virion*

DENV has a relatively simple structure. Virions are small spherical particles, 40 to 50 nm in diameter, that contain three structural proteins: the nucleocapsid protein C (12–14 kD); a small nonglycosylated

B. *The Replicative Cycle*

1. *Binding and Penetration*

Virus binding to a cell surface receptor mediated by a viral attachment protein (VAP) is the first step in the infection process, leading to the subsequent virus penetration to the host cell. The identification of the VAP in the virion and its counterpart, the cellular receptor, is required not only to understand virus replication but also tissue tropism and pathogenesis. In the case of DENV, two general mechanisms for virus binding and uptake are known. The most extensively studied mechanism involves the binding of virus-antibody complexes (formed in the presence of subneutralizing amounts of antibody) to Fc-receptor positive cells via the Fc portion of immunoglobulin G (Littaua *et al.*, 1990). This entry mechanism may play a role in development of DHF and DSS as a consequence of sequential infections with different DENV serotypes. The primary infection in patients lacking DENV antibodies or the infection of cells without Fc receptors is mediated by an antibody-independent mechanism that has only recently started to be extensively studied and is still unresolved.

As for other flaviviruses, the E protein has been identified as the VAP for DENV. The E protein derived from culture fluids of DENV-4-infected cells was shown to attach to different cell types including Vero, LLCMK2, HepG2, L929, MDBK, and human endothelial cells (Anderson *et al.*, 1992). This study has also evidenced the important role of E protein in controlling infection and determining cell and tissue tropism because the degree of E-binding correlated with cell susceptibility to the virus. Later, Chen *et al.* (1996) found that a recombinant chimeric form of DENV-2 E protein bound specifically to Vero, CHO, human endothelial, and human glial cells, confirming that the binding profile was in accordance with cell susceptibility to virus replication.

By contrast to the certain involvement of E protein as a VAP, the identity of the cellular receptor for DENV is at present controversial. The ability of arthropod-borne flaviviruses to replicate in cells of both vertebrate and invertebrate origin suggests either the presence of a single ubiquitous receptor or the likelihood of divergent cell receptors participating in virus attachment. In particular, DENV replicates in a wide variety of primary and continuous cell cultures derived from many mammalian, avian, and arthropod tissues. Several reports have implicated both proteins and glycosaminoglycans (GAGs) as receptor candidate molecules, suggesting a dependence on the type of host cell and virus serotype for the initial interaction DENV cell.

Among the proteins reported as putative DENV receptors, not fully characterized trypsin-susceptible proteins were described as responsible for binding of DENV-2 to human monocytes (Daughaday *et al.*, 1981) and DENV-1 to human hepatoma HepG2 cells and simian Vero cells (Marianneau *et al.*, 1996). In addition, four membrane proteins with apparent molecular masses of 27, 45, 67, and 87 kDa were identified as possible receptors for DENV-2 in human macrophages (Moreno-Altamirano *et al.*, 2002), and a 65 kDa trypsin-sensible protein in human and mouse neuroblastoma cells bound DENV-2 (Ramos-Castañeda *et al.*, 1997). The four serotypes of DENV were found to bind to the myelomonocytic cell line HL60 and the non-EBV transformed B cell line BM13674, with a different degree of affinity in the order DENV-2 > DENV-3 > DENV-1 > DENV-4, and the proteinaeous nature of the receptor on the membranes of these cells for DENV-2 was also shown (Bielefeldt-Ohmann, 1998). Furthermore, a very recent report of Navarro-Sanchez *et al.* (2003) has shown that the binding of mosquito-grown DENV to human dendritic cells occurs through the cell surface molecule called dendritic cell-specific ICAM3-grabbing nonintegrin (DC-SIGN). This protein is a C-type lectin specific for high-mannose-type carbohydrates. There are two potential N-linked glycosylation sites on each E subunit at the residues Asn-153 and Asn-67. DENV serotypes were found heterogeneous in their use of glycosylation sites, but the attached carbohydrates were described as the high-mannose-type (Johnson *et al.*, 1994) and required for viral entry. For mosquito cells, two glycoproteins of 40 and 45 kDa present on the surface of C6/36 cells were identified as putative receptors for DENV-4 binding (Salas-Benito and del Angel, 1997), whereas two other polypeptides of 80 and 67 kDa were shown to be involved in DENV-2 binding to the same cells (Muñoz *et al.*, 1998).

In contrast to the mentioned reports identifying protein molecules as DENV receptors, an involvement of heparan sulfate (HS) was demonstrated for attachment of recombinant DENV-2 E protein to Vero and CHO cells (Chen *et al.*, 1997) and attachment of DENV-2 virions to BHK cells (Hung *et al.*, 1999), Vero and CHO cells (Germi *et al.*, 2002), and human hepatocytes (Hilgard and Stockert, 2000). HS is one of the more ubiquitous members of molecules of the GAG family, found both on the cell surface and in the extracellular matrix. Many diverse viruses have been shown to interact with HS for target cell binding (Spillmann, 2001). The DENV interaction with GAG, however, is unusual for its specificity for a highly sulphated form of HS (Chen *et al.*, 1997). Experimental approaches based on the inhibition of DENV binding by treatment of cells with GAG lyases, desulfation of cellular

HS, or treatment of the virus with heparin supported the hypothesis that HS could act directly as DENV receptor. Furthermore, an involvement of HS during attachment and entry has also been demonstrated for other arthropod-borne flaviviruses, such as yellow fever virus (YFV) (Germi *et al.*, 2002), tick-borne encephalitis virus (TBEV) (Kroschewski *et al.*, 2003), and Murray Valley encephalitis virus (MVEV) (Lee and Lobigs, 2000), as well as for hepatitis C virus (HCV), member of the *Hepacivirus* genus of Flaviviridae (Cribier *et al.*, 1998). In another studies, however, HS was not found necessary, and, in addition, enzymatic removal of HS increased viral attachment to certain human leukocyte cells (Bielefeldt-Ohmann *et al.*, 2001). Thus, a plausible mechanism emerging from these conflicting data is an entry multistep process consisting of the sequential interaction of the envelope E protein with several target molecules on the cell membrane: HS may serve primarily to concentrate virus particles on the cell surface to facilitate the subsequent interaction with a high-affinity second receptor of protein nature. This hypothesis was supported by Martínez-Barragán and del Angel (2001) who have shown the binding of radiolabeled DENV-4 particles to Vero cell GAGs as well as to a 74 kDa surface glycoprotein, suggesting that HS may be the primary receptor and then other molecules, such as the 74 kDa protein, might participate as coreceptors for viral entry. It must be considered that even though HS seems to be a major determinant of DENV attachment on HS-expressing cells, alternative molecules less abundant than HS may act not only as coreceptors but also as initial receptors. A similar situation has also been found for other HS-binding viruses, such as for herpes simplex virus (Spear *et al.*, 2000).

The E protein not only mediates virus binding to cell receptors but also the subsequent membrane fusion step, apparently triggered by conformational changes produced in this protein at the acidic environment of the endosomes. As already outlined for receptor identification, the mechanism of penetration in *Flavivirus* has also been a subject of controversy. Although electron microscopic studies have shown that DENV-2 penetrated directly into the cytoplasm of C6/36 and BHK cells by fusion of the virion envelope with the plasma membrane at physiologic pH (Hase *et al.*, 1989; Lim and Ng, 1999), it is generally accepted that for productive DENV infection, viral uptake occurs through receptor-mediated endocytosis. Early evidences of this mode of entry were provided by experiments of virus inhibition with acidotropic agents as well as by the formation of syncytia by cell-to-cell fusion of mosquito cells infected with DENV exposed at low acidic pH (Heinz *et al.*, 1994; Summers *et al.*, 1989; Randolph and Stollar, 1990). More

recently, the entry of the *Flavivirus* Japanese encephalitis virus (JEV) was shown to take place by a clathrin-dependent endocytic pathway leading to infection (Nawa *et al.*, 2003).

To better understand the molecular interactions that lead to entry of DENV to the cell, the structure of the DENV-2 virion by cryo-electron microscopy and the crystal structure of its E protein have been recently reported (Kuhn *et al.*, 2002; Modis *et al.*, 2003). As expected, DENV-2 closely resembles the E protein of TBEV, the first *Flavivirus* protein characterized at atomic level (Rey *et al.*, 1995) but with slight differences. In the virion envelope, E forms head-to-tail linked homodimers that lie parallel to the virion surface, and as a consequence of this horizontal orientation, E has an outer and an inner surface. Each monomer contains three structural domains predominantly constituted by β strands and connected by hinge regions. Domain I is the central domain that organizes the structure; domain II is an elongated dimerization domain that contains the fusion peptide (residues 98 to 111); and domain III is an immunoglobulin-like structure proposed to contain the putative receptor binding site at residues 382–385. Accordingly, domain III has been previously proposed as the primary DENV receptor-binding motif because monoclonal antibodies that bind to domain III are blockers of virus adsorption (Crill and Roehrig, 2001), and GAG-binding motifs as possible antireceptors for HS were identified within domain III (Chen *et al.*, 1997). The fusion peptide in domain II is buried at the inner surface and becomes exposed as consequence of the conformational changes initiated by exposure to low pH. The main induced changes imply dissociation of the E homodimers followed by an irreversible rearrangement into homotrimers and motions at the interface between domains I and II, leading to the creation of a hydrophobic exterior to allow the projection of the fusion peptide from domain II toward the target membrane. According to their structural properties, the E *Flavivirus* protein and the E1 *Alphavirus* protein have been defined as a new class of viral fusion proteins, class II, in opposition to the class I viral fusion proteins that are present in orthomyxoviruses, paramyxoviruses, retroviruses, and filoviruses (Heinz and Allison, 2001).

2. Translation, Proteolytic Processing, and RNA Replication

The first event of biosynthesis in DENV infected cells is translation of the genome into a polyprotein, which is co- and post-translationally processed to produce the three structural proteins C, M, and E and seven nonstructural (NS) proteins. The order of these products in the polyprotein is NH₂-C-prM-E-NS1-NS2A-NS2B-NS3-NS4A-NS4B-NS5-COOH (Fig. 1), where prM is a precursor of M.

Following entry and fusion, nucleocapsids transit into the cytoplasm and associate with ribosomes to initiate translation. Once a small polypeptide is synthesized, the complex RNA-ribosomes-nascent protein docks at the rough endoplasmic reticulum (ER) through the membrane anchor signals in C protein, and then translation and processing of viral protein continues in association with the ER.

As indicated in Fig. 1, polyprotein processing is performed by the combined activity of cellular and viral proteases. With only one exception (the cleavage at the NS1-NS2A junction), all primary cleavages are performed either by a host-cell signal peptidase resident in the ER (cleavages at C-prM, prM-E, E-NS1, and NS4A-NS4B junctions) or by a viral serine protease composed of NS3 and NS2B (cleavages at NS2A-NS2B, NS2B-NS3, NS3-NS4A, and NS4B-NS5 junctions) (Chambers *et al.*, 1990). The cleavage at NS1-NS2A occurs soon after synthesis by an still unknown ER-resident host protease (Falgout and Markoff, 1995).

NS proteins are involved in different functions of the replicative cycle. NS1, NS3, and NS5 are the major NS proteins. NS1 is a glycoprotein peripherally associated with membranes, which forms homodimers apparently functional for virus replication. The colocalization of NS1 with double-stranded RNA and other evidences implicate NS1 in RNA replication (Mackenzie *et al.*, 1996), but its precise role in this process is unclear. Aside from its replicative function, NS1 is secreted from infected cells and is responsible for inducing a strong and protective immune response (Falgout *et al.*, 1990).

NS3 is a multifunctional polypeptide with several enzymatic activities related to polyprotein processing and RNA replication. The previously mentioned serine protease activity has been the most widely studied; the active form is a complex of NS3 and NS2B, with the catalytic residues contained in the N-terminal one-third of NS3 (Falgout *et al.*, 1991). In addition to the already mentioned cleavages at protein junctions in the polyprotein, the viral serine protease is also responsible of internal cleavages in C, NS2A, NS3, and NS4A, but the significance of this internal cleavage is presently unknown. The remaining part (2/3) of NS3 comprises an RNA triphosphatase, which may contribute to RNA capping (Wengler and Wengler, 1993), and RNA helicase and nucleoside triphosphatase (NTPase) activities (Cui *et al.*, 1998; Li *et al.*, 1999). The NTPase/helicase activity may separate nascent RNA strands from the template as well as unwind the secondary structures located at the UTR regions to initiate RNA synthesis, as suggested by the evidence of binding of NS3 to stem-loop structures at the 3'-UTR (Cui *et al.*, 1998).

NS5 is the most conserved flavivirus protein, with activity of RNA-dependent RNA polymerase located at its C-terminal domain and a methyltransferase motif in the N-terminal domain, probably involved in viral RNA capping (Koonin, 1993; Tan *et al.*, 1996).

NS2A, NS2B, NS4A, and NS4B are four small hydrophobic proteins that are associated to membranes. As described, NS2B and NS3 form the serine protease complex. The precise functions of NS2A, NS4A, and NS4B are unknown, but based on their cellular localization, NS2A and NS4A are proposed to be involved in RNA replication (Mackenzie *et al.*, 1998).

Following translation and processing of the viral proteins, most of the NS proteins associate to the 3'-UTR of viral RNA to form a replication complex (RC) for RNA synthesis (Lindenbach and Rice, 2001). RNA replication begins with the synthesis of a genome-length minus strand RNA to originate a double-stranded RNA or replicative form (RF). The minus strand RNA of the RF serves as a template for the synthesis of genomic plus strand RNA, which takes place in the form of a replicative intermediate (RI) consisting of multiple nascent plus strands growing on an individual minus strand. Thus, viral RNA synthesis is asymmetric, with a plus strand accumulation greater than that of minus strand (Lindenbach and Rice, 2001).

A unique feature typical of *Flavivirus* infected cells is the extensive proliferation and reorganization of rough and smooth cellular membranes in the perinuclear region, leading to the formation of subcellular membranes structures where the different processes of the multiplication cycle take place in a compartmentalized scheme. These specialized membranous structures are called convoluted membranes/paracrystalline arrays (CM/PC) and vesicle packets (VP) (Lindenbach and Rice, 2001). The cleavage of the polyprotein by cellular signal peptidase occurs in the ER lumen, while the remaining cleavages seem to be performed at the CM/PC, where the viral protease complex NS3/NS2B and NS4A colocalize (Westaway *et al.*, 1997). In contrast, the localization site of the RC for RNA replication is the VP, where the proteins NS1, NS3, NS5, NS2A, and NS4A as well as the RF are located, with the newly formed viral genomic RNAs oriented outward and the RF located inside the vesicles (Mackenzie *et al.*, 1999).

3. Assembly and Budding

Virion assembly begins with the association of the protein C with genomic RNA on the cytosolic face of the ER membrane. Electron microscopic studies have demonstrated that fully formed DENV virions appear within vesicles of the ER, suggesting that nucleocapsids

acquire the envelope by budding from the ER membrane into the lumen (Lindenbach and Rice, 2001). Later, particles are transported through the secretory pathway to the cell surface for release.

The DENV virion is first assembled as an immature particle that contains prM noncovalently associated with E in a heterodimeric complex. During virion egress through the exocytic pathway, glycan trimming and processing of E and prM takes place. These post-translational modifications are essential for the proper folding of glycoprotein and the secretion of mature virions. Finally, prM is cleaved by the Golgi enzyme furin to form the structural M protein and the pr peptide, which is secreted to the medium (Murray *et al.*, 1993; Stadler *et al.*, 1997). The apparent function of prM in the heterodimer is to stabilize the pH-sensitive epitopes on the E protein and protect the E protein from undergoing conformational changes during transport of virions through the acidic compartments in the exocytic pathway. After the late cleavage of prM, the pH-dependent fusion ability of E is activated while the E homodimers are formed in virus particles before their release from the cell.

VI. VIRAL INHIBITORS

There is no any specific antiviral therapy for DENV infections. Supportive medical care and symptomatic treatment through hydration are the most important aids to patients and to improve survival in the severe forms of disease. But, different classes of viral inhibitors have been studied for their antiviral properties, largely in cell culture systems due to the troubles with flavivirus animal models. The main classes of compounds reported active against DENV *in vitro* infection are presented in Table I.

A. In Vitro Studies

1. Inhibitors of Viral Binding and Entry

The blockade of virus binding is very valuable as an antiviral therapeutic strategy because it allows the establishment of a first barrier to suppress infection. In fact, the functional significance of the initial interaction of E protein and the target cell in DENV infectivity has been clearly indicated by reports demonstrating that soluble recombinant E protein was able to inhibit DENV-2 infection and plaque formation on mammalian cells (Chen *et al.*, 1996; Chiu and Yang, 2003).

TABLE I

IN VITRO ANTIVIRAL ACTIVITY OF VARIOUS CLASSES OF COMPOUNDS AGAINST DENV

Compound	DENV serotype
<u>Polyanionic substances</u>	
Heparin	DENV-2 ^a
Suramin	DENV-2 ^b
DL-galactan hybrids	DENV-2 ^c
λ -, μ/ν -, and κ/ι -carrageenans	DENV-2 ^d
Polyoxotugstates	DENV-2 ^e
<u>IMPDH inhibitors</u>	
Ribavirin	DENV-1, -2, -3, -4 ^f
Ribamidine analogues	DENV-4 ^g
Tiazofurin, selenazofurin, EICAR	DENV-2 ^h
Mycophenolic acid	DENV-2 ⁱ
VX-497	DENV-1 ^j
<u>OMP decarboxylase inhibitors</u>	
6-azauridine	DENV-1, -2, -4 ^k
<u>Interferons</u>	
Interferon α , β , or γ	DENV-1, -2, -4 ^l
<u>Antisense oligonucleotides</u>	
C-5 propyne substituted phosphorothioate oligonucleotides	DENV-2 ^m
<u>α-glucosidase inhibitors</u>	
Castanospermine, deoxynojirimycin	DENV-1 ⁿ
N-nonyl-deoxinojirimycin	DENV-2 ^o

^a Chen *et al.* (1997); Germi *et al.* (2002); Hung *et al.* (1999); Lin *et al.* (2002).^b Chen *et al.* (1997).^c Pujol *et al.* (2002).^d Damonte *et al.* (2002).^e Shigeta *et al.* (2003).^f Crance *et al.* (2003); Diamond *et al.* (2002); Koff *et al.* (1982); Markland *et al.* (2000).^g Gabrielsen *et al.* (1992).^h Leyssen *et al.* (2000).ⁱ Diamond *et al.* (2002); Leyssen *et al.* (2000)^j Markland *et al.* (2000).^k Crance *et al.* (2003).^l Crance *et al.* (2003); Diamond and Harris (2001).^m Raviprakash *et al.* (1995).ⁿ Courageot *et al.* (2000).^o Wu *et al.* (2002).

Since the finding of highly sulphated HS as a putative primary receptor for DENV, polyanionic compounds have turned attractive types of candidates into inhibitors of DENV infectivity targeted to interfere with the E–HS interaction. The effectiveness of heparin, a close structural homologue of HS, and the polysulfonate pharmaceutical suramin to competitively inhibit infection of Vero cells by DENV-2, as shown by reduction of viral-induced cytopathic effects, was precisely in support of the initial hypothesis of HS as DENV receptor (Chen *et al.*, 1997). In addition, these investigators determined that the minimum size structure of the polysulfate required to occupy the E protein binding site was a heparin-derived deca-saccharide, which was similar in potency to heparin with IC_{50} (inhibitory concentration 50%) values of $0.3 \mu\text{g/ml}$. A structure-activity relationship study carried out to examine the E-binding ability of different heparin-like polyanions, including small polyanions, GAGs, and persulfated GAGs, has confirmed the need of a minimum chain size equivalent to the heparin deca-saccharide as well as high-charge density and structural flexibility for optimal interaction between the polyanion and the E protein (Marks *et al.*, 2001). Taking account of this information may be helpful for the design of new DENV binding/entry inhibitors with maximum antiviral effectiveness.

Other investigators also confirmed the ability of heparin to prevent DENV-2 binding to Vero cells (Germi *et al.*, 2002) and BHK cells (Hung *et al.*, 1999). Data from Hung *et al.* (1999) indicated that blockade of interaction with HS not only affected binding but also DENV penetration and also showed for the first time the virucidal activity of heparin against DENV-2. Direct incubation of the virions with this drug resulted in inactivation of infectivity with still higher effectiveness than the blockade in virus binding because the concentration required to inactivate 50% virions was as low as $0.01 \mu\text{g/ml}$ (equivalent to 0.002 U/ml). This interesting property may make this type of compound useful as a disinfectant.

Whether HS is used by all four serotypes to bind to host cells has yet to be demonstrated. A differential susceptibility of DENV serotypes to heparin inhibition, however, has been shown: by virus yield reduction assay in BHK cells, DENV-2 was highly inhibited ($IC_{50} = 0.3\text{--}3 \mu\text{g/ml}$, according to viral strain) as previously reported for this serotype, but the suppression of heparin on DENV-1, DENV-3, and DENV-4 was much less significant (<50% reduction in virus yield up to $100 \mu\text{g/ml}$ heparin) (Lin *et al.*, 2002). At present, it is not known if this differential susceptibility is due either to a poor replication of serotypes 1, 3, and 4 in cultured cells or to a variation in receptor usage. DENV-2 is the better adapted virus to grow *in vitro*, and it is the routinely used viral serotype in most biologic, biochemical, and molecular studies. The certain chance of reinfection in

humans by different viral serotypes with the consequent severe clinical manifestations make the antiviral compound against DENV to be effective against the four serotypes mandatory.

Aside of heparinoids, the demonstration of anti-DENV activity was extended to other types of polyanions with very promising results. Sulfated polysaccharides extracted from sea algae have been reported as potent inhibitors of other HS-binding viruses, such as HSV, CMV, and HIV (reviewed in Witvrouw and de Clercq, 1997; Damonte *et al.*, 2004). The effective compounds included galactans, agarans, carrageenans, mannans, xylo-mannans, fucoidans, and fucans. Accordingly, diverse structural types of homogeneous algal polysaccharides were assayed and found effective to block DENV infection. A novel series of DL-galactan hybrids extracted from the red seaweed *Gymnogongrus torulosus* and the λ -carrageenan 1T1, the μ/ν -carrageenan 1C3, and the κ/ι -type 1C1, from the seaweed *Gigartina skottsbergii* inhibited the replication of DENV-2 in Vero cells at concentrations that were up to 5000-fold lower than the cytotoxic concentrations (Pujol *et al.*, 2002; Damonte *et al.*, 2002). The compounds had no detrimental effects on cell viability or growth in stationary or actively dividing cells. In addition, the lack of significant anticoagulant properties was another advantage shown by these DL-galactans and carrageenans when compared with heparin and its derivatives. The main target for antiviral activity of these natural polysaccharides was virus adsorption, as expected, but interestingly they also showed a variable level of direct inactivating effect on virions, with virucidal concentration 50% values of 4.5–17.5-fold exceeding the IC₅₀s obtained by plaque reduction assay. An additional hallmark is the fact that these selective antiviral polysulfates can be obtained from natural sources, the sea algae, and thus they can be prepared and made available in large quantities at low cost. To this point, it must be noticed that both homogeneous purified compounds as well as crude polysaccharide extracts are highly active and selective anti-DENV agents (Damonte *et al.*, unpublished results).

Polyoxometalates are inorganic polyanionic substances formed principally by an oxide anion and early transitional metal cations, such as tungsten, molybdenum, antimony, vanadium, and others. The ammonium 21-tungsto-9-antimoniate HPA-23 was one of the first compounds of this class showing a wide spectrum of activity against DNA and RNA viruses, including the flaviviruses DENV and Kunjin virus (Bartholomeusz *et al.*, 1994). Recently, polyoxotungstates substituted with vanadium or titanium were found to be inhibitors of DENV-2 multiplication in Vero cells at IC₅₀, ranging from 0.45 to 61.5 μ M

(Shigeta *et al.*, 2003). Although not proven, polyoxotungstates are suspected to mainly inhibit DENV binding.

Another class of molecules that may act as inhibitors of binding are lectins, which block specific sugar residues in the envelope glycoprotein involved in receptor interaction. The lectins concanavalin A (which binds to α -linked terminal mannose residues) and wheat germ agglutinin (which recognizes acetylglucosamine on N-linked glycans) were inhibitors of DENV-2 by blockade of the viral binding and penetration in BHK cells (Hung *et al.*, 1999). The soluble ectodomain of the lectin DC-SIGN, a putative receptor for DENV in dendritic cells, was also an inhibitor of virus infection (Navarro-Sanchez *et al.*, 2003).

Among probable early inhibitors of the replicative cycle of DENV, two of the initial compounds studied more than two decades ago as anti-DENV agents were amantadine hydrochloride and rimantadine hydrochloride, known as blockers of influenza virus uncoating. Both compounds were found to inhibit the multiplication of the four serotypes of DENV in monkey LLC-MK2 cells, and the growth of DENV-2 in human and monkey peripheral blood leukocytes was also significantly reduced in the presence of amantadine or rimantadine (Koff *et al.*, 1980, 1981). Maximal inhibition of DENV replication was observed when the drugs were added immediately after adsorption, confirming an effect on the early entry/uncoating process. However, no further studies about the efficacy of this type of drug against flaviviruses have been reported. More recent works with another type of *Flavivirus*, JEV, have introduced the use of pharmacological agents affecting the endocytic pathway as probable entry inhibitors. Chlorpromazine, a neuroleptic drug with wide clinical use and an ability to inhibit the clathrin-dependent endocytosis, affected productive JEV infection in Vero cells without decreasing cell viability (Nawa *et al.*, 2003).

An important finding in the recent work about the DENV E protein structure is the identification of a binding pocket that can accommodate a hydrophobic ligand, in particular the detergent β -N-octylglucoside added during crystallization bound to the pocket (Modis *et al.*, 2003). Mutations altering the pH of the E conformational change necessary to trigger membrane fusion map to this pocket. This opens new perspectives in the future search of DENV entry inhibitors because the pocket can be a potential site for small molecules, which inserted at that position, might inhibit the conformational change required for fusion and then block infection. This strategy may be similar to that of WIN anticoronavirus compounds interacting with

the canyon of the capsid to block the structural transition required for virus entry (McKinlay and Pevear, 1992).

2. *Inhibitors of Intracellular Virus Multiplication*

The attempts to find antiviral substances able to block the intracellular multiplication of DENV and flaviviruses in general have been mainly focused on the screening of probable inhibitors of cellular factors required for RNA synthesis, as has occurred for other RNA viruses. One of the most investigated compounds for anti-DENV antiviral effect is ribavirin. Ribavirin (1- β -D-ribofuranosyl-1,2,4-triazole-3-carboxamide) is a guanosine analogue with a broad spectrum of antiviral activity against RNA and DNA viruses. Three different mechanisms for the *in vitro* antiviral activity of ribavirin have been proposed. After phosphorylation to ribavirin 5'-monophosphate, the main interaction is a competitive inhibition of inosine monophosphate dehydrogenase (IMPDH); by blocking the conversion of IMP to xanthosine monophosphate (XMP), a precursor molecule in the biosynthesis of GTP and dGTP, ribavirin depleted the intracellular GTP pool (Streeter *et al.*, 1973). Ribavirin can also be phosphorylated to its 5'-triphosphate, and in this form, can affect either the initiation of viral mRNAs or the elongation of viral RNAs by competitive inhibition of mRNA-capping enzymes or viral polymerases, respectively (Gilbert and Knight, 1986; Goswami *et al.*, 1979). Another recently proposed mechanism of action for ribavirin is its action as a mutagen, pushing RNA viruses to a critically high mutation rate and driving the virus population into the called "error catastrophe" (Crotty *et al.*, 2000). The high error rate of RNA viruses due to the low fidelity of RNA polymerases has been proposed as an evolutionary advantage, but a small increase in the error rate, produced by ribavirin, may lead to a lethal loss of genome viability and virus infectivity. It was shown that the antipolio virus activity of ribavirin correlated with its mutagenic effect, supporting that the primary mode of the drug's action in this system may be "error catastrophe" (Crotty *et al.*, 2001). The multiple mechanisms of action of ribavirin also include *in vivo* indirect immune-mediated activities (Tam *et al.*, 2002).

Ribavirin has been used to treat human patients infected with respiratory syncytial virus (reviewed in Wyde, 1998) and the arenavirus Lassa virus (McCormick *et al.*, 1986). In combination with interferon α , ribavirin is also one of the current therapies approved for treatment of chronic or acute hepatitis C virus infections (Davis *et al.*, 1998; McHutchison *et al.*, 1998; Walker *et al.*, 2003). In contrast, the antiviral effect of ribavirin against DENV is very weak. Several

investigators have reported the inhibitory effect *in vitro* of ribavirin against the four serotypes of DENV in monkey kidney and human hepatoma cell lines, but a high concentration of the compound was required, and the selectivity was low in growing cells due to cytostatic action (Crance *et al.*, 2003; Markland *et al.*, 2000; Koff *et al.*, 1982; Diamond *et al.*, 2002). Similar results about a consistent but modest *in vitro* antiviral action of ribavirin was reported for other members of the genus *Flavivirus*, including the human pathogens YFV, JEV, and West Nile virus (WNV) (Crance *et al.*, 2003; Huggins *et al.*, 1984; Jordan *et al.*, 2000; Neyts *et al.*, 1996). The inhibitory effects were completely reversed by the addition of exogenous guanosine, indicating that the antiviral effect of ribavirin in *Flavivirus* infected cells was mainly exerted through competitive inhibition of IMPDH (Koff *et al.*, 1982; Neyts *et al.*, 1996; Diamond *et al.*, 2002).

Other competitive inhibitors of IMPDH were also assayed for antiviral effect on DENV, JEV, and YFV infection. The evaluated substances comprised compounds chemically related to ribavirin, such as analogues of its 3-carboxamide derivative ribamidine, thiazole C-nucleoside tiazofurin (2- β -D-ribofuranosyl-thiazole-4-carboxamide), selenium analogue selenazofurin (2- β -D-ribofuranosyl-selenazole-4-carboxamide), and the 5-ethynyl ribavirin analogue EICAR (5-ethynyl-1- β -D-ribofuranosyl-imidazole-4-carboxamide). Most of these compounds were found to be equally or more potent antiviral agents against flaviviruses than ribavirin, but they had a marked cytostatic effect (Gabrielsen *et al.*, 1992; Huggins *et al.*, 1984; Leyssen *et al.*, 2000; Neyts *et al.*, 1996).

The importance of IMPDH as a target for flavivirus therapy was confirmed through the evaluation of uncompetitive inhibitors of the enzyme: the phenyloxazole derivative VX-497 ((*S*)-*N*-3-[3-(3-methoxy-4-oxazol-5-yl-phenyl)-ureido]-benzyl-carbamic acid tetrahydrofuran-3-yl-ester) showed modest antiviral activity against DENV (Markland *et al.*, 2000), whereas mycophenolic acid was a very potent inhibitor of DENV, WNV, and YFV (Diamond *et al.*, 2002; Morrey *et al.*, 2002; Neyts *et al.*, 1996). MPA showed a 65-fold greater potency than ribavirin against DENV-2 in human hepatoma cell lines, with IC₅₀ values in the range of 0.3 to 1.9 μ M, and MPA also decreased the levels of virus production more than 6 log. Because the inhibitory effects of MPA are reversed by guanosine, its antiviral activity depends on its capacity to deplete intracellular guanosine levels by inhibition of IMPDH. A quantitative RT-PCR assay demonstrated that MPA abrogated *in vitro* DENV infection by preventing synthesis and accumulation of viral RNA (Diamond *et al.*, 2002). The morpholinoethylester of MPA, named Mofetil, has clinical use as an immunosuppressive agent to prevent the

rejection of transplanted organs (Lipsky, 1996). The high effectiveness of MPA to block *in vitro* DENV infection (linked to the low toxicity showed in humans by Mofetil) (Taylor *et al.*, 1994) turn this drug into a very attractive compound to treat human DENV infections. A serious drawback to the perspective of therapeutic trials with MPA or its derivatives, however, is given by the immunosuppressive potential of the drug linked to the immunopathogenesis of DHF syndrome.

Several classes of nucleoside analogues targeted to other enzymes in the nucleic acid metabolism have also been assayed as potential DENV inhibitors. Among tested compounds, orotidine monophosphatase (OMP) decarboxylase inhibitors were found the most active to block flavivirus multiplication. OMP decarboxylase is an essential enzyme in the pyrimidine metabolism for the conversion of OMP to UMP. The inhibitors of OMP decarboxylase pyrazofurin (3-(β -D-ribofuranosyl)-4-hydroxy-pyrazole-5-carboxamide) and 6-azauridine and derivatives were endowed with antiviral activity against DENV-1, DENV-2, DENV-4, YFV, JEV, WNV, and other flaviviruses, but they were also endowed with cytostatic activity (Neyts *et al.*, 1996; Morrey *et al.*, 2002; Crance *et al.*, 2003).

Among nonspecific inhibitors of viral replication, the interferon system represents the innate antiviral response provided by the host cell. Interferons α and β are secreted by virus-infected cells and exhibit antiproliferative, antiviral, and immunomodulatory properties. IFN- γ is secreted by activated T lymphocytes and NK cells and has antiviral activity directly through the induction of diverse molecules and indirectly through enhanced antigen presentation and the induction of apoptosis. The effects of the different types of interferons on *in vitro* DENV infection were studied. Recombinant interferon α was found to be a very selective inhibitor of DENV-1, DENV-2, and DENV-4 replication on Vero cells, with IC₅₀ values in the range of 10.6 to 16.9 UI/ml and selectivity indices greater than 500 in quiescent and growing cells (Crance *et al.*, 2003). Diamond *et al.* (2000) demonstrated that the infection of human cells, including hepatoma cells, primary fibroblasts, erythroleukemic cells, and myeloid cells, by DENV-2 was prevented by pretreatment of cells with interferon α or β . The protection was exerted on both antibody-independent and antibody-dependent pathways of human cell infection. Interferon γ had a more variable effect because it inhibited antibody-independent infection with lower efficacy than interferon α or β , but it had irrelevant inhibitory effect or enhanced antibody-dependent infection. These results are in agreement with the controversial role of interferon γ in pathogenesis of DENV infection proposed by different studies (Rothman and Ennis, 1999).

Several experimental approaches demonstrated that interferon β and γ prevented DENV infection by inhibiting the translation of the input strand of viral RNA, probably disrupting a step subsequent to the binding of ribosomes and the initiation of translation (Diamond and Harris, 2001). The mode of anti-DENV effect appeared independent of the interferon-induced protein kinase activated by double-stranded RNA (PKR) and would be a novel mechanism for interferon action. Previously, the only suggested mechanisms for the inhibition of the Flaviviridae members by interferon acted through the production of nitric oxide in JEV infection (Lin *et al.*, 1997) and PKR in HCV infection (Gale *et al.*, 1997). Due to the blockade of an early stage in DENV life cycle, interferon protection was restricted to *de novo* viral infection but could not impede an established infection (Diamond *et al.*, 2000). Interestingly, the effect of interferon on a superinfecting DENV of a different serotype was assessed: when DENV-2 infected cells were exposed to interferon and then superinfected with DENV-4, the replication of the superinfecting serotype was abolished (Diamond and Harris, 2001).

Given the higher efficacy of the combined therapy with interferon α and ribavirin for hepatitis C treatment in comparison to the monotherapy with either interferon α or ribavirin alone, the *in vitro* combination of these two drugs was considered for other members of Flaviviridae. The analysis of the combination of interferon α and ribavirin revealed synergistic interactions against YFV as well as the pestivirus bovine viral diarrhea virus (Buckwold *et al.*, 2003).

In the intracellular stage of DENV replicative cycle several targets related to RNA synthesis seem to be adequate for chemotherapeutic strategies (Section V.B.2). In recent years, the rationale design of drugs directed to those specific viral targets appears as an expanding approach to find specific antiviral compounds for any viral agent. These DENV targets include RNA-dependent RNA polymerase activity (in NS5) to prevent RNA strand elongation; putatives RNA triphosphatase activity (in NS3) and methyltransferase activity (in NS5) to prevent RNA capping; and RNA helicase-NTPase activity (in NS3) to prevent unwinding of RNA strands. In addition, conserved structures in the UTR regions of genomic RNA are probably involved in initiation and/or regulation of RNA synthesis.

An antiviral assay based on the measure of the RNA-dependent RNA polymerase activity from extracts of DENV infected cells has been developed and proposed to test the specific inhibitory activity on RNA synthesis of potential anti-*Flavivirus* agents (Bartholomeusz *et al.*, 1994). A molecular approach to screen for molecules that block

the intramolecular interaction between the putative domains of the RNA-dependent RNA polymerase of DENV NS5 as well as the intermolecular interaction between NS5 and the helicase NS3 has also been recently intended, reporting a modified yeast two-hybrid assay to quantify the strength interaction between two protein domains and the alteration in this interaction by specific inhibitors (Vasudevan *et al.*, 2001). On this line of rationale design of antiviral molecules, molecular modeling studies have lead to the synthesis of heterocycles as well as nucleoside and nucleotide analogues, directed toward the potential inhibition of the NTPase/helicase activities of other members of Flaviviridae, including West Nile virus (WNV), JEV, and HCV (Borowski *et al.*, 2002; Zhang *et al.*, 2003). These studies have shown that the ATPase and helicase activities of WNV and HCV seem to be uncoupled and thus may be modulated independently from each other by a mechanism operating on the level of the enzyme. In particular, the imidazo [4,5-d] pyridazine derivative HMC-HO4 was found to inhibit WNV replication in cell culture with similar potency as the inhibition of the helicase activity of the viral enzyme (Borowski *et al.*, 2002). The selective inhibition of the unwinding activity of the NTPase/helicase of WNV is an initial finding for the development of a specific chemotherapeutic strategy for flaviviruses. Much research, however, is still needed to generate enough information and be able to design drugs specifically targeted to the different motifs of viral enzymes involved in RNA synthesis.

The serine protease domain of NS3 protein is also believed to be a main target for antiviral therapy, given its central role in the replicative cycle to produce the individual viral polypeptides. The protease of DENV has been cloned and expressed, and site-directed mutagenesis has been used to study the residues in the catalytic site (Valle and Falgout, 1998), a starting point to design peptidomimetics to block the enzyme. No studies about inhibitors targeted to DENV protease, however, have been reported.

Another selective antiviral approach based on gene targeting through short oligonucleotides has received increasing attention in the last years. Antisense oligonucleotides are generally considered as inhibitors of viral mRNA translation because of their ability to form duplexes with complementary sequences of the viral mRNA. For DENV, the duplex is directly formed with the input viral genome. This strategy was assayed against DENV-2 infection of LLCMK/2 cells by microinjection of three-classes of antisense oligonucleotides targeted to five different regions along DENV-2 genome (Raviprakash *et al.*, 1995). Unmodified phosphodiester oligonucleotides as well as the corresponding phosphorothioate

oligonucleotides, in which an oxygen atom in the phosphodiester linkage is replaced by a sulfur atom, were found ineffective to inhibit DENV-2 replication. These results are in accordance with the negative results reported by Tolou *et al.* (1996) for phosphorothioate oligonucleotides targeted to different regions of the DENV genome. By contrast, novel modified phosphorothioate oligonucleotides with the C-5 of uridines and cytidines replaced by propynyl groups caused a significant viral inhibition. Among the five target regions tested along the DENV genome, antisense oligonucleotide directed against the 5'-sequence spanning the translation initiation region of the viral genome was the most effective inhibitor, followed by the antisense oligonucleotide directed against a target in the 3'-UTR (Raviprakash *et al.*, 1995). Many features of antisense oligonucleotide technology concerning the optimization of bioavailability, cellular permeation or delivery system, intracellular stability to nuclease degradation, and specific and greater affinity for the target sequence still remain to be addressed, however.

3. Maturation Inhibitors

The post-translational glycosylation processing of viral glycoproteins has been pursued as a target for chemotherapeutic intervention in enveloped viruses (Mehta *et al.*, 1998). During the synthesis of N-linked glycoproteins, the oligosaccharide core Glc₃Man₉GlcNAc₂ added to the growing polypeptide in the ER is then modified by enzymes in the ER and the Golgi to originate the high mannose and complex structures found in glycoproteins. The processing events involve the sequential trimming of the glucose residues on the precursor by two enzymes: α -glucosidase I removes the terminal glucose, and α -glucosidase II removes the remaining glucoses. Several iminosugar derivatives are inhibitors of α -glucosidases, preventing the glucose trimming, and have been reported to have antiviral effects on DENV. Castanospermine (CST) and deoxynojirimycin (DNJ) reduced the production of infective particles of DENV-1 in neuroblastoma cells in a dose-dependent manner without affecting cell integrity (Courageot *et al.*, 2000). The inhibition of glucose trimming affected the correct folding of glycoproteins prM and E without preventing the heterodimeric association, but the complexes prM-E appeared to be unstable, leading to a blockade in particle assembly and a nonproductive infection. The iminosugar *N*-nonyl-DNJ (NN-DNJ), a 9-carbon alkyl derivative of DNJ, was also found to suppress the multiplication of DENV-2 in BHK cells due to an interference in the interaction of the untrimmed glycoproteins with the ER chaperone Calnexin (Wu *et al.*, 2002).

Based on the differential susceptibility and selectivity shown by enveloped viruses to glucosidase inhibitors, it has been proposed that viruses acquiring their lipid envelopes and glycoproteins from intracellular membranes, such as ER and Golgi, may be extremely dependent on the ER glucosidases (Block and Jordan, 2002). As shown, the morphogenesis and release of viruses like DENV from infected cells are prevented with concentrations of glucosidase inhibitors having little or no toxicity to the cell, indicating a major effect of inhibitors on viral glycoprotein secretion with respect to host-cell glycoproteins. In addition, in a mouse model of lethal challenge by infection with JEV, oral delivery of NN-DNJ at a dose of 200 mg/kg/day increased the survival rate to 47% compared to 7% for the untreated group (Wu *et al.*, 2002), opening good perspectives for this type of compound.

4. Other Miscellaneous Inhibitors

A new potential pharmacological target for the control of *Flavivirus* infection is the inhibition of virus replication through the prevention of virus-associated apoptosis of infected cells. DENV has been shown to induce infected cells to undergo apoptotic cell death, one of the mechanisms responsible for the severe cytopathic effects induced by DENV in some infected cells (Avirutnan *et al.*, 1998; Despres *et al.*, 1998). Liao *et al.* (2001) demonstrated that aspirin and its metabolite sodium salicylate, a commonly prescribed drug with wide pharmacological activities, at 1–5 mM concentrations compatible with the amount in the sera of patients undergoing anti-inflammatory therapy, specifically inhibited JEV and DENV-2 replication as well as virus induced apoptosis in infected BHK cells. The mechanism by which salicylates suppress flavivirus infection seems to involve a specific p38 mitogen-activated protein (MAP) kinase inhibitor. This *in vitro* result is not easily transferred to the *in vivo* situation because it is known that salicylates exert a notorious antiplatelet function originating an increase in bleeding time, a collateral effect totally contraindicated for DHF or DSS patients. Aside from these considerations, this study has identified an interesting point to combat DENV infections.

The search for compounds with antiviral activity against flaviviruses in natural sources has not been limited to the mentioned sulfated polysaccharides extracted from seaweed. Screening studies about the antiviral effect on DENV of several natural products have increased in recent years with positive results. Aqueous extracts of neem (*Azadirachta indica* Juss) leaves, traditionally used as curative against certain fungal and bacterial diseases, exhibited a protective effect against the infection of C6/36 cells with DENV-2 in

a dose-dependent manner, probably through inhibition of an early stage of virus replication (Parida *et al.*, 2002). Antiviral activity against DENV was also exhibited by chemically characterized plant and marine products of diverse structure: two metabolites named gymnochrome D and isogymnochrome D isolated from the marine invertebrate crinoid *Gymnocrinus richeri* exerted a dose-dependent inhibitory effect *in vitro* on DENV-1 (Laille *et al.*, 1998); the flavonoids glabranine and 7-O-methyl-glabranine isolated from the Mexican plants *Tephrosia* sp were highly potent anti-DENV-2 compounds (Sánchez *et al.*, 2000), and the essential oils extracted from the aromatic plants *Artemisia douglasiana* and *Eupatorium patens* of Argentina displayed virucidal activity against suspensions of DENV-2 (García *et al.*, 2003). The precise mode of action of these compounds is not yet fully elucidated, but the results obtained in these few studies indicate good perspectives for products of natural origin that are nontoxic and inexpensive to treat millions of people suffering from DENV diseases worldwide, particularly in Third World countries.

B. In Vivo Systems

The limitations of the available animal models of DENV infection have restricted the adequate *in vivo* evaluation of compounds with *in vitro* proved antiviral activity. Primates can be infected with DENV and develop a measurable viremia after inoculation, but they do not develop the disease signs that occur in humans. In addition, the cost and the restricted availability of these animals strongly limit their use for antiviral trials. Rodents are effectively infected only by intracerebral inoculation, causing encephalitis, which is not a feature of the human disease. Peripheral inoculation of immunocompetent or severe combined immunodeficient (SCID) mice with DENV does not cause disease.

As a consequence, at present there are no very exciting reports of compounds exhibiting effective antiviral action *in vivo*. The efficacy of ribavirin against DENV infection could not be demonstrated in animal experimental infections. Prophylactic treatment of rhesus monkeys infected with DENV-1 had no significant effect on the level and duration of viremia (Malinoski *et al.*, 1990). In BALB/c mice, the intraperitoneal administration of ribavirin had no effect on the survival of animals intracerebrally inoculated with DENV-2, but intraperitoneal treatment with ribavirin 2',3',5'-triacetate, a lipophilic analogue of ribavirin, caused a significant increase in survival time and rate (Koff *et al.*, 1983). Ribavirin was also not effective in the course

of YFV infection in monkeys (Huggins, 1989). In contrast, interferon and interferon inducers were found active in experimental infections with several flaviviruses, including YFV infection in monkeys (Stephen *et al.*, 1977), St. Louis encephalitis virus infection in mice (Brooks and Phillpotts, 1999), JEV infection in mice and hamsters (Taylor *et al.*, 1980), and Modoc virus infection in mice (Leyssen *et al.*, 2003). Although a very effective inhibition against DENV *in vitro* infection is exerted by interferon, the use of interferon and interferon inducers is a point of discussion, as the pathogenesis of DENV-induced disease, particularly DHF and DSS, is not totally elucidated (Rothman and Ennis, 1999).

Several attempts were made to establish a small murine model for DENV infection by peripheral inoculation; the presently reported DENV animal models consist of:

- SCID mice reconstituted with human peripheral blood lymphocytes (hu-PBL-SCID mice); after intraperitoneal infection with DENV-1, only some of these mice showed sensitivity to DENV-1 (Wu *et al.*, 1995).
- SCID mice engrafted with human erythroleukemia K562 cells (K562-SCID mice); infection of the abdominal mass tumor with DENV-1 to DENV-4 serotypes produced neurological signs of paralysis and variable levels of mortality rates (Lin *et al.*, 1998)
- SCID mice transplanted with the human hepatocarcinoma HepG2 cells; after infection with DENV-2, the animals showed some clinical, haematological, histopathological, and virological similarities to human DENV infection (An *et al.*, 1999).
- Mice lacking the interferon α/β and interferon γ receptor genes (AG129 mice); the intraperitoneal administration of DENV-2 produced disease, virus replication, and death (Johnson and Roehrig, 1999).

There are still no reports about the evaluation of probable anti-DENV agents in any of these murine models, probably due to the complexity of their management.

Another alternative proposal is the use of the virus Modoc (MODV) as a surrogate system to evaluate antiviral strategies against human flaviviruses. MODV is a murine virus belonging to the nonvector cluster of the genus *Flavivirus*, with sequence similarity to arthropod-borne flaviviruses. Models of infection with MODV have been described in SCID mice and hamsters by peripheral routes, inducing encephalitis and mortality (Leyssen *et al.*, 2001). The final testing of the antiviral compound in an animal model with the human virus DENV cannot be avoided.

VII. STRATEGIES FOR VACCINE DEVELOPMENT

Several promising vaccine candidates are currently in human clinical trials, but up to date, there are no commercial vaccines available for dengue. Although there have been many efforts over the last six decades to produce a vaccine, progress has been slow. One of the reasons for this delay is the already mentioned lack of good animal models to study DF and DHF. Thus, the development of safe and potent vaccines still represents a challenge for the coming years (reviewed in Cardoso, 1998; Jacobs and Young, 2003; Pugachev *et al.*, 2003; Pang, 2003).

Recent studies about the immune response elicited by DENV pointed out the importance of the immune system in the control of infection but also its probable involvement in pathogenesis, as seen previously (Morens, 1994). Hence, vaccines should induce well-balanced immune responses with the production of specific antibodies against the virus as well as encourage cellular immunity; vaccines should avoid undesirable effects that are associated with such immune responses (Baize *et al.*, 2001). Any reliable dengue vaccine must provide complete protection against not just one but all four serotypes (Guzman, 1998). Immunity acquired from natural infection is specific for each serotype, and as many as three different serotype infections have been reported in one individual. For this reason, a tetravalent vaccine may likely be needed (Kinney and Huang, 2001; Lopez Antunano and Mota, 2000).

Different strategies for the development of dengue vaccines include live attenuated and inactivated viruses, recombinant subunits, protein expression in *Escherichia coli*, recombinant baculoviruses, recombinant poxviruses, chimeric viruses derived from infectious cDNA clones of DENV, and naked DNA vaccines.

Live attenuated vaccines were first tested in monkeys (Angsubhakorn, 1994; Halstead *et al.*, 1984; Marchette *et al.*, 1990). These vaccines stimulated the production of neutralizing antibodies and also conferred protection to the vaccinated animals against challenge with homologous and heterologous strains of DENV. Because of their safety and avirulence in monkeys, live vaccines were recommended for human trials. Although investigations into dengue vaccines have been supported by the WHO for the past 20 years, only in the late 20th and early 21st centuries were live attenuated vaccines tested in human volunteers (Dharakul *et al.*, 1994; Edelman *et al.*, 1994; Rothman *et al.*, 2001; Vaughn *et al.*, 1996). Currently, two tetravalent live attenuated vaccines developed in Thailand and the United States are in phase II clinical trials. The Thai project, initiated in 1976, was

originally developed at Mahidol University, Bangkok, and is licensed to Aventis Pasteur of Lyon, France (Bhamarapavati and Sutee, 2000; Sabchareon *et al.*, 2002). Safety and efficacy trials are ongoing and show that the vaccine is safe and protects up to 90% of recipients from all four serotypes. The second dengue tetravalent live attenuated vaccine was developed at the Walter Reed Army Institute of Research in Silver Spring, Maryland, and is licensed to Glaxo Smith Kline Biologicals in Rixensart, Belgium (Halstead and Deen, 2002). Both vaccines are based on living, weakened DENV, selected by growing all four serotypes in nonhuman tissue cultures (Alvarez *et al.*, 2001; Petriccioni, 1976). Initial results obtained in phase I and II trials have raised two major concerns: adverse reactions, although mild with monovalent vaccines, were more frequent and significantly more severe with a tetravalent vaccine, and when the tetravalent formulation was administered, neutralizing antibodies were predominantly directed against DENV-3. Other live attenuated candidate vaccines are being created in which virulence genes are deleted (Durbin *et al.*, 2001; Whitehead *et al.*, 2003). A low level of reactogenicity and a high degree of immunogenicity were observed in adult human volunteers.

On the other hand, an approach used to overcome the problem of safety and reversion to virulence of the attenuated vaccines is the use of killed vaccines. The infectious agent is inactivated using different methodology (chemical inactivation or radiation) so that it cannot replicate in the host, without altering the immunogenicity of the protective antigens (Putnak *et al.*, 1996). Experiments carried out with inactivated DENV-2 demonstrated that the virus retained its antigenicity and was immunogenic in mice and rhesus monkeys, eliciting high titers of DENV-2 neutralizing antibodies. Moreover, mice were completely protected against challenge with the virulent virus, and monkeys showed absence or a significant reduction in viremia after challenge with homologous virus. Some drawbacks of inactivated vaccines are that they are not very immunogenic, so they need to be combined with adjuvants to improve their efficacy, and also an incomplete inactivation may cause a field outbreak of the disease.

A different approach for protecting people who live in an endemic area of developing countries is using synthetic flavivirus peptides that may be introduced into human skin using a lotion containing peptides ("peplotion") and substances capable of enhancing the penetration to reach Langerhans cells (Becker, 1994). The peptide-treated Langerhans cells are able to migrate and induce the cellular immune response in the lymph nodes (Taweekhaisupapong *et al.*, 1996). In this way, the priming of CD8⁺ cytotoxic T cells may provide cellular immune

protection from infection without inducing the humoral immune response, which can lead to the shock syndrome in DF patients.

As mentioned, a rapid growth on molecular knowledge on flaviviruses has registered in the last decade. On the basis of this information, several potential recombinant subunit vaccines are being developed and appear to be effective experimentally (Konishi and Fujii, 2002; Simmons *et al.*, 2001; Venugopal and Gould, 1994). Various expression vectors are being used, including *E. coli* (Srivastava *et al.*, 1995), baculovirus (Chan *et al.*, 2002; Feighny *et al.*, 1994; Qu *et al.*, 1993; Velzing *et al.*, 1999), and vaccinia virus (Falgout *et al.*, 1990; Hahn *et al.*, 1990; Parrish *et al.*, 1991). Moderate levels of neutralizing antibodies and anamnestic response after challenge with DENV were achieved in mice and monkeys. Unfortunately, no satisfactory results have been obtained in humans.

Several studies are ongoing to develop dengue vaccines using antigens from structural proteins, particularly the E and the prM proteins as well as the nonstructural proteins NS1 and NS3, with recombinant DNA technology (Bray *et al.*, 1996; Butrapet *et al.*, 2002; Chen *et al.*, 1995; Huang *et al.*, 1999, 2000). In this respect, the YFV 17D vaccine has been used as a backbone to generate chimeric viruses into which prM and E genes of the four DENV serotypes could be inserted (Caufour *et al.*, 2001; Chambers *et al.*, 2003; Guirakhoo *et al.*, 2002; van der Most *et al.*, 2000). The E protein of the chimeric virus contains protective antigens of DENV, while the remaining part of the viral genome remains YFV and is responsible for replication. The chimeric virus replicates inside cells at a rate similar to YFV 17D. The advantage of the approach is that strong immunity results only to the target DENV and not to YFV. High replication efficiency, genomic stability, attenuation phenotype, and induction of protective immunity in mice and monkeys suggest that this approach may result in safer, live-attenuated, controlled vaccines. The Chimerivax platform (developed by Acambis of Cambridge, UK) has been used to construct chimeric JEV and DENV that are in different phases of development. (Barrett, 2001; Monath *et al.*, 2002). Although attenuated live virus vaccines are promising, more study is needed.

Another type of dengue vaccine to enter clinical trials was developed using what is known as naked DNA technology (Chang *et al.*, 2001; Kochel *et al.*, 2000; Konishi *et al.*, 2000; Putnak *et al.*, 2003; Raviprakash *et al.*, 2001). This vaccine differs from attenuated vaccines in that it does not introduce the virus into the host body but only introduces its DNA. Vaccination with naked DNA mimics the immune response following natural infection, with the induction of virus neutralizing antibodies and MHC class I and II restricted cell-mediated immune responses.

Recently, a gene shuffling (Molecular Breeding) approach developed by MaxyGen is being explored under a collaborative development agreement for producing a tetravalent dengue DNA vaccine using a single plasmid construct (Stemmer, 2002).

Strategies for optimizing the DNA vaccines include the testing of different delivery devices that may augment the immune response (Peachman *et al.*, 2003; Trimble *et al.*, 2003). Animals vaccinated with the Biojector device, which delivers DNA more efficiently to dendritic skin cells, tended to maintain higher antibody levels than those vaccinated with needle and syringe. The gene gun was also evaluated in rhesus macaques for the delivery of smaller doses of DNA (1–2 μg), resulting in the induction of low-titered neutralizing antibodies and complete to partial protection. It was suggested that low antibody titers following three inoculations might indicate an important role for T cell immunity in protection with the DNA vaccines. The potential advantages of DNA vaccines are that infectious viruses do not need to be used, the vaccines are easy to produce, and they are relatively stable. There is a safeguard in that the vaccine cannot revert in the host body, causing a full-blown infection. However, the naked DNA vaccine is not yet robust and may not provide sufficient immunity. Other concerns include risk of damage to human chromosomes, resulting in cancer, as well as risk of an anti-DNA response, resulting in autoimmune disorders.

In November 2002, a meeting of the Task Force on Clinical Trials of Dengue Vaccines, which was part of the Initiative for Vaccine Research (IVR) and was cosponsored by the Pediatric Dengue Vaccine Initiative (PDVI), provided recommendations and guidance in the areas of vaccine development and testing. Some recommendations were (i) establishing banks for vaccine testing reagents; (ii) supporting development of better correlates of protection, animal models (e.g., primate testing), and the human challenge model; (iii) promoting more studies in the area of immune correlates of protection (e.g., T cell responses and antibody responses after vaccination and natural infection); (iv) providing standard reagents (sera and viruses) for measuring antibodies against dengue and RNA standards for measuring flavivirus burden by PCR methods; and (v) establishing standards for tetravalent dengue vaccines as well as setting up vaccine working groups (WHO, 2003). In the same way, the WHO proposed a set of guidelines for the production and quality control of live attenuated dengue vaccine (LAV) candidates. These guidelines should cover all LAV made by classical and molecular approaches, including virus characterization (e.g., sequence, attenuation markers) for master and production seeds,

permissible residual levels of cellular DNA for vaccines produced in certified Vero cells, and the stability (e.g., thermostability) of vaccine products (WHO, 2002, 2003).

VIII. CONCLUDING REMARKS

Even though the global incidence of DF and DHF occurring in the last decades has increased these diseases still remain largely neglected in that there are no specific vaccines or chemotherapy regimens for their prevention and treatment. The fact that most of the millions of people infected regimens with DENV-associated diseases inhabit Third-World countries is certainly a reason for addressing the neglect. However, scientists are starting to remedy this problem, and research is being devoted to improving the knowledge of the structural characteristics of virion components as well as the intimate mechanisms of the DENV replication cycle, which is key information for chemotherapeutic intervention. As reviewed in this chapter, the life cycle of DENV presents a series of stages representing potential targets for antiviral drug discovery. The *in vitro* screening of diverse classes of compounds allowed the identification of effective inhibitors of the initial viral binding and entry, the intracellular processes of translation, transcription and genome replication, and the late steps of virion maturation. Furthermore, data on the crystal structure of virion E glycoprotein and the active domains of *Flavivirus* crucial enzymes such as protease, RNA polymerase, and helicase, are starting to be obtained and will allow the rationale design of drugs to block these biomolecules. Intensive research has also been focused on the design of chimeric viruses or naked DNA to obtain a safe vaccine that will protect against the four serotypes of DENV. In addition, new small animal models have been developed to overcome the current limitations for the *in vivo* testing of promising *in vitro* DENV inhibitors or candidate vaccines. Altogether, these different approaches seem to guarantee a better future perspective to combat infections with DENV and members of *Flavivirus* in general.

ACKNOWLEDGMENTS

Research in the authors' laboratory was supported by Agencia Nacional de Promoción Científica y Tecnológica (ANPCyT) and the University of Buenos Aires, Argentina.

REFERENCES

- Alvarez, M., Guzman, M. G., Pupo, M., Morier, L., Bravo, J., and Rodriguez, R. (2001). Study of biologic attributes of Cuban dengue 2 virus after serial passage in primary dog kidney cells. *Int. J. Infect. Dis.* **5**:35–39.
- An, J., Kimura-Kuroda, J., Hirabayashi, Y., and Yasui, K. (1999). Development of a novel mouse model for dengue virus infection. *Virology* **263**:70–77.
- Anderson, R., King, A. D., and Innis, B. L. (1992). Correlation of E protein binding with cell susceptibility to dengue 4 virus infection. *J. Gen. Virol.* **73**:2155–2159.
- Angsubhakorn, S., Yoksan, S., Pradermwong, A., Nitatpattana, N., Sahaphong, S., and Bhamarapravati, N. (1994). Dengue-3 (16562) PGMK 33 vaccine: Neurovirulence, viremia, and immune responses in *Macaca fascicularis*. *Southeast Asian J. Trop. Med. Public Health* **25**:554–559.
- Avirutnan, P., Malasit, P., Seliger, B., Bhakdi, S., and Husmann, M. (1998). Dengue virus infection of human endothelial cells leads to chemokine production, complement activation, and apoptosis. *J. Immunol.* **161**:6338–6346.
- Baize, S., Marianneau, P., Georges-Courbot, M. C., and Deubel, V. (2001). Recent advances in vaccines against viral haemorrhagic fevers. *Curr. Opin. Infect. Dis.* **14**:513–518.
- Barrett, A. D. (2001). Current status of *Flavivirus* vaccines. *Ann. N. Y. Acad. Sci.* **951**:262–271.
- Bartholomeusz, A., Tomlinson, E., Wright, P. J., Birch, C., Locarnini, S., Weigold, H., Marcuccio, S., and Holan, G. (1994). Use of a *Flavivirus* RNA-dependent RNA polymerase assay to investigate the antiviral activity of selected compounds. *Antivir. Res.* **24**:341–350.
- Becker, Y. (1994). Dengue fever virus and Japanese encephalitis virus synthetic peptides, with motifs to fit HLA class I haplotypes prevalent in human populations in endemic regions, can be used for application to skin Langerhans cells to prime antiviral CD8⁺ cytotoxic T cells (CTLs)—A novel approach to the protection of humans. *Virus Genes.* **9**:33–45.
- Bhamarapravati, N., and Sutee, Y. (2000). Live attenuated tetravalent dengue vaccine. *Vaccine* **18**:44–47.
- Bielefeldt-Ohmann, H. (1997). Pathogenesis of dengue virus diseases: Missing pieces in the jigsaw. *Trends Microbiol.* **5**:409–413.
- Bielefeldt-Ohmann, H. (1998). Analysis of antibody-independent binding of dengue viruses and dengue virus envelope protein to human myelomonocytic cells and B lymphocytes. *Virus Res.* **57**:63–79.
- Bielefeldt-Ohmann, H., Meyer, M., Fitzpatrick, D. R., and Mackenzie, J. S. (2001). Dengue virus binding to human leukocyte cell lines: Receptor usage differs between cell types and virus strains. *Virus Res.* **73**:81–89.
- Block, T. M., and Jordan, R. (2002). Iminosugars as possible broad spectrum antihepatitis virus agents: The glucovirs and alkovirs. *Antiviral Chem. Chemother.* **12**:317–325.
- Borowski, P., Lang, M., Haag, A., Schmitz, H., Choe, J., Chen, H. M., and Hosmane, R. S. (2002). Characterization of imidazo [4,5]-pyridazine nucleosides as modulators of unwinding reaction mediated by West Nile virus nucleoside triphosphatase/helicase: Evidence for activity on the level of substrate and/or enzyme. *Antimicrob. Agents Chemother.* **46**:1231–1239.
- Bray, M., Men, R., and Lai, C. J. (1996). Monkeys immunized with intertypic chimeric dengue viruses are protected against wild-type virus challenge. *J. Virol.* **70**:4162–4166.

- Brooks, T. J. G., and Phillpotts, R. J. (1999). Interferon- α protects mice against lethal infection with St. Louis encephalitis virus delivered by the aerosol and subcutaneous routes. *Antivir. Res.* **41**:57–64.
- Buckwold, V. E., Wei, J., Wenzel-Mathers, M., and Russell, J. (2003). Synergistic *in vitro* interactions between alpha interferon and ribavirin against bovine viral diarrhea virus and yellow fever virus as surrogate models of hepatitis C virus replication. *Antimicrob. Agents Chemother.* **47**:2293–2298.
- Butrapet, S., Rabablt, J., Angsubhakorn, S., Wiriyarat, W., Huang, C., Kinney, R., Punyim, S., and Bhamarapavati, N. (2002). Chimeric dengue type 2/type 1 viruses induce immune responses in cynomolgus monkeys. *Southeast Asian J. Trop. Med. Public Health* **33**:589–599.
- Cahour, A., Pletnev, A., Vazielle, F. M., Rosen, L., and Lai, C. J. (1995). Growth-restricted plaque virus mutants containing deletions in the 5'-noncoding region of the RNA genome. *Virology* **207**:68–76.
- Calisher, C. H. (1988). Antigenic classification and taxonomy of flaviviruses (family Flaviviridae) emphasizing a universal system for the taxonomy of viruses causing tick-borne encephalitis. *Acta Virol.* **32**:469–478.
- Calisher, C. H., Karabatsos, N., Dalrymple, J. M., Shope, R. E., Porterfield, J. S., Eastway, E. G., and Brandt, W. E. (1989). Antigenic relationships between flaviviruses as determined by cross-neutralization tests with polyclonal antisera. *J. Gen. Virol.* **70**:37–43.
- Cardosa, M. J. (1998). Dengue vaccine design: Issues and challenges. *Br. Med. Bull.* **54**:395–405.
- Caufour, P. S., Motta, M. C., Yamamura, A. M., Vazquez, S., Ferreira, I. I., Jabor, A. V., Bonaldo, M. C., Freire, M. S., and Galler, R. (2001). Construction, characterization, and immunogenicity of recombinant yellow fever 17D-dengue type 2 viruses. *Virus Res.* **79**:1–14.
- Chambers, T. J., Hahn, C. S., Galler, R., and Rice, C. M. (1990). *Flavivirus* genome organization, expression, and replication. *Annu. Rev. Microbiol.* **44**:649–668.
- Chambers, T. J., Liang, Y., Droll, D. A., Schlesinger, J. J., Davidson, A. D., Wright, P. J., and Jiang, X. (2003). Yellow fever virus/dengue-2 virus and yellow fever virus/dengue-4 virus chimeras: Biological characterization, immunogenicity, and protection against dengue encephalitis in the mouse model. *J. Virol.* **77**:3655–3668.
- Chan, L. C., Young, P. R., Bletchly, C., and Reid, S. (2002). Production of the baculovirus-expressed dengue virus glycoprotein NS1 can be improved dramatically with optimised regimes for fed-batch cultures and the addition of the insect moulting hormone, 20-Hydroxyecdysone. *J. Virol. Methods* **105**:87–98.
- Chang, G. J., Davis, B. S., Hunt, A. R., Holmes, D. A., and Kuno, G. (2001). *Flavivirus* DNA vaccines: Current status and potential. *Annals N.Y. Acad. Sci.* **951**:272–285.
- Chen, W., Kawano, H., Men, R., Clark, D., and Lai, C. J. (1995). Construction of intertypic chimeric dengue viruses exhibiting type 3 antigenicity and neurovirulence for mice. *J. Virol.* **69**:5186–5190.
- Chen, Y., Maguire, T., Hileman, R. E., Fromm, J. R., Esko, J. D., Linhardt, R. J., and Marks, R. M. (1997). Dengue virus infectivity depends on envelope protein binding to target cell heparan sulfate. *Nature Medicine* **3**:866–871.
- Chen, Y., Maguire, T., and Marks, R. M. (1996). Demonstration of binding of dengue virus envelope protein to target cells. *J. Virol.* **70**:8765–8772.
- Chevillon, C., and Failloux, A. B. (2003). Questions on viral population biology to complete dengue puzzle. *Trends Microbiol.* **11**:415–421.

- Chiu, M. W., and Yang, Y. L. (2003). Blocking the dengue virus 2 infections on BHK-21 cells with purified recombinant dengue virus 2 E protein expressed in *Escherichia coli*. *Biochem. Biophys. Res. Commun.* **309**:672–678.
- Clarke, D. H., and Casals, J. (1965). Arboviruses; Group B. In “Viral and rickettsial infections of man” (F. L. Horsfall and I. Tamm, eds.). Lippincott, Philadelphia.
- Courageot, M. P., Frenkiel, M. P., Duarte Dos Santos, C., Deubel, V., and Despres, P. (2000). α -glucosidase inhibitors reduce dengue virus production by affecting the initial steps of virion morphogenesis in the endoplasmic reticulum. *J. Virol.* **74**:564–572.
- Crance, J. M., Scaramozzino, N., Jouan, A., and Garin, D. (2003). Interferon, ribavirin, 6-azauridine, and glycyrrhizin: Antiviral compounds active against pathogenic flaviviruses. *Antivir. Res.* **58**:73–79.
- Cribier, B., Schmitt, C., Kirn, A., and Stoll-Keller, F. (1998). Inhibition of hepatitis C virus adsorption to peripheral blood mononuclear cells by dextran sulfate. *Arch. Virol.* **143**:375–379.
- Crill, W. D., and Roehrig, J. T. (2001). Monoclonal antibodies that bind to domain III of dengue virus E glycoprotein are the most efficient blockers of virus adsorption to Vero cells. *J. Virol.* **75**:7769–7773.
- Crotty, S., Cameron, C. E., and Andino, R. (2001). RNA virus error catastrophe: Direct molecular test by using ribavirin. *Proc. Natl. Acad. Sci. USA* **98**:6895–6900.
- Crotty, S., Maag, D., Arnold, J. J., Zhong, W., Lau, J. Y. N., Hong, Z., Andino, R., and Cameron, C. E. (2000). The broad-spectrum antiviral ribonucleotide, ribavirin, is an RNA virus mutagen. *Nature Med.* **6**:1375–1379.
- Cui, T., Sugrue, R. J., Xu, Q., Lee, A. K., Chan, Y. C., and Fu, J. (1998). Recombinant dengue virus type 1 NS3 protein exhibits specific viral RNA binding and NTPase activity regulated by the NS5 protein. *Virology* **246**:409–417.
- Damonte, E. B., Matulewicz, M. C., and Cerezo, A. S. (2004, In press). Sulfated seaweed polysaccharides as antiviral agents. *Curr. Med. Chem.*
- Damonte, E. B., Pujol, C. A., Nocedal, M., Ciancia, M., Matulewicz, M. C., and Cerezo, A. S. (2002). Potent and selective inhibition of dengue virus by carrageenans. *Antivir. Res.* **53**:A49.
- Daughaday, C. C., Brandt, W. E., McCown, J. M., and Russell, P. K. (1981). Evidence for two mechanisms of dengue virus infection of adherent human monocytes: Trypsin-sensitive virus receptors and trypsin-resistant immune complex receptors. *Infect. Immun.* **32**:469–473.
- Davis, G. L., Esteban Mur, R., Rustgi, V., Hoefs, J., Gordon, S. C., Trepo, C., Shiffman, M. L., Zeuzem, S., Craxi, A., Ling, M. H., and Albrecht, J. (1998). Interferon alfa-2b alone or in combination with ribavirin for the treatment of relapse of chronic hepatitis C. International Hepatitis Interventional Therapy Group. *N. Engl. J. Med.* **339**:1493–1499.
- Deo, Y. M., Graciano, R. F., Repp, R., and van der Winkel, J. G. (1997). Clinical significance of IgG Fc receptors and Fc gamma R-directed immunotherapies. *Immunol. Today* **18**:127–135.
- Despres, P., Frenkiel, M. P., Ceccaldi, P. E., Duarte Dos Santos, C., and Deubel, V. (1998). Apoptosis in the mouse central nervous system in response to infection with mouse-neurovirulent dengue viruses. *J. Virol.* **72**:823–829.
- Dharakul, T., Kurane, I., Bhamarapravati, N., Yoksan, S., Vaughn, D. W., Hoke, C. H., and Ennis, F. A. (1994). Dengue virus-specific memory T cell responses in human volunteers receiving a live attenuated dengue virus type 2 candidate vaccine. *J. Infect. Dis.* **170**:27–33.

- Diamond, M. S., and Harris, E. (2001). Interferon inhibits dengue virus infection by preventing translation of viral RNA through a PKR-independent mechanism. *Virology* **289**:297–311.
- Diamond, M. S., Roberts, T., Edgil, D., Lu, B., Ernst, J., and Harris, E. (2000). Modulation of dengue virus infection in human cells by alpha, beta, and gamma interferons. *J. Virol.* **74**:4957–4966.
- Diamond, M. S., Zachariah, M., and Harris, E. (2002). Mycophenolic acid inhibits dengue virus infection by preventing replication of viral RNA. *Virology* **304**:211–221.
- Drake, J. W. (1993). Rates of spontaneous mutation among RNA viruses. *Proc. Natl. Acad. Sci. USA* **90**:4171–4175.
- Durbin, A. P., Karron, R. A., Sun, W., Vaughn, D. W., Reynolds, M. J., Perreault, J. R., Thumar, B., Men, R., Lai, C. J., Elkins, W. R., Chanock, R. M., Murphy, B. R., and Whitehead, S. S. (2001). Attenuation and immunogenicity in humans of a live dengue virus type-4 vaccine candidate with a 30 nucleotide deletion in its 3'-untranslated region. *Am. J. Trop. Med. Hyg.* **65**:405–413.
- Edelman, R., Tacket, C. O., Wasserman, S. S., Vaughn, D. W., Eckels, K. H., Dubois, D. R., Summers, P. L., and Hoke, C. H. (1994). A live attenuated dengue-1 vaccine candidate (45AZ5) passaged in primary dog kidney cell culture is attenuated and immunogenic for humans. *J. Infect. Dis.* **170**:1448–1455.
- Falgout, B., Bray, M., Schlessinger, J. J., and Lai, C. J. (1990). Immunization of mice with recombinant vaccinia virus expressing authentic dengue virus nonstructural protein NS1 protects against lethal dengue virus encephalitis. *J. Virol.* **64**:4356–4363.
- Falgout, B., and Markoff, L. (1995). Evidence that *Flavivirus* NS1-NS2A cleavage is mediated by a membrane-bound host protease in the endoplasmic reticulum. *J. Virol.* **69**:7232–7243.
- Falgout, B., Pethel, M., Zhang, Y. M., and Lai, C. J. (1991). Both nonstructural proteins NS2B and NS3 are required for the proteolytic processing of dengue virus nonstructural proteins. *J. Virol.* **65**:2034–2042.
- Feighny, R., Burrous, J., and Putnak, R. (1994). Dengue type-2 virus envelope protein made using recombinant baculovirus protects mice against virus challenge. *Am. J. Trop. Med. Hyg.* **50**:322–328.
- Gabrielsen, B., Phelan, M. J., Barthel-Rosa, L., See, C., Huggins, J. W., Kefauver, D. F., Monath, T. P., Ussery, M. A., Chmurny, G. N., Schubert, E. M., Upadhya, K., Kwong, C., Carter, D. A., Secrist, J. A., III, Kirsi, J. J., Shannon, W. M., Sidwell, R. W., Kini, G. D., and Robins, R. K. (1992). Synthesis and antiviral evaluation of N-carboxamidine-substituted analogues of 1 β -D-ribofuranosyl-1,2,4-triazole-3-carboxamidine hydrochloride. *J. Med. Chem.* **35**:3231–3238.
- Gale, M. J., Jr., Korth, M. J., Tang, N. M., Tan, S. L., Hopkins, D. A., Dever, T. E., Polyak, S. J., Gretch, D. R., and Katze, M. G. (1997). Evidence that hepatitis C virus resistance to interferon is mediated through repression of the PKR protein kinase by the nonstructural 5A protein. *Virology* **230**:217–227.
- García, C. C., Talarico, L. B., Almeida, N., Colombres, S., Duschatzky, C., and Damonte, E. B. (2003). Virucidal activity of essential oils from aromatic plants of San Luis, Argentina. *Phytother. Res.* **17**:1073–1075.
- Germi, R., Crance, J. M., Garin, D., Guimet, J., Lortat-Jacob, H., Ruigrok, R. W. H., Zarski, J. P., and Drouet, E. (2002). Heparan sulfate-mediated binding of infectious dengue virus type 2 and yellow fever virus. *Virology* **292**:162–168.
- Gilbert, B. E., and Knight, V. (1986). Biochemistry and clinical application of ribavirin. *Antimicrob. Agents Chemother.* **30**:201–205.

- Goswami, B. B., Borek, E., Sharma, O. K., Fujitaki, J., and Smith, R. A. (1979). The broad spectrum antiviral agent ribavirin inhibits capping of mRNA. *Biochem. Biophys. Res. Commun.* **89**:830–836.
- Gubler, D. J. (2002). Epidemic dengue/dengue hemorrhagic fever as a public health, social, and economic problem in the 21st century. *Trends Microbiol.* **10**:100–103.
- Gubler, D. J., and Meltzer, M. (1999). The impact of dengue/dengue hemorrhagic fever on the developing world. *Adv. Virus Res.* **53**:35–70.
- Gubler, D. J., and Trent, D. W. (1994). Emergence of epidemic dengue/dengue hemorrhagic fever as public health problem in the Americas. *Infect. Agents Dis.* **2**:383–393.
- Guirakhoo, F., Pugachev, K., Arroyo, J., Miller, C., Zhang, Z. X., Weltzin, R., Georgakopoulos, K., Catalan, J., Ocran, S., Draper, K., and Monath, T. P. (2002). Viremia and immunogenicity in nonhuman primates of a tetravalent yellow fever-dengue chimeric vaccine: Genetic reconstructions, dose adjustment, and antibody responses against wild-type dengue virus isolates. *Virology* **298**:146–159.
- Guzman, M. G. (1998). Advances in the development of a vaccine against dengue. *Acta Cient. Venez.* **49**:38–45.
- Hahn, Y. S., Lenches, E. M., Galler, R., Rice, C. M., Dalrymple, J., and Strauss, J. H. (1990). Expression of the structural proteins of dengue 2 virus and yellow fever virus by recombinant vaccinia viruses. *Arch. Virol.* **115**:251–65.
- Halstead, S. B. (1988). Pathogenesis of dengue: Challenges to molecular biology. *Science* **239**:476–481.
- Halstead, S. B., and Deen, J. (2002). The future of dengue vaccines. *Lancet* **360**:1243–1245.
- Halstead, S. B., Eckels, K. H., Putvatana, R., Larsen, L. K., and Marchette, N. J. (1984). Selection of attenuated dengue 4 viruses by serial passage in primary kidney cells. IV. Characterization of a vaccine candidate in fetal rhesus lung cells. *Am. J. Trop. Med. Hyg.* **33**:679–683.
- Hase, T., Summers, P. L., and Eckels, K. H. (1989). *Flavivirus* entry into cultured mosquito cells and human peripheral blood monocytes. *Arch. Virol.* **104**:129–143.
- Heinz, F. X., and Allison, S. L. (2001). The machinery for *Flavivirus* fusion with host cell membranes. *Curr. Opin. Microbiol.* **4**:450–455.
- Heinz, F. X., Auer, G., Stiasny, K., Holzmann, H., Mandl, C., Guirakhoo, F., and Kunz, C. (1994). The interactions of the *Flavivirus* envelope proteins: Implications for virus entry and release. *Arch. Virol.* **Suppl. 9**:339–348.
- Henchal, E. A., and Putnak, T. R. (1990). The dengue viruses. *Clin. Microbiol. Rev.* **4**:376–396.
- Hilgard, P., and Stockert, R. (2000). Heparan sulfate proteoglycans initiate dengue virus infection of hepatocytes. *Hepatology* **32**:1069–1077.
- Holmes, E. C., and Burch, S. (2000). The causes and consequences of genetic variation in dengue virus. *Trends Microbiol.* **8**:74–77.
- Huang, C. Y., Butrapet, S., Pierro, D. J., Chang, G. J., Hunt, A. R., Bhamarapravati, N., Gubler, D. J., and Kinney, R. M. (2000). Chimeric dengue type 2 (vaccine strain PDK-53)/dengue type 1 virus as a potential candidate dengue type 1 virus vaccine. *J. Virol.* **74**:3020–3028.
- Huang, J. H., Wey, J. J., Sun, Y. C., Chin, C., Chien, L. J., and Wu, Y. C. (1999). Antibody responses to an immunodominant nonstructural 1 synthetic peptide in patients with dengue fever and dengue hemorrhagic fever. *J. Med. Virol.* **57**:1–8.
- Huggins, J. W. (1989). Prospects for treatment of viral hemorrhagic fevers with ribavirin, a broad spectrum antiviral drug. *Rev. Infect. Dis.* **11Suppl. 4**: S750–761.

- Huggins, J. W., Robins, R. K., and Canonico, P. G. (1984). Synergistic antiviral effects of ribavirin and the C-nucleoside analogs tiazofurin and selenazofurin against togaviruses, bunyaviruses, and arenaviruses. *Antimicrob. Agents Chemother.* **26**:476–480.
- Hung, S. L., Lee, P. L., Chen, H. W., Chen, L. K., Kao, C. L., and King, C. C. (1999). Analysis of the steps involved in dengue virus entry into host cells. *Virology* **257**:156–167.
- Jacobs, M., and Young, P. (2003). Dengue vaccines: Preparing to roll back dengue. *Curr. Opin. Investig. Drugs* **4**:168–171.
- Johnson, A. J., Guirakhoo, F., and Roehrig, J. T. (1994). The envelope glycoproteins of dengue 1 and dengue 2 viruses grown in mosquito cells differ in their utilization of potential glycosylation sites. *Virology* **203**:241–249.
- Johnson, A. J., and Roehrig, J. T. (1999). New mouse model for dengue virus vaccine testing. *J. Virol.* **73**:783–786.
- Jordan, I., Briese, T., Fischer, N., Lau, J. Y.-N., and Lipkin, W. I. (2000). Ribavirin inhibits West Nile virus replication and cytopathic effect in neural cells. *J. Infect. Dis.* **182**:1214–1217.
- Kalayanarooj, S., Vaughn, D. W., Ninmannitya, S., Green, S., Suntayakorn, S., Kunen-trasai, N., Viramitrachai, W., Ratanachueke, S., Kiatpolpoj, S., Innis, B. L., Rothman, A. L., Nisalak, A., and Ennis, F. A. (1997). Early clinical and laboratory indicators of acute dengue illness. *J. Infect. Dis.* **176**:313–3121.
- Kautner, I., Robinson, M., and Kuhnle, U. (1997). Dengue virus infection: Epidemiology, pathogenesis, clinical presentation, diagnosis, and prevention. *J. Pediatr.* **131**:516–524.
- Kinney, R. M., and Huang, C. Y. (2001). Development of new vaccines against dengue fever and Japanese encephalitis. *Intervirology* **44**:176–197.
- Kliks, S. C., Nisalak, A., Brandt, W. E., Wahl, L., and Burke, D. S. (1989). Antibody-dependent enhancement of dengue virus growth in human monocytes as a risk factor for dengue hemorrhagic fever. *Am. J. Trop. Med. Hyg.* **40**:444–451.
- Kochel, T. J., Raviprakash, K., Hayes, C. G., Watts, D. M., Russell, K. L., Gozalo, A. S., Phillips, I. A., Ewing, D. F., Murphy, G. S., and Porter, K. R. (2000). A dengue virus serotype-1 DNA vaccine induces virus neutralizing antibodies and provides protection from viral challenge in Aotus monkeys. *Vaccine* **18**:3166–3173.
- Koff, W. C., Elm, J. L., Jr, and Halstead, S. B. (1980). Inhibition of dengue virus replication by amantadine hydrochloride. *Antimicrob. Agents Chemother.* **18**:125–129.
- Koff, W. C., Elm, J. L., Jr, and Halstead, S. B. (1981). Suppression of dengue virus replication *in vitro* by rimantadine hydrochloride. *Am. J. Trop. Med. Hyg.* **30**:184–189.
- Koff, W. C., Elm, J. L., Jr, and Halstead, S. B. (1982). Antiviral effects of ribavirin and 6-mercapto-9-tetrahydro-2-furylpyrimidine against dengue viruses *in vitro*. *Antivir. Res.* **2**:69–79.
- Koff, W. C., Pratt, R. D., Elm, J. L., Jr., Venkateshan, C. N., and Halstead, S. B. (1983). Treatment of intracranial dengue virus infections in mice with a lipophilic derivative of ribavirin. *Antimicrob. Agents Chemother.* **24**:134–136.
- Konishi, E., and Fujii, A. (2002). Dengue type 2 virus subviral extracellular particles produced by a stably transfected mammalian cell line and their evaluation for a subunit vaccine. *Vaccine* **20**:1058–1067.
- Konishi, E., Yamaoka, M., Kurane, I., and Mason, P. W. (2000). A DNA vaccine expressing dengue type 2 virus premembrane and envelope genes induces neutralizing antibody and memory B cells in mice. *Vaccine* **18**:1133–1139.

- Koonin, E. V. (1993). Computer-assisted identification of a putative methyltransferase domain in NS5 protein of flaviviruses and $\lambda 2$ protein of *Reovirus*. *J. Gen. Virol.* **74**:733–740.
- Kroschewski, H., Allison, S. L., Heinz, F. X., and Mandl, C. W. (2003). Role of heparan sulfate for attachment and entry of tick-borne encephalitis virus. *Virology* **308**:92–100.
- Kuhn, R. J., Zhang, W., Rossmann, M. G., Pletnev, S. V., Corver, J., Lenches, E., Jones, C. T., Mukhopadhyay, S., Chipman, P. R., Strauss, E. G., Baker, T. S., and Strauss, J. H. (2002). Structure of dengue virus: Implications for *Flavivirus* organization maturation, and fusion. *Cell* **108**:717–725.
- Kuno, G., Chang, G. J., Tsuchiya, K. R., Karabatsos, N., and Cropp, C. B. (1998). Phylogeny of the genus *Flavivirus*. *J. Virol.* **72**:73–83.
- Kurane, I., and Ennis, F. E. (1992). Immunity and immunopathology in dengue virus infections. *Semin. Immunol.* **4**:121–127.
- Kurane, I., and Ennis, F. A. (1994). Cytokines in dengue virus infections: Role of cytokines in the pathogenesis of dengue hemorrhagic fever. *Semin. Virol.* **5**:443–448.
- Laille, M., Gerald, F., and Debitus, C. (1998). *In vitro* antiviral activity on dengue virus of marine natural products. *Cell. Mol. Life Sci.* **54**:167–170.
- Lee, E., and Lobigs, M. (2000). Substitutions at the putative receptor-binding site of an encephalitic *Flavivirus* alter virulence and host-cell tropism and reveal a role for glycosaminoglycans in entry. *J. Virol.* **74**:8867–8875.
- Leitmeyer, K. C., Vaughn, D. W., Watts, D. M., Salas, R., Villalobos de Chacon, I., Ramos, C., and Rico-Hesse, R. (1999). Dengue virus structural differences that correlate with pathogenesis. *J. Virol.* **73**:4738–4747.
- Leysen, P., de Clercq, E., and Neyts, J. (2000). Perspectives for the treatment of infections with Flaviviridae. *Clin. Microbiol. Rev.* **13**:67–82.
- Leysen, P., Drosten, C., Paning, M., Charlier, N., Paeshuyse, J., de Clercq, E., and Neyts, J. (2003). Interferons, interferon inducers, and interferon-ribavirin in treatment of *Flavivirus*-induced encephalitis in mice. *Antimicrob. Agents Chemother.* **47**:777–782.
- Leysen, P., van Lommel, A., Drosten, C., Schmitz, H., De Clercq, E., and Neyts, J. (2001). A novel model for the study of the therapy of *Flavivirus* infections using the Modoc virus. *Virology* **279**:27–37.
- Li, H. T., Clum, S., You, S. H., Ebner, K. E., and Padmanabhan, R. (1999). The serine protease and RNA-stimulated nucleoside triphosphatase and RNA helicase functional domains of dengue virus type 2 NS3 converge within a region of 20 amino acids. *J. Virol.* **73**:3108–3116.
- Liao, C. L., Lin, Y. L., Wu, B. C., Tsao, C. H., Wang, M. C., Liu, C. I., Huang, Y. L., Chen, J. H., Wang, J. P., and Chen, L. K. (2001). Salicylates inhibit *Flavivirus* replication independently of blocking nuclear factor kappa B activation. *J. Virol.* **75**:7828–7839.
- Lim, H. Y., and Ng, M. L. (1999). A different mode of entry by dengue-2 neutralisation escape mutant virus. *Arch. Virol.* **144**:989–995.
- Lin, Y. L., Huang, Y. L., Ma, S. H., Yeh, C. T., Chiou, S. Y., Chen, L. K., and Liao, C. L. (1997). Inhibition of Japanese encephalitis virus infection by nitric oxide. Antiviral effect of nitric oxide on RNA virus replication. *J. Virol.* **71**:5227–5235.
- Lin, Y. L., Lei, H. Y., Lin, Y. S., Yeh, T. M., Chen, S. H., and Liu, H. S. (2002). Heparin inhibits dengue 2 virus infection of five human liver cell lines. *Antivir. Res.* **56**:93–96.
- Lin, Y. L., Liao, C. L., Chen, L. K., Yeh, C. T., Liu, C. I., Ma, S. H., Huang, Y. Y., Huang, Y. L., Kao, C. L., and King, C. C. (1998). Study of dengue virus infection in SCID mice engrafted with human K562 cells. *J. Virol.* **72**:9729–9737.

- Lindenbach, B. D., and Rice, C. M. (2001). Flaviviridae: The viruses and their replication. In "Fundamental virology" (D. M. Knipe and P. M. Howley, eds.). Lippincott Williams & Wilkins, Philadelphia.
- Lipsky, J. J. (1996). Mycophenolate mophetil. *Lancet* **348**:1357–1359.
- Littaua, R., Kurane, I., and Ennis, F. A. (1990). Human: IgG Fc receptor II mediates antibody-dependent enhancement of dengue virus infection. *J. Immunol.* **144**:3183–3186.
- Lopez Antunano, F. J., and Mota, J. (2000). Development of immunizing agents against dengue. *Rev. Panam. Salud Publica.* **7**:285–292.
- Mackenzie, J. M., Jones, M. K., and Westaway, E. G. (1999). Markers for trans-Golgi membranes and the intermediate compartment localize to induced membranes with distinct replication functions in *Flavivirus*-infected cells. *J. Virol.* **73**:9555–9567.
- Mackenzie, J. M., Jones, M. K., and Young, P. R. (1996). Immunolocalisation of the dengue virus nonstructural glycoprotein NS1 suggests a role in viral RNA replication. *Virology* **220**:232–240.
- Mackenzie, J. M., Khromykh, A. A., Jones, M. K., and Westaway, E. G. (1998). Subcellular localization and some biochemical properties of the *Flavivirus* Kunjin nonstructural proteins NS2A and NS4A. *Virology* **245**:203–215.
- Malinoski, F. J., Hasty, S. E., Ussery, M. A., and Dalrymple, J. M. (1990). Prophylactic ribavirin treatment of dengue type 1 infection in rhesus monkeys. *Antivir. Res.* **13**:139–150.
- Marchette, N. J., Dubois, D. R., Larsen, L. K., Summers, P. L., Kraiselburd, E. G., Gubler, D. J., and Eckels, K. H. (1990). Preparation of an attenuated dengue 4 (341750 Carib) virus vaccine. I. Pre-clinical studies. *Am. J. Trop. Med. Hyg.* **43**:212–218.
- Marianneau, P., Mégret, F., Olivier, R., Morens, D. M., and Deubel, V. (1996). Dengue 1 virus binding to human hepatoma HepG2 and simian Vero cell surfaces differs. *J. Gen. Virol.* **77**:2547–2554.
- Markland, W., McQuaid, T. J., Jain, J., and Kwong, A. D. (2000). Broad-spectrum antiviral activity of the IMP dehydrogenase inhibitor VX-497: A comparison with ribavirin and demonstration of antiviral additivity with alpha interferon. *Antimicrob. Agents Chemother.* **44**:859–866.
- Marks, R. M., Lu, H., Sundaresan, R., Toida, T., Suzuki, A., Imanari, T., Hernáiz, M. J., and Linhardt, R. J. (2001). Probing the interaction of dengue virus envelope protein with heparin: Assessment of glycosaminoglycan-derived inhibitors. *J. Med. Chem.* **44**:2178–2187.
- Martínez-Barragán, J. J., and del Angel, R. M. (2001). Identification of a putative coreceptor on Vero cells that participates in dengue 4 virus infection. *J. Virol.* **75**:7818–7827.
- McCormick, J. B., King, I. J., Webb, P. A., Scribner, C. L., Craven, R. B., Johnson, K. M., Elliott, L. H., and Belmont Williams, R. (1986). Lassa fever. Effective therapy with ribavirin. *N. Engl. J. Med.* **314**:20–26.
- McHutchison, J. G., Gordon, S. C., Schiff, E. R., Schiffman, M. L., Lee, W. M., Rustgi, V. K., Goodman, Z. D., Ling, M. H., Cort, S., and Albrecht, J. K. (1998). Interferon alfa-2b alone or in combination with ribavirin as initial treatment for chronic hepatitis C. *N. Engl. J. Med.* **339**:1485–1492.
- McKinlay, M. A., and Pevear, D. C. (1992). Treatment of the picornavirus common cold by inhibitors of viral uncoating and attachment. *Annu. Rev. Microbiol.* **46**:635–654.
- Mehta, A., Zitzmann, N., Rudd, P. M., Block, T. M., and Dwek, R. A. (1998). Alpha-Glucosidase inhibitors as potential broad-based antiviral agents. *FEBS Lett.* **430**:17–22.

- Modis, Y., Ogata, S., Clements, D., and Harrison, S. C. (2003). A ligand-binding pocket in the dengue virus envelope glycoprotein. *Proc. Natl. Acad. Sci. USA* **100**:6986–6991.
- Monath, T. P., McCarthy, K., Bedford, P., Johnson, C. T., Nichols, R., Yoksan, S., Marchesani, R., Knauber, M., Wells, K. H., Arroyo, J., and Guirakhoo, F. (2002). Clinical proof of principle for Chimeri Vax: Recombinant live, attenuated vaccines against *Flavivirus* infections. *Vaccine* **20**:1004–1018.
- Moreno-Altamirano, M. M. B., Sánchez-García, F. J., and Muñoz, M. L. (2002). Non Fc receptor-mediated infection of human macrophages by dengue virus serotype 2. *J. Gen. Virol.* **83**:1123–1130.
- Morens, D. M. (1994). Antibody-dependent enhancement of infection and the pathogenesis of viral disease. *Clin. Infect. Dis.* **19**:500–512.
- Morrey, J. D., Smeed, D. F., Sidwell, R. W., and Tseng, C. (2002). Identification of active antiviral compounds against a New York isolate of West Nile virus. *Antivir. Res.* **55**:107–116.
- Muñoz, M. L., Cisneros, A., Cruz, J., Das, P., Tovar, R., and Ortega, A. (1998). Putative dengue virus receptors from mosquito cells. *FEMS Microbiol. Lett.* **168**:251–258.
- Murray, J. M., Askov, J. G., and Wright, P. J. (1993). Processing of the dengue virus type 2 proteins prM and C-prM. *J. Gen. Virol.* **74**:175–182.
- Navarro-Sanchez, E., Altmeyer, R., Amara, A., Schwartz, O., Fieschi, F., Virelizier, J. L., Arenzana-Seisdedos, F., and Despres, P. (2003). Dendritic-cell-specific ICAM3-grabbing nonintegrin is essential for productive infection of human dendritic cells by mosquito-cell-derived dengue viruses. *EMBO Rep.* **4**:723–728.
- Nawa, M., Takasaki, T., Yamada, K. I., Kurane, I., and Akatsuka, T. (2003). Interference in Japanese encephalitis virus infection of Vero cells by a cationic amphiphilic drug, chlorpromazine. *J. Gen. Virol.* **84**:1737–1741.
- Neyts, J., Meerbach, A., McKenna, P., and de Clercq, E. (1996). Use of the yellow fever virus vaccine strain 17D for the study of strategies for the treatment of yellow fever virus infections. *Antivir. Res.* **30**:125–132.
- Pang, T. (2003). Vaccines for the prevention of neglected diseases-dengue fever. *Curr. Opin. Biotechnol.* **14**:332–336.
- Parida, M. M., Upadhyay, C., Pandya, G., and Jana, A. M. (2002). Inhibitory potential of neem (*Azadirachta indica* Juss) leaves on dengue virus type 2 replication. *J. Ethnopharmacol.* **79**:273–278.
- Parrish, C. R., Woo, W. S., and Wright, P. J. (1991). Expression of the NS1 gene of dengue virus type 2 using vaccinia virus. Dimerisation of the NS1 glycoprotein. *Arch. Virol.* **117**:279–286.
- Peachman, K. K., Rao, M., and Alving, C. R. (2003). Immunization with DNA through the skin. *Methods* **31**:232–242.
- Petricciani, J. C. (1976). Nonhuman primate diploid cells for vaccine production. *Dev. Biol. Stand.* **37**:21–25.
- Pugachev, K. V., Guirakhoo, F., Trent, D. W., and Monath, T. P. (2003). Traditional and novel approaches to *Flavivirus* vaccines. *Int. J. Parasitol.* **33**:567–582.
- Pujol, C. A., Estévez, J. M., Carlucci, M. J., Ciancia, M., Cerezo, A. S., and Damonte, E. B. (2002). Novel DL-galactan hybrids from the red seaweed *Gymnogongrus torulosus* are potent inhibitors of herpes simplex virus and dengue virus. *Antiviral Chem. Chemother.* **13**:83–89.
- Putnak, R., Barvir, D. A., Burrous, J. M., Dubois, D. R., D'Andrea, V. M., Hoke, C. H., Sadoff, J. C., and Eckels, K. H. (1996). Development of a purified, inactivated, dengue 2 virus vaccine prototype in Vero cells: Immunogenicity and protection in mice and rhesus monkeys. *J. Infect. Dis.* **174**:1176–1184.

- Putnak, R., Fuller, J., VanderZanden, L., Innis, B. L., and Vaughn, D. W. (2003). Vaccination of rhesus macaques against dengue 2 virus with a plasmid DNA vaccine encoding the viral premembrane and envelope genes. *Am. J. Trop. Med. Hyg.* **68**:469–476.
- Qu, X., Chen, W., Maguire, T., and Austin, F. (1993). Immunoreactivity and protective effects in mice of a recombinant dengue 2 Tonga virus NS1 protein produced in a baculovirus expression system. *J. Gen. Virol.* **74**:89–97.
- Ramos-Castañeda, J., Imbert, J. L., Barron, B. L., and Ramos, C. (1997). A 65-kDa trypsin sensible membrane cell protein as a possible receptor for dengue virus in cultured neuroblastoma cells. *J. Neurovirol.* **3**:435–440.
- Randolph, V. B., and Stollar, V. (1990). Low pH-induced cell fusion in *Flavivirus*-infected *Aedes albopictus* cell cultures. *J. Gen. Virol.* **71**:1845–1850.
- Raviprakash, K., Liu, K., Matteucci, M., Wagner, R., Riffenburgh, R., and Carl, M. (1995). Inhibition of dengue virus by novel, modified antisense oligonucleotides. *J. Virol.* **69**:69–74.
- Raviprakash, K., Marques, E., Ewing, D., Lu, Y., Phillips, I., Porter, K. R., Kochel, T. J., August, T. J., Hayes, C. G., and Murphy, G. S. (2001). Synergistic neutralizing antibody response to a dengue virus type 2 DNA vaccine by incorporation of lysosome-associated membrane protein sequences and use of plasmid expressing GM-CSF. *Virology* **290**:74–82.
- Rey, F. A., Heinz, F. X., Mandl, C., Kunz, C., and Harrison, S. G. (1995). The envelope glycoprotein from tick-borne encephalitis virus at 2 Å resolution. *Nature* **375**:291–298.
- Rico-Hesse, R. (1990). Molecular evolution and distribution of dengue viruses type 1 and 2 in nature. *Virology* **174**:479–493.
- Rico-Hesse, R., Harrison, L. M., Nisalak, A., Vaughn, D. W., Kalayanarooj, S., Green, S., Rothman, A. L., and Ennis, F. A. (1998). Molecular evolution of dengue type 2 virus in Thailand. *Am. J. Trop. Med. Hyg.* **58**:96–101.
- Rico-Hesse, R., Harrison, L. M., Salas, R. A., Tovar, D., Nisalak, A., Ramos, C., Boshell, J., de Mesa, M. T., Nogueira, R. M., and de Rosa, A. T. (1997). Origins of dengue type 2 viruses associated with increased pathogenicity in the Americas. *Virology* **230**:244–251.
- Rosen, L. (1977). The Emperor's new clothes revisited, or reflections on the pathogenesis of dengue hemorrhagic fever. *Am. J. Trop. Med. Hyg.* **26**:337–343.
- Rothman, A. L., and Ennis, F. A. (1999). Immunopathogenesis of dengue hemorrhagic fever. *Virology* **257**:1–6.
- Rothman, A. L., Kanesa-Thanan, N., West, K., Janus, J., Saluzzo, J. F., and Ennis, F. A. (2001). Induction of T lymphocyte responses to dengue virus by a candidate tetravalent live attenuated dengue virus vaccine. *Vaccine* **19**:4694–4699.
- Sabchareon, A., Lang, J., Chanthavanich, P., Yoksan, S., Forrat, R., Attanath, P., Sirivichayakul, C., Pengsaa, K., Pojjaroen-Anant, C., Chokeyindachai, W., Jagsudee, A., Saluzzo, J. F., and Bhamarapavati, N. (2002). Safety and immunogenicity of tetravalent live-attenuated dengue vaccines in Thai adult volunteers: Role of serotype concentration, ratio, and multiple doses. *Am. J. Trop. Med. Hyg.* **66**:264–272.
- Salas-Benito, J. S., and del Angel, R. M. (1997). Identification of two surface proteins from C6/36 cells that bind dengue type 4 virus. *J. Virol.* **71**:7246–7252.
- Sánchez, I., Gómez-Garibay, F., Taboada, J., and Ruiz, B. H. (2000). Antiviral effect of flavonoids on the dengue virus. *Phytother. Res.* **14**:89–92.
- Shigeta, S., Mori, S., Kodama, E., Kodama, J., Takahashi, K., and Yamase, T. (2003). Broad-spectrum anti-RNA virus activities of titanium and vanadium substituted polyoxotungstates. *Antivir. Res.* **58**:265–271.

- Simmons, M., Murphy, G. S., Kochel, T., Raviprakash, K., and Hayes, C. G. (2001). Characterization of antibody responses to combinations of a dengue 2 DNA and dengue 2 recombinant subunit vaccine. *Am. J. Trop. Med. Hyg.* **65**:420–426.
- Spear, P. G., Eisenberg, R. J., and Cohen, G. H. (2000). Three classes of cell surface receptors for alpha-herpes virus entry. *Virology* **275**:1–8.
- Spillmann, D. (2001). Heparan sulfate: Anchor for viral intruders? *Biochimie* **83**:811–817.
- Srivastava, A. K., Putnak, J. R., Warren, R. L., and Hoke, C. H., Jr. (1995). Mice immunized with a dengue type 2 virus E and NS1 fusion protein made in *Escherichia coli* are protected against lethal dengue virus infection. *Vaccine* **13**:1251–1258.
- Stadler, K., Allison, S. L., Schlich, J., and Heinz, F. X. (1997). Proteolytic activation of tick-borne encephalitis virus by furin. *J. Virol.* **71**:8475–8481.
- Stemmer, W. P. (2002). Molecular breeding of genes, pathways, and genomes by DNA shuffling. *Scientific World Journal* **2**:130–131.
- Stephen, E. L., Sammons, M. L., Pannier, W. L., Baron, S., Spertzel, R. O., and Levy, H. B. (1977). Effect of a nuclease-resistant derivative of polyriboinosinic-polyribocytidylic acid complex on yellow fever in rhesus monkeys (*Macaca mulatta*). *J. Infect. Dis.* **136**:122–126.
- Streeter, D. G., Witkowski, J. T., Khare, G. P., Sidwell, R. W., Bauer, R. J., Robins, R. K., and Simon, L. N. (1973). Mechanism of action of 1-(-D-ribofuranosyl-1,2,4-triazole-3-carboxamide) (Virazole), a new broad-spectrum antiviral agent. *Proc. Natl. Acad. Sci. USA* **70**:1174–1178.
- Summers, P. L., Cohen, W. H., Ruiz, M. M., Hase, T., and Eckels, K. H. (1989). Flaviviruses can mediate fusion from without in *Aedes albopictus* mosquito cell cultures. *Virus Res.* **12**:383–392.
- Tam, R. C., Lau, J. Y. N., and Hong, Z. (2002). Mechanisms of action of ribavirin in antiviral therapies. *Antiviral Chem. Chemother.* **12**:261–272.
- Tan, B. H., Fu, J., Sugrue, R. J., Yap, E. H., Chan, Y. C., and Tan, Y. H. (1996). Recombinant dengue type 1 virus NS5 protein expressed in *Escherichia coli* exhibits RNA-dependent RNA polymerase activity. *Virology* **216**:317–325.
- Taweekhaisupapong, S., Sriurairatana, S., Angsubhakorn, S., Yoksan, S., and Bhamrapravati, N. (1996). *In Vivo* and *in vitro* studies on the morphological change in the monkey epidermal Langerhans cells following exposure to dengue 2 (16681) virus. *Southeast Asian J. Trop. Med. Public Health* **27**:664–672.
- Taylor, D. O., Ensley, R. D., Olsen, S. L., Dunn, D., and Renlund, D. G. (1994). Mycophenolate mofetil (RS-61443): Preclinical, clinical, and three-year experience in heart transplantation. *J. Heart Lung Transpl.* **13**:571–582.
- Taylor, J. L., Schoenherr, C., and Grossberg, S. E. (1980). Protection against Japanese encephalitis virus in mice and hamsters by treatment with carboxymethyl-acridanone, a potent interferon inducer. *J. Infect. Dis.* **142**:394–399.
- Tolou, H., Puggelli, H., Tock, F., and Durand, J. P. (1996). Partial inhibition of yellow fever virus replication *in vitro* with different phosphorothioate oligodeoxyribonucleotides. *Acta Virol.* **40**:73–79.
- Trimble, C., Lin, C. T., Hung, C. F., Pai, S., Juang, J., He, L., Gillison, M., Pardoll, D., Wu, L., and Wu, T. C. (2003). Comparison of the CD8⁺ T cell responses and antitumor effects generated by DNA vaccine administered through gene gun, biojector, and syringe. *Vaccine* **21**:4036–4042.
- Valle, R. P., and Falgout, B. (1998). Mutagenesis of the NS3 protease of dengue virus type 2. *J. Virol.* **72**:624–632.

- van der Most, R. G., Murali-Krishna, K., Ahmed, R., and Strauss, J. H. (2000). Chimeric yellow fever/dengue virus as a candidate dengue vaccine: Quantitation of the dengue virus-specific CD8 T cell response. *J. Virol.* **74**:8094–8101.
- Vasudevan, S. G., Johansson, M., Brooks, A. J., Llewellyn, L. E., and Jans, D. A. (2001). Characterisation of inter- and intra-molecular interactions of the dengue virus RNA-dependent RNA polymerase as potential drug targets. *Farmacology* **56**:33–36.
- Vaughn, D. W., Hoke, C. H., Jr, Yoksan, S., LaChance, R., Innis, B. L., Rice, R. M., and Bhamarapavati, N. (1996). Testing of a dengue 2 live-attenuated vaccine (strain 16681 PDK 53) in ten American volunteers. *Vaccine* **14**:329–336.
- Velzing, J., Groen, J., Drouet, M. T., van Amerongen, G., Copra, C., Osterhaus, A. D., and Deubel, V. (1999). Induction of protective immunity against dengue virus type 2: Comparison of candidate live-attenuated and recombinant vaccines. *Vaccine* **17**:1312–1320.
- Venugopal, K., and Gould, E. A. (1994). Towards a new generation of *Flavivirus* vaccines. *Vaccine* **12**:966–975.
- Walker, M. P., Appleby, T. C., Zhong, W., Lau, J. Y. N., and Hong, Z. (2003). Hepatitis C virus therapies: Current treatments, targets, and future perspectives. *Antiviral Chem. Chemother.* **14**:1–21.
- Walport, M. J., and Taylor, P. R. (1997). Immunology: What is the proximal cause of inflammation? *Curr. Biol.* **7**:R41–R43.
- Wang, W. K., Lee, C. N., Kao, C. L., Lin, Y. L., and King, C. C. (2000). Quantitative competitive reverse transcription-PCR for quantification of dengue virus RNA. *J. Clin. Microbiol.* **38**:3306–3310.
- Wang, W. K., Lin, S. R., Lee, C. M., King, C. C., and Chang, S. C. (2002). Dengue type 3 virus in plasma is a population of closely related genomes: Quasispecies. *J. Virol.* **76**:4662–4665.
- Watts, D. M., Porter, K. R., Putvatana, P., Vazquez, B., Calampa, C., Hayes, C. G., and Halstead, S. B. (1999). Failure of secondary infection with American genotype dengue 2 to cause dengue hemorrhagic fever. *Lancet* **354**:1431–1434.
- Wengler, G., and Wengler, G. (1993). The NS3 nonstructural protein of flaviviruses contains an RNA triphosphatase activity. *Virology* **197**:265–273.
- Westaway, E. G., Mackenzie, J. M., Kenney, M. T., and Khromykh, A. A. (1997). Ultrastructure of Kunjin virus-induced infected cells: Colocalization of NS1 and NS3 with double-stranded RNA, and of NS2B with NS3, in virus-induced membrane structures. *J. Virol.* **71**:6650–6661.
- Whitehead, S. S., Falgout, B., Hanley, K. A., Blaney, J. E., Jr, Markoff, L., and Murphy, B. R. (2003). A live, attenuated dengue virus type 1 vaccine candidate with a 30-nucleotide deletion in the 3'-untranslated region is highly attenuated and immunogenic in monkeys. *J. Virol.* **77**:1653–1657.
- WHO(2002). *Guidelines for the evaluation of dengue vaccines in population exposed to natural infection*. <http://www.who.int/tdr/publications/publications/pdf/dengueguidelines.pdf>.
- WHO(2003). Report of the Steering Committee on dengue and other flaviviruses vaccines. [//www.who.int/vaccine_research/diseases/dengue/en/dengue2003minutes_sc.pdf](http://www.who.int/vaccine_research/diseases/dengue/en/dengue2003minutes_sc.pdf).
- Witvrouw, M., and de Clercq, E. (1997). Sulfated polysaccharides extracted from sea algae as potential antiviral drugs. *Gen. Pharmacol.* **29**:497–511.
- Worobey, M., Rambaut, A., and Holmes, E. C. (1999). Widespread intrasero-type recombination in natural populations of dengue virus. *Proc. Natl. Acad. Sci. USA* **96**:7352–7357.

- Wu, S. F., Lee, C. J., Liao, C. L., Dwek, R. A., Zitzmann, N., and Lin, Y. L. (2002). Antiviral effects of an iminosugar derivative on *Flavivirus* infections. *J. Virol.* **76**:3596–3604.
- Wu, S. J., Hayes, C. G., Dubois, D. R., Windheuser, M. G., Kang, Y. H., Watts, D. M., and Sieckmann, D. G. (1995). Evaluation of the severe combined immunodeficient (SCID) mouse as an animal model for dengue viral infection. *Am. J. Trop. Med. Hyg.* **52**:468–476.
- Wyde, P. R. (1998). Respiratory syncytial virus (RSV) disease and prospects for its control. *Antivir. Res.* **39**:63–79.
- Zeng, L., Falgout, B., and Markoff, L. (1998). Identification of specific nucleotide sequences within the conserved 3'-SL in the dengue type 2 virus genome required for replication. *J. Virol.* **72**:7510–7522.
- Zhang, N., Chen, H. M., Koch, V., Schmitz, H., Liao, C. L., Bretner, M., Bhadti, V. S., Fatto Naso, R. B., Hosmane, R. S., and Borowski, P. (2003). Ring-expanded ("fat") nucleoside and nucleotide analogues exhibit potent *in vitro* activity against Flaviviridae NTPases/helicases, including those of the West Nile virus, hepatitis C virus, and Japanese encephalitis virus. *J. Med. Chem.* **46**:4149–4164.

This Page Intentionally Left Blank

BACTERIOPHAGE T4: STRUCTURE, ASSEMBLY, AND INITIATION INFECTION STUDIED IN THREE DIMENSIONS¹

Vadim V. Mesyanzhinov

Shemyakin-Ovchinnikov Institute of Bioorganic Chemistry of
the Russian Academy of Sciences
16/10 Miklukho-Maklaya S., 117997
Moscow, Russia

- I. Introduction
- II. Bacteriophage T4 Head Structure and Assembly
 - A. Structure
 - B. Assembly of the Head
 - C. DNA Packaging
 - D. Two-Dimensional Structural Studies
 - E. Three-Dimensional Structural Studies
- III. The Tail
- IV. The Fibers
 - A. The X-Ray Structure of STFs
 - B. Fibrin
- V. The Baseplate Structure
 - A. Structure of Baseplate Proteins
 - B. Overall Tail Tube–Baseplate Structure
 - C. Location of Baseplate Proteins with Known Atomic Structures
 - D. Identification of Other Baseplate Proteins
- VI. Structure of the Star-Shaped Baseplate
- VII. The Mechanism of the Baseplate Conformational Transition and Initiation of the Infection
- VIII. Conclusion
- References

I. INTRODUCTION

Bacteriophage T4 is a double-stranded DNA (dsDNA) contractile-tailed virus that infects the *Escherichia coli* strains. The T4-like subgroup of *Myoviridae* (Ackermann, 1999) is widely spread, propagates on a broad range of bacterial hosts that grow in diverse environments, and represents one of the most numerically abundant genetic domains in the biosphere (Brussow and Hendrix, 2002). Studies of the

¹ Dedicated to Professor Eduard Kellenberger on occasion of the 50th anniversary of his pioneering research on bacteriophage T4 structure and morphogenesis.

evolution of the phages and their impact in natural ecosystems are now flourishing (Hendrix, 2002; Hendrix *et al.*, 1999; Wommack and Colwell, 2000).

During the past five decades, bacteriophage T4 has provided an experimental model system for combining genetic, biochemical, and structural research to understand the mechanisms controlling assembly and morphogenesis of complex biologic systems and viruses (Kellenberger, 1966, 1980, 1990; Wood, 1980). The principles realized in the T4 assembly can be encountered in a broader range of cell biology processes, including cytoskeleton biology, signaling pathways, transcription, protein trafficking, and assembly of other viruses.

The AT-rich (65.5%) T4 genome of 168,903 bps has 289 open reading frame encoded proteins, 8 t-RNA genes, and at least 2 other genes that encode small but stable RNAs of unknown function (Kutter *et al.*, 1993; Miller *et al.*, 2003). More than 150 T4 genes have been characterized by genetic analysis or by the analysis of cloned gene products, but only 62 genes are “essential” under standard laboratory conditions.

Among known viruses studied on the molecular level, the virion of bacteriophage T4 is extremely structurally complex (Fig. 1). The T4 virion is built by more than 1500 protein subunits that represent about 50 different gene products. Of these, 24 gene products are involved in the head assembly, 22 in the tail assembly, and 6 in formation of the tail fibers. More than 10 other genes code for scaffolding, which involves catalytic and chaperone-like proteins that assist in protein folding and protein assembly but that are not present in the assembled infectious virion particle. The mature T4 particle consists of a 1150-Å long and 850-Å wide prolate head encapsidating a single molecule of genomic dsDNA; a 1000-Å long and 210-Å diameter contractile tail formed on a 500-Å diameter baseplate; and six long tail fibers (LTFs) of 1450 Å attached to the baseplate (Eiserling and Black, 1994). Bacteriophage T4 assembly occurs by one of the most complex processes so far extensively characterized at the molecular level using a combination of electron microscopy, genetics, and biochemical approaches. As was established a long time ago, a T4 head, a tail, LTFs, and whiskers are assembled via four independent pathways and joined together to form a mature infectious virion (Edgar and Lielausis, 1968; Wood *et al.*, 1968). Many of the steps in the T4 assembly could proceed by complementation *in vitro*, with production of infectious particles when extracts of the mutant-infected cells that produce different phage components are incubated together (Edgar and Lielausis, 1968; Edgar and Wood, 1966). In addition, phage components isolated from one mutant could be assayed for ability to complement each other to correct the defective function.

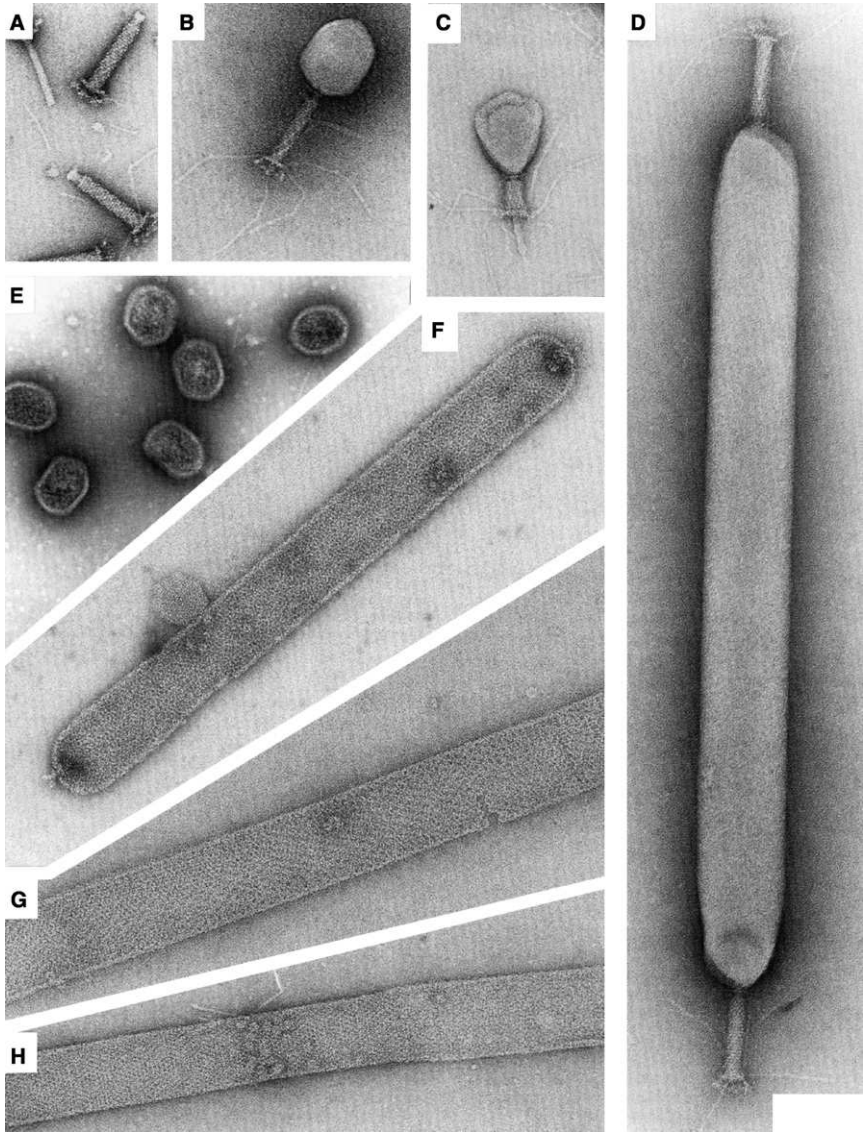


FIG. 1. Electron micrographs of negatively stained bacteriophage T4-related particles: (A) Purified phage T4 tails. (B) Mature bacteriophage T4 with extended tail. (C) Mature phage T4 treated with 5 M of urea, causing the tail to contract. (D) Bacteriophage T4 *hoc*⁻*soc*⁻ giant particle. (E) Bacteriophage T4 proheads, the so-called τ -particles (Aebi *et al.*, 1974), consisting of an inner core predominantly made of gp22 and an outer shell made of gp23. (F) A *21am-23ptg-can* giant T4 prohead. (G) A *21am-22am* superlattice-type prohead. (H) Hybrid unexpanded/expanded gp23* polyhead after limited proteolysis with gp8 protease. Scale bar: 100 nm (A–H). From Müller *et al.* (1994).

Most of the T4 genes that code structural proteins are expressed during the latter half of the infectious cycle, and they are largely clustered. Because all proteins of the T4 particle are synthesized simultaneously, the order of their assembly cannot result from the temporal regulation of gene products synthesis but must be controlled at the level of protein interaction (Kellenberger, 1976). The level of finished T4 parts does not appear to exert feedback controls on their production level or on the production of other components. Instead, the T4 genetic system appears to be settled to produce components in fixed relative amounts with tails and tail fibers in excess over heads, presumably maximizing the probability that assembled heads containing the genomic DNA will become converted to infectious particles (Wood, 1980).

Recent breakthroughs in X-ray crystallography and cryo-electron microscopy (Adrian *et al.*, 1984; Dubochet *et al.*, 1988; Rossmann *et al.*, 2001) have made it possible to extend the structural knowledge of T4 to a higher resolution. Success of Michael Rossmann's laboratory in determining the atomic structures of a number of T4 virion proteins, such as gene product (gp) whiskers antigen control (*wac*) or fibrin (Strelkov *et al.*, 1997, 1998; Tao *et al.*, 1997), gp8 (Leiman *et al.*, 2003), gp9 (Kostyuchenko *et al.*, 1999), gp11 (Leiman *et al.*, 2000), gp5-gp27 complex (Kanamaru *et al.*, 2002), and Mark van Raaij's group success in solving the gp12 structure (Thomassen *et al.*, 2003; van Raaij *et al.*, 2001) provided insight into the processes that link the initial recognition of the tail fibers of the host receptors with the subsequent injection of the viral DNA into the host. Latest developments in cryo-electron microscopy and three-dimensional (3-D) image reconstruction (Kostyuchenko *et al.*, 2003) have explained further the regulation of the T4 assembly pathways and the functioning of infection machinery.

The stepping stones for this review are the chapters of Kellenberger (1990), Black *et al.* (1994), Coombs and Arisaka (1994), Wood *et al.* (1994), and Leiman *et al.* (2003), and Rossmann *et al.* (2004). This review aims to summarize briefly the current knowledge of the T4 structure and assembly pathways and to point out the most significant recent results in this area. Furthermore, as the chapter author, I will concentrate on the T4 head structure present data on the individual T4 proteins whose spatial structures were successfully solved recently by X-ray crystallography at atomic resolution. Finally, I attempt to describe the quasi-atomic structure of the T4 baseplate, a multiprotein nanomachine, which controls host-cell recognition and attachment, tail sheath contraction, and viral DNA ejection into cell. The T4 baseplate employs a novel structural element, a rigid molecular cell-puncturing

device that contains a lysozyme domain. Its functions are to penetrate the outer cell membrane and to disrupt the peptidoglycan layer for subsequent injection of viral DNA into the host cell.

II. BACTERIOPHAGE T4 HEAD STRUCTURE AND ASSEMBLY

A. Structure

The head of phage T4, or capsid, represents geometrically an elongated icosahedron composed of more than 3000 protein subunits encoded by at least 12 gene products (Table I). This prolate wild-type capsid of triangulation class $T = 13$ *laevo* is elongated along a fivefold axis of symmetry (Aebi *et al.*, 1974). The T value represents the number of elementary triangles of the underlying hexagonal net required

TABLE I
PROTEIN COMPOSITIONS OF THE T4 PROHEAD AND MATURE HEAD^a

Gene	Prohead		Head		Location
	Length (aa)	Copy no	Length (aa)	Copy no	
23	521	930	422	930	Major capsid protein
20	524	12	524	12	Portal vertex
24	427	55	407	55	Fivefold vertices
<i>soc</i>	80	0	80	810	Outer capsid surface
<i>hoc</i>	376	0	376	155	Outer capsid surface
22	269	576	cleaved	—	Internal (scaffold)
21	212	72	cleaved	—	Internal (scaffold)
IPIII	194	370	cleaved	—	Internal (scaffold)
IPI	95	360	cleaved	—	Internal (scaffold)
IPII	100	360	cleaved	—	Internal (scaffold)
<i>alt</i>	682	40	682	40	Internal (portal vertex)
68	141	240	—	0	Internal
67	80	341	cleaved	—	Internal

^a Modified from Black *et al.* (1994) and Leiman *et al.* (2003).

Copy numbers of the shell proteins are derived from the EM studies of Baschong *et al.* (1991), Fokine *et al.* (2004), Iwasaki *et al.* (2000), and Olson *et al.* (2001).

Copy numbers of the internal proteins are based on the SDS-PAGE analysis of Onorato *et al.* (1978) and Isobe *et al.* (1976).

to cover one facet of an isometric icosahedron (Caspar and Klug, 1962). The T number is restricted to values in the sequence $h^2 + hk + h^2$ (e.g., 1, 3, 4, 9, 12, 13, 16, etc.) by the requirement that its facets must be equilateral triangles. The number of capsomers arranged on this surface lattice is given by $10T + 2$, of which 12 are associated with vertices. Discrete increments of axial elongation can be characterized geometrically by a Q number, an integer of any positive value that represents the corresponding ratio of areas for the triangular side facets of the elongated icosahedron. The number of capsomers in that case is $5(T + Q) + 2$. The Q number of the wild-type T4 capsid is 20 (Fokine *et al.*, 2004).

In total, the mature T4 capsid contains 930 subunits of gp23* (* is a gp23 protein proteolytically processed during capsid maturation), a major capsid protein, and 55 subunits of gp24*. Their pentamers occupy 11 vertices of the icosahedron (Olson *et al.*, 2001) and 12 subunits of gp20 located at unique portal vertex required for DNA packaging and subsequent attachment of the tail. The T4 capsid shell is decorated on the outside with *gphoc* (highly antigenic outer capsid protein) and *gpsoc* (small outer capsid protein) (Baschong *et al.*, 1988; Ishii and Yanagida, 1977; Ishii *et al.*, 1978). The latter two proteins are nonessential for head morphogenesis, and they both are absent in the T2 phage (Ishii *et al.*, 1978; Steven *et al.*, 1991).

A number of mutations in the genes controlling head assembly leads to formation of heads having a normal T number of 13 with different Q numbers: isometric ($Q = T = 13$), petites or intermediates ($Q = 17$), normal ($Q = 20$), and giants ($Q > 20$) as shown in Fig. 1D (Black *et al.*, 1994). Capsid-related tubular polymorphic variants of the unprocessed form of gp23, assembled in certain mutant infections, are called “polyheads” that do not contain DNA (Fig. 1G). These polyheads can usually be purified from lysates of *E. coli* cells after infections with phages carrying conditionally lethal mutants (i.e., amber, *am* or temperature sensitive, *ts*) in genes 21 (coding for the T4PPase), 20 (head–tail connector protein), and/or 22 (major prohead scaffolding core protein) affecting normal capsid assembly. These tubular structures are open-ended and not closed with hemispherical caps; elongated polymorphs of the latter kind are referred to as giant proheads or giant capsids (Fig. 1D and F) (reviewed in Black *et al.*, 1994). The surface lattices of the polyheads relate to lattices of the prohead by polymorphic variation. They represent cylindrical closures of the same hexagonal net that is folded in the prohead into a prolate icosahedral shell. However, polyheads have diameters that are typically about 20 to 30% smaller than that of a prohead (Steven *et al.*, 1976; Yanagida *et al.*, 1970).

B. Assembly of the Head

The T4 head assembly occurs via a number of the discrete intermediate stages: first, a DNA-free precursor, or prohead is assembled by a complex cell membrane-nucleated polymerization process. The prohead is then processed proteolytically. Next, the genomic DNA is packaged in a process that requires ATP energy; finally, head maturation is completed. As it has been pointed out (Black *et al.*, 1994), studies of T4 head morphogenesis have resulted in the discovery of novel assembly mechanisms. These include: (i) the prohead scaffolding core, a transition internal structure that is eliminated from the assembled prohead; (ii) the proteolytic regulation of the assembly pathway; (iii) the packaging of DNA into a preformed prohead using energy of the ATP hydrolysis; (iv) an assembly pathway controlled in time by sequential protein-protein interactions that activate required enzymatic activities; (v) large-scale conformational changes of the assembled capsid proteins that modulate stability and internal volume of the capsid, and (vi) the folding of the gp23 polypeptide chain that is controlled by the host GroEL chaperonin in cooperation with T4 gp31, which completely substitutes the *E. coli* GroES in the infected cells (reviewed in Ang *et al.*, 2000; Richardson *et al.*, 1998). In spite of low sequence identity (below 15%), gp31 of T4 and GroES of *E. coli* both have similar folds assembled to donut-shaped heptamers that serve as a cap for the GroEL protein-folding chamber. It is unclear why T4 uses its own encoded cochaperonin to fold the major capsid protein. Presumably, the volume of the GroEL/GroES chamber is insufficient to accommodate a gp23 monomer, and hence, gp23 requires gp31, which might provide a folding chamber of a larger volume.

Assembly of the T4 prohead starts with the formation of the gp20-gp40 membrane-spanning initiation complex at the inner side of the cytoplasmic membrane (Laemmli *et al.*, 1970). Protein gp40 is not present in the assembled heads, and it is required to initiate the assembly process of gp20 (Hsiao and Black, 1978). Subsequently, other proteins attach to the gp20-gp40 complex and form a prohead (Table I). This prohead consists of an internal core made up of the major core protein gp22; the minor head proteins gp21 (a serine-type protease), gp67, and gp68; and the so-called internal proteins IPI, IPII, and IPIII (Onorato *et al.*, 1978; Showe and Black, 1973). However, IPI and IPII are dispensable for the prohead assembly. In the absence of IPIII, about half of the gp23 molecules are assembled into polyheads and half into phages. In summary, a morphogenetically correct T4 prohead could be assembled from an irreducible set of four gene products: gp20,

gp22, gp67, and gp23. Addition of gp40, IPIII, and 24 improves the efficiency of prohead assembly, and gp21 is required to ensure that correctly formed proheads mature into capsids.

The molecular mechanisms determining the shape and size of the T4 prohead represent a challenging problem. Eduard Kellenberger (1969, 1972) proposed two mechanisms based on the interaction of internal core and shell, a template and Vernier models, which might determine the size of a large icosahedral viral capsid (reviewed in Black *et al.*, 1994; Lane and Eiserling, 1990). The template model accounts for the shape of the prohead, dictated by that of the underlying scaffolding core. The Vernier model assumes a Vernier-type matching between the core and the shell of growing prohead. When the core and shell correspond exactly, elongation is terminated. In contrast to these models based on geometric constraints, the "kinetic" model of Showe and Onorato (1978) proposed that length regulation is based on the relative kinetics of assembly of the core and the prohead shell.

Genetic data show that the isometric and intermediate-length (petite) heads are associated only with mutations in the genes 22, 67, and 68 coded core proteins (Keller *et al.*, 1988; Paulson *et al.*, 1976; Volker *et al.*, 1982a,b). All isometric and intermediate T4 heads have the same length as normal prolate heads. This suggests that the scaffolding core is the primary determinant of the width or T number.

The major capsid protein gp23 is a functionally rather complex molecule whose detailed interactions and conformational changes during capsid assembly are far from being understood. Clearly, gp23 has form-determining properties and can assemble into several distinct forms. Several studies (reviewed in Black *et al.*, 1994; Lane and Eiserling, 1990) reported two large mutation classes in gene 23: the *pt* mutations lead to the production of the isometric heads (petite), and the *ptg* mutations produce both petite and giant capsids. The *ptg* mutations were mapped at 10 different loci arranged in three rather narrow clusters of gene 23: cluster 1 (residues 66 to 97), cluster 2 (residues 268 to 287), and cluster 3 (residues 457 to 461) (Doermann *et al.*, 1973). These three regions of gp23 have been shown to have homology with gp24. A class of point mutations in gene 23, called 24-bypass (*byp24*) mutations, compensate for deficiency in the vertex protein, gp24, by substituting gp23 (McNicol *et al.*, 1977).

Current data suggest that the primary determinant of both prohead width and length is its morphogenetic core, and it is likely that the core and shell grow concurrently (Black *et al.*, 1994). However, it is unclear what determines the prolate form of the core. Based on a major core component, gp22, a model was proposed for the normal prolate T4

core by Engel *et al.* (1982). The authors suggested that the length of the core is determined by the way in which six filamentous strands of gp22 molecules are wound around a common axis to form a prolate ellipsoid. Such strands had previously been detected in giant proheads and polyhead core (Paulson and Laemmli, 1977). The gp22 sequence has a high propensity to fold into α -helices, and gp22 predominantly forms the coiled-coil strands (Mesyanzhinov *et al.*, 1990). Future crystallographic study of scaffolding core and shell proteins in combination with detailed 3-D high-resolution analysis of the gp23 assembled structures corresponding to distant maturation steps of the T4 capsid should provide important information for understanding the molecular principles and mechanisms underlying the T4 head assembly and the switching between different functional states of supramolecular structures.

A region of the amino acid sequence of a catalytic core component, gp21, reveals a homology to the active site of serine proteases, with His substituting for Ser in gp21 (Keller and Bickle, 1986). Upon completion of the assembly of the T4 prohead, inactive gp21 zymogen is converted to the active T4PPase by slow cleavage (Showe *et al.*, 1976), which, in turn, degrades the scaffold proteins into small peptides. How the gp21-to-T4PPase conversion is initiated is not yet known. As it was proposed in McNicol *et al.* (1997) and Onorato *et al.* (1978), one distinct possibility is that gp24 might be the proteinase activator, acting when it occupies the vertices of the assembling prohead. The T4 gene *lip* (late inhibitor of proteinase) that is located between the head gene 24 and the baseplate gene 25 (Kaliman *et al.*, 1990) might also participate in regulation of gp21PPase activity in the assembled prohead.

Being activated, the T4PPase specifically cleaves the 65-residue-long amino-terminal " Δ -piece" from the 521-residue-long gp23 (56 kDa) molecule (Parker *et al.*, 1984), thus yielding the 48.7-kDa gp23 (Laemmli, 1970). A small piece of the gp24 sequence (2.2 kDa) is also cleaved under the prohead-head maturation, but the portal protein gp20 is not cleaved. The T4PPase catalyzes all of the prohead maturation cleavages at a consensus Leu(Ile)-Xxx-Glu recognition site. Moreover, a high-order structure of cleaved proteins must limit cleavage on these sites, and some such sequences are not cleaved in certain prohead targets (Black *et al.*, 1994). Most of small peptides produced by T4PPase are expelled from the prohead, thus providing space necessary to accommodate the genomic DNA during packaging.

After cleavage of the gp23 Δ -piece, the near-hexagonal capsid lattice expands from 112 to 130 Å, thus increasing the capsid volume by

roughly 50% (Aebi *et al.*, 1974, 1977) and thereby exposing the *hoc* and *soc* binding sites on the gp23* lattice (Aebi *et al.*, 1977; Ishii and Yanagida, 1977). Concomitant with this expansion of the gp23* lattice, which involves rotation of the gp23* protomers, and translocation of at least two distinct epitopes from one capsid site to the other (Aebi *et al.*, 1974; Kistler *et al.*, 1978, 1982; Steven and Carrascosa, 1979; Steven *et al.*, 1991), packaging of the genomic DNA occurs.

C. DNA Packaging

The proteolytically processed prohead released from the cytoplasmic membrane is capable of DNA packaging. DNA packaging requires the terminase (packaging-linkage) proteins that link long, replicated concatameric DNA into a mature prohead at the portal vertex, that act enzymatically during translocation DNA, and that cut DNA following packaging. Two partially overlapping T4 late genes, 16 and 17, code the terminase proteins. The phage T4 terminase holoenzyme subunit apparently consists of multiple copies of the large subunit, gp17, and a small subunit, gp16 (Rao and Black, 1988). The large subunit possesses the prohead-binding and putative DNA-translocation ATPase activities, while the small subunit regulates the large gp17 subunit activities and conveys specific DNA recognition (Kuebler and Rao, 1998; Leffers and Rao, 2000; Lin and Black, 1998; Lin *et al.*, 1997).

It has been proposed that the terminase large subunits of bacteriophages can assume different conformational states (Guo *et al.*, 1987; Hwang and Feiss, 1995; Lin *et al.*, 1999). Some of the properties of gp17 and other large subunit terminase proteins suggest that they fit criteria to be included in a class of intrinsically unstructured proteins (Bright *et al.*, 2001; Wright and Dyson, 1999). Thus gp17 (i) interacts with multiple proteins, including gp16, gp20, gp32, and gp55 (Malys *et al.*, 2002) and presumably DNA; (ii) binds and hydrolyzes ATP; (iii) is highly susceptible to proteolysis; and (iv) exists in multiple interconvertible conformational states. The gp16 small subunit interaction is most important for conversion to a highly active and catalytic form. Analysis of the gp17 complexes separated from gp16 on glycerol gradients, however, showed that a prolonged enhanced ATPase activity persisted after exposure to gp16, suggesting that constant interaction of two proteins may not be required during packaging (Baumann and Black, 2003). Probably other protein interactions may be necessary to lock the gp17 protein into specific conformations for packaging.

It was proposed that the DNA packaging apparatus represents a rotary motor powered by ATP hydrolysis (Hendrix, 1978; Simpson *et al.*, 2000). The DNA is a movable central spindle of the motor surrounded by a dodecameric portal protein serving as a ball race between the DNA spindle and the fivefold symmetric capsid vertex, to which the ATPase terminase complex is attached. The forces that act on individual DNA molecules that are being packaged into the heads of bacteriophage $\phi 29$ have been measured and show that the $\phi 29$ portal protein generates one of the strongest known molecular motors (Smith *et al.*, 2001). Although the sequence homology between the connector proteins from different tailed bacteriophages is rather low (less than 20%), they all have similar cone-shaped dodecameric structure and are functioning similarly (Driedonks *et al.*, 1981; Kochan *et al.*, 1984; Lurz *et al.*, 2001; Simpson *et al.*, 2000; Valpuesta *et al.*, 1992). Furthermore, the connectors from small phage $\phi 29$ (19.3-kbp genome) and lambda (48.5-kbp genome) are interchangeable (Donate *et al.*, 1990).

The length of the T4 packaged DNA is proportional to the volume of the head; the so-called “head-full” mechanism yields circularly permuted and terminally redundant viral chromosomes. Mutants with altered lengths of the capsid are capable of DNA packaging (Eiserling *et al.*, 1970; Lane *et al.*, 1990; Uhlenhop *et al.*, 1974). The isometric heads contain only about 70% of the genome, whereas the giants can contain more than a dozen of the genomic sequences repeated along a single dsDNA molecule. The termination of packaging is probably regulated by mechanical stress applied to the portal complex. Upon completion of DNA packaging, the gp16–gp17 terminase complex dissociates from the head.

Finally, one molecule of *hoc* and six molecules of *soc* per each gp23* capsomer are bound to the T4 capsid (Aebi *et al.*, 1977). The head maturation is completed by gp13, gp14, gp2, and gp4. These proteins presumably bind to the portal vertex formed by 12 subunits of gp20, and they are required for subsequent attachment of the assembled tail. The tails do not attach to the empty but otherwise mature heads, and a DNA-mediated interaction is probably involved in the joining head–tail process.

D. Two-Dimensional Structural Studies

The strong tendency of gp23, the isolated major T4 capsid protein, to assemble into polyheads has prevented determination of its structure by X-ray crystallography at high resolution. Other capsid proteins also

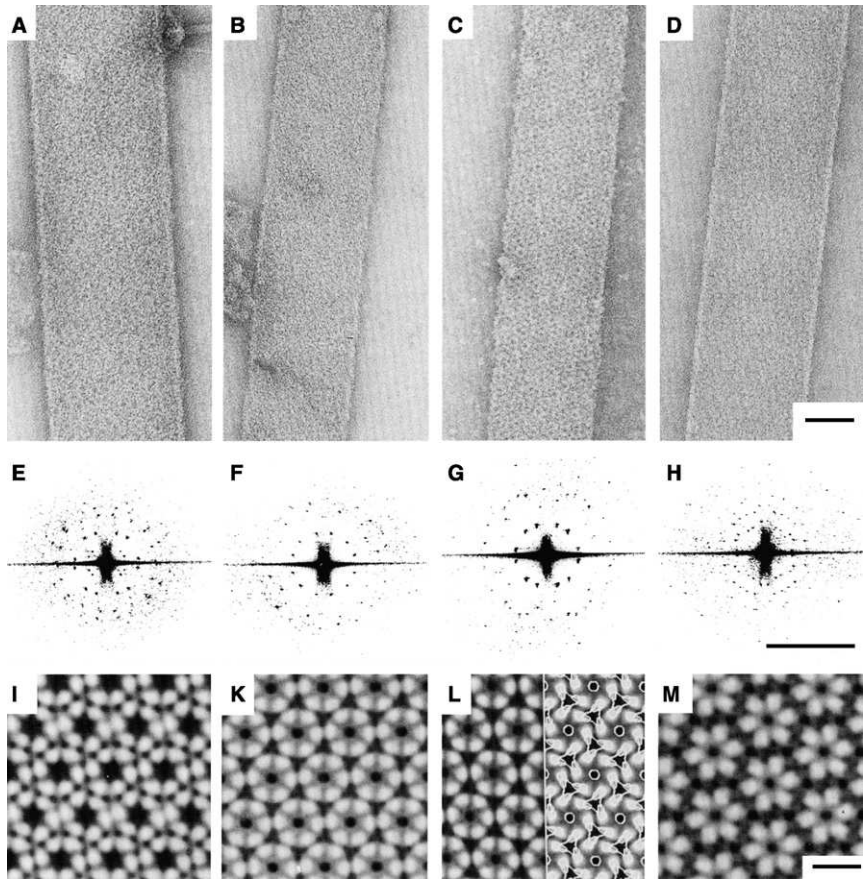


FIG. 2. Electron micrograph areas (A–D), optical diffraction patterns (E–H), and correlation averages (I–M) of *in vitro* matured (i.e., gp23* or gp23+ containing, gp23* containing expanded) prohead-like superlattice-type polyheads. (A) Prohead-like polyhead. (B) Unexpanded gp23* containing polyhead after a 25-min incubation with V8 protease. (C) unexpanded gp23+ containing polyhead after a 30-min incubation with either V8 protease or trypsin. (D) The gp23* containing polyhead after *in vitro* expansion of the gp23* lattice from about 11 to 13 nm. (E–H) Corresponding representative optical diffraction patterns. (L, M) The top and bottom halves of spread-flattened polyheads that were first quasi-optically filtered and the resulting single-sided filtrations that were correlation averaged. (I) Correlation-averaged prohead-like polyheads revealing a superlattice-type surface lattice. (K) Correlation-averaged gp23* and gp23+. (L) Superlattice-type polyheads now revealing a normal lattice type, near-hexagonal surface lattice. (M) Correlation-averaged gp23* superlattice-type polyhead after expansion of its near-hexagonal gp23* lattice. The contours superimposed onto the right half of the cleaved/unexpanded gp23+ lattice in Fig. 2L represent the difference map of the gp23-containing prohead-like and gp23+ containing cleaved/unexpanded polyhead lattice. The Δ -piece

have a strong tendency to form large aggregates *in vitro*. Conformational states during T4 capsid maturation, however, have been studied extensively by a variety of EM (electron microscopy) and image processing approaches. In particular, the extended polysheaths, tubular polyheads, and giant proheads and capsids, which flatten uniformly on the grid, present regular two-dimensional (2-D) arrays of capsomers that are readily amenable to image processing (Aebi *et al.*, 1974; DeRosier and Klug, 1972). Quasi-optical filtration followed by correlation averaging of negatively stained 2-D crystalline arrays of several proteins offered an attractive approach to structural studies at the molecular level (Aebi *et al.*, 1973, 1981; Buhle *et al.*, 1983). This method was used successfully in several laboratories to understand details of the process of bacteriophage T4 head morphogenesis and maturation properties of the capsid-like assemblies such as polyheads and giant phages (Aebi *et al.*, 1974, 1977; Laemmli *et al.*, 1976; Steven *et al.*, 1991).

Cleavage and expansion *in vitro* of the major capsid protein gp23 using prohead-like T4 polyheads, produced by 20am–21am, 21am–22am, and 20am–21am–22am mutants (Fig. 1G and H), was used as a model system to better understand distinct intermediate stages during capsid maturation (Müller *et al.*, 1994a). In a first step, the 65-residue-long amino-terminal “ Δ -piece” was cleaved by *Staphylococcus aureus* V8 protease at exactly the same position (i.e., between amino acids 65 and 66) at which the phage-coded T4PPase cleaves (Parker *et al.*, 1984), to yield mature gp23* without affecting a second potential cleavage site between residues 142 and 143. Negatively stained samples of cleaved polyheads revealed a near-hexagonal lattice with a 112-Å lattice constant (Fig. 2). One-sided correlation averages of these cleaved/unexpanded polyheads yielded capsomers that were rounder than those of prohead-like (i.e., uncleaved) control polyheads, with distinct trimers of mass (specifically, trimers of the Δ -pieces in the area where three protomers are shared among three different capsomers) removed, as revealed by difference maps computed from the correlation averages. Quantitative expansion of the 112-Å near-hexagonal lattice into the 130-Å near-hexagonal lattice characteristic of mature phage heads could be induced by pelleting the cleaved/unexpanded polyheads and resuspending them in water.



removed by the action of the V8 protease appears to mediate the trimeric intercapsomere interaction (i.e., triangular contours), whereas the Δ -piece is found near the site of the dimeric intercapsomere interaction (i.e., the blobs defining the corners of the triangles). Scale bars: 50 nm (A–D), (2.5 nm) – (E–H), and 10 nm (I–M). From Müller *et al.* (1994).

It is evident that the conformational state of the Δ -piece plays a pivotal role in mediating expansion of the gp23* lattice: (i) cleavage of prohead-like polyheads with V8 protease in a second site between residues 142 and 143 or with trypsin between residues 143 and 144 to gp23⁺ (41 kDa) render the polyheads unexpandable, indicating that the presence of the Δ -piece is in need for expansion; (ii) in difference maps computed from correlation-averaged unexpanded gp23* and gp23⁺ polyhead lattices, the 142-residue-long amino-terminal Δ' -piece has been localized near the dimeric intercapsomer contact that stabilizes the expanded gp23* polyhead lattice; (iii) upon expansion, gp23* polyheads assume a conformation that renders them resistant to further cleavage by either V8 protease or trypsin; (iv) extensive reorganization of the Δ' -piece upon expansion of the gp23* polyhead lattice has also been demonstrated by immunoelectron microscopy using a peptide antibody against residues 139–146 recognizing an epitope within the Δ' -piece (Steven *et al.*, 1991). Accordingly, during expansion, residues 139–146 are translocated from the outer to the inner surface of the polyhead lattice. Taken together, these observations indicate that the Δ' -piece is implicated in an intercapsomer contact necessary to stabilize the expanded gp23* polyhead lattice.

E. Three-Dimensional Structural Studies

Cryo-electron microscopy and 3-D image reconstruction methods provide reliable high-resolution information about structural organization of viral capsids (Baker *et al.*, 1999; Rossmann *et al.*, 2001). The rapid cooling to near liquid nitrogen temperature prevents the formation of ice crystals in the biologic samples (like virus particles), preserves their structure, and also “freezes” the molecules in the middle of reaction. One of the most promising applications of cryo-electron microscopy is time-resolved imaging that allows snapshots of the macromolecular complexes as a reaction or as a conformational transition. (Fuller *et al.*, 1995; Heymann *et al.*, 2003).

A cryo-electron microscopy approach has been applied to study the isometric T4 capsids. Maps that are 3-D of the empty isometric T4 capsids with and without *gpsoc* (Iwasaki *et al.*, 2000) and DNA-filled capsids (Olson *et al.*, 2001) have been determined at 27-Å and at 15-Å resolution, respectively. The capsid diameter varies from about 970 Å along the fivefold axes to about 880 Å along the threefold and twofold axes (Fig. 3). The shell of about 30-Å thickness, as expected for a $T = 13$ particle, is composed of 120 hexamers of gp23* and 12 pentamers of gp24*. The *gpsoc* is a rod-like molecule ($\sim 39 \times 27 \times 14$ Å) that forms a

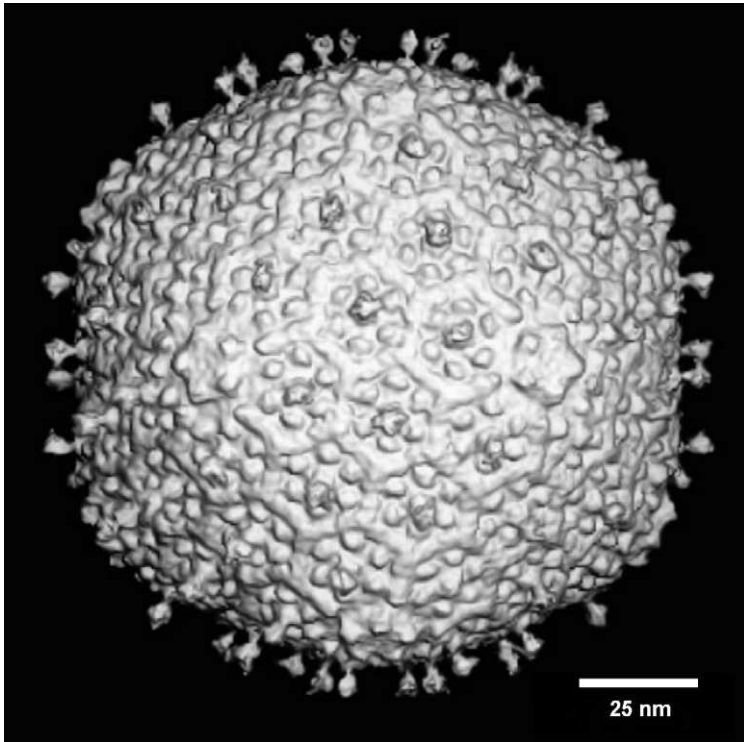


FIG. 3. Shaded-surface representation of the 3-D cryo-electron microscopy reconstruction of the T4 isometric capsids. The view is along a twofold axis of the icosahedron. The prominent balloon-shaped projections are *gp24** molecules. A total of 120 *gp24** molecules extend outward from the center of each *gp23** hexamer in the capsid. From Olson *et al.* (2001).

continuous mesh on the surface of *gp23** hexamers (Figs. 3 and 4). Every *gpsoc* molecule binds between two *gp23** subunits but not between *gp23** and *gp24** (Fig. 3), and, therefore, *gpsoc* does not bind around the *gp24** pentamers. The *gpsoc* forms trimers at the meeting points of three *gp23** hexamers.

The failure of *gp24** to bind *gpsoc* provides a possible explanation for the property of osmotic shock resistance (Os), which was mapped in gene 24 (Leibo *et al.*, 1979). It was speculated that Os-resistant mutant *gp24** might have acquired the ability to bind *gpsoc*, thus stabilizing the capsid (Iwasaki *et al.*, 2000).

*Gp24** is a balloon-shaped molecule. It extends to about 50 Å away from the shell surface (Fig. 3). Its protruding part is composed of two

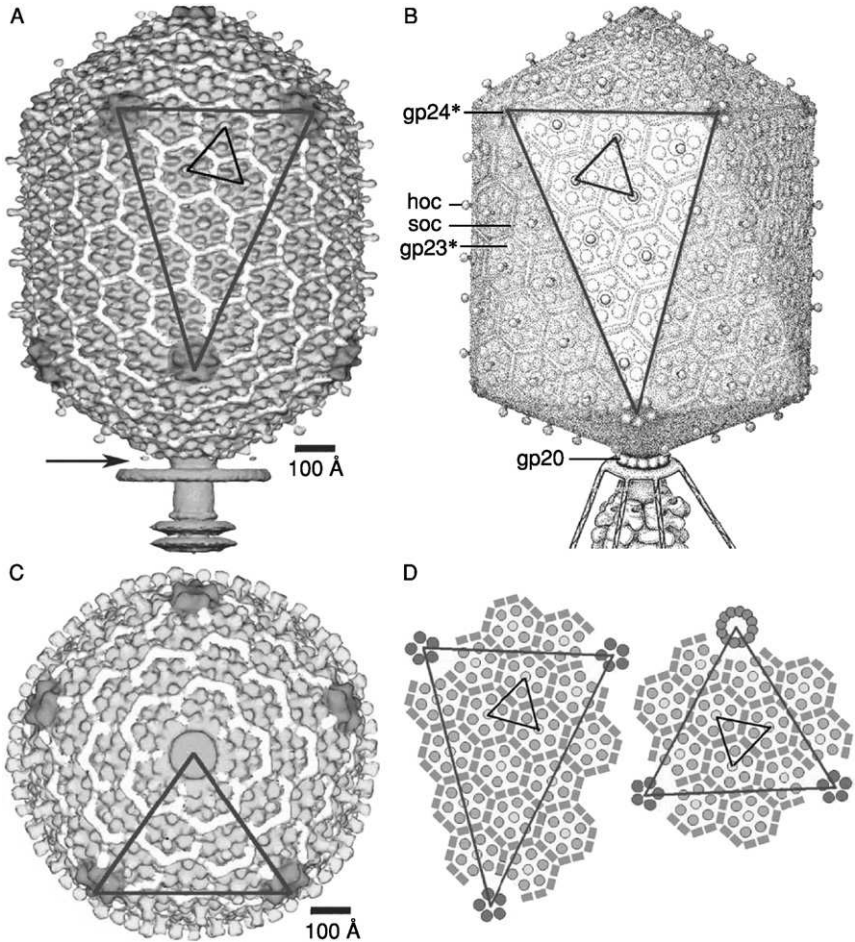


Fig. 4. (Adopted from Fokine *et al.*, 2004). Structure of the bacteriophage T4 head ($T_{end} = 13$ laevo, $T_{mid} = 20$, $h_1 = 3$, $k_1 = 1$, $h_2 = 4$, and $k_2 = 2$) compared with the previously proposed model ($T_{end} = 13$ laevo, $T_{mid} = 21$, $h_1 = 3$, $k_1 = 1$, $h_2 = 3$, and $k_2 = 3$) (Baschong *et al.*, 1988; Eiserling and Black, 1994). The facet triangles are shown in blue and the basic triangles are shown in black as appropriate. (A) Shaded surface representation of the cryo-EM reconstruction viewed perpendicular to the fivefold axis. gp23* is shown in blue, gp24* is in magenta, soc is in white, hoc is in yellow, and the tail is in green. (B) Model of the previously proposed T4 head structure (adapted from Eiserling and Black, 1994). (C) View of the reconstruction along the fivefold axis with the portal vertex toward the observer; the tail has been cut away at the level shown by the black arrow in A. Proteins are colored as described for A. (D, Left) Schematic representation of the distribution of proteins in the elongated midsection facet. (D, Right) Schematic representation of an end-cap facet. Proteins are colored as described for A except the soc molecules are shown as gray rectangles. A and C were prepared with the help of the programs DINO (www.dino3d.org) and POVRAY (www.povray.org). (See Color Insert.)

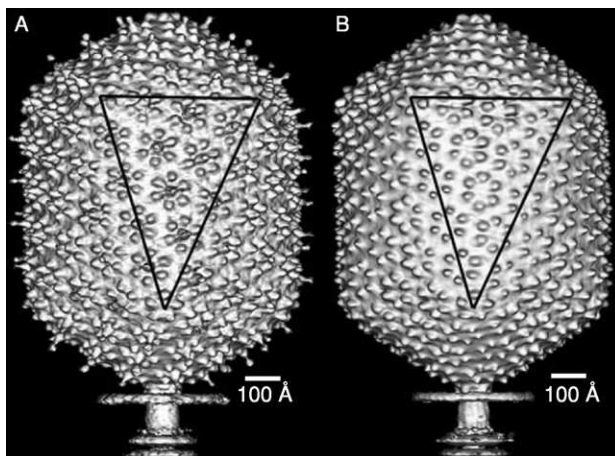


Fig. 5. (Adopted from Fokine *et al.*, 2004). Shaded surface representations of the *soc*- (A) and *hoc-soc-* (B) reconstructions. A facet triangle is shown.

domains: a rounded base (~ 19 Å high) and a globular head (~ 20 Å wide and 24 Å high) connected by a thin neck region. The overall mass of the protrusion is about 12 kDa, suggesting that up to 2/3 of *gp_{hoc}* might be inserted in the center of each *gp_{23*}* hexamer.

Recently, the 3-D structure of the T4 prolate head of the mature virus, using cryo-electron microscopy and image reconstruction techniques has been determined to 22 Å resolution (Fokine *et al.*, 2004). The T4 capsid has a hexagonal surface lattice characterized by the triangulation numbers $T_{end} = 13$ *laevo* for the icosahedral caps and Q or $T_{mid} = 20$ for the midsection (Fig. 4). Hexamers of the major capsid protein *gp_{23*}* and pentamers of the vertex protein *gp_{24*}*, as well as the outer surface proteins *hoc* and *soc*, are clearly evident in the reconstruction. In addition, the binding sites and shape of the *hoc* and *soc* proteins have been established by analysis of the T4 structure of the head when *soc* or *hoc* and *soc* are missing (Fig. 5).

III. THE TAIL

Products of at least 22 genes are involved in assembly of the T4 phage tail (Table II) that uses the stored energy of the assembled contractile sheath and the packaged DNA to eject the genome into the host. The assembly pathway of the tail is based on strictly ordered

TABLE II
T4 BACTERIOPHAGE TAIL PROTEINS IN ORDER OF
APPEARANCE IN THE T4 GENETIC MAP^a

Gene	Length (aa)	Copy no.	Location
3	176	6	Tail tube terminator
53	196	6	Wedge
5	575	3	Hub
6	660	12	Wedge
7	1032	6	Wedge-vertex
8	334	12	Wedge
9	288	18	Wedge-vertex
10	602	18	Wedge-pin
11	219	18	Wedge-pin
12	527	18	Short-tail fiber
15	272	6	Tail terminator
18	659	138	Tail sheath
19	163	138	Tail tube
25	132	6	Wedge
26	208	nd ^{*b}	Hub and chaperone?
27	391	3	Hub
28	177	nd ^{*b}	Hub
29	590	6	Tail tube
48	364	6	Baseplate
54	320	6	Baseplate
<i>td</i>	286	3	Hub?
<i>frd</i>	193	6	Wedge?

^a Modified from Coombs and Arisaka (1994) and Leiman *et al.* (2003a). Data of Copy no. for gp18 and gp19 are from Leiman *et al.* (2004).

^b The nd* stands for "not determined."

sequential interactions of proteins (Ferguson and Coombs, 2000; Kikuchi and King, 1975a,b,c; Plishker *et al.*, 1983; Watts *et al.*, 1990; Zhao *et al.*, 2000). The baseplate, a remarkably complex multiprotein structure that serves as a control unit of T4 infection, is assembled first. The baseplate is composed of about 150 subunits of at least 16 different gene products, many of which are oligomeric (Table II). The baseplate is assembled from six identical wedges that surround a central hub (Coombs and Arisaka, 1994). The T4 gp11 (the STF-connecting protein), gp10, gp7, gp8, gp6, gp53, and gp25 combined

sequentially to build up a wedge. The central hub is formed by gp5, gp27 (Kanamaru *et al.*, 2002), and gp29. Assembly of the baseplate is completed by attaching gp9, the STF-connecting protein, STFs, gp48, and gp54. The last two proteins are required to initiate polymerization of the tail tube, a channel for DNA ejection. The tail tube is terminated with gp3 (King, 1968; Vianelli *et al.*, 2000). The tail tube serves as a template for assembly of gp18 that formed the contractile tail sheath. The length of the tail tube is probably determined by gp29, the “ruler protein” or template (Abuladze *et al.*, 1994), that also participates in assembly of the baseplate (Kikuchi and King, 1975c). The length of the tail sheath is determined by the tube. In the absence of the tail tube that is built of 138 subunits (Leiman *et al.*, 2004) of gp19 of 18.5 kDa, gp18 assembles into long polysheaths with a structure similar in several aspects to the contracted state (Kellenberger and Boy de la Tour, 1964; Moody, 1973). Both the tail tube and the tail sheath have helical symmetry with a pitch of 40.6 Å and successive subunits repeated every 17.7° (DeRosier and Klug, 1968; Lepault and Leonard, 1985; Moody and Makowski, 1981).

The assembly of the tail is completed by a gp15 hexamer that binds to the last ring of the tail sheath (Zhao *et al.*, 2003). The tail associates with the head after DNA packaging. After the phage head is joined to a LTF-less tail, six gpwac (fibrin) molecules attached to the neck of the virion form a ring embracing it (“collar”), and thin filaments protrud from the collar (“whiskers”). Whiskers help with attachment the baseplate of other fibrous proteins, the LTFs, which interact with the receptors on the bacterial surface.

An assembled T4 tail sheath represents a metastable supramolecular structure that undergoes conformational changes after phages bind to the LPS receptors on a host cell. During irreversible contraction, the length of tail sheath decreases from 980 to 360 Å, and its outer diameter increases from 210 to 270 Å (Coombs and Arisaka, 1994).

IV. THE FIBERS

Certain viruses, like adeno and reoviruses, as well as many bacteriophages use fibrous proteins to recognize their host receptors. The T4 has three types of fibrous proteins: the long tail fibers (LTFs), the short tail fibers (STFs), and whiskers. The T4 LTFs, which are about 1450 Å in length and only about 40 Å in diameter, are primary adsorption devices (Goldberg *et al.*, 1994; Kellenberger *et al.*, 1965). Each LTF fiber consists of rigid proximal halves encoded by gene 34 and distal

ones encoded by gene 37. These halves are connected by gp35 and gp36 that form a hinge region (Cerritelli *et al.*, 1996; Wood *et al.*, 1994). The proteins that formed the LTF are homotrimers, except for gp35 that is assembled as a monomer (Cerritelli *et al.*, 1996). The N-terminal of gp34 forms the baseplate-binding bulge, and the C-terminal of gp37 binds to a cell receptor. The amino acid sequences of the T4 fibers are composed of a repeating motif common to gp34, gp37, and gp12, with intervening sequences of different lengths (Fig. 6). The C-terminal sequences of gp37 and gp12 are slightly homologous presumably because both bind to the LPS receptors.

Two phage-encoded chaperones, gp57A and gp38, are required for assembly of both LTF's proximal and distal parts. However, gp38 is a structural component for the T2 phage distal part of LTF. It binds to the tip of gp37 and is responsible for receptor recognition (Henning and Hashemolhosseini, 1994). The gp57A is also required for trimerization of gp12 *in vitro* and *in vivo* (Matsui *et al.*, 1997). Another two assembly-assisted proteins, gp63 and *gpwac*, participate in the attachment of the LTFs to the baseplate (Terzaghi *et al.*, 1979; Wood *et al.*, 1978).

A. The X-Ray Structure of STF_s

The STF is a club-shaped molecule of about 340 Å long, consisting of a parallel, in-register assembled trimer of gp12 of 527 residues per polypeptide chain (Mason and Haselkorn, 1972; Makhov *et al.*, 1993). STF_s are attached to baseplate by the N-terminal thin part, while the C termini bind to the host-cell receptors (Makhov *et al.*, 1993). The structure of a heat and protease-stable domain of the STF that contains the LPS binding site was recently determined by X-ray crystallography (Protein Data Bank (PDB) codes 1H6W and 1OCY). (Thomassen *et al.*, 2003; van Raaij *et al.*, 2001). Initially, a 33-kDa proteolytic fragment consisting of residues 85–396 and 518–527 was crystallized, but residues 85–245 were invisible in the crystal structure (van Raaij *et al.*, 2001). The ordered residues 246–396 and 518–527 have revealed new folding motifs. Residues 246–289 form an N-terminal region held together by intertwined strands and a central, mainly hydrophobic, core. Residues 290–327 form a central right-handed triple β-helix (Fig. 6B), a structure reminiscent of, but different from, the adenovirus triple β-spiral (van Raaij *et al.*, 2001).

The treatment of STF_s by trypsin in the presence of zinc ions resulted in a 45-kDa fragment (Thomassen *et al.*, 2003). The X-ray crystallography of this fragment at 1.5 Å resolution reveals the

structure of the C-terminal part of the molecule containing the putative LPS-binding site that presumably is formed by cluster of basic and aromatic residues. The C-terminal has a novel “knitted” fold consisting of three extensively intertwined gp12 monomers. The intertwining of the receptor binding domain represents a case of a 3-D “domain swapping” phenomena found in several proteins (Liu and Eisenberg, 2002; Liu *et al.*, 2002). The STF residues 399–472, containing β -strands F–M and α -helix III, have been “swapped” to the neighboring monomer, leading to cyclic trimerization (Fig. 7C).

The C-terminal domain has a metal-binding site that contains a zinc ion coordinated by six His residues in a stable octahedral conformation (Fig. 8). Since the T4 STFs have no enzymatic activity, unlike the trimeric P22 phage tail spike (Steinbacher *et al.*, 1994), zinc probably increases the stability of the C terminus or its need for proper assembly of gp12 trimer.

B. Fibritin

Another T4 fibrous protein, the whisker fibers (*gpwac*, or “fibritin” as it was renamed in our group), is attached to the neck, and formed by gp13 and gp14. In the T4 genome, gene *wac* is located between upstream gene 12 and downstream gene 13. Fibritin belongs to a specific class of accessory proteins acting in the phage assembly as a bicomplementary template. It performs a chaperone function accelerating the connection of the distal parts of LTFs to their proximal parts (Terzaghi *et al.*, 1979). Being a structural component of the mature phage particle (Coombs and Eiserling, 1977), fibritin also works as a primitive molecular sensor (Conley and Wood, 1975). Under conditions unfavorable for phage growth (low temperature), it holds long fibers in a fixed position, raised to the tail and capsid, keeping virus particles noninfectious.

The sequence of the *gpwac* polypeptide chain of 487 residues exhibits a pattern specific for α -helical coiled–coil proteins. It is characterized by the presence of a heptad repeat (**a**-b-c-**d**-e-f-g)_n (Sobolev and Mesyanzhinov, 1991), with the **a** and **d** positions preferentially occupied by apolar residues and the *e* and *g* positions often occupied by charged residues. Such a motif, a characteristic feature of coiled–coils, is widely distributed (Cohen and Parry, 1994). A major part of the *gpwac* sequence, starting around residue 50 and ending at residue 460, divides into 13 continuous coiled–coil regions that are linked by the short segments without heptad repeats (Efimov *et al.*, 1994). Analysis has shown also that fibritin is a homotrimer assembled in

parallel and attached to the T4 neck by the terminal domain (Efimov *et al.*, 1994).

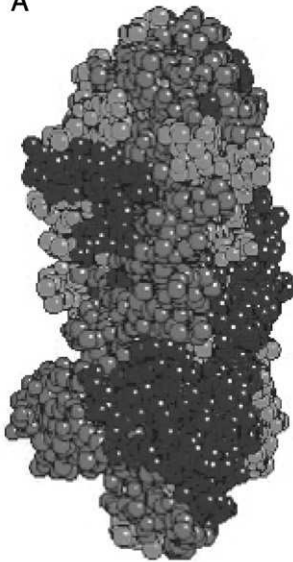
Recombinant fibrinitins truncated at the N termini, expressed in *E. coli* from plasmids, were soluble and assembled into rigid filamentous particles, and, according to CD spectroscopy, exhibited a high content of α -helical secondary structure. Surprisingly, recombinant fibrinitin with short (18 residues) and C-terminal deletion was completely insoluble, forming nonspecific aggregates (Boudko *et al.*, 2002; Efimov *et al.*, 1994; Letarov *et al.*, 1999). We called the C-terminal domain a “foldon” or folding nucleus, a unit required for fibrinitin folding and assembly, providing correct alignment of three subunits. Foldon is a protein unit that forms on the initial steps of folding (Yu and King, 1984) and that remains intact even after it is isolated or transferred into other proteins (Inaba *et al.*, 2000; Panchenko *et al.*, 1996; Wakasugi *et al.*, 1994; Yanagawa *et al.*, 1993).

It is difficult to crystallize the entire length of fibrinitin, which is a rather flexible protein needed to accomplish its functions in the phage. However, several N-terminally truncated mutants were successfully crystallized (Strelkov *et al.*, 1997), and structures of two of them, fibrinitin E (Fig. 9) and fibrinitin M, were solved to atomic resolution by X-ray crystallography (PDB codes 1aaO and 1AVY, respectively) (Strelkov *et al.*, 1998; Tao *et al.*, 1997). Fibrinitin E is a truncated molecule that comprises the last 119 residues and fibrinitin M of the last 74 residues. The structures successfully confirmed early predictions for fibrinitin as a parallel trimeric coiled-coil with a small β -structural domain at the C terminus.

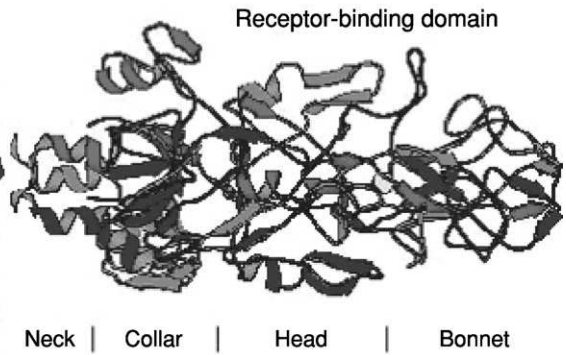
Three coiled-coil segments of fibrinitin E are separated by two loops: residues Gly386–Gly391 form the first one (L10), and the second one (L11) contains the residues Asn404–Gly417 (Tao *et al.*, 1997). Structure of fibrinitin E showed that loops do not interrupt coiled-coil continuation—the helical segments started at position **d** and ended at position **a** of a heptad repeat. Such an arrangement makes coiled-coil continuous—downstream helices almost exactly follow the continuation of the preceding ones (Fig. 10).

The C-terminal domain or foldon (Fig. 11) is a β -annulus-like structure formed by the last 30 C-terminal residues from each of the trimer subunits. The X-ray structure of fibrinitin E demonstrated that foldon residues form extensive hydrophobic and some polar interactions within and between subunits. The role of a foldon as a folding nucleus and its stabilizing action have been used recently to design several chimera proteins, including the T4 phage STFs and LTFs (Miroshnikov *et al.*, 1998, 2000), short collagen fragments (Boudko *et al.*, 2002b; Frank

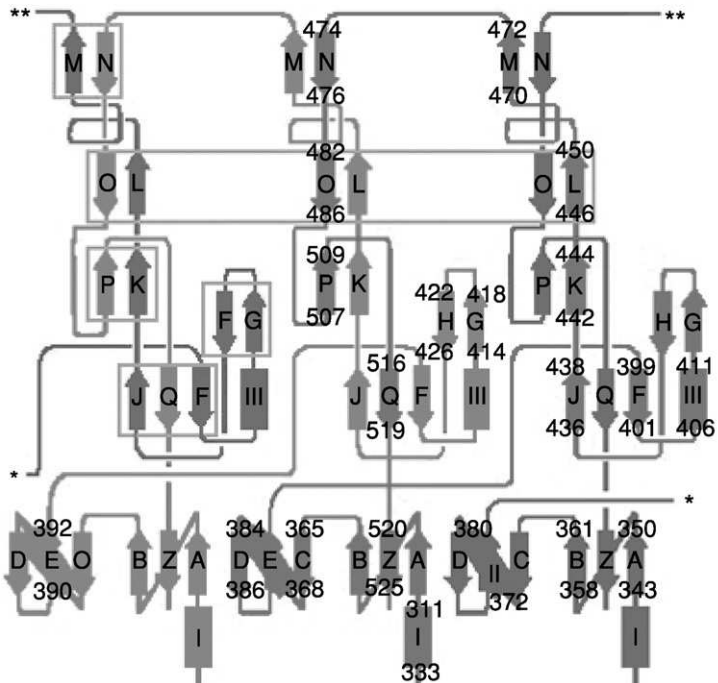
A



B



C



et al., 2001; Stetefeld *et al.*, 2003), the human adenovirus type 5 fiber protein (Kashentseva, *et al.*, 2002; Krasnykh *et al.*, 2001), and a stable trimeric form of a 140-kD protein of HIV-1 (Yang *et al.*, 2002). Such *de novo* engineered proteins can be used for a variety of applications, including the study of receptor-ligand recognition.

V. THE BASEPLATE STRUCTURE

Practically every assembled T4 particle is able to infect an *E. coli* host cell, probably as a consequence of a contractile tail sheath–baseplate complex. The baseplate is the control center of the viral infectivity, that communicates between the tail fibers, which sense host-cell receptors,

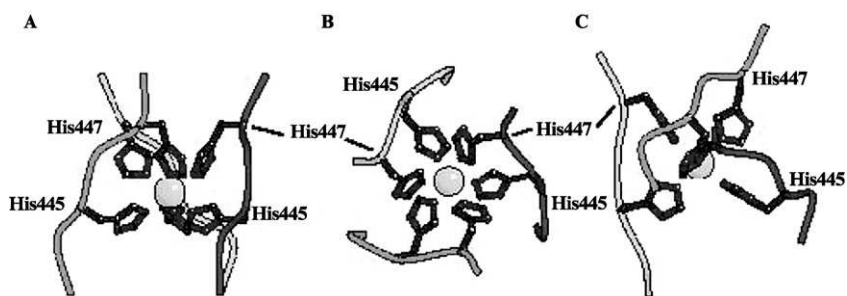


FIG. 8. (A) The zinc ion in the center of the receptor-binding domain. Shown are the main chains of the three monomers (residues 443–448 in each case) in yellow, red, and green and the side chains of the ligating His residues. The coordination is octahedral with Zn–His445 NE2 distance of 2.22 Å and a Zn–His447 NE2 distance of 2.25 Å. (B) Views from the top down the threefold axis. (C) View down one of the fourfold axes of the octahedron formed by the NE2 atoms of the six ligating His residues. From Thomassen *et al.* (2003). (See Color Insert.)

FIG. 7. Structure of the ordered region of the 45-kDa fragment of STF. (A) Space-filling model of the structure illustrating the extensive intertwining in the receptor-binding domain. (B) Ribbon diagram in the same orientation as Fig. 7A. At the bottom is shown the neck region (the α -helical residues 336–339) and the middle collar region (residues 340–396 plus 518–527); at the top is shown the metal-containing receptor-binding domain (residues 397–517), which is divided into the head and bonnet. (C) Topology diagram. Alpha-helices are marked I, II, and III, and β -strands are A to Q (excluding I) and Z. Beginning and end residues of the secondary structure elements are numbered in one of the monomers (not always the same one to avoid overlaps). Gray boxes surround the six-stranded β -barrel domain and the other smaller β -sheets. In the 3-D structure, the blue loops marked with a * connect, as do those marked **. From Thomassen *et al.* (2003). (See Color Insert.)

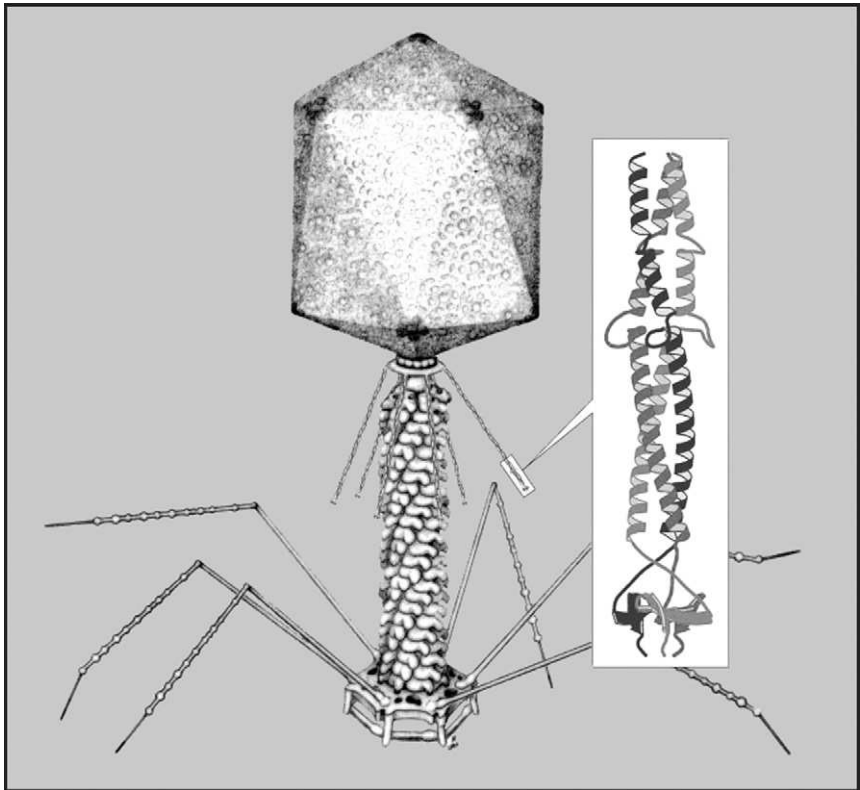


FIG. 9. Bacteriophage T4, with the fibrin whiskers shown in color (Tao *et al.*, 1997). On the right is an enlarged ribbon diagram of fibrin E. (See Color Insert.)

and the tail sheath, which contracts to eject the viral DNA into the host. Understanding of the baseplate structure, a multiprotein machine, is a challenging problem.

Crowther *et al.* (1977) were able to establish the approximate position of gp9, gp11, and STF by comparing negative-stained electron microscopy images of the wild-type and mutant baseplates that lacked respective proteins. Using chemical cross-linking and a gold-labeled antibody, the contacts between neighboring baseplate proteins were studied (Watts and Coombs, 1990; Watts *et al.*, 1990). Other electron microscopy studies using image processing (Makhov *et al.*, 1993; Veprintseva *et al.*, 1980) indicated that the STFs are located around the edge of the hexagonal baseplate and are either fully extended along the edge or are folded back upon themselves.

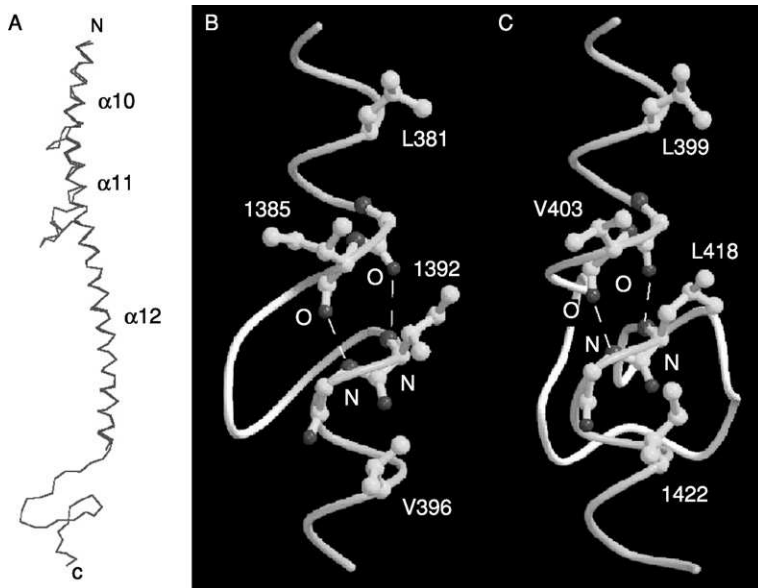


FIG. 10. Insertion loops in the coiled-coil region of fibrin E. (A) Superposition of the fibrin E C α backbone (blue) onto an ideal structure (red), which is calculated from parameters defining helix α -12. (B, C) The arrangement of hydrophobic side chains and hydrogen bonds at the insertion loops L10 and L11 (the two chains are rotated by 50° and 100° about the coiled-coil axis relative to Fig. 10A, respectively). From Tao *et al.* (1997). (See Color Insert.)

A. Structure of Baseplate Proteins

1. Protein gp9

The gp9 is a structural protein of the T4 baseplate that connects the LTFs (Crowther, 1980; Urig *et al.*, 1983). The association of the proximal part of the LTFs with gp9 is helped by the T4 encoded chaperone-like protein, gp63 (Wood and Conley, 1979). After attachment of the LTFs to the LPS receptors on an *E. coli* cell surface, gp9 initiates a baseplate structural transition to a six-pointed star with subsequent tail sheath contraction and injection of the T4 DNA into the cell (Crowther *et al.*, 1977). Protein gp9 also has stabilizing action on the baseplate, preventing its abortive triggering (Crowther, 1980).

Another gp9 function is to allow for the “up” and “down” movements of the LTFs. When the LTFs are attached to the baseplate, they can adopt two distinct configurations, designated as “up” and “down” (Kellenberger *et al.*, 1965). In the down position, the LTFs are extended

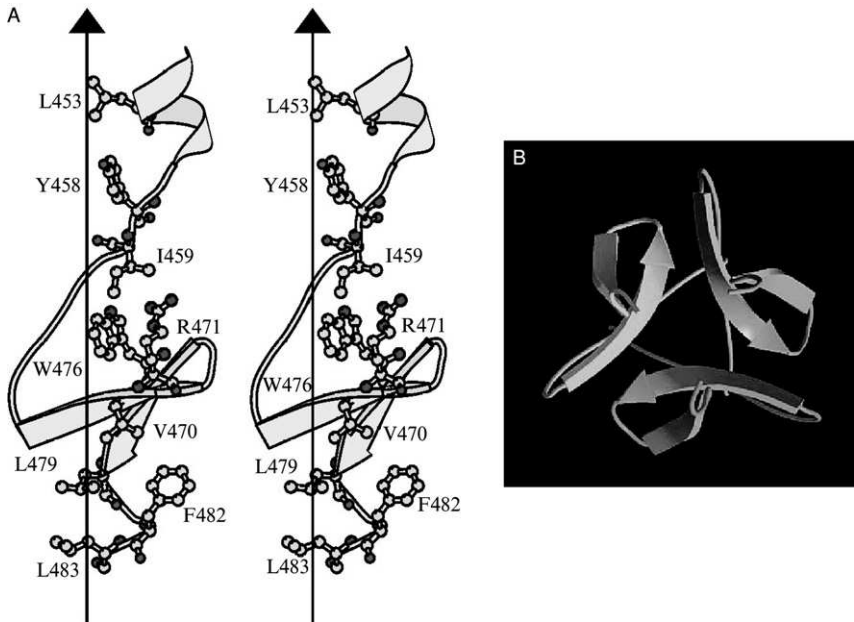


FIG. 11. The C-terminal domain (foldon) of fibrin E. (A) Stereo diagram of the C-terminal domain of a fibrin E subunit. The side chains shown are those located in the hydrophobic interior formed at the interface between three symmetrically related subunits. The vertical line shows the trimer axis. Atoms are shown in standard colors. (B) Ribbon diagram of the C-terminal domain looking along the trimer axis; each subunit is shown in a different color. From Tao *et al.* (1997). (See Color Insert.)

and able to interact with their cell surface receptors and initiate infection. At acidic pH or low temperature, the LTFs are retracted into the up configuration and are close to the tail sheath of the virus particle. In the latter case, the virus is not infectious because the distal parts of the LTFs, which recognize the LPS receptors, are not able to interact with the bacterial cell surface. At optimal conditions when T4 phage has highest infectivity, equilibrium exists between the up and down configurations. Kellenberger *et al.* (1996) suggested that the baseplate determines the collective behavior of the LTFs by fixing the hinge angle around which the fibers can oscillate freely. Hence, gp9 might be required to regulate the up and down positions of the LTFs.

Recombinant gp9 expressed in *E. coli* cells from a plasmid vector is functionally active and is able to incorporate into the gp9 defective particles, converting them into an infectious phage *in vitro* (Navruzbekov *et al.*, 1999). The structure of gp9 has been solved to

2.3-Å resolution by X-ray crystallography (PDB code 1QEX). (Kostyuchenko *et al.*, 1999). Functionally active protein, like phage P22 tail-spike protein (Betts and King, 1999), is a SDS-resistant trimer assembled in parallel, with overall dimensions of $60 \times 60 \times 130$ Å (Fig. 12). The X-ray crystallographic data show that the gp9 polypeptide chain of 288 amino acid residues forms a trimer with three discrete domains: the N-terminal coiled-coil (residues Met1–Gln59 in which residues Thr20–Asn40 formed a coiled-coil structure with two Phe residues in a hydrophobic core), middle coil (Ile60–Pro164), and C-terminal coil (Ala175–Gln288).

The N-terminal sequence (Met1–Thr20) has an irregular secondary structure that folds down antiparallel to the coiled-coil structure in the direction of the middle domain. The middle domain is a seven-stranded β -sandwich. It represents a unique protein fold that does not form essential interactions between monomers in the trimer. The C-terminal domain is an eight-stranded, antiparallel β -barrel with a slight resemblance to the jelly-roll virus capsid structure found in

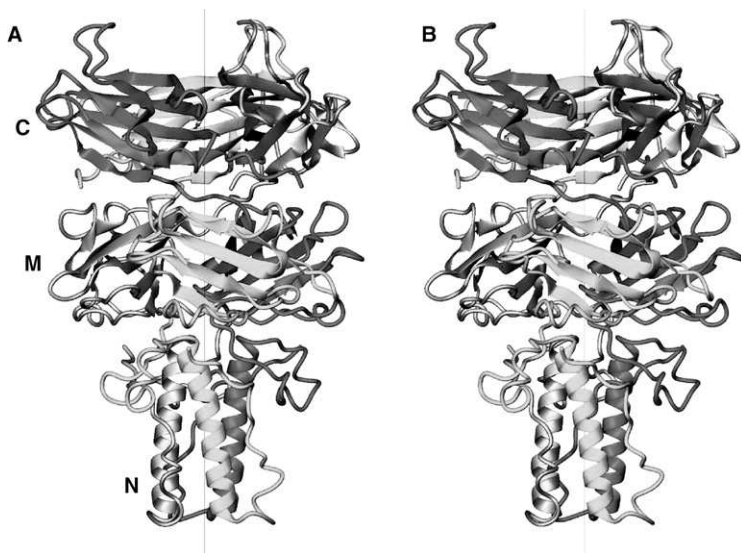


FIG. 12. Crystal structure of gp9. (A) Stereo view of the trimer structure solved by X-ray crystallography. The N-terminal, middle, and C-terminal domains are designated by letters N, M, and C, respectively. (B) Ribbon diagram of the gp9 trimer looking along the trimer axis from the coiled-coil part. [This figure was drawn by S. V. Strelkov using the program DINO (<http://www.dino3d.org>)]. From Kostyuchenko *et al.* (1999). (See Color Insert.)

numerous plant and animal viruses (Liljas, 1999; Rossmann and Johnson, 1989). Residues Met167–Ser173 connect the middle domain with the C-terminal domain by an extended chain that makes hydrogen bonds with neighboring monomers and may provide mobility of the domains relative to each other (Kostyuchenko *et al.*, 1999). The N-terminal and middle finger domains are on the same side of the trimer threefold axis. However, the C-terminal domain has been rotated near Pro174 by approximately 120° around the triad axis relative to the N-terminal and middle finger domains (Kostyuchenko *et al.*, 1999). The change in position of the C-terminal domain gives rise to a swapping domain topology (Liu and Eisenberg, 2002) of the three adjacent monomers in the gp9 trimeric protein like in the STFs.

The C-terminal apex of the gp9 trimer has a diameter of about 60 Å. The charge distribution, looking along the threefold axis, shows three symmetrically related clusters of high negative charge arising from the sequence Glu243-Thr-Glu-Glu-Asp-Glu. This loop might be required to bind the LTF to the gp9.

2. Protein gp11

The gp11 protein is required for assembly of the STFs into the baseplate (Edgar and Lielausis, 1968). Both gp11 and gp12 can be added to otherwise complete 11^- virus particles to produce an infectious phage, indicating that gp11 binds to the baseplate's periphery. Crowther *et al.* (1977) compared the negatively stained electron microscopy micrographs of the native and $gp11^-$ baseplates and concluded that gp11 is located at the outer rim. The gp11 forms an equimolar complex with gp10 [(gp10)₃ – (gp11)₃] *in vitro*, which is active in the *in vivo* complementation (Zhao *et al.*, 2000).

The crystal structure of recombinant gp11 active in *in vitro* complementation (Kurochkina *et al.*, 2001) was determined to 2.0-Å resolution as shown in Figs. 13 and 14 (PDB number 1EL6) (Leiman *et al.*, 2000). The refined atomic model of gp11 consists of 208 out of 218 residues (Ser12 to Ala219). The gp11 is a homotrimer with approximate dimensions $78 \times 78 \times 72$ Å. Each gp11 monomer has three domains: the first is the N-terminal α -helical domain (residues 12–64), the second is the middle or distal domain “finger” (residues 80–188), and the third C-terminal domain is formed by residues 65–79 and 189–219 (Fig. 13). A search for folds homologous to gp11 using the program DALI (Holm and Sander, 1993) have shown no significant similarity to any other structure in the PDB.

The N-terminal α -helical domain of gp11 forms a parallel, trimeric coiled-coil (Fig. 14). This domain of 12-residue-long is located at the center of the molecule and is surrounded by the three NSC-related finger domains and the three C-terminal domains. The finger domain (Fig. 13) is a seven-stranded, antiparallel, and skewed β -roll containing one long α -helix.

The threefold-related C-terminal domains of gp11 monomers generate a threefold β -annulus structure that appears in proteins of small plant viruses (Abad-Zapatero *et al.*, 1980; Harrison *et al.*, 1978). The bacteriophage T4 fibritin has also a similar threefold β -annulus domain functioning as a foldon (Letarov *et al.*, 1999; Tao *et al.*, 1997). The formation of this structure is promoted by an inter-C-terminal domain within the trimer (Fig. 15). The hydrogen-bonding network of the gp11 C-terminal domain is more extensive than in T4 fibritin. There is an external hydrophobic region on each annulus in both structures. These similarities suggest that this domain is essential for gp11 trimerization as well.

3. Protein gp8

The gp8 is also a structural protein of the baseplate wedge (Kikuchi and King, 1975a). The gp8 monomer has 334 residues (Efimov *et al.*, 1990). Analytical ultracentrifugation and cross-linking analysis indicate that gp8 is a dimer in solution (Shneider *et al.*, 2001; Watts and Coombs, 1989). On the stage of wedge assembly, gp8 binds to the (gp11)₃-(gp10)₃-gp7 complex, creating a binding site for gp6. The assembly pathway is strictly ordered, and gp8 does not form a complex with gp10 in the absence of gp7 (Plishker *et al.*, 1988). Although only the LTFs and STF were shown to interact with the host-cell receptors (Riede, 1987; Wilson *et al.*, 1970), mutations in several baseplate proteins, including gp8, can influence the host preferences of T4 phage of different *E. coli* strains (Georgopoulos *et al.*, 1977).

A 2.0-Å resolution X-ray structure of gp8 shows that the two-domain protein forms a dimer in which each monomer consists of a three-layered β -sandwich with two loops, each containing an α -helix at the opposite sides of the sandwich shown in Fig. 16 (PDB numbers 1N80, 1N8B, and 1N7Z). (Leiman *et al.*, 2003). The monomer structure can be divided into two domains: residues 1–87 and 246–334 forming domain I and residues 88–245 forming domain II. A search for folds homologous to gp8 showed no significant similarity to any other structure in the PDB.

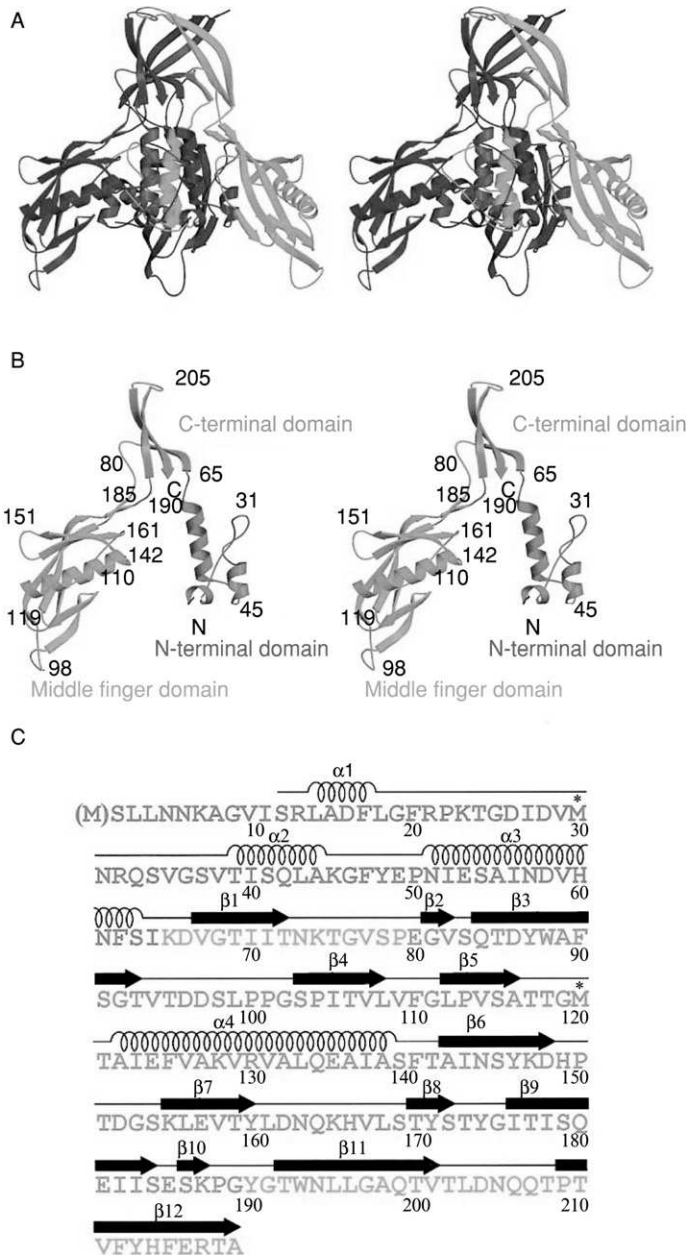


FIG. 13. X-ray structure of gp11. (A) Stereo ribbon diagram of the gp11 trimer. The monomers A, B, and C are colored red, green, and blue, respectively. (B) Stereo ribbon

4. The gp27–gp5 Complex Structure

Proteins gp5 and gp27 have been identified as the structural proteins of the baseplate central hub (Kikuchi and King, 1975c). These proteins formed a stable complex *in vivo* and *in vitro*. The lysozyme activity of the T4 baseplate was attributed to the lysozyme domain of gp5 required for digestion of the cellular peptidoglycan layer during the initial stages of infection (Nakagawa *et al.*, 1985). Protein gp5, therefore, was called a “tail lysozyme” that has 43% sequence identity with the cytoplasmic soluble T4 lysozyme, coded by gene *e* (Matthews and Remington, 1974). After incorporation into the baseplate, gp5 undergoes a self-cleavage between Ser351 and Ala352. Both resulting parts, the N-terminal (gp5*) and the C-terminal (gp5C) (Fig. 17), remain in the phage particle (Kanamaru *et al.*, 1999). The gp5 C-terminal domain, gp5C, is a SDS-resistant trimer containing 11

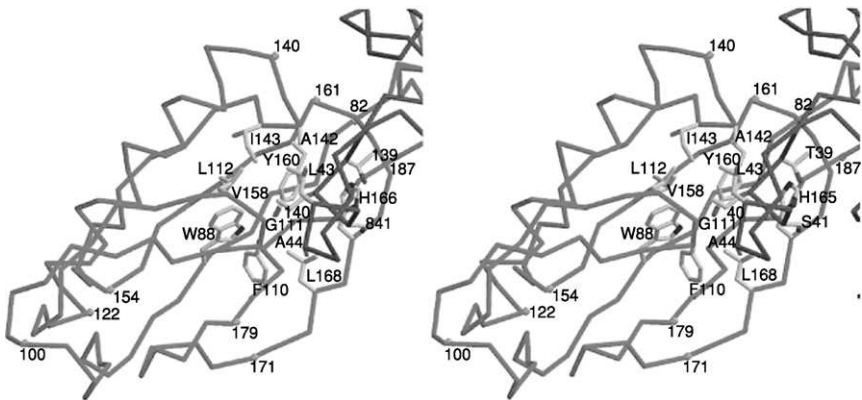


FIG. 14. The gp11 finger domain. Stereoscopic view of the interactions (white residues) between the finger domain of monomer B (green) with the N-terminal domain helix $\alpha 2$ of monomer A (red). Orange labels identify strategic positions in the finger domain. The backbone color code is as in Figs. 13A and 13B. Reprinted from Leiman *et al.* (2000). (See Color Insert.)

←

diagram of the gp11 monomer with the N terminus shown in light blue, the C terminus in orange, and the middle finger domain in olive green. Amino acid sequence numbers are indicated at strategic locations. (C) Amino acid sequence of gp11. Secondary structure elements are shown above the sequence entries. The domains are colored as in Fig. 14A. The Se-labeled Met residues are marked with an asterisk. The post-translationally cleaved formyl-methionine residue is in parentheses. Reprinted from Leiman *et al.* (2000). (See Color Insert.)

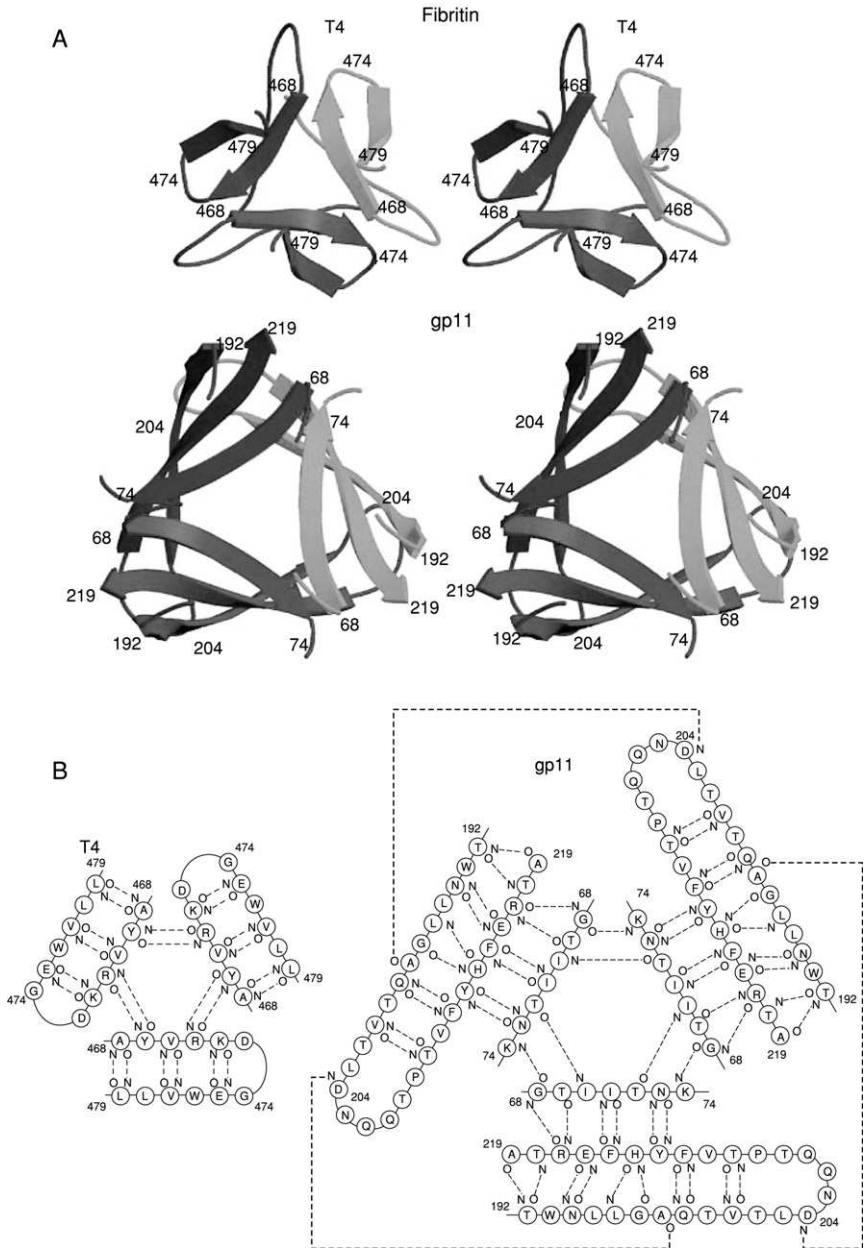


FIG. 15. Comparison of the structures of T4 fibrin and gp11. (A) Stereoscopic view of the similar C-terminal, β -annulus domains of fibrin (Top) and the gp11 trimer (Bottom).

ValXGlyXXXXX octapeptide repeats (Kanamaru *et al.*, 1999; Mosig *et al.*, 1989). Protein gp5C is responsible for trimerization of the entire gp5–gp27 complex that consists of nine polypeptide chains (gp27-gp5*-gp5C)₃ once the cleavage of gp5 has occurred (Kanamaru *et al.*, 1999) (Fig. 17).

The structure of the gp5–gp27 complex has been determined to 2.9 Å resolution as shown in Fig. 18 (PDB number 1K28) (Kanamaru *et al.*, 2002). The overall structure of this complex resembles a 190-Å long torch. The gp27 trimer form the torch's cylindrical "head," and the gp5C trimer represents the "handle." Three gp27 monomers are assembled into a hollow cylinder with a length of 60 Å and internal and external diameters of about 30 Å and 80 Å, respectively. This structure encompasses the three N-terminal domains of gp5* to which the trimeric gp5C is attached. The C-terminal parts of the three gp5C chains are intertwined and folded into a rigid β -helical prism. The middle lysozyme domains surrounded the amino end of the prism. The gp27 monomer of 319 residues is folded into four domains (Fig. 18B). Two domains (residues 2–111 and residues 207–239 plus residues 307–368) created a torus-like structure at the top of the gp5–gp27 complex torch. These two gp27 domains have similar seven- or eight-stranded, anti-parallel β -barrel structures and can be superimposed onto each other with RMSD of 2.4 Å between the equivalence C α atoms. Therefore, the top of the gp27 cylinder is terminated with a pseudo-sixfold-symmetric torus. Although there is no significant sequence similarity between these domains (4% sequence identity only), their external surfaces are mostly hydrophobic, and the charge distributions are similar (Fig. 18C). Thus, the gp27 trimer can form an interface between the hexameric baseplate and trimeric gp5. The internal and external surfaces of the gp27 cylinder match the dimensions of the tail tube, suggesting that the gp27 trimer may serve as an extension to the 90-Å-diameter tail tube. The other two gp27 domains, formed by residues 112–206 and residues 240–306 plus 359–376, bind to the two adjacent N-terminal domains of gp5*, thus promoting assembly of the oligomeric gp5–gp27 complex. The interface between gp27 and gp5* is formed by complementary polar and charged residues, with the surface of gp27 being mostly positively charged and the surface of gp5* being mostly negatively charged.



The different monomers are colored red, blue, and green. (B) The hydrogen-bonding network in the β -annulus of fibrin (Left) and gp11 (Right). Reprinted from Leiman *et al.* (2000). (See Color Insert.)

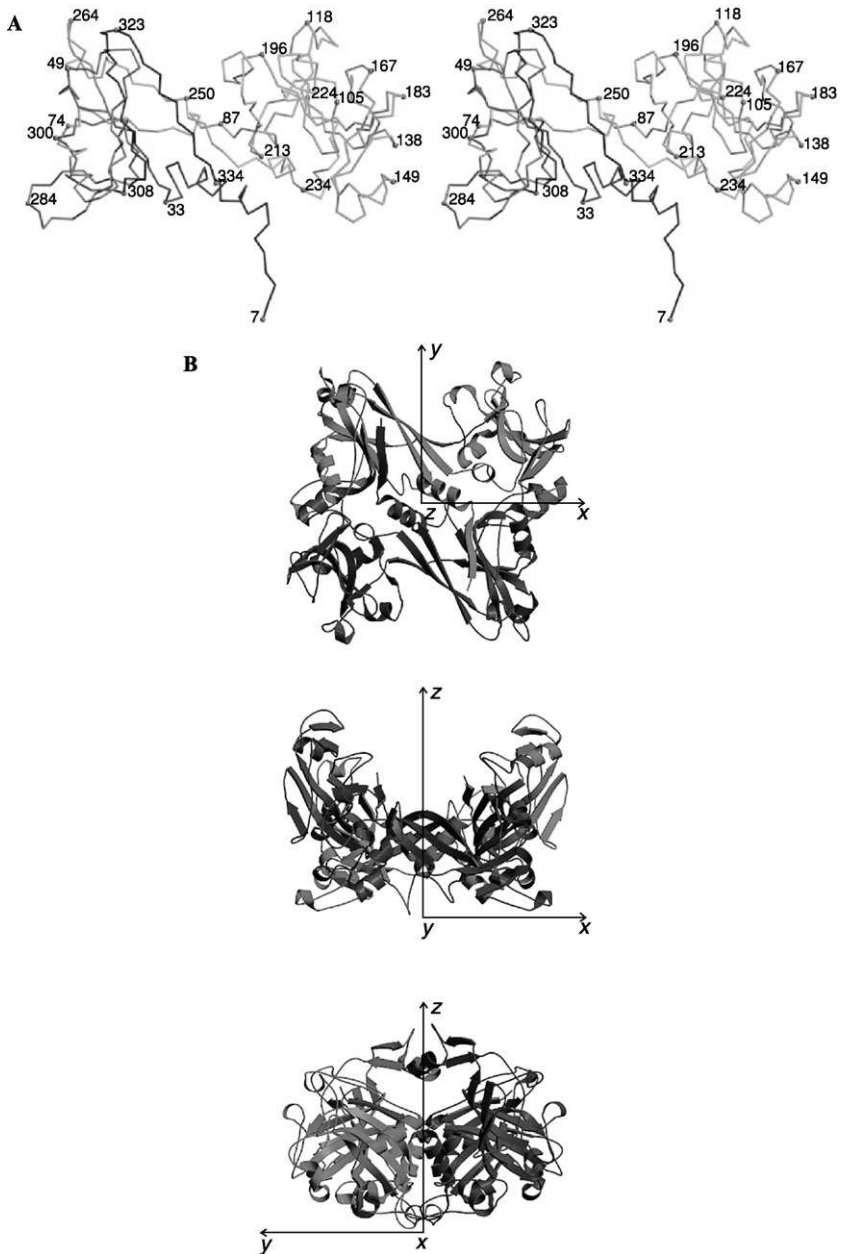


FIG. 16. The gp8 structure. (A) A stereo diagram of the gp8 monomer C α trace with the N terminus in blue, the C terminus in red, and the intermediate residues changing color in spectral order. Amino acid sequence numbers are indicated at strategic locations.

The gp5* monomer has two domains, an N-terminal and a lysozyme (Fig. 18A). The N-terminal domain (residues 1–129) is a five-stranded, antiparallel β -barrel and has the oligonucleotide/oligosaccharide-binding (OB) fold (Murzin and Chothia, 1992). In the OB-type proteins, the OB-binding interface usually contains a cluster of aromatic and

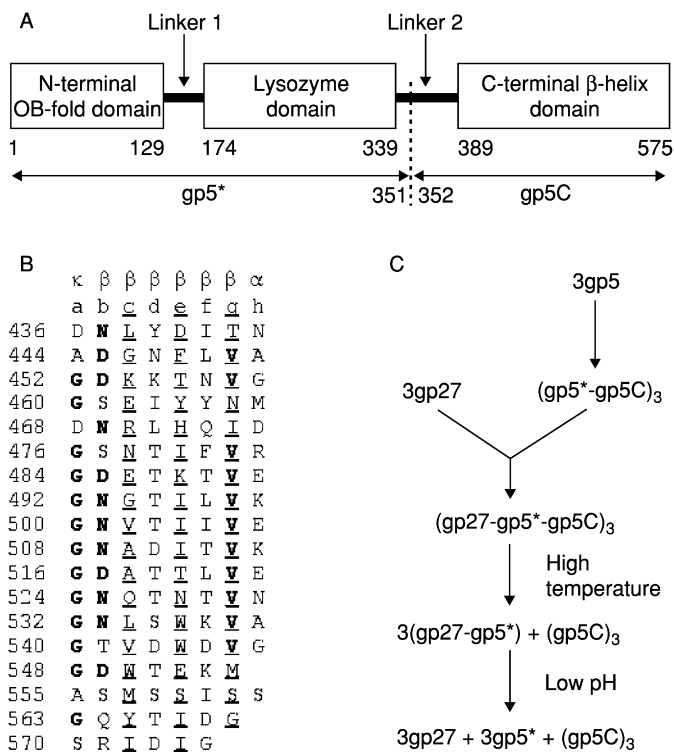


FIG. 17. Assembly of the gp5–gp27 complex. (A) Domain organization within the gp5 monomer. The maturation cleavage is indicated by the dotted line. Initial and final residue numbers are shown for each domain. (B) Alignment of the octapeptide units comprising the intertwined part of the C-terminal β -helix domain of gp5. Conserved residues are in bold print; residues facing the inside are underlined. The main chain dihedral angle configuration of each residue in the octapeptide is indicated at the top by κ (kink), β (sheet), and α (helix). (C) Assembly of gp5 and gp27 into the hub and needle of the baseplate. Reprinted from Kanamaru *et al.* (2002) with permission.

(B) A ribbon diagram of the gp8 dimer. Three orthogonal orientations are shown. The two monomers are colored red and blue. Reprinted from Leiman *et al.* (2003a). (See Color Insert.)

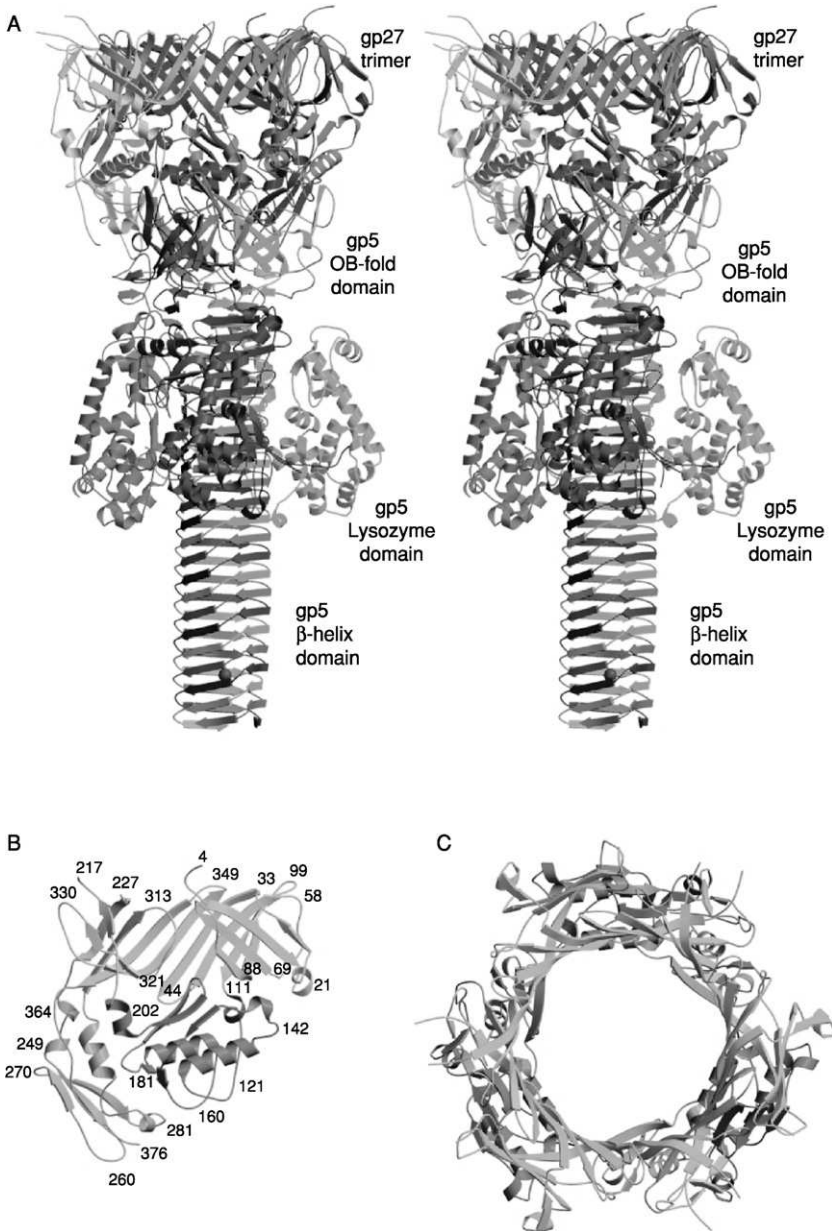


FIG. 18. Structure of the gp5–gp27 complex. (A) Ribbon stereo diagram. The three gp5 monomers are colored red, green, and blue. The three gp27 monomers are colored yellow, gray, and purple. The metal ion within gp5C is shown in pink. The phosphate is hidden

positively charged residues. Residues of these types, such as Trp10, Arg81, Tyr83, His85 and Tyr100, form interactions between the threefold-related gp5 N-terminal domains. The surface that is formed by these residues roughly corresponds to the lactose-binding site in an OB fold protein heat-labile enterotoxin (LT). Although the sequence identity between the enterotoxin LT and the gp5 N-terminal domain is only 4%, they can be superimposed onto each other with RMSD of 2.7 Å between 52 structurally equivalent C α atoms (Kanamaru *et al.*, 2002; Leiman, 2003). The putative oligosaccharide-binding region in the N-terminal domain of gp5 suggests that this domain might facilitate binding of gp5* to oligosaccharides of the periplasmic peptidoglycan layer for its digestion by the lysozyme domain. Furthermore, to activate the oligosaccharide-binding interface, gp5* may separate from the baseplate when the tail tube enters the periplasmic space.

The gp5 lysozyme domain, located on the periphery of the central β -helix, is connected to the N-terminal domain via linker 1 and to gp5C via linker 2, which contains the cleavage site between gp5* and gp5C (Fig. 17A). The exact location of the cleavage site is not visible in the crystal structure because seven residues upstream and nine residues downstream of the cleavage site are disordered.

The structures of the gp5 lysozyme domain and T4L (Kuroki *et al.*, 1993) can be superimposed onto each other with RMSD of 1.1 Å, except for five extra residues in gp5. The two residues, Val211-Arg212, are located near the catalytic cleft exit, while other three-residue insertions, Asn232-Pro233-Gly234, are located in close proximity to the β -helix. Both enzymes have identical residues in their active sites, suggesting that the enzymatic mechanism is the same and that both molecules probably have a common evolutionary origin. Structural comparison with T4L also shows that residues Pro363-Ala364-Asp365, belonging to linker 2, bind into three of the four peptide binding sites on the threefold-related neighboring subunit of gp5, but they leave the catalytic polysaccharide-binding cleft open to solution. This peptide-binding site is used by the peptidoglycan substrate in T4L. The other side of the polysaccharide-binding cleft is sterically blocked by the β -helix. These observations explain the lack of activity of the trimeric (gp5*-gp5C)₃ complex compared to monomeric gp5* (Kanamaru *et al.*, 1999).



behind the lysozyme domain. (B) The structure of the gp27 monomer with its 4 domains colored cyan, pink, light green, and gold along the polypeptide chain. Residue numbers are indicated in strategic locations. (C) Top view of the gp27 cylinder with the cyan and green domains forming a hexagonal torus. Reprinted from Kanamaru *et al.* (2002) with permission. (See Color Insert.)

The most remarkable part of gp5 is the triple-stranded β -helix, formed by three chains of gp5C wound around a central crystallographic threefold axis and creating an equilateral triangular prism, which is 110 Å in length and, on average, 28 Å in diameter (Fig. 19). The β -strands run roughly orthogonal to the prism axis. Each face of the prism has a slight left-handed twist (-3° per β -strand), as is usually observed in the β -sheets. The width of the prism face narrows gradually from 33 Å at the amino end to 25 Å at the C-terminal end and creates a pointed needle-like structure. This narrowing is caused by a decrease in size of the external side chains and by the internal Met554 and Met557 residues, which break the octapeptide repeat near the tip of the helix (Fig. 17C).

The first five β -strands of gp5C (residues 389–435) form an antiparallel β -sheet, creating one of the three prism faces. A similar β -sheet prism domain has been observed in the central portion of the phage P22 tail spike protein (Seckler, 1998; Steinbacher *et al.*, 1994). Unlike the hydrophobic interior of the P22 tail spike, however, the interior of gp5 β -sheet prism is mostly polar. The succeeding 18 gp5 β -strands form a three-start β -helix. Each chain makes six complete turns along the helix length. These intertwined strands (residues 436–575) generate a remarkably smooth continuation of the nonintertwined N-terminal β -sheet prism (residues 389–435) (Fig. 19).

The octapeptide sequence of the intertwined part of the β -helix (residues **a** through **h**) has Gly residues at position **a**, Asn or Asp residues at position **b**, Val residues at position **g**, and polar or charged residues at position **h** (Fig. 17B). Residues **b** through **g** form the extended β -strands that run at an angle of 75° with respect to the helix axis (Fig. 19), whereas the Gly residues at position **a** and residues at position **h** kink the polypeptide chain by about 130° clockwise.

The inside of the β -helix is progressively more hydrophobic toward its C-terminal tip. The middle part of the helix has a pore containing at least 42 water molecules bound to polar and charged side chains. The helix is stabilized by two ions situated on the helix symmetry axis. Three Lys454 residues coordinate an anion, which is probably a phosphate (HPO_4^{2-}) as judged by the size of the density peak and the threefold symmetry of the amino acid environment. The other ion is a cation with a van der Waals radius larger than 2 Å and coordinated by three Glu552 residues. Potential candidates are Na, Mg, K, and Ca. This ion is buried in the hydrophobic environment where it neutralizes the negative charge of three Glu552 residues (Fig. 19B), and it is presumably required for proper folding of the protein.

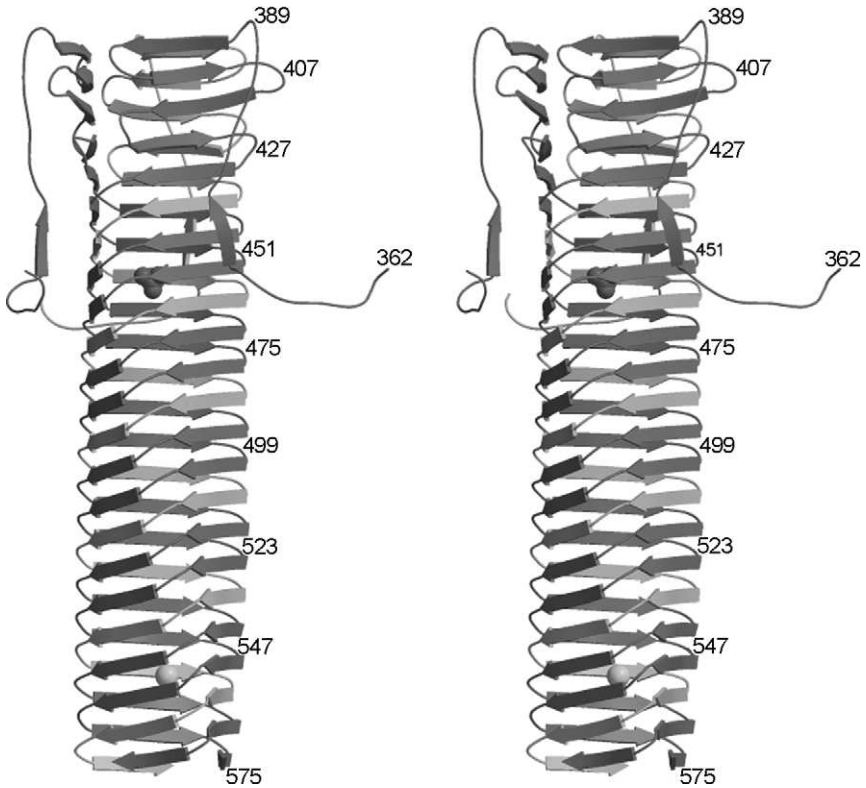


Fig. 19. Stereo diagram of the gp5 C-terminal domain (Rossmann *et al.*, 2004). The three gp5 chains are colored red, green and blue. The residue numbers are indicated in strategic locations. The metal and phosphate ions, stabilizing the internal contacts in the β -helix, are shown as yellow and magenta spheres, respectively.

The triple-stranded β -helix fold has also been observed in the structure of the bacteriophage T4 gp12 that forms the STF's (van Raaij *et al.*, 2001) (Fig. 7). Although the ribbon diagrams of the gp5 and gp12 β -helices look very similar, their structures have different properties. The gp5 β -helix has a well-defined octapeptide repeat with a common motif (Fig. 18B), whereas the gp12 helix lacks a repeating sequence motif. Moreover, the strands in the gp12 helix vary slightly in length (five to seven residues per strand), having a consensus of six residues. The inside of the gp12 helix is mainly hydrophobic, whereas the inside of the gp5 helix presents hydrophobic, polar, and charged patches. In addition, the gp5 helix contains water molecules and ions. It is unclear whether the two β -helices have a common evolutionary origin, but the

gp5 helix is designed to be a mechanically more rigid structure than the gp12 helix, which makes gp5 suitable as a molecular needle for puncturing the host membrane.

The structure of the gp5–gp27 complex suggests its function. The trimeric gp5–gp27 complex forms the central hub of the hexagonal baseplate. The gp27 cylinder is an extension of the tail tube that is continued by the three N-terminal domains of gp5 and terminated with a sharp tip formed by the β -helix. The three lysozyme domains surround the β -helix and are inactive until the infection starts. The 30 Å-diameter pore, formed by the gp27 cylinder, is large enough to accommodate a dsDNA molecule passing through it.

B. Overall Tail Tube–Baseplate Structure

For the first time, a 3-D structure based on a cryo-electron microscopy reconstruction of the baseplate with the attached tail tube was determined to a resolution of 12 Å (Kostyuchenko *et al.*, 2003). The baseplate–tail tube complex is produced by a double T4 amber-mutant that is defective in synthesis of gp18, the tail sheath protein, and gp23, the major capsid protein. A modified form of the program SPIDER (Frank *et al.*, 1996) was used to process the 945 selected particle images, to search for and refine the particle orientations, and, finally, to generate the 3-D reconstruction.

Based on the 3-D reconstruction data, it was possible to identify precisely the location of six oligomeric proteins whose X-ray crystallographic structures had been determined previously to atomic resolution (gp9, gp8, gp11, gp12, gp5, and gp27) (Kanamara *et al.*, 2002; Kostyuchenko *et al.*, 1999; Leiman *et al.*, 2000, 2003a; Thomassen *et al.*, 2003; van Raaij *et al.*, 2001). In addition, using previous genetic, biochemical, and structural data (Kikuchi and King, 1975c; Plishker and Berget, 1984; Watts *et al.*, 1990; Zhao *et al.*, 2000), another four structural proteins (gp7, gp10, gp48 or gp54, and gp19) were identified and their overall shape determined (Leiman, 2003).

Contrary to the earlier planar models of the baseplate as a hexagonal structure (Coombs and Arisaka, 1994; Crowther *et al.*, 1997), the cryo-electron microscopy reconstruction showed that the baseplate is dome-shaped. It is about 270 Å in length and 520 Å at its widest diameter around the dome's base (Fig. 20). The helical tail tube extends 940 Å from the top of the baseplate, and it has an outer diameter of 96 Å and an inner diameter of 43 Å. The rim of the dome is formed by six symmetry-related, arrow-like fibrous proteins about 340 Å in length and about 40 Å in width. At the center of the dome, along the

dome axis, is a needle-like structure of about 105 Å in length and 38 Å in width that was previously identified as belonging to the gp5–gp27 complex, a cell-puncturing device (Kanamaru *et al.*, 2002).

C. Location of Baseplate Proteins with Known Atomic Structures

The crystal structures of the individual oligomeric proteins fit well into the cryo-electron microscopy structures of the native baseplate (Kostyuchenko *et al.*, 2003). Thus, the regulation of the baseplate assembly is apparently based not on conformational changes of assembled proteins but is most probably the result of new site generation of the interaction proteins.

Although identification and positioning of the proteins with known X-ray structures (gp8, gp9, gp11, gp12, and gp5–gp27) in the cryo-electron microscopy density by visual inspection has been relatively easy, systematic computer searches have been carried out, not only to confirm the location of these proteins, but also to provide an assessment of the quality of the cryo-electron microscopy reconstruction and to determine the absolute hand of the map. The hand determination using the gp8, gp11, and gp12 crystal structures, for which the absolute hand was known, gave consistent results. However, fitting the gp5–gp27 complex gave little discrimination. Fitting of the gp5–gp27 complex into the cryo-electron microscopy density of the baseplate showed additional density at the tip of the gp5 β -structure, suggesting the presence of another protein with an approximate molecular mass of 23 kDa (Fig. 20D). This density may correspond to the hub protein gp26 of 23.4 kDa, whose presence in the baseplate remains uncertain (Leiman, 2003).

The STF is a club-shaped, flexible molecule about 340 Å in length (Makhov *et al.*, 1993). Six arrow-like structures around the rim of the dome (Fig. 20) are strongly reminiscent of the negatively stained image of an STF (Makhov *et al.*, 1993) and could be readily fitted with the crystal atomic structure of a trimeric C-terminal fragment (residues 246–527) of the STF (Fig. 21A). The shaft of the arrow head is kinked, changing its direction by about 90°, bending around gp11 (Fig. 20); its N terminus is attached to the next counterclockwise-associated arrow-head when viewed from the tail toward the head (Fig. 20C and 21A). Thus, the STFs packaging under the baseplate is consistent with one of the two possible arrangements suggested earlier based on analysis of images produced by conventional electron microscopy (Makhov *et al.*, 1993). The total length of the STF cryo-electron microscopy density is

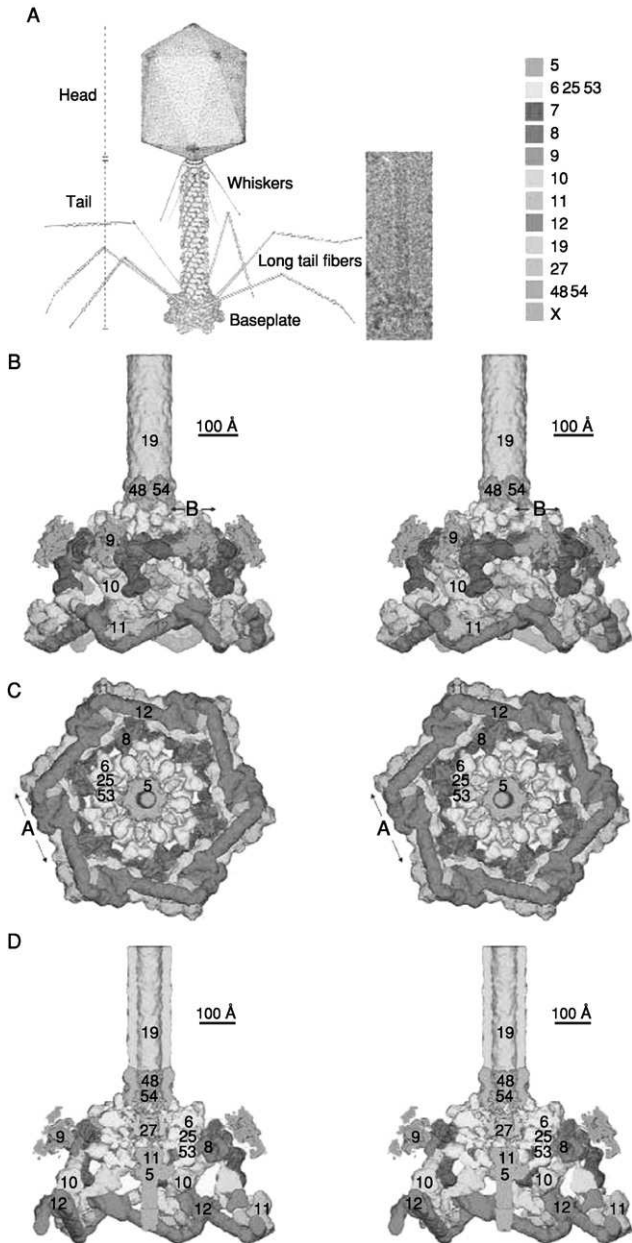


FIG. 20. Structure of the baseplate–tail tube complex. (A). Model of the T4 virus modified from Eislering and Black (1994) to include the new structural data. Also shown

about 340 Å. The known crystal structure of the C-terminal fragment is about 150 Å in length and includes an “arrowhead” domain that is 80 Å in length.

Apparently, the stability of the hexagonal baseplate is maintained by the interactions of the STFs with each other and gp11. In the absence of the STFs, the baseplate could easily switch to the star-shaped conformation (Crowther *et al.*, 1977). The garland of six STF wound around the gp11 vertices would seem to be a metastable configuration. On initiation of infection, the dissociation of the STFs garland should trigger the structural reorganization of the baseplate.

The structure of the three-fingered gp11 molecule (Leiman *et al.*, 2000) was recognized as being located at the vertices of the hexagonal rim of the baseplate dome (Fig. 20B). The gp11 trimer associates with the STFs (Fig. 22A) and a domain of another protein (Fig. 22B) that was identified as gp10, which is clamped between the three fingers of gp11. The kink of each STF is attached to the space between

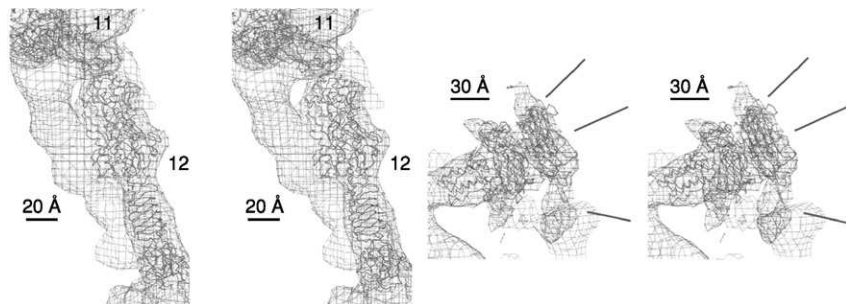


FIG. 21. Fit of the crystal structures, shown as $C\alpha$ traces, into the cryo-electron microscopy density. (A) The STFs (magenta) and a part of gp11 (cyan) viewed as area A in Fig. 20. (B) Protein gp9 (green) viewed as area B in Fig. 20. An intermediate and two extreme directions of the LTFs, as suggested by the orientations of the gp9 trimer, are shown as green, red, and blue lines, respectively. The orientation of the tail axis is vertical and is situated behind the display. Reprinted from Kostyuchenko *et al.* (2003) with permission. (See Color Insert.)

is a Cryo-EM image of the baseplate–tail tube complex. (B) Side view; (C) End view; (D) Cross-section. The baseplate and proximal part of the tail tube are shown. Colors identify proteins labeled with their respective gene numbers: spring green, gp5; beige, gp6+gp25+gp53; red, putative gp7; dark blue, gp8; green, gp9; yellow, putative gp10; cyan, gp11; magenta, gp12; salmon, gp19; sky blue, gp27; pink, putative gp48 or gp54; orange, unidentified protein X at the tip of gp5. The letters A and B correspond to areas viewed in Figs. 20A and 20B, respectively. Reprinted from Kostyuchenko *et al.* (2003) with permission. (See Color Insert.)

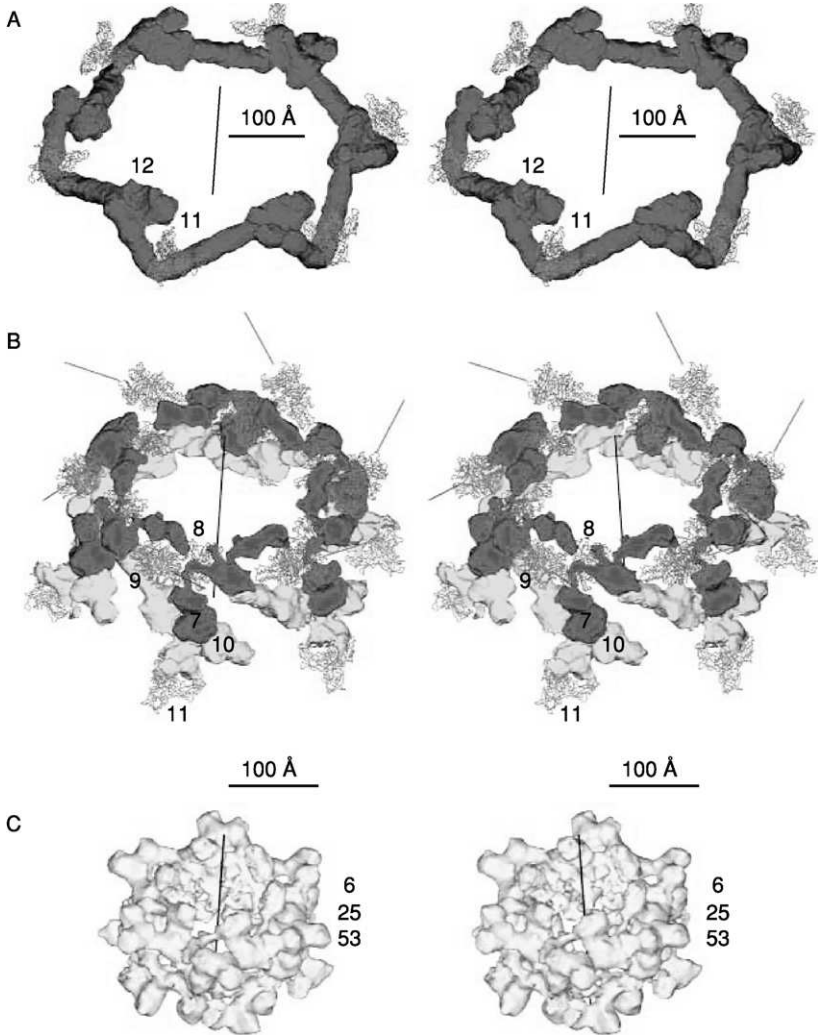


FIG. 22. Details of the baseplate structure. Proteins are labeled with their respective gene numbers. (A) The garland of the STF's (magenta) with gp11 structures (cyan $C\alpha$ -trace) at the kinks of the gp12 fibers. The black line represents the sixfold axis of the baseplate. (B) The baseplate "pins" composed of gp7 (red), gp8 (dark blue $C\alpha$ -trace), gp10 (yellow), and gp11 (cyan $C\alpha$ -trace). Shown also is gp9 (green $C\alpha$ -trace), the LTF attachment protein, with a green line along its threefold axis representing the direction of the long tail fibers. (C) Unassigned density around the center of the baseplate representing gp6, gp25, and gp53. Reprinted from Kostyuchenko *et al.* (2003) with permission. (See Color Insert.)

the central head domain and one of the fingers of the gp11 trimer (Fig. 22A). This arrangement is consistent with the baseplate assembly pathway in which the binding of the gp11 trimer is a prerequisite for the attachment of the STF to the baseplate (Kikuchi and King, 1975c). Although the C-terminal domains of gp11 and gp12 lack superimposable structural similarities, van Raaij *et al.* (2001) found that the arrangement of some of their β -strands is analogous, suggesting that gp11 may also perform the function of gp12-binding of the cellular LPS.

The four-footed structure of the gp8 dimer (Leiman *et al.*, 2003) was clearly recognizable in the baseplate 3-D reconstruction. The gp8 dimers located on the inside of the upper part of the baseplate dome, with their centers of mass at a radius of 139 Å (Fig. 20C), are in agreement with the previously published radius of approximately 130 Å determined by EM using immunogold labeling (Watts *et al.*, 1990).

The gp9 trimer is required for attachment of the long tail fibers to the baseplate (Crowther *et al.*, 1977). Using immunogold-labeling electron microscopy, it was shown that gp9 is located at the baseplate periphery near gp7 and gp10 (Coombs and Arisaka, 1994). The gp9⁻ phage particles lack the long tail fibers (Urige *et al.*, 1983) but can be complemented with recombinant gp9 to produce infectious fibered phage (Navruzbekov *et al.*, 1999). On Fig. 20B, there is a visible region of fragmented density on the upper outer edge of the 3-D image of the baseplate, about 180 Å from the baseplate axis. This density corresponds to the shape of the gp9 trimer (Kostyuchenko *et al.*, 1999), consistent with its rough location observed in negatively stained electron microscopy micrographs (Crowther *et al.*, 1977). This density, however, has an average value of less than one-half of that of the other fitted crystal structures and lacks accurate trimeric symmetry. The overall shape of the gp9 density suggests that the protein can pivot up to approximately 55° about a radial axis of the baseplate, perpendicular to the threefold axis of gp9 (Fig. 21B). The N-terminal coiled-coil domain of gp9 is associated with identified gp7 in the upper rim of the baseplate, whereas the C-terminal domain forms the colinear LTF attachment site.

D. Identification of Other Baseplate Proteins

Negatively stained electron microscopy micrographs have shown that the baseplate has six pins at the vertices, running roughly parallel to the long axis of the phage (Crowther *et al.*, 1977), although these are not readily apparent in the present cryo-electron microscopy

high-resolution 3-D reconstruction. These pins had been associated with gp7, gp8, gp10, and gp11 (Watts *et al.*, 1990). The 3-D map, however, has a density at each vertex that could be ascribed as the pins, running from the top of the dome near gp9, connecting with gp8, and then to gp11 (Fig. 22B). The parts of this density that have a triangular cross-section were assigned to be the gp10 trimer. This putative gp10 density also interacts with the three gp11 fingers, the N-terminal end of one STF molecule, and the C-terminal “arrow-head” of a symmetrically related STF molecule. The volume of the uninterpreted density in each pin corresponds to about 280 kDa, consistent with three gp10s subunits and one copy of gp7. The gp7 density consists of three connected domains, one of which interacts with the LTF attachment protein, gp9. The component of the pin density, associated with gp8 on the exterior of the baseplate (Watts *et al.*, 1990), was assigned to be gp7 (Kostyuchenko *et al.*, 2003) (Fig. 20 and 22B).

The gp54 of 35 kDa and gp48 of 40 kDa are necessary for initiation of tail tube and tail sheath assembly (Kikuchi and King, 1975c; Meezan and Wood, 1971). Attachment of gp48 precedes attachment of gp54 to the baseplate (King, 1971). The gp48 forms a 100-Å diameter platform on top of the baseplate, whereas attachment of gp54 to the baseplate does not change its morphology as observed by negative staining electron microscopy (King, 1971). Hence, density at the top and outside of the dome, where the tail tube and baseplate join, is likely to be the site of gp54 and gp48 (Figs. 20B and 20D). The volume of this density suggests that the associated monomer might have a molecular mass of 33 kDa, which would be consistent with the presence of at least gp48 or gp54. This protein connects the end of the tail tube with the top of the gp27 cylinder, a part of the cell-puncturing device. Furthermore, this protein creates a cap to the gp27 cylinder, thus also acting as a stopper to the end of the tail tube.

The remaining unassigned proteins in the baseplate are gp6 (molecular mass 74 kDa, with 6 or 12 copies per baseplate), gp25 (molecular mass 15.1 kDa, with 6 copies per baseplate), and gp53 (molecular mass 23 kDa, with 6 copies per baseplate). Removal of all the assigned protein density from the baseplate–tail tube reconstruction (Fig. 22C) gives a total volume per wedge corresponding to a molecular mass of 166 kDa. The proteins in the uninterpreted density presumably provide the nucleation site for the tail sheath polymerization. They form a platform on top of the baseplate, which resembles a layer of the tail sheath subunits, gp18 (King, 1971).

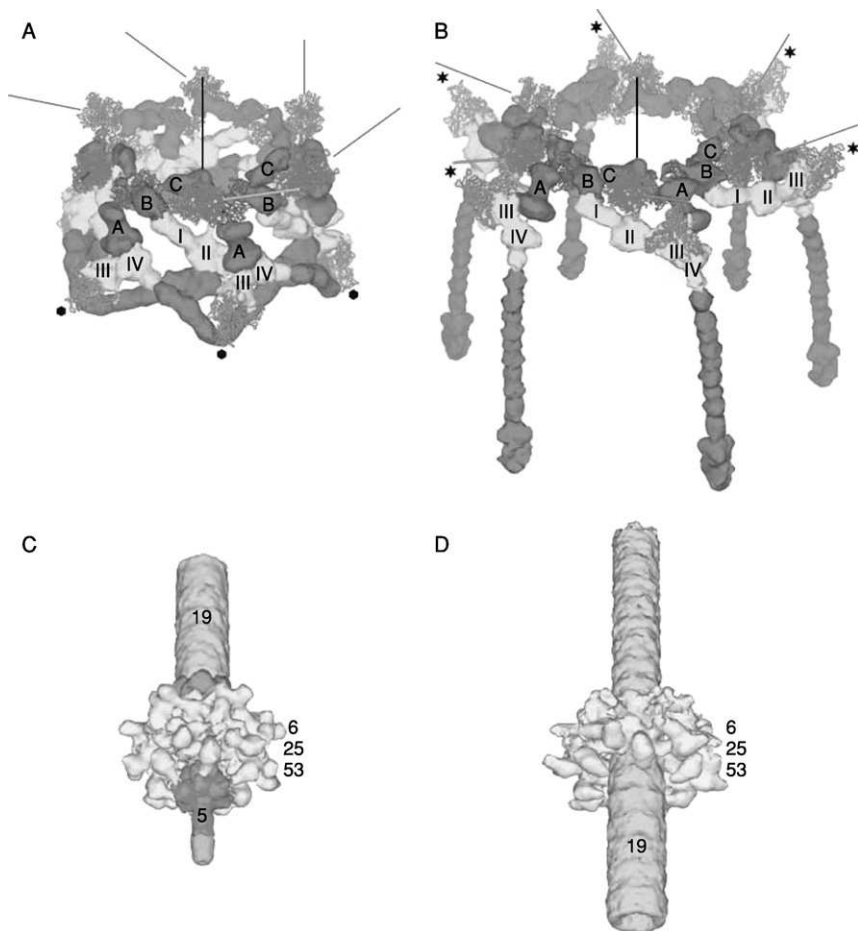


Fig. 23. Comparison of the baseplate in the two conformations (Leiman *et al.*, 2004). (A and B) Structure of the periphery of the baseplate in the hexagonal and star conformations, respectively. Colors identify different proteins: gp7 (red), gp8 (blue), gp9 (green), gp10 (yellow), gp11 (cyan), and gp12 (magenta). Three baseplate proteins (gp8, gp9, and gp11), with the available complete crystal structures, are shown as $C\alpha$ traces. The density of the short tail fibers in the star conformation is based on the crystal structure of the receptor binding, C-terminal fragment of gp12 (Thomassen *et al.*, 2003) and on the corresponding density from the hexagonal conformation of the baseplate. Directions of the long tail fibers are indicated with gray rods. The three domains of gp7 are labeled with letters A, B, and C. The four domains of gp10 are labeled with Roman numbers I through IV. The C-terminal domain of gp11 is labeled with a black hexagon or black star in the hexagonal or star conformations, respectively. The baseplate 6-fold axis is indicated by a black line. (C and D) Structure of the proteins surrounding the hub in the hexagonal and star conformations. The proteins are colored as follows: spring green, gp5; pink, gp19; sky blue, gp27; violet, putative gp48 or gp54; beige, gp6-gp25-gp53; orange, unidentified protein at the tip of gp5. A part of the tail tube is shown in both conformations for clarity. (See Color Insert.)

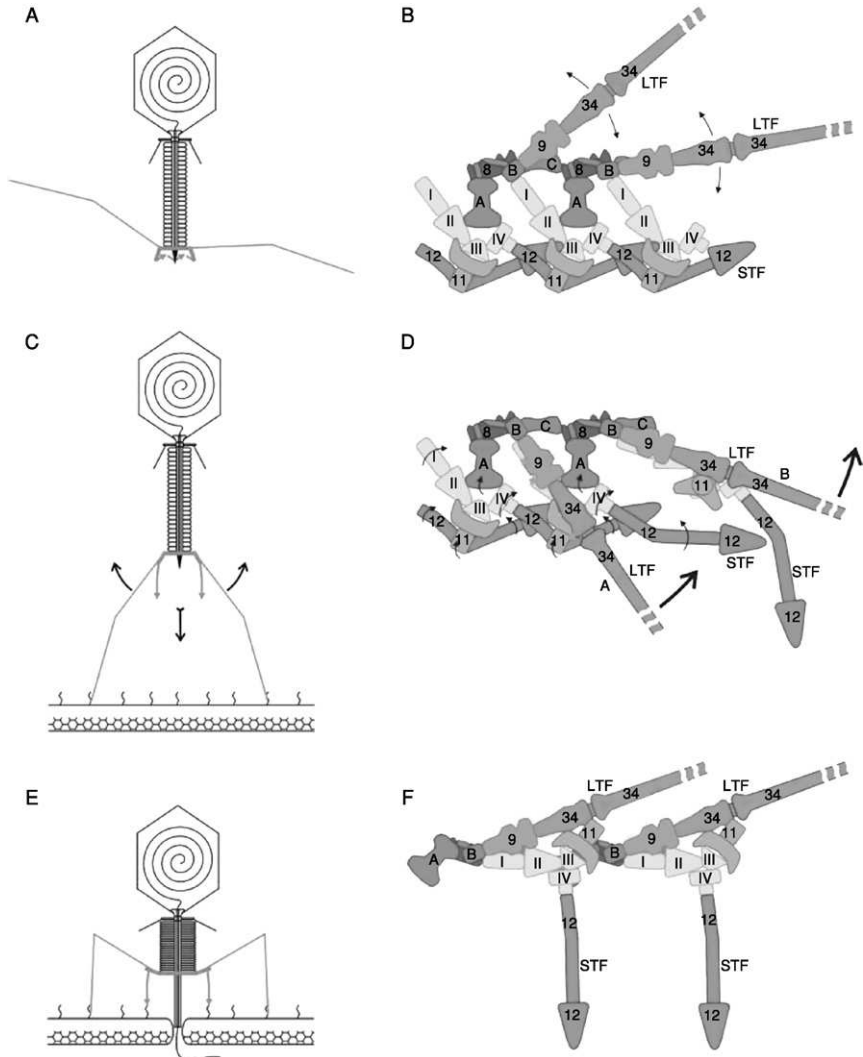


Fig. 24. (Leiman *et al.*, 2004). Baseplate conformational switch schematics. (A and B) The phage is free in solution. The LTFs are extended and oscillate around their midpoint position. The movements of the fibers are indicated with black arrows. The proteins are labeled with their corresponding gene numbers and colored as in Fig. 23. Domains of gp7 and gp10 are labeled as in Fig. 23. (C and D) The LTFs attach to their surface receptors and adapt the “down” conformation. The fiber labeled “A” and its corresponding attachment protein gp9 interact with gp11 and with gp10, respectively. These interactions, labeled with orange stars, probably initiate the conformational switch of the baseplate. The black arrows indicate tentative domain movements and rotations, which have been

The tail tube is a rather featureless cylindrical structure composed of sixfold symmetric, 40.6-Å-thick rings. When helical symmetry constraints were applied by assuming a right-handed twist of 17.7° between rings as determined by Moody and Makowski (1981), the cylinder seemed to have a six-start helix with a left-handed twist of 42.3°. This is the same as a right-handed twist of 17.7° for this sixfold symmetric molecular arrangement. In contrast to the baseplate–tail tube complexes isolated by Duda *et al.* (1986), the tail tube in 3-D reconstructions has no density in its internal channel (Kostyuchenko *et al.*, 2003). This channel density could correspond to gp29, the ruler protein (Abuladze *et al.*, 1994), which might have been lost during purification baseplate–tail tube complexes.

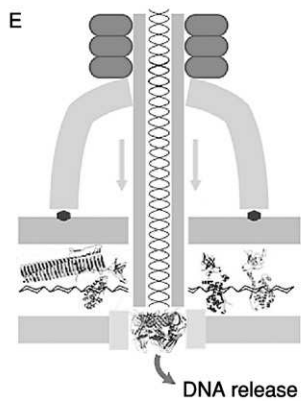
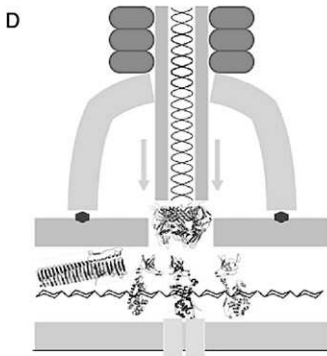
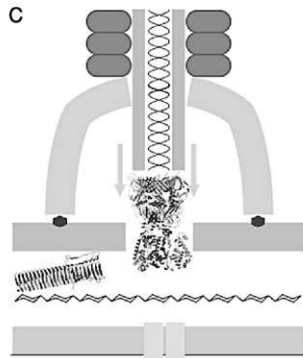
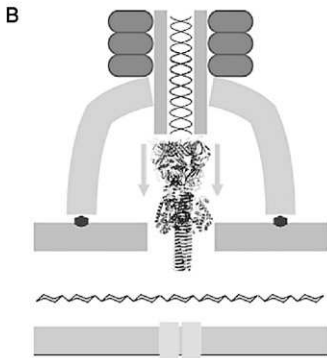
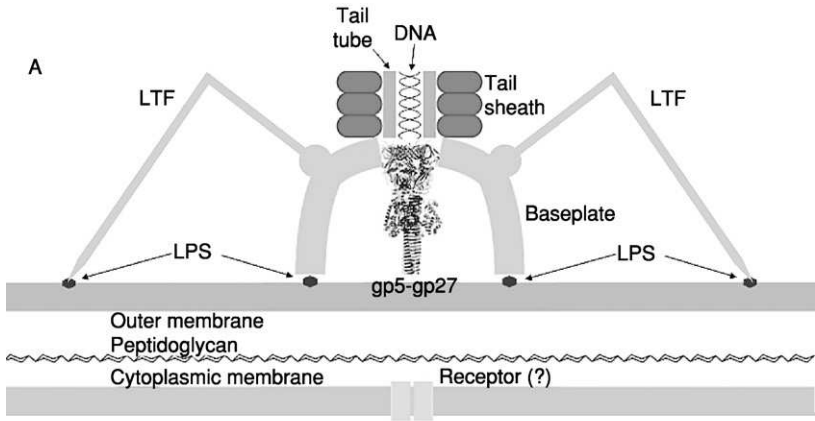
VI. STRUCTURE OF THE STAR-SHAPED BASEPLATE

Short treatment of bacteriophage T4 with 3 to 5 M of urea at neutral pH resulted in the baseplate transformation to a star-shape and subsequent tail sheath contraction (Müller *et al.*, 1994b; To *et al.*, 1969). The cryo-electron microscopy micrographs of 2580 phage particles with contracted tails treated a short time with 3 M of urea were taken and digitized (Leiman, 2004).

The star-shaped baseplate is significantly flatter and wider than the one in the dome-shaped conformation (Kostyuchenko *et al.*, 2003). Upon completion of the switch, the baseplate diameter increases from 520 to 610 Å and the height decreases from 270 to 120 Å (Fig. 23). Nevertheless, both structures consist of the same proteins. Although the overall conformational transition of the baseplate is quite large, the shapes of the component proteins have changed little in the two states. Most proteins or their domains appeared to move as rigid bodies. In the dome-shaped structure, the STF is associated colinearly with a domain of the gp10 (Kostyuchenko *et al.*, 2003). In the star-shaped baseplate, this domain points down toward the potential host-cell surface and has an extension of about 80 Å (Fig. 23). The structure of gp7 in the star-shaped baseplate resembles the one in the dome-shaped and is



derived from the comparison of the two terminal conformations. The fiber labeled “B” has advanced along the conformational switch pathway so that gp11 is now seen along its three-fold axis and the STF is partially extended in preparation for binding to its receptor. The thick red arrows indicate the projected movements of the fibers and the baseplate. (E and F) The conformational switch is complete; the STFs have bound their receptors and the tail sheath has contracted. The phage has initiated DNA transfer into the cell. (See Color Insert.)



composed of three large domains. The overall shapes of these domains are almost unchanged in the two conformations, but their orientations are somewhat different. The largest, dumbbell-looking domain, connecting gp10 to gp8, swivels from an almost vertical to a nearly horizontal orientation (Fig. 23). As a result, the major arrow-like domain of gp10 changes its orientation from being at about 45° with respect to the baseplate sixfold axis to nearly orthogonal to it. Compared to the native conformation, these rearrangements lead to flattening and widening of the star-shaped baseplate (Leiman *et al.*, 2004).

The proximal part of the LTFs emanates from the star-shaped baseplate (Fig. 23). Only about a 230-Å-long stretch of the 1,440-Å-long fiber is ordered in the cryo-electron microscopy map. LTFs are attached colinearly with gp9 and also have a lateral interaction with gp11. Orientation of the gp11 trimer is also changed (Fig. 23). In the dome-shape baseplate, the gp11 trimer axis forms a 144° angle with respect to the baseplate sixfold axis; in the star-shaped structure, the gp11 axis has a 48° angle. In the native state, the STF's are bound to gp11 under the baseplate, and the LTF's oscillate in search of a potential receptor.

VII. THE MECHANISM OF THE BASEPLATE CONFORMATIONAL TRANSITION AND INITIATION OF THE INFECTION

The 3-D structures of the T4 baseplate (Kanamaru *et al.*, 2002; Kostyuchenko *et al.*, 2003; Leiman *et al.*, 2004) lead to a predicted mechanism of infection that might relate to the infection processes in many Myoviridae and Siphoviridae bacteriophages (Leiman, 2003) (Fig. 24). The T4 phage initiates infection of *E. coli* by recognizing the LPS cell surface receptors with the distal ends of its LTFs. The recognition signal is then transmitted to the baseplate attachment protein, gp9, and then to the baseplate itself.

Depending on environmental conditions, the LTFs can be extended or retracted and aligned along the tail sheath (Kellenberger *et al.*, 1965, 1996). Such changes are consistent with the observed variable



FIG. 25. T4 infection process. (A) Phage attaching the baseplate to the cell surface. (B) Tail contraction causing the gp5 needle to puncture the outer cell membrane. (C) The gp5C dissociating from the tail tube, thus activating the three lysozyme domains. (D) The lysozyme domains creating an opening in the peptidoglycan layer. (E) The gp27 associating with a receptor on the inner membrane and initiating the release of DNA into the cytoplasm. For simplification, the LTFs are not shown in B through E. (Leiman *et al.*, 2003b). (See Color Insert.)

orientation of gp9, where the trimeric LTFs attach to gp9 colinearly with the gp9 threefold axis (Fig. 22B). The recognition of the LPS receptor by the tips of the LTFs can be transmitted to the baseplate via primary changes of the gp9 conformation. It is known that the structure of gp9 can be affected by its environment. For example, the crystal structure of gp9 at pH 7.5 (Kostyuchenko *et al.*, 1999) when compared to the crystal structure at pH 4.0 (S. V. Strelkov, 2004; personal communication) shows a rotation of the C-terminal domain by about 20° relative to the middle domain.

The tangential orientation of the gp9 trimer axis (Fig. 22B) suggests that angular as well as directional changes might have a substantial impact, transmitting the signal first to gp7 and gp8, then to gp10 and eventually to gp11 sitting on the kink of the STFs. The association of gp11 with gp12 shows that a rotation of gp11 around its threefold axis would direct the STFs arrowheads toward the host-cell surface that allow them to bind the LPS receptors. The LTFs in the oscillation Browning process should bind laterally to the gp11 trimers, grab them, and pull the pins outward, which should lead to dissociation of the STFs from gp11 and subsequently should break the garland arrangement. The dissociation of the STFs garland allows the baseplate pins to move outward, expanding the star-shaped structure from about 520 Å to 740 Å in diameter as is observed on *in vivo* infection or after urea treatment *in vitro* (Crowther *et al.*, 1977; Leiman *et al.*, 2004). The impact of the gp9 conformational changes on the surrounding gp7 and gp8 molecules should also affect the central platform on the top of the dome and associated tail sheath, causing tail sheath contraction and conformational changes of gp18, which proceeds as a domino effect (Moody, 1973).

The contracted tail sheath drives the T4 particle closer to the cell surface and, therefore, exerts a force onto the tail tube directed toward the cell membrane (Fig. 25). This mechanical force is transmitted through the gp27 cylinder and the N-terminal domain of gp5 to the β -helix needle, causing the latter to puncture the outer membrane. As the tail sheath contraction progresses, the β -helix needle spans the entire 40Å width of the outer membrane, thereby enlarging the pore in the membrane. Subsequently, when the β -helix rigid needle comes into contact with the periplasmic peptidoglycan layer, it should dissociate from the tip of the tail tube, thus activating the gp5 lysozyme domain. The latter dissociates from the gp27 cylinder and locally digests the cell wall, permitting the tail tube to contact the cytoplasmic membrane. The gp27 trimer, sitting on the tip of the tail tube, probably interacts with a specific receptor on the membrane. This event initiates release

of DNA from the phage head through the tail tube into the host cell. The involvement of the receptor in transfer of the T4 DNA into the infected cell is supported by the relatively high rate of the transfer. Rates as high as 4000 bp/sec have been observed (Letellier *et al.*, 2003), which is much higher than the rate for passive transfer.

VIII. CONCLUSION

After a glorious history as one of the primary tools that established the foundation of molecular biology, studies of bacteriophages viruses, including T4 phage, is undergoing a renaissance (Campbell, 2003). As indicated by the example of the 3-D structure of baseplate and individual proteins, the T4 bacteriophage is especially attractive in the deeper exploration of basic biologic questions, such as those concerning molecular machines, evolution of protein domains, and virus infectivity. Future 3-D structural studies of the T4 assembly stages should improve the understanding of how protein–protein and protein–nucleic acid interactions control the function of this very complex virus and allow analogies to be made with other viruses and related biologic machines.

ACKNOWLEDGMENTS

Special thanks and credit are given to the graduate students Victor Kostyuchenko, Petr Leiman, Andrei Letarov, Grisha Navruzbekov, Sergei Strelkov, Sergei Boudko, Mikhail Shneider, and Kostya Miroshnikov as well as to my colleagues Lidia Kurochkina and Nina Sykilinda. I am deeply grateful to Professor Michael G. Rossmann for his continuous effort and interest in T4 phage. I also appreciate Professor Josef I. Atabekov for his valuable advice. Work of our laboratory was supported in part by a Howard Hughes Medical Institute grant for collaboration with Michael G. Rossmann, by a grant of the Human Frontiers Science Program (together with Michael G. Rossmann and Fumio Arisaka), and by a grant of the Russian Fund for Basic Research.

REFERENCES

- Abad Zapatero, C., Abdel-Meguid, S. S., Johnson, J. E., Leslie, A. G., Raiment, I., Rossmann, M. G., Suck, D., and Tsukihara, T. (1980). Structure of southern bean mosaic virus at 2.8 Å resolution. *Nature* **286**:33–39.
- Abuladze, N. K., Gingery, M., Tsai, J., and Eiserling, F. A. (1994). Tail length determination in bacteriophage T4. *Virology* **199**:301–310.
- Ackermann, H.-W. (1999). Tailed bacteriophages: The order Caudovirales. *Adv. Viral Res.* **51**:135–201.

- Adrian, M., Dubochet, J., Lepault, J., and McDowell, A. W. (1984). Cryo-electron microscopy of viruses. *Nature* **308**:32–36.
- Aebi, U., Smith, P. R., Dubochet, J., Henry, C., and Kellenberger, E. (1973). A study of the structure of the T-layers of *Bacillus brevis*. *J. Supramol. Struct.* **1**:498–522.
- Aebi, U., Bijlenga, R. K. L., van den Broek, J., van den Broek, R., Eiserling, F., Kellenberger, C., Kellenberger, E., Mesyanzhinov, V., Müller, L., Showe, M., Smith, R., and Steven, A. (1974). The transformation of τ particles into T4 heads. II. Transformations of the surface lattice and related observations on form determination. *J. Supramol. Struct.* **2**:253–275.
- Aebi, U., van Driel, R., Bijlenga, R. K. L., Ten Heggeler, B., van der Broek, R., Steven, A., and Smith, P. R. (1977). Capsid fine structure of T-even bacteriophages: Binding and localization of two dispensable capsid proteins into P23 surface lattice. *J. Mol. Biol.* **110**:687–698.
- Aebi, U., Fowler, W. E., Isenberg, G., Pollard, T. D., and Smith, P. R. (1981). Crystalline actin sheets: Their structure and polymorphism. *J. Cell Biol.* **91**:340–351.
- Ang, D., Keppel, F., Klein, G., Richardson, A., and Georgopoulos, C. (2000). Genetic analysis of bacteriophage-encoded cochaperonins. *Ann. Rev. Genetics* **34**:439–456.
- Baker, T. S., Olson, N. H., and Fuller, S. D. (1999). Adding the third dimension to virus life cycles: Three-dimensional reconstruction of icosahedral viruses from cryo-electron micrographs. *Microbiol. Mol. Biol. Rev.* **63**:862–922.
- Baschong, W., Aebi, U., Baschong-Preschianotto, C., Dubochet, J., Landmann, L., Kellenberger, E., and Wurtz, R. (1988). Head structure of bacteriophages T2 and T4. *J. Ultrastruct. Mol. Struct. Res.* **99**:189–202.
- Baschong, W., Baschong-Preschianotto, C., Engel, A., Kellenberger, E., Lustig, A., Reichelt, R., Zulauf, M., and Aebi, U. (1991). Mass analysis of bacteriophage T4 proheads and mature heads by scanning transmission electron microscopy and hydrodynamic measurements. *J. Struct. Biol.* **106**:93–101.
- Baumann, R. G., and Black, L. W. (2003). Isolation and characterization of T4 bacteriophage gp17 terminase, a large subunit multimer with enhanced ATPase activity. *J. Biol. Chem.* **278**:4618–4627.
- Betts, S., and King, J. (1999). There's a right way and a wrong way: *In vivo* and *in vitro* folding, misfolding, and subunit assembly of the P22 tail spike. *Structure Folding Des.* **7**:R131–R139.
- Black, L. W., Showe, M. K., and Steven, A. C. (1994). Morphogenesis of the bacteriophage T4 head. In "Molecular Biology of Bacteriophage T4" (J. D. Karam, ed.). American Society for Microbiology, Washington, DC.
- Boudko, S. P., Londer, Y. Y., Letarov, A. V., Sernova, N. V., Engel, J., and Mesyanzhinov, V. V. (2002a). Domain organization, folding, and stability of bacteriophage T4 fibritin, a segmented coiled-coil protein. *Eur. J. Biochem.* **269**:833–841.
- Boudko, S., Frank, S., Kammerer, R. A., Stetefeld, J., Schulthess, T., Landwehr, R., Lustig, A., Bachinger, H. P., and Engel, J. (2002b). Nucleation and propagation of the collagen triple helix in single-chain and trimerized peptides: Transition from third- to first-order kinetics. *J. Mol. Biol.* **317**:459–470.
- Bright, J. N., Woolf, T. B., and Hoh, J. H. (2001). Predicting properties of intrinsically unstructured proteins. *Progr. Biophys. Mol. Biol.* **76**:131–173.
- Brussow, H., and Hendrix, R. W. (2002). Phage genomics: Small is beautiful. *Cell* **108**:13–16.
- Buhle, E. L., Knox, B., Serpersu, E., and Aebi, U. (1983). The structure of the Ca²⁺-ATPase as revealed by electron microscopy and image processing of ordered arrays. *J. Ultrastruct. Res.* **85**:186–203.

- Campbell, A. (2003). The future of bacteriophage biology. *Nature Rev. Genetics* **4**:471–477.
- Caspar, D. L. D., and Klug, A. (1962). Physical principles in the construction of regular viruses. *Cold Spring Harbor Symp. Quant. Biol.* **27**:1–24.
- Cerritelli, M. E., Wall, J. S., Simon, M. N., Conway, J. F., and Steven, A. C. (1996). Stoichiometry and domain organization of the long tail-fiber of bacteriophage T4: A hinged viral adhesin. *J. Mol. Biol.* **260**:767–780.
- Cohen, C., and Parry, D. A. (1994). Alpha-helical coiled coils: More facts and better predictions. *Science* **263**:488–489.
- Conley, M. P., and Wood, W. B. (1975). Bacteriophage T4 whiskers: A rudimentary environment-sensing device. *Proc. Natl. Acad. Sci. USA* **72**:3701–3705.
- Coombs, M. P., and Eiserling, F. A. (1977). Studies on the structure, protein composition, and assembly of the neck of bacteriophage T4. *J. Mol. Biol.* **116**:375–405.
- Coombs, D. H., and Arisaka, F. (1994). T4 tail structure and function. In “Molecular Biology of Bacteriophage T4” (J. D. Karam, ed.). American Society for Microbiology, Washington, DC.
- Crowther, R. A., Lenk, E. V., Kikuchi, Y., and King, J. (1977). Molecular reorganization in the hexagon to star transition of the baseplate of bacteriophage T4. *J. Mol. Biol.* **116**:489–523.
- Crowther, R. A. (1980). Mutants of bacteriophage T4 that produce infective fibreless particles. *J. Mol. Biol.* **137**:159–174.
- DeRosier, D. J., and Klug, A. (1968). Reconstruction of three-dimensional structures from electron micrographs. *Nature (London)* **217**:130–134.
- Doermann, A. H., Eiserling, F. A., and Boeher, L. (1973). Genetic control of capsid length in bacteriophage T4. I. Isolation and preliminary description of four new mutants. *J. Virol.* **12**:374–385.
- Donate, L. E., Murialdo, H., and Carrascosa, J. L. (1990). Production of lambda-phi 29 phage chimeras. *Virology* **179**:936–940.
- Driedonks, R. A., Engel, A., Ten Heggeler, B., and van Driel, R. (1981). Gene 20 product of bacteriophage T4 its purification and structure. *J. Mol. Biol.* **152**:641–662.
- Dubochet, J., Adrian, M., Chang, J. J., Homo, J. C., Lepault, J., McDowell, A. W., and Schultz, P. (1988). Cryo-electron microscopy of vitrified specimens. *Q. Rev. Biophys.* **21**:129–228.
- Duda, R. L., Gingery, M., and Eiserling, F. A. (1986). Potential length determiner and DNA injection protein is extruded from bacteriophage T4 tail tubes *in vitro*. *Virology* **151**:296–314.
- Edgar, R. S., and Wood, W. B. (1966). Morphogenesis of bacteriophage T4 in extracts of mutant-infected cells. *Proc. Natl. Acad. Sci. USA* **55**:498–505.
- Edgar, R. S., and Lielausis, I. (1968). Some steps in the assembly of bacteriophage T4. *J. Mol. Biol.* **32**:263–276.
- Efimov, V. P., Prilipov, A. G., and Mesyanzhinov, V. V. (1990). Nucleotide sequences of bacteriophage T4 genes 6, 7, and 8. *Nucleic Acids Res.* **18**:5313.
- Efimov, V. P., Nepluev, I. V., Sobolev, B. N., Zurabishvili, T. G., Schulthess, T., Lustig, A., Engel, J., Haener, M., Aebi, U., Venyaminov, S. Yu., Potekhin, S. A., and Mesyanzhinov, V. V. (1994). Fibrin encoded by bacteriophage T4 gene *wac* has a parallel triple-stranded alpha-helical coiled-coil structure. *J. Mol. Biol.* **242**:470–486.
- Eiserling, F. A., Geiduschek, E. P., Epstein, R. H., and Metter, E. J. (1970). Capsid size and deoxyribonucleic acid length: The petite variants of bacteriophage T4. *J. Virol.* **6**:865–876.

- Eiserling, F. A., and Black, L. W. (1994). Pathways in T4 morphogenesis. In "Molecular Biology of Bacteriophage T4" (J. D. Karam, ed.). American Society for Microbiology, Washington, DC.
- Engel, A., van Driel, R., and Driedonks, R. (1982). A proposed structures of the prolate phage T4 prehead core. *J. Ultrastruct. Res.* **80**:12–22.
- Ferguson, P. L., and Coombs, D. H. (2000). Pulse-chase analysis of the *in vivo* assembly of the bacteriophage T4 tail. *J. Mol. Biol.* **297**:99–117.
- Fokine, A., Chipman, P. R., Leiman, P. G., Mesyanzhinov, V. V., Rao, V. B., and Rossmann, M. G. (2004). Molecular architecture of the prolate head of bacteriophage T4. *Proc. Natl. Acad. Sci. USA* **101**:6003–6008.
- Frank, J., Radermacher, M., Penczek, P., Zhu, J., Li, Y., Ladjadj, M., and Leith, A. (1996). SPIDER and WEB: Processing and visualization of images in 3-D electron microscopy and related fields. *J. Struct. Biol.* **116**:190–199.
- Frank, S., Kammerer, R. A., Mechling, D., Schulthess, T., Landwehr, R., Bann, J., Guo, Y., Lustig, A., Bachinger, H. P., and Engel, J. (2001). Stabilisation of short collagen-like triple helices by protein engineering. *J. Mol. Biol.* **308**:1081–1089.
- Fuller, S. D., Berriman, J. A., Butcher, S. J., and Gowen, B. E. (1995). Low pH induces swiveling of the glycoprotein heterodimers in the Semliki Forest virus spike complex. *Cell* **81**:715–725.
- Georgopoulos, C. P., Georgiou, M., Selzer, G., and Eisen, H. (1977). Bacteriophage T4 mutants which propagate on *E. coli* K12 but not on *E. coli* B. *Experientia* **33**:1157–1158.
- Goldberg, E., Grinius, L., and Letellier, L. (1994). Recognition, attachment, and injection. In "Molecular Biology of Bacteriophage T4" (J. D. Karam, ed.). American Society for Microbiology, Washington, DC.
- Guo, P., Peterson, C., and Anderson, D. (1987). Prohead and DNA-gp3-dependent ATPase activity of the DNA packaging protein gp16 of bacteriophage phi 29. *J. Mol. Biol.* **197**:229–236.
- Harrison, S. C., Olson, A. J., Scutt, C. E., Winkler, F. K., and Bricogne, G. (1978). Tomato bushy stunt virus at 2.9 Å resolution. *Nature* **276**:368–373.
- Hendrix, R. W. (1978). Symmetry mismatch and DNA packaging in large bacteriophages. *Proc. Natl. Acad. Sci. USA* **75**:4779–4783.
- Hendrix, R. W. (2002). Bacteriophages: Evolution of the majority. *Theor. Popul. Biol.* **61**:471–480.
- Hendrix, R. W., Smith, M. C. M., Burns, R. N., Ford, M. E., and Hatfull, G. F. (1999). Evolutionary relationships among diverse bacteriophages and prophages: All the world's a phage. *Proc. Natl. Acad. Sci. USA* **96**:2192–2197.
- Henning, U., and Hashemolhosseini, S. (1994). Receptor recognition by T-even-type coliphages. In "Molecular Biology of Bacteriophage T4" (J. D. Karam, ed.). American Society for Microbiology, Washington, DC.
- Heymann, J. B., Cheng, N., Newcomb, W. W., Trus, B. L., Brown, J. C., and Steven, A. C. (2003). Dynamics of herpes simplex virus capsid maturation visualized by time-lapse cryo-electron microscopy. *Nat. Struct. Biol.* **10**:334–341.
- Holm, L., and Sander, C. (1993). Protein structure comparison by alignment of distance matrices. *J. Mol. Biol.* **233**:123–138.
- Hsiao, C. L., and Black, L. W. (1978). Head morphogenesis of bacteriophage T4. II. The role of gene 40 in initiation prehead assembly. *Virology* **91**:15–25.
- Hwang, Y., and Feiss, M. (1995). A defined system for *in vitro* lambda DNA packaging. *Virology* **211**:367–376.

- Inaba, K., Kobayashi, N., and Fersht, A. R. (2000). Conversion of two-state to multi-state folding on fusion of two protein foldons. *J. Mol. Biol.* **302**:219–233.
- Ishii, T., Yamaguchi, Y., and Yanagida, M. (1978). Binding of the structural protein *soc* to the head shell of bacteriophage T4. *J. Mol. Biol.* **120**:533–544.
- Ishii, T., and Yanagida, M. (1977). The two dispensable structural proteins (*soc* and *hoc*) of the T4 phage capsid: Their properties, isolation, and characterization of defective mutants and their binding with the defective heads *in vitro*. *J. Mol. Biol.* **109**:487–514.
- Isobe, E., Black, L. W., and Tsugita, A. (1976). Protein cleavage during virus assembly: A novel specificity of assembly dependent cleavage in bacteriophage T4. *Proc. Natl. Acad. Sci. USA* **73**:4205–4209.
- Iwasaki, K., Trus, B. L., Wingfield, P. T., Cheng, N., Campusano, G., Rao, V. B., and Steven, A. C. (2000). Molecular architecture of bacteriophage T4 capsid: Vertex structure and bimodal binding of the stabilizing accessory protein. *Soc. Virology* **271**:321–333.
- Kaliman, A. V., Khasanova, M. A., Kryukov, V. M., Tanyashin, V. I., and Bayev, A. A. (1990). The nucleotide sequence of the region of bacteriophage T4 *inh(lip)-hoc* genes. *Nucleic Acids Res.* **18**:4277.
- Kanamaru, S., Gassner, N. C., Ye, N., Takeda, S., and Arisaka, F. (1999). The C-terminal fragment of the precursor tail lysozyme of bacteriophage T4 stays as a structural component of the baseplate after cleavage. *J. Bacteriol.* **181**:2739–2744.
- Kanamaru, S., Leiman, P. G., Kostyuchenko, V. A., Chipman, P. R., Mesyanzhinov, V. V., Arisaka, F., and Rossmann, M. G. (2002). *Nature* **415**:553–557.
- Kashentseva, E. A., Seki, T., Curiel, D. T., and Dmitriev, I. P. (2002). Adenovirus targeting to c-erbB-2 oncoprotein by single-chain antibody fused to trimeric form of adenovirus receptor ectodomain. *Cancer Res.* **62**:609–616.
- Kellenberger, E. (1966). Control mechanisms in bacteriophage morphogenesis. In “Ciba Foundation Symposium on Principles of Biomolecular Organization” (G. E. W. Wolstenholme and M. O’Connor, eds.). Churchill, London.
- Kellenberger, E. (1969). Polymorphic assemblies of the same virus protein subunits. In “Symmetry and Function of Biological Systems at the Macromolecular Level” (A. Engstrom and B. Strandberg, eds.). John Wiley and Sons, New York.
- Kellenberger, E. (1972). Assembly in biological systems and mechanisms of length determination in protein assemblies. In “Polymerization in Biological Systems Ciba Foundation Symposium 7” (G. E. W. Wolstenholme and M. O’Connor, eds.). Churchill, London.
- Kellenberger, E. (1976). DNA viruses: Cooperativity and regulation through conformational changes as features of phage assembly. *Phylos. Trans. R. Soc. Lond. B. Biol. Sci.* **27**:3–13.
- Kellenberger, E. (1980). DNA viruses: Cooperativity and regulation through conformational changes as features of phage assembly. *Biosystems* **12**:201–223.
- Kellenberger, E. (1990). Form determination of the heads of bacteriophages. *Eur. J. Biochem.* **190**:233–248.
- Kellenberger, E., and Boy de la Tour, E. (1964). On the fine structure of normal and polymerized tail sheath of phage T4. *J. Ultrastruct. Res.* **11**:545–563.
- Kellenberger, E., Bolle, A., Boy de la Tour, E., Epstein, R. H., Franklin, N. C., Jerne, N. K., Reale-Scafati, A., Sechaud, J., Benet, I., Goldstein, D., and Lauffer, M. A. (1965). Functions and properties related to the tail fibers of bacteriophage T4. *Virology* **26**:419–440.

- Kellenberger, E., Stauffer, E., Haner, M., Lustig, A., and Karamata, D. (1996). Mechanism of the long tail-fiber deployment of bacteriophages T-even and its role in adsorption, infection, and sedimentation. *Biophys. Chem.* **59**:41–59.
- Keller, B., and Bickle, T. A. (1986). The nucleotide sequence of gene 21 of bacteriophage T4 coding for the prohead protease. *Gene* **49**:245–251.
- Keller, B., Dubochet, J., Andrian, M., Maeder, M., Wurtz, M., and Kellenberger, E. (1988). Length and shape variants of the bacteriophage T4 head: Mutations in the scaffolding core genes 68 and 22. *J. Virol.* **62**:2960–2969.
- Kikuchi, Y., and King, J. (1975a). Genetic control of bacteriophage T4 baseplate morphogenesis. I. Sequential assembly of the major precursor *in vivo* and *in vitro*. *J. Mol. Biol.* **99**:645–672.
- Kikuchi, Y., and King, J. (1975b). Genetic control of bacteriophage T4 baseplate morphogenesis. II. Mutants unable to form the central part of the baseplate. *J. Mol. Biol.* **99**:673–694.
- Kikuchi, Y., and King, J. (1975c). Genetic control of bacteriophage T4 baseplate morphogenesis. III. Formation of the central plug and overall assembly pathway. *J. Mol. Biol.* **99**:695–716.
- King, J. (1968). Assembly of the tail of bacteriophage T4. *J. Mol. Biol.* **32**:231–262.
- King, J. (1971). Bacteriophage T4 tail assembly: Four steps in core formation. *J. Mol. Biol.* **58**:693–709.
- Kistler, J., Aebi, U., Onorato, L., Ten Heggeler, B., and Show, M. (1978). Structural changes during the transformation of T4 polyheads. I. Characterization of the initial and final states by Fab-fragment labeling of freeze-dried and shadowed preparations. *J. Mol. Biol.* **126**:571–589.
- Kistler, J., Showe, M., Carrascosa, J. L., Stirmer, B., and Onorato-Showe, L. (1982). Structural changes during the transformation of bacteriophage T4 polyheads. II. Evidence that a conformational change in the major capsid protein precedes the expansion. *J. Mol. Biol.* **162**:607–622.
- Kochan, J., Carrascosa, J. L., and Murialdo, H. (1984). Bacteriophage lambda preconnectors. Purification and structure. *J. Mol. Biol.* **174**:433–447.
- Kostyuchenko, V. A., Navruzbekov, G. A., Kurochkina, L. P., Strelkov, S. V., Mesyanzhinov, V. V., and Rossmann, M. G. (1999). The structure of bacteriophage T4 gene product 9: The trigger for tail contraction. *Structure Fold. Des.* **7**:1213–1222.
- Kostyuchenko, V. A., Leiman, P. G., Chipman, P. R., Kanamaru, S., van Raaij, M. J., Arisaka, F., Mesyanzhinov, V. V., and Rossmann, M. G. (2003). Three-dimensional structure of bacteriophage T4 baseplate. *Nat. Struct. Biol.* **10**:688–693.
- Krasnykh, V., Belousova, N., Korokhov, N., Mikheeva, G., and Curiel, D. T. (2001). Genetic targeting of an adenovirus vector via replacement of the fiber protein with the phage T4 fibrin. *J. Virol.* **75**:4176–4183.
- Kuebler, D., and Rao, V. B. (1998). Functional analysis of the DNA-packaging/terminase protein gp17 from bacteriophage T4. *J. Mol. Biol.* **281**:803–814.
- Kurochkina, L. P., Leiman, P. G., Venyaminov, S. Y., and Mesyanzhinov, V. V. (2001). Expression and properties of bacteriophage T4 gene product 11. *Biochemistry (Mosc)*. **66**:141–146.
- Kuroki, R., Weaver, L. H., and Matthews, B. W. (1993). A covalent enzyme-substrate intermediate with saccharide distortion in a mutant T4 lysozyme. *Science* **262**:2030–2033.
- Kutter, E., Guttman, B., Batts, D., Peterson, S., Djavakhishvili, T., Stidham, T., Arisaka, F., Mesyanzhinov, V., Ruger, W., and Mosig, G. (1993). Genomic map of bacteriophage T4. In “Genomic Maps” (S. J. O’Brien, ed.). Cold Spring Harbor Laboratory Press, New York.

- Laemmli, U. K. (1970). Cleavage of structural proteins during the assembly of the head of bacteriophage T4. *Nature* **227**:680–685.
- Laemmli, U. K., Molbert, E., Showe, M., and Kellenberger, E. (1970). Form determining function of the genes required for the assembly of the head of bacteriophage T4. *J. Mol. Biol.* **49**:99–113.
- Laemmli, U. K., Amos, L. A., and Klug, A. (1976). Correlation between structural transformation and cleavage of the the major head protein of bacteriophage T4. *Cell* **7**:191–203.
- Lane, T., and Eiserling, F. (1990). Genetic control of capsid length in bacteriophage T4. VII. A model of length regulation based on DNA size. *J. Struct. Biol.* **104**:9–23.
- Lane, T., Serwer, P., Hayes, S. J., and Eiserling, F. (1990). Quantized viral DNA packaging revealed by rotating gel electrophoresis. *Virology* **174**:472–478.
- Leibo, S. P., Kellenberger, E., Kelenberger-van der Kamp, C., Frey, T. G., and Sternberg, C. M. (1979). Gene 29-controlled osmotic shock resistance in bacteriophage T4: Probable multiple gene function. *J. Virol.* **30**:327–338.
- Leffers, G., and Rao, V. B. (2000). Biochemical characterization of an ATPase activity associated with the large packaging subunit gp17 from bacteriophage T4. *J. Biol. Chem.* **275**:37127–37136.
- Leiman, P. G. (2003). Purdue University “Structure of the bacteriophage T4 baseplate”. Ph.D. thesis.
- Leiman, P. G., Kostyuchenko, V. A., Shneider, M. M., Kurochkina, L. P., Mesyanzhinov, V. V., and Rossmann, M. G. (2000). Structure of bacteriophage T4 gene product 11, the interface between the baseplate and short tail fibers. *J. Mol. Biol.* **301**:975–985.
- Leiman, P. G., Shneider, M. M., Kostyuchenko, V. A., Chipman, P. R., Mesyanzhinov, V. V., and Rossmann, M. G. (2003a). Structure and location of gene product 8 in the bacteriophage T4 baseplate. *J. Mol. Biol.* **328**:821–833.
- Leiman, P. G., Kanamaru, S., Mesyanzhinov, V. V., Arisaka, F., and Rossmann, M. G. (2003b). Structure and morphogenesis of bacteriophage T4. *Cell Mol. Life Sci.* **60**:2356–2370.
- Leiman, P. G., Chipman, P. R., Kostyuchenko, V. A., Mesyanzhinov, V. V., and Rossmann, M. G. (2004). Three-dimensional rearrangement of proteins in the tail of bacteriophage t4 on infection of its host. *Cell.* **118**:419–429.
- Lepault, J., and Leonard, K. (1985). Three-dimensional structure of unstained frozen-hydrated extended tails of bacteriophage T4. *J. Mol. Biol.* **182**:431–441.
- Letarov, A. V., Londer, Y. Y., Boudko, S. P., and Mesyanzhinov, V. V. (1999). The carboxy-terminal domain initiates trimerization of bacteriophage T4 fibritin. *Biochemistry (Mosc)* **64**:817–823.
- Letellier, L., Boulanger, P., de Frutos, M., and Jacquot, P. (2003). Channeling phage DNA through membranes: From *in vivo* to *in vitro*. *Res. Microbiol.* **154**:283–287.
- Liljas, L. (1999). Virus assembly. *Curr. Opin. Struct. Biol.* **9**:129–134.
- Lin, H., and Black, L. W. (1998). DNA requirements *in vivo* for DNA packaging. *Virology* **242**:118–127.
- Lin, H., Simon, M. N., and Black, L. W. (1997). Purification and characterization of the small subunit of phage T4 terminase, gp16, required for DNA packaging. *J. Biol. Chem.* **272**:3495–3501.
- Lin, H., Rao, V. B., and Black, L. W. (1999). Analysis of capsid portal protein and terminase functional domains: Interaction sites required for DNA packaging in bacteriophage T4. *J. Mol. Biol.* **289**:249–260.
- Liu, Y., and Eisenberg, D. (2002). 3-D domain swapping: As domains continue to swap. *Protein Sci.* **11**:1285–1299.

- Liu, Y., Gotte, G., Libonati, M., and Eisenberg, D. (2002). Structures of the two 3-D domain-swapped RNase A trimers. *Protein Sci.* **11**:371–380.
- Lurz, R., Orlova, E. V., Gunther, D., Dube, P., Droge, A., Weise, F., van Heel, M., and Tavares, P. (2001). Structural organisation of the head-to-tail interface of a bacterial virus. *J. Mol. Biol.* **310**:1027–1037.
- Malys, N., Chang, D. Y., Baumann, R. G., Xie, D., and Black, L. W. (2002). A bipartite bacteriophage T4 *soc* and *hoc* randomized peptide display library: Detection and analysis of T4 terminase (gp17) and late σ factor (gp55) interaction. *J. Mol. Biol.* **319**:289–304.
- Makhov, A. M., Trus, B. L., Conway, J. F., Simon, M. N., Zurabishvili, T. G., Mesyanzhinov, V. V., and Steven, A. C. (1993). The short tail-fiber of bacteriophage T4: Molecular structure and a mechanism for its conformational transition. *Virology* **194**:117–127.
- Mason, W. S., and Haselkorn, R. (1972). Product of T4 gene 12. *J. Mol. Biol.* **66**:445–469.
- Matsui, T., Griniuviene, B., Goldberg, E., Tsugita, A., Tanaka, N., and Arisaka, F. (1997). Isolation and characterization of a molecular chaperone, gp57A, of bacteriophage T4. *J. Bacteriol.* **179**:1846–1851.
- Matthews, B. W., and Remington, S. J. (1974). The three-dimensional structure of the lysozyme from bacteriophage T4. *Proc. Natl. Acad. Sci. USA* **71**:4178–4182.
- McNicol, A. A., Simon, L. D., and Black, L. W. (1997). A mutation which bypasses the requirement for p24 in bacteriophage T4 capsid morphogenesis. *J. Mol. Biol.* **116**:261–283.
- Meezan, E., and Wood, W. B. (1971). The sequence of gene product interaction in bacteriophage T4 tail core assembly. *J. Mol. Biol.* **58**:685–692.
- Mesyanzhinov, V. V., Sobolev, B. N., Marusich, E. I., Prilipov, A. G., and Efimov, V. P. (1990). A proposed structure of bacteriophage T4 gene product 22—A major prohead scaffolding core protein. *J. Struct. Biol.* **104**:24–31.
- Miller, E. S., Kutter, E., Mosig, G., Arisaka, F., Kunisawa, T., and Ruger, W. (2003). Bacteriophage T4 genome. *Microbiol. Mol. Biol. Rev.* **67**:86–156.
- Miroshnikov, K. A., Marusich, E. I., Cerritelli, M. E., Cheng, N., Hyde, C. C., Steven, A. C., and Mesyanzhinov, V. V. (1998). Engineering trimeric fibrous proteins based on bacteriophage T4 adhesins. *Protein Eng.* **11**:329–332.
- Miroshnikov, K. A., Sernova, N. V., Shneider, M. M., and Mesyanzhinov, V. V. (2000). Transformation of a fragment of beta-structural bacteriophage T4 adhesin to stable alpha-helical trimer. *Biochemistry (Mosc.)* **65**:1346–1351.
- Moody, M. F. (1973). Sheath of bacteriophage T4. III. Contraction mechanism deduced from partially contracted sheaths. *J. Mol. Biol.* **80**:613–635.
- Moody, M. F., and Makowski, L. (1981). X-ray diffraction study of tail-tubes from bacteriophage T2L. *J. Mol. Biol.* **150**:217–244.
- Mosig, G., Lin, G. W., Franklin, J., and Fan, W. H. (1989). Functional relationships and structural determinants of two bacteriophage T4 lysozymes: A soluble (gene *e*) and a baseplate-associated (gene 5) protein. *New Biol.* **1**:171–179.
- Müller, M., Mesyanzhinov, V. V., and Aebi, U. (1994a). *In vitro* maturation of prehead-like bacteriophage T4 polyheads: Structural changes accompanying proteolytic cleavage and lattice expansion. *J. Struct. Biol.* **112**:199–215.
- Müller, M., Aebi, U., and Engel, A. (1994b). Biochemical and structural characterization of contractile MM phage tails: A comparison with T4 bacteriophage tails. *J. Struct. Biol.* **112**:11–31.
- Murzin, A. G., and Chothia, C. (1992). Protein architecture: New superfamilies. *Curr. Opin. Struct. Biol.* **2**:895–903.

- Nakagawa, H., Arisaka, F., and Ishii, S. (1985). Isolation and characterization of the bacteriophage T4 tail-associated lysozyme. *J. Virol.* **54**:460–466.
- Navruzbekov, G. A., Kurochkina, L. P., Kostyuchenko, V. A., Zurabishvili, T. G., Venyaminov, S. Y., and Mesyanzhinov, V. V. (1999). *Biochemistry (Mosc.)* **64**:1499–1506.
- Olson, N. H., Gingery, M., Eiserling, F. A., and Baker, T. S. (2001). The structure of isometric capsids of bacteriophage T4. *Virology* **279**:385–391.
- Onorato, L., Stirmer, B., and Showe, M. K. (1978). Isolation and characterization of bacteriophage T4 mutant preheads. *J. Virol.* **27**:409–426.
- Panchenko, A. R., Luthy-Schulten, Z., and Wolynes, P. G. (1996). Foldons, protein structural modules, and exons. *Proc. Natl. Acad. Sci. USA* **93**:2008–2013.
- Parker, M. L., Christensen, A. C., Boosman, A., Stockard, J., Young, E. T., and Doermann, A. H. (1984). Nucleotide sequence of bacteriophage T4 gene 23 and the amino acids sequence of its products. *J. Mol. Biol.* **180**:399–416.
- Paulson, J. R., and Laemmli, U. K. (1977). Morphogenetic core of the bacteriophage T4 head. Structure of the core in polyheads. *J. Mol. Biol.* **111**:459–485.
- Paulson, J. R., Lazaroff, S., and Laemmli, U. K. (1976). Head length determination in bacteriophage T4: The role of core protein P22. *J. Mol. Biol.* **103**:99–109.
- Plishker, M. F., and Berget, P. B. (1984). Isolation and characterization of precursors in bacteriophage T4 baseplate assembly. III. The carboxyl termini of protein P11 are required for assembly activity. *J. Mol. Biol.* **178**:699–709.
- Plishker, M. F., Chidambaram, M., and Berget, P. B. (1983). Isolation and characterization of precursors in bacteriophage T4 baseplate assembly. II. Purification of the protein products of genes 10 and 11 and the *in vitro* formation of the P(10/11) complex. *J. Mol. Biol.* **170**:119–135.
- Plishker, M. F., Rangwala, S. H., and Berget, P. B. (1988). Isolation of bacteriophage T4 baseplate proteins P7 and P8 and *in vitro* formation of the P10/P7/P8 assembly intermediate. *J. Virol.* **62**:400–406.
- Rao, V. B., and Black, L. W. (1988). Cloning, overexpression, and purification of the terminase proteins gp16 and gp17 of bacteriophage T4. Construction of a defined *in vitro* DNA packaging system using purified terminase proteins. *J. Mol. Biol.* **200**:475–488.
- Richardson, A., Landry, S. J., and Georgopoulos, C. (1998). The ins and outs of a molecular chaperone machine. *Trends Biochem. Sci.* **23**:138–143.
- Riede, I. (1987). Receptor specificity of the short tail fibers (gp12) of T-even type *Escherichia coli* phages. *Mol. Gen. Genet.* **206**:110–115.
- Rossmann, M. G., and Johnson, J. E. (1989). Icosahedral RNA virus structure. *Annu. Rev. Biochem.* **58**:533–573.
- Rossmann, M. G., Mesyanzhinov, V. V., Arisaka, F., and Leiman, P. G. (2004). The bacteriophage T4 DNA injection machine. *Curr. Opin. Struct. Biol.* **14**:171–180.
- Rossmann, M. G., Bernal, R., and Pletnev, S. V. (2001). Combining electron microscopic with X-ray crystallographic structures. *J. Struct. Biol.* **136**:190–200.
- Sandmeier, H., Iida, S., and Arber, W. (1992). DNA inversion regions Min of plasmid p15B and Cin of bacteriophage P1: Evolution of bacteriophage tail fiber genes. *J. Bacteriol.* **174**:3936–3944.
- Seckler, R. (1998). Folding and function of repetitive structure in the homotrimeric phage P22 tail spike protein. *J. Struct. Biol.* **122**:216–222.
- Shneider, M. M., Boudko, S. P., Lustig, A., and Mesyanzhinov, V. V. (2001). Properties of bacteriophage T4 baseplate protein encoded by gene 8. *Biochemistry (Mosc)* **66**:693–697.

- Showe, M. K., and Black, L. W. (1973). Assembly core of bacteriophage T4: An intermediate in head formation. *J. Mol. Biol.* **107**:35–54.
- Showe, Isobe, E., and Onorato, L. (1976). Bacteriophage T4 prohead proteinase. I. Purification and properties of a bacteriophage enzyme which cleaves the capsid precursor proteins. *J. Mol. Biol.* **107**:55–89.
- Showe, M. K., and Onorato, L. (1978). Kinetic factors and form determination of the head of bacteriophage T4. *Proc. Natl. Acad. Sci. USA* **75**:4165–4169.
- Simpson, A. A., Tao, Y., Leiman, P. G., Badasso, M. O., He, Y., Jardine, P. J., Olson, N. H., Morais, M. C., Grimes, S., Anderson, D. L., Baker, T. S., and Rossmann, M. G. (2000). *Nature* **408**:745–750.
- Sobolev, B. N., and Mesyanzhinov, V. V. (1991). The *wac* gene product of bacteriophage T4 contains coiled-coil structural patterns. *J. Biomol. Struct. Dyn.* **8**:953–965.
- Smith, D. E., Tans, S. J., Smith, S. B., Grimes, S., Anderson, D. L., and Bustamante, C. (2001). The bacteriophage straight phi29 portal motor can package DNA against a large internal force. *Nature* **413**:748–752.
- Steinbacher, S., Seckler, R., Miller, S., Steipe, B., Huber, R., and Reinemer, P. (1994). Crystal structure of P22 tail spike protein: Interdigitated subunits in a thermostable. *Science* **265**:383–386.
- Stetefeld, J., Frank, S., Jenny, M., Schulthess, T., Kammerer, R. A., Boudko, S., Landwehr, R., Okuyama, K., and Engel, J. (2003). Collagen stabilization at atomic level: Crystal structure of designed (Gly-Pro-Pro) 10-foldon. *Structure (Camb.)* **11**:339–346.
- Steven, A. C., and Carrascosa, J. L. (1979). Proteolytic cleavage and structural transformation: Their relationship in bacteriophage T4 capsid maturation. *J. Supramol. Struct.* **10**:1–11.
- Steven, A. C., Couture, E., Aebi, U., and Showe, M. (1976). Structure of T4 polyheads. II. A pathway of polyhead transformations as a model for T4 capsid maturation. *J. Mol. Biol.* **106**:187–221.
- Steven, A. C., Bauer, A. C., Bisher, M. E., Robey, F. A., and Black, L. W. (1991). The maturation-dependent conformational change of phage T4 capsid involves the translocation of specific epitopes between the inner and outer capsid surfaces. *J. Struct. Biol.* **106**:221–236.
- Strelkov, S. V., Tao, Y., Rossmann, M. G., Kurochkina, L. P., Shneider, M. M., and Mesyanzhinov, V. V. (1997). Preliminary crystallographic studies of bacteriophage T4 fibrin confirm a trimeric coiled-coil structure. *Virology* **219**:190–194.
- Strelkov, S. V., Tao, Y., Shneider, M. M., Mesyanzhinov, V. V., and Rossmann, M. G. (1998). Structure of bacteriophage T4 fibrin M: A troublesome packing arrangement. *Acta Crystallogr. D Biol. Crystallogr.* **D54**:805–816.
- Tao, Y., Strelkov, S. V., Mesyanzhinov, V. V., and Rossmann, M. G. (1997). Structure of bacteriophage T4 fibrin: A segmented coiled-coil and the role of the C-terminal domain. *Structure* **5**:789–798.
- Terzaghi, B. E., Terzaghi, E., and Coombs, D. (1979). Mutational alteration of the T4D tail fiber attachment protein. *J. Mol. Biol.* **127**:1–14.
- Thomassen, E., Gielen, G., Schutz, M., Schoehn, G., Abrahams, J. P., Miller, S., and van Raaij, M. J. (2003). The structure of the receptor-binding domain of the bacteriophage T4 short tail fiber reveals a knitted trimeric metal-binding fold. *J. Mol. Biol.* **331**:361–373.
- To, C. M., Kellenberger, E., and Eisenstark, A. (1969). Disassembly of T-even bacteriophage into structural parts and subunits. *J. Mol. Biol.* **46**:493–511.

- Uhlenhopp, E. L., Zimm, B. H., and Cummings, D. J. (1974). Structural aberrations in T-even bacteriophage. VI. Molecular weight of DNA from giant heads. *J. Mol. Biol.* **89**:689–702.
- Urig, M. A., Brown, S. M., Tedesco, P., and Wood, W. B. (1983). Attachment of tail fibers in bacteriophage T4 assembly. Identification of the baseplate protein to which tail fibers attach. *J. Mol. Biol.* **169**:427–437.
- Valpuesta, J. M., Fujisawa, H., Marco, S., Carazo, J. M., and Carrascosa, J. L. (1992). Three-dimensional structure of T3 connector purified from overexpressing bacteria. *J. Mol. Biol.* **224**:103–112.
- van Raaij, M. J., Schoehn, G., Burda, M. R., and Miller, S. (2001). Crystal structure of a heat and protease-stable part of the bacteriophage T4 short tail fiber. *J. Mol. Biol.* **314**:1137–1146.
- Vepintseva, O. D., Deev, A. A., Ivanitskii, G. R., Kuninskii, A. S., and Khusainov, A. A. (1980). Aberrant form of T4 phage reorganization. *Dokl. Akad. Nauk SSSR.* **254**:496–499.
- Vianelli, A., Wang, G. R., Gingery, M., Duda, R. L., Eiserling, F. A., and Goldberg, E. B. (2000). Bacteriophage T4 self-assembly: Localization of gp3 and its role in determining tail length. *J. Bacteriol.* **182**:680–688.
- Volker, T. A., Gafner, J., Bickle, T. A., and Showe, M. K. (1982a). Gene 67, a new essential bacteriophage T4 gene codes for a pre-head core component, PIP. I. Genetic mapping and DNA sequence. *J. Mol. Biol.* **161**:479–489.
- Volker, T. A., Kuhn, A., Showe, M. K., and Bickle, T. A. (1982b). Gene 67, a new essential bacteriophage T4 gene codes for a pre-head core component, PIP. II. The construction *in vitro* of unconditionally lethal mutants and their maintenance. *J. Mol. Biol.* **161**:491–504.
- Wakasugi, K., Isimori, K., Imai, K., Wada, Y., and Morishima, A. (1994). “Module” substitution in hemoglobin subunits *J. Biol. Chem.* **269**:18750–18756.
- Watts, N. R., and Coombs, D. H. (1989). Analysis of near-neighbor contacts in bacteriophage T4 wedges and hubless baseplates by using a cleavable chemical cross-linker. *J. Virol.* **63**:2427–2436.
- Watts, N. R., and Coombs, D. H. (1990). Structure of the bacteriophage T4 baseplate as determined by chemical cross-linking. *J. Virol.* **64**:143–154.
- Watts, N. R., Hainfeld, J., and Coombs, D. H. (1990). Localization of the proteins gp7, gp8, and gp10 in the bacteriophage T4 baseplate with colloidal gold:F(ab)₂ and undecagold:Fab’ conjugates. *J. Mol. Biol.* **216**:315–325.
- Wilson, J. H., Luftig, R. B., and Wood, W. B. (1970). Interaction of bacteriophage T4 tail fiber components with a lipopolysaccharide fraction from *Escherichia coli*. *J. Mol. Biol.* **51**:423–434.
- Wommack, K. E., and Colwell, R. R. (2000). Virioplankton: viruses in aquatic ecosystems. *Microbiol. Mol. Biol. Rev.* **64**:69–144.
- Wood, W. B. (1980). Bacteriophage T4 morphogenesis as a model for assembly of subcellular structures. *Q. Rev. Biol.* **55**:353–367.
- Wood, W. B., and Conley, M. P. (1979). Attachment of tail fibers in bacteriophage T4 assembly: Role of the phage whiskers. *J. Mol. Biol.* **127**:15–29.
- Wood, W. B., Edgar, R. S., King, J., Lielausis, I., and Henninger, M. (1968). Bacteriophage assembly. *Fed. Proc.* **27**:1160–1166.
- Wood, W. B., Conley, M. P., Lyle, H. L., and Dickson, R. C. (1978). Attachment of tail fibers in bacteriophage T4 assembly. Purification, properties, and site of action of the accessory protein coded by gene 63. *J. Biol. Chem.* **253**:2437–2445.

- Wood, W. B., Eiserling, F. A., and Crowther, R. A. (1994). Long tail fibers: Genes, proteins, structure, and assembly. In "Molecular Biology of Bacteriophage T4" (J. D. Karam, ed.). American Society for Microbiology, Washington, DC.
- Wright, P. E., and Dyson, H. J. (1999). Intrinsically unstructured proteins: Reassessing the protein structure-function paradigm. *J. Mol. Biol.* **293**:321–331.
- Yanagida, M. D., Boy de la Tour, E., Alff-Steinberger, C., and Kellenberger, E. (1970). Studies on the morphopoiesis of the of the head of bacteriophage T-even. VIII. Multi-layered polyheads. *J. Mol. Biol.* **50**:35–58.
- Yanagawa, H., Yoshida, K., Torigoe, C., Prak, J. S., Sato, K., Shirai, T., and Go, M. (1993). Protein anatomy: Functional roles of barnase module. *J. Biol. Chem.* **268**:5861–5865.
- Yang, X., Lee, J., Mahony, E. M., Kwong, P. D., Wyatt, R., and Sodroski, J. (2002). Highly stable trimers formed by human immunodeficiency virus type 1 envelope glycoproteins fused with the trimeric motif of T4 bacteriophage fibritin. *J. Virol.* **76**:4634–4642.
- Yu, M.-H., and King, J. (1984). Single amino acid substitutions influencing the folding pathway of the phage P22 tail spike endorhamnosidase. *Proc. Natl. Acad. Sci. USA* **81**:6584–6588.
- Zhao, L., Kanamaru, S., Chaidirek, C., and Arisaka, F. (2003). P15 and P3, the tail completion proteins of bacteriophage T4, both form hexameric rings. *J. Bacteriol.* **185**:1693–1700.
- Zhao, L., Takeda, S., Leiman, P. G., and Arisaka, F. (2000). Stoichiometry and intersubunit interaction of the wedge initiation complex, gp10-gp11, of bacteriophage T4. *Biochim. Biophys. Acta* **1479**:286–292.

GENOMIC ORGANIZATION, BIOLOGY, AND DIAGNOSIS OF TAURA SYNDROME VIRUS AND YELLOWHEAD VIRUS OF PENAEID SHRIMP

Arun K. Dhar,^{*} Jeff A. Cowley,[†] Kenneth W. Hasson,[‡] and
Peter J. Walker[†]

^{*}Department of Biology, San Diego State University
San Diego, California 92182

[†]CSIRO Livestock Industries, Queensland Bioscience Precinct
St. Lucia, Queensland 4067

[‡]Texas Veterinary Medical Diagnostic Laboratory
College Station, Texas 77841

- I. Introduction
- II. Taura Syndrome Disease
 - A. History
 - B. Clinical Signs, Transmission, and Disease Cycle
 - C. Physical Properties of Taura Syndrome Virus
 - D. Genome Organization and Gene Expression of Taura Syndrome Virus
 - E. Comparison of Genome Organization of TSV with Insect and Mammalian Picornaviruses
 - F. Genetic Diversity of Taura Syndrome Virus
 - G. Diagnosis of Taura Syndrome Virus
- III. Yellowhead Disease
 - A. History, Clinical Signs, and Transmission
 - B. Physical Properties of Yellowhead Virus
 - C. Genome Organization and Gene Expression of Yellowhead Virus
 - D. Relationship of Yellowhead Virus with Gill-Associated Virus
 - E. Diagnosis of Yellowhead Virus
- IV. Concluding Remarks
- References

I. INTRODUCTION

Over the past two decades, shrimp aquaculture has transformed into a major industry worldwide, providing jobs for millions of people directly and indirectly. As shrimp farming expands globally, it faces a growing number of challenges. Among these, diseases caused by viruses have been recognized as a major threat to the long-term sustainability of this industry. The first shrimp virus was isolated by Couch from wild shrimp (*Penaeus duorarum*) collected from the Florida Gulf Coast in the early 1970s (Couch, 1974a,b). Since then, more than 20

viruses have been reported to infect shrimp (Lightner, 1996a), and the list is growing. Many of these viruses have caused serious diseases in penaeid shrimp, resulting in significant economic losses to commercial shrimp farmers. The three most detrimental shrimp viruses are white spot syndrome virus (WSSV), yellowhead virus (YHV), and Taura syndrome virus (TSV), all of which have caused serious epizootics in various regions of Asia and are considered notifiable by the Office International de Epizooties (OIE, 2002). In the Western Hemisphere, the shrimp industry has suffered catastrophic losses due to both WSSV and TSV; however, losses due to YHV have not been reported (Lightner *et al.*, 1997b; Tu *et al.*, 1999; Yu and Song, 2000). Several reviews describing the histopathology, diagnostic methods, and epidemiology of these important viral disease have been published in recent years (Flegel, 1997; Lightner, 1996b; Lightner and Redman, 1998; Loh *et al.*, 1997). These are valuable references for researchers interested in shrimp viruses. The present review is focused on two viruses, TSV and YHV, with a major emphasis on the genome organization of these viruses.

II. TAURA SYNDROME DISEASE

A. History

The designation of TSV, the causative agent of Taura syndrome (TS), as a notifiable disease by the OIE amply reflects the serious nature of this viral agent and the deleterious economic impact it has inflicted on shrimp farming in the Americas (Brock, 1997; Brock *et al.*, 1995, 1997; Hasson *et al.*, 1995, 1999a,b; Lightner, 1995, 1996a,b; Lightner *et al.*, 1995, 1997a,b; OIE, 2002) and, more recently, in Taiwan (Tu *et al.*, 1999; Yu and Song, 2000). Of the approximately 20 known viral diseases of penaeid shrimp, TS is possibly one of the most controversial in terms of its disputed etiology (Brock *et al.*, 1995; Hasson, 1998; Hasson *et al.*, 1995, 1999a,b; Lightner, 1996a,b, 1998, 1999). Hence, a review of this disease would be incomplete without explaining the cause of this dispute and how it contributed to the unobstructed spread of TSV throughout the Western Hemisphere between 1992 to 1996 (Hasson *et al.*, 1999a). The resulting panzootic cost to the shrimp farming industry in the Americas was an estimated \$1.2–2 billion in lost revenue (Brock, 1997; Hasson, 1998; Hasson *et al.*, 1999a; Lightner, 1995, 1996; Lightner *et al.*, 1995, 1996b).

Ecuadorian investigators first recognized TS as a new disease, both clinically and histologically, in Pacific white shrimp (*Penaeus*

vannamei) farms located along the mouth of the Taura river basin (Guayas Province, Ecuador) during the summer of 1992 (Brock *et al.*, 1995, 1997; Jimenez, 1992; Lightner *et al.*, 1994; Wigglesworth, 1994). They named the disease after the Taura region where the first outbreaks were detected (Jimenez, 1992; Wigglesworth, 1994). The cause of TS was initially attributed to the toxic effects of two systemic fungicides: Tilt (Propiconazole, Ciba-Geigy) and Calixin (Tridemorph, BASF). These fungicides were being sprayed on local banana plantations to control Black Leaf Wilt disease, a serious banana plant fungal infection (Brock *et al.*, 1995; Hasson, 1998; Intriago *et al.*, 1997a,b; Lightner *et al.*, 1994; Stern, 1995; Wigglesworth, 1994). Because initial disease occurrence in adjacent shrimp farms coincided with periods of heavy rainfall, it was assumed that fungicide-contaminated runoff from the plantations was the direct cause of the shrimp die-offs (Jimenez, 1992; Lightner *et al.*, 1994; Wigglesworth, 1994). This hypothesized toxic etiology for the shrimp losses persisted in the popular press through early 1995. No confirmatory scientific evidence, however, was forthcoming to support this theory (Anonymous, 1995; Barniol, 1995; Brock *et al.*, 1995; Hasson, 1998; Hasson *et al.*, 1995; Intriago *et al.*, 1995a,b; Jimenez *et al.*, 1995; Lightner *et al.*, 1994, 1995). During the 2 years following its discovery, TS spread west through Ecuador's most concentrated shrimp farming region, southward into *P. vannamei* farms of Northern Peru, and northward into *P. vannamei* farms located on the Pacific Coast of Colombia (Brock *et al.*, 1995; Hasson *et al.*, 1999a; Lightner *et al.*, 1994; Wigglesworth, 1994). In these latter two regions, there were neither banana plantations nor application of the two accused fungicides. All prior and subsequent attempts to experimentally induce TS by either water borne, oral, or injection-mediated exposure to Tilt and Calixin failed to reproduce the clinical signs and histological lesions associated with the disease (Brock *et al.*, 1995, 1997; Hasson, 1998; Hasson *et al.*, 1995; Lightner, 1996a; Lightner *et al.*, 1994, 1995, 1996c). As a result, investigators began to question the toxic etiology hypothesis and pursue other possible causes. A third widely used banana plant fungicide in Ecuador, called Benlate O. D. (Benomyl, DuPont), was also tested as a possible cause of TS and, as with Tilt and Calixin, failed to induce the disease (Lightner *et al.*, 1996c). During May 1994, two separate outbreaks of TS occurred among cultured *P. vannamei* on Oahu, Hawaii, representing the first incursion of this disease into the United States (Brock *et al.*, 1995). Within 5 months of these two outbreaks, experimental *per os* induction of the disease was accomplished (Brock *et al.*, 1995), a previously uncharacterized virus (named Taura syndrome virus) was

independently identified by two separate labs within the United States (Brock *et al.*, 1995; Hasson *et al.*, 1995; Lightner *et al.*, 1995), and the newly recognized virus was then shown to be the cause of TS through fulfillment of River's postulates (Hasson *et al.*, 1995). Although a viral etiology for TS had now been scientifically established, leaders of the Ecuadorian shrimp farming industry maintained that the disease had a toxic etiology in support of their ongoing litigation against the producers of Tilt (Ciba-Geigy, personal communication, 1995). The conflicting information regarding the etiology of TS left shrimp growers throughout the Americas confused or indifferent about the true causative nature of the disease, and no regulations to restrict international movement of live shrimp stocks were implemented. As a result, the disease was spread throughout the Western Hemisphere through sales of TSV-infected postlarvae and broodstock. At the end of 1996, 13 of the 14 shrimp farming countries in the Americas were infected with TSV (Brock *et al.*, 1995; Hasson, 1998; Hasson *et al.*, 1999a; Lightner, 1995, 1996a; Zarain-Herzberg and Ascencio-Valle, 2001). In 1999, Ecuadorian researchers conceded that TSV had been present in Ecuador since 1994 but maintained that the shrimp losses suffered by their industry during 1992 and 1993 were caused by toxic fungicides (Intriago *et al.*, 1997a,b; Jimenez *et al.*, 2000). This was contrary to the fact that these early outbreaks were clinically and histologically identical to TSV-induced epizootics and scientifically demonstrated to be TSV-caused (Bonami *et al.*, 1997; Brock *et al.*, 1995; Hasson *et al.*, 1995, 1999a; Lightner, 1995, 1996a, 1998; Lightner *et al.*, 1995). During 1999, the Ecuadorian shrimp farming community abandoned their position that Tilt and Calixin were the cause of TS and currently claim that the fungicide, Benlate O.D., is the actual etiologic agent of the disease. Thus, the ongoing controversy persists and now moves into its eleventh year.

B. Clinical Signs, Transmission, and Disease Cycle

1. Clinical Signs

The clinical signs of acute TSV infection in farmed *P. vannamei* include lethargy, anorexia, opaque musculature, atactic swimming behavior, flaccid bodies, soft cuticles, and chromatophore expansion resulting in reddening of the uropods, appendages, and general body (Brock *et al.*, 1995; Hasson *et al.*, 1995; Lightner, 1995, 1996a; Lightner *et al.*, 1994, 1995) (Fig. 1). Development of red coloration from chromatophore expansion is believed to be linked to pigment (carotenoids) incorporation resulting from the consumption of phytoplankton and is

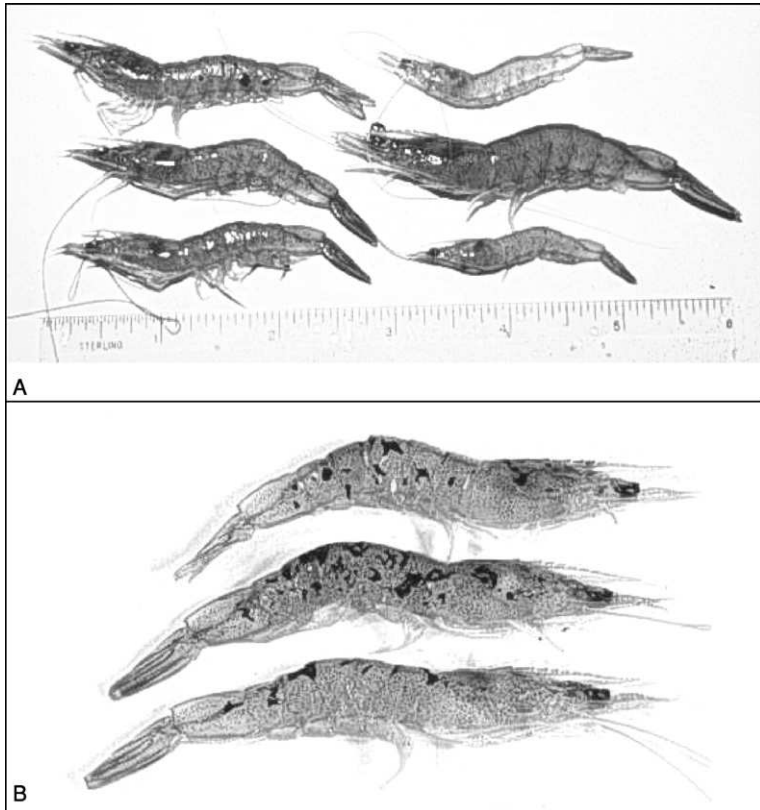


FIG 1. Farmed *Penaeus vannamei* juveniles originating from two separate TSV epizootics. (A) Signs of TSV acute phase infection. The shrimp in the upper right corner is healthy and translucent. The remaining five shrimp are acutely infected with TSV and display an overall darker coloration, typically ranging from lavender to red, due to chromatophore expansion (B) Signs of TSV transition phase infection. The cephalothorax and tail of these three shrimp display multifocal melanized lesions that indicate a transition phase TSV infection. These lesions identify foci of cuticular epithelium that were destroyed during the acute phase infection and are now in the process of resolving. (See Color Insert.)

not observed in experimentally infected *P. vannamei* that are maintained in clear water systems on artificial diets (Brock *et al.*, 1995; Hasson *et al.*, 1995; Lightner *et al.*, 1994, 1995). Naturally and experimentally infected shrimp that survive the acute phase infection develop grossly visible, multifocal, melanized lesions on the cephalothorax, tail, and appendages (Brock *et al.*, 1995; Hasson *et al.*, 1995; Lightner *et al.*, 1994) (Fig. 1).

These lesions are characteristic of a transition phase of TSV infection (Hasson *et al.*, 1999b) (Section II,B,3). TSV typically strikes *P. vannamei* in late postlarval to early juvenile stages between 15 to 40 days poststocking of production or nursery ponds, but TSV is also capable of causing serious disease in subadult and adult *P. vannamei* (Brock *et al.*, 1995; Lightner, 1996a; Lightner *et al.*, 1994; Lotz, 1997; Wigglesworth, 1994). Infected *P. vannamei* generally die within 1 week of disease onset with cumulative mortalities typically ranging from 60 to 95% (Brock *et al.*, 1995, 1997; Hasson *et al.*, 1995; Lightner, 1995, 1996a; Lightner *et al.*, 1994, 1995; Wigglesworth, 1994). As with other mass mortalities in shrimp farms, whether due to an infectious or noninfectious agent, the flocking of sea birds over a stricken pond as they feed on the numerous dead and dying shrimp often signals a TSV epizootic (Brock *et al.*, 1997; Garza *et al.*, 1997). Similar TSV clinical signs and mortality data have been reported for *P. stylirostris* (Pacific blue shrimp) stocks (Robles-Sikisaka *et al.*, 2002) that were widely farmed in Mexico during 1996 to 2000 (Clifford, 2000) and, prior to 1999, considered TSV resistant (Brock *et al.*, 1995). Robles-Sikisaka *et al.* (2002) and Erickson *et al.* (2002) demonstrated that TSV epizootics among *L. stylirostris* stocks in Mexico were the result of a new emerging strain or serotype of TSV (Section II,F).

2. Transmission

The different modes of TSV transmission have been examined to a limited extent (Table I). Vertical transmission of this virus has been hypothesized to occur based on anecdotal information but not

TABLE I
VECTORS OF TSV

A. Short-range transmission (within ponds)
• Cannibalism of acute or chronically infected moribund or dead shrimp
• Waterborne
B. Medium-range transmission (between ponds and farms)
• Sea birds
• Water boatmen (<i>T. reticulata</i>)
• Chronically infected shrimp
• Wild infected postlarvae
C. Long-range transmission (between countries)
• Live infected postlarvae and broodstock
• Frozen infected shrimp

demonstrated (Lightner, 1995; Lightner and Redman, 1998). Dissemination of the virus within a pond or tank results from cannibalism of infected moribund or dead shrimp by healthy shrimp, resulting in rapid exponential spread of the virus within the exposed population (Brock *et al.*, 1995; Hasson *et al.*, 1995). Work by Prior and Browdy (2000) showed that TSV remains pathogenic in decaying *P. vannamei* shrimp carcasses for up to 3 weeks following death and can serve as a source for renewed outbreaks if consumed by TSV-susceptible shrimp. In the same study, water borne transmission of TSV was demonstrated to occur for up to 48 hr following the peak mortality period of an experimentally induced TSV epizootic. Chronically infected *P. vannamei* harbor infectious TSV within both the lymphoid organ (LO) and hemolymph for at least 8–12 months postinfection, representing a potential source of renewed outbreaks if cannibalized (Hasson, 1998; Hasson *et al.*, 1995, 1999c). As a result, persistence of TSV in a farm or a given region may be due to the presence of chronically infected shrimp living within ponds, canals, or adjacent estuaries.

The transmission of TSV between ponds or farms has been attributed to seabirds, predominantly gulls, and a flying aquatic insect commonly known as the water boatmen (*Trichocorixa reticulata*) (Garza *et al.*, 1997; Hasson *et al.*, 1995; Lightner, 1995, 1996a). Garza *et al.* (1997) demonstrated that sea gull feces collected from the banks of TSV infected ponds in Texas during the 1995 TSV epizootic contained infectious TSV. They hypothesized that shrimp eating birds transmit TSV to other ponds or farms through defecation of TSV infected feces with subsequent ingestion of the infected fecal matter by scavenging shrimp. Water boatmen are commonly found in large numbers in shrimp farms. They possess a sucking proboscis and will prey on small postlarval shrimp (Hasson *et al.*, 1995; Lightner, 1995, 1996a,b). Limited histological and TSV *in situ* hybridization (ISH) analyses of experimentally exposed and wild water boatmen samples indicate that these insects transport TSV within their intestinal contents but are not directly infected by the virus (Hasson, unpublished data; Lightner, 1996a,b). Similar to sea birds, water boatmen are believed to be capable of disseminating infectious virus through their fecal matter, or, perhaps they spread the virus upon death when they are consumed by shrimp. Similar to the water boatmen, red drum (*Sciaenops ocellatus*), blue crabs (*Callinectes sapidus*), grass shrimp (*Palaemonetes* sp.), and sea trout (*Cynoscion nebulosus*) are not infected by the virus as indicated by experimental TSV *per os* exposure and histological analyses (Erickson *et al.*, 1997). However, the possibility of fecal transmission of TSV by these potential vectors was not examined.

TSV is considered endemic in countries along the Pacific coast, ranging from northern Peru up through Mexico (Brock *et al.*, 1995, 1997; Hasson *et al.*, 1999a; Lightner, 1995, 1996a,b; Zarain-Herzberg and Ascencio-Valle, 2001). Acute and/or chronic disease has been detected in wild *P. vannamei* postlarvae collected in Ecuador and in broodstock captured off of Honduras, El Salvador, and southern Mexico (Brock *et al.*, 1997; Lightner, 1995, 1996a,b). Hence, wild postlarvae and broodstock of unknown health history are potential TSV vectors, should be avoided by shrimp growers, and represent another means by which the virus can be transmitted either locally or between countries.

The movement of TSV between countries has mainly been attributed to the sale and export of live postlarvae and adult shrimp with acute or chronic TSV infections (Brock *et al.*, 1997; Hasson *et al.*, 1999a; Lightner, 1995, 1996a,b, 1999; Lightner *et al.*, 1997b). This is the principal means by which TSV was introduced into shrimp farming nations within the Western Hemisphere during 1992 to 1996 and the manner by which the disease entered Taiwan in 1998 (Hasson *et al.*, 1999a; Tu *et al.*, 1999; Yu *et al.*, 2000). The ability of TSV to withstand long-term freezing without loss of infectivity makes frozen shrimp another potential vector of this disease (Hasson *et al.*, 1995; Lightner, 1995). Thus, virus spread between countries can occur if a frozen infected product is used as bait for fishing (Lightner, 1995; Prior *et al.*, 2001) or if shrimp processing plant wastes are carelessly introduced into local water ways (Lightner, 1995; Lightner *et al.*, 1996b, 1997b).

The principal penaeid host of TSV is *P. vannamei*, which is the predominant marine penaeid species farmed in the Americas and which has been introduced into Asia (Jory, 1995; Tu *et al.*, 1999). TSV causes serious disease in postlarval, juvenile, and adult shrimp of this species, but has not been reported in *P. vannamei* smaller than those in the postlarval (PL) 11 stage (Brock *et al.*, 1995; Lightner, 1996a; Lightner *et al.*, 1995, 1997a; Lotz, 1997). The American penaeids *P. stylirostris*, *P. schmitti*, *P. setiferus*, *P. duorarum*, and *P. aztecus* can also be infected by TSV. However, serious acute TSV infections have only been reported for the PL and juvenile stages of *P. setiferus* (Overstreet *et al.*, 1997), juvenile stages of *P. schmitti* (Brock *et al.*, 1997; Lightner, 1996a) and, most recently, in postlarval and juvenile *P. stylirostris* (Erickson *et al.*, 2002; Robles-Sikisaka *et al.*, 2002). Findings of TSV-tolerant *P. setiferus* juveniles suggest that different strains of this species are more TSV resistant than others (Erickson *et al.*, 1997; Hasson, 1998; Overstreet *et al.*, 1997). Similarly, TSV-resistant strains of specific pathogen-free (SPF) *P. vannamei* have been developed through selective breeding

programs initiated and run by the U.S. Marine Shrimp Farming Consortium as a strategy to combat this disease (Argue *et al.*, 2002; Carr *et al.*, 1997; Lightner, 1995). Limited TSV infectivity studies conducted on the Asian penaeid species *P. monodon*, *P. japonicus*, and *P. chinensis* suggest that all three species are moderately susceptible to the virus as juveniles (Brock *et al.*, 1997; Hasson, 1998; Overstreet *et al.*, 1997). However, TSV can mutate, and a recently described new strain of TSV was found to cause severe infection-induced losses in populations of farmed *P. stylirostris*, a species that was previously considered TSV-refractive or tolerant. This finding is troubling as it suggests that all species of shrimp currently deemed refractive or resistant to the disease may be infected if additional TSV strains or serotypes emerge (Brock *et al.*, 1995; Erickson *et al.*, 2002; Robles-Sikisaka *et al.*, 2002).

3. Disease Cycle

Initial descriptions of TSV lesion pathogenesis were incomplete and based on routine histological analyses of either naturally infected *P. vannamei* from farms or experimentally infected shrimp obtained from short-term infectivity studies (Brock *et al.*, 1995; Hasson *et al.*, 1995; Jimenez, 1992; Lightner *et al.*, 1994, 1995). The cyclic nature of a TSV infection was later determined through histological and ISH analyses of experimentally infected *P. vannamei* juveniles and found to consist of three overlapping yet clinically and histologically distinct phases. The cycle consists of a per acute to acute phase, a short transition phase, and a long-term chronic phase (Hasson *et al.*, 1999b,c). Lotz *et al.* (2003) have divided the disease cycle into five states (uninfected susceptible, prepatently or latently infected, acutely infected, chronically infected, and dead infected shrimp) for the purpose of describing the epizootiology of the disease in mathematical terms. For the purpose of this review, the three phases of TSV infection cycle will be described (Fig. 2).

The clinical signs of an acute phase infection were described earlier. During this period, beginning as early as 24 h postexposure and lasting between 7 to 10 days, virus-induced mortalities peak, and the infected population suffers its highest losses as shown in Fig. 2, phase 1 (Hasson *et al.*, 1999b; Lotz *et al.*, 2003). The predominant cell type targeted by TSV is the cuticular epithelium of the foregut, gills, appendages, hindgut, and general body cuticle (Brock *et al.*, 1995; Hasson *et al.*, 1995; Jimenez, 1992; Lightner, 1995, 1996a; Lightner *et al.*, 1994, 1995). Lesions may extend into underlying subcuticular connective tissue and striated muscle (Brock *et al.*, 1995; Hasson *et al.*, 1995, 1999b; Lightner *et al.*, 1994, 1995). In severe cases, the antennal

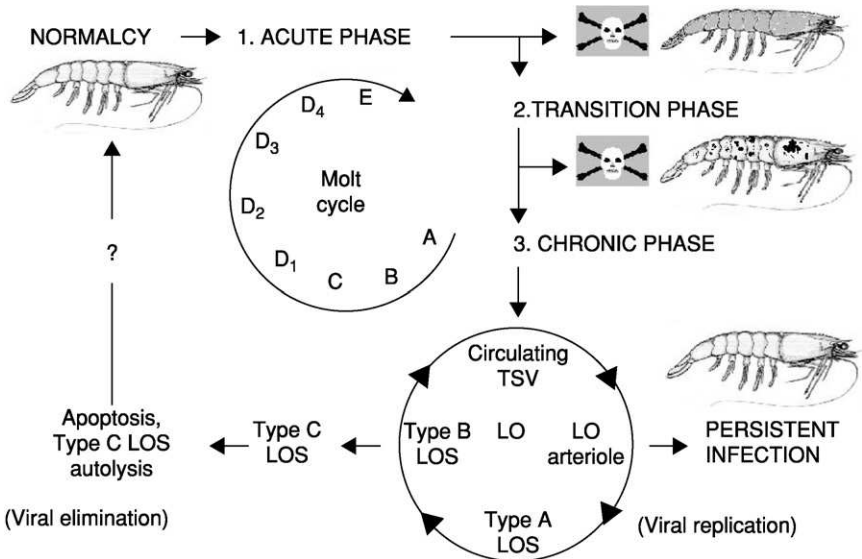


FIG 2. Hypothesized TSV disease cycle in juvenile *Penaeus vannamei* (Phase 1: The acute phase infection targets the cuticular epithelium and subcutis, killing about 60–95% of susceptible shrimp that typically die in preecdysis or postecdysis (stages D₄ or E) and display marked chromatophore expansion. Phase 2: Acute phase survivors enter the transition phase, which is characterized by grossly visible multifocal melanized lesions covering the body, moderate mortality, delay of molt, infrequent acute phase epithelial lesions, sequestering of circulating TSV by hemocytes within the walls of lymphoid organ (LO) arterioles, and interstitial LO spheroid formation. Phase 3: The chronic phase infection begins following molt (postecdysis, stage A) with marked LO spheroid development and LO hypertrophy, with a cessation of mortalities and a return of normal behavior and appearance. Pinocytosis of circulating TSV virions by hemocytes initiates LO spheroid production and morphogenesis beginning with the type A morphotype. Viral replication within the type A LO spheroid produces the vacuolated and necrotic type B form with release of TSV back into the circulatory system, reinitiating spheroid production within the LO and resulting in a persistent chronic infection. Alternatively, the type B spheroid hemocytes may undergo apoptosis and transform into the type C morphotype, resulting in viral elimination with the possibility of the shrimp host returning to a TSV-free state (normalcy). The final outcome of a TSV infection (viral persistence versus elimination) is believed to be largely dependent on the immunological, nutritional, and overall health status of the shrimp. Disease cycle is adapted from Hasson *et al.* (1999b,c); molt cycle adapted from Roer and Dillaman (1993).

gland, hematopoietic tissue, testes, and ovaries may also be infected (Hasson *et al.*, 1999b; Verlee Breland, GCRL, personal communication, 1997). Acutely infected epithelial cells detach from the underlying stroma and assume a spherical shape; cell lysis follows with the liberation of virions into the circulatory system (Hasson, 1998; Hasson *et al.*,

1999b). Histologically, TSV induces a distinctive acute phase lesion consisting of necrotic epithelial cells that display highly basophilic pyknotic and karyorrhectic nuclei, marked cytoplasmic eosinophilia, and variably staining and sized cytoplasmic inclusion bodies (Brock *et al.*, 1995; Hasson *et al.*, 1995, 1999b; Jimenez, 1992; Lightner, 1994, 1995; Lightner *et al.*, 1995). Collectively, these characteristics produce the aptly termed “peppered” or “buckshot laden” appearing histological lesion, which is considered pathognomonic for an acute phase TSV infection (Fig. 3A) (Brock *et al.*, 1995; Hasson *et al.*, 1995, 1999b; Jimenez, 1992; Lightner, 1994, 1995; Lightner *et al.*, 1995). Infection and lysis of the cuticular epithelium does not elicit an immediate

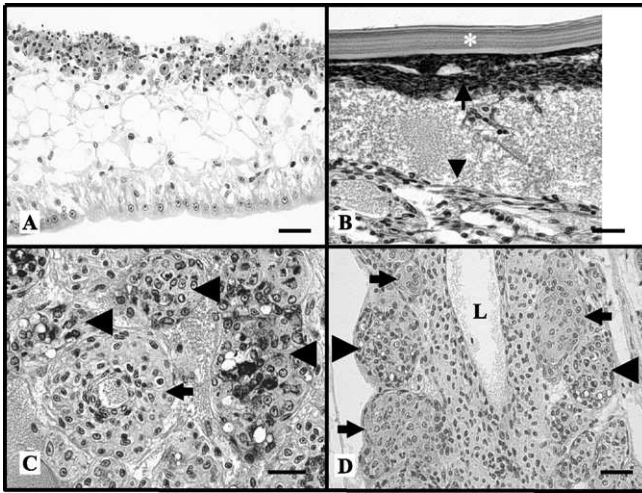


FIG 3. Photomicrographs of naturally occurring acute, transition, and chronic phase TSV infections in *Penaeus vannamei* by routine histology. (A) Head appendage illustrating a pathognomonic severe segmental acute phase TSV infection of the cuticular epithelium and subcutis (Top). The “peppered” appearance of the lesion is principally due to nuclear pyknosis, karyorrhexis, and karyolysis. Normal uninfected epithelium is present for comparison (Bottom). The surrounding cuticle is absent due to sectioning artifact. (B) A transition phase TSV lesion within the region of the cuticular epithelium and subcuticular connective tissue of a tail segment. A layer of melanized (brown) hemocytic infiltrates (small arrow), located immediately below the exocuticle (*), has replaced the virus-killed epithelium. Edema and fibrous tissue are evident (large arrow head), further indicative of ongoing wound repair. (C) High magnification of the lymphoid organ of a chronically infected shrimp showing a normal arteriole in cross-section (small arrow) and three basophilic type B spheroids (large arrow heads). (D) Type A (small arrow) and type B (large arrow head) spheroids bordering the walls of the subgastric artery in the same shrimp described in Fig. 3C. L = Lumen. Hematoxylin and eosin stain. Bar = 30 μm . (See Color Insert.)

inflammatory response and typically occurs in late premolt or early postmolt stages in *P. vannamei* (Brock *et al.*, 1995; Hasson *et al.*, 1995, 1997, 1999a,b; Lightner, 1996a; Lightner *et al.*, 1994, 1995). Dead shrimp with partially sloughed cuticles are commonly observed during this phase. It is possible that the combined porosity of the cuticle and increased metabolic activity of the epithelium that occurs just prior to and during ecdysis results in increased virus accessibility to epithelial cells whose activated state makes them conducive to viral replication (Hasson, 1998).

Shrimp surviving the acute phase infection enter a brief transitional phase, as shown in Fig. 2 as phase 2, which shares characteristics of both the acute and chronic phases and effectively links them together (Hasson *et al.*, 1999b). The transition phase is characterized by declining mortalities and marked by grossly visible multifocal melanized lesions of the cephalothorax and tail. The histological characteristics include infrequent scattered acute phase epithelial lesions, normal appearing lymphoid organ (LO) arterioles (tubules) that display a diffuse TSV probe positive signal by *in situ* hybridization (ISH), and the initiation of spheroid development within the LO. The grossly visible melanized lesions within the cuticular epithelium consist of hemocytic infiltrates and represent foci of resolving acute phase lesions (Fig. 3B). *P. vannamei* with transition phase infections are grossly and histologically detectable in experimentally infected stocks about 4 days following *per os* exposure to TSV, and this phase has a duration of about 5 days. Transition phase shrimp are lethargic and anorexic, presumably because all resources are devoted to wound repair and recovery. The end of the transition phase and initiation of the chronic phase infection is signaled by resumption of the molt cycle and the shedding of the melanized exoskeleton (Hasson *et al.*, 1995, 1999b,c).

A chronic TSV infection, shown in Fig. 2 as phase 3, begins about 6 days postinfection and was found to have a minimum duration of 8 to 12 months in experimentally infected *P. vannamei* (Hasson, 1998; Hasson *et al.*, 1999c; Jeff Lotz, personal communication, 1997). The characteristics of a chronic TSV infection include a cessation of mortalities, absence of disease signs, and resumption of normal feeding and swimming behavior. Histologically, the hallmark of a chronic TSV infection is the presence of numerous spheroids located within both the interstices of a hypertrophied lymphoid organ and along the external surface of the subgastric artery (Fig. 3C and D). Infrequent numbers of ectopic spheroids are also found associated with tegmental glands located within connective tissues of the cephalothorax and appendages. Spheroids consist of phagocytic semigranular and granular hemocytes

with a high apoptotic index (Anggraeni and Owens, 2000). Routine histology and ISH analyses were used to track the development of spheroids in time-course sampled *P. vannamei* juveniles with experimentally induced chronic TSV infections during a 12-month study (Hasson *et al.*, 1999c). To summarize briefly, spheroid development begins during the transition phase following active pinocytosis and sequestering of circulating TSV particles by resident or transient phagocytic hemocytes located in the walls of the LO arterioles. These activated hemocytes are believed to migrate into the LO interstitium where they form aggregates with other TSV-activated hemocytes. The resulting spheroid is characterized by a well-delineated, lightly basophilic, and variably sized and shaped solid mass of hemocytes. Furthermore, spheroids undergo successive morphological changes and produce three distinct forms that were named morphotypes A, B, and C. The first LO spheroid morphotype to appear, type A, consists of a homogenous mass of hemocytes that is, typically, TSV negative by ISH analysis, presumably containing undetectable levels of virus. The subsequent morphotype to develop, type B, displays multifocal cytoplasmic vacuolization and moderate to numerous necrotic foci that are consistently TSV positive by ISH, indicating ongoing viral replication. The terminal morphotype, type C, displays morphological characteristics of apoptotic cells that are TSV negative by ISH and eventually disappear through combined autolysis and resorption. Continued replication of TSV in type B spheroids with concurrent release of the virus into the shrimp circulatory system perpetuates spheroid production in the LO in a cyclic fashion and induces a persistent infection as shown in Fig. 2, phase 3. In contrast, the progressive transformation of the type B to the type C morphotype, with resultant TSV elimination by apoptosis, could return the shrimp host to a TSV-free state (normalcy). Based on these results and published information on LO physiology, Hasson *et al.* (1999c) proposed that spheroid development in marine shrimp represents a cell-mediated immune response as first suggested by Kondo *et al.* (1994). Further, the function of the LO is to remove biotic and abiotic substances from the hemolymph of the shrimp host that are otherwise too small to illicit an encapsulation response (Hasson *et al.*, 1999c). This same hypothesis has been advanced and supported by more recent studies involving the effects of both viral and bacterial infections on the LO (Anggraeni *et al.*, 2000; Soowannayan *et al.*, 2002; van de Braak *et al.*, 2002). The possible outcomes of a chronic TSV infection include a return to normalcy through the complete elimination of TSV via apoptosis or persistence of a chronic state infection due to continued viral replication. Which of these two

competing processes will prevail within the LO probably depends on the nutritional, immunological, and overall health status of the host (Hasson, 1998; Hasson *et al.*, 1999c).

C. Physical Properties of Taura Syndrome Virus

Initial isolation and characterization work was conducted on sucrose and cesium chloride gradient-purified TSV isolated from *P. vannamei* originating from naturally occurring epizootics in Ecuador (1993) and Hawaii (1994) by Hasson *et al.* (1995). These isolates were found to have icosahedral symmetry (Fig. 4), had a diameter of 31–32 nm and a buoyant density of 1.337 g/ml, were nonenveloped, and replicated within the cytoplasm of host cells. These characteristics suggested that TSV corresponded to either Nodaviridae or Picornaviridae. Subsequent work by Bonami *et al.* (1997) demonstrated that TSV possesses a linear positive-sense ssRNA genome of about 9kb, three major (55, 40, and 24 kDa) and one minor (58 kDa) polypeptides composing the capsid, and an extracted genomic RNA that is itself

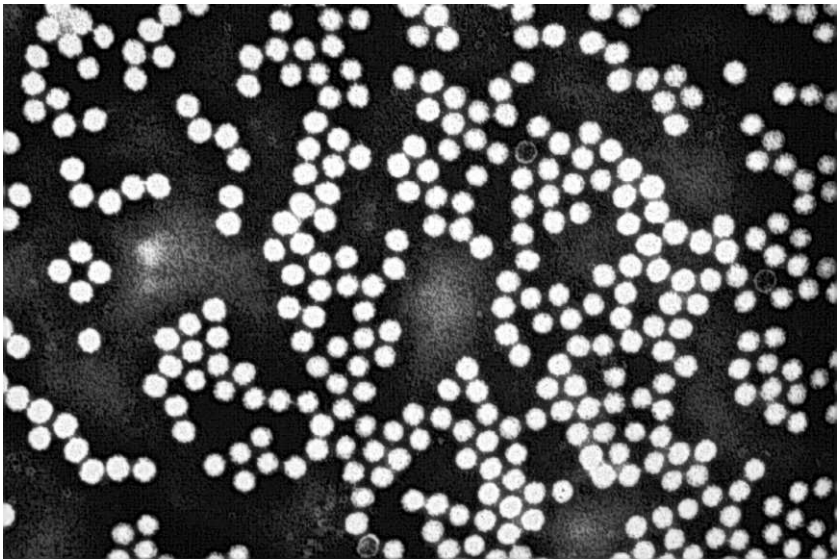


FIG 4. Transmission electron micrograph illustrating CsCl gradient-purified and negatively stained (with 2% PTA) TSV particles isolated from farmed *Penaeus vannamei* originating from Ecuador. The icosahedral viral particles are 31 to 32 nm in diameter and are nonenveloped.

infectious. This latter finding was suggestive of a genome with a polyadenylated 3'-end and the ability to act as a polycistronic mRNA. Collectively, these characteristics justified the classification of TSV as a *Picornavirus* and similarities to insect picornaviruses were discussed by Bonami *et al.* (1997). Subsequent sequence analysis of a cloned segment of the 3'-end of the TSV genome (3728 bp) by Robles-Sikisaka *et al.* (2001) provided further molecular evidence that TSV is similar to other insect picornaviruses. Work conducted by Mari *et al.* (2002) determined the complete sequence of the TSV genome (10,205 nucleotides) and classified the virus as a member of a newly designated group, cricket paralysis-like viruses, in Picornaviridae (van Regenmortel *et al.*, 2000). This group of insect viruses, together with TSV, share similarities with the picornaviruses but are sufficiently different to be grouped separately (Mari *et al.*, 2002).

D. Genome Organization and Gene Expression of *Taura* Syndrome Virus

The TSV genome comprises a single-stranded RNA of positive polarity with a 3'-poly(A) tail (Bonami *et al.*, 1997). The genome is 10,205 nucleotides (nt) long with a 5'-untranslated region of 377 nt and a 3'-untranslated region of 226 nt (Mari *et al.*, 2002). There are two open reading frames (ORFs) in the TSV genome. ORF1 is 6324 nt long and encodes a 2107 amino acid (aa) polyprotein with a molecular mass of 234 kDa. ORF2 is 3036 nt long and encodes a 1011 aa polypeptide with a molecular mass of 112 kDa (Mari *et al.*, 2002). There is an intergenic region of 226 nt between the two ORFs. ORF1 encodes nonstructural proteins, and ORF2 encodes the virion structural proteins (Mari *et al.*, 2002; Robles-Sikisaka *et al.*, 2001). The ORF1 nonstructural proteins contain sequence motifs that correspond to the conserved motifs of a helicase (NTP-binding protein), a protease, and a RNA-dependent RNA polymerase (RdRp) (Fig. 5). The RNA helicase consensus sequence, Gx₄GK, is present at ORF1 amino acid positions 752 to 758, and the TSV helicase domain shows significant similarity with the cognate domain of insect picorna-like viruses (*Drosophila* C virus, DCV; *Rhopalosiphum padi* virus, RhPV; *Plautia stali* intestinal virus, PSIV; black queen cell virus, BQCV; *Triatoma* virus of the fungus *Triatoma infestans*, TrV; and *Himetobi* P virus, HiPV). The protease domain in the TSV ORF1-encoded polypeptide resides between amino acid residues 1380 to 1570. It also shows similarity with the 3C protease of insect picorna-like viruses as well as other positive-sense RNA viruses of the Picornaviridae, Sequiviridae, and Comoviridae that

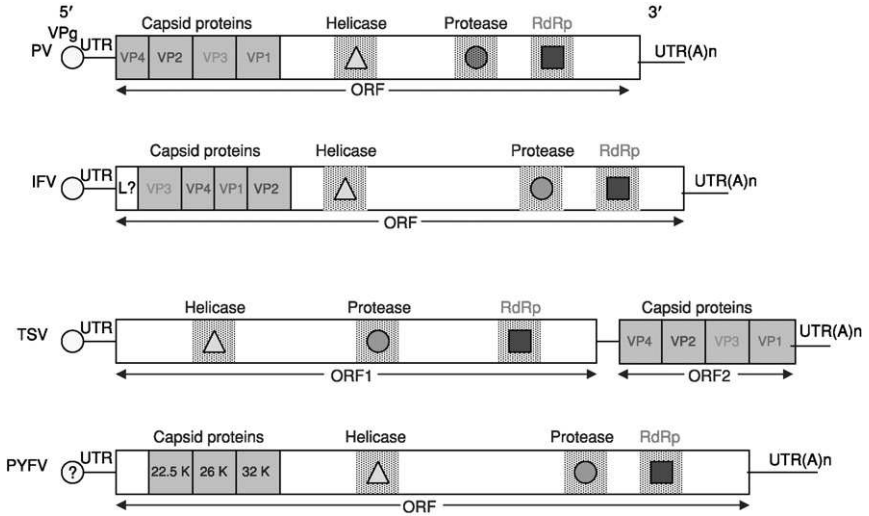


FIG 5. A schematic representation of the genome organization of mammalian and insect picornaviruses and plant RNA viruses. ORF = Open reading frame, UTR = Untranslated region, VPg = Genome linked protein, and ? = The unconfirmed presence of VPg. The helicase (Δ), protease (\circ), and the RNA-dependent RNA polymerase (\blacksquare) regions are indicated. (See Color Insert.)

have a conserved (GxCG) protease motif (Gorbalenya *et al.*, 1989). In TSV, the protease motif is partially conserved with Gly being replaced by Cys. However, like other picornaviruses, the His-Asp-Cys catalytic triad in the protease domain is conserved in TSV (Mari *et al.*, 2002).

The C-terminal region of TSV ORF1 contains the RdRp domain. Multiple alignment of the TSV RdRp domain with homologous domains of other positive-sense RNA viruses is shown in Fig. 6. There are eight conserved motifs in the RdRp (Koonin, 1991) preserved in all insect picorna-like viruses along with picornaviruses of mammalian and plant origin (Fig. 5). Among these, motifs 1, 5, 6, and 7 are more conserved than other motifs, and it has been suggested that these highly conserved motifs might constitute sites for RNA binding (Koonin, 1991). Phylogenetic analysis using the Maximum Likelihood method categorizes picornaviruses into two major clusters (Fig. 7). One cluster contains insect and mammalian picornaviruses and the other the plant picornaviruses. In the first cluster, insect picornaviruses possessing a dicistronic genome (see subsequent paragraphs for detail) group together; in this group, TSV clusters with DCV and cricket paralysis virus (CrPV). The second subcluster contains two groups:

one group includes sacbrood virus (SBV) of honeybee and infectious flacherie virus (IFV) of silkworm, the genome organization of which shares more similarities with mammalian than insect picornaviruses, and the other group includes mammalian picornaviruses (Fig. 7).

In addition to helicase, protease, and RdRp motifs, the TSV genome contains a short aa sequence at the N-terminal end of ORF1 (positions 166 to 230) that shows significant similarity with the inhibition of apoptosis (IAP) proteins found in mammals, yeast, insects, and some DNA viruses (Mari *et al.*, 2002). No other RNA viruses are known to contain such an IAP motif. TSV-infected shrimp that survive the initial acute infection enter into a long-term chronic phase infection (Fig. 2) (Hasson *et al.*, 1999b,c). It remains to be seen if the TSV-encoded peptides containing the IAP motif play any role in evading the host immune system, thus enabling the virus to replicate during the long-term chronic phase infection.

TSV ORF2 contains the capsid proteins. TSV virions contain three major proteins designated as VP1 to VP3 (55, 40, and 24 kDa) and one minor protein (58 kDa) designated as VP0, polypeptide (Bonami *et al.*, 1997). The N termini of VP1 to VP3 have been sequenced, and the order of these proteins in ORF2 was found to be VP2, VP1, and VP3 (Mari *et al.*, 2002). The N-terminal sequence of VP0 has not been determined, and it has been hypothesized that it might be processed from ORF2 in a manner similar to PSIV, an insect picorna-like virus infecting the brown-winged green bug (*Plautia stali*) (Sasaki *et al.*, 1998). The five amino acid motif containing the VP2/VP1 cleavage site in TSV is conserved in insect picornaviruses: TSV (GF↓SKD), PSIV (GF↓SKP), DCV (GF↓SKP), and RhPV (GW↓SKP) (Robles-Sikisaka *et al.*, 2001). The presumed VP1 and VP3 cleavage site in TSV (H↓A) is partially conserved with those used by insect picornaviruses Q↓(A,S,V) (Mari *et al.*, 2002).

A BLASTP search using the ORF2 1011 aa sequence of TSV showed 39 to 43% similarity with the cognate ORF of insect picornaviruses including RhPV (213/482 aa overlap, $E = 2e^{-24}$), TrV (231/584 aa overlap, $E = 2e^{-20}$), DCV (230/581 aa overlap, $E = 3e^{-19}$), PSIV (162/402 aa overlap, $E = 4e^{-16}$), CrPV (56/136 aa overlap, $E = 2e^{-04}$), and HiPV (230/580 aa overlap, $E = 1e^{-15}$) (Robles-Sikisaka *et al.*, 2001). These similarities encompass TSV VP1 and VP2 capsid proteins. A multiple alignment of TSV VP1 and VP2 amino acid sequences with the homologous proteins of insect and mammalian picornaviruses is shown in Fig. 8. A small RNA virus infecting aphids (*Acyrtosiphon pisum* virus, APV) (van der Wilk *et al.*, 1997) has recently been reported to have a genome like those of other insect-infecting RNA viruses that contain

two long ORFs with its virion proteins encoded in the 3'-ORF. The TSV capsid protein sequences, however, show no significant similarity to that of APV.

Northern blot analysis, using total RNA from tail muscle of TSV-infected *P. stylirostris* and radio-labeled probe to a genomic region containing the TSV capsid genes, detected a single transcript of about 10 kb. This suggests that the capsid protein gene is not transcribed as a subgenomic RNA and that the capsid proteins might be translated from the full-length transcript (Robles-Sikisaka *et al.*, 2001). This distinguishes TSV from many positive-stranded RNA viruses (e.g., species of Calciviridae and Togaviridae) in which the capsid proteins encoded in the 3'-end of the genome are generally translated from a subgenomic RNA (Murphy *et al.*, 1995). The TSV transcriptional strategy, however, is similar to insect picornaviruses like RhPV, PSIV, and HiPV, which do not produce a subgenomic RNA for the expression of their capsid proteins encoded in the ORF at the 3'-end of the viral genome.

E. Comparison of Genome Organization of TSV with Insect and Mammalian Picornaviruses

Many picornaviruses have been isolated from a wide range of insect species. Based on their biologic and biophysical properties as well as genome organization data, these viruses were classified as members of a newly designated group, as cricket paralysis-like viruses, in the



FIG 6. Multiple alignment of amino acid sequence of RdRp genes of picornaviruses using the ClustalX program. The alignment is shaded (using up to a 50% consensus) with gray and black indicating similar and identical residues, respectively. The numbers 1 through 8 above the alignment indicate locations of the conserved motifs. A total of 17 *Picornavirus* species were used for the multiple alignment. These include cricket paralysis virus (CrPV; AF218039), *Drosophila C* virus (DCV; AF014388), acute bee paralysis virus (ABPV; NC002548), *Rhopalosiphum padi* virus (RhPV; AF022937), sacbrood virus (SBV; AF092924), *Plautia stali* intestinal virus (PSIV; AB006531), black queen cell virus (BQCV; AF183905), *Triatoma* virus (TrV; AF178440), himetobi P virus (HiPV; AB017037), infectious flacherie virus (IFV; AB000906), and Taura syndrome virus (TSV; F277675). In addition to insect picornaviruses, the RdRp sequences of the following mammalian picornaviruses were taken for phylogenetic analysis: foot-and-mouth disease virus (FMDV; P03305), human echovirus (EV; AF311938), and hepatitis A virus (HAV; BAA35107). The RdRp sequences of positive-strand RNA viruses infecting plants that were included for the multiple alignment were rice tungro spherical virus (RTSV; A46112), Parsnip yellow fleck virus (PYFV; Q05057), and cowpea mosaic virus (CPMV; P03600). (See Color Insert.)

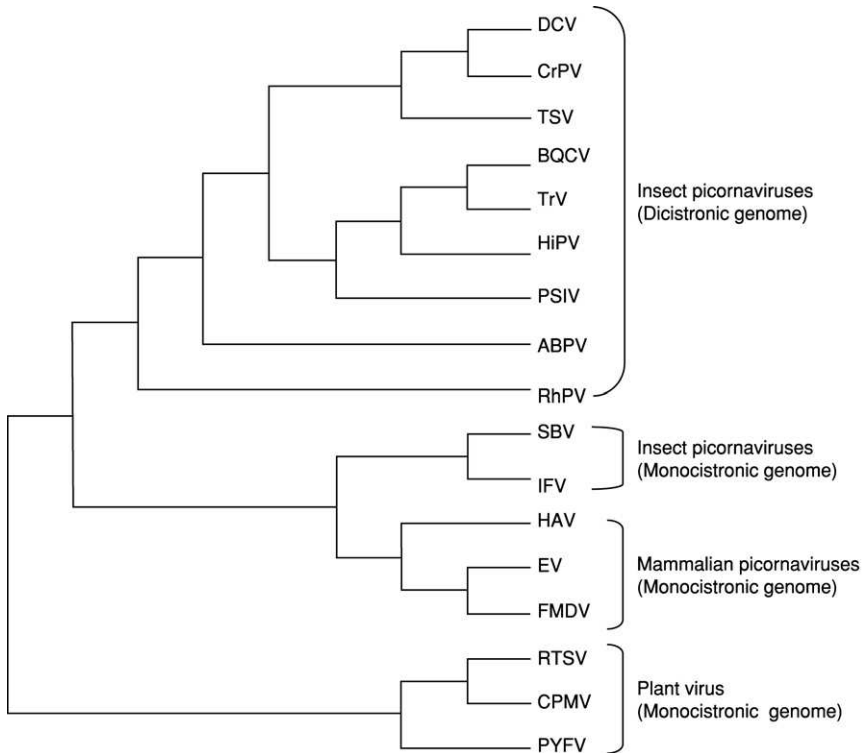


FIG 7. Maximum likelihood phylogenetic tree of picornaviruses infecting insects and mammalian hosts using the amino acid sequence of the RNA-dependent RNA polymerase gene. Plant RNA viruses were used as the out-group. The list of the virus species used for the phylogenetic analysis is the same as used for the multiple alignment of the RdRP gene. The plant picornaviruses were used as an out-group for the phylogenetic analysis. The DNA substitution model used for the analysis was the Hasegawa-Kishino-Yano 85 + I + G; proportion of transitions/transversions was 0.9308; nucleotide frequencies were A = 0.28990, C = 0.19290, G = 0.21940, T = 0.29780; proportion of invariable sites equaled 0.0346; were shape parameter was 2.3891; and the log likelihood of the tree was 15706.94.

family Picornaviridae with CrPV as the type species of this group (Christian and Scotti, 1998; van Regenmortel *et al.*, 2000). Genomes of a number of these viruses have now been sequenced. These include CrPV (AF218039), DCV (AF014388), and acute bee paralysis virus (ABPV, NC002548); BQCV (AF183905), and SBV (AF092924) of honeybees; RhPV (AF022937), PSIV (AB006531), TrV (AF178440), and

HiPV (AB017037); as well as IFV (AB000906) and TSV of shrimp (F277675). Among these viruses, the genome organizations of IFV and SBV were found to be similar to that of mammalian picornaviruses. They contain a single long ORF with the capsid proteins located at the N-terminal end and the nonstructural proteins at the C-terminal end. In contrast, the genomes of CrPV, DCV, RhPV, PSIV, HiPV, TrV, and TSV contain two long ORFs (ORF1 and ORF2) separated by a intergenic region. The 5'-end of ORF1 contains the nonstructural proteins, and the 3'-end of ORF2 contains the capsid proteins (Fig. 5). All of these viruses show greater sequence similarity to each other than with any of the mammalian picornaviruses. In addition, the insect picornaviruses that possess dicistronic genomes have two unique features. First, no subgenomic RNA is produced for translation of the capsid proteins, and second, the coat protein cistron appears to lack an initiating methionine, suggesting that the coat protein is translated through internal initiation and mediated by an internal ribosomal entry site (IRES). Functional IRES elements have been identified in the intergenic region of CrPV and PSIV (Sasaki and Nakashima, 1999; Wilson *et al.*, 2000), and cap-independent translation in PSIV ORF2 has been demonstrated *in vitro* using a rabbit reticulocyte lysate (Sasaki and Nakashima, 2000). In CrPV, the initiation codon for IRES-mediated translation was identified as CCU, whereas in PSIV and RhPV, the initiation codon was found to be CUU. It has been shown that the CCU/CUU triplets are part of the inverted repeat sequence of the IRES elements that form RNA pseudo-knot structures essential for IRES activity (Sasaki and Nakashima, 1999; Wilson *et al.*, 2000). In TSV, although there is an in-frame methionine in ORF2, N-terminal sequencing of the VP2 capsid protein identified an Ala at the terminal position in the sequenced protein (ANPVEIDNFDTT) (Mari *et al.*, 2002). The Ala codon is preceded by both a Pro (CCU) and a Met (AUG) codon (MPANPVE). For Met to be the initiation codon for TSV ORF2, MP residues would need to be removed from the mature protein. Such post-translational processing has never been found in eukaryotes, and it is likely that TSV employs an IRES-mediated cap-independent mechanism for translation of the structural proteins, which is similar to the insect picornaviruses.

In cells infected with insect picornaviruses like DCV, it has been shown that structural proteins are produced in vast excess over nonstructural proteins (Moore *et al.*, 1980, 1981). This contrasts to what has been observed in cells infected with human picornavirus, where equimolar amounts of structural and nonstructural proteins are produced

(Ruckert, 1996). The IRES-mediated translation of the coat proteins in insect picornaviruses with dicistronic genomes, therefore, provides a mechanistic explanation for the abundance of structural compared to nonstructural proteins in infected cells. Thus, the translation of the two distinct polyproteins (ORF1 and ORF2) appears to be independently controlled. This contrasts to the picornaviruses encoding a single ORF in which a single polyprotein is post-translationally processed to generate both the structural and nonstructural proteins (Ruckert, 1996).

F. Genetic Diversity of Taura Syndrome Virus

During the summers of 1999 and 2000, TSV epizootics occurred frequently among *P. stylirostris* shrimp farmed in Mexico. TSV-infected shrimp presented severe acute-phase histological lesions accompanied by high mortality. These shrimp were virus positive by RT-PCR and by ISH but negative by immunohistochemistry (IHC) analyses using a TSV-specific monoclonal antibody (mAb) (Hasson, unpublished data). Severe acute-phase TSV lesions in *P. stylirostris* were observed on only one previous occasion in 1997 in a diagnostic case from Nicaragua (Hasson, unpublished data). Because *P. stylirostris* are characteristically TSV-tolerant, it was speculated that the epizootics in Mexico might have been due to the emergence of a previously unrecognized TSV strain (Hasson, unpublished data). Subsequently, TSV isolates were collected from 16 different farms in Mexico (Sinaloa and Sonora) and then compared with isolates from the United States (Texas and Hawaii), Taiwan, and Nicaragua (Robles-Sikisaka *et al.*, 2002). TSV VP1 and VP2 gene regions were amplified by RT-PCR and sequenced. Both VP1 and VP2 coding sequences showed some conservative and nonconservative amino acid replacements among the isolates (Fig. 9). Among these changes, nonconservative replacements of S→A (polar uncharged to nonpolar hydrophobic) in VP1 (Fig. 9A) and Q→K (polar uncharged to positively charged) in VP2 (Fig. 9B) occurred in quite a few isolates. These nonconservative replacements may alter antigenic epitopes involved in antibody binding and contribute to the serological differences identified. Changes in antigenicity and host adaptability resulting from point mutations in the coat protein genes have been reported in mammalian picornaviruses, such as coxsackie virus B4 (Halim and Ramsingh, 2000), encephalomyocarditis virus (Nelsen-Salz *et al.*, 1996), human influenza A virus (Fitch *et al.*, 1991), and foot-and-mouth disease virus

A

```

1
80
Tx1  FAAPVGLAVAMANWWRGNINLNLRFQAKTQYHQCRLLVQYLPYGSQVPIESILSQIIDISQVDDKGIIDIAFPSPVYPNKWM
Tx2  .....
Hi1  .....S.....
Hi2  .....S.....
Tw1  .....S.....
Tw2  .....S.....
Sin1  .....S.....
Sin6A .....S.....
Sin6B .....S.....
Son1A .....S.....
Son6A .....S.....
Son6B .....S.....
Son7A .....S.....
Son7B .....S.....
Son2B .....S.....
Son9A .....S.....
Son10B .....S.....
Sin2C .....S.....
Sin2A .....L.....
Sin4A .....L.....
Son4A .....L.....
Son4B .....L.....
Son5A .....L.....
Son5B .....L.....
Son8A .....L.....
Son8B .....L.....
Son10A .....L.....
Sin4B .....
Sin5A .....
Sin5B .....
Sin5C .....
Son1B .....
Son2A .....

```

```

81
169
Tx1  RVIDPAKVGYTADCAPGRIVISVLNPLISASTVSPNIVMYPWVWNSNLEVAEPGLAKAAIGFNYPADVPEEPTFSVTRAPVSGILFTL
Tx2  .....
Hi1  .....
Hi2  .....
Tw1  .....H.....A.....
Tw2  .....H.....A.....
Sin1  .....
Sin6A .....
Sin6B .....
Son1A .....
Son6A .....
Son6B .....
Son7A .....
Son7B .....
Son2B .....
Son9A .....
Son10B .....
Sin2C .....
Sin2A .....
Son1B .....
Son4A .....
Son4B .....
Son5A .....S.L.....
Son5B .....
Son8A .....
Son8B .....
Son10A .....
Sin4A .....A.....
Sin4B .....A.....A.....
Sin5A .....A.....A.....
Sin5B .....A.....A.....
Sin5C .....A.....A.....
Son2A .....A.....A.....

```

FIG 9. (continued)

B

	1		80
Tx1	MSNKLANIAYMRCDYEVTVRVQATPFLQGALWLNKMKNAKQTSIIIRRTLTEHLRSITSPFGIEMNLQSEARAITLSIPYT		
Tx2		
Hi1		
Hi2		
Tw1		
Tw2		
Sin2B		
Sin4B		
Son3		
Son4A		
Son5A		
Son5C		
Son8A		
Son8B		
Sin5B		
Sin5C		
Son2B		
Son7A		
Sin2C		
Sin3		
Sin6A		
Sin6B		
Son1A		
Son1B		
Son6A		
Son7B		
Son9A		
Son9B		
Son10A		
Son10B		V.....

	81		169
Tx1	SELQVFNPRNVNMLNSIRLSVLSQLQGPEDVESASYSIYGRLNKIKLYGHAPSVTSSVYPSTQSGYDDDCPIVHAGTDEDSSKQGIIVSR		
Tx2		
Hi1		
Hi2		
Tw1		
Tw2		
Sin2B	V.....	
Sin4B	K.....	
Son3	K.....	
Son4A	K.....	
Son5A	K.....	
Son5C	K.....	
Son8A	K.....	
Son8B	K.....	
Sin5B		F.....
Sin5C		F.....
Son2B		F.....
Son7A		Y.....W.....
Sin2C		
Sin3		
Sin6A		
Sin6B		
Son1A		
Son1B		H.....
Son6A		
Son7B		
Son9A		
Son9B		
Son10A		
Son10B		

FIG 9. Multiple alignment of predicted amino acid sequences. (A) VP1 sequence. (B) VP2 sequence. Capsid protein genes of TSV isolates were collected from the United States (H₁ = Hawaii, T_x = Texas), Mexico (Son = Sonora, Sin = Sinaloa), and Taiwan (Tw). Identical amino acid is indicated by a dot. Adapted from Robles-Sikisaka *et al.* (2002) with permission.

(Haydon *et al.*, 2001; Mateu *et al.*, 1988). It remains to be seen if point mutations in VP1 and VP2 genes provide TSV a selective advantage for host adaptability or increased virulence.

TSV-infected shrimp collected from the United States, Taiwan, Mexico, and Nicaragua were analyzed by hematoxylin and eosin-phloxine (H&E) histology and IHC using a TSV-specific mAb. Although all *P. vannamei* and *P. stylirostris* collected from the United States (Texas and Hawaii isolates), Taiwan, Mexico, and Nicaragua showed acute- or chronic-phase TSV infections by H&E histology, IHC produced positive signals with the isolates from Taiwan, Texas, and Hawaii but not the isolates from Mexico and Nicaragua. This suggests that more than one isolate is prevalent in TSV endemic regions (Fig. 10). A similar finding has also been published by Erickson *et al.* (2002). These authors reported that the virus could be detected in all three of their isolates collected from Mexico and from the United States (Hawaii) by Western blot, immunodot blot, and IHC analyses using a TSV polyclonal antibody. However, when IHC analyses were conducted using mAb 1A1, only two of three Mexican isolates and the Hawaiian isolate reacted positively, indicating the presence of more than one isolate in TSV epizootic areas. The epitope recognized by mAb 1A1 was putatively localized to the TSV VP1 protein (Erickson *et al.*, 2002).

RNA viruses have been found to exist as a mixture of related yet heterogeneous genome sequences (known as “quasi-species”) due to lack of effective proofreading activity of RNA polymerase (Domingo and Holland, 1997). Therefore, the existence of TSV strains comprising more than one dominant genotype in infected shrimp populations is not surprising. However, the history of TSV epizootics in Mexico suggests another possibility. When TSV epizootics in Mexico reached a peak in 1996, farmers started switching from culturing TSV-susceptible *P. vannamei* to TSV-resistant *P. stylirostris*. This resulted in the decline of TSV epizootics, and by 1998, shrimp production in Mexico (Sinaloa) appeared to have stabilized (Zarain-Herzberg and Ascencio-Valle, 2001). The replacement of *P. vannamei* with *P. stylirostris* in shrimp farms in Mexico might have contributed to the development of a new strain(s) of TSV as the virus adapted to a new host species. As live postlarvae and adult shrimp are transported from one country to another and across the continents, TSV has spread into new areas where it was not previously present (Tu *et al.*, 1999; Yu and Song, 2000). It is, therefore, possible that as naive shrimp populations are exposed to TSV, virus and host selection will evolve, which might result in the emergence of a new and possibly more virulent strain with devastating consequences.

G. Diagnosis of Taura Syndrome Virus

1. Bioassay

TSV infection can be induced by exposing specific pathogen-free (SPF) juvenile shrimp (*P. vannamei*, Kona stock) to TSV-suspect shrimp either by following oral or injection routes (OIE, 2003). Confirmation of TSV presence is then accomplished through analysis of the dying shrimp using histological or molecular methods. The *per os* challenge protocol involves feeding chopped carcasses of suspect shrimp to SPF juveniles in small tanks. TSV-positive indicator shrimp, as identified by gross signs and histopathology, appear within 3 to 4 days post-challenge, and significant mortalities occur within 3 to 8 days. The injection protocol involves homogenizing TSV-suspect shrimp head tissues or whole shrimp in TN buffer or sterile 2% saline solution. Following centrifugation of the homogenate, the clarified supernatant is diluted to 1:10 to 1:100 in sterile 2% saline and filter sterilized, and then 10–20 μ l/g body weight is injected intramuscularly into the third tail segment of the shrimp. If the inoculum contains TSV, shrimp begin dying within 1 to 2 days although inocula containing less TSV may take longer to induce mortalities (OIE, 2003).

2. Histological and Immunological Methods

A variety of histological, immunological, and molecular diagnostic techniques are available for the detection of TSV, and these are thoroughly reviewed elsewhere (Lightner, 1996b, 1999; Lightner *et al.*, 1998). Routine H&E histology of Davidson's AFA-preserved shrimp tissue (Bell and Lightner, 1988; Humason, 1972) is a standard diagnostic tool used for the identification of TSV-induced pathology. Observation of the pathognomonic acute-phase lesion in cuticular epithelium (Fig. 3A) by light microscopy is sufficient to make a definitive diagnosis of TSV infection (Brock *et al.*, 1995, 1997; Hasson *et al.*, 1995, 1997, 1999a,b; Lightner, 1995, 1996a,b; Lightner *et al.*, 1994, 1995).

An ISH method for detecting TSV in shrimp tissue has been developed that employs two TSV-specific, digoxigenin-labeled cDNA probes (1.3 and 1.5 kb) complementary to the TSV genome (Mari *et al.*, 1998). Positive ISH reactions in shrimp histological sections produce a blue-black precipitate within the cytoplasm of TSV-infected cells. One advantage of ISH over routine H&E histology is the greater diagnostic sensitivity, as TSV can be detected in shrimp with mild acute infections that may not be obvious by routine histology. In addition, ISH can

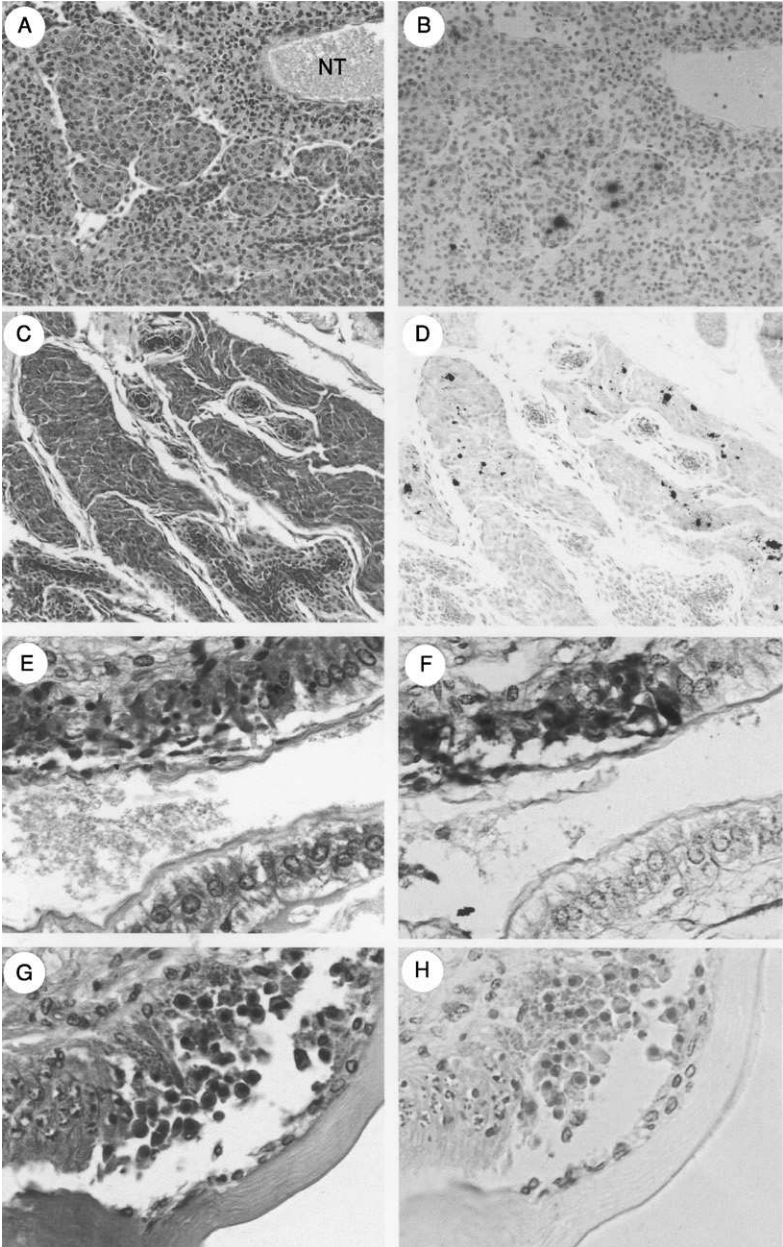


FIG 10. (*continued*)

detect TSV both in asymptomatic and chronically-infected shrimp in which the only histological abnormality is the presence of ectopic or LO spheroids. As LO spheroid development has been associated with at least six different shrimp viral diseases, demonstration of TSV in spheroids by ISH is necessary for a confirmatory diagnosis of this disease (Hasson *et al.*, 1999c). Overfixation of TSV-infected shrimp tissue with Davidson's AFA fixative can result in acid hydrolysis of RNA and produce false-negative ISH results. This problem can be avoided by using a fixation time of 24 hr and prompt tissue embedding or preservation in a neutral pH fixative (Hasson *et al.*, 1997).

An ELISA-based dot blot test for the detection of TSV capsid protein by use of a TSV-specific monoclonal antibody has been described (Poulos *et al.*, 1999), and the procedure has been modified for the IHC detection of TSV in histological sections (Dr. Luis Matheu Wyld, personal communication, 1998). IHC has advantages over ISH in that it is a rapid assay (4 hr versus 36 hr for ISH), more economical, and its TSV detection sensitivity is equivalent to ISH assay. The principle drawback with this technique is that the current commercially available antibody detects the original TSV type strain or isotype but not the Mexican strain identified in *L. stylirostris* (Erickson *et al.*, 2002; Robles-Sikisaka *et al.*, 2002).



FIG 10. Photomicrographs of consecutive acute or chronic phase TSV-infected tissue sections following analysis by H&E histology (Left column) and immunohistochemistry utilizing a TSV-specific mAb (Right column). (A, B) Lymphoid organ (LO) of a *P. vannamei* juvenile chronically infected with the 1995 Texas TSV isolate. Numerous LO spheroids are located to the left of and below a normal LO tubule (NT) and contain strong multifocal IHC positive signals (blue-black precipitate) (Davidson's fixative, 20X). (C, D) LO of a *P. stylirostris* juvenile submitted by a farm in Taiwan, 2000, and displaying a chronic TSV infection. Small normal LO tubules are surrounded by large, irregularly shaped LO spheroids, that display multifocal IHC positive signals similar to Fig. 10B (Davidson's fixative, 20X). (E, F) Midsagittal section through the anterior stomach of a *P. vannamei* juvenile infected with the 1994 Hawaii TSV isolate. The upper halves of the photos display a typical acute phase TSV infection of the cuticular epithelium (note pyknotic nuclei), and the lower halves illustrate normal uninfected epithelium. TSV presence in the necrotic region is denoted by the strong IHC signal (R-F fixative, 60X). (G, H) Midsagittal section through the paragnath of a *P. stylirostris* juvenile submitted by a farm in Mexico (Sonora), 2000. The pathodiagnostic acute phase TSV lesion is characterized by nuclear pyknosis, cytoplasmic eosinophilia, and detachment of the infected cuticular epithelial cells from the surrounding matrix in contrast to normal uninfected epithelium located to the far left. IHC analysis produced a negative result denoted by the absence of blue-black precipitate (Davidson's fixative, 60X). Histological sections were stained with H and E. Sections analyzed by IHC were counterstained with Bismarck brown. Adapted from Robles-Sikisaka *et al.* (2002) with permission. (See Color Insert.)

Detection of viruses by their propagation in cell lines is a routine diagnostic tool used in clinical virology laboratories (Lightner and Redman, 1998; Toullec, 1999). A variety of shrimp primary cell cultures have been developed, but an immortalized shrimp cell line has yet to be achieved. As a result, diagnosticians continue to rely on *in vivo* bioassays for shrimp virus detection and amplification (Lightner, 1996a; Lightner and Redman, 1998; Toullec, 1999). A crustacean cell line established from crayfish (*Orconecte limosus*) neuronal cells has been reported (Neumann *et al.*, 2000) and is available from the American Type Culture Collection (ATCC). There have been no reported attempts, however, to propagate TSV or other shrimp viruses using this cell line.

3. RT-PCR and Real-Time RT-PCR

An RT-PCR method has been described for the detection of TSV in hemolymph (Nunan *et al.*, 1998), and the sequences of primers (9195F and 9992R) used to amplify a 231-bp region of the VP2 gene are given in Table II. Compared to TSV diagnosis based on clinical signs, histopathology and bioassays that are both labor intensive and time consuming, RT-PCR provides a nonlethal diagnostic method that is both rapid and highly sensitive.

Recently, real-time RT-PCR methods using either SYBR Green dye (Dhar *et al.*, 2002; Moullisseaux *et al.*, 2003) and the TaqMan probe (Tang *et al.*, 2003) have been developed for the rapid detection and quantification of TSV. The real-time PCR assay measures the amplicon accumulation during the exponential phase of the reaction. Amplification profiles and the dissociation curves obtained for a TSV-infected and a healthy shrimp sample together with those obtained for an endogenous shrimp gene, elongation factor-1 α , are shown in Fig. 11. The amplification profile indicates a significant increase in fluorescence at 31.25 cycles (recorded as the cycle threshold value [Ct] value) in the TSV-infected sample but not the control sample (Fig. 11A). However, both healthy and TSV infected samples provided equivalent amplification of elongation factor-1 α (Fig. 11C). The dissociation curves of the TSV and elongation factor-1 α amplicons had peaks at expected temperature, confirming the specificities of these amplicons (Figs 11B and D). The SYBR Green RT-PCR is very sensitive, highly specific, and has a wide dynamic range of detection. It will be very useful for detecting subclinical infection and has a high throughput potential for screening broodstock and other samples for TSV (Dhar *et al.*, 2002).

A real-time RT-PCR assay using TaqMan probe has been described by Tang *et al.* (2003). The method is very sensitive and highly specific

in detecting TSV. The high specificity of TaqMan RT-PCR is achieved by the use of a target-specific, dually labeled fluorogenic probe that hybridizes to the template between the PCR primers and is cleaved during polymerase extension by its 5'-exonuclease activity (Holland *et al.*, 1991). TaqMan probes, however, are currently quite expensive. Unlike a real-time assay using the TaqMan probe, SYBR Green real-time RT-PCR does not require an additional probe. The diagnostic specificity of SYBR Green real-time RT-PCR is achieved by analyzing the dissociation curve of the target amplicon. However, in TaqMan RT-PCR, both TSV and endogenous shrimp targets can be amplified simultaneously using probes with different fluorogenic tags, which is not possible in SYBR Green RT-PCR.

III. YELLOWHEAD DISEASE

A. History, Clinical Signs, and Transmission

Yellowhead disease (YHD) syndrome (*Hua leung*) was first observed in 1990 in black tiger shrimp (*Penaeus monodon*) farmed in central Thailand (Limsuwan, 1991). By 1992, the disease had spread to shrimp farming regions on the east and west coasts of the Gulf of Thailand, where YHD has remained enzootic (Boonyaratpalin *et al.*, 1993; Limsuwan, 1991). The occurrence and severity of YHD outbreaks in Thailand appeared to diminish following the emergence of white spot syndrome virus (WSSV) in 1994, and yellowhead virus (YHV) or related viruses have since been commonly detected in healthy shrimp (Flegel, 1997; Pasharawipas *et al.*, 1997). Although the origins of YHV remain unclear, a review of particle morphology, morphogenesis, and histopathology has suggested that the collapse of the shrimp farming industry in Taiwan in the late 1980s may have been due to YHV rather than *monodon* baculoviruses as had been reported at that time (Chantanachookin *et al.*, 1993; Chen and Kou, 1989).

In early descriptions of YHD in Thailand, *P. monodon* with severe signs displayed a pale or bleached body appearance and a yellowish discoloration of the cephalothorax. This latter sign, from which the name YHD is derived, was due to yellowing of the hepatopancreas (HP), which was typically swollen and soft compared to the normal brown HP of healthy shrimp, and due to a yellow-brownish discoloration of gills (Boonyaratpalin *et al.*, 1993; Chantanachookin *et al.*, 1993; Flegel *et al.*, 1995b; Limsuwan, 1991). Juvenile to subadult shrimp were susceptible to YHD, and mortalities were observed to

TABLE II
LIST OF PRIMERS USED FOR THE DETECTION OF TSV, YHV, AND GAV BY CONVENTIONAL AND REAL-TIME RT-PCR

Virus/control gene	Primer	Primer sequence (5'–3')	Amplicon size (bp)
Conventional RT-PCR:			
TSV	9195F	For: TCAATGAGAGCTTGGTCC	231 ^a
	9992R	Rev: AAGTAGACAGCCGCGCTT	
YHV	10F	For: CCGCTAATTTCAAACTACG	135 ^b
	144R	Rev: AAGGTGTTATGTCGAGGAAGT	
YHV	273F	For: CAAGATCTCACGGCAACTCA	273 ^c
	273R	Rev: CCGACGAGAGTGTTAGGAGG	
YHV and GAV	GY1	For: GACATCACTCCAGACAACATCTG	794 ^d
	GY4	Rev: GTGAAGTCCATGTGTGTGAGACG	
YHV	GY2	For: CATCTGTCCAGAAGGCGTCTATGA	277 ^e
	Y3	Rev: ACGCTCTGTGACAAGCATGAAGTT	
GAV	GY2	For: CATCTGTCCAGAAGGCGTCTATGA	406 ^f
	G6	Rev: GTAGTAGAGACGAGTGACACCTAT	
Real-time RT-PCR:			
SYBR Green real-time RT-PCR:			
TSV	112F	For: CTGTTTGTAACACTACCTCCTGGAATT	50 ^g
	162R	Rev: TGATAACAACAACCAGTGGAGGACTAA	
	004F	For: ATGAGAGCTTGGTCCTGGACTTC	78 ^h
	081R	Rev: CCCAATCACTAATCAGAATGTAGTGC	

YHV	141F	For: CGTCCCGGCAATTGTGAT	65 ⁱ
	206R	Rev: CCAGTGACGTTTCGATGCAATA	
	912F	For: TCAATGAGTTCAATGACGTCGAA	50 ^j
	962R	Rev: GAATGGTATCACCGTTCAGTGTCTT	
	399F	For: ATCGGCACAGGAGCAGACA	98 ^k
	496R	Rev: GTAACCCCGGCCATGACTT	
Taqman RT-PCR: TSV	1004F	For: TTGGGCACCAAACGACATT	72 ^l
	1075R	Rev: GGGAGCTTAAACTGGACACACTGT	
		Probe: CAGCACTGACGCACAATATTCGAGCATC	
Internal control gene:	25F	For: TCGCCGAAGCTGCTGACCAAGA	55 ^m
EF-1 α	79R	Rev: CCGGCTTCCAGTTCCTTACC	

^a Nunan *et al.* (1998); ^b Wongteerasupaya *et al.* (1997); ^c Tang and Lightner (1999); ^{d,e,f} Cowley *et al.* (2003); ^{g,i} Dhar *et al.* (2002); ^{j,h,k,m} Mouillesseaux *et al.* (2003); ^l Tang *et al.* (2003).

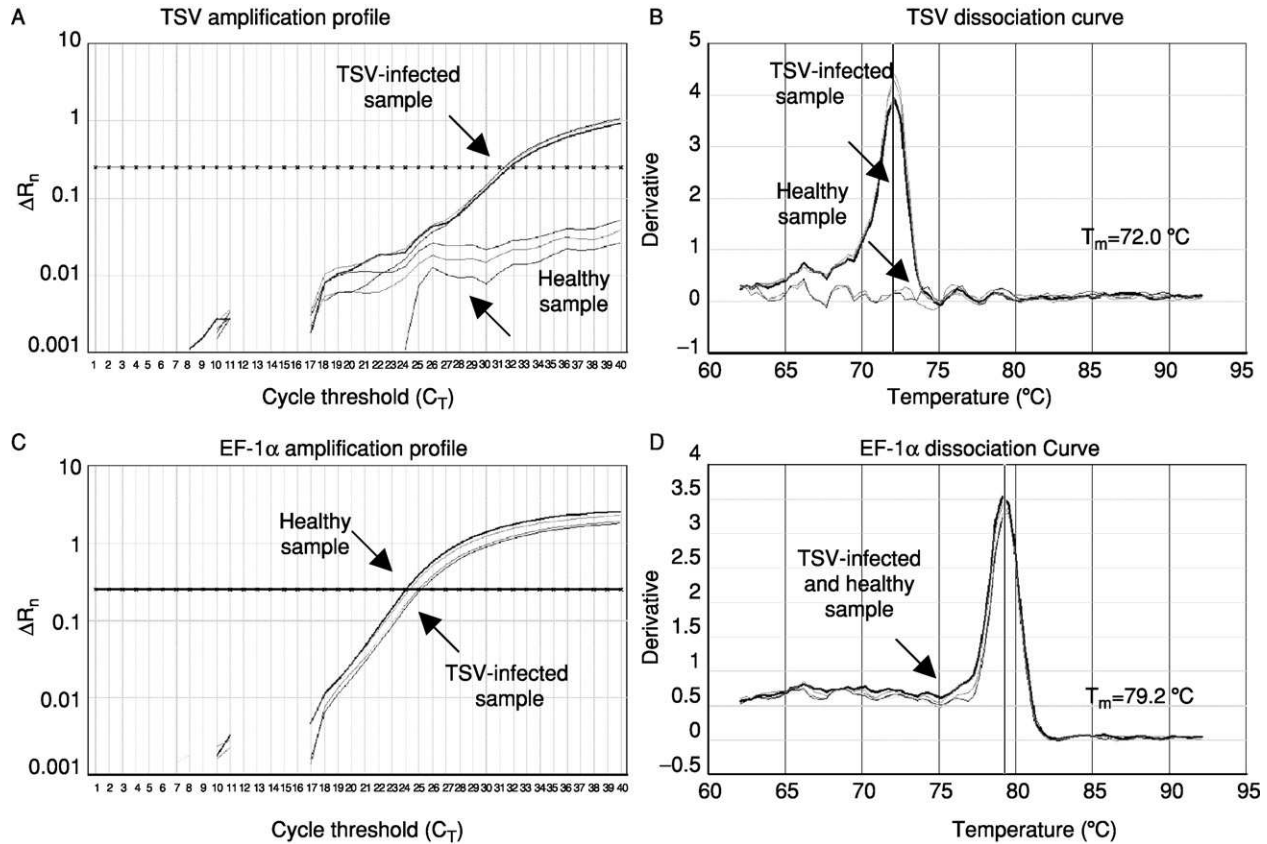


FIG 11. The amplification plots and the corresponding dissociation curves of TSV and EF-1 α genes from a TSV-infected shrimp and a healthy shrimp. The melting temperature (T_m) of each amplicon is shown alongside its dissociation curve. Adapted from Dhar *et al.* (2002) with permission.

occur within hours of shrimp displaying clinical symptoms. Original outbreaks were associated with complete pond losses within 3 to 5 days of the first signs of YHD (Limsuwan, 1991). The appearance of gross signs and the congregation of moribund shrimp near the surface at the pond edges were commonly preceded by a period of high-feed consumption followed by an abrupt cessation of feeding (Boonyaratpalin *et al.*, 1993; Limsuwan, 1991).

Subsequent to the initial outbreaks in Thailand (Limsuwan, 1991), YHV infection has been reported to occur wherever *P. monodon* is cultured in Southeast Asia and the Indo-Pacific. Countries in which YHV has been reported include China (Lightner, 1996), the Philippines (Albaladejo *et al.*, 1998; Natividad *et al.*, 1999), Taiwan (Wang and Chang, 2000), Indonesia (Rukyani, 2000), Malaysia (Yang *et al.*, 2000), Vietnam (Khoa *et al.*, 2000), India (Mohan *et al.*, 1998), and Sri Lanka (Siriwardena, 2000). In 1993, a virus morphologically identical to YHV was detected in the lymphoid organs of healthy wild and farmed *P. monodon* in Queensland, Australia, and was given the name lymphoid organ virus (LOV) (Spann *et al.*, 1995). In 1995 to 1996 an apparently pathogenic form of this virus was detected in high levels in the gills of moribund farmed *P. monodon* displaying YHD-like histopathology and was named gill-associated virus (GAV) (Spann *et al.*, 1997). It is now evident that LOV and GAV represent the same virus observed in chronic and acute phases of infection (Spann *et al.*, 2003; Walker *et al.*, 2001), and gill-associated virus has become the accepted name for the agent.

The natural occurrence of YHV infections in other penaeid shrimp or crustaceans appears to be uncommon. A yellowhead-like virus has been reported in *Penaeus japonicus* farmed in Taiwan (Wang *et al.*, 1996). There is some evidence, based on the transmission of YHD to *P. monodon*, that krill (*Acetes* sp.) and small wild shrimp (*Palaemon styliferus*) from *P. monodon* ponds can carry YHV (Flegel *et al.*, 1995b, 1997a). Histopathology consistent with YHV infection was reported in diseased *P. setiferus*, which were also infected with WSSV, at a farm in Texas in 1995 (Lightner *et al.*, 1997b). The infections were suspected to have originated from water-borne waste produced at a nearby facility processing *P. monodon* imported from Asia. However, descriptions of YHV infections based on histopathology alone need to be viewed with caution because it has recently been shown that WSSV can cause severe lymphoid organ and connective tissue necrosis in *P. setiferus* and *P. vannamei* that is similar to and can be easily confused for YHV (Pantoja and Lightner, 2003). Apart from one other unconfirmed report of the detection of YHV protein in a *P. setiferus* using an immunoblotting technique (Loh *et al.*, 1998), there is no evidence that YHV is

currently present in Western Hemisphere shrimp. Extensive RT-PCR screening of shrimp species indigenous to Australia has identified that GAV is highly prevalent in eastern coast *P. monodon* but, except for some very low-level infections detected in *Penaeus esculentus* that had been cocultivated in a pond with *P. monodon*, is not apparent in other shrimp species (Walker *et al.*, 2001).

Experimental transmission studies by feeding or direct injection have shown that YHV has the potential to infect wild shrimp, *Euphasia superba* and *Palaemon setiferus*, commonly found in ponds (Flegel *et al.*, 1995a, 1997) and cause disease of varying severity in several species of farmed shrimp. Shrimp species to which YHV can be transmitted include *Penaeus merguensis* and *Metapenaeus ensis* (Chantanachookin *et al.*, 1993), species *Penaeus vannamei* and *Penaeus stylirostris* (Lightner *et al.*, 1998; Lu *et al.*, 1994, 1997), and species *Penaeus setiferus*, *Penaeus aztecus*, and *Penaeus duorarum* (Lightner *et al.*, 1998) indigenous to the Western Hemisphere. In Australia, GAV has been transmitted experimentally to *Penaeus japonicus*, *Penaeus esculentus*, and *Penaeus merguensis* and, as reported for YHV (Lightner *et al.*, 1998), species and age affects the severity of disease signs (Spann *et al.*, 2000, 2003).

YHV has been transmitted horizontally to *P. monodon* and other species via several routes, including exposure to free water-borne virus particles generated from filtered tissue extracts, cohabitation, and cannibalism of infected carcasses (Flegel *et al.*, 1995a; Lightner, 1996; Lightner *et al.*, 1998). Transmission by ingestion has been demonstrated from the late postlarval (PL) stages onward. These infectivity studies demonstrated that PL₂₀ were quite susceptible, dying 7 to 10 days post-challenge, whereas no mortality occurred in similarly exposed PL₁₅ shrimp (Flegel *et al.*, 1995b). The ingestion of tissues of *P. monodon* infected with YHV or GAV has proven to be an efficient route of virus transmission to other penaeid shrimp (Lightner *et al.*, 1998; Lu *et al.*, 1997; Walker *et al.*, 2001). Transmission of YHV to *P. monodon* has also been demonstrated by ingestion of infected *Acetes* sp. and *P. styliiferus* (Flegel *et al.*, 1995a, 1997a).

There is no direct experimental data to demonstrate that YHV is transmitted vertically. It was recognized soon after the first reports of YHD that subclinical carriers might transmit infections to progeny (Chantanachookin *et al.*, 1993). Screening of Thai broodstock by electron microscopy, however, identified a low prevalence of YHV infection, which suggested that vertical transmission could not account for the widespread disease (Flegel *et al.*, 1997b). There are also no reports of the direct detection of YHV infection in the reproductive organs of

P. monodon broodstock. More recently, a genotypic variant distinct from YHV and GAV has been detected by PCR in high (~55%) prevalence in healthy *P. monodon* PL1-15 postlarvae from hatcheries in Vietnam (Phan, 2001), suggesting that this virus may be perpetuated in farmed stocks by vertical transmission from broodstock. In the case of GAV, there is substantial evidence that vertical transmission contributes to the high (>96%) infection prevalence detected in wild and farmed *P. monodon* from the East Coast of Australia (Cowley *et al.*, 2000a; Spann *et al.*, 1995; Walker *et al.*, 2001). GAV has been detected by RT-PCR in spermatophores and mature ovaries of healthy broodstock and in spermatophore secretions by ISH (Walker *et al.*, 2001), and mature virus particles have been observed by TEM in the spermatophore seminal fluid of adult males reared in captivity (Cowley *et al.*, 2003). Moreover, if one considers the probable ancient origins of GAV (Cowley and Walker, 2002), the origin of progenitor penaeid shrimp dating back more than 500 million years (Siveter *et al.*, 2001) and the limited natural host range, it seems likely that GAV/YHV and other related viruses may have coevolved with *P. monodon*. The maintenance of a subclinical infection state perpetuated via vertical transmission is a common feature of the biology and coevolution of invertebrate viruses.

B. Physical Properties of Yellowhead Virus

Electron microscopy of tissue sections from *P. monodon* displaying YHD clinical signs identified enveloped, bacilliform YHV virions (40–60 nm × 150–200 nm) with rounded ends (Boonyaratpalin *et al.*, 1993; Chantanachookin *et al.*, 1993). Diffuse projections approximately 8 nm thick and 11 nm in length extend from the envelope surface (Wang and Chang, 2000; Wongteerasupaya *et al.*, 1995) (Fig. 12). Negatively stained virus purified from hemolymph in sucrose density gradients display narrowed envelopes extending from particle ends (Wang and Chang, 2000; Wongteerasupaya *et al.*, 1995), and virions with long envelope extensions joined to form doughnut-shaped structures (Nadala *et al.*, 1997a). The origin of these envelope extensions and their role in YHV particle morphogenesis is not clear. Although apparently unique in structure, YHV virions appear to resemble more closely those of toroviruses than other known viruses.

The YHV nucleocapsid has helical symmetry and comprises a coiled filament of 16–30 nm diameter with periodicity of 5–7 nm (Boonyaratpalin *et al.*, 1993; Chantanachookin *et al.*, 1993; Nadala *et al.*, 1997a; Wang and Chang, 2000). Filamentous nucleocapsid precursors approximately 15 nm in diameter and of variable length

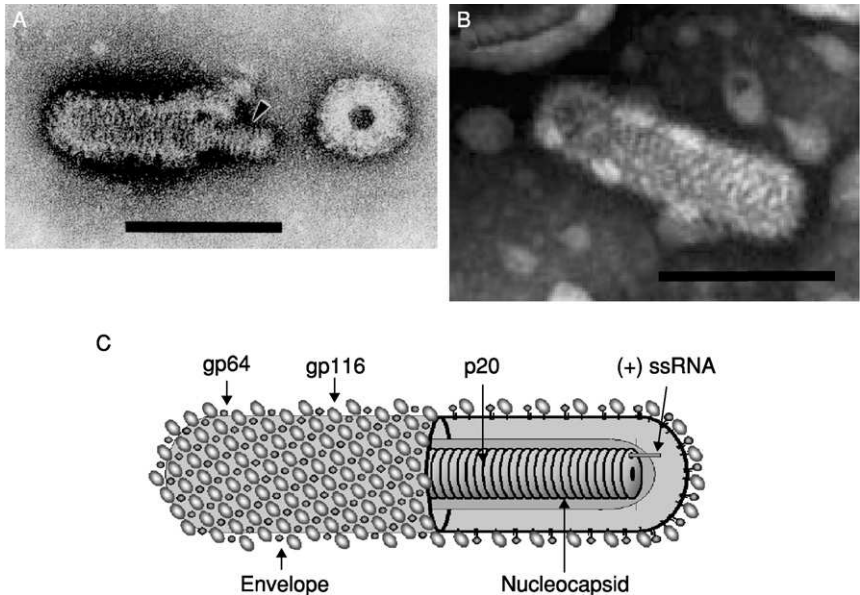


FIG 12. Transmission electron micrographs of negative-stained virions. (A) YHV virion. An arrow highlights the internal nucleocapsid. (B) GAV virion. (C) Schematic illustration of the *Okavirus* virion. Bars a = 100 nm. Electron micrographs (A) From Nadala *et al.* (1997a) and (B) from Spann *et al.* (1995); reproduced with permission. (See Color Insert.)

(80–450 nm) occur abundantly in the cytoplasm of infected cells. Nucleocapsids acquire envelopes by intracytoplasmic budding at membranes of the endoplasmic reticulum from which it is presumed the trilaminar lipid envelope of virions is derived. The long nucleocapsid precursors appear to generate elongated enveloped virion precursors that subsequently fragment into discrete rod-shaped virions (Chantanachookin *et al.*, 1993). Purified YHV virions paired end to end with an appearance suggesting they may have arisen by fragmentation of longer virions have also been reported (Wongteerasupaya *et al.*, 1995). Nucleocapsid precursors and mature enveloped virions are characteristically observed throughout the cytoplasm of infected cells and often within membranous vesicles in which budded virions often align in paracrystalline arrays (Boonyaratpalin *et al.*, 1993; Chantanachookin *et al.*, 1993). Virions have also been observed near or between the outer and inner nuclear membranes (Chantanachookin *et al.*, 1993; Wang and Chang, 2000) in proximity to cytoplasmic nucleocapsid filaments, suggesting that virion maturation can sometimes

occur at these membranes. Virions have also been observed budding from the cytoplasmic membrane (Boonyaratpalin *et al.*, 1993), as has also been observed in GAV-infected cells (Spann *et al.*, 1995, 1997).

YHV virions have a buoyant density in sucrose of 1.18–1.20 g/ml (Nadala *et al.*, 1997a). The lower estimation (1.154–1.162 g/ml) reported by Wang and Chang (2000) appears due to particles not being centrifuged to equilibrium density. Transmission experiments have shown that YHV extracts can remain infectious for at least 72 hr in sea water, and it has been reported that about 30 ppm calcium hypochlorite is an effective disinfectant (Flegel *et al.*, 1995b). Other physicochemical properties, including virion pH stability and sensitivity to other chemical agents, have yet to be reported for YHV.

YHV virions purified by sucrose density gradient centrifugation were initially reported to possess three major and one minor structural protein M_r 135, 67, 22 kDa, and 170 kDa, respectively (Nadala *et al.*, 1997b). Subsequent analyses employing Coomassie blue rather than silver staining identified only three proteins of M_r 110–116, 63–64, and 20 kDa (Jitrapakdee *et al.*, 2003; Wang and Chang, 2000). A method employing sodium metaperiodate oxidization of protein-linked carbohydrate followed by the detection of the oxidized carbohydrates using biotin-linked-hydrazide and streptavidin-horseradish peroxidase has been used to determine the glycosylation status of the virion proteins. Using this approach, Nadala *et al.* (1997b) showed that the 135-kDa protein was glycosylated, and Jitrapakdee *et al.* (2003) subsequently detected carbohydrates in both larger (116 and 64 kDa) proteins. As a low concentration of metaperiodate used at low temperature preferentially oxidizes terminal sialic acid residues, it is possible such residues are more prevalent in the 116–135-kDa protein and that differences in methodology contributed to this discrepancy in carbohydrate detection. Jitrapakdee *et al.* (2003) also employed a thymol- H_2SO_4 carbohydrate detection method dependent on the presence of hexosyl, hexuronosyl, or pentosyl residues (Racusen, 1979) to confirm that both larger YHV virion proteins were glycosylated, and these were designated gp116 and gp64 (Table III).

It is likely the gp116 and gp64 glycoproteins form the projections emanating from the envelope of the virion. However, direct evidence for this using immuno-electron microscopy and monoclonal antibodies (mAbs) generated to semipurified YHV (Sithigorngul *et al.*, 2000, 2002) has been obtained only for gp116 (Soowannayan *et al.*, 2003). Immuno-gold labeling with mAb V3-2B, which binds to the gp116 structural glycoprotein in Western blots, deposited gold particles on the envelope periphery of purified virions. Virions were not labeled with mAb Y18

TABLE III
PUTATIVE FUNCTIONS AND PROTEIN SIZE ESTIMATES OF THE YHV STRUCTURAL PROTEINS

Large spike glycoprotein	S1	gp116 ^a	110–135 kDa ^b
Small spike glycoprotein	S2	gp64	63–67 kDa
Nucleocapsid protein	N	p20	20–22 kDa

^a Nomenclature from Jitrapakdee *et al.* (2003).

^b Apparent M_r values determined by electrophoresis (Jitrapakdee *et al.*, 2003; Nadala *et al.*, 1997a; Sithigorngul *et al.*, 2002; Wang and Chang, 2000).

specific to the gp64 structural glycoprotein, and it may be that the antigenic epitope targeted by this antibody is internal to the protein structure and thus inaccessible. The mAb Y19 specific to the small (20–22 kDa) structural protein also did not bind to intact virions. However, when used on ultra-thin tissue sections, gold particles were observed to bind to free filamentous nucleocapsids in addition to the internal, electron dense, virion nucleocapsids (Soowannayan *et al.*, 2003). The binding of MAb Y19 to nucleocapsids, which would be inaccessible in purified virions, suggests that the nonglycosylated p20 protein is likely to be the virion nucleocapsid protein. The predicted functional roles of the three YHV structural proteins are listed in Table III.

The first report on the nature of the YHV genome isolated from purified virions indicated that it comprised RNA rather than DNA (Wongteerasupaya *et al.*, 1995). This finding contradicted earlier taxonomic descriptions of YHV, based on particle morphology and association with nuclear membranes, as a granulosis-type baculovirus (Boonyaratpalin *et al.*, 1993; Chantanachookin *et al.*, 1993). Nadala *et al.* (1997a) subsequently showed that the YHV genome comprised an unsegmented single-stranded RNA of at least 22 kb. Because no proteins were detected following *in vitro* translation of virion RNA, the genome was tentatively assigned to have negative-sense polarity (Nadala *et al.*, 1997a). However, Tang and Lightner (1999) subsequently isolated RNA from clarified hemolymph presumed to contain mature extracellular virions as a template for cDNA synthesis reactions employing primers of complementary polarities. A PCR product was only obtained for cDNA synthesized using primers that were antisense to a continuous open reading frame (ORF), indicating YHV genomic RNA was likely to be of positive-sense polarity. By *in situ* hybridization (ISH), YHV in shrimp tissues was also only detected using RNA probes synthesized in antisense to ORFs encoded in three independent cDNA clones. However, as the antisense RNA probes would also have

detected YHV mRNA, these data are inconclusive. Subsequent comparisons of genome sequence, organization, and coding strategy have resolved that YHV, like GAV, is most closely related to the (+) RNA viruses of the order Nidovirales (Cowley and Walker, 2002; Cowley *et al.*, 2000b, 2001, 2002a; Sittidilokratna *et al.*, 2002).

C. Genome Organization and Gene Expression of Yellowhead Virus

The International Committee on Taxonomy of Viruses (ICTV) has recently ratified the classification of YHV, together with GAV as a type species in new genus *Okavirus* of the new family Roniviridae within the Nidovirales (Mayo, 2002; Walker *et al.*, 2003). The name *Okavirus* is derived from the observation that the viruses are commonly detected in the shrimp lymphoid or “Oka” organ. Roniviridae (sigla rod-shaped *nidovirus*) recognizes their distinctive rod-shaped virion morphology (Cowley and Walker, 2002; Cowley *et al.*, 2000b; Mayo, 2002). Classification within the Nidovirales was supported by identified phylogenetic relationships between GAV and nidoviruses in the viral replicase genes in the 5'-terminal 20-kb region of the GAV (+) ssRNA genome (Cowley *et al.*, 2000b; González *et al.*, 2003; Gorbalenya *et al.*, 2002). The discovery that GAV synthesizes 3'-coterminal subgenomic (sg) mRNAs (Cowley *et al.*, 2002a) consistent with the gene transcription strategy used by coronaviruses, toroviruses, and arteriviruses, also supports taxonomic classification in the Nidovirales.

YHV and GAV possess a (+) sense ssRNA genome that is 3'-polyadenylated (Cowley and Walker, 2002; Cowley *et al.*, 2000b; Jitrapakdee *et al.*, 2003). Sequences of YHV genome regions encompassing the approximately 8-kb ORF1b (Sittidilokratna *et al.*, 2002) and approximately 5-kb ORF3 genes (Jitrapakdee *et al.*, 2003) have been reported. Short sequences within the ORF1b gene targeted by RT-PCR tests have also been described (Cowley *et al.*, 2000a; Soowannayan *et al.*, 2003; Tang and Lightner, 1999; Wongteerasupaya *et al.*, 1997). Because the complete sequence of the YHV genome has yet to be reported, known information on gene organization will be described in relation to that determined for the 26,235-nt (+) ssRNA genome of the closely related GAV (Cowley and Walker, 2002, Cowley *et al.*, 1999, 2001, 2000b). The GAV genome is organized into 5 ORFs ordered 5'-ORF1a/ORF1b-ORF2-ORF3-ORF4-[A]_n-3' (Cowley and Walker, 2002). The GAV and YHV genome structures are shown in Fig. 13. The details of the intergenic region (IGR) lengths and the lengths and deduced molecular masses of the predicted gene ORFs are listed in Table IV.

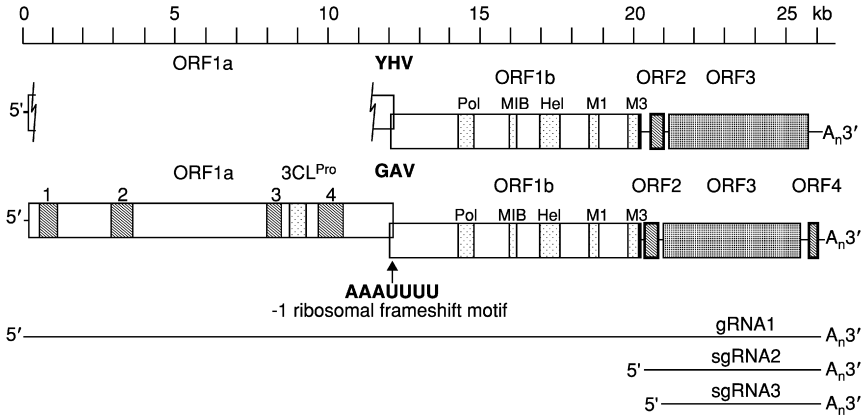


FIG 13. Organization of the complete 26,235 nt (+) ssRNA genome of GAV and the ORF1b and structural genes of YHV. The relative positions of four regions (1–4) containing clusters of hydrophobic residues and the 3C-like proteinase (3CL^{Pro}) are indicated in ORF1a in addition to the SDD polymerase (Pol), the three metal ion binding (MIB) domains, helicase (Hel), and motif 1 (M1) and 3 (M3) domains in ORF1b. The AAAUUUU slippery sequence in the ORF1a–1b overlap that precedes an RNA pseudo-knot and is the site of -1 ribosomal frameshifting to generate the pp1ab replicase polyprotein is identified. As ORF4 in GAV is truncated to 20 amino acids in YHV due to an insertion generating a stop codon, this ORF is not indicated in YHV. The full-length gRNA and the two subgenomic (sg)mRNAs with 5'-termini mapping to the intergenic regions upstream of ORF2 and ORF3 of GAV are also shown.

The 5'-terminal 20-kb portion of the GAV genome is occupied by a large replicase gene comprising two long ORFs [ORF1a (12,248 nt) and ORF1b (7942 nt)], which overlap by 99 nt (Cowley *et al.*, 2000b). Although ORF1a continues to the putative 5'-end of the genome, the first inframe putative initiation codon (AUG) resides 68 nt downstream of the 5'-terminal "A" nucleotide determined using a 5'-rapid amplification of cDNA ends (RACE) technique. The putative initiation codon is in a highly favorable context for translation initiation (Kozak, 1986), suggesting that the upstream region is untranslated (Cowley *et al.*, 2000b). The 5'-terminal 152-nt sequence of the YHV genomic RNA has also been determined using the 5'-RACE method (Cowley and Sittidilokratna, unpublished data). In this region, the YHV sequence is 87.5% identical to GAV. The terminal 19 nt are absolutely conserved, and a 3-nt insertion occurs in the putative YHV untranslated region upstream of the ORF1a start codon (Fig. 14). Experimental data have demonstrated that translation of the putative polyprotein pp1ab of

TABLE IV
THE DETAILS OF THE INTERGENIC REGION (IGR) LENGTHS AND THE LENGTHS AND DEDUCED
MOLECULAR MASSES OF THE PREDICTED ORFs IN GAV AND YHV GENOMES^a

Genome region	Nucleotide		Amino acid		kDa	
	GAV	YHV	GAV	YHV	GAV	YHV
5'-genomic UTR	68	71				
ORF1ab-ORF2 IGR						
ORF2-ORF3 IGR	57	54				
ORF3-ORF4 IGR	256	297				
ORF1a			4060	ND ^b	460.3	ND ^b
ORF1b			2646	2618	302.5	299.3
ORF2			144	146	15.9	16.2
ORF3			1640	1666	182.0	185.7
ORF4			83	20	9.6	ND ^b

^a Information of YHV reproduced from Sittidilokratna (2003) with permission.

^b ND means not determined.

YHV 5'	-ACGUUACGUUCCACGUACUAUUCCACUGCACUCAAAUAAACCUUUUAUACCCGUUUUCAAU	60
GAV 5'UA.....UCA.....U...C---.A.....C.G	57
	E L L	
	M E P F Q V L S L L A T S F S L	
YHV	CGUUACCGACCAUGGAACCUUUUCAGGUUCUAUCGUUGUUGGCAACAUCUUCAGUCUAC	120
GAVU.....G.....G.....U.....C.....CU	117
	F	
	L L L L R I L D R G T T V L S A V R	
YHV	UCCUAUUGCUUAGGAUCCUAGACCGCGGCACG <u>ACUGUUCUGUCUGCCGUCAGA</u>	173
GAVC.....U..... <u>ACUGUUCUGUCUGCCGUCAGA</u>	170

FIG 14. Alignment of the 5'-terminal sequences of the genomic RNA of YHV and GAV determined by sequence analysis of multiple clones generated using a 5'-RACE method (Cowley *et al.*, 2000b). The coding sequence of the predicted N terminus of the pp1ab replicase polyprotein encoded by the ORF1a/1b gene is indicated, and amino acid and nucleotide variations in GAV are shown above and below the YHV sequences, respectively. The region targeted by the 5'-RACE antisense primer is underlined.

GAV is facilitated by a-1 ribosomal frameshift element employing an AAAUUUU "slippery" sequence that immediately precedes a predicted complex RNA pseudo-knot (Cowley *et al.*, 2002a). As shown in Fig. 15 and compared to that of GAV, the -1 ribosomal frameshift element in the ORF1a/ORF1b overlap of YHV has few (11/188 nt = 9.3%) differences, and 3 of 4 nt changes in predicted base-paired sequences are either commensurate or preserve the predicted RNA folding structure

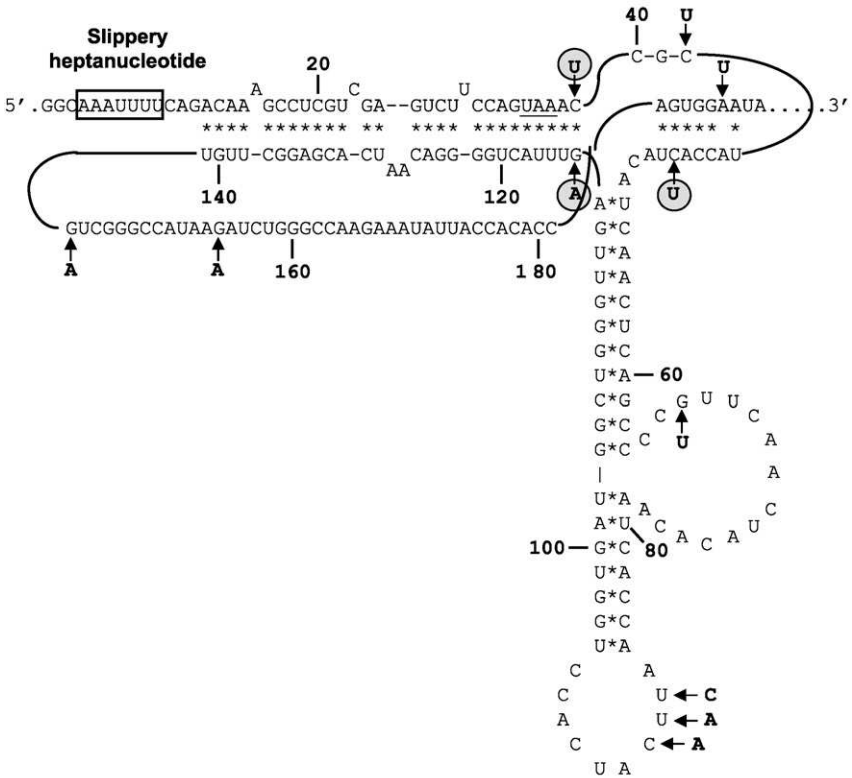


FIG 15. Schematic representation of the -1 ribosomal frameshift site and predicted RNA pseudo-knot in the YHV ORF1a/ORF1b overlap region used for translation of pplab replicase polyprotein. Sequence differences to GAV are shown (arrows), and compensatory nucleotide changes that maintain base pairing in the pseudo-knot structure are circled.

(Sittidilokratna *et al.*, 2002). Compared to the GAV ORF1b sequence that overlaps ORF1a by 99 nt (33 aa), the YHV ORF1b/ORF1a overlap is trimmed to 36 nt (12 aa) by the presence of a UGA stop codon 3 nt upstream of the AAAUUUU frameshift motif. In both viruses, -1 frameshifting at this motif is predicted to occur at the Phe (F) codon in ORF1a (AAAUUUU) and ORF1b (AAAUUUU) to generate the ORF1a/ORF1b read-through sequence-HEANFSDK- (Cowley *et al.*, 2000b; Sittidilokratna *et al.*, 2002).

The replicase gene encoding ORF1a (4060 aa) and ORF1b (2646 aa) in GAV can thus generate two polyproteins, pp1a (460 kDa) and a

C-terminally extended pp1ab (759 kDa), likely to be generated in lower abundance as -1 ribosomal frameshifting occurs at about 24% efficiency (Cowley *et al.*, 2000b, 2002a). As in other nidoviruses, the pp1ab replicase polyprotein is expected to be involved in genome replication and transcription of the 3'-coterminal sgmRNAs required for efficient translation of the viral structural proteins (Cowley *et al.*, 2002a). Sequence analysis of pp1a identified four regions with clusters of hydrophobic residues predicted to contain multiple transmembrane (TM) domains. Hydrophobic regions 3 and 4 (Fig. 13) flank a putative chymotrypsin-like (3C-like) proteinase (3CL^{pro}) domain, which was the only pp1a region with detectable similarity to other nidoviruses (Cowley *et al.*, 2000b; Ziebuhr *et al.*, 2003). A recombinant GAV 3CL^{pro} has been shown to cleave at sites in pp1a (²⁸²⁷LVTHE ↓ VRTGN²⁸³⁶) and in the C terminus of pp1ab (⁶⁴⁴¹KVNHE ↓ LYHVA⁶⁴⁵⁰), and the tentative consensus sequence VxHE ↓ (L, V) has been proposed (Ziebuhr *et al.*, 2003). Several other potential 3CL^{pro} cleavage sites in pp1ab with this motif have yet to be confirmed. However, this cleavage site specificity and other structural characteristics defined by the GAV 3CL^{pro} sequence indicate that it is distinct from those currently known for mammalian or plant pathogens and bridges an evolutionary gap between the distantly related proteinases of coronaviruses and plant potyviruses (Ziebuhr *et al.*, 2003).

Sequence comparison of the 2646 aa ORF1b coding sequence identified homologues of nidovirus RNA-dependent RNA polymerase (RdRp), metal ion binding (MIB), helicase, and the motif 1 and motif 3 (C-terminal) domains (de Vries *et al.*, 1997). Although very little similarity occurs elsewhere in the RdRp, the functional domains are shared with the supergroup 1 (+) RNA viruses (Koonin, 1991), and the conserved amino acids are completely preserved in GAV (Cowley *et al.*, 2000b) and YHV (Sittidilokratna *et al.*, 2002). This includes the SDD, rather than GDD, RdRp core motif, which is unique to nidoviruses. Downstream of the polymerase in YHV and GAV is a cluster of three MIB or zinc finger motifs characteristic of TFIIIA-like fingers (Gorbalenya *et al.*, 1989) based on the spacings within each block of four Cys/His residues and on the positioning of surrounding aromatic residues. The helicase domain contains the Pur NTP-binding motifs A (GppGtGKT/S) and B (DE) characteristic of the dsRNA duplex unwinding enzymes of nidoviruses and other RNA viruses (Gorbalenya and Koonin, 1989). Limited homology is also detectable in two domains, described as motifs 1 and 3 in coronaviruses and toroviruses (de Vries *et al.*, 1997), between the helicase and C terminus of the ORF1b coding sequence of YHV and GAV (Cowley *et al.*, 2000b;

Sittidilokratna *et al.*, 2002). The significance of this will only become apparent when the function of these nidovirus motifs is better understood.

Compared to GAV, the YHV ORF1b sequence contains a 9-nt (3-codon) insertion in the region between the polymerase and metal-ion binding (MIB) domains, a codon deletion downstream of the helicase domain, and a codon insertion immediately preceding the stop codon (Sittidilokratna *et al.*, 2002). Overall, the ORF1b amino acid coding sequences of the two viruses are 88.9% identical. Their sequences in the functional motifs of the RdRp and helicase domains, however, are almost identical, and the putative active Cys and His residues of the three MIB motifs are absolutely preserved. A phylogenetic tree constructed using the ORF1b RNA-dependent RNA polymerase (RdRp) domain of YHV and GAV showing the distant evolutionary relationship of these okaviruses of the Roniviridae to members of the Coronaviridae (coronaviruses and toroviruses) and the Arteriviridae is shown in Fig. 16.

The GAV ORF2 gene encodes a 144-aa (16.0-kDa, pI = 9.75) protein that contains 19 (13%) proline residues and is highly hydrophilic, containing 20 (14%) basic and 13 (9%) acidic amino acids (Cowley *et al.*, 2004b). The 146-aa ORF2 (16.3 kDa) sequence determined for YHV is 83.6% identical and possesses a similar overall charge structure to GAV ORF2 (Sittidilokratna, 2003). Immuno-gold labeling of free and virion encapsidated nucleocapsids of GAV by antibodies to a synthetic ORF2 peptide and a recombinant ORF2 protein indicates that the ORF2 gene product is likely to be the viral nucleocapsid protein (Cowley *et al.*, 2004b). GAV ORF2 antibodies cross-react with the YHV p20 structural protein, and antibodies to YHV p20 have also been shown to bind to nucleocapsids (Soowannayan *et al.*, in press). The genome organization of GAV and YHV is thus distinct from the vertebrate nidoviruses in which the nucleocapsid protein gene resides in the near 3'-terminal genome region downstream of genes encoding the structural glycoproteins and integral membrane (M) protein (de Vries *et al.*, 1997).

The YHV ORF3 gene encodes a 1666-aa (185.7-kDa) protein that contains six highly hydrophobic regions that are likely to be trans-membrane domains and has the predicted membrane topology shown in Fig. 17 (Jitrapakdee *et al.*, 2003). The cognate 1640-aa (182-kDa) protein encoded by the GAV ORF3 gene has an identical hydropathic profile (Cowley and Walker, 2002) and overall displays 75% identity to YHV ORF3. The N-terminal sequence analyses have shown that the YHV virion gp116 and gp64 proteins are encoded in the ORF3 gene

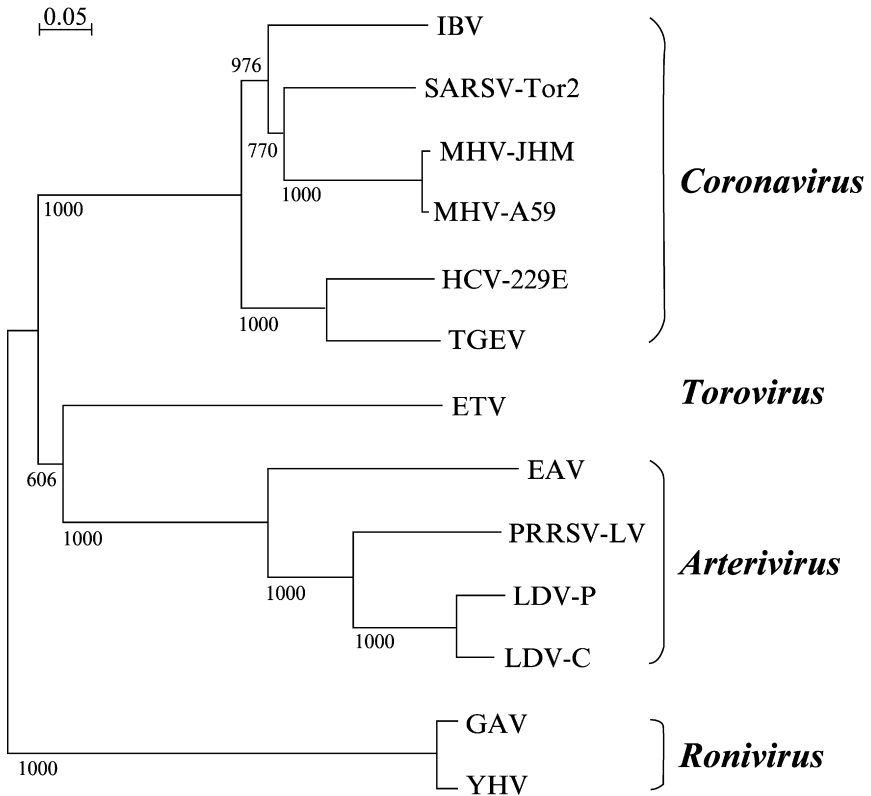


FIG 16. Phylogenetic tree generated using the Clustal X1.81 program employing the Gonnet protein weight matrix for pairwise and multiple alignments and the YHV ORF1b polymerase (RdRp) domain (AAL14793) encompassing residues ⁶²⁵IPKIS...IERVF⁹⁰⁷. The YHV RdRp was aligned to the cognate domains in the pp1ab replicase polyproteins of the *Ronivirus* GAV (AAF82690) as well as species of *Coronavirus* including avian infectious bronchitis virus (IBV, NP_006134), SARSV strain Tor2 (AAP41036), murine hepatitis virus (MHV) strains JHM (VFIHJH) and A59 (CAA36202), human *Coronavirus* strain (HCV strain 229E, Q05002), and porcine transmissible gastroenteritis virus (TGEV strain Purdue, Q91W06). In addition, the alignment was extended to the Berne equine *Torovirus* (ETV, P18458) as well as species of *Arterivirus* including equine arteritis virus (EAV, NP_705590), the porcine reproductive and respiratory syndrome Lelystad virus (PRRSV-LV, Q04561), and the lactate dehydrogenase-elevating virus (LDV) strains P (AAA85664) and C (NP_065671). Bootstrap values are for 1000 independent alignments.

and generated by post-translational processing from a precursor polyprotein (Jitrapakdee *et al.*, 2003). The N terminus of gp116 is generated by cleavage immediately downstream of transmembrane domain 3 motif Ala-Phe-Ala²²⁸, and the N terminus of gp64 is

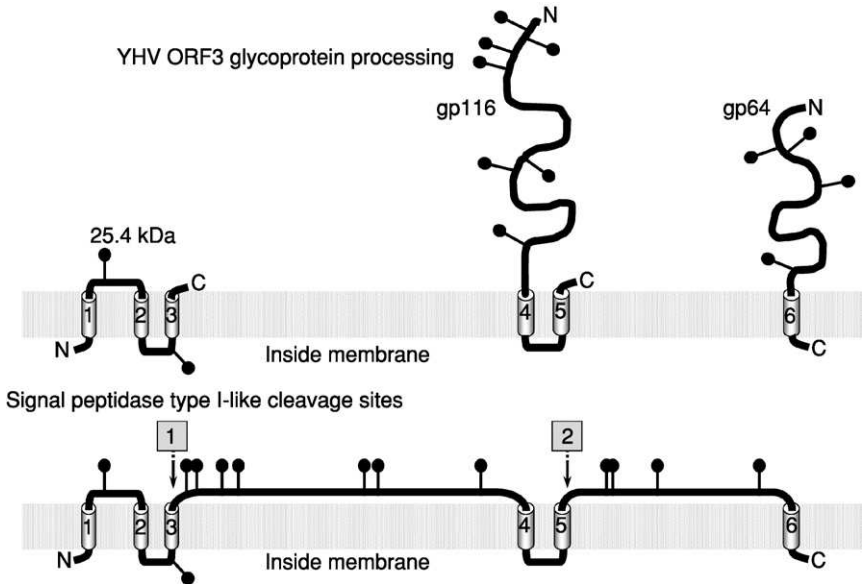


FIG 17. Predicted membrane topology of the YHV ORF3 glycoprotein showing the relative positions of 6 predicted transmembrane (TM) domains and 13 predicted N-linked glycosylation sites. Signal peptidase type I-like cleavage sites that map to residues at the C-terminal side of TM domains 3 and 5 are indicated. The topology of the putative 25.4-kDa triple membrane spanning protein and the gp116 and gp64 structural glycoproteins of YHV generated by cleavage is indicated.

generated by cleavage immediately after the transmembrane domain 5 motif Ala-Ser-Ala¹¹²⁷. Such Ala-X-Ala motifs commonly occur in pre-protein signal sequences where they act as a cleavage target for signal peptidase 1 (Carlos *et al.*, 2000), suggesting that ORF3 transmembrane domains 3 and 5 may function as efficient internal signal sequences for a type I-like signal peptidase. The fate of the predicted amino-terminal 25.4-kDa product of the ORF3 polyprotein generated by cleavage at Ala²²⁸ is not known. No protein of this mass has been detected in purified YHV virions (Jitrapakdee *et al.*, 2003; Nadala *et al.*, 1997b; Wang and Chang, 2000), and specific antibodies are not yet available to detect its expression in infected cells. Although this putative 25.4 kDa protein's function is unknown, it contains three putative membrane spanning domains just as do the nonglycosylated membrane (M) glycoproteins of coronaviruses (Cavanagh, 1995), toroviruses (den Boon *et al.*, 1991), and arteriviruses (Snijder and Meulenberg, 1998). However, its predicted membrane topology infers

an N_{cyt}C_{exo} orientation, which is the reverse of that predicted for the M proteins of vertebrate nidoviruses.

Based on the predicted membrane topology of ORF3, it is probable that (i) gp116 is a polytopic type III transmembrane glycoprotein anchored in the virion envelope by transmembrane domains 4 and 5 with the carboxy-terminus protruding outward and that (ii) gp64 is a type I transmembrane glycoprotein anchored by the C-terminal transmembrane domain 6 of ORF3 (Jitrapakdee *et al.*, 2003). Although gp116 (26 Cys) and gp64 (24 Cys) contain numerous cysteine residues, there is no evidence of intermolecular covalent linkage of these glycoproteins in virions. The lower calculated mass of gp116 (101.7 kDa) and gp64 (58.6 kDa) deduced from the ORF3 sequence is consistent with these proteins being extensively glycosylated at most potential N-linked sites in gp116 (7 sites) and gp64 (4 sites) (Jitrapakdee *et al.*, 2003). Additional analyses, however, are required to determine which of these are used and if any of several predicted O-linked glycosylation sites in gp116 are used.

The 638-nt sequence between ORF3 and the 3'-poly (A) tail of GAV contains a short ORF4 (83 aa = 9.6 kDa) commencing 256 nt downstream of ORF3 (Cowley and Walker, 2002). In YHV, an ORF4 homologue resides 298 nt downstream of ORF3 but only extends 20 amino acids due to a U insertion generating a UAA stop codon (Sittidilokratna, 2003). Because no sgmRNA for ORF4 has been detected in Northern blots, it is unlikely that an ORF4 protein is translated in abundance. However, evidence of ORF4 expression in shrimp tissues at very low levels has been obtained by immuno-histochemistry using antiserum to a GAV ORF4 synthetic peptide (Cowley *et al.*, unpublished data).

In GAV, the intergenic regions (IGRs) upstream of ORF2 (93 nt) and ORF3 (57 nt) contain a highly conserved sequence of 32 nt in which there is a continuous stretch of 26 identical nucleotides (Cowley *et al.*, 2002a). The putative 256-nt intergenic region upstream of ORF4 contains sequences with very limited homology to the two upstream IGRs. In YHV, the IGR upstream of ORF2 is 260 nt longer than in GAV (Sittidilokratna *et al.*, 2002), and sequences flanking a 46-nt (84.8% identity) core sequence conserved in GAV are dissimilar. The 54-nt IGR upstream of YHV ORF3 contains a continuous stretch of 40 nt identical to GAV (Sittidilokratna, 2003). As in GAV, the putative 297-nt IGR upstream of the equivalent ORF4 start site in YHV contains AU-rich sequences, and 40/41 nt in the region immediately upstream of ORF4 are identical (Sittidilokratna, 2003). An alignment of the YHV and GAV IGR sequences encompassing the 5'-terminal position of sgmRNA2 and sgmRNA3 determined for GAV, in addition to a site in

the IGR upstream of ORF4 with limited homology to the conserved promoter elements in the two upstream IGRs, is shown in Fig. 18.

Northern blots in combination with primer extension and 5'-RACE analyses identified two GAV sgmRNAs with 5'-AC termini, in common with the 5'-AC termini of the genomic RNA (Cowley *et al.*, 2000b), that mapped to common 5'-AC sites central to the conserved IGR sequences (Cowley *et al.*, 2002a). This was supported by the identification of intracellular dsRNA replicative intermediates of about 22, 5.8 and 5.2 kbp that approximate the size of genomic RNA1, sgmRNA2, and sgmRNA3, respectively (Cowley *et al.*, 2002a). More recently, a 5'-RACE technique dependent on the presence of 7-methyl-guanosine triphosphate-(^{m7}Gppp)-cap has confirmed the 5'-AC termini of the GAV genomic and sgmRNAs and shown them to be capped (Cowley, unpublished data). The absence of the 5'-leader derived from the 5'-end of the genomic RNA distinguishes GAV from coronaviruses (Sawicki and Sawicki, 1999), arteriviruses (van Marle *et al.*, 1999), and, to a lesser extent, the Berne torovirus (van Vliet *et al.*, 2002). In the latter, only the longest of its four sgmRNAs contains a 5'-leader sequence. No discrete or abundant sgmRNA has been found to initiate in the untranslated sequence upstream of ORF4, which likely explains why it is not translated in abundance. As already described, the genomic IGR sequences encompassing the presumed sgmRNA2 and three transcription start sites are highly conserved between YHV and GAV. It is also noteworthy that, in alignments with the two other IGRs, the single nucleotide variation (U in YHV and G in GAV) in the 41-nt stretch upstream ORF4 occurs at the cognate position of the A residue deduced to be the 5'-terminal nucleotide in sgmRNA2 and sgmRNA3 (Cowley *et al.*, 2002b; Sittidilokratna, 2003). The 5'-AC termini of the genomic RNA and the two sgmRNAs of GAV, and likely YHV, suggest

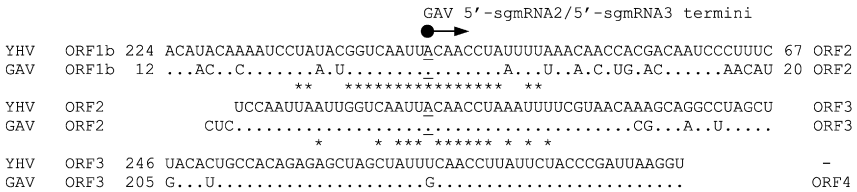


FIG 18. Alignment of the YHV and GAV IGR sequences between the ORF1b-ORF2, ORF2-ORF3, and ORF3-ORF4 genes. Only nucleotide variations in GAV compared to YHV are shown. Conserved nucleotides between the different intergenic sequences are indicated (*), and numbers to the right and left of the sequences indicate the distance to upstream and downstream ORFs. The 5'A terminal positions, determined for GAV and predicted for YHV, sgmRNA2, and sgmRNA3 are underlined.

that the absence of an A nucleotide at this position may critically affect the synthesis of a sgRNA4 for the efficient translation of ORF4. Therefore, if the expression of ORF4 is not essential to virus replication in its crustacean hosts, mutations interrupting its open reading frame, as detected in YHV (Sittidilokratna, 2003), could accumulate without detriment to virus fitness.

D. Relationship of Yellowhead Virus with Gill-Associated Virus

A bleached appearance of the body and yellowing of the cephalothorax is only sometimes apparent in farmed *P. monodon* with acute YHD and generalized reddening of common in experimental infections (Chantanachookin *et al.*, 1993). In original farm outbreaks of acute GAV-related disease, cephalothorax yellowing was not apparent and shrimp typically displayed generalized reddening of the body and gills, which can be reproduced experimentally (Spann *et al.*, 1997). YHV appears to be more virulent than GAV in that mortalities can reach 100% within 3 to 4 days in farmed stocks or during experimental infections (Chantanachookin *et al.*, 1993; Limsuwan, 1991). However, for GAV, mortalities commonly occur in experimentally infected *P. monodon* over 7 to 14 days, and farm outbreaks often present as a chronic disease involving the progressive appearance of relatively low numbers of moribund shrimp. These infected shrimp usually display shell and gill fouling as well as damaged and melanized appendages, and they gather at the pond edges (Callinan *et al.*, 2003b; Owens, 1997; Spann *et al.*, 1997; Spann *et al.* unpublished data). No direct comparisons of the pathogenicity of these two related viruses, however, have been reported. Furthermore, meaningful comparisons between YHV and GAV are difficult because inoculum doses have not been standardized in quantal assays, and, in some cases, inocula may have been contaminated with other pathogens.

Although the tissue distribution and histopathology seen in YHV and GAV infections are similar, available reports suggest that there are some differences. High levels of free mature YHV virions accumulate in hemolymph (Nadala *et al.*, 1997b; Wongteersupaya *et al.*, 1995), whereas it has proved difficult to purify GAV from hemolymph (Spann *et al.*, unpublished data). Moreover, intensely basophilic inclusions characteristically seen in the lymphoid organ and elsewhere in YHV-infected shrimp are not as evident for GAV (Spann *et al.*, 1997). Although GAV has been identified in the eye of *P. monodon* (Smith, 2000) where it appears to cause lesions reported as retinopathy (Callinan

et al., 2003a), as of yet there are no reports of similar pathology caused by YHV.

Accumulated data now indicate that the reference isolates of YHV from Thailand and GAV from Australia represent two of five distinct genotypes (Cowley *et al.*, 1999; Phan, 2001; Soowannayan *et al.*, 2003; Walker *et al.*, 2001; Wijegoonawardane and Walker, unpublished data) in what has been described as a yellowhead (YH)-complex of viruses (Walker *et al.*, 2001). One of the genotypic variants, with 92% identity to GAV and 83% identity to the reference YHV genotype in the ORF1b gene helicase C-terminal domain, has been found in healthy *P. monodon* broodstock and postlarvae from hatcheries in Vietnam (Phan, 2001; Walker *et al.*, 2001). A variant with 92% identity to GAV and 80% identity to YHV in another ORF1b gene region has been detected in healthy *P. monodon* broodstock from Thailand (Soowannayan *et al.*, 2003). Based on the identity levels to the YHV and GAV reference isolates, it is likely these viruses fall within the same genotype. Sequence comparison of the 577-nt ORF1b region spanned by the GAV5/6 PCR primers originally identified 85% identity between GAV from Australia and a YHV isolate from Thailand (Cowley *et al.*, 1999, 2000a). This GAV region displays similar (83%) identity to the YHV ORF1b sequence determined by Sittidilokratna *et al.* (2002) using a reference Thai YHV isolate derived from diseased shrimp. However, the YHV sequence reported by Cowley *et al.* (1999) is only 85% identical to that reported by Sittidilokratna *et al.* (2002), indicating that it represents a fourth genotype as distantly related to the reference Thai YHV isolate as it is to GAV. Moreover, sequence differences between this variant and the reference YHV genotype might explain why RT-PCR using the GAV5/6 primers generated an amplicon with this YHV genotype (Cowley *et al.*, 2000a) but failed to amplify the reference YHV genotype (Cowley *et al.*, unpublished data). Molecular epidemiological studies have recently identified a fifth YHV genotype in healthy *P. monodon* broodstock from India (Wijegoonawardane and Walker, unpublished data) that is almost equally divergent from GAV (81% identity) and the other three YHV genotypes (80–83% identity) currently recognized within the YH complex of viruses.

E. Diagnosis of Yellowhead Virus

1. Histopathology

The viruses that compose the YH complex (YHV and GAV) produce necrotic lesions in multiple tissues that permit a presumptive diagnosis of this disease by routine H&E histology (Boonyaratpalin *et al.*,

1993; Chantanachookin *et al.*, 1993; Lightner, 1996a; Nash *et al.*, 1995; OIE, 2003; Spann *et al.*, 1997). Both naturally occurring and experimentally induced YHV infections have been reported in a variety of penaeids including *P. monodon*, *P. japonicus*, *P. vannamei*, *P. setiferus*, *P. aztecus*, and *P. duorarum* (Chantanachookin *et al.*, 1993; Lightner, 1996a; Lightner *et al.*, 1998; Lu *et al.*, 1994; OIE, 2003). The target tissues of YHV are of mesodermal and ectodermal origins and include the LO, hemocytes, fixed phagocytes (heart, gill, and hepatopancreas), hematopoietic tissue, cuticular epithelium, and spongy connective tissues (Fig. 19). Affected cells typically display severe necrosis characterized by nuclear pyknosis, karyorrhexis or karyolysis, cytoplasmic eosinophilia, and basophilic cytoplasmic inclusions

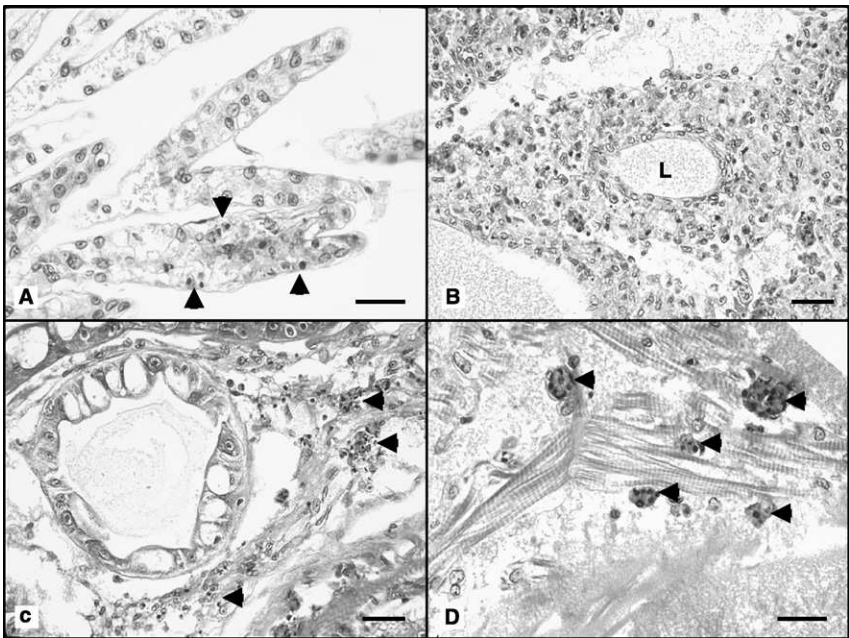


FIG 19. Photomicrographs of tissues from *Penaeus stylirostris* juvenile with an experimentally induced acute yellowhead virus (Thai strain) infection. (A) Mild YHV-infected gill lamellae displaying multifocal necrotic cells with pyknotic nuclei (arrow heads) and cytoplasmic eosinophilia (B) Severe diffuse necrosis of the stromal matrix cells in the walls of a lymphoid organ arteriole. The numerous basophilic spheres consist of pyknotic nuclei and presumptive inclusion bodies (L = arteriole lumen). (C) Multifocal necrosis (arrow heads) within the intertubular hemal sinuses of the hepatopancreas. (D) Aggregates of necrotic cells, presumably fixed phagocytes (arrow heads), within the heart (Hematoxylin and Eosin stain). Bar: 30 μ m. (See Color Insert.)

(Boonyaratpalin *et al.*, 1993; Chantanachookin *et al.*, 1993; Lightner, 1996a; Lu *et al.*, 1994; Nash *et al.*, 1995; OIE, 2003; Spann *et al.*, 1997; Wang and Chang, 2000). These morphological characteristics appear to be caused by apoptosis (Khanobdee *et al.*, 2002) and are very similar to those observed in TSV-infected cuticular epithelial cells. However, the two diseases are easily differentiated as YHV infects a broader range of tissues when compared to TSV (Hasson, 1998; Hasson *et al.*, 1999a,b; Lightner, 1996a). Most notable among the tissues affected by YHV is the LO in which the virus induces a severe diffuse necrosis of the stromal matrix cells in the walls of the LO arterioles (tubules). This pathology is one of the hallmarks of YHD and is not observed in TSV-infected shrimp. The observation of solitary or multiple necrotic fixed phagocytes or hemocytes within the hemal spaces of the heart, hepatopancreas, gills, antennal gland, and connective tissues further aids in histologically differentiating YHV from TSV-caused infections (Boonyaratpalin *et al.*, 1993; Chantanachookin *et al.*, 1993; Lightner, 1996a; Lu *et al.*, 1995a; Nash *et al.*, 1995; OIE, 2003; Spann *et al.*, 1997). Histological lesions that are morphologically similar to those induced by YHV, particularly within the LO, have also been reported for infections caused by WSSV, *Vibrio penaeicida*, and a systemic Rickettsia-like bacterium found in Madagascar (Mermoud *et al.*, 1998; Nunan *et al.*, 2003; Pantoja and Lightner, 2001). Hence, confirmation of a YHV or GAV infection by another diagnostic method (i.e., RT-PCR, ISH, or TEM) is necessary to support presumptive histological findings.

Gill-associated virus is a part of the YHV complex and was described in farmed *P. monodon* from Australia (Spann *et al.*, 1997). By ISH, there is comparable extensive tissue distribution of virus in *P. monodon* acutely infected with either YHV (Tang and Lightner, 1999) or GAV (Spann *et al.*, 2003; Tang *et al.*, 2002). Histologically, GAV differs from YHV in that the lesions are limited to the gills and the lymphoid organ (OIE, 2003; Spann *et al.*, 1997). Similar to TSV, GAV can induce a chronic state infection in *P. monodon* where the only histologic abnormality is the presence of spheroids within the LO (OIE, 2003; Spann *et al.*, 1995; Walker *et al.*, 2003). As in all cases of virus-induced LO spheroids, the causative agent cannot be identified by routine histology, and some other form of diagnostic analysis (i.e., ISH, RT-PCR, or IHC) is required to make this determination.

2. Immunodetection

A nitrocellulose enzyme immunoassay (NC-EIA) using rabbit polyclonal YHV antibody has been described for the detection of YHV (Lu *et al.*, 1996). The gill tissue was found to be a good source for

the NC-EIA and the detection limit of NC-EIA was 0.4 ng of viral protein. Subsequently, a modified dot-blot NC-EIA using horseradish peroxidase (HRP)-conjugated YHV-specific polyclonal antibody was developed by Nadala and Loh (2000). This assay is very simple and has a potential for screening field samples. A Western blot method capable of detecting YHV in shrimp hemolymph sample has been described by Nadala *et al.* (1997b). Using this method, a 135-kDa protein and a 170-kDa protein of YHV was detected in hemolymph at 64 hr post-infection, and a 135-kDa protein was detected in YHV-infected primary lymphoid organ cell culture 4 days post-infection. The Western blot assay is highly specific and is recommended by the OIE as a confirmatory diagnostic method for YHV detection in combination with *in situ* nucleic acid hybridization, transmission electron microscopy (TEM), and RT-PCR (OIE, 2003). A YHV-specific monoclonal antibody (mAbV3-2B) was used for the detection of the virus by immunohistochemical examination and by Western blot analysis (Sithigorngul *et al.*, 2000). The mAb showed YHV-specific immunoreactivities in the cytoplasm of gill tissues and in hemocytes and detected a 135-kDa protein in Western blots (Sithigorngul *et al.*, 2000).

3. RT-PCR and Real-Time RT-PCR

The first protocol for YHV detection by RT-PCR was described by Wongteerasupaya *et al.* (1997). The primer sequences have been provided in Table II. The RT-PCR amplifies a 135-bp region in the ORF1b gene (Cowley *et al.*, 1999; Sittidilokratna *et al.*, 2002), and the method has a sensitivity of approximately 0.01 pg of YHV RNA ($\sim 10^3$ genomes). Tang and Lightner (1999) also described an RT-PCR method using YHV-specific primers amplifying a 273-bp ORF1b gene region upstream of the 135-bp amplicon; the test detected YHV in the hemolymph of infected shrimp (Table II). An RT-nested PCR has also been described for GAV (Cowley *et al.*, 2000a), and recently, Cowley *et al.* (2004b) have described another nested RT-PCR that is highly sensitive and capable of differentiating YHV from GAV. The latter method involves amplification of a 749-bp ORF1b region of either YHV or GAV in the first step of PCR. In the second step of PCR, either a 406-bp cDNA is amplified from GAV or a 277-bp cDNA is amplified from YHV using GAV- and YHV-specific primers (Fig. 20, Table II). The two-step PCR was found to be about 1000-fold more sensitive than the one-step PCR, and the detection limit was found to be 10 fg of total cellular RNA. Amplification of both the 406-bp and 277-bp products from the same sample allows the identification of dual infections with YHV and GAV (Cowley *et al.*, 2004a).

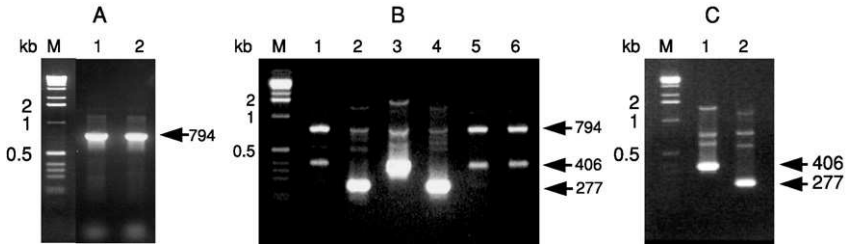


FIG 20. Amplification of GAV and YHV RNA by RT-PCR followed by nested PCR with various primer combinations. (A) PCR amplification (primer pair GY1–GY4) of a 794-bp product from cDNA synthesized from reference GAV (lane 1) and YHV (lane 2) RNA using primer GY5. (B) Nested PCR amplification of RT-PCR products from GAV (lanes 1–3) and YHV (lanes 4–6) using primer pairs GY2–Y3 (lanes 1 and 4), GY2–G3 (lanes 2 and 5), and GY2–G6 (lanes 3 and 6). (C) Nested PCR amplification of a 406-bp GAV-specific product (lane 1) or 277-bp YHV-specific product (lane 2) using the multiplexed primer set GY2–Y3/G6. PCR products (10 μ l) were resolved in a 2% agarose-TAE gel containing 0.5 μ g/ml ethidium bromide. M: 1-kb DNA ladder (Invitrogen). Reproduced from Cowley *et al.* (2004a), with permission.

Real-time RT-PCR methods for the detection and quantification of YHV RNA using SYBR Green chemistry have recently been described (Dhar *et al.*, 2002; Mouillesseaux *et al.*, 2003). The methods vary in the length of the amplicon (50 to 98 bp) generated using YHV-specific primers (Table II). The method is capable of detecting down to a single-copy equivalent of the YHV genome and has a wide dynamic range of detection. The amplification plots and the corresponding dissociation curves of a YHV amplicon and a shrimp internal control gene are shown in Fig. 21. The specificity of the YHV amplicon is confirmed by examining the dissociation curves. A dissociation curve with a single peak at expected melting temperature indicates the amplification target amplicon. Because each amplicon has a unique melting temperature, primers based on a conserved region in the genome will be useful to amplify all the genotypes of YHV/GAV complex, whereas primers based on the variable region of the genome will be useful in identifying different genotypes of YHV–GAV complex. In addition, due to the lack of an immortalized shrimp cell line, quantification of the virus is difficult. Although YHV has been cultivated in a primary cell line from the lymphoid organ of *P. vannamei* (Lu *et al.*, 1995b) or *P. monodon* (Chen and Wang, 1999), the need to prepare cultures from shrimp with an unknown background presents a problem for standardization of the virus assay. This limitation can be overcome by real-time RT-PCR. In addition, real-time RT-PCR could be used to detect subclinical infection, measure the viral load, and determine the tissue tropism for YHV

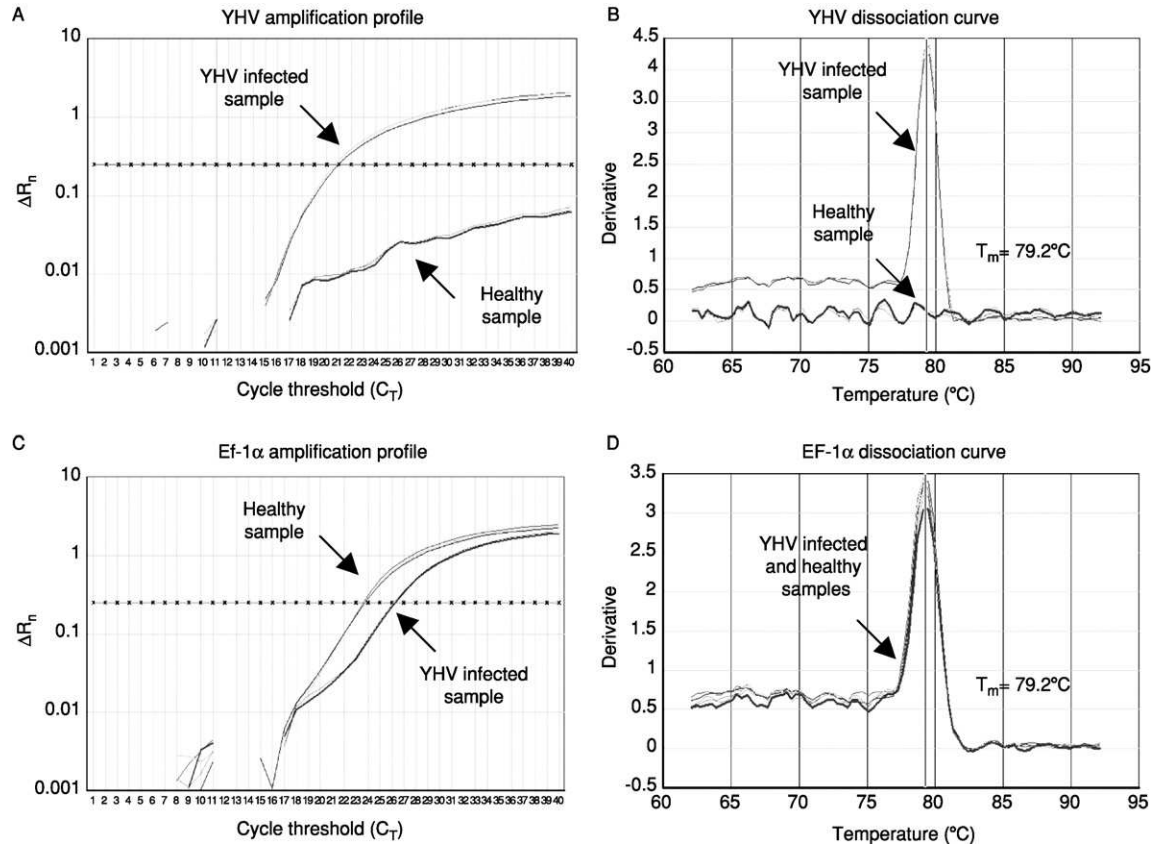


FIG. 21. The amplification plots and the corresponding dissociation curves of YHV and EF-1 α genes from a TSV infected shrimp and a healthy shrimp. The melting temperature (T_m) of each amplicon is shown alongside its dissociation curve. Adapted from Dhar *et al.* (2002) with permission.

and GAV. Although real-time RT-PCR may not be feasible for routine field testing due to high cost, sophisticated instrumentation, and the required technical expertise, it would be useful for testing broodstock to ensure their virus-free status and monitoring of live and frozen shrimp that are sold within and between countries with the objective of preventing the further spread of these viruses.

IV. CONCLUDING REMARKS

Taura syndrome and yellowhead diseases have had a profound economic and social impact in the developing nations of East Asia and the Americas where they have threatened the long-term sustainability of numerous shrimp culture industries. A variety of management strategies, including virus exclusion or prevention through the use of specific pathogen-free (SPF) and/or specific pathogen-resistant (SPR) stocks, have been attempted (Lightner, 1999). However, the ability of RNA viruses, such as TSV and YHV, to mutate and adapt to previously resistant hosts makes their control and exclusion particularly difficult. Advances in the areas of TSV and YHV detection have facilitated the development of highly sensitive and disease-specific molecular diagnostic tools that permit the nonlethal detection of subclinically infected shrimp populations. This enables farmers to identify and eliminate contaminated stocks and, thus, limit the spread of these viral diseases.

There has been significant progress in understanding the general biology of both TS and YHD and in developing methods for the detection of TSV and YHV. However, many of the processes involved in viral replication and translation of the viral encoded genes remain to be determined. The molecular mechanisms used for the initiation and regulation of viral RNA synthesis and the regulation of translation and processing of the nonstructural and structural polyproteins encoded by the TSV and YHV will be the subjects of future studies. Studying these processes will be critical toward understanding the molecular basis of TSV and YHV pathogenesis.

Another area that has received very little attention is the pathogen defense or immune response of shrimp against viral diseases. Information pertaining to shrimp genes that might be involved in the pathogenesis of TSV and YHV and viral diseases in general remains elusive. Most studies on the immunity of shrimp and crustaceans have focused in general on bacterial and fungal pathogens, and little is known about how crustaceans respond to viral infections. Although no host cellular genes involved in TSV and YHV pathogenesis have been identified so

far, a number of immune genes in shrimp that might be involved in WSSV pathogenesis have been identified by using mRNA differential display (Astrofsky *et al.*, 2002; Luo *et al.*, 2003), expressed sequence tag analysis (Rojtinnakorn *et al.*, 2002; Roux *et al.*, 2002), and cDNA microarray analysis (Dhar *et al.*, 2003). Functional genomics approaches, using shrimp cDNA microarrays coupled with targeted gene silencing by dsRNA interference, should prove useful in identifying the genes and the molecular events governing viral pathogenesis in TSV and YHV.

ACKNOWLEDGMENTS

Arun K. Dhar would like to thank Refugio Robles-Sikisaka and Kate Licon for their help in preparing the manuscript. Research work of Dhar is funded by grants from Advanced Bionutrition Corporation, Columbia, Maryland, and the California Sea Grant Program, California. Kenneth W. Hasson would like to thank Dr. Patricia Varner, Mr. Daniel Areola, and Dr. John Reagor of TVMDL for their editorial comments on portions of the manuscript and image scanning assistance.

REFERENCES

- Albaladejo, J. D., Tapay, L. M., Migo, V. P., Alfafara, C. G., Somga, J. R., Mayo, S. L., Miranda, R. C., Natividad, K., Magbanua, F. O., Itami, T., Matsumura, M., Nadala, E. C. B., Jr., and Loh, P. C. (1998). Screening for shrimp viruses in the Philippines. In "Advances in Shrimp Biotechnology" (T. W. Flegel, ed.). National Center for Genetic Engineering and Biotechnology, Bangkok, Thailand.
- Anggraeni, M. S., and Owens, L. (2000). The haemocytic origin of lymphoid organ spheroid cells in the penaeid prawn *Penaeus monodon*. *Dis. Aqua. Org.* **40**:85–92.
- Anonymous (1995). Mortalidades en Texas no es síndrome de Taura. *Panorama Acuicola* **1**:1 and 6.
- Argue, B. J., Arce, S. M., Lotz, J. M., and Moss, S. M. (2002). Selective breeding of pacific white shrimp (*Litopenaeus vannamei*) for growth and resistance to Taura syndrome virus. *Aquaculture* **204**:447–460.
- Astrofsky, A., Roux, M. M., Klimpel, K. R., Fox, J. G., and Dhar, A. K. (2002). Identification of differentially expressed genes in Pacific blue shrimp (*Penaeus stylirostris*) in response to challenge with white spot virus (WSSV). *Arch. Virol.* **147**:1799–1812.
- Barniol, R. (1995). Etiología del síndrome de Taura: La tesis Ecuatoriana. *Acuicultura del Ecuador* **10**:7–11.
- Bell, T. A., and Lightner, D. V. (1988). "A Handbook of Normal Penaeid Shrimp Histology." World Aquaculture Society, Baton Rouge, LA.
- Bonami, J. R., Hasson, K. W., Mari, J., Poulos, B. T., and Lightner, D. V. (1997). Taura syndrome of marine penaeid shrimp: Characterization of the viral agent. *J. Gen. Virol.* **78**:313–319.
- Boonyaratpalin, S., Supamataya, K., Kasornchnadra, J., Direkbusarakom, S., Aekpanithanpong, U., and Chantanachookin, C. (1993). Non-occluded baculo-like virus, the causative agent of yellow-head disease in the black tiger shrimp (*Penaeus monodon*). *Fish Pathol.* **28**:103–109.

- Brock, J. A. (1997). Special topic review: Taura syndrome, a disease important to shrimp farms in the Americas. *World J. Microbiol. Biotechnol.* **13**:415–418.
- Brock, J. A., Gose, R., Lightner, D. V., and Hasson, K. W. (1995). An overview on Taura syndrome, an important disease of farmed *Penaeus vannamei*. In “Swimming Through Troubled Water” (C. L. Browdy and J. S. Hopkins, eds.). *Proceedings of the Special Session on Shrimp Farming Aquaculture*, World Aquaculture Society, Baton Rouge, LA.
- Brock, J. A., Gose, R. B., Lightner, D. V., and Hasson, K. W. (1997). Recent developments and an overview of Taura syndrome of farmed shrimp in the Americas. In “Diseases in Asian Aquaculture III” (T. W. Flegel and I. H. MacRae, eds.). Fish Health Section Asian Fisheries Society, Manila, Philippines.
- Callinan, R. B., Jiang, L., Smith, P. T., and Soowannayan, C. (2003a). Fatal, virus-associated peripheral neuropathy and retinopathy in farmed *Penaeus monodon* in eastern Australia. *Dis. Aquat. Org.* **53**:181–193.
- Callinan, R. B., and Jiang, L. (2003b). Fatal, virus-associated peripheral neuropathy and retinopathy in farmed *Penaeus monodon* in eastern Australia. *Dis. Aquat. Org.* **53**:195–202.
- Carlos, J. L., Paetzel, M., Brubaker, G., Karla, A., Ashwell, C. M., Lively, M. O., Cao, G., Bullinger, P., and Dalbey, R. E. (2000). The role of the membrane-spanning domain of type I signal peptidases in substrate cleavage site selection. *Biol. Chem.* **275**:38813–38822.
- Carr, W. H., Fjalestad, K. T., Lotz, J. M., Oyama, R. N., Godin, D. M., Chang, C. P. L., Segura, F. J., Roddy, S. C., and Sweeney, J. N. (1997). Advances in selective breeding for growth performance and disease resistance in specific pathogen-free (SPF) pacific white shrimp, *Penaeus vannamei*. *Linking Science to Sustainable Industry Development, Annual International Conference and Exposition of the World Aquaculture Society Vol 52*:68.
- Cavanagh, D. (1995). The coronavirus surface glycoprotein. In “The Coronaviridae” (S. G. Siddell, ed.). Plenum Press, New York.
- Chantanachookin, C. S., Boonyaratpalin, J., Kasornchnadra, S., Direkbusarakom, U., Ekpanithanpong, K., Supamataya, S., Sriurairatana, T., and Flegel, W. (1993). Histology and ultrastructure reveal a new granulosis-like virus in *Penaeus monodon* affected by yellowhead disease. *Dis. Aqua. Org.* **17**:145–157.
- Chen, S. N., and Kou, G. H. (1989). Infection of cultured cells from the lymphoid organ of *Penaeus monodon* Fabricius by monodon-type baculovirus. *J. Fish Dis.* **12**:73–76.
- Chen, S. N., and Wang, C. S. (1999). Establishment of cell culture systems from penaeid shrimp and their susceptibility to white spot disease and yellowhead viruses. *Methods Cell. Sci.* **21**:199–206.
- Clifford, H. (2000). Shrimp farming in Mexico: Recent developments. *Glob. Aquaculture Adv.* **3**:79–81.
- Christian, P. D., and Scotti, P. D. (1998). Picorna-like viruses of insects. In “The Insect Viruses” (L. K. Miller and K. A. Ball, eds.). Plenum Press, New York.
- Couch, J. A. (1974a). Free and occluded virus similar to *Baculovirus* in hepatopancreas of pink shrimp. *Nature* **247**:229–231.
- Couch, J. A. (1974b). An enzootic nuclear polyhydrosis virus of pink shrimp: Ultrastructure, prevalence, and enhancement. *J. Inv. Pathol.* **24**:311–331.
- Cowley, J. A., and Walker, P. J. (2002). The complete genome sequence of gill-associated virus of *Penaeus monodon* prawns indicates a gene organisation unique among nidoviruses. *Arch. Virol.* **147**:1977–1987.
- Cowley, J. A., Dimmock, C. M., Wongteerasupaya, C., Boonsaeng, V., Panyim, S., and Walker, P. J. (1999). Yellowhead virus from Thailand and gill-associated virus from

- Australia are closely related but distinct prawn viruses. *Dis. Aquat. Org.* **36**:153–157.
- Cowley, J. A., Dimmock, C. M., Spann, K. M., and Walker, P. J. (2000a). Detection of Australian gill-associated virus (GAV) and lymphoid organ virus (LOV) of *Penaeus monodon* by RT-nested PCR. *Dis. Aquat. Org.* **39**:159–167.
- Cowley, J. A., Dimmock, C. M., Spann, K. M., and Walker, P. J. (2000b). Gill-associated virus of *Penaeus monodon* prawns: An invertebrate virus with ORF1a and ORF1b genes related to arteri- and coronaviruses. *J. Gen. Virol.* **81**:1473–1484.
- Cowley, J. A., Dimmock, C. M., Spann, K. M., and Walker, P. J. (2001). Gill-associated virus of *Penaeus monodon* prawns. Molecular evidence for the first invertebrate nidovirus. *Adv. Exp. Med. Biol.* **494**:43–48.
- Cowley, J. A., Dimmock, C. M., and Walker, P. J. (2002a). Gill-associated nidovirus of *Penaeus monodon* prawns transcribes 3'-coterminally subgenomic mRNAs that do not possess 5'-leader sequences. *J. Gen. Virol.* **83**:927–935.
- Cowley, J. A., Hall, M. R., Cadogan, L. C., Spann, K. M., and Walker, P. J. (2002b). Vertical transmission of gill-associated virus (GAV) in the black tiger prawn *Penaeus monodon*. *Dis. Aquat. Org.* **50**:95–104.
- Cowley, J. A., Cadogan, L. C., Wongteerasupaya, C., Hodgson, R. A., J., Boonsaeng, V., Walker, P. J. (2004a). Multiplex RT-nested PCR differentiation of gill-associated virus (Australia) from yellowhead virus (Thailand) of *Penaeus monodon*. *J. Virol. Methods* **17**: 49–59.
- Cowley, J. A., Cadogan, L. C., Spann, K. M., Sittidilokratna, N., Walker, P. J. (2004b). The gene encoding the nucleocapsid protein of gill-associated nidovirus of *Penaeus monodon* prawns is located upstream of the glycoprotein gene. *J. Virol.* **78**: 8935–8941.
- de Vries, A. A. F., Horzinek, M. C., Rottier, P. J. M., and de Groot, R. J. (1997). The genome organization of the *Nidovirales*: Similarities and differences between arteri-, toro-, and coronaviruses. *Seminars Virol.* **8**:33–47.
- den Boon, J. A., Snijder, E. J., Locker, J. K., Horzinek, M. C., and Rottier, P. J. (1991). Another triple-spanning envelope protein among intracellularly budding RNA viruses: The torovirus E protein. *Virology* **182**:655–663.
- Dhar, A. K., Roux, M. M., and Klimpel, K. R. (2002). Quantitative assay for measuring the Taura syndrome virus (TSV) and yellowhead virus (YHV) load in shrimp by real-time RT-PCR using SYBR Green chemistry. *J. Virol. Methods* **104**:69–82.
- Dhar, A. K., Dettori, A., Roux, M. R., Klimpel, K. R., and Read, B. (2003). Use of cDNA microarray to isolate the differentially expressed genes in white spot syndrome virus (WSSV) infected shrimp (*Penaeus stylirostris*). *Arch. Virol.* **148**:2381–2396.
- Domingo, E., and Holland, J. J. (1997). RNA virus mutation and fitness for survival. *Annu. Rev. Microbiol.* **51**:151–178.
- Erickson, H., Lawrence, A. L., Gregg, K. L., Frelier, P. F., Lotz, J. M., and McKee, D. A. (1997). Sensitivity of *Penaeus vannamei*, *Sciaenops ocellatus*, *Cynoscion nebulosus*, *Palaemonetes* sp., and *Callinectes sapidus* to Taura syndrome virus infected tissue. *Linking Science to Sustainable Industry Development, Annual International Conference and Exposition of the World Aquaculture Society* Vol **52**:140.
- Erickson, H., Zarain-Herberg, M., and Lightner, D. V. (2002). Detection of Taura syndrome virus (TSV) strain differences using selected diagnostic methods: Diagnostic implications in penaeid shrimp. *Dis. Aqua. Org.* **52**:1–10.
- Fitch, W. M., Leiter, J. M., Li, X. O., and Palese, P. (1991). Positive Darwinian evolution in human influenza A viruses. *Proc. Natl. Acad. Sci.* **88**:4270–4274.
- Flegel, T. W. (1997). Special topic review: Major viral diseases of the black tiger prawn (*Penaeus monodon*) in Thailand. *World J. Microbiol. Biotechnol.* **13**:433–442.

- Flegel, T. W., Fegan, D. F., and Sriurairatana, S. (1995a). Environmental control of infectious shrimp diseases in Thailand. In "Diseases in Asian Aquaculture II" (M. Shariff, R. P. Subasinghe, and J. R. Arthur, eds.). Asian Fisheries Society, Manila, Philippines.
- Flegel, T. W., Sriurairatana, S., Wongterasupaya, C., Boonsaeng, V., Panyim, S., and Withyachumnarnkul, B. (1995b). Progress in characterization and control of yellowhead virus of *Penaeus monodon*. In "Swimming Through Troubled Water" (C. L. Braudy and J. S. Hopkins, eds.). Proceedings of the Special Session on Shrimp Farming Aquaculture, World Aquaculture Society, Baton Rouge, LA.
- Flegel, T. W., Boonyaratpalin, S., and Withyachumnarnkul, B. (1997a). Current status of research on yellowhead virus and white spot virus in Thailand. In "Diseases in Asian Aquaculture III" (T. W. Flegel and I. H. MacRae, eds.), pp. 285–296. Fish Health Section. Asian Fisheries Society, Manila, Philippines.
- Flegel, T. W., Sriurairatana, S., Morrison, D. J., and Waiyakrutha, N. (1997b). *Penaeus monodon* captured broodstock surveyed for yellowhead virus and other pathogens by electron microscopy. In "Shrimp Biotechnology in Thailand" (T. W. Flegel, P. Menasveta, and S. Paisarnrat, eds.), National Center for Genetic Engineering and Biotechnology, Bangkok, Thailand, pp. 37–43.
- Garza, J. R., Hasson, K. W., Poulos, B. T., Redman, R. M., White, B. L., and Lightner, D. V. (1997). Demonstration of infectious Taura syndrome virus in the feces of sea gulls collected during an epizootic in Texas. *J. Aquat. Animal Health* **9**:156–159.
- González, J. M., Gomez-Puertas, P., Cavanagh, D., Gorbalenya, A. E., and Enjuanes, L. (2003). A comparative sequence analysis to revise the current taxonomy of the family Coronaviridae. *Arch. Virol.* **148**:2207–2235.
- Gorbalenya, A. E., and Koonin, E. V. (1989). Viral proteins containing the purine NTP-binding sequence pattern. *Nucl. Acids. Res.* **17**:4847–4861.
- Gorbalenya, A. E., Blinov, V. M., Donchenko, A. P., and Koonin, E. V. (1989). An NTP-binding motif is the most conserved sequence in a highly diverged monophyletic group of proteins involved in positive strand RNA viral replication. *J. Mol. Evol.* **28**:256–268.
- Gorbalenya, A. E., Pringle, F. M., Zeddarn, J. L., Luke, B. T., Cameron, C. E., Kalmakoff, J., Hanzlik, T. N., Gordon, K. H., and Ward, V. K. (2002). The palm subdomain-based active site is internally permuted in viral RNA-dependent RNA polymerases of an ancient lineage. *J. Mol. Biol.* **324**:47–62.
- Halim, S., and Ramsingh, A. I. (2000). A point mutation in VP1 of coxsackie virus B4 alters antigenicity. *Virology* **269**:86–94.
- Hasson, K. W., Lightner, D. V., Poulos, B. T., Redman, R. M., White, B. L., Brock, J. A., and Bonami, J. R. (1995). Taura Syndrome in *Penaeus vannamei*: Demonstration of a viral etiology. *Dis. Aqua. Org.* **23**:115–126.
- Hasson, K. W., Hasson, J., Aubert, H., Redman, R. M., and Lightner, D. V. (1997). A new RNA-friendly fixative for the preservation of penaeid shrimp samples for virological detection using cDNA genomic probes. *J. Virol. Methods* **66**:227–236.
- Hasson, K. W. (1998). Taura Syndrome in Marine Penaeid Shrimp: Discovery of the Viral Agent and Disease Characterization Studies. Ph.D. diss. University of Arizona, Tucson.
- Hasson, K. W., Lightner, D. V., Mohney, L. L., Redman, R. M., Poulos, B. T., Mari, J., Bonami, J. R., and Brock, J. A. (1999a). The geographic distribution of Taura syndrome virus (TSV) in the Americas: Determination by histopathology and *in situ* hybridization using TSV-specific cDNA probes. *Aquaculture* **171**:13–26.

- Hasson, K. W., Lightner, D. V., Mohny, L. L., Redman, R. M., Poulos, B. T., and White, B. L. (1999b). Taura syndrome virus (TSV) lesion development and the disease cycle in the Pacific white shrimp *Penaeus vannamei*. *Dis. Aqua. Org.* **36**:81–93.
- Hasson, K. W., Lightner, D. V., Mohny, L. L., Redman, R. M., Poulos, B. T., and White, B. L. (1999c). Role of lymphoid organ spheroids in chronic Taura syndrome virus (TSV) infections in *Penaeus vannamei*. *Dis. Aqua. Org.* **38**:93–105.
- Haydon, D. T., Bastos, A. D., Knowles, N. J., and Samuel, A. R. (2001). Evidence for positive selection in foot-and-mouth disease virus capsid genes from field isolates. *Genetics* **157**:7–15.
- Holland, P. M., Abramson, R. D., Watson, R., and Gelfand, G. H. (1991). Detection of specific polymerase chain reaction product by utilizing the 5'–3' exonuclease activity of *Thermus aquaticus* activity. *Proc. Natl. Acad. Sci. USA* **88**:7276–7280.
- Humason, G. L. (1972). "Animal Tissue Techniques," 3rd Ed. W. H. Freeman and Company, San Francisco.
- Intriago, P., Espinoza, J., Jimenez, R., Machuca, M., Barniol, R., Krauss, E., and Salvador, X. (1995a). Taura syndrome, a toxicity syndrome of *Penaeus vannamei* in Ecuador. *Annual International Conference and Exposition of the World Aquaculture Society*, p. 143.
- Intriago, P., Jimenez, R., Machuca, M., Barniol, R., Krauss, E., and Salvador, X. (1995b). Demonstracion de la etiologia toxica del sindrome de Taura. *Tercero Congreso Ecuatoriano de Acuicultura*, p. 23.
- Intriago, P., Jimenez, R., Machuca, M., Barniol, R., Krauss, E., and Salvador, X. (1997a). Evidencias bioquimicas y experimentales que apoyan la naturaleza toxica del sindrome de Taura en *Penaeus vannamei* (Crustacea decapoda) en el Ecuador. *Panorama Acuicola* **2**:22–23.
- Intriago, P., Jimenez, R., Machuca, M., Barniol, R., Krauss, E., and Salvador, X. (1997b). Experiments on toxicosis as the cause of Taura syndrome in *Penaeus vannamei* (Crustacea decapoda) in Ecuador. In "Diseases in Asian Aquaculture III" (T. W. Flegel and I. H. MacRae, eds.). Fish Health Section, Asian Fisheries Society, Manila, Philippines.
- Jimenez, R. (1992). Sindrome de taura (Resumen). *Acua. Ecuador* **1**:1–16.
- Jimenez, R., Machuca, M., and Barniol, L. (1995). Taura syndrome: Epizootiology and histopathology of a mortality toxicity syndrome of penaeid shrimp in Ecuador. *Annual International Conference and Exposition of the World Aquaculture Society*, p. 147.
- Jimenez, R., Barniol, R., Barniol, L., and Machuca, M. (2000). Periodic occurrence of epithelial viral necrosis outbreaks in *Penaeus vannamei* in Ecuador. *Dis. Aqua. Org.* **42**:91–99.
- Jitrapakdee, S., Unajak, S., Sittidilokratna, N., Hodgson, R. A. J., Cowley, J. A., Walker, P. J., Panyim, S., and Boonsaeng, V. (2003). Identification and analysis of gp116 and gp64 structural glycoproteins of yellowhead nidovirus of *Penaeus monodon* shrimp. *J. Gen. Virol.* **84**:863–873.
- Jory, D. (1995). Global situation and current megatrends in marine shrimp farming. *Aquaculture* **21**:74–83.
- Khanobdee, K., Soowannayan, C., Flegel, T. W., Ubol, S., and Withyachumnarnkul, B. (2002). Evidence for apoptotic correlated with mortality in the giant black tiger shrimp *Penaeus monodon* infected with yellowhead virus. *Dis. Aquat. Org.* **48**:79–90.
- Khoa, L. V., Hao, N. V., and Huong, L. T. L. (2000). Vietnam. In "Thematic Review on Management Strategies for Major Diseases in Shrimp Aquaculture" (J. R. Arthur, D. Fegan, and R. Subasinghe, eds.). FAO, Rome, Italy.
- Koonin, E. V. (1991). The phylogeny of RNA-dependent RNA polymerases of positive-strand RNA viruses. *J. Gen. Virol.* **72**:2197–2206.

- Kondo, M., Itami, T., Takahashi, Y., Fuji, R., and Tomonga, S. (1994). Structure and function of the lymphoid organ in the Kuruma prawn. *Dev. Comp. Immunol.* **18**(Suppl. 1):109.
- Kozak, M. (1986). Point mutations define a sequence flanking the AUG initiator codon that modulates translation by eukaryotic ribosomes. *Cell* **44**:283–292.
- Lightner, D. V. (1995). Taura syndrome: An economically important viral disease impacting the shrimp farming industries of the Americas including the United States. *Proceedings of the Ninety-Ninth Annual Meeting USAHA*, pp. 36–62.
- Lightner, D. V. (1996a). A Handbook of Shrimp Pathology and Diagnostic Procedures for Diseases of Cultured Penaeid Shrimp. World Aquaculture Society, Baton Rouge, LA.
- Lightner, D. V. (1996b). Epizootiology, distribution, and the impact on international trade of two penaeid shrimp viruses in the Americas. *Rev. Sci. Off. Int. Epiz.* **5**:579–601.
- Lightner, D. V. (1999). The penaeid shrimp viruses TSV, IHNV, WSSV, and YHV: Current status in the Americas, available diagnostic methods, and management strategies. *J. Appl. Aquaculture* **9**:27–51.
- Lightner, D. V., and Redman, R. M. (1998). Shrimp diseases and current diagnostic methods. *Aquaculture* **164**:201–220.
- Lightner, D. V., Jones, L. S., and Ware, G. W. (1994). *Proceedings of the Taura Syndrome Workshop*. Executive summary, submitted reports, and transcribed notes.
- Lightner, D. V., Redman, R. M., Hasson, K. W., and Pantoja, C. R. (1995). Taura syndrome in *Penaeus vannamei*: Histopathology and ultrastructure. *Dis. Aqua. Org.* **21**:53–59.
- Lightner, D. V., Hasson, K. W., White, B. L., and Redman, R. M. (1996). Chronic toxicological and histopathological studies with benomyl in *Penaeus vannamei* (Crustacea: Decapoda). *Aquat. Toxicol.* **34**:105–118.
- Lightner, D. V., Redman, R. M., Poulos, B. T., Nunan, L. M., Mari, J. L., Hasson, K. W., and Bonami, J. R. (1997a). Taura syndrome: Etiology, pathology, hosts, geographic distribution, and detection methods. *New approaches to viral diseases of aquatic animals, Proceedings of the NRAI Workshop*, pp. 190–205.
- Lightner, D. V., Redman, R. M., Poulos, B. T., Nunan, L. M., Mari, J. L., and Hasson, K. W. (1997b). Risk of spread of penaeid shrimp viruses in the Americas by the international movement of live and frozen shrimp. *Rev. Sci. Off. int. Epiz.* **16**:146–160.
- Lightner, D. V., Hasson, K. W., White, B. L., and Redman, R. M. (1998). Experimental infection of Western Hemisphere penaeid shrimp with Asian white spot syndrome virus and Asian yellowhead virus. *J. Aquat. Anim. Health* **10**:271–281.
- Limsuwan, C. (1991). “Handbook for Cultivation of Black Tiger Prawns.” Tansetakit, Bangkok, Thailand.
- Loh, P. C., Tapay, L. M., Lu, Y., and Nadala, E. C. B., Jr. (1997). Viral pathogens of the penaeid shrimp. *Adv. Virus Res.* **48**:263–312.
- Loh, P. C., Cesar, E., Nadala, B., Jr., Tapay, L. M., and Lu, Y. (1998). Recent developments in immunologically based and cell culture protocols for the specific detection of shrimp viral pathogens. In “Advances in Shrimp Biotechnology” (T. W. Flegel, ed.). National Center for Genetic Engineering and Biotechnology, Bangkok, Thailand.
- Lotz, J. (1997). Effect of host size on virulence of Taura virus to the marine shrimp *Penaeus vannamei* (Crustacea: Penaeidae). *Dis. Aquat. Org.* **30**:45–51.
- Lotz, J., Flowers, A. M., and Breland, V. (2003). A model of Taura syndrome virus (TSV) epidemics in *Litopenaeus vannamei*. *J. Invert. Pathology* **83**:168–176.
- Lu, Y., Tapay, L. M., Brock, J. A., and Loh, P. C. (1994). Infection of the yellowhead baculo-like virus (YBV) in two species of penaeid shrimp, *Penaeus stylirostris* (Simpson) and *Penaeus vannamei* (Boone). *J. Fish Dis.* **17**:649–656.

- Lu, Y., Tapay, L. M., Loh, P. C., Brock, J. A., and Gose, R. B. (1995a). Distribution of yellowhead virus in selected tissues and organs of penaeid shrimp *Penaeus vannamei*. *Dis. Aquat. Org.* **23**:67–70.
- Lu, Y., Tapay, L. M., Loh, P. C., Brock, J. A., and Gose, R. B. (1995b). Development of a quantal assay in primary shrimp cell culture for yellowhead baculovirus (YBV) of penaeid shrimp. *J. Virol. Methods* **52**:231–236.
- Lu, Y., Tapay, L. M., and Loh, P. C. (1996). Development of a nitrocellulose-enzyme immunoassay (NC-EIA) for the detection of yellowhead virus from penaeid shrimp. *J. Fish Dis.* **19**:9–13.
- Lu, Y., Tapay, L. M., Gose, R. B., Brock, J. A., and Loh, P. C. (1997). Infectivity of yellowhead virus (YHV) and the Chinese baculo-like virus (CBV) in two species of penaeid shrimp, *Penaeus stylirostris* (Stimpson) and *Penaeus vannamei* (Boone). In "Diseases in Asian Aquaculture III" (T. W. Flegel and I. H. MacRae, eds.). Asian Fisheries Society, Manila, Philippines.
- Luo, T., Zhang, X., Shao, Z., and Xu, X. (2003). *PmAV*, a novel gene involved in virus resistance of shrimp *Penaeus monodon*. *FEBS Lett.* **551**:53–57.
- Mateu, M. G., Silva, D. A., Rocha, E., de Braum, D. L., Alonso, A., Enjuanes, L., Domingo, E., and Barahona, H. (1988). Extensive antigenic heterogeneity of foot-and-mouth disease virus serotype C. *Virology* **167**:113–124.
- Mari, J., Bonami, J. R., and Lightner, D. V. (1998). Taura syndrome of penaeid shrimp: Cloning of viral genome fragments and development of specific gene probes. *Dis. Aquat. Org.* **33**:11–17.
- Mari, J., Poulos, B. T., Lightner, D. V., and Bonami, J. R. (2002). Shrimp Taura syndrome virus: Economic characterization and similarity with members of the genus of cricket paralysis-like viruses. *J. Gen. Virol.* **83**:915–926.
- Mayo, M. A. (2002). A summary of taxonomic changes recently approved by ICTV. *Arch. Virol.* **147**:1655–1656.
- Mermoud, I., Costa, R., Ferre, O., Goarant, C., and Haffner, P. (1998). Syndrome 93' in New Caledonian outdoor rearing ponds of *Penaeus stylirostris*: History and description of three major outbreaks. *Aquaculture* **164**:323–325.
- Mohan, C. V., Shankar, K. M., Kulkarni, S., and Sudha, P. M. (1998). Histopathology of cultured shrimp showing gross signs of yellowhead syndrome and white spot syndrome during 1994 Indian epizootics. *Dis. Aquat. Org.* **34**:9–12.
- Moore, N. F., Kearns, A., and Pullin, J. S. K. (1980). Characterization of cricket paralysis virus-induced polypeptides in *Drosophila* cells. *J. Virol.* **33**:1–9.
- Moore, N. F., Reavy, B., and Pullin, J. S. K. (1981). Processing of cricket paralysis virus-induced polypeptides in *Drosophila* cells: Production of high molecular weight polypeptides by treatment with iodoacetamide. *Arch. Virol.* **68**:1–8.
- Moulliseseaux, K. P., Klimpel, K. R., and Dhar, A. K. (2003). Improvement in the specificity and sensitivity of detection for the Taura syndrome virus and yellowhead virus of penaeid shrimp by increasing the amplicon size in SYBR Green real-time RT-PCR. *J. Virol. Methods* **111**:121–127.
- Murphy, F. A., Fauquet, C. M., Bishop, D. H. L., Ghabrial, S. A., Jarvis, A. W., Martelli, G. P., Mayo, M. A., Summers, M. D. (eds.). (1995). Virus taxonomy, classification, and nomenclature of viruses. Sixth report of the international committee of taxonomy of viruses. *Arch. Virol.* **10** Suppl, Springer-Verlag, New York.
- Nadala, E. C. B., Jr., Tapay, L. M., and Loh, P. C. (1997a). Yellowhead virus: A rhabdovirus-like pathogen of penaeid shrimp. *Dis. Aquat. Org.* **31**:141–146.

- Nadala, E. C. B., Jr., Tapay, L. M., Cao, S., and Loh, P. C. (1997b). Detection of yellowhead virus and Chinese baculovirus in penaeid shrimp by the Western blot technique. *J. Virol. Methods* **69**:39–44.
- Nadala, E. C. B., Jr., and Loh, P. C. (2000). Dot-blot nitrocellulose enzyme immunoassays for the detection of white spot virus and yellowhead virus of penaeid shrimp. *J. Virol. Methods* **84**:175–179.
- Nash, G., Arkarjamon, A., and Withyachumnarnkul, B. (1995). Histological and rapid haemocytic diagnosis of yellowhead disease in *Penaeus monodon*. In “Diseases in Asian Aquaculture II” (M. Shariff, J. R. Arthur, and R. P. Subasinghe, eds.). Fish Health Section, Asian Fisheries Society, Manila, Philippines.
- Natividad, K., Magbanua, F. O., Migo, V. P., Alfara, C. G., Albaladejo, J. D., Nadala, E. C. B., Jr., Loh, P. C., and Tapay, L. M. (1999). Evidence of yellowhead virus in cultured black tiger shrimp (*Penaeus monodon* Fabricius) from selected shrimp farms in the Philippines. *Fourth Symposium on Diseases in Asian Aquaculture*, p. 60.
- Nelsen-Salz, B., Zimmermann, A., Wickert, S., Arnold, G., Botta, A., Eggers, H. J., and Kruppenbacher, J. P. (1996). Analysis of sequence and pathogenic properties of two variants of encephalomyocarditis virus differing in a single amino acid in VP1. *Virus Res.* **41**:109–122.
- Neumann, T., Kaiser, H. E., and Rath, F. W. (2000). A permanent cell line of the crayfish *Orconecte limosus* as a potential model in comparative oncology. *In vivo* **14**:691–698.
- Nunan, L. M., Poulos, B. T., and Lightner, D. V. (1998). Reverse transcription polymerase chain reaction (RT-PCR) used for the detection of Taura syndrome virus (TSV) in experimentally infected shrimp. *Dis. Aquat. Org.* **34**:87–91.
- Nunan, L., Poulos, B., Redman, R., Le Groumellec, M., and Lightner, D. V. (2003). Molecular detection methods developed for a systemic rickettsia-like bacterium (RLB) in *Penaeus monodon* (Decapoda: Crustacea). *Dis. Aquat. Org.* **53**:15–23.
- OIE Fish Disease Commission (2002). *International Aquatic Animal Health Code*. 5th ed. Office International des Epizooties, Paris.
- OIE Fish Disease Commission (2003). Yellowhead disease. Chap. 4.1.3 in Manual of diagnostic tests for aquatic animals. http://www.oie.int/eng/normes/fmanual/A_summry.htm.
- Overstreet, R. M., Lightner, D. V., Hasson, K. W., McIlwain, S., and Lotz, J. (1997). Susceptibility to TSV of some penaeid shrimp native to the Gulf of Mexico and southeast Atlantic Ocean. *J. Invert. Path* **69**:165–176.
- Owens, L. (1997). Special topic review: The history of the emergence of viruses in the Australian prawn industry. *World J. Microbiol. Biotechnol.* **13**:427–431.
- Pantoja, C., and Lightner, D. V. (2001). Necrosis due to WSSV can mimic YHV lesions in lymphoid organ of penaeid shrimp. *Advocate* **4**:15.
- Pantoja, C. R., and Lightner, D. V. (2003). Similarity between the histopathology of white spot syndrome virus and yellowhead syndrome virus and its relevance to diagnosis of YHV disease in the Americas. *Aquaculture* **218**:47–54.
- Pasharawipas, T., Flegel, T. W., Sriurairatana, S., and Morrison, D. J. (1997). Latent yellowhead infections in *Penaeus monodon* and implications regarding disease resistance or tolerance. In “Shrimp Biotechnology in Thailand” (T. W. Flegel, P. Menasveta, and S. Paisarnrat, eds.). National Center for Biotechnology and Genetic Engineering, Bangkok, Thailand.
- Phan, Y. T. N. (2001). Prevalence and coprevalence of white spot syndrome virus (WSSV) and yellowhead complex viruses (YHV-complex) in cultured giant tiger prawn (*Penaeus monodon*) in Vietnam. Master thesis. University of Queensland, Brisbane.

- Poulos, B. T., Kibler, R., Bradley-Dunlop, D., Mohney, L. L., and Lightner, D. V. (1999). Production and use of antibodies for the detection of the Taura syndrome virus in penaeid shrimp. *Dis. Aquat. Org.* **37**:99–106.
- Prior, S., and Browdy, C. L. (2000). Postmortem persistence of white spot and Taura syndrome viruses in water and tissue. *Proceedings for the Annual Conference of the World Aquaculture Society*, p. 397.
- Prior, S., Segars, A., and Browdy, C. L. (2001). A preliminary assessment of live and frozen bait shrimp indicators and/or vectors of shrimp viruses. *The International and Triennial Conference and Exposition of the World Aquaculture Society*, p. 541.
- Racusen, D. (1979). Glycoprotein detection in polyacrylamide gel with thymol and sulfuric acid. *Anal. Biochem.* **99**:474–476.
- Robles-Sikisaka, R., Garcia, D. K., Klimpel, K. R., and Dhar, A. K. (2001). Nucleotide sequence of 3'-end of the genome of Taura syndrome virus of shrimp suggests that it is related to insect picornaviruses. *Arch. Virol.* **46**:941–952.
- Robles-Sikisaka, R., Hasson, K. W., Garcia, D. K., Brovont, K. E., Cleveland, K., Klimpel, K. R., and Dhar, A. K. (2002). Genetic variation and immunohistochemical differences among geographic isolates of Taura syndrome virus of penaeid shrimp. *J. Gen. Virol.* **83**:3123–3130.
- Roer, R. D., and Dillaman, R. M. (1993). Molt-related change in integumental structure and function. In "The Crustacean Integument: Morphology and Biochemistry" (M. N. Horst and J. A. Freeman, eds.). CRC Press, Boca Raton, LA.
- Rojtinnakorn, J., Hirono, I., Itami, T., Takahashi, Y., and Aoki, T. (2002). Gene expression in hemocytes of kuruma prawn, *Penaeus japonicus*, in response to infection with WSSV by EST approach. *Fish Shellfish Immunol.* **13**:69–83.
- Roux, M. M., Pain, A., Klimpel, K. R., and Dhar, A. K. (2002). Lipopolysaccharide and β -1,3-glucan-binding gene is upregulated in white spot virus (WSSV) infected in shrimp (*Penaeus stylirostris*). *J. Virol.* **76**:7140–7149.
- Ruckert, R. R. (1996). Picornaviridae: The viruses and their replication. In "Field virology" (B. N. Fields, D. N. Knipe, and P. M. Howley, eds.). Lippincott-Raven, Philadelphia, PA.
- Rukyani, A. (2000). Indonesia. In "Thematic Review on Management Strategies for Major Diseases in Shrimp Aquaculture" (J. R. Arthur, D. Fegan, and R. Subasinghe, eds.). FAO, Rome, Italy.
- Sasaki, J., and Nakashima, N. (1999). Translation initiation at the CUU codon is mediated by the internal ribosomal entry site of an insect picorna-like virus *in vitro*. *J. Virol.* **73**:1219–1226.
- Sasaki, J., and Nakashima, N. (2000). Methionine-independent initiation of translation in the capsid protein of an insect RNA virus. *Proc. Natl. Acad. Sci.* **97**:1512–1515.
- Sasaki, J., Nakashima, N., Saito, H., and Noda, H. (1998). An insect picorna-like virus, *Plautia stali* intestine virus, has genes of capsid proteins in the 3'-part of the genome. *Virology* **244**:50–58.
- Sawicki, S. G., and Sawicki, D. L. (1999). A new model for coronavirus transcription. *Adv. Exp. Med. Biol.* **440**:215–219.
- Siriwardena, P. P. G. S. N. (2000). Sri Lanka. In "Thematic Review on Management Strategies for Major Diseases in Shrimp Aquaculture" (J. R. Arthur, D. Fegan, and R. Subasinghe, eds.). FAO, Rome, Italy.
- Sithigorngul, P., Chauchuwong, P., Sithigorngul, W., Longyant, S., Chaivisuthangkura, P., and Menasveta, P. (2000). Development of a monoclonal antibody specific to yellowhead virus (YHV) from *Penaeus monodon*. *Dis. Aquat. Org.* **42**:27–34.

- Sithigorngul, P., Rukpratanporn, S., Longyant, S., Chaivisuthangkura, P., Sithigorngul, W., and Menasveta, P. (2002). Monoclonal antibodies specific to yellowhead virus (YHV) of *Penaeus monodon*. *Dis. Aquat. Org.* **49**:71–76.
- Sittidilokratna, N. (2003). Analysis of the YHV Genome and Expression of Recombinant Glycoprotein. gp116. Ph.D. diss. Mahidol University, Bangkok.
- Sittidilokratna, N., Hodgson, R. A. J., Cowley, J. A., Jitrapakdee, S., Boonsaeng, V., Panyim, S., and Walker, P. J. (2002). Complete ORF1b-gene sequence indicates yellowhead virus is an invertebrate nidovirus. *Dis. Aquat. Org.* **50**:87–93.
- Siveter, D. J., Williams, M., and Waloszek, D. (2001). A phosphatocopid crustacean with appendages from the Lower Cambrian. *Science* **293**:479–481.
- Smith, P. T. (2000). Diseases of the eye of farmed shrimp *Penaeus monodon*. *Dis. Aquat. Org.* **43**:159–173.
- Snijder, E. J., and Meulenberg, J. J. M. (1998). The molecular biology of arteriviruses. *J. Gen. Virol.* **79**:961–979.
- Soowannayan, C., Sithigorngul, P., and Flegel, T. W. (2002). Use of a specific monoclonal antibody to determine tissue tropism of yellowhead virus (YHV) of *Penaeus monodon* by *in situ* immunohistochemistry. *Fish Science* **68**(Suppl. 1):805–809.
- Soowannayan, C., Flegel, T. W., Sithigorngul, P., Slater, J., Hyatt, A., Crammeri, S., Wise, T., Crane, M. S. J., Cowley, J. A., McCulloch, R. J., and Walker, P. J. (2003). Detection and differentiation of yellowhead complex viruses using monoclonal antibodies. *Dis. Aquat. Org.* **57**:193–200.
- Spann, K. M., Vickers, J. E., and Lester, R. J. G. (1995). Lymphoid organ virus of *Penaeus monodon* from Australia. *Dis. Aquat. Org.* **23**:127–134.
- Spann, K. M., Cowley, J. A., Walker, P. J., and Lester, R. J. G. (1997). A yellowhead-like virus from *Penaeus monodon* in Australia. *Dis. Aquat. Org.* **31**:169–179.
- Spann, K. M., Donaldson, R. A., Cowley, J. A., and Walker, P. J. (2000). Differences in the susceptibility of some penaeid prawn species to gill-associated virus (GAV) infection. *Dis. Aquat. Org.* **4**:221–225.
- Spann, K. M., McCulloch, R. J., Cowley, J. A., East, I. J., and Walker, P. J. (2003). Detection of gill-associated virus (GAV) by *in situ* hybridization during acute and chronic infections of *Penaeus monodon* and *P. esculentus*. *Dis. Aquat. Org.* **56**:1–10.
- Stern, S. (1995). Swimming through troubled waters in shrimp farming: Ecuador country review. In “Swimming through Troubled Water” (C. L. Browdy and J. S. Hopkins, eds.). Proceedings of the Special Session on Shrimp Farming Aquaculture, World Aquaculture Society, Baton Rouge, LA.
- Tang, K. F. J., and Lightner, D. V. (1999). A yellowhead virus gene probe: Nucleotide sequence and application for *in situ* hybridization. *Dis. Aquat. Org.* **35**:165–173.
- Tang, K. F. J., Spann, K. M., Owens, L., and Lightner, D. V. (2002). *In situ* detection of Australian gill-associated virus with a yellowhead virus gene probe. *Aquaculture* **205**:1–5.
- Tang, K. F. J., Wang, J., and Lightner, D. V. (2003). Quantitation of Taura syndrome virus by real-time RT-PCR with a TaqMan assay. *J. Virol. Methods* **115**:109–114.
- Toullec, J. (1999). Crustacean primary cell culture: A technical approach. *Methods Cell Sci.* **21**:193–198.
- Tu, C., Huang, H., Chuang, S., Hsu, J., Kuo, S., Li, N., Hsu, T., Li, M., and Lin, S. (1999). Taura syndrome in pacific white shrimp *Penaeus vannamei* cultured in Taiwan. *Dis. Aquat. Org.* **38**:159–161.
- van de Braak, C. B. T., Botterblom, M. H. A., Taverne, N., Van Muiswinkel, W. B., Rombut, J. H. W. M., and van der Knapp, W. P. W. (2002). The roles of hemocytes and the lymphoid organ in the clearance of injected *Vibrio* bacteria in *Penaeus monodon* shrimp. *Fish Shell. Immunol.* **13**:293–309.

- van der Wilk, F., Dullemans, A. M., Verbeek, M., and van den Heuvel, J. F. (1997). Nucleotide sequence and genomic organization of *Acyrtosiphon pisum* virus. *Virology* **238**:353–362.
- van Marle, G., Dobbe, J. C., Gulyaev, A. P., Luytjes, W., Spaan, W. J. M., and Snijder, E. J. (1999). Arterivirus discontinuous mRNA transcription is guided by base pairing between sense and antisense transcription-regulating sequences. *Proc. Natl. Acad. Sci. USA* **96**:12056–12061.
- van Regenmortel, M. H. V., Fauquet, C. M., Bishop, D. H. L., Carstens, E. B., Estes, M. K., Lemon, S. M., Maniloff, J., Mayo, M. A., McGeoch, D. J., Pringle, C. R., and Wickner, R. B. (2000). "Virus Taxonomy: The Classification and Nomenclature of Viruses." *The seventh Report of the International Committee on Taxonomy of Viruses*. Academic Press, San Diego, CA.
- van Vliet, A. L., Smits, S. L., Rottier, P. J., and de Groot, R. J. (2002). Discontinuous and nondiscontinuous subgenomic RNA transcription in a nidovirus. *EMBO J.* **21**:6571–6580.
- Walker, P. J., Cowley, J. A., Spann, K. M., Hodgson, R. A. J., Hall, M. R., and Withyachumnarnkul, B. (2001). Yellowhead complex viruses: Transmission cycles and topographical distribution in the Asia-Pacific region. In "The New Wave" (C. L. Browdy and D. E. Jory, eds.). *Proceedings of the Special Session on Sustainable Shrimp Culture*. The World Aquaculture Society, Baton Rouge, LA.
- Walker, P. J., Flegel, T. W., Boonsaeng, V., Lightner, D. V., Tang, K. F. J., Loh, P. C., Chang, P. S., Bonami, J. R., Cowley, J. A., Snijder, E. J., and Enjuanes, L. (2003). Roniviridae. Taxonomic structure of the family. In "Virus Taxonomy, Eighth Report of the International Committee on Taxonomy of Viruses" (M. H. V. van Regenmortel, C. M. Fauquet, D. H. L. Bishop, E. B. Estes, S. M. Lemon, J. Maniloff, M. A. Mayo, D. J. McGeoch, C. R. Pringle, and R. B. Wickner, eds.). Academic Press, San Diego, CA.
- Wang, C. S., Tang, K. J., Kuo, G. H., and Chen, S. N. (1996). Yellowhead disease-like virus infection in the Kuruma shrimp *Penaeus japonicus* cultured in Taiwan. *Fish. Pathol.* **31**:177–182.
- Wang, Y. C., and Chang, P. S. (2000). Yellowhead virus infection in the giant tiger prawn *Penaeus monodon* cultured in Taiwan. *Fish. Pathol.* **35**:1–10.
- Wigglesworth, J. (1994). Taura Syndrome hits Ecuador farms. *Fish Farmer* **17**:30–31.
- Wilson, J. E., Powell, M. J., Hoover, S. E., and Sarnow, P. (2000). Naturally occurring dicistronic cricket paralysis virus RNA is regulated by two internal ribosomal entry sites. *Mol. Cell. Biol.* **20**:4990–4999.
- Wongteerasupaya, C., Boonsaeng, V., Panyim, S., Tassanakajon, A., Withyachumnarnkul, B., and Flegel, T. W. (1997). Detection of yellowhead virus (YHV) of *Penaeus monodon* by RT-PCR amplification. *Dis. Aquat. Org.* **31**:181–186.
- Wongteerasupaya, C., Sriurairatana, S., Vickers, J. E., Anutara, A., Boonsaeng, V., Panyim, S., Tassanakajon, A., Withyachumnarnkul, B., and Flegel, T. W. (1995). Yellowhead virus of *Penaeus monodon* is an RNA virus. *Dis. Aquat. Org.* **22**:45–50.
- Yang, Y. G., Shariff, M., Lee, L. K., and Hassan, M. D. (2000). Malaysia. In "Thematic Review on Management Strategies for Major Diseases in Shrimp Aquaculture" (J. R. Arthur, D. Fegan, and R. Subasinghe, eds.). FAO, Rome, Italy.
- Yu, C., and Song, Y. (2000). Outbreaks of Taura syndrome in Pacific white shrimp *Penaeus vannamei* cultured in Taiwan. *Fish Pathol.* **35**:21–24.
- Zarain-Herzberg, M., and Ascencio-Valle, F. (2001). Taura syndrome in Mexico: Follow-up study in shrimp farms of Sinaloa. *Aquaculture* **193**:1–9.
- Ziebuhr, J., Bayer, S., Cowley, J. A., and Gorbalenya, A. E. (2003). The 3C-like proteinase of an invertebrate nidovirus links coronavirus and potyvirus homologs. *J. Virol.* **77**:1415–1426.

This Page Intentionally Left Blank

VIRUSES OF THE CHESTNUT BLIGHT FUNGUS, *CRYPHONECTRIA PARASITICA*

Bradley I. Hillman* and Nobuhiro Suzuki†

*Department of Plant Biology and Pathology, Rutgers University, New Brunswick
New Jersey 08901

†Research Institute for Bioresources, Okayama University
Okayama 710-0046, Japan

- I. Introduction
 - II. Fungi as Hosts for Virus Infection
 - III. History of *C. parasitica* as a Virus Host
 - IV. Viruses as the Cause of Hypovirulence and a Description of CHV1
 - V. General Properties and Procedures for Studying *C. parasitica* Viruses
 - A. Isolation of dsRNA
 - B. Virulence Tests
 - C. Asexual and Sexual Sporulation
 - D. Transfection and Transformation
 - VI. Structure and Characteristics of the CHV1 Genome
 - A. Overview of CHV1 RNA Genome Structure and Replication
 - B. 5'- and 3'-Noncoding Sequences of CHV1
 - C. Coding Sequences of CHV1
 - VII. Host Genes and Signaling Pathways Affected by CHV1 Infection
 - VIII. Other *Cryphonectria* Hypoviruses
 - A. CHV2
 - B. CHV3
 - C. CHV4
 - IX. Defective and Satellite RNAs of Hypoviruses
 - X. Other Viruses of *C. parasitica*
 - A. Two Reoviruses
 - B. Mitochondrial Viruses: The *Narnaviridae*
 - C. Partially Characterized Viruses
 - XI. Population Biology and Evolution of *Cryphonectria* Viruses
 - A. Molecular Evolution of Hypoviruses
 - B. Population Biology of *Cryphonectria* Viruses
 - C. Lateral Transfer and Origins of *Cryphonectria* Viruses
 - XII. Conclusions
- References

Viruses of *Cryphonectria parasitica* have been studied for more than 30 years because of their association with biologic control of the filamentous fungus that causes chestnut blight. One virus, *Cryphonectria hypovirus* 1 (CHV1), has been studied intensively and its manipulation has led to the discovery of considerable information about specific

host-virus interactions. CHV1 was the prototype for description of the virus family *Hypoviridae*, the first virus family described whose members have no capsid. Three other virus species within this family as well as many strains of those species have since been identified. The different species vary in their genome organizations, in the degree to which they alter fungal virulence and phenotype, and in their natural occurrence. In addition to viruses in the family *Hypoviridae*, several other virus families have been identified in *Cryphonectria*. These have been less important from the standpoint of the natural history of the fungus and its biologic control but are important from a virological perspective. Among the most notable are viruses in the families *Reoviridae*, *Narnaviridae*, and *Chrysoviridae*. Hence, the filamentous fungus causing chestnut blight has become a rich source for the study of diverse viruses in a widespread and easily manipulable haploid organism.

I. INTRODUCTION

Viruses are an integral component of eukaryotic hosts, but fungal viruses have been given less attention than other viruses. The number of economically important hosts in which fungal viruses cause serious disease is relatively low. When other eukaryotes such as plants and vertebrates suffer from virus infections, the effects are often of immediate economic or social significance: food supplies are compromised or the population is affected with illnesses. Although fungi contribute to the food supply, their contribution is somewhat more minor and less direct—yeasts are used for bread, wine, and beer production, and filamentous fungi are used for production of cheese, enzymes, and drugs. Virus infections may reduce the effectiveness of fungi in their role as food producers, but viruses rarely present problems that cannot be overcome simply by cleaning up cultures. Fungi have a greater impact on food supply in their roles as plant pathogens. They are the most important group of plant pathogens, so their infection by viruses may be beneficial to humans when infection results in depression of fungi populations. Similarly, fungi cause diseases of vertebrates, and suppression of these organisms is desirable. This highlights two other key features of fungal viruses: they are often asymptomatic in their fungal hosts, and they tend to be transmitted only by hyphal fusion (anastomosis) or vertically through sexual or asexual spores. These properties are fortunate from the standpoint of the roles of viruses as pathogens of fungi viewed beneficial to humans, but these properties

are also unfortunate from the standpoint of their potential as biological control agents for pathogenic fungi.

The history of fungal virology is still relatively young and much less well developed than that of other viruses. Plant and animal viruses were well known as disease-causing agents and had been characterized as different from other microbes by the turn of the 20th century. Bacterial viruses were well known by the early 20th century and were an integral part of the development of modern genetics and molecular biology. Fungal viruses, however, were not characterized until the 1950s, and there are few laboratories with fungal virology as the primary research area.

This chapter focuses especially on viruses that infect *C. parasitica*. A few examples are included from other systems, but these are not meant to provide a broad review of fungal virology. For broader reviews, the reader is directed to Buck (1998) and Ghabrial (1994). For other reviews on *C. parasitica*, see Anagnostakis (1982, 1987), MacDonald and Fulbright (1991), and Milgroom (1995). Several reviews specifically cover *Cryphonectria hypovirus* 1 or CHV1 (Dawe and Nuss, 2001; Nuss, 1992, 1996, 2000).

II. FUNGI AS HOSTS FOR VIRUS INFECTION

Most fungi are culturable and are therefore relatively easy to work with as experimental hosts for virus infection. Of the fungal hosts, yeasts are the most tractable. They grow as colonies that are selectable by a number of methods on solid media and complete sexual reproduction cycles rapidly and efficiently. Yeasts are natural hosts to several viruses that have been well characterized. Unfortunately, yeasts have not yet proven to be good experimental hosts for fungal viruses. Most of the work that has been done with yeast viruses has been with naturally infected strains, limiting the flexibility of yeasts as virus hosts. Surprisingly, though, yeasts are beginning to be useful as hosts for the study of plant and vertebrate viruses. Several single-stranded RNA (ssRNA) viruses have been shown to replicate in yeast when introduced as nucleic acid constructs (e.g., Janda and Ahlquist, 1993; Price *et al.*, 2000), and this host has provided important details of RNA virus replication.

Filamentous fungi that are well-defined in genetic and molecular terms and that show versatile growth characteristics are the most useful for the study of viruses and their infection processes. Desirable characteristics include: (i) ability to grow rapidly in culture (some

fungi grow very slowly or are dimorphic and fall naturally into a yeast phase); (ii) stability of growth (some fungi sector often or naturally lose virulence in culture); (iii) ability to reproduce sexually (many fungi are “imperfect” with no known natural or experimental sexual cycle, limiting genetic studies); (iv) ability to reproduce through spores asexually (often a useful way to obtain virus-free, isogenic cultures from naturally infected isolates); and (v) ability to be transformed easily. A number of other characteristics are also desirable in a fungal host: (i) extensive knowledge of host genetics, genomics, developmental, and molecular biology; (ii) understanding of the population structure and evolutionary biology of the host; and (iii) economic importance of the fungal host.

Fulfillment of Koch’s postulates for a virus requires unequivocal demonstration that it is the agent causing a particular disease. This has been difficult with fungal viruses because most have been transmitted only by anastomosis (Fig. 1). In such experiments, the virus is not purified, and Koch’s postulates are not fulfilled. No matter how carefully experiments involving anastomosis are performed, they cannot overcome this shortcoming. Within the last 10 years, infection of fungi with purified particles and especially RNA has become feasible in

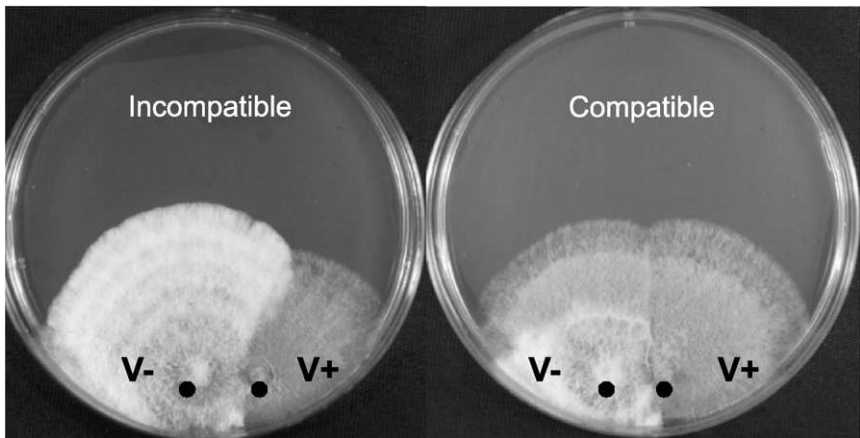


FIG 1. Vegetative incompatibility as a barrier to virus transmission in *C. parasitica*. (Left) Formation of a barrage between incompatible virus-containing and virus-free isolates. Acquisition by a virus-free isolate of phenotype is not associated with infection. (Right) Anastomosis between compatible virus-containing and virus-free isolates. Anastomosis allows acquisition by virus-free isolate of phenotype associated with infection. Isolates were placed on the edge of culture dishes at marked spots and allowed to grow for 1 week.

some cases. The recent progress with *Cryphonectria* viruses from the standpoint of host-pathogen interactions has resulted from the ability to fulfill Koch's postulates and manipulate the viral genome as well as the fungal genome.

III. HISTORY OF *C. PARASITICA* AS A VIRUS HOST

At the turn of the 20th century, Beijerinck was performing experiments that would convince most scientists of the fundamental difference between viruses and other microbes. At the same time, a filamentous fungus was beginning to destroy the chestnut stands native to eastern North America (Anagnostakis, 1987). The fungus was originally identified as *Diaporthe* sp. and was later renamed *Endothia parasitica* (Shear and Stevens, 1917). Barr would later reexamine the genus *Endothia* and place *E. parasitica* in the closely related genus *Cryphonectria* (Barr, 1978). *C. parasitica* had arrived into the native American chestnut (*Castanea dentata*) growing region most probably on Japanese chestnuts (*Castanea crenata*). Such trees are highly resistant to the fungus and were most likely not identified as diseased. *C. parasitica* quickly ravaged the American chestnut population, killing virtually all of the highly susceptible trees. By the time the fungus arrived in Europe in the late 1930s, foresters were well aware of its destructive potential (Heiniger and Rigling, 1994). Several factors combined to prevent a recurrence of a pandemic. First, European chestnut (*Castanea sativa*) is somewhat less susceptible to *C. parasitica* than American chestnut; second, the coppices in which chestnut are grown in much of Europe are more conducive to disease control; and finally, a virus that entered the European population at an early stage slowed the epidemic (Heiniger and Rigling, 1994). The virus would later come to be known as *Cryphonectria hypovirus* 1 (CHV1) and has been the subject of the most intense scrutiny of any filamentous fungal virus. In the course of investigating this fungus, however, it has become apparent that *C. parasitica* serves as host to a broad array of viruses, some of that are closely related to CHV1 and others that are not.

IV. VIRUSES AS THE CAUSE OF HYPOVIRULENCE AND A DESCRIPTION OF CHV1

In 1951, the Italian plant pathologist Antonio Biraghi noted that some infected European chestnut trees in Italy appeared to be recovering and had cankers that were morphologically distinct but that

did not result in death of the infected tree (Biraghi, 1951). French scientist Jean Grente noted that fungal strains isolated from these non-lethal cankers were morphologically distinct from fungal strains associated with lethal cankers (Grente, 1965; Grente and Berthelay-Sauret, 1978). They were white in color, sporulated little if at all, and grew more slowly than the fast growing, orange, profusely sporulating cultures normally isolated from dying trees. This turned out to be an important observation from the standpoint of biologic control of the fungus and working with the virus—the infected fungus is easily distinguishable from its virus-free counterpart. Grente took advantage of this feature to demonstrate that under the right conditions, the diseased phenotype could be acquired by a normal-looking strain following contact with a diseased strain. He coined the term *transmissible hypovirulence* for this phenomenon.

Given that *C. parasitica* generally causes cankers from a single point of infection on a tree, it was quickly recognized that hypovirulent strains able to transmit the agent responsible for the diseased phenotype may be useful for control of this fungus, which had been recalcitrant to chemical control. A program for control of *C. parasitica* using hypovirulent isolates was initiated in several chestnut growing regions of Europe and remains active today. A major factor in the success of this program turned out to be the relatively low level of diversity within the European *C. parasitica* population (Anagnostakis *et al.*, 1986; Milgroom and Cortesi, 1999). This low level of diversity was reflected in the low number of different vegetative compatibility groups found in the population, allowing for relatively efficient virus transfer within the population.

In the late 1960s, scientists in the United States became aware of the relative success of hypovirulence research in Europe, and a program was initiated to try to implement the same type of control in the American chestnut population. A group at the Connecticut Agricultural Experiment Station led by Dr. Peter Day spearheaded the research, which was initiated with the same hypovirulent strains as those used in Europe. The remaining member of the original research group, Dr. Sandy Anagnostakis, has written very useful reviews that summarize early work on hypovirulence and this period (Anagnostakis, 1982, 1987). It was quickly recognized that the situation in North America was more complex than the situation in Europe: the American fungal population was more diverse than the European population, and transmission of the agent responsible for the distinct hypovirulent phenotype from a particular strain to another strain in the American population was more of a rare event. Despite the practical problems,

the Connecticut group was the first to focus considerable energy into determining the basis for hypovirulence. This research was initiated at a time when virology was well developed as a science but the molecular biology of RNA viruses was not. The first and most important molecular observation about hypovirulent fungal strains was that they contain double-stranded RNA (dsRNA), which was not observed in virulent fungal isolates (Anagnostakis and Day, 1979; van Alfen *et al.*, 1975). This suggested that the agents responsible for hypovirulence are viral in nature; however, no classical virus particles could be isolated. Instead, pleomorphic vesicles that appeared to contain dsRNA were identified (Dodds, 1978, 1980).

Further investigation of the molecular properties of the virus-like agents associated with hypovirulence of *C. parasitica*, now classified in the virus family *Hypoviridae* (Hillman *et al.*, 2000b), was hampered by the limitations of the system and fungal viruses in general. The pleomorphic particles that were isolated from hypovirulent fungal isolates contained no discernable protein component, and they were difficult to purify (Hansen *et al.*, 1985) (Fig. 2). Most critically, infectivity could not be demonstrated under any of the conditions examined by various researchers. This included attempts to infect with the pleomorphic

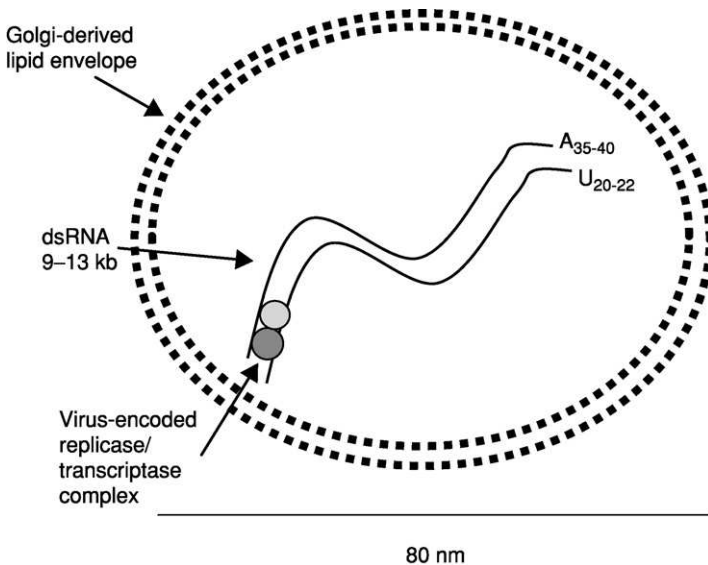


FIG 2. Diagram of a vesicle associated with viruses in the family Hypoviridae. Most details are from studies of CHV1, as described in the text. Redrawn from Hillman *et al.* (2000b).

particles and with purified dsRNA to virus-free fungal cultures and protoplasts isolated from those cultures. Not until the development of infectious transcripts of RNA viruses and application to this system in the early 1990s was the infectivity of one of the *C. parasitica* viruses demonstrated (see next paragraph).

It is no accident that early experiments with European hypovirulent cultures yielded positive results fairly quickly because there are several characteristics of CHV1-infected *C. parasitica* cultures that render them particularly well suited for studying virus-induced hypovirulence. As already noted, the European hypovirulent isolates are dramatically different from virulent isolates—they are white, in contrast to the orange-colored uninfected *C. parasitica* isolates, and can thus be identified within a few days of infection. Furthermore, this phenotype is extremely stable in a fungal background that is also very stable (Anagnostakis, 1981). Such stability is not always the case; many filamentous fungi sector abundantly, and virus-associated symptoms are difficult to discern, let alone to confirm experimentally with confidence. The fact that the early work was performed in Europe, where there are few vegetative incompatibility groups of *C. parasitica* and a high probability of being able to transmit virus among strains, further facilitated early experiments (Anagnostakis and Kranz, 1987; Anagnostakis *et al.*, 1986; Cortesi *et al.*, 2001, 1996; Milgroom and Cortesi, 1999). The European isolates contain a great deal of dsRNA compared to many fungal viruses: recovery of dsRNA is generally in the range of 3–8 $\mu\text{g/g}$ tissue (wet weight), and yields of 10–20 $\mu\text{g/g}$ tissue are common (Dodds, 1980; Hillman, unpublished data; Hillman *et al.*, 1990). These yields are much higher than those from *C. parasitica* isolates infected with most other viruses of this type, which may be up to 50- to 100-fold less. Working with such high yields of dsRNA greatly eases confirmation of dsRNA presence in newly infected tissue and facilitates experiments requiring dsRNA as starting material. In these respects, *C. parasitica* isolates infected with CHV1-type viruses show parallels with other experimental models of historical importance such as tobacco mosaic virus (TMV), which causes dramatic and consistent symptoms in its plant host and accumulates to high concentration in infected plants (Hull, 2002).

Although most research on chestnut blight viruses and hypovirulence has been done with CHV1, the genus *Hypovirus* of the family *Hypoviridae* is now recognized to contain four species that vary in genome organization, sequence relationships, and effects on the fungal host. These are referred to in the vernacular as hypoviruses. Following the convention used for many other fungal viruses, the species were

designated as CHV1, CHV2, CHV3, and CHV4 in chronological order of their complete sequence characterization and determination that they represented individual species (Fig. 3). When the family was described in 1995 in the Sixth Report of the International Committee on Taxonomy of Viruses (Hillman *et al.*, 1995), it represented the first virus family whose members did not contain a capsid. One other such family, the *Narnaviridae*, has been described since then. This property is common among fungal viruses, and other such families will undoubtedly be described in the future. A schematic summary of the range of dsRNA elements discussed in this chapter and their relative effects on the host fungus is presented in Fig. 4.

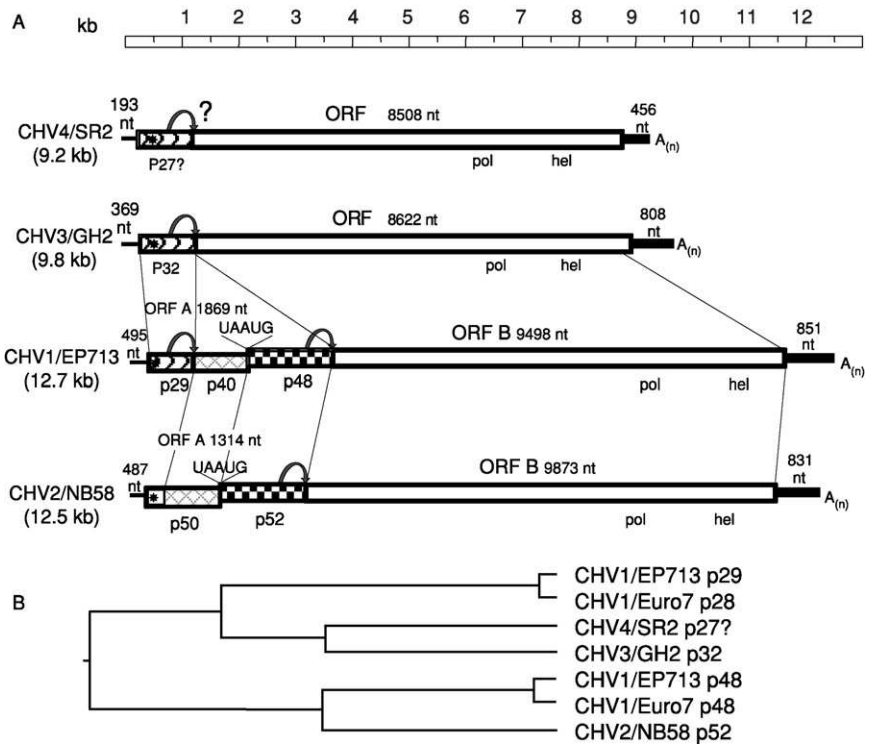


FIG 3. Individual species of genus *Hypovirus*. (A) Schematic diagrams of genome organizations of the four species of the family Hypoviridae. (B) Neighbor-joining tree showing relationships among papain-like proteinase sequences of hypoviruses. The putative CHV4 p27 has not yet been shown have proteinase activity (shown by the ?) but is based on sequence alignments. Adapted from Hillman *et al.* (2000a).

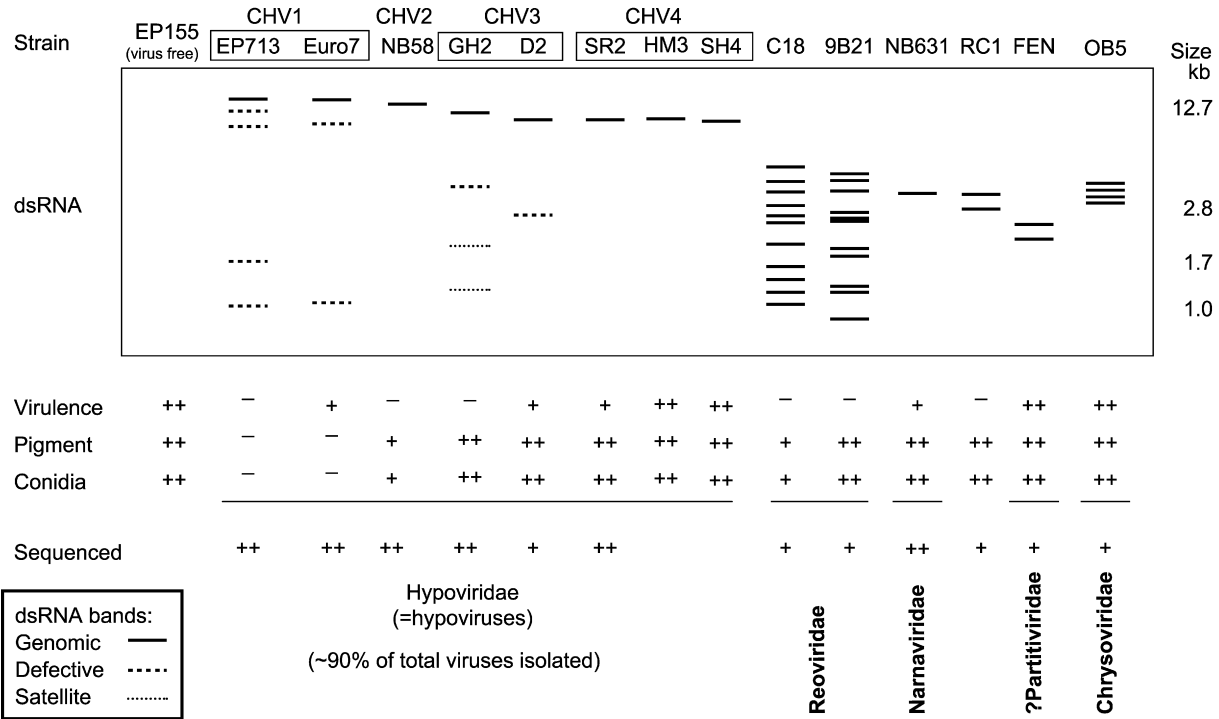


FIG 4. Diagram of composite gel showing relative mobilities of dsRNAs isolated from different virus-infected strains of *C. parasitica* and selected properties of the strains. Virulence, orange pigment, and conidia production are relative to EP155, the most commonly used virus-free strain, and are summarized from various studies.

V. GENERAL PROPERTIES AND PROCEDURES FOR STUDYING *C. PARASITICA* VIRUSES

This section briefly describes a few methods that are central to *C. parasitica* virus research.

A. Isolation of dsRNA

Almost all viruses of filamentous fungi are positive-stranded RNA or dsRNA viruses, so screening for presence of dsRNA, which could either be in viral genomes or replicative forms, is a rapid way to assess virus presence directly from infected fungal tissue. A number of methods have been used to do this, most of them derivative of the simplified cellulose column procedure (Hillman *et al.*, 1990; Morris and Dodds, 1979). For large numbers of samples, anti-dsRNA monoclonal antibodies have been used (Peever *et al.*, 1997). These only provide information about dsRNA presence or absence, rendering the antibodies of limited value as an analytical tool for examining virus diversity.

B. Virulence Tests

C. parasitica is a canker pathogen, and the natural way to assess virulence of individual isolates is to inoculate them to live trees. Such assays are usually not feasible, and rapid laboratory virulence tests are preferred. Excised stem assays most closely mimic inoculation of intact stems, and this can be done in a variety of ways (Elliston, 1978; Jaynes and Elliston, 1980; Lee *et al.*, 1992). The fungus also grows rapidly and makes lesions on apple fruits, and these provide a readily available substitute suitable for many studies (Fulbright, 1984).

C. Asexual and Sexual Sporulation

C. parasitica sporulates asexually very readily during infection and in culture, and the species does so in response to light and nutritional stimuli (Hillman *et al.*, 1990; Larson and Nuss, 1994). Sexual sporulation usually requires mating between two isolates of different mating types and has been initiated successfully only on chestnut stems or related tree species (Anagnostakis, 1979; Marra and Milgroom, 2001). Inoculation to harvesting of ascospores generally takes 6 to 12 weeks, considerably longer than yeast or *Neurospora*, but is a reliable genetic tool.

D. Transfection and Transformation

Transfection and transformation of *C. parasitica* are initiated with protoplasts, which are relatively easy to make from rapidly growing liquid cultures. A number of antibiotics can be used as selectable markers for transformation, and stable transformants can be obtained within a few days (Churchill *et al.*, 1990). Stable transformation to initiate infection with a full-length cDNA clone of a hypovirus genome was accomplished in 1992 (Choi and Nuss, 1992a). Shortly after this experiment, a transfection method was developed taking advantage of the rapid regeneration of protoplasts and anastomosis to form a single colony (Chen *et al.*, 1994). These methods allow for rapid introduction of foreign genes, knockout or knockdown of host genes, or introduction of certain viruses into new host backgrounds (Fig. 5).

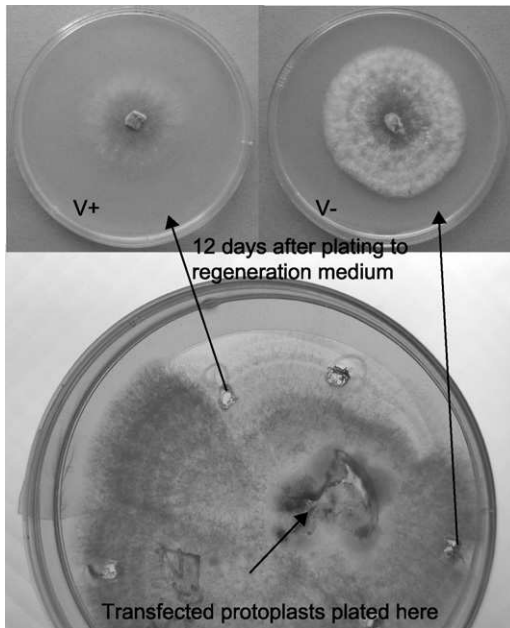


FIG 5. Transfection of *C. parasitica*. (Bottom) Fungal protoplasts transfected with a virus (in this case, the 9B21 reovirus) were plated to a regeneration medium in a small pool, then allowed to grow into a single colony as described by Chen and Nuss (1994). (Top) Subcultures from different regions of the primary transfectant colony. These may or may not contain a virus; those containing a virus are stably infected.

VI. STRUCTURE AND CHARACTERISTICS OF THE CHV1 GENOME

A. Overview of CHV1 RNA Genome Structure and Replication

The white, hypovirulent strain EP713 was made in the Connecticut Agricultural Experiment Station in the early 1970s by anastomosis of a French hypovirulent strain with a North American virus-free strain; thus, the virus, now called CHV1/EP713, is of French origin, whereas the genetic background of the host is American (Anagnostakis and Day, 1979). The genome organization of the CHV1/EP713 was determined in the beginning of 1990s (Shapira *et al.*, 1991b). As first predicted based on elements of the genome structure for the related virus that later became known as CHV3/GH2 (Smart *et al.*, 1999; Tartaglia *et al.*, 1986), the genome organization of CHV1/EP713 resembled a positive-strand RNA virus. Thus, the genome organization is described in those terms. The 12,712 nucleotide CHV1/EP713 genome is composed of a 5'-495-nt noncoding sequence, 11,406-nt coding region, 3'-851-nt noncoding sequence, and a templated poly(A) tract (Fig. 3). As a component of the dsRNA, the average size of the poly(A) tract was estimated to be 35 residues (Hiremath *et al.*, 1986), and the complementary poly(U) tract was estimated to be 20 residues (Hillman *et al.*, 1989). Because these determinations were made in different laboratories with different methodologies, it is not known whether this size difference is significant. The size of the poly(A) tract as a component of ssRNA transcripts has not been determined. The poly(A)-containing strand has two continuous open reading frames, ORF A (623 codons) and ORF B (3166 codons), encoding two polyproteins, p69 and the large ORF B polyprotein. Although replication-associated RNA polymerase and helicase domains are contained within ORF B, there is considerably more information about the expression and functions of the ORF A proteins. Each of the polyproteins encodes a papain-like proteinase, p29 and p48 at the N-terminal portion, that release cotranslationally from their cognate precursors. The p29 and p48 proteinases are paralogs presumably derived through gene duplication (Koonin *et al.*, 1991) though it is currently not clear which was the progenitor protein. In addition to the p29 proteinase, ORF A encodes a basic protein, p40. ORF B encodes the RNA-dependent RNA polymerase and RNA helicase domains in addition to the p48 proteinase, but little is known about further processing events of the ORF B polyprotein and specific protein functions. The polyprotein B is thought to be translated from viral full-length transcript by a termination/reinitiation mechanism mediated by the UAAUG pentamer as in the case for the dicistronic

influenza B virus RNA segment 7 (Horvath *et al.*, 1990), a mechanism that appears to be shared with CHV2 (Hillman *et al.*, 1994). In addition to the full-length genome, small internally deleted and defective interfering-like RNAs are detected in infected mycelia (Shapira *et al.*, 1991a) and discussed in Section IX.

CHV1 RNA replication is likely to occur in cytoplasmic vesicles composed of host-derived lipid membranous layers (Hansen *et al.*, 1985; Newhouse *et al.*, 1983, 1990), other host components, and virus-encoded replicase proteins. The vesicles are specifically produced in infected fungal cells, often surrounded by rough endoplasmic reticulum (ER) (Newhouse *et al.*, 1983), and encapsulate viral dsRNA. As demonstrated biochemically by Fahima *et al.* (1993), purified infection-specific vesicles are active in the synthesis of both plus-sense (transcription) and minus-sense (replication) viral RNA strands. Given the evolutionary relatedness between hypoviruses and positive-stranded RNA potyviruses (Choi *et al.*, 1991a; Koonin *et al.*, 1991), it was of interest to examine the relative accumulation of positive- and negative-stranded RNA. Fahima *et al.* (1993) reported that vesicles isolated from CHV1/EP713-infected mycelia produced both full-length positive- and negative-strand RNAs at ratios of between 2 and 8, which is consistent with the value (2 to 4) estimated for the *in vivo* accumulation using real-time PCR (Suzuki and Nuss, 2002). Thus, the positive- to negative-stranded RNA ratios observed for hypoviruses both *in vitro* and *in vivo* are much lower than the values of 20 to 75 generally accepted for a productive infection by positive-stranded RNA viruses that are phylogenetically similar to CHV1 (Baltimore, 1969; Tam and Messner, 1999). The persistent nature of hypovirus infections and the absence of a capsid protein may contribute to the lower positive-to-negative-stranded ratio, consistent with findings from other positive-strand RNA viruses.

B. 5'- and 3'-Noncoding Sequences of CHV1

Early in its characterization, the CHV1/EP713 genome was recognized to contain extensive 5'- and 3'-noncoding regions (Rae *et al.*, 1989). The 3'-noncoding region remains uncharacterized in terms of structure–function relationships. The 495-residue 5'-noncoding region contains seven AUG codons with in-frame termination sequences shortly downstream, thus reminiscent of internal ribosome entry site (IRES) sequences identified in related picornaviruses and other viruses (reviewed in Hellen and Sarnow, 2001). Constructs containing the 5'-noncoding sequence did not result in protein products for *in vitro* translation studies, but removal of this sequence results in efficient

translation *in vitro* (Rae *et al.*, 1989). *In vivo* studies in which the 5'-noncoding region was fused to green fluorescent protein (GFP) or to β -glucuronidase (GUS) also consistently resulted in no protein expression, while similar constructs lacking this element resulted in efficient expression of the reporter genes (Foglia and Hillman, unpublished data). However, it is now known that residues 496–567, the first 72 nucleotides of ORF A, are required for viability of infectious cDNA clones (Section VI.C), leading to conjecture that these constitute part of an IRES. Many such elements are now known to extend into adjacent ORFs (reviewed in Lu and Wimmer, 1996), consistent with results for CHV1. The other hypovirus terminal elements differ in length (Fig. 3), but all examined thus far contain three or more minicistrons and appear to be IRES elements.

C. Coding Sequences of CHV1

1. Multifunctional Papain-like Cystein Proteinase, p29

Like the similar HC-Pro of plant-infecting potyviruses, CHV1/EP713 p29 contains at least three functional domains and has a variety of effects on virus–host interactions. Functions assigned to p29 thus far include virus viability, autoproteolysis, suppression of host processes (e.g., laccase production, pigmentation, conidiation, elevation of virus RNA replication, and vertical transmission of virus through conidia). The 72 nucleotide coding sequence at the 5'-end of the p29 gene is essential for virus viability and has been conjectured to be part of the IRES element already discussed (Suzuki *et al.*, 2000), whereas the rest of the p29 coding domain is dispensable for virus replication (Craven *et al.*, 1993). The region adjacent to the N-terminal essential domain, Gly²⁵ through Gln⁷³, is involved in symptom expression as well as in virus replication and transmission. The C-terminal half of p29 contains the catalytic Cys¹⁶² and His²¹⁵ residues required for cotranslational self-cleavage from the precursor polyprotein p69 (Choi *et al.*, 1991a,b).

A variety of studies have been done to show that expression of p29 *in cis* or *in trans* leads to reduced sporulation and pigmentation and enhancement of viral RNA accumulation and transmission through conidia. Before the availability of infectious cDNA constructs to examine CHV1, *C. parasitica* was transformed with cDNA constructs expressing individual viral proteins. Such studies led to the finding that p29 proteolytic processing occurred *in vivo* and that p29 alone suppressed pigmentation and asexual sporulation even in the absence of

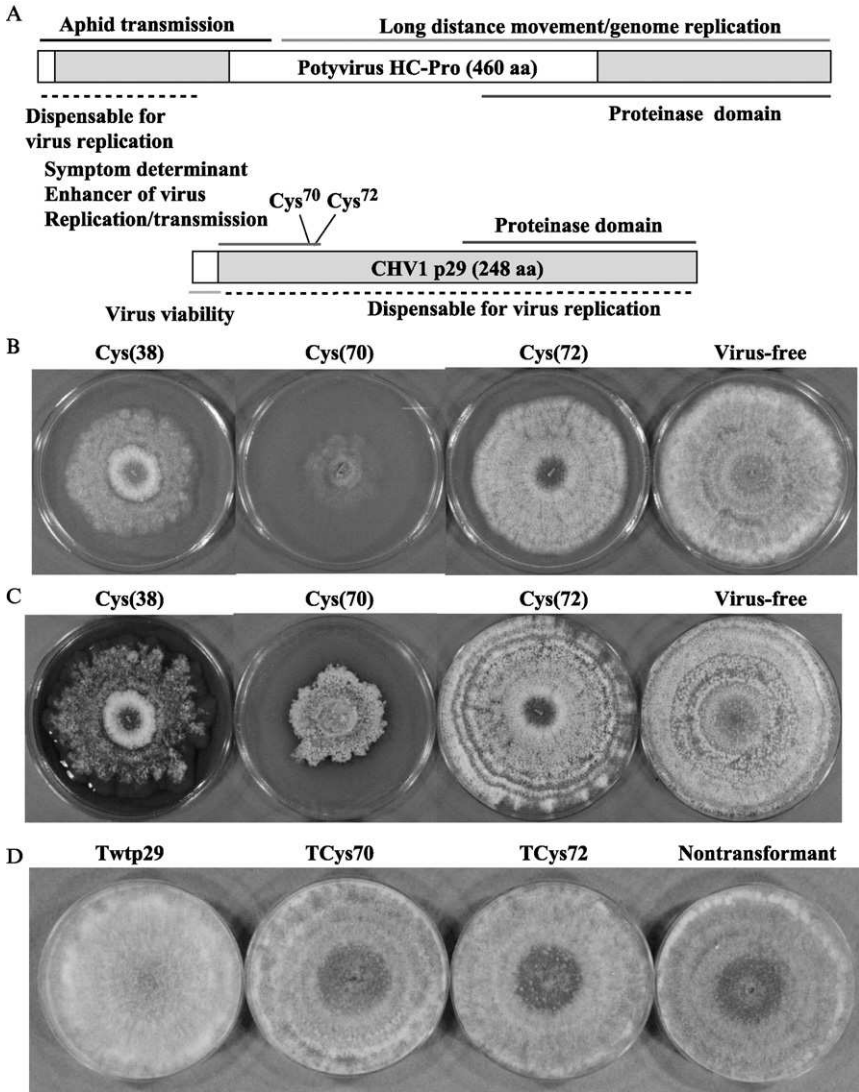


FIG 6. Comparison of CHV1 p29 and potyviral HC-Pro and effects of p29 site-directed mutations on colony morphology. (A) Functional domains of CHV1 p29 and potyviral HC-Pro (Kasschau *et al.*, 1997; Kasschau and Carrington, 2001). Pale boxes represent corresponding regions that share amino acid (aa) sequence similarity (Koonin *et al.*, 1991). (B) Phenotypic characters resulting from p29 cysteine mutants at 1 week following transfection. (C) Same phenotypic characters 1 month following transfection. Virus-free EP155 spheroplasts were transfected with RNA transcripts derived from Cys(38),

active virus infection (Choi and Nuss, 1992b; Craven *et al.*, 1993). Craven *et al.* (1993) demonstrated that the ability of p29 to modify the fungal phenotype required release from a larger polyprotein but did not require its intrinsic papain-like proteolytic activity. Deletion of p29 as well as the C-terminal portion of ORF A, p40, resulted in some reduction in viral RNA and virus transmission through asexual spores, and these functions can be complemented in Δ p29 mutants by expression of p29 *in trans* (Suzuki and Nuss, 2002; Suzuki *et al.*, 2003). Using a series of p29 deletion mutants, Suzuki *et al.* (1999) showed that the N-terminal region from Gly²⁵ through Gln⁷³ is a symptom determinant responsible for suppression of pigmentation and conidiation through *in cis* activity. This region contains four cysteine residues that are conserved among p29 homologues of all CHV1 strains examined to date as well as in potyviral HC-Pro. Two of the four residues, Cys⁷⁰ and Cys⁷², played pivotal roles in the ability of p29 to act as a symptom determinant in the context of infectious viral cDNA clones (Suzuki *et al.*, 1999) (Fig. 6) as well as in Δ p40 backgrounds (Suzuki and Nuss, unpublished). In these experiments, recombinant virus with Cys⁷⁰→Gly resulted in greatly distorted colony morphology and reduced colony growth on solid PDA media as well as in liquid PDB media. After prolonged growth, colonies infected with Cys⁷⁰→Gly mutants sporulated profusely, in contrast to their wild-type (wt) counterparts (Fig. 6C). In contrast, infection with recombinant virus in which Gly was substituted for Cys⁷² resulted in colony morphologies that were indistinguishable from the Δ p29 virus-infected strains (Fig. 6C). Mutation at residues 70 and 72 also abolished the *in trans* activity of p29 to alter phenotypic characters. That is, transformants (TCys70, TCys72) with the coding domains for mutant p29 containing Cys⁷⁰→Gly or Cys⁷²→Gly showed the same phenotype as nontransformants (Fig. 6D) in the presence or absence of virus replication. Results of combined transformation and transfection studies with mutant p29 proteins showed that its ability to suppress pigmentation and asexual sporulation is linked to its ability to elevate virus replication and transmission, and Cys⁷⁰ and Cys⁷² within the symptom determinant, Phe²⁵-Gln⁷³, are very likely to be responsible for all of the *in cis* and



Cys(70), and Cys(72) mutant viral cDNAs that have Cys-to-Gly substitutions at p29 positions Cys³⁸, Cys⁷⁰, and Cys⁷², respectively. Colonies infected with Cys(38) and Cys(72) are indistinguishable from colonies infected with wild-type and Δ p29 viruses. (D) Cultures of EP155 that are 1 week old and transformed with only the coding sequences of wild-type (Twtp29), p29Cys70 (TCys70), and p29Cys72 (TCys72) are shown.

in trans activities assigned to p29. Mutation at Cys⁷² results in defects for all the actions of wild-type p29, whereas mutant p29 with Cys⁷⁰→Gly has a qualitatively different role in symptom expression and viral RNA accumulation when expressed *in cis*.

Although the p29 protein of CHV1 negatively impacts its own ecological fitness by depressing sporulation, it paradoxically would appear to increase its fitness by elevating transmission frequency on a per spore basis under laboratory conditions. Such transmission would clearly have a major impact on the overall ecology and fitness of host and virus. Of course, this would have practical impact on these viruses as biocontrol agents. Rate of virus transmission through conidia depends on combinations of virus strains, fungal host strains, and, when grown *in vitro*, culture conditions (Elliston, 1985; Enebak *et al.*, 1994b). One of the unknown factors is the extent to which the tree host—the natural substrate for the fungus—affects virus transmission. Transmission efficiency of CHV1/EP713 is 5% for *C. radicalis* and 86% for *C. havanensis* under moderate light conditions, but 100 and 66% for the same virus–host combinations under high light conditions (Chen *et al.*, 1996a). Peever *et al.* (2000) found that the rate for different CHV1/*C. parasitica* combinations varied in a small range from 95 to 100%. Further studies are required to determine whether virus-encoded protein-mediated to enhancement of virus transmission is seen for other hypovirus–host combinations and what host and other viral factors affect transmission.

Parallels between CHV1 p29 and potyviral HC-Pro (Fig. 6A), the first identified viral suppressor of a cellular post-transcriptional gene silencing (PTGS) antiviral defense response (Anandalakshmi *et al.*, 1998; Kasschau and Carrington, 1998), are noteworthy. These include (i) moderate levels of amino acid sequence similarities, including the conserved N-terminal cysteines and papain-like protease catalytic and cleavage domains (Choi *et al.*, 1991a; Koonin *et al.*, 1991); (ii) functional roles in viral replication processes and symptom expression (Suzuki and Nuss, 2002; Suzuki *et al.*, 2003); and (iii) the ability to alter host developmental processes when expressed in the absence of virus infection (Anandalakshmi *et al.*, 2000; Craven *et al.*, 1993; Suzuki *et al.*, 2003). These lead to a prediction that p29 exerts its multifunctional role through suppression of a host PTGS antiviral defense response, just as many of the functional roles assigned to HC-Pro in viral genome amplification, vascular virus movement, and symptom severity rely on HC-Pro-mediated suppression of PTGS (Kasschau and Carrington, 1998).

2. A Basic Protein, p40, Derived from the C-Terminal Portion of p69

The highly basic nature of p40 ($pK_a = 11.96$) and conservation between CHV1 and CHV2 (Hillman *et al.*, 1994) suggested an essential role of this protein in viral RNA binding or replication. Detailed examination of the roles of the ORF was made possible by the surprising observation that the ORF was dispensable for virus replication (Suzuki *et al.*, 2000). Deletion of the p40 coding domain was accompanied by significant reduction in viral RNA accumulation and vertical transmission. Gain of function analysis was used to map the p40 functional domain to a region extending from Thr²⁸⁸ to Arg³¹². The severity of virus-mediated phenotypic suppression by p40 deletion and gain of function mutants was directly related to the accumulation of viral RNA. Deletion of p40 had little effect on virus-mediated hypovirulence, but virus-mediated suppression of several other host processes was significantly affected (Suzuki *et al.*, 2000).

The phenotypic consequences of p40 deletion are strikingly similar to those reported for deletion of p29 but with several distinctions. For example, deletion of p29 causes a reduction in the level of virus-mediated suppression of laccase activity (Craven *et al.*, 1993), while deletion of p40 does not (Suzuki and Nuss, 2002). Deletion of p29 also showed greater effect on sporulation and viral replication (Suzuki and Nuss, 2002). The similarities to potyviral HC-Pro already noted for p29 have not been identified in p40 (Suzuki and Nuss, 2002; Suzuki *et al.*, 1999).

Unlike p29, p40 does not function *in trans* as a symptom determinant or to enhance RNA accumulation. Protein p29 is likely to alter host phenotype directly through action of the protein on host factors and indirectly by contributing to viral RNA accumulation (Section VI.C.1). In contrast, p40 appears to act indirectly through its accessory role in amplifying viral RNA in a highly *cis*-preferential fashion. It was proposed that p40 promotes expression of ORF B by facilitating ribosome termination and reinitiation at the UAAUG pentanucleotide that contains the ORF A/ORF B boundary (Shapira *et al.*, 1991b). This hypothesis was supported by the finding that all *in vitro* engineered deletion mutants of CHV1 that lacked p40 activity underwent compensatory mutations that converted the genome organization from dicistronic to monocistronic (Suzuki and Nuss, 2002). Conversion to the monocistronic configuration would increase ORF B expression and, consequently, promote replication efficiency. Monocistronic progeny viruses have never been recovered from dicistronic mutant viruses that contained the p40 activity domain, suggesting that conversion to

a monocistronic configuration provides no advantage, or is even deleterious, in the context of the p40 activity domain.

The four species of the family *Hypoviridae* differ in organization (Hillman *et al.*, 2000) (Fig. 3). CHV1 and CHV2 viruses, which have the dicistronic ORF A/ORF B genome architecture, both encode p40 homologues. In contrast, CHV3 and CHV4 viruses, which have monocistronic genomes, lack the p40 counterpart. These combined observations have led to the suggestion that p40 functions *in cis*, perhaps contranationally, to enhance ORF B expression and thereby viral RNA replication by facilitating ribosome termination/reinitiation at the UAAUG pentanucleotide and ORF A/ORF B junction (Suzuki *et al.*, 2003).

3. ORF B Domains

Although ORF B of CHV1 occupies more than 2/3 of the coding region on the viral genome, surprisingly little is known about its expression and regulation. Like picornaviruses, plant potyviruses replicate to high titers and have a single ORF whose individual genes are expressed exclusively via proteolytic processing *in cis* or *in trans*. Therefore, all gene products accumulate in equimolar amounts regardless of their genomic positions. Because of high levels of expression, proteolytic processing has been relatively straightforward to study *in vitro* as well as *in vivo*, leading to a clear understanding of potyvirus gene expression strategies (reviewed in Dougherty and Semler, 1993; Reichmann *et al.*, 1992). Although the RNA polymerase and helicase domains were identified shortly after the CHV1/EP713 genome was sequenced (Koonin *et al.*, 1991; Shapira *et al.*, 1991b), only the N-terminal p48 was shown to be cleaved from the rest of the polyprotein (Shapira and Nuss, 1991). Using antibodies raised against recombinant protein representing the core RNA polymerase domain, Fahima *et al.* (1993, 1994) identified an 87-kDa protein that copurified with viral dsRNA-containing vesicles and with polymerase activity. No potential cleavage sites, however, were identified, and to our knowledge there have been no further reports of cleavage sites downstream from the p48 cleavage site.

Insights into CHV1 ORF B domains involved in symptom expression were gained through recombination experiments using two viral strains with over 90% overall amino acid sequence identity, a different approach than those used for functional analysis of p29 and p40 (Chen and Nuss, 1999; Chen *et al.*, 2000). The more severe strain of CHV1/EP713 and mild strain of CHV1/Euro7 were originally isolated from superficial cankers in southern France in 1966 and in northern Italy in 1977, respectively. Although both strains reduced orange pigmentation,

CHV1/Euro7 caused less severe phenotypic alterations than CHV1/EP713. Colonies infected with the CHV1/Euro7 grew slightly faster on solid synthetic medium than corresponding virus-free strains (Chen and Nuss, 1999), while CHV1/EP713-infected colonies grew more slowly. Colonies containing CHV1/Euro7 showed moderate levels of conidial formation and virulence as well as incited cankers with a number of conidia-containing stromata, comparable to cankers caused by virus-free isogenic strains. This result contrasts with the finding that CHV1/Euro7 altered only slightly cAMP-regulated host gene expression and laccase activity (Parsley *et al.*, 2002) which contrasts with the substantial reduction by CHV1/EP713 (Chen *et al.*, 1996b).

Virus recombination experiments were performed following establishment of an infectious cDNA clone of CHV1/Euro7 as had been done with CHV1/EP713 (Chen and Nuss, 1999). When swapping the ORF A and ORF B coding domains of the two viruses, the ORF B coding domain was identified as the major contributor to phenotype. By exchanging domains within ORF B in the chimeric viruses, Chen *et al.* (2000) mapped domains responsible for canker size (2363–5310) and pustule formation on dormant chestnut stems (5311–9904). The domain responsible for alteration of cAMP-dependent signaling (5311–9897) was also identified (Parsley *et al.*, 2002). These studies demonstrated that hypoviruses can be fine-tuned to optimize the interaction between the pathogenic fungus and its plant host and for enhanced ecological fitness.

Replication-competent ORF B deletion mutant viruses are currently unavailable, hampering further functional analysis. Of course, such experiments are ongoing to try to assign functional roles to ORF B domains. In fact, mutants lacking the ORF B proteinase, p48, in the context of Δ p40 and Δ p69 backgrounds resulted in no detectable virus RNA accumulation (Suzuki and Nuss, unpublished data). Furthermore, ORF A-engineered replication-competent vector constructs with heterologous inserts upstream of the p48 coding domain underwent deletion of foreign inserts by 9 weeks post-transfection, but these deletions never included the p48 coding region (ORF B polyprotein). Introduction of foreign genes into viral genomes often leads to deletion of neighboring dispensable viral sequences as well as foreign sequences (Dolja *et al.*, 1993; Rabindran and Dawson, 2001). This was not the case for CHV1 recombinants, suggesting that p48 is essential. Elucidation of ORF B polyprotein processing should provide target candidates for analyses with recombinant viruses and transgenic fungal isolates.

VII. HOST GENES AND SIGNALING PATHWAYS AFFECTED BY CHV1 INFECTION

Hypoviruses initiate persistent rather than acute infections of their fungal hosts, and, thus, some of the complications inherent in acute virus–host defense responses can be avoided by their study (Nuss, 1996). In addition to the reverse genetics systems described previously, the robust transformation protocol available for the host fungus (Churchill *et al.*, 1990) allows for foreign gene expression (Choi and Nuss, 1992b) or targeted disruption of endogenous genes by homologous recombination-mediated gene replacement (Gao and Nuss, 1996; Zhang *et al.*, 1993). A recent milestone was the establishment of an EST library of host genes and its use in microarray analysis to study regulatory pathways underlying virus–host interactions in a moderate throughput manner (Allen, 2003; Dawe *et al.*, 2003). Initial identification of specific host genes and/or key signaling cascades that were perturbed by CHV1 was reviewed by Nuss (1996) and more recently by Dawe and Nuss (2001).

With the conventional Northern blot approach, several genes were reported to respond to CHV1 infection. The Mat-2 mating type pheromone precursor genes, *Mf2/1* and *Mf2/2* (Powell and van Alfen, 1987; Zhang *et al.*, 1998), were first shown to be reduced in mRNA accumulation, most likely causing the female fertility defect. Also shown to be down-regulated were genes responsible for enzymatic activities, such as laccase, *lac-1* (polyphenol oxidase) (Choi *et al.*, 1992; Larson *et al.*, 1992; Rigling *et al.*, 1989), and cellobiohydrolase, *cbh-1* (Kazmierczak *et al.*, 1996; Wang and Nuss, 1995). The gene for cryparin, a cell wall hydrophobin (*crp-1*), was also shown to be down-regulated by CHV1 infection (Kazmierczak *et al.*, 1996). As an extension of these studies, mRNA differential display was used by Chen *et al.* (1996b) to identify over 400 RT-PCR products either up-(296 products) or down-regulated (127 products) by virus infection. Among the 296 PCR amplicons, product 13-1, whose function is unknown, has been used in a promoter-GFP reporter construct to monitor perturbation of the cAMP-mediated signaling (Parsley *et al.*, 2002). Kang *et al.* (2000) used a similar differential display approach to estimate that 20% of the total host genes are affected by CHV1 infection.

These studies were followed recently by moderate-throughput studies aimed at examining a larger subset of genes. Dawe *et al.* (2003) developed a *C. parasitica* EST library/database by compiling 4,200 sequence files and cataloging 2,200 unique genes. The database covers approximately 20 to 25% of total *C. parasitica* genes, assuming that

the total number of *C. parasitica* genes is similar to the 10,082 predicted for closely related *Neurospora crassa* (Galagan *et al.*, 2003). Function assignment by simple database search using BLASTX analysis and subsequent classification according to molecular function and biologic process showed that these genes broadly represent the entire population of expressed genes of *C. parasitica*. The EST collection was used for microarray analysis to identify a number of genes up- or down-regulated by infection with CHV1/EP713 (Allen, 2003). Of the 295 genes (13% of the total genes deposited with the library), 132 were increased and 163 were decreased in abundance. Genes whose expression was constitutively up-regulated included stress response genes, such as homologues of HSP70 and glutathione-S-transferase (GST), and transmethylation-involved genes, such as S-adenosyl-L-methionine synthetase and S-adenosyl-L-homocysteine hydrolase. Examples of down-regulated genes included three transcriptional regulatory factors. Functional roles of these genes in virus replication, symptom expression, antihost defense response of CHV1, fungal host defense against CHV1 infection, and fungal pathogenicity warrant further investigation. This system is now well poised for exploration of transcriptional profiles during infection with the different viruses described later in this chapter (Sections VIII, X).

Based on the pleiotropic effects of CHV1 infection, a link between CHV1 infection and the heterotrimeric G protein signaling pathway was proposed (Dawe and Nuss, 2001). This pathway is prevalent in eukaryotic cells and plays essential roles in perception of smell, taste, and light; cell growth and differentiation; embryogenesis; and development in response to extracellular stimuli (Gutkind, 1998). The current working model is that CHV1 causes reduced accumulation of a Gi- α subunit (which possesses inhibitory activities on adenylylcyclase activity). CPG-1, one of the three G protein α subunits identified in the organism, partially neutralizes inhibitory effects by CPG-1 on adenylylcyclase and elevates cAMP levels in mycelia, which then leads to alterations in transcription profiles and macroscopic colony phenotype. Supporting this model are the following observations: (i) CPG-1 is decreased post-translationally in CHV1-infected cells (Choi *et al.*, 1995); (ii) disruption of *cpg-1* partially mimics the CHV1-infected phenotype (Gao and Nuss, 1996); (iii) about 65% of genes affected by CHV1 infection behave similarly in fungal strains with *cpg-1* cosuppressed (Chen *et al.*, 1996b); and (iv) cAMP, a second messenger of the G protein signaling cascade, is increased in fungal colonies infected with CHV1, such as in colonies cosuppressed for *cpg-1* (Chen *et al.*, 1996b).

The G protein-linked signal pathways have been shown to play pivotal roles in the virulence of phytopathogenic fungi (e.g., in *Ustilago*, *Magnaporthe*, and *Fusarium*) (Lengeler *et al.*, 2000). Functional analyses of other G protein signal transduction-associated proteins of *C. parasitica*, such as the two other G protein α subunits of CPG-2 and CPG-3 (Choi *et al.*, 1995; Parsley *et al.*, 2003), a beta subunit CPGB-1 (Kasahara and Nuss, 1997), and a BDM-1 related to the mammalian phosducin (Kasahara *et al.*, 2000), should contribute to the picture of the G protein's perturbation by CHV1 and elucidation of the pathogenicity of other fungi.

CHV1 also disturbs the IP₃-calcium signaling second messenger system, which positively regulates transcription of *lac-1* to reduce lacase accumulation in the host (Larson *et al.*, 1992). The IP₃-calcium pathway is assumed to be linked upstream to the CPG-1 cascade. Reduction in CPG-1 by CHV1 infection may elevate cAMP levels, activate cAMP-dependent protein kinase, and then inhibit the activities of the effector, phospholipase C, which thus impairs IP₃ generation and Ca₂ mobilization (Gao and Nuss, 1996).

The mitogen activated protein (MAP) kinase cascade is another key regulatory pathway highly conserved in eukaryotic cells. In response to external stimuli, this pathway governs a wide range of biologic processes, such as mating and pseudohyphal growth in yeast, fungal pathogenicity, cell division and differentiation, and apoptosis in mammalian cells. Recently Kim and coworkers characterized two MAP kinase genes of *C. parasitica*: *cpmk-1* (Park *et al.*, 2003) and *cpmk-2* (Jung *et al.*, 2003). The genes *cpmk-1* and *cpmk-2* showed highest sequence identities to *osm-1* and *pmk-1* from the rice blast fungus, *Magnaporthe grisea*. The OSM-1 regulates cellular turgor during hyperosmotic stress but not during appressorium-mediated plant infection (Dixon *et al.*, 1999), while PMK-1 is essential for appressorium formation and infectious hyphae growth. Intriguingly, the CpMK-1 pathway is affected by CHV1 infection particularly in hyperosmotic conditions. Disruption of *cpmk-1* results in a phenotype with a subset of hypovirulence-associated traits, including partial reduction in virulence. These observations suggest that in addition to the G protein signaling pathway, the MAP kinase regulatory cascade is involved in CHV1 symptom expression. It remains unclear whether the two signal transduction pathways independently contribute to the virus-mediated alterations in host phenotype and transcript profile or if there is cross talk between them.

The second MAP kinase pathway, CpMK-2, is not affected by infection with CHV1 (Jung *et al.*, 2003). The *cpmk-2*-null mutant strains

manifest almost all the phenotypic alterations shown by the *cpg-1* disruptant. These results suggest that the MAP kinase and G protein signaling pathways may be interconnected in *C. parasitica*, as has been shown for other organisms (Gutkind, 1998; Lengeler *et al.*, 2000).

A Ser/Thr protein kinase CpPK-1 that was up-regulated by CHV1 infection was recently characterized by Kim *et al.* (2002). The transgenically increased expression of *cppk-1* resulted in a subset of hypovirulence-associated traits such as repressed pigmentation, suppressed conidiation, and female sterility, which are accompanied by a reduction of the pheromone genes *Mf2/1* and *Mf2/2*. These results suggest that up-regulation of the CpPK-1-associated signaling pathway in response to CHV1 infection causes alterations in the host transcriptional profile and phenotypic characters.

Broad questions concerning CHV1-affected signaling pathways include: (i) which viral factor(s) interfere with the signaling pathways? (ii) with what do those viral factors interact? (iii) how and at which step do the key signal transduction cascades interplay? Unraveling secondary transcriptional regulation will also be an interesting future challenge.

VIII. OTHER *CRYPHONECTRIA* HYPOVIRUSES

A. CHV2

Cryphonectria hypovirus 2 (CHV2) was the second hypovirus completely characterized and formally named but was not the second one identified. In 1988, Peter Bedker, a forest pathologist from Rutgers University, isolated several *C. parasitica* cultures from a population of American chestnut in eastern New Jersey. Among the cultures were several that were morphologically distinct from their virulent counterparts. These isolates were brown, had slow growing mycelium that was distinctly thin, and were extremely debilitated when inoculated to chestnut stems (Bedker, 1989; Chung *et al.*, 1994; Hillman *et al.*, 1992). In fact, when tested against other hypovirulent isolates, these were equally or more debilitated than any tested up to that time. The hypovirulent isolates from New Jersey were also morphologically distinguishable from other hypovirulent cultures, including others identified in North America (Fulbright *et al.*, 1983) (Section VIII.B).

The dsRNA isolated from the brown, hypovirulent cultures from New Jersey was resolved as a single gel band of about 12 kb, a similar size to the genomic dsRNA of CHV1 but without the smaller defective

RNAs normally present in CHV1-infected cultures (Hillman *et al.*, 1992). Hybridization analysis with dsRNA and a series of cDNA clones representing the CHV2/NB58 genome was used to examine the relationships between CHV2 and other hypovirulence-associated viruses (Hillman *et al.*, 1992). Several clones representing the 3'-proximal portion of the CHV2 genome hybridized to CHV1 dsRNA, but no hybridization was observed on the 5'-proximal half, and no other heterologous dsRNA hybridized. This suggested that CHV1 and 2 were fairly closely related and that the 3'-proximal half of the genome was more conserved than the 5'-proximal half. Sequence and translation analysis of the CHV2 genome showed that it was similar in many respects to the CHV1 genome, with the conserved RNA polymerase and helicase domains residing on the 3'-proximal half and these sequences being easily aligned. However, the 5'-proximal sequences were much more difficult or impossible to align, and CHV2 lacked the ORF A proteinase, one of the two papain-like protease paralogues present in CHV1. It was demonstrated, however, that the ORF B proteinase of CHV2 is functional (Hillman *et al.*, 1994) (Fig. 3). The brown phenotype of CHV2 and absence of an ORF A proteinase homologue was consistent with the evidence that expression of the ORF A proteinase of CHV1/EP713 alone as a nuclear gene in transgenic, virus-free isolates results in a white phenotype reminiscent of the infected culture. A cystein-rich region similar to that in CHV1 was identified at the N terminus of the CHV2 ORF A protein, p50, with the remainder occupied by a basic domain homologous to CHV1 p40. Thus, CHV2 ORF A is substantially similar in molecular terms to a natural version of functional deletion mutants identified for CHV1, and cultures infected with these viruses are also similar phenotypically (Craven *et al.*, 1993; Suzuki *et al.*, 1999).

Until the mid-1990s, the small population in New Jersey was the only place CHV2 had been identified. In a survey of Asian chestnut blight isolates, however, Peever *et al.* (1998) identified three *C. parasitica* isolates from southern China that had similar phenotypic characteristics and dsRNA that hybridized with CHV2-derived cDNA clones. These were the only isolates of more than 260 examined in that study that contained CHV2 dsRNA. Sequences of the CHV2 isolates identified in China were very similar to the U.S. isolates, indicating a close relationship between the two. Several questions were raised by these findings. (i) First why is this virus so limited in distribution? The answer here may be simply that CHV2 has very low ecological fitness. Although it sporulates more profusely than CHV1-infected isolates (Smart *et al.*, 1999), the virus is transmitted in only 2 to 5% of conidia

and not through ascospores (Hillman, unpublished data), so vertical transmission is predicted to be very poor in a natural setting. Furthermore, the extreme debilitation of *C. parasitica* isolates infected with this virus would be predicted to substantially reduce their competitiveness (ii) Second did CHV2 travel directly from China to the United States? Multiple importations of *C. parasitica* from Asia are assumed, and there are records of chestnut trees being imported into the United States since the late 1800s (Anagnostakis, 1992, 2001). It is possible that CHV2 became established only in a small, localized area proximal to the initial site of importation but failed to spread more broadly.

B. CHV3

Following up on reports of the work with transmissible hypovirulence from Connecticut, hypovirulent strains of *C. parasitica* were identified in Michigan in the early 1980s (Fulbright, 1984; Fulbright *et al.*, 1983) and later in Canada (McKeen, 1995; Melzer and Boland, 1999). The virus that came to be named CHV3/GH2 was the first of the Michigan viruses studied in detail, and it turned out to be quite different from the European viruses (Fulbright, 1990). Colony morphology of such isolates in culture was aberrant, often with lobed margins, but there was no apparent reduction in pigmentation and little reduction in sporulation or laccase activity (Durbahn, 1992, Smart *et al.*, 1999). When Don Nuss began to turn his attention from *Wound tumor virus* to hypovirulence-associated viruses in the mid-1980s, the first subject of his studies was CHV3/GH2. Shortly after publication of the study demonstrating the complexity of the CHV3/GH2 genome (Tartaglia *et al.*, 1986), Nuss's lab group began focusing on CHV1 for the reasons mentioned earlier: that is, CHV1 is a much more tractable virus system. Chris Smart did much of the initial molecular characterization of the CHV3/GH2 genome with Fulbright and Nuss (Durbahn, 1992), and it was completed in the Hillman laboratory (Hillman *et al.*, 2000; Smart *et al.*, 1999; Yuan, 1999; Yuan and Hillman, 2001).

Characterization of the CHV3 genome revealed the surprising finding of a single ORF rather than two, as had been found in CHV1 and 2 (Smart *et al.*, 1999) (Fig. 3). Examination of the N-terminal sequence of the single ORF showed the presence of a homologue of the CHV1 p29 proteinase, the only proteinase predicted on the CHV3 sequence. By *in vitro* translation, the predicted 32-kD protein was shown to cleave autoproteolytically, and the cleavage site was mapped by mutagenesis (Yuan and Hillman, 2001). Studies of ORF B with

recombinant CHV1 viruses previously described help shed light on the biology of CHV3. At least some functional difference between CHV1 p29 and CHV3 p32 is indicated by the different phenotypes elicited by the two proteins. CHV3-infected cultures do not show the great reduction in pigment production sporulation associated with CHV1 and p29 (Smart *et al.*, 1999). The activity of p32 has not been examined using recombinant virus or transformation.

C. CHV4

The first indication that there was a CHV species distinct from others that had already been characterized came from a study of dsRNA-containing isolates of *C. parasitica* from the Appalachian range in North America that showed little evidence of hypovirulence and little difference in colony morphology relative to virus-free strains (Enebak *et al.*, 1994b). A more expansive study of *C. parasitica* isolates showed that the virus in these asymptomatic isolates was prevalent throughout the natural chestnut range in North America (Peever *et al.*, 1997). This led to the subsequent characterization of the most recently described member of the Hypoviridae family, CHV4 (Linder-Basso, 2002; Linder-Basso *et al.*, submitted). Viruses in this species are most difficult to work with because they often cause no symptoms in their fungal host and because the dsRNA titer is very low; thus, large-scale experiments with large sample sizes are problematic. As relatively little molecular analysis of CHV4 has been done, many questions about this virus species remain about genome expression and specific effects on the fungal host. For example, amino acid alignments of the N-terminal domain of CHV4 that is positionally homologous to CHV1 p29 and CHV3 p32 suggest that CHV4 is also most likely a papain-like proteinase, but this is not clear from the alignments, and it has not yet been demonstrated by *in vitro* translation (Linder-Basso, 2002).

One of the intriguing features of the CHV4 genome is the presence of a glycosyltransferase domain homologue in the 5'-proximal third of the genome (Linder-Basso, 2002; Linder-Basso *et al.*, submitted). A similar region is also present at the same position of the CHV3 genome, but no such domain is present in either CHV1 or 2. It is tempting to speculate that this domain is involved with vesicle trafficking of these hypoviruses, but their function is unknown. Regardless of the function of this domain, its presence in only two of the four hypovirus species suggests that its function either is specific to CHV3 and 4 or is met in other ways in CHV1 and 2.

IX. DEFECTIVE AND SATELLITE RNAs OF HYPOVIRUSES

Defective and satellite RNAs are associated with several hypoviruses, but careful studies on their origins and biologic effects are mostly lacking. Early molecular studies revealed the presence of defective RNAs associated with CHV1 (Hiremath *et al.*, 1986, 1988) and both defective and satellite RNAs associated with CHV3 (Tartaglia *et al.*, 1986). To date, no satellite RNAs have been reported for any CHV1 isolate; however, small (<2 kb, called S-dsRNA) and large (>8 kb, called M-dsRNA) defective RNAs have been a hallmark of many CHV1 isolates (Shapira *et al.*, 1991a). Although these defective dsRNAs often segregate independently in single conidial isolates, they have not proved to be stable in continued passage or transmission experiments, and there has not been a reproducibly demonstrable effect of these defective RNAs on virus symptoms (Hillman and Nuss, 1988, unpublished data). Molecular investigation of CHV1/EP713-defective RNAs revealed that they represent heterogeneous populations (Shapira *et al.*, 1991a). The sequence breakpoints of the M-dsRNAs have not been reported, but these dsRNAs appear to contain at least the 5'-terminal 3.5 kb and the 3'-terminal 3.5 kb of the viral genome. Sequences of three clones representing S-dsRNAs of less than 0.7 kb revealed that each contain approximately 150 nucleotides of the viral 5'-terminal sequence and 450 nucleotides of the 3'-terminal sequence. All three clones were slightly different at the breakpoints, two of them containing a nontemplate sequence of unknown origin (Shapira *et al.*, 1991a). Studies with infectious transcripts of CHV1 genomic RNA appear to reinforce the conclusions from naturally infected isolates: defective RNAs are generated *de novo* following infection with genomic RNA alone, but there may be differences in the defective RNA composition among independent transfectants (Chen *et al.*, 1994; Choi and Nuss, 1992a; Suzuki, unpublished data).

In contrast to the CHV1 defective RNAs, the CHV3 defective and satellite RNAs appear to be more homogeneous and stable components. Continued subculture of CHV3/GH2, which contains one satellite and one defective RNA (Hillman *et al.*, 2000; Tartaglia *et al.*, 1986), does not appear to affect the overall dsRNA composition. Sequence analysis of these molecules has confirmed the stability of these subviral RNAs. The CHV3/GH2 defective RNA contains two discontinuities and is only 90% identical to the sequence of the genomic RNA (Fig. 7). The CHV3/GH2 defective RNA contains a continuous ORF that encodes a functional proteinase and a complete helicase domain, suggesting a mechanism for

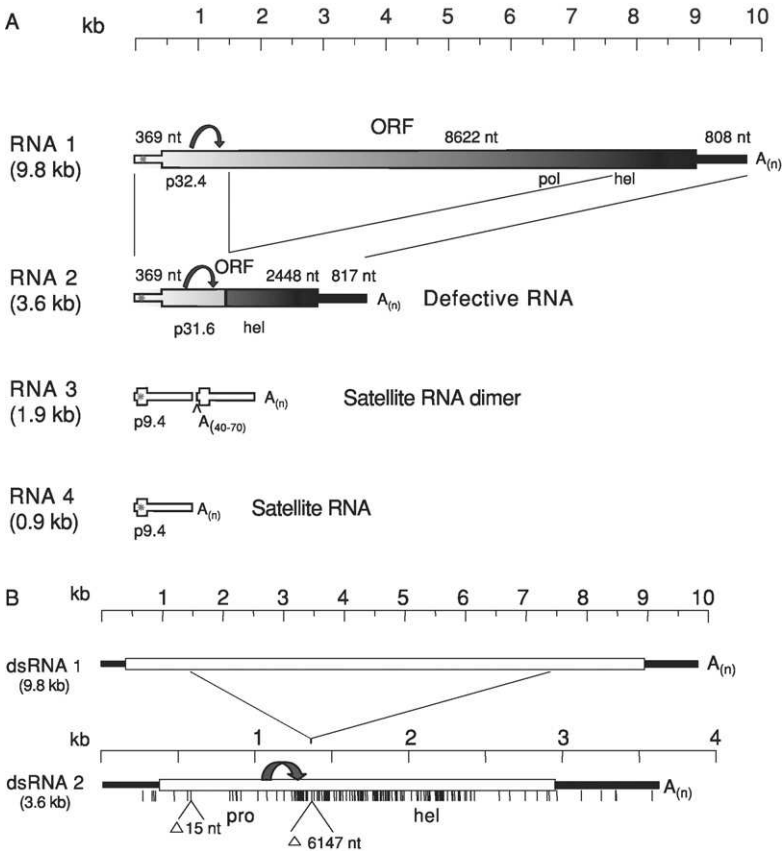


FIG 7. Genomic, satellite, and defective RNAs of CHV3/GH2. (A) Genome organizations. Arrows show proteinase cleavage sites; the light * on RNAs1–4 indicates position of sequence shared among all RNAs. (B) Distribution of nucleotide differences between genomic (upper) and defective (lower) RNAs. Redrawn from Hillman *et al.* (2000a).

its preferential amplification (Hillman *et al.*, 2000a; Yuan and Hillman, 2001).

The satellite RNA from CHV3/GH2 does not cross-hybridize with genomic or defective RNAs, but regions of sequence identity near the 5'-end suggest that it likely was derived at least in part from the CHV3 genomic RNA (Hillman *et al.*, 2000a). Similar satellites have been identified in a number of different CHV3 isolates and in some CHV4 isolates (Hillman *et al.*, 2000a; Melzer and Boland, 1999; Paul and Fulbright, 1988; Yuan and Hillman, unpublished data; Milgroom

personal communication, 2001). Two satellite RNAs from other CHV3 isolates that have been sequenced completely or partially show little difference from the CHV3/GH2 satellite sequence, indicating a common origin for these satellites (Yuan, 1999; Yuan and Hillman, unpublished data). As with the CHV1 defective RNAs, there is no indication that either the defective or satellite RNAs of CHV3 have any effect on virus symptoms; however, infectious cDNA clones are not available and critical infectivity studies have not yet been done.

X. OTHER VIRUSES OF *C. PARASITICA*

A. *Two Reoviruses*

In the early 1990s, two viruses were identified in *C. parasitica* isolates from West Virginia that had features consistent with their characterization as reoviruses: each contained 11 segments of dsRNA in approximately equimolar amounts, the dsRNA segments segregated in an all-or-none fashion in single conidial isolates, and the dsRNA segments did not cross-hybridize with each other. Particles approximately the size and appearance of reovirus cores were identified though initial purifications were poor (Enebak, 1992; Enebak *et al.*, 1994a). Initial research was performed largely on the virus from *C. parasitica* strain C-18. The virus in this isolate has proven somewhat difficult to work with because it is easily lost from culture. The reason for this is still unknown, but this loss occurs in different host backgrounds. Little work was done on these viruses for several years; when the projects were taken up again, another reovirus-containing strain from the same geographic region, 9B21, was chosen because it had a more dramatic phenotype and because the 9B21 virus was stable. The 9B21 virus was purified, and a complete cDNA library was synthesized and sequenced, confirming that it is a reovirus (Hillman *et al.*, 2004; Supyani, Hillman, and Suzuki, unpublished data) (Fig. 8).

A particularly interesting feature of the 9B21 reovirus is that it results in a phenotype that is quite distinct from the CHV1 phenotype: virulence is reduced substantially, but pigmentation and sporulation are reduced little if at all (Hillman *et al.*, 2004). Interestingly, purified particles from infected cultures were also infectious when introduced to protoplasts of *C. parasitica* isolates of different genetic backgrounds (Hillman *et al.*, 2004), a property unusual among fungal viruses. The complete 26-kb sequence of the 9B21 reovirus shows that its closest relative is a similar virus recently characterized from the ascomycete

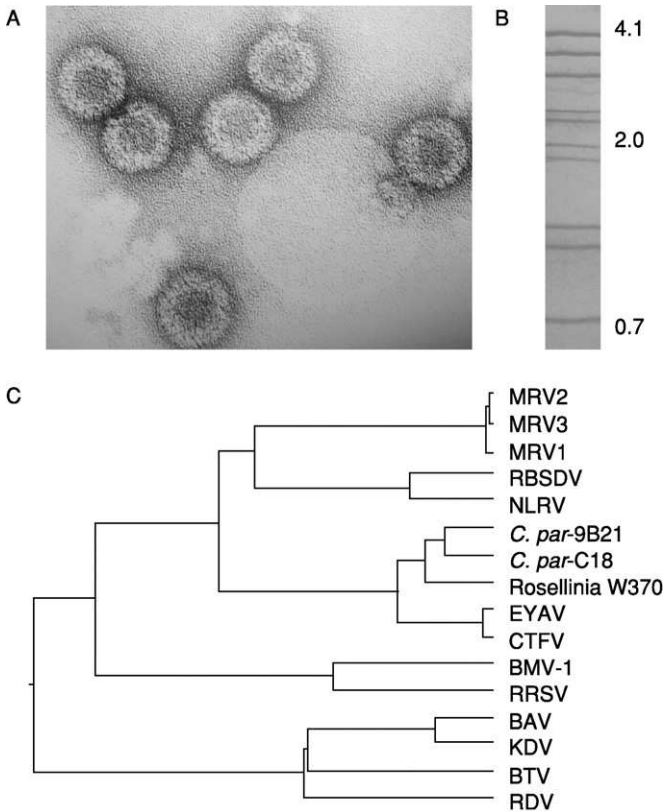


FIG 8. Properties of a *C. parasitica* reovirus. (A) Electron micrograph of particles isolated from *C. parasitica* strain 9B21 (Kondo, Hillman, and Suzuki, 2002, unpublished data). (B) The dsRNA purified from the particle-containing fraction. (C) Unrooted neighbor-joining tree of alignments performed with Clustal V of selected reovirus RNA-dependent RNA polymerase amino acid sequences. Accession numbers and abbreviations are *C. parasitica* reoviruses 9B21 (AY277888) and C18 (*C. par*-9B21 and *C. par*-C18) (Festa and Hillman, 2004, unpublished data); *Rosellinia* W370 (AB102674); *Mammalian reovirus 1* (MRV1; NC004271); *Mammalian reovirus 2* (MRV2; NC004272); *Mammalian reovirus 3* (MRV3; NC004282); *Rice Black streak dwarf virus* (RBSDV; AY144568); *Nilaparvata ligulans reovirus* (NLRV; D49693); *Bluetongue virus* (BTV; P13840); *Banna virus* (BAV; NC004211); *Kadipiro virus* (KV; NC004210); *Rice ragged stunt virus* (RRSV; NC003749); *Bombyx mori virus 1* (BMV-1; NC004138); *Rice dwarf virus* (RDV; Q02119); *Eyach virus* (EYAV; NC003696); and *Colorado tick fever virus* (CTFV; AF004181).

Rosellinia necatrix (Osaki *et al.*, 2002; Wei *et al.*, 2003) but that it is also very closely related to members of the *Coltivirus* genus of the family *Reoviridae*, which includes the tick-borne human pathogen *Colorado tick fever virus* (CTFV) (Attoui *et al.*, 2002). In fact, although

the fungal viruses will be placed in a new genus (Mertens *et al.*, in press), they are sufficiently closely related to CTFV that they likely would have been placed in the same genus were it not for the very different natures of the hosts (Fig. 8C). Excluding the virus families that contain retrotransposons, the family *Reoviridae* is now unique in having members that infect vertebrate, invertebrate, plant, and fungal hosts.

The recent continued characterization and sequencing of the C-18 virus shows that it is surprisingly distinct from the 9B21 virus. Although both viruses have 11 segments of dsRNA, the relative segment sizes in the two viruses are different (reviewed in Ghabrial, 1994, Fig. 16). Many of the homologous segments of the two viruses do not cross-hybridize, and the overall degree of nucleotide sequence identity of the two viruses appears to be less than 50% (Festa and Hillman, 2004, unpublished data). Thus, although the two viruses were isolated only 20 miles apart from each other, they are much more distantly related than, for example, *Mammalian reovirus* 1, 2, and 3 are from each other (Mertens *et al.*, 2000). Other properties of the two viruses are similar, including particle infectivity, but there are significant differences in details.

The fungal reoviruses will doubtless prove to be excellent models for reovirus host/pathogen interactions. Although the same obstacles will be faced in the production of infectious cDNA clones as have been faced with other reoviruses, the rapid growth cycle and ease of transformation of the host coupled with the ability to introduce the viruses easily by transfection give considerable advantage to these viruses as targets for study.

B. Mitochondrial Viruses: The Narnaviridae

In the examination of *C. parasitica* isolates from American chestnut in New Jersey, U.S.A., a very small (<3 kb) dsRNA was identified. The isolate bearing this small dsRNA, designated NB631, was mildly debilitated, growing slightly more slowly and causing slightly less disease than dsRNA-free strains from the same area. Cloning and sequencing of the dsRNA revealed that an ORF could be deduced only if mitochondrial codon usage was invoked (i.e., assuming that UAG encodes tryptophan) (Polashock and Hillman, 1994). This suggested that the dsRNA must be mitochondrial. Although they had not been characterized in detail, the debilitating or D elements of *Ophiostoma ulmi* were known to be associated with mitochondria (Rogers *et al.*, 1987). Localization experiments confirmed that the NB631 dsRNA was

predominately in the mitochondrial fraction, and sexual crosses demonstrated that the element was maternally inherited, as would be expected for a mitochondrial element.

Transmission experiments demonstrated that, like other hypovirulence-associated dsRNAs, NB631 dsRNA was passed from infected to uninfected mycelium by anastomosis (Polashock and Hillman, 1994). With passage of the dsRNA, the mild debilitation was seen in the recipient strains. Thus, the following questions arose: is the population of mitochondria in the virus-free recipient strain replaced by infected mitochondria, or does mitochondrial fusion take place? Answers to these questions were especially important in light of the finding that senescing mitochondria could cause hypovirulence in *C. parasitica* (Baidyaroy *et al.*, 2000; Mananti *et al.*, 1993). Experiments to critically examine the effects of the dsRNA element on the fungus were not so straightforward. All of the single conidial isolates from infected isolates contained virus, so isogenic strains with and without virus could not be generated through single spore isolation (Polashock and Hillman, 1994). When virus was transmitted by hyphal fusion, the resulting recipient strains all contained mitochondria that were recombinants of the donor and recipient strains. Therefore, the mildly debilitated phenotype of NB631 could not reliably be attributed only to the virus (Polashock *et al.*, 1997). Attempts to initiate infection by transformation with DNA constructs or by transfection with RNA generated from cDNA clones have not been successful (Polashock and Hillman, unpublished data).

A new virus family, the *Narnaviridae* was described to accommodate the NB631 virus, *Ophiostoma* mitochondrial viruses, and related yeast viruses. The yeast viruses are found in the cytoplasm rather than in mitochondria and were placed in the genus *Narnavirus*, whereas the mitochondrial viruses such as the NB631 virus were placed in the *Mitovirus* genus (Wickner *et al.*, 2000). The genus now includes five species and five tentative species (Buck *et al.*, in press). The *C. parasitica* virus has been designated *Cryphonectria mitovirus* 1/NB631 (CMV1/NB631). Genome organizations, relationships, and selected properties of some of the RdRp supergroup 2 viruses related to CMV1/NB631 are illustrated in Fig. 9. It is interesting that this group includes another fungal virus, *Diaporthe* RNA virus, which appears to be membrane associated (Preisig *et al.*, 2000) and includes a plant virus group with members whose replication is known to be associated with mitochondria (Weber-Lotfi *et al.*, 2002) as well as another plant virus group whose members lack a capsid protein (Murant *et al.*, 2000).

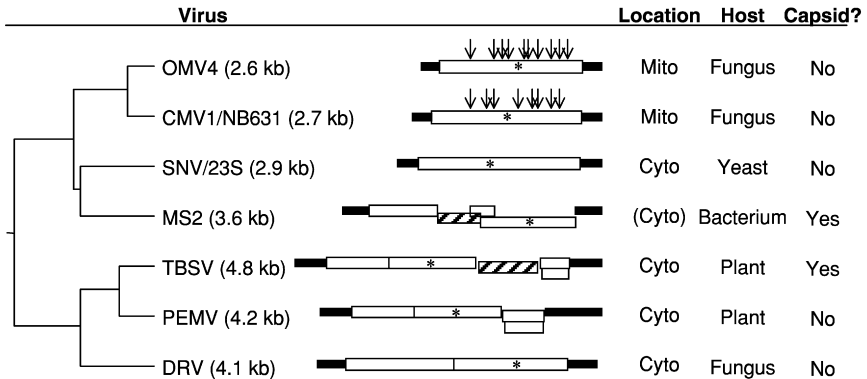


FIG 9. Properties of a *C. parasitica* mitochondrial virus CMV/NB631 (L31849; family *Narnaviridae*) compared to closely and distantly related viruses of the RdRp supergroup 2. The following is a list of abbreviation definitions and accession numbers: OMV4 (*Ophiostoma mitovirus* 4; CAB42652; family *Narnaviridae*); SNV/23S (*Saccharomyces narnavirus* 23S; NC_004050; family *Narnaviridae*); MS2 (phage MS2; NC_001417; family *Leviviridae*); TBSV *Tomato bushy stunt virus*; NC_001554; family *Tombusviridae*; PEMV (*Pea enation mosaic virus*, NC_003853; genus *Umbravirus*); DRV (*Diaporthe* RNA virus; NC_001278).

C. Partially Characterized Viruses

A number of viruses of *Cryphonectria* have been identified and partially characterized. Some of these have little or no effect on their hosts, but others are somewhat debilitating. Peever *et al.* (1998) identified two small dsRNA species in several *C. parasitica* isolates from China that suggest a virus of the *Partitiviridae* family. This virus is asymptomatic in the host, is transmitted to near 100% of conidial progeny, but is not transmitted to ascospore progeny (Hillman, unpublished data). These properties are in keeping with other members of this family of extremely simple viruses that encode only a capsid protein and RNA polymerase from their two segments (Ghabrial and Hillman, 1999).

Another virus that is asymptomatic in *Cryphonectria* contains four segments of dsRNA within isometric particles that sediment as a single peak in sucrose gradients. The virus has not been found naturally in isolates of *C. parasitica* but rather in several isolates of a new unnamed species that was found to be sympatric with *C. parasitica* in several areas of Japan. Partial sequence analysis of dsRNA isolated from virus particles from isolate OB5-11 indicates that this virus is a member of the new family *Chrysoviridae* (Dyrek and Hillman, 2002, unpublished

data). Until recently, *Chrysovirus* was a genus of the family *Partitiviridae*, but presence of four dsRNA segments that encode polypeptides and distinct RdRp sequences led to the description of the new family (Ghabrial, in press).

Finally, a virus that has a substantial effect on fungal virulence but remains poorly understood at the molecular level was identified in isolate RC1 from Michigan. Strain RC1 is deeply pigmented, slow growing, and reduced in virulence (Durbahn, 1992). Two dsRNA molecules were associated with strain RC1: one of approximately 2.8 kb and another of 1.6 kb (Fulbright, 1984; Fulbright *et al.*, 1983; Smart and Fulbright, 1995). The larger of the two was in a similar size range to the mitovirus from isolate NB631, but there is no evidence that the RC1 virus is associated with mitochondria. Furthermore, sequence analysis from a portion of the genome has revealed no significant similarity with mitoviruses (Hillman, unpublished data).

XI. POPULATION BIOLOGY AND EVOLUTION OF *CRYPHONECTRIA* VIRUSES

A. *Molecular Evolution of Hypoviruses*

Cryphonectria viruses are interesting from the standpoint of population biology and evolution of viruses. The viruses are one component of a host-parasite-parasite system; therefore, evolution of any of the three components will affect evolution of the other two. Only recently have the tools become available to examine either the fungal host or its viruses.

No thorough study of hypovirus evolution has yet been done, and many questions concerning the evolution of this group remain. In their initial description of the relationship of CHV1 to plant potyviruses, Koonin *et al.* (1991) suggested five major evolutionary steps required for evolution of a hypovirus genome from a potyvirus genome. Regardless of the genome structure of the progenitor virus, two of the five steps are pertinent to discussion of hypovirus genome evolution itself: duplication of the HC-Pro homologue and emergence of the termination codon between ORF A and B (numbers as in Koonin *et al.*, 1991). Results already described suggest that evolution of the p40 homologue and the emergence of the UAAUG termination/initiation sequence are linked evolutionary steps although it remains unclear which of the two proteinase paralogs is the progenitor and which is derived from duplication. Positive-strand RNA viruses have a propensity to recombine, and recombination among hypoviruses has been demonstrated (Carbone *et al.*, 2004; Linder-Basso, 2002; Linder-Basso *et al.*,

submitted), so it is equally plausible that the proteinase gene duplication arose by intermolecular or intramolecular recombination. The two hypovirus species found commonly in North America, CHV3 and CHV4, both have a single ORF genome structure. Interestingly, hypoviruses with single ORF genome organizations have not been identified in Asia, presumably where the fungus and hypoviruses began to coevolve, suggesting that if they exist in that location, they are not common (Milgroom, personal communication, 2003; Peever *et al.*, 1998). An interesting possibility is that, for yet unknown reasons, the single ORF viruses had selective advantage during the rapid spread of their fungal host through the North American chestnut population, but CHV1 was more fit for slow movement through the resistant chestnut population in Asia. A more prosaic explanation is that the prevalence of the different virus types in different regions simply reflects expansion of small founder populations.

B. Population Biology of Cryphonectria Viruses

C. parasitica is a fascinating system for examining evolution of a fungal virus in a rapidly moving epidemic although, in many ways, it is a *post mortem* system because the active phase of the epidemic has come and gone. Elegant work has been done on the evolution of the fungus in a similar system, the Dutch elm disease fungus, *Ophiostoma ulmi*, and *O. novo-ulmi* (Brasier, 1988, 2001; Cole *et al.*, 2000). There is considerable information on different viruses in this fungus (e.g., Hong *et al.*, 1998, 1999) although specifics of virus evolution are not yet understood.

One of the greatest problems with population studies that attempt to accurately reflect the natural evolution of *C. parasitica* viruses is that the populations in Europe and North America have been tampered with for many years. Shortly after the chestnut blight epidemic took hold in North America, efforts to determine the origin of the fungus and its relationships to similar fungi were initiated. These efforts included deliberate inoculations of trees in the wild with *C. parasitica* isolates from China (Shear and Stevens, 1917). Furthermore, in attempts aimed at biologic control, fungal strains bearing viruses that have not evolved in a given ecosystem have been introduced into new areas. Anecdotal examples of such deliberate introductions abound, particularly in the 1970s and 1980s. In North America, scientists studying hypovirulence and biologic control were often contacted by a nursery grower or homeowner for treatment of a dying American chestnut. The hypovirulent strain provided for treatment may have

contained a virus that evolved thousands of miles away. If established, such a virus serves as a reservoir of RNA for recombination with other viruses that did coevolve in that area. In some cases, such releases are well documented, but in others they are not (Anagnostakis, 1987; Anagnostakis and Waggoner, 1981; Anagnostakis *et al.*, 1998; MacDonald and Fulbright, 1991). Virus-bearing strains cultivated in North America also have been released in other countries, including China. This again serves to confound analysis of the natural population of the fungus and its viruses.

The first tools available to examine chestnut blight fungal populations were vegetative compatibility for examining the fungal isolates (Anagnostakis, 1977) and phenotype changes or dsRNA banding patterns for examining the viruses (Anagnostakis, 1981; Anagnostakis and Day, 1979; Elliston, 1985). These were blunt instruments with which to approach complex problems although they have been used to great advantage in these and later experiments (Milgroom and Cortesi, 1999; Milgroom *et al.*, 1990). Vegetative incompatibility genes segregating independently resulted in more than 100 "anastomosis groups," so even tests to determine an anastomosis group were time consuming and often difficult to interpret. In many cases, dsRNA banding patterns are not stable because of defective or satellite RNAs that may be lost or gained upon subculture and transmission.

Work on the fungal populations took a major step forward when Michael Milgroom developed fingerprinting methods to examine the *Cryphonectria* population structure (Milgroom *et al.*, 1992). These methods were applied to populations in North America, Europe, and Asia (Heiniger and Rigling, 1994; Milgroom, 1995; Milgroom and Lipari, 1995; Milgroom *et al.*, 1992). These studies indicate that the fungus was likely introduced into North America from Japan rather than China. The European fungal population is also more closely related to the Japanese population although it could not be determined whether the original introduction into Europe was from Japan or North America (Milgroom *et al.*, 1996). Unfortunately, these methods have not found application on the scale of local populations.

C. Lateral Transfer and Origins of Cryphonectria Viruses

Multiple virus introductions must have occurred in *C. parasitica*. It is unreasonable to believe that all the viruses were present at the time of speciation of the fungus and have evolved since that time. Although fungi have chitinous cell walls and vegetative incompatibility barriers

that prevent free horizontal gene flow, such horizontal transfer may occur and may be common. In a study examining transmission and evolution of CHV1 in Asia and in the laboratory, Liu *et al.* (2003) identified another *Cryphonectria* sp., as of yet unnamed, that is sympatric with *C. parasitica* and that was also infected with CHV1. Phylogenetic analysis of virus and host was used to try to distinguish among hypotheses of interspecies transmission (that the virus moved across illegitimate anastomosal connections), cospeciation (that the virus was present at the time of speciation and evolved subsequently), and ancestral polymorphism (that polymorphisms present in the virus population prior to speciation were maintained after speciation). Examination of viral sequences from two naturally CHV1-infected isolates of *Cryphonectria* sp. revealed that they were substantially different from each other and that their phylogenies did not correspond to phylogenies inferred from ITS sequence trees of the fungi, suggesting interspecies transmission as the most likely scenario. Laboratory experiments demonstrated that the virus could be transmitted by anastomosis in the same manner as it is among *C. parasitica* isolates.

Circumstantial evidence for horizontal transfer in another ascomycete system was provided in recent work with viruses of the pathogen *Sclerotinia* (Melzer *et al.*, 2002). Laboratory anastomosis experiments similar to those described above demonstrated that the virus could in some cases move from one *Sclerotinia* species to another. In a separate study, determination of the sequence of a *Sclerotinia* dsRNA showed that it was nearly identical to one of the dsRNAs in *O. novo-ulmi* (Deng *et al.*, 2003). Finally, experimental expansion of fungal host range of recombinant viruses is being demonstrated with increasing frequency (Moleleki *et al.*, 2003; Sasaki *et al.*, 2002; van Heerden *et al.*, 2001). Presumably, such relationships among fungal viruses and evidence for natural expansion of host range will become more common as more fungal virus sequences are determined.

In addition to lateral transfer from related fungi, the idea of introduction of viruses into this fungus directly from unrelated sympatric organisms, such as associated arthropods, must be considered. Several of the viruses found in *C. parasitica* have relatives with invertebrate vectors (Hillman *et al.*, 2004; Koonin *et al.*, 1991). There is no evidence for such lateral transfer across kingdoms as a recent event, but the close association of arthropods with the fungus would provide the type of environment required for such a transfer to occur (Nannelli *et al.*, 1999; Wendt *et al.*, 1983).

XII. CONCLUSIONS

The study of many isolates of *C. parasitica* from chestnut growing regions worldwide has led to the definition of this as the premier system in which to examine viruses of filamentous fungi at the molecular and population levels. A great number of isolates have been screened for dsRNA, and it is not unreasonable to presume that eight or more families of viruses will have been identified in this fungus once characterization of viruses in existing cultures is complete. This system will continue to provide great insight into eukaryotic viruses, their ecology, and details of their infection processes.

ACKNOWLEDGMENTS

The authors are grateful to Dr. Don Nuss and Dae-Hyuk Kim for sending us reprints and preprints and thank Drs. D. Nuss, D. H. Kim, Salah Bouzoubba, and Shin Kasahara for fruitful discussions. Portions of the CHV1 section were adapted from Suzuki and Nuss (2002) and Suzuki *et al.* (2003).

REFERENCES

- Allen, T. D., Dawes, A. L., and Nuss, D. L. (2003). Use of cDNA microarrays to monitor transcriptional responses of the chestnut blight fungus *Cryphonectria parasitica* to infection by virulence-attenuating hypoviruses. *Eukaryot. Cell* **2**:1253–1265.
- Anagnostakis, S. L. (1977). Vegetative incompatibility in *Endothia parasitica*. *Exper. Mycol.* **1**:306–316.
- Anagnostakis, S. L. (1979). Sexual reproduction of *Endothia parasitica* in the laboratory. *Mycologia* **71**:213–215.
- Anagnostakis, S. L. (1981). Stability of double-stranded RNA components of *Endothia parasitica* through transfer and subculture. *Exper. Mycol.* **5**:236–242.
- Anagnostakis, S. L. (1982). Biological control of chestnut blight. *Science* **215**:466–471.
- Anagnostakis, S. L. (1987). Chestnut blight: The classical problem of an introduced pathogen. *Mycologia* **79**:23–37.
- Anagnostakis, S. L. (1992). Chestnuts and the introduction of chestnut blight. *Annu. Rep. Northern Nut Growers Assoc.* **83**:39–42.
- Anagnostakis, S. L. (2001). The effects of multiple importations of pests and pathogens on a native tree. *Biol. Invasions* **3**:245–254.
- Anagnostakis, S. L., Chen, B., Geletka, L. M., and Nuss, D. L. (1998). Hypovirus transmission to ascospore progeny by field-released transgenic hypovirulent strains of *Cryphonectria parasitica*. *Phytopathology* **88**:598–604.
- Anagnostakis, S. L., and Day, P. R. (1979). Hypovirulence conversion in *Endothia parasitica*. *Phytopathology* **69**:1226–1229.
- Anagnostakis, S. L., Hau, B., and Kranz, J. (1986). Diversity of vegetative compatibility groups of *Cryphonectria parasitica* in Connecticut and Europe. *Plant Disease* **70**:536–538.

- Anagnostakis, S. L., and Kranz, J. (1987). Population dynamics of *Cryphonectria parasitica* in a mixed-hardwood forest in Connecticut. *Phytopathology* **77**:751–754.
- Anagnostakis, S. L., and Waggoner, P. E. (1981). Hypovirulence, vegetative incompatibility, and the growth of cankers of chestnut blight. *Phytopathology* **71**:1198–1202.
- Anandalakshmi, R., Marathe, R., Ge, X., Herr, J. M., Jr., Mau, C., Mallory, A., Pruss, G., Bowman, L., and Vance, V. B. (2000). A calmodulin-related protein that suppresses post-transcriptional gene silencing in plants. *Science* **290**(5489):142–144.
- Anandalakshmi, R., Pruss, G. J., Ge, X., Marathe, R., Mallory, A. C., Smith, T. H., and Vance, V. B. (1998). A viral suppressor of gene silencing in plants. *Proc. Natl. Acad. Sci. USA* **95**:13079–13084.
- Attoui, H., Mohd Jaafar, F., Biagini, P., Cantaloube, J. F., de Micco, P., Murphy, F. A., and de Lamballerie, X. (2002). Genus *Cultivirus* (family Reoviridae): Genomic and morphologic characterization of Old World and New World viruses. *Arch. Virol.* **147**:533–561.
- Baidyaroy, D., Huber, D. H., Fulbright, D. W., and Bertrand, H. (2000). Transmissible mitochondrial hypovirulence in a natural population of *Cryphonectria parasitica*. *Mol. Plant Microbe Interact.* **13**:88–95.
- Baltimore, D. (1969). The replication of picornaviruses. In “The Biochemistry of Viruses” (H. B. Levy, ed.). Marcel Dekker, New York.
- Barr, M. E. (1978). The *Diaportheales* of North America with emphasis on *Gnomonia* and its segregates. *Mycol. Mem.* **7**:1–232.
- Bedker, P. J. (1989). Hypovirulent strains of *Cryphonectria parasitica* in New Jersey. *Phytopathology* **79**:1142.
- Biraghi, A. (1951). Caratteri di resistenza in *Castanea sativa* nei confronti di *Endothia parasitica*. *Boll. Staz. Patol. Veget.* **8**:5.
- Brasier, C. M. (1988). Rapid changes in the genetic structure of epidemic populations of *Ophiostoma ulmi*. *Nature* **332**:538–541.
- Brasier, C. M. (2001). Rapid evolution of introduced plant pathogens via interspecific hybridization. *BioScience* **51**:123–133.
- Buck, K. W. (1998). Molecular variability of viruses of fungi. In “Molecular Variability of Fungal Pathogens” (P. D. Bridge, Y. Couteaudier, and J. M. Clarkson, eds.). CABI International, Wallingford, United Kingdom.
- Buck, K. W., Esteban, R., and Hillman, B. I. (In press). Narnaviridae. In “Virus Taxonomy: Eighth Report of the International Committee for the Taxonomy of Viruses” (C. M. Fauquet, J. Maniloff, M. A. Mayo, U. Desselberger, and A. Balls, eds.) Academic Press, New York.
- Carbone, I., Liu, Y.-C., Hillman, B. I., and Milgroom, M. G. (2004). Recombination and migration of *Cryphonectria hypovirus 1* as inferred from gene genealogies and the coalescent. *Genetics* **166**:1611–1629.
- Chen, B., Chen, C.-H., Bowman, B. H., and Nuss, D. L. (1996a). Phenotypic changes associated with wild-type and mutant hypovirus RNA transfection of plant pathogenic fungi phylogenetically related to *Cryphonectria parasitica*. *Phytopathology* **86**:301–310.
- Chen, B., Choi, G. H., and Nuss, D. L. (1994). Attenuation of fungal virulence by synthetic infectious hypovirus transcripts. *Science* **264**:1762–1764.
- Chen, B., Gau, S., Choi, G. H., and Nuss, D. L. (1996b). Extensive alteration of fungal gene transcript accumulation and elevation of G protein-regulated cAMP levels by a virulence-attenuating hypovirus. *Proc. Natl. Acad. Sci. USA* **93**:7996–8000.
- Chen, B., Geletka, L. M., and Nuss, D. L. (2000). Using chimeric hypoviruses to fine-tune the interaction between a pathogenic fungus and its plant host. *J. Virol.* **74**:7562–7567.

- Chen, B., and Nuss, D. L. (1999). Infectious cDNA clone of hypovirus CHV1/Euro7: A comparative virology approach to investigate virus-mediated hypovirulence of the chestnut blight fungus *Cryphonectria parasitica*. *J. Virol.* **73**:985–992.
- Choi, G. H., Chen, B., and Nuss, D. L. (1995). Virus-mediated or transgenic suppression of a G-protein alpha subunit and attenuation of fungal virulence. *Proc. Natl. Acad. Sci. USA* **92**:305–309.
- Choi, G. H., Larson, T. G., and Nuss, D. L. (1992). Molecular analysis of the laccase gene from the chestnut blight fungus and selective suppression of its expression in an isogenic hypovirulent strain. *Molec. Plant Microbe Interac.* **5**:119–128.
- Choi, G. H., and Nuss, D. L. (1992a). Hypovirulence of chestnut blight fungus conferred by an infectious viral cDNA. *Science* **257**:800–803.
- Choi, G. H., and Nuss, D. L. (1992b). A viral gene confers hypovirulence-associated traits to the chestnut blight fungus. *EMBO J.* **11**:473–477.
- Choi, G. H., Pawlyk, D. M., and Nuss, D. L. (1991a). The autocatalytic protease p29 encoded by a hypovirulence-associated virus of the chestnut blight fungus resembles the potyvirus-encoded protease HC-Pro. *Virology* **183**:747–752.
- Choi, G. H., Shapira, R., and Nuss, D. L. (1991b). Cotranslational autoproteolysis involved in gene expression from a double-stranded RNA genetic element associated with hypovirulence of the chestnut blight fungus. *Proc. Natl. Acad. Sci. USA* **88**:1167–1171.
- Chung, P. H., Bedker, P. J., and Hillman, B. I. (1994). Diversity of *Cryphonectria parasitica* hypovirulence-associated double-stranded RNAs within a chestnut population in New Jersey. *Phytopathology* **84**:984–990.
- Churchill, A. C. L., Ciuffetti, L. M., Hansen, D. R., van Etten, H. D., and van Alfen, N. K. (1990). Transformation of the fungal pathogen *Cryphonectria parasitica* with a variety of heterologous plasmids. *Curr. Genet.* **17**:25–31.
- Cole, T. E., Hong, Y., Brasier, C. M., and Buck, K. W. (2000). Detection of an RNA-dependent RNA polymerase in mitochondria from a mitovirus-infected isolate of the Dutch elm disease fungus, *Ophiostoma novo-ulmi*. *Virology* **268**:239–243.
- Cortesi, P., McCulloch, C. E., Song, H., Lin, H., and Milgroom, M. G. (2001). Genetic control of horizontal virus transmission in the chestnut blight fungus, *Cryphonectria parasitica*. *Genetics* **159**:107–118.
- Cortesi, P., Milgroom, M. G., and Bisiach, M. (1996). Distribution and diversity of vegetative compatibility types in subpopulations of *Cryphonectria parasitica* in Italy. *Mycol. Res.* **100**:1087–1093.
- Craven, M. G., Pawlyk, D. M., Choi, G. H., and Nuss, D. L. (1993). Papain-like protease p29 as a symptom determinant encoded by a hypovirulence-associated virus of the chestnut blight fungus. *J. Virol.* **67**:6513–6521.
- Dawe, A. L., McMains, V. C., Panglao, M., Kasahara, S., Chen, B., and Nuss, D. L. (2003). An ordered collection of expressed sequences from *Cryphonectria parasitica* and evidence of genomic microsynteny with *Neurospora crassa* and *Magnaporthe grisea*. *Microbiology* **149**:2373–2384.
- Dawe, A. L., and Nuss, D. L. (2001). Hypoviruses and chestnut blight: Exploiting viruses to understand and modulate fungal pathogenesis. *Annu. Rev. Genet.* **35**:1–29.
- Deng, F., Xu, R., and Boland, G. J. (2003). Hypovirulence-associated dsRNA from *Sclerotinia homeocarpon* is conspecific with *Ophiostoma novo-ulmi* mitovirus 3a-Ld. *Phytopathology* **93**:1407–1414.
- Dixon, K. P., Xu, J. R., Smirnov, N., and Talbot, N. J. (1999). Independent signaling pathways regulate cellular turgor during hyperosmotic stress and appressorium-mediated plant infection by *Magnaporthe grisea*. *Plant Cell* **11**:2045–2058.

- Dodds, J. A. (1978). Double-stranded RNAs and virus-like particles in *Endothia parasitica*. *Proc. American Chestnut Symposium*, 122 pages.
- Dodds, J. A. (1980). Association of type 1 viral-like dsRNA with club-shaped particles in hypovirulent strains of *Endothia parasitica*. *Virology* **107**:1–12.
- Dolja, V. V., Herndon, K. L., Pirone, T. P., and Carrington, J. C. (1993). Spontaneous mutagenesis of a plant potyvirus genome after insertion of a foreign gene. *J. Virol.* **67**:5968–5975.
- Dougherty, W. G., and Semler, B. L. (1993). Expression of virus-encoded proteinases: Functional and structural similarities with cellular enzymes. *Microbio. Rev.* **57**:781–822.
- Durbahn, C. M. (1992). Molecular characterization of ds RNA associated with hypovirulence in Michigan isolates of *Cryphonectria parasitica*. Ph.D. diss. Michigan State University, East Lansing.
- Elliston, J. E. (1978). Pathogenicity and sporulation of normal and diseased strains of *Endothia parasitica* in American chestnut. *Proc. American Chestnut Symposium*, 122 pages.
- Elliston, J. E. (1985). Preliminary evidence for two debilitating cytoplasmic agents in a strain of *Endothia parasitica* from western Michigan. *Phytopathology* **75**:170–173.
- Enebak, S. A. (1992). Characterization of dsRNA-containing strains of *Cryphonectria parasitica* recovered from the central Appalachian. Ph.D. diss. West Virginia University, Morgantown.
- Enebak, S. A., Hillman, B. I., and MacDonald, W. L. (1994a). A hypovirulent isolate of *Cryphonectria parasitica* with multiple genetically unique dsRNA elements. *Molec. Plant Microbe Interac.* **7**:590–595.
- Enebak, S. A., MacDonald, W. L., and Hillman, B. I. (1994b). Effect of dsRNA associated with isolates of *Cryphonectria parasitica* from the central Appalachians and their relatedness to other dsRNAs from North America and Europe. *Phytopathology* **84**:528–534.
- Fahima, T., Kazmierczak, P., Hansen, D. R., Pfeiffer, P., and van Alfen, N. K. (1993). Membrane-associated replication of an unencapsidated double-strand RNA of the fungus, *Cryphonectria parasitica*. *Virology* **195**:81–89.
- Fahima, T., Wu, Y., Zhang, L., and van Alfen, N. K. (1994). Identification of the putative RNA polymerase of *Cryphonectria* hypovirus in a solubilized replication complex. *J. Virol.* **68**:6116–6119.
- Fulbright, D. W. (1984). Effect of eliminating dsRNA in hypovirulent *Endothia parasitica*. *Phytopathology* **74**:722–724.
- Fulbright, D. W. (1990). Molecular basis for hypovirulence and its ecological relationships. In "New Directions in Biological Control" (R. Baker and P. Dunn, eds.). Alan R. Liss, New York.
- Fulbright, D. W., Weidlich, W. H., Haufler, K. Z., Thomas, C. S., and Paul, C. P. (1983). Chestnut blight and recovering American chestnut trees in Michigan. *Can. J. Bot.* **61**:3144–3171.
- Galagan, J. E., Calvo, S. E., Borkovich, K. A., Selker, E. U., Read, N. D., Jaffe, D., FitzHugh, W., Ma, L. J., Smirnov, S., Purcell, S., Rehman, B., Elkins, T., Engels, R., Wang, S., Nielsen, C. B., Butler, J., Endrizzi, M., Qui, D., Ianakiev, P., Bell-Pedersen, D., Nelson, M. A., Werner-Washburne, M., Selitrennikoff, C. P., Kinsey, J. A., Braun, E. L., Zelter, A., Schulte, U., Kothe, G. O., Jedd, G., Mewes, W., Staben, C., Marcotte, E., Greenberg, D., Roy, A., Foley, K., Naylor, J., Stange-Thomann, N., Barrett, R., Gnerre, S., Kamal, M., Kamvysselis, M., Mauceli, E., Bielke, C., Rudd, S., Frishman, D., Krystofova, S., Rasmussen, C., Metzner, R. L., Perkins, D. D., Kroken, S.,

- Cogoni, C., Macino, G., Catcheside, D., Li, W., Pratt, R. J., Osmani, S. A., DeSouza, C. P., Glass, L., Orbach, M. J., Berglund, J. A., Voelker, R., Yarden, O., Plamann, M., Seiler, S., Dunlap, J., Radford, A., Aramayo, R., Natvig, D. O., Alex, L. A., Mannhaupt, G., Ebbole, D. J., Freitag, M., Paulsen, I., Sachs, M. S., Lander, E. S., Nusbaum, C., and Birren, B. (2003). The genome sequence of the filamentous fungus *Neurospora crassa*. *Nature* **422**:859–868.
- Gao, S., and Nuss, D. L. (1996). Distinct roles for two G protein alpha subunits in fungal virulence, morphology, and reproduction revealed by targeted gene disruption. *Proc. Natl. Acad. Sci. USA* **93**:14122–14127.
- Ghabrial, S. A. (1994). New developments in fungal virology. *Adv. Virus Res.* **43**:303–338.
- Ghabrial, S. A., Chrysoviridae (In press). In “Virus Taxonomy: Eighth Report of the International Committee for the Taxonomy of Viruses” (C. M. Fauquet, J. Maniloff, M. A. Mayo, U. Desselberger, and A. Ball eds.). Academic Press, New York.
- Ghabrial, S. A., and Hillman, B. I. (1999). Partitiviruses—Fungal (Partitiviridae). In “Encyclopedia of Virology,” Vol. 2. Academic Press, New York.
- Grente, J. (1965). Les formes hypovirulentes d'*Endothia parasitica* et les espoirs de lutte contre le chancre du chataignier. *C. R. Acad. Agric. France* **51**:1033–1037.
- Grente, J., and Berthelay-Sauret, S. (1978). Biological control of chestnut blight in France. *Proc. American Chestnut Symposium*, 122 pages.
- Gutkind, J. S. (1998). The pathways connecting G protein-coupled receptors to the nucleus through divergent mitogen-activated protein kinase cascades. *J. Biol. Chem.* **273**:1839–1842.
- Hansen, D. R., van Alfen, N. K., Gillies, K., and Powell, N. A. (1985). Naked dsRNA associated with hypovirulence of *Endothia parasitica* is packaged in fungal vesicles. *J. Gen. Virol.* **66**:2605–2614.
- Heiniger, U., and Rigling, D. (1994). Biological control of chestnut blight in Europe. *Annu. Rev. Phytopathol.* **32**:581–599.
- Hellen, C. U. T., and Sarnow, P. (2001). Internal ribosome entry sites in eukaryotic mRNA molecules. *Genes Dev.* **15**:1593–1612.
- Hillman, B. I., Foglia, R., and Yuan, W. (2000a). Satellite and defective RNAs of *Cryphonectria hypovirus* 3-Grand Haven 2, a virus species in the family Hypoviridae with a single open reading frame. *Virology* **276**:181–189.
- Hillman, B. I., Fulbright, D. W., Nuss, D. L., and van Alfen, N. K. (1995). Hypoviridae. In “Sixth Report of the International Committee for the Taxonomy of Viruses” (F. A. Murphy, ed.). Springer-Verlag, New York.
- Hillman, B. I., Fulbright, D. W., Nuss, D. L., and van Alfen, N. K. (2000b). Hypoviridae. In “Virus Taxonomy: Seventh Report of the International Committee for the Taxonomy of Viruses” (M. H. V. van Regenmortel, C. M. Fauquet, D. H. L. Bishop, E. B. Carstens, M. K. Estes, S. M. Lemon, J. Maniloff, M. A. Mayo, D. J. McGeoch, C. R. Pringle, and R. B. Wickner, eds.). Academic Press, San Diego.
- Hillman, B. I., Halpern, B. T., and Brown, M. P. (1994). A viral dsRNA element of the chestnut blight fungus with a distinct genetic organization. *Virology* **201**:241–250.
- Hillman, B. I., Rae, B. P., Tartaglia, J., and Nuss, D. L. (1989). Elucidating the structure and function of double-stranded RNA genetic elements associated with biological control of chestnut blight. *Molecular Biology of Plant-Pathogen Interaction. Proceedings of the UCLA Symposium* **101**:59–70.
- Hillman, B. I., Shapira, R., and Nuss, D. L. (1990). Hypovirulence-associated suppression of host functions in *Cryphonectria parasitica* can be partially relieved by high light intensity. *Phytopathology* **80**:950–956.

- Hillman, B. I., Supyani, S., Kondo, H., and Suzuki, N. (2004). A reovirus of the fungus *Cryphonectria parasitica* that is infectious as particles and related to the *Coltivirus* genus of animal pathogens. *J. Virol.* **78**:892–898.
- Hillman, B. I., Tian, Y., Bedker, P. J., and Brown, M. P. (1992). A North American hypovirulent isolate of the chestnut blight fungus with European isolate-related dsRNA. *J. Gen. Virol.* **73**:681–686.
- Hiremath, S., L'Hostis, B., Ghabrial, S. A., and Rhoads, R. E. (1986). Terminal structure of hypovirulence-associated dsRNA in the chestnut blight fungus *Endothia parasitica*. *Nucl. Acids Res.* **14**:9877–9896.
- Hiremath, S., Nuss, D., Ghabrial, S. A., and Rhoads, R. E. (1988). Molecular cloning of hypovirulence-associated double-stranded RNA in *Endothia parasitica* and detection of sequence-related single-stranded RNA. *J. Gen. Virol.* **69**:2441–2453.
- Hong, Y., Cole, T. E., Brasier, C. M., and Buck, K. W. (1998). Evolutionary relationships among putative RNA-dependent RNA polymerases encoded by a mitochondrial virus-like RNA in the Dutch elm disease fungus, *Ophiostoma novo-ulmi*, by other viruses and virus-like RNAs and by the *Arabidopsis* mitochondrial genome. *Virology* **246**:158–169.
- Hong, Y., Dover, S. L., Cole, T. E., Brasier, C. M., and Buck, K. W. (1999). Multiple mitochondrial viruses in an isolate of the Dutch elm disease fungus, *Ophiostoma novo-ulmi*. *Virology* **258**:118–127.
- Horvath, C. M., Williams, M. A., and Lamb, R. A. (1990). Eukaryotic coupled translation of tandem cistrons: Identification of the influenza B virus BM2 polypeptide. *EMBO J.* **9**:2639–2647.
- Hull, R. (2002). In "Matthews' Plant Virology," 4th Ed. Academic Press, San Diego.
- Janda, M., and Ahlquist, P. (1993). RNA-dependent replication, transcription, and persistence of bromo mosaic virus RNA replicons in *S. cerevisiae*. *Cell* **72**:961–970.
- Jaynes, R. A., and Elliston, J. E. (1980). Pathogenicity and canker control by mixtures of hypovirulent strains of *Endothia parasitica* in American chestnut. *Phytopathology* **70**:453–456.
- Jung, H. J., Mo, A. Y., Kim, S. K., Kwon, B. R., Cha, B. J., and Kim, D. H. (2003). Cloning and characterization of ERK homologue, CpMK2, from *Cryphonectria parasitica*. *Phytopathology* **93**:S42.
- Kang, H.-S., Choi, J.-W., Park, S.-M., Cha, B., Yang, M.-S., and Kim, D.-H. (2000). Ordered differential display from *Cryphonectria parasitica*. *Plant Pathol. J.* **16**:142–146.
- Kasahara, S., and Nuss, D. L. (1997). Targeted disruption of a fungal G protein beta subunit gene results in increased vegetative growth but reduced virulence. *Mol. Plant Microbe Interact.* **10**:984–993.
- Kasahara, S., Wang, P., and Nuss, D. L. (2000). Identification of *bdm-1*, a gene involved in G protein beta-subunit function and alpha-subunit accumulation. *Proc. Natl. Acad. Sci. USA* **97**:412–417.
- Kasschau, K. D., and Carrington, J. C. (1998). A counterdefensive strategy of plant viruses: Suppression of post-transcriptional gene silencing. *Cell* **95**:461–470.
- Kasschau, K. D., and Carrington, J. C. (2001). Long-distance movement and replication maintenance functions correlate with silencing suppression activity of potyviral HC-Pro. *Virology* **285**:71–81.
- Kasschau, K. D., Cronin, S., and Carrington, J. C. (1997). Genome amplification and long-distance movement functions associated with the central domain of tobacco etch potyvirus helper component-proteinase. *Virology* **228**:251–262.

- Kazmierczak, P., Pfeiffer, P., Zhang, L., and van Alfen, N. K. (1996). Transcriptional repression of specific host genes by the mycovirus *Cryphonectria hypovirus 1*. *J. Virol.* **70**:1137–1142.
- Kim, M. J., Choi, J. W., Park, S. M., Cha, B. J., Yang, M. S., and Kim, D. H. (2002). Characterization of a fungal protein kinase from *Cryphonectria parasitica* and its transcriptional up-regulation by hypovirus. *Mol. Microbiol.* **45**:933–941.
- Koonin, E. V., Choi, G. H., Nuss, D. L., Shapira, R., and Carrington, J. C. (1991). Evidence for common ancestry of a chestnut blight hypovirulence-associated double-stranded RNA and a group of positive-strand RNA plant viruses. *Proc. Natl. Acad. Sci. USA* **88**:10647–10651.
- Larson, T. G., Choi, G. H., and Nuss, D. L. (1992). Regulatory pathways governing modulation of fungal gene expression by a virulence-attenuating mycovirus. *EMBO J.* **11**:4539–4548.
- Larson, T. G., and Nuss, D. L. (1994). Altered transcriptional response to nutrient availability in hypovirus-infected chestnut blight fungus. *EMBO J.* **13**:5616–5623.
- Lee, J. K., Tattar, T. A., Berman, P. M., and Mount, M. S. (1992). A rapid method for testing the virulence of *Cryphonectria parasitica* using excised bark and wood of American chestnut. *Phytopathology* **82**:1454–1456.
- Lengeler, K. B., Davidson, R. C., D'Souza, C., Harashima, T., Shen, W. C., Wang, P., Pan, X., Waugh, M., and Heitman, J. (2000). Signal transduction cascades regulating fungal development and virulence. *Microbiol. Mol. Biol. Rev.* **64**:746–785.
- Linder-Basso, D. (2002). Viruses and transposons of the chestnut blight fungus, *Cryphonectria parasitica*: Tools to examine virulence, fungal diversity, and evolution. Ph.D. diss. Rutgers University, New Brunswick, NJ.
- Linder-Basso D., Dynek, J., Hillman, B. I. Genome analysis of *Cryphonectria hypovirus 4*, the most common hypovirus species in North America. Submitted.
- Liu, Y.-C., Linder-Basso, D., Hillman, B. I., Kaneko, S., and Milgroom, M. G. (2003). Evidence for interspecies transmission of viruses in natural populations of filamentous fungi in the genus *Cryphonectria*. *Molec. Ecol.* **12**:1619–1628.
- Lu, H.-H., and Wimmer, E. (1996). Poliovirus chimeras replicating under the translational control of genetic elements of hepatitis C virus reveal unusual properties of the internal ribosomal entry site of hepatitis C virus. *Proc. Natl. Acad. Sci. USA* **93**:1412–1417.
- MacDonald, W. L., and Fulbright, D. W. (1991). Biological control of chestnut blight: Use and limitation of transmissible hypovirulence. *Plant Dis.* **75**:656–661.
- Mananti, N., Bertrand, H., Monteiro-Vitorello, C. M., and Fulbright, D. W. (1993). Elevated mitochondrial alternative oxidase activity in dsRNA-free, hypovirulent isolates of *Cryphonectria parasitica*. *Phys. Mol. Plant Pathol.* **42**:455–463.
- Marra, R. E., and Milgroom, M. G. (2001). The mating system of the fungus *Cryphonectria parasitica*: Selfing and self-incompatibility. *Heredity* **86**:134–143.
- McKeen, C. D. (1995). Chestnut blight in Ontario: Past and present status. *Can. J. Plant Pathol.* **17**:295–304.
- Melzer, M. S., and Boland, G. J. (1999). CHV3-type dsRNAs and the GH2 genotype in a population of *Cryphonectria parasitica* in Ontario. *Can. J. Plant Pathol.* **21**:248–255.
- Melzer, M. S., Ikeda, S. S., and Boland, G. J. (2002). Interspecific transmission of double-stranded RNA and hypovirulence from *Sclerotinia sclerotiorum* to *S. minor*. *Phytopathology* **92**:780–784.
- Mertens, P. P. et al. (2000). Reoviridae. "Virus Taxonomy: Seventh Report of the International Committee for the Taxonomy of Viruses" (E. M. H. V. van Regenmortel, C. M. Fauquet, D. H. L. Bishop, E. B. Carstens, M. K. Estes, S. M. Cimon, J. Maniloff, M. A.

- Mayo, D. J. McGeoch, G. R. Pringle, and R. B. Wickner, eds.). Academic Press, New York.
- Mertens, P. P., Hillman, B. I., Suzuki, N. (In press). Mycoreovirus. In "Virus Taxonomy: Eighth Report of the International Committee for the Taxonomy of Viruses" (C. M. Fauquet, J. Maniloff, M. A. Mayo, U. Desselberger, and A. J. Balls, eds.). Academic Press, New York.
- Milgroom, M. G. (1995). Population biology of the chestnut blight fungus, *Cryphonectria parasitica*. *Can. J. Bot.* **73**(Suppl. 1):S311–S319.
- Milgroom, M. G., and Cortesi, P. (1999). Analysis of population structure of the chestnut blight fungus based on vegetative incompatibility genotypes. *Proc. Natl. Acad. Sci. USA* **96**:10518–10523.
- Milgroom, M. G., and Lipari, S. E. (1995). Population differentiation in the chestnut blight fungus, *Cryphonectria parasitica*, in eastern North America. *Phytopathology* **85**:155–160.
- Milgroom, M. G., Lipari, S. E., and Powell, W. A. (1992). DNA fingerprinting and analysis of population structures of the chestnut blight fungus, *Cryphonectria parasitica*. *Genetics* **131**:297–306.
- Milgroom, M. G., Lipari, S. E., and Wang, K. (1992). Comparison of genetic diversity in the chestnut blight fungus, *Cryphonectria (Endothia) parasitica*, from China and the U.S. *Mycol. Res.* **96**:1114–1120.
- Milgroom, M. G., MacDonald, W. L., and Double, M. L. (1990). Spatial pattern analysis of vegetative compatibility groups in the chestnut blight fungus, *Cryphonectria parasitica*. *Can. J. Bot.* **69**:1407–1413.
- Milgroom, M. G., Wang, K., Zhou, Y., Lipari, S. E., and Kaneno, S. (1996). Intercontinental population structure of the chestnut blight fungus, *Cryphonectria parasitica*. *Mycologia* **88**:179–190.
- Moleleki, N., van Heerden, S. W., Wingfield, M. J., Wingfield, B. D., and Preisig, O. (2003). Transfection of *Diaporthe perijuncta* with *Diaporthe* RNA Virus. *Appl. Environ. Microbiol.* **69**:3952–3956.
- Morris, T. J., and Dodds, J. A. (1979). Isolation and analysis of double-stranded RNA from virus-infected plant and fungal tissue. *Phytopathology* **69**:854–858.
- Murant, A. F., Robinson, D. J., Taliany, M. E., de Zoeten, G. A., Falk, B. W., Gibbs, M. J., Pietersen, G., and Waterhouse, P. M. (2000). Genus *Umbravirus*. In "Virus Taxonomy: Seventh Report of the International Committee for the Taxonomy of Viruses" (E. M. H. V. van Regenmortel, C. M. Fauquet, D. H. L. Bishop, E. B. Carstens, M. K. Estes, S. M. Cimon, J. Maniloff, M. A. Mayo, D. J. McGeoch, G. R. Pringle, and R. B. Wickner, eds.). Academic Press, New York.
- Nannelli, R., Turchetti, T., and Maresi, G. (1999). *Corticoulous mites* (Acari) as potential vectors of *Cryphonectria parasitica* (Murr.) Barr hypovirulent strains. *Internat. J. Acarol.* **24**:237–244.
- Newhouse, J. R., Hoch, H. C., and MacDonald, W. L. (1983). The ultrastructure of *Endothia parasitica*. Comparison of a virulent with a hypovirulent isolate. *Can. J. Bot.* **61**:389–399.
- Newhouse, J. R., MacDonald, W. L., and Hoch, H. C. (1990). Virus-like particles in hyphae and conidia of European hypovirulent (dsRNA-containing) strains of *Cryphonectria parasitica*. *Can. J. Bot.* **68**:90–101.
- Nuss, D. L. (1992). Biological control of chestnut blight: An example of virus-mediated attenuation of fungal pathogenesis. *Microbiol. Rev.* **56**:561–576.
- Nuss, D. L. (1996). Using hypoviruses to probe and perturb signal transduction processes underlying fungal pathogenesis. *Plant Cell* **8**:1846–1853.

- Nuss, D. L. (2000). Hypovirulence and chestnut blight: From the field to the laboratory and back. In "Fungal Pathology" (J. W. Kronstad, ed.). Kluwer, The Hague, Netherlands.
- Osaki, H., Wei, C. Z., Arakawa, M., Iwanami, T., Nomura, K., Matsumoto, N., and Ohtsu, Y. (2002). Nucleotide sequences of double-stranded RNA segments from a hypovirulent strain of the white root rot fungus *Rosellinia necatrix*: Possibility of the first member of the Reoviridae from fungus. *Virus Genes* **25**:101–710.
- Park, S. M., Kim, E. S., Kim, M. J., Yang, M. S., and Kim, D. H. (2003). Cloning and characterization of ERK homologue, CpMK1, from *Cryphonectria parasitica*. *Phytopathology* **93**:S69.
- Parsley, T. B., Chen, B., Geletka, L. M., and Nuss, D. L. (2002). Differential modulation of cellular signaling pathways by mild and severe hypovirus strains. *Eukaryot. Cell* **1**:401–413.
- Parsley, T. B., Segers, G. C., Nuss, D. L., and Dawe, A. L. (2003). Analysis of altered G protein subunit accumulation in *Cryphonectria parasitica* reveals a third G-alpha homologue. *Curr. Genet.* **43**:24–33.
- Paul, C. P., and Fulbright, D. W. (1988). Double-stranded RNA molecules from Michigan hypovirulent isolates of *Endothia parasitica* vary in size and sequence homology. *Phytopathology* **78**:751–755.
- Peever, T. L., Liu, Y.-C., Cortesi, P., and Milgroom, M. G. (2000). Variation in tolerance and virulence in the chestnut blight fungus-hypovirus interaction. *Appl. Environ. Microbiol.* **66**:4863–4869.
- Peever, T. L., Liu, Y.-C., and Milgroom, M. G. (1997). Diversity of hypoviruses and other double-stranded RNAs of *Cryphonectria parasitica* in North America. *Phytopathology* **87**:1026–1033.
- Peever, T. L., Liu, Y.-C., Wang, K., Hillman, B. I., Foglia, R., and Milgroom, M. G. (1998). Incidence and diversity of double-stranded RNAs occurring in the chestnut blight fungus, *Cryphonectria parasitica*, in China and Japan. *Phytopathology* **88**:811–817.
- Polashock, J. J., and Hillman, B. I. (1994). A small mitochondrial double-stranded (ds) RNA element associated with a hypovirulent strain of the chestnut blight fungus and ancestrally related to yeast cytoplasmic T and W dsRNAs. *Proc. Natl. Acad. Sci. USA* **91**:8680–8684.
- Polashock, J. P., Bedker, P. J., and Hillman, B. I. (1997). Movement of a small mitochondrial double-stranded (ds) RNA element of *Cryphonectria parasitica*: Ascospore inheritance and implications for mitochondrial recombination. *Mol. Gen. Genet.* **256**:566–571.
- Powell, W. A., and van Alfen, N. K. (1987). Differential accumulation of poly(A)+ RNA between virulent and double-stranded RNA-induced hypovirulent strains of *Cryphonectria (Endothia) parasitica*. *Molec. Cell. Biol.* **7**:3688–3693.
- Preisig, O., Moleleki, N., Smit, W. A., Wingfield, B. D., and Wingfield, M. J. (2000). A novel RNA mycovirus in a hypovirulent isolate of the plant pathogen *Diaporthe ambigua*. *J. Gen. Virol.* **81**:3107–3114.
- Price, B. D., Roeder, M., and Ahlquist, P. (2000). DNA-directed expression of functional flock house virus RNA1 derivatives in *Saccharomyces cerevisiae*, heterologous gene expression, and selective effects on subgenomic mRNA synthesis. *J. Virol.* **74**:11724–11733.
- Rabindran, S., and Dawson, W. O. (2001). Assessment of recombinants that arise from the use of a TMV-based transient expression vector. *Virology* **284**:182–189.
- Rae, B. P., Hillman, B. I., Tartaglia, J., and Nuss, D. L. (1989). Characterization of double-stranded RNA genetic elements associated with biological control of chestnut

- blight: Organization of terminal domains and identification of gene products. *EMBO J.* **8**:657–663.
- Reichmann, J. L., Lain, S., and Garcia, J. A. (1992). Highlights and prospects of potyvirus molecular biology. *J. Gen. Virol.* **73**:1–16.
- Rigling, D., Heiniger, U., and Hohl, H. R. (1989). Reduction of laccase activity in dsRNA-containing hypovirulent strains of *Cryphonectria (Endothia) parasitica*. *Phytopathology* **79**:219–223.
- Rogers, H. J., Buck, K. W., and Brasier, C. M. (1987). A mitochondrial target for the double-stranded RNAs in diseased isolates of the fungus that causes Dutch elm disease. *Nature* **329**:558–560.
- Sasaki, A., Onoue, M., Kanematsu, S., Suzuki, K., Miyanishi, M., Suzuki, N., Nuss, D. L., and Yoshida, K. (2002). Extending chestnut blight hypovirus host range within diarthrales by biolistic delivery of viral cDNA. *Mol. Plant Microbe Interact.* **15**:780–789.
- Shapira, R., Choi, G. H., Hillman, B. I., and Nuss, D. L. (1991a). The contribution of defective RNAs to the complexity of viral-encoded double-stranded RNA populations present in hypovirulent strains of the chestnut blight fungus, *Cryphonectria parasitica*. *EMBO J.* **10**:741–746.
- Shapira, R., Choi, G. H., and Nuss, D. L. (1991b). Virus-like genetic organization and expression strategy for a double-stranded RNA genetic element associated with biological control of chestnut blight. *EMBO J.* **10**:731–739.
- Shapira, R., and Nuss, D. L. (1991). Gene expression by a hypovirulence-associated virus of the chestnut blight fungus involves two papain-like protease activities. *J. Biol. Chem.* **266**:19419–19425.
- Shear, C. L., and Stevens, N. E. (1917). *Endothia parasitica* and related species. *United States Department of Agriculture bulletin* 380, 82 pages.
- Smart, C. D., and Fulbright, D. W. (1995). Characterization of a strain of *Cryphonectria parasitica* doubly infected with hypovirulence-associated dsRNA viruses. *Phytopathology* **85**:491–494.
- Smart, C. D., Yuan, W., Foglia, R., Nuss, D. L., Fulbright, D. W., and Hillman, B. I. (1999). *Cryphonectria hypovirus* 3-GH2, a virus species in the family Hypoviridae with a single open reading frame. *Virology* **265**:66–73.
- Suzuki, N., Chen, B., and Nuss, D. L. (1999). Mapping of a hypovirus p29 protease symptom determinant domain with sequence similarity to potyvirus HC-Pro protease. *J. Virol.* **73**:9478–9484.
- Suzuki, N., Geletka, L. M., and Nuss, D. L. (2000). Essential and dispensable virus-encoded replication elements revealed by efforts to develop hypoviruses as gene expression vectors. *J. Virol.* **74**:7568–7577.
- Suzuki, N., Maruyama, K., Moriyama, M., and Nuss, D. L. (2003). Hypovirus papain-like protease p29 functions *in trans* to enhance viral double-stranded RNA accumulation and vertical transmission. *J. Virol.* **77**:11697–11707.
- Suzuki, N., and Nuss, D. L. (2002). Contribution of protein p40 to hypovirus-mediated modulation of fungal host phenotype and viral RNA accumulation. *J. Virol.* **76**:7747–7759.
- Tam, P. E., and Messner, R. P. (1999). Molecular mechanisms of coxsackie virus persistence in chronic inflammatory myopathy: Viral RNA persists through formation of a double-stranded complex without associated genomic mutations or evolution. *J. Virol.* **73**:10113–10121.
- Tartaglia, J., Paul, C. P., Fulbright, D. W., and Nuss, D. L. (1986). Structural properties of double-stranded RNAs associated with biological control of chestnut blight fungus. *Proc. Natl. Acad. Sci. USA* **83**:9109–9113.

- van Alfen, N. K., Jaynes, R. A., Anagnostakis, S. L., and Day, P. R. (1975). Chestnut blight: Biological control by transmissible hypovirulence in *Endothia parasitica*. *Science* **189**:890–891.
- van Heerden, S. W., Geletka, L. M., Preisig, O., Nuss, D. L., Wingfield, B. D., and Wingfield, M. J. (2001). Characterization of South African *Cryphonectria cubensis* isolates infected with a *C. parasitica* hypovirus. *Phytopathology* **91**:628–632.
- Wang, P., and Nuss, D. L. (1995). Induction of a *Cryphonectria parasitica* cellobiohydrolase I gene is suppressed by hypovirus infection and regulated by a GTP-binding-protein-linked signaling pathway involved in fungal pathogenesis. *Proc. Natl. Acad. Sci. USA* **92**:11529–11533.
- Weber-Lotfi, F., Dietrich, A., Russo, M., and Rubino, L. (2002). Mitochondrial targeting and membrane anchoring of a viral replicase in plant and yeast cells. *J. Virol.* **76**:10485–10496.
- Wei, C. Z., Osaki, H., Iwanami, T., Matsumoto, N., and Ohtsu, Y. (2003). Molecular characterization of dsRNA segments 2 and 5 and electron microscopy of a novel reovirus from a hypovirulent isolate, W370, of the plant pathogen *Rosellinia necatrix*. *J. Gen. Virol.* **84**:2431–2437.
- Wendt, R., Weidhaas, J., Griffin, G. J., and Elkins, J. R. (1983). Association of *Endothia parasitica* with mites isolated from cankers on American chestnut trees. *Plant Dis.* **67**:757–758.
- Wickner, R. B., Esteban, R., and Hillman, B. I. (2000). Narnaviridae. In “Virus Taxonomy: Seventh Report of the International Committee on Taxonomy of Viruses” (M. H. V. Van Regenmortel, C. Fauquet, D. Bishop, E. Carsten, M. Estes, S. M. Lemon, J. Maniloff, D. Mayo, D. McGeoch, C. Pringle, and R. B. Wickner, eds.). Academic Press, San Diego.
- Yuan, W. (1999). Genome structure and analysis of two hypoviruses in the chestnut blight fungus, *Cryphonectria parasitica*, from North America. Masters' thesis. Rutgers University, New Brunswick, NJ.
- Yuan, W., and Hillman, B. I. (2001). *In vitro* translational analysis of genomic, defective, and satellite RNAs of *Cryphonectria hypovirus* 3-GH2. *Virology* **281**:117–123.
- Zhang, L., Baasiri, R. A., and van Alfen, N. K. (1998). Viral repression of fungal pheromone precursor gene expression. *Mol. Cell. Biol.* **18**:953–959.
- Zhang, L., Churchill, A. C. L., Kazmierczak, P., Kim, D.-H., and van Alfen, N. K. (1993). Hypovirulence-associated traits induced by a mycovirus of *Cryphonectria parasitica* are mimicked by targeted inactivation of a host gene. *Mol. Cell. Biol.* **13**:7782–7792.

INDEX

A

- A. aegypti*, 246
- ABPV. *See* Acute bee paralysis virus
- ACAD. *See* Activated T cell autonomous death
- Acetes*, 387
- Actinomycin D, 91
- Activated T cell autonomous death (ACAD), 199, 201–202
- Activation-induced cell death (AICD), 199, 200–201
 - caspace activation in, 201
- Acute bee paralysis virus (ABPV), 372
- Adaptive immunity, 183
- Agglutinin, 258
- AICD. *See* Activation-induced cell death
- Alternative reading frame proteins (ARF), 75–76
- Amino acids, 79
- Amphiphysin II
 - NS5A and, 125–126
- Anamnestic immunity, 183
- Anastomosis, 426, 456
- Antibodies
 - classes of, 186–187
 - efficacy of, 187–190
 - in human viral diseases, 188
 - long-term production of, 190–191
 - viral infection combat and, 185–186
- Antigen
 - cytokines and, 212
 - levels of, 209–210
 - T cell production and, 213
- Antigen specificity, 183
- Antigen-presenting cells (APC), 196
 - B cells as, 190
 - CD40 pathway and, 217–218
 - downregulation of, 197
 - in immune response, 193
- Antigens
 - T cells triggered by, 208–209

- Antiviral functions
 - of CD8⁺ T cells, 206–207
- APC. *See* Antigen-presenting cells
- Apoptosis, 199–200
 - prevention of, 265
- Arboviruses, 240
- Arenaviruses, 259
- ARF. *See* Alternative reading frame proteins
- Asian chestnut blight isolates, 448
- Assembly
 - of DENV, 253–254
- ATP
 - NTPase activity and, 117
 - transphosphorylases, 118
- ATP hydrolysis, 297
- AUG codons, 100
- Avihepadnaviruses
 - as HBV models, 6–7
 - in-frame preC region of, 20

B

- B cell lines, 90
- B cell receptor (BcR), 184
- B cells
 - class switching, 192
 - maturation, 191–192
 - memory, 190
 - T cells helping, 216
- Bacteriophage T4
 - baseplate conformational transition in, 339–341
 - baseplate structure of, 311–312
 - cryo-electron microscopy of, 290
 - definition of, 287–288
 - DNA packaging of, 296–297
 - electron micrographs of, 289, 298
 - fibers of, 305–306
 - fibrin E diagram, 312
 - fibrin of, 308–311
 - genome of, 288

- Bacteriophage T4 (*continued*)
 gp11 and, 320
 head assembly of, 293–296
 head structure of, 291–292
 hexagon and star conformations
 of, 335
 history of, 288
 immunoelectron microscopy of, 300
 infection process of, 338
 initiation of baseplates, 336
 LTFs of, 305–306, 309
 mature capsid of, 292
 mutations in head of, 292
 protein composition of head of, 291
 quasi-optical filtration of, 299
 receptor-binding domain of, 310
 repeat segments of, 307
 shield surface representation of, 301
 star-shaped baseplate of, 337–339
 STFs of, 305–306, 309
 tail assembly of, 305
 tail of, 303–305
 tail proteins of, 304
 tail-tube baseplate structure of,
 328–329
 three-dimensional structural studies
 of, 300–303
 threefold axis of, 302
 two-dimensional structural studies of,
 297–300
 virion of, 288
 x-ray crystallography of, 290
- Baculovirus, 270
 granulosis-type, 392
- Bafilomycin A₁, 41
- Bak, 201
- Baseplate conformational transition
 initiation of, 336
 in T4, 339–341
- Baseplate proteins
 identifying, 333–337
 location of, 329–333
 structure of, 313–328
- Baseplate structure
 details of, 332
 of T4, 311
- Baseplate-tail tube complex, 330
- Bax, 201
- Bcl-2, 201
- Bcl-x_L, 201
- BcR. *See* B cell receptor
- Benlate O.D., 355, 356
- BH3-only proteins, 201
- BHK cells, 250, 256
- Biojector device, 271
- Black Leaf Wild disease, 355
- B-lymphocytes, 183
- BQCV, 372
- Budding
 of DENV, 253–254
byp24 mutations, 294
- Bystander antiviral effects
 of CD4⁺ T cells, 220
- C**
- C. havanesis*, 440
- C ORF, 8, 10
 precore proteins and, 20
- C protein, 252
- C. radicalis*, 440
- C6/36 cells, 250
- Calixin, 355, 356
- Calnexin, 264
- Capsid proteins
 amino acid sequences of, 373
 core proteins and, 15
 at N-terminal, 374
 structure and assembly of, 16–20
 TSV ORF2, 369
- Carboxypeptidase D (CPD), 2, 36, 39
 in plasma membrane, 40
- Castanospermine (CST), 264
- cccDNA, 13
 L proteins and, 36–37
 regulation of, 45
- CC-chemokine receptor 7 (CCR7), 197,
 203, 204
 effector functions expressed by, 205
- CCR7. *See* CC-chemokine receptor 7
- CD4, 94
- CD11a, 197
- CD25, 197
- CD40 pathway
 APC licensing via, 217–218
- CD44, 197
- CD62L, 198, 204
- CD69, 197
- CD81, 95, 98

- Cell culture adaptation
 HCV, 134–130
 mutations, 136–137
- Cell culture systems
 HCV, 89–93
- Cell entry
 HCV, 93–99
- CHBV. *See* Crane HBV
- Chemical cross-linking
 of baseplate proteins, 312
- Chemotherapy
 DHBV as model for, 52–53
- Chestnut blight viruses
 Asian, 448
 research on, 430–431
- Chimpanzee
 HCV in, 87
- CHO cells, 249
- Chromatophore expansion, 356
- CHV1. *See* *Cryphonectria hypovirus* 1
- CHV2. *See* *Cryphonectria hypovirus* 2
- CHV3. *See* *Cryphonectria hypovirus* 3
- CHV4. *See* *Cryphonectria hypovirus* 4
- Cis*-acting RNA element (CRE)
 role of, 114
- Clinical features
 of DENV, 242–243
- CM/PC. *See* Convoluted membranes/
 paracrystalline arrays
- CMV, 215
- Colorado tick fever virus (CTFV), 454
- Coltivirus*es, 454
- Concanavalin A, 258
- Contraction phase
 of CD8⁺ T cells, 198–202
- Convoluted membranes/paracrystalline
 arrays (CM/PC), 253
- Core protein
 capsid proteins and, 15
 E1 protein interaction with, 133
 encoding of, 8
 functions of DHBV, 12–16
 hydrophobic domains in, 127
 liquid droplet interaction with, 80
 localization of, 79
 recombinantly expressed, 16–17
- Cosin-phloxine, 378
- Coxsackie virus, 215, 222
 B4, 375
- CPD. *See* Carboxypeptidase D
- CpMK-2, 446–447
- CpPK-1, 447
- Crane HBV (CHBV), 6
- CRCs. *See* Crude replication complexes
- CRE. *See* *Cis*-acting RNA element
- Cross-linking analysis
 of gp8, 317
- CrPV, 372, 374
- Crude replication complexes (CRCs),
 121–122
 preparing, 126–127
- Cryo-electron microscopy, 18
 of bacteriophage T4, 290, 300
 bacteriophage T4 shield surface
 representation, 301
 of STFs, 331
- Cryphonectria hypovirus* 1 (CHV1),
 423–424
 coding sequences of, 437–443
 defective RNAs of, 451–453
 description of, 427–432
 EP713, 442–443
 Euro 7, 442–443
 genome structure, 435–436
 noncoding sequences of, 436–437
 Northern blot analysis of, 444
 ORF B domains of, 442–443
 replication of, 435–436
 signaling pathways affected by, 444–447
- Cryphonectria hypovirus* 2 (CHV2)
 discovery of, 447–448
 ORF of, 448
- Cryphonectria hypovirus* 3 (CHV3)
 defective RNAs of, 451–453
 discovery of, 449
 genome characterization of, 449
 genomic RNAs of, 452
 ORF of, 449–450, 459
 satellite RNAs of, 451–453
- Cryphonectria hypovirus* 4 (CHV4)
 discovery of, 450
 genome organization of, 450
 ORF of, 459
- Cryphonectria mitovirus*, 456
- Cryphonectria parasitica*, 423–424, 427
 dsRNA isolation, 433
 history of, as virus host, 427
 infected strains of, 432
 lateral transfer of, 460–462
 mitochondrial viruses, 457

- Cryphonectria parasitica* (continued)
 narnaviridae effecting, 455–457
 partially characterized viruses,
 457–458
 population biology of, 459–460
 reoviruses effecting, 453–455
 sporulation, 433
 transfection and transformation of, 434
 virulence tests, 433
 virus transmission in, 426
- CST. *See* Castanospermine
- C-terminal, 18
 of β -helix, 326
 cleavage product, 77–78
 of DHBV, 13
 E1 signal peptide, 78
 of fibrin E, 314
 of gp5, 319–321
 of gp9, 315–316
 of gp11, 316–317
 hydrophobic membrane anchors, 80
 metal-binding site of, 308
 of NS2, 76
 of p69, 441–442
 of TM2, 31
 of TSV ORF1, 368
- CTFV. *See* Colorado tick fever virus
- CTL. *See* Cytotoxic T lymphocytes
- C-type lectin, 94
- CV-1, 91
- Cys107, 20
- Cysresidues, 20
- Cytidines, 264
- Cytokines
 antigen contact and, 212
 duck, 48–50
 role of, in hepadnaviral infection,
 46–48
 secretion of, 206
 T cell initiated production of, 221
 toxic, 222
- Cytotoxic T lymphocytes (CTL), 46–47

D

- DC-SIGN, 96, 258
- DCV, 372, 374
- Defective RNAs
 of hypoviruses, 451–453
- Dengue fever (DF), 239
 cause of, 242
 epidemics of, 245, 246
- Dengue hemorrhagic disease
 (DHF), 240
- Dengue virus (DENV), 239
 assembly, 253–254
 binding and penetration, 248–251
 budding, 253–254
 classification of, 240–241
 clinical features of, 242–243
 domains of, 251
 genetic variation in, 244–245
 as global reemerging agent, 245–246
 inhibitors of, 265–266
 intracellular virus multiplication of,
 259–264
 life cycle of, 241
 maturation inhibitors of, 264–265
 organization of, 247
 pathogenesis of, 243–244
 proteolytic processing of, 251–253
 receptors, 249
 Rhesus monkeys with, 266–267
 RNA replication of, 251–253
 SCID mice with, 266–267
 small murine model for, 267
 translation of, 251–253
 vaccine development for, 268–272
 viral binding inhibitors, 254–259
 virion of, 246–247
in vitro antiviral activity, 255
in vivo systems of infection,
 266–267
- DENV. *See* Dengue virus
- Deoxynojirimycin (DNJ), 264
- DF. *See* Dengue fever
- DHBc
 functions of, 12–16
 HBc v., 14
 recombinant expression of, 18
- DHBcAg, 20–21
- DHBV. *See* Duck hepatitis B virus
- DHF. *See* Dengue hemorrhagic disease
- Diaportha*, 456
- Direct antiviral effects
 of CD4⁺ T cells, 219–220
- DNA oligonucleotide primers, 27–28
- DNA packaging
 of bacteriophage T4, 296–297

DNA synthesis, 12
 RNA template degradation and, 28
 DNA templates
 switching, 28
 DNJ. *See* Deoxyojirimycin
 dsRNA
 isolation of, in *C. parasitica*, 433
 Duck hepatitis B virus (DHBV)
 age/dose-dependence of infection
 outcome of, 43–44
 animal virus model, 2
 capsid structure of, 17
 as chemotherapy model, 52–53
 core protein functions of, 12–16
 core protein structure of, 18
 C-terminal of, 13–14
 cytokines in, 50–52
 early steps of infection with, 40–42
 envelope of, 33, 34
 envelope proteins of, 31
 experimental *in vivo* infection,
 43–46
 as HBV animal models, 6–7
 HBV virion compared with, 8
 hepadnaviral transduction vectors
 and, 53–54
 as host response model, 46–53
 host-range studies of, 42–43
 internalization of, 41
 kinetics of infection of, 38–40
 major envelope proteins, 30
 mutants, 45–46
 mutations in P protein of, 23–24
 ORFs of, 8, 10
 P protein activation of, 25–26
 reverse transcriptase of, 22
 schematic comparison of HBV
 with, 9
 subviral particles of, 33–35
 SVPs of, 40
in vitro infection of, 37–43
 DuIFN, 48–49
 recombinant, 51

E

E proteins, 247, 254, 258–259, 270
 as VAP, 248
 X-ray crystal structure of, 83
 E1 proteins, 76, 78, 80–81
 core protein interaction with, 133
 expression of, 98
 folding process of, 81
 location of, 83
 membrane topology of, 127–128
 transmembrane domains of, 82–83
 E1/E2 heterodimers, 94, 131
 E2 proteins, 76, 80–81
 coexpression of, 81
 expression of, 98
 function of, 95
 membrane topology of, 127–128
 P1 position of, 103
 structural model of, 83
 transmembrane domains of, 82–83
 EBV, 215
 Effector functions
 CCR7⁺ cells expressing, 205
 EICAR, 260
 Electron micrographs
 of bacteriophage T4, 289, 298
 of baseplate proteins, 333–334
 of *P. monodon*, 389
 ELISA. *See* Enzyme-linked
 immunosorbent assay
 ELISA-based dot blot test, 381–382
 ELISPOT technique, 191
 EMCV. *See* Encephalomyocarditis virus
 Encephalomyocarditis virus
 (EMCV), 92
 Endoplasmic reticulum (ER)
 C-terminal E1 signal peptide and, 78
 C-terminal polypeptide, 82
 stress, 140
 Envelope proteins
 mutational analysis of, 16
 structure and function of, 29–32
 transmembrane topologies of, 32–33
 Enzyme-linked immunosorbent assay
 (ELISA), 72
 ER. *See* Endoplasmic reticulum
 Erythroderma, 242
Escherichia coli, 268, 270, 293,
 309, 311
 gp9 expressed in, 313–314
 NS2-3 domains expressed in
 Expansion phase
 of CD4⁺ T cells, 213
 of CD8⁺ T cells, 195–198

F

- FasL molecule, 200, 206
- Fc receptors, 185
- Fibrin
 - of bacteriophage T4, 308–311
 - crystallizing, 309
 - C-terminal domain of, 314
 - diagram of, 312
 - insertion loops of, 313
 - recombinant, 309
 - x-ray structure of, 309
- Filamentous fungi, 425–426
- Finger domain
 - of gp11, 319
- Flavivirus*, 73, 107, 239, 240–241, 250, 251, 253, 258, 261, 265, 269
 - proteinase activity in, 110
- Frameshift proteins, 75–76, 102
- Fungal viruses, 424
- Fungi
 - as hosts for virus infection, 425–427
- Fusion peptides, 41–42
- Fusion proteins, 26

G

- G protein-linked signal pathways, 446
- G133E, 45
- Gamma activation site (GAS), 141
- GAV. *See* Gill-associated virus
- GB virus A (GBV-A), 73
- GB virus B (GBV-B), 73
 - propagation of, 86
- GB virus C (GBV-C), 73
- GBP, 49
- Gene expression
 - of TSV, 367–371
 - of YHV, 393–403
- Genetic diversity
 - of DENV, 244–245
- Genome maturation
 - of P protein, 27–29
- Genome organization
 - CHV1, 435–436
 - of GAV, 394
 - schematic representation of, 368
 - of TSV, 367–370
 - of YHV, 393–403

- Gill-associated virus (GAV)
 - amplification of, 408
 - discovery of, 387
 - 5′terminal sequences of, 395
 - IGR of, 395, 401
 - ORF sequence alignment of, 402
 - ORF1b sequence of, 396
 - ORF2 gene of, 398
 - in *P. monodon*, 406
 - primers for detection of, 384, 385
 - ssRNA genomes of, 393
 - virion of, 390
 - YHV and, 403–404
- Global reemerging agents
 - DENV as, 245–246
- Globalization
 - of health issues, 245
- Glu552 residues, 326
- Glutathione-s-transferase (GST), 445
- Glycoproteins
 - HCV, 81–82
 - processing of, 264
- Glycosaminoglycans (GAGs), 248
- gp3, 305
- gp5, 305
 - C-terminal of, 319–321
 - lysozyme domain of, 325, 340
 - N-terminal domain of, 323–325, 340
 - terminal structure of, 327
 - triple-stranded β helix of, 326
- gp6, 304–305, 334
- gp7, 304–305, 317, 340
- gp8, 304–305, 340
 - four-footed, 333
 - structure of, 317
- gp9, 312
 - crystal structure of, 315
 - C-terminal of, 315–316
 - function of, 313–314
 - LTFs and, 332–333
 - N-terminal sequence of, 315
 - structure of, 313–316
 - tangential orientation of, 340
- gp10, 304–305, 317, 340
 - STFs and, 337
- gp11, 304–305, 313, 340
 - bacteriophage T4 and, 320
 - crystal structure of, 316
 - C-terminal of, 317

- finger domain of, 319
 - N-terminal of, 316
 - structure of, 316–317
 - three-fingered, 331–333
 - x-ray structure of, 318
 - gp12, 305
 - gp13
 - fibrin attached to, 308
 - gp14
 - fibrin attached to, 308
 - gp16, 296
 - terminase, 297
 - gp17
 - properties of, 296
 - terminase, 297
 - gp20, 292, 296
 - gp20-gp40 membrane
 - assembly of, 293
 - gp21
 - serine proteases and, 295
 - gp21PPase
 - regulation of, 295
 - gp22
 - 288–289
 - sequence of, 295
 - gp23
 - cleavage of, 295–296
 - expansion of, 299
 - hexamers of, 301
 - polyhead lattice of, 300
 - properties of, 294
 - structure of, 297
 - yielding, 299
 - gp24
 - gpsoc binding and, 301
 - gp25, 304–305, 334
 - gp27, 305
 - cylinder, 340
 - trimer, 319–321
 - gp27-gp5 complex, 329
 - assembly of, 323
 - ribbon stereo diagram of, 324
 - structure of, 319–328
 - gp29, 304–305
 - gp31, 293
 - gp32, 296
 - gp34
 - N-terminal of, 306
 - gp35, 306
 - gp36, 306
 - gp37
 - C-terminal of, 306
 - gp48, 305
 - gp53, 304, 334
 - gp54, 305, 334
 - gp55, 296
 - gp64, 399–400
 - gp116, 399
 - N-terminus of, 399
 - gp*hoc*, 292
 - structure of, 301–303
 - gpsoc
 - gp24 and, 301
 - Granulosis-type baculovirus, 392
 - GroES, 293
 - GST. *See* Glutathione-s-transferase
 - GTP binding sites
 - in NS5B, 123
 - Gymnochrome D, 266
 - Gymnogongrus*, 257
- ## H
- H chains, 184–185
 - HBc
 - DHBC v., 14
 - HBV. *See* Hepatitis B virus
 - HBV transgenic mice, 4, 47
 - IFN- γ in, 52
 - HCMV, 215
 - HCV. *See* Hepatitis C virus
 - Helicase, 369
 - metal ion binding, 397
 - Hematoxylin, 378
 - Hemolymph
 - YHV in, 403
 - Hepacivirus*, 73, 250
 - Hepadnaviruses, 2
 - assembly of, 34–35
 - cytokines in, 46–48
 - host range of, 42–43
 - infectious cycle of, 7–12
 - M protein of, 30
 - P proteins of, 21–29
 - pgRNA reverse transcription in, 19
 - replication of, 51
 - schematic of, 11
 - transduction vectors of, 53–54
 - Heparin, 256

- Hepatitis B virus (HBV)
 assembly of envelope of, 35–36
 capsid structure of, 17
 definition of, 1
 DHBV as chemotherapy/vaccination
 model, 52–53
 DHBV virion compared with, 8
 in ducks, 6–7
 molecular biology of, 2
 non-primate orthohepadnaviruses
 models of, 5–6
 NS5B RdRp, 119–124
 precore proteins of, 20–21
 primate orthohepadnavirus models
 of, 3–5
 schematic comparison of DHBV with, 9
 spherical SVPs of, 34
 subviral particles of, 33–35
 surface proteins, 31
 TM2 in translocation of, 33
 in tupaias, 88
 vaccination for, 1–2
- Hepatitis C virus (HCV), 250
 antiviral therapies for, 146–149
 cell culture adaptation in, 134–139
 cell culture systems, 89–93
 cell entry, 93–99
 cell lines infected by, 90
 Cis-acting RNA sequences in, 111–115
 cloning of, 72
 coding regions of, 105
 coding sequence of, 114
 Con-1 genome, 136
 cytopathic effects exerted by, 139–140
 experimental systems, 86–87
 genomic organization of, 74–78
 host-cell permissiveness in, 134–139
 immune response, 140–146
 immunofluorescence assays of, 90
 immunoglobulins and, 85
 interferons in, 146–147
 membrane topology of, 125
 MHC in, 141
mus musculus domesticus models, 88
 NS3/4A proteinase complex in,
 108–111
 ORF, 101
 in *P. troglodytes*, 87–89
 particle formation, 133
 PKR in, 142–143
 polyprotein cleavage in, 108
 processing pathways of, 75
 proteins, 77
 proteolytic processing of structural
 proteins, 103–104
 receptor candidates for, 93–99
 replication complex of, 126–127
 replication cycle of, 84
 replication rates of, 73
 replicon structure, 92
 replicon system of, 91–92
 ribavirin in, 146–147
 RNA replication in, 115–116, 124–126
 RNA translation, 99–103
 serum constituents bound by, 85
 small interfering RNAs and, 147–148
 structural proteins of, 78–83
 symptoms of, 72–73
 transmission of, 72–73
 in Trimeria mouse, 88, 89
 viral protein membrane topology,
 127–132
 virus assembly and release, 132–134
in vivo models for replication of,
 87–89
 Western blot analysis of, 90
- Hepatocyte viruses
 bloodstream entry of, 40–41
 Hepatoma cell lines, 4
 HepG2, 4, 91, 248, 249
 as receptor candidate, 95–96
 Heptad repeats, 310
 Heterotrimeric G proteins, 445
 HiPV, 374
 Histological diagnosis
 of TSV, 379–382
 HL60, 249
 Homologous regions
 of T4 tail fiber, 307
 Horizontal transfer, 461
 Host-Cell factors
 in HCV RNA replication, 124–126
 Host-Cell permissiveness
 HCV, 134–130
 HPA-23, 257
 HS, 256–257
 Hsp40, 25
 Hsp70, 25
 Hsp90, 25, 107
 in *in vitro* P protein activation, 26–27

- Huh7, 4, 79, 91–92, 135
 replicon cells, 138
- Human immunodeficiency virus (HIV), 182
- Human vesicle-associated and membrane-protein associated protein (hVAP-A)
 expression of, 125
- hVAP-A. *See* Human vesicle-associated and membrane-protein associated protein
- Hydrophilic domains, 79
- Hyphal fusion, 456
- Hypoviridae
 defective RNAs of, 451–453
 identifying, 447
 molecular evolution of, 458–459
 organization of, 442
 satellite RNAs of, 451–453
 vesicles associated with, 429
- Hypoviruses*, 430–431
 individual species of, 431

I

- IAP motifs, 369
- ICCS. *See* Intracellular cytokine staining
- IFF-1, 49
- IFN regulatory factor-3
 NS3/4A and, 145
- IFN- α , 143
 duck, 48–49
 PEG conjugated, 74
- IFN- γ , 47, 141, 203, 206, 215, 261
 duck, 49
 in HBV transgenic mice, 52
 synthesis of, 210
 T cell initiated production of, 209–210, 211
- Ig. *See* Immunoglobulin
- IGR. *See* Intergenic region
- IHC. *See* Immunohistochemistry
- IL-2, 197, 202, 215, 217
 duck, 49–50
- IL-16
 duck, 50
- IL-18
 duck, 50
- Immune response
 CD4⁺ T lymphocytes and, 211–213
 CD8⁺ lymphocytes in, 194–195
 classifying, 183
 HCV, 140–146
 lymphocytes in, 184–185
 overview of, 182–183
- Immunodetection
 of YHV, 406–407
- Immunodot blot analysis
 of TSV, 378
- Immunoelectron microscopy
 of bacteriophage T4, 300
- Immunofluorescence assays
 of HCV, 90
- Immunoglobulin (Ig), 184
 A, 186
 biologic features of, 187
 D, 186
 E, 186
 Fc portion of, 248
 G, 186
 HCV and, 85
 M, 186, 192
 secretion of, 191
- Immunohistochemistry (IHC), 375
- Immunological diagnosis
 of TSV, 379–382
- Immunopathology
 definition of, 221
- IMPDH. *See* Inosine monophosphate dehydrogenase
- In vivo* models
 of HCV, 87–89
- Influenza, 215, 218
- Initiative for Vaccine Research (IVR), 271
- Innate immunity, 183
- Inosine monophosphate dehydrogenase (IMPDH), 259
 inhibitors of, 260
- Insertion loops
 of fibrin E, 313
- Interferon system, 261
 in HCV, 146–147
- Intergenic region (IGR)
 in GAV, 395, 401
 in YHV, 395
- Internal ribosome entry site (IRES), 74, 99, 111, 139

Intracellular cytokine staining
 (ICCS), 203
 Intracellular virus multiplication
 of DENV, 259–264
 IP₃-calcium signaling, 446
 IPV, 374
 IRES elements, 374
 IRES. *See* Internal ribosome entry site
 ISH methods
 for TSV diagnosis, 379–380
 Isogymnochrome D, 266
 IVR. *See* Initiative for Vaccine Research

J

J-domain proteins, 27

K

K1846T substitution
 in NS4B, 135
 Koch's postulates, 426

L

L chains, 184–185
 L protein
 functional roles of, 36–37
 preS domains of, 16
 structure and function of, 29–32
 transmembrane topologies of, 32–33
 L929, 248
 Langerhans cells
 peptide-treated, 269
 Large extracellular loop (LEL), 95
 Lassa virus, 259
 Lateral transfer
 of *C. parviticus*, 460–462
 LCMV, 207, 218
 antibodies, 189
 T cell response to, 196
 LCMV TcR transgenic mice, 203
 LDLr, 96, 98
 Liquid droplet
 core protein interactions with, 80
 Liver sinusoidal endothelial cells (LSEC)
 in hepatocyte cultures, 39–40

LLCMK2, 248
 LO spheroid monotypes, 365, 381
 Long tail fibers (LTF)
 gp9 and, 331–333
 in oscillation Browning process, 340
 proximal part of, 339
 of T4, 305–306, 309
 LPS receptors, 305
 LSEC. *See* Liver sinusoidal endothelial
 cells
 L-SIGN, 96
 LTF. *See* Long tail fibers
 Lymphocytes
 in antiviral immune response,
 184–185
 Lymphotoxin, 215
 Lys454 residues, 327
 Lysosomotropic agents, 42
 Lysozyme domains, 291
 of gp5, 325, 340

M

mAb. *See* Monoclonal antibodies
 Major histocompatibility complex
 (MHC), 190
 class I/II molecules, 193, 220
 distribution and function of, 194
 expression of, 195–196
 in HCV, 141
 purging of, 219
 TcR interaction with, 208
 MAP kinase activation, 37
 MAP. *See* Mitogen-activated protein
 Maximum Likelihood method, 368
 MCMV, 215
 MDBK, 248
 Meg-Gly. *See* N-terminal myristoylation
 signal
 Memory B cells
 as antigen presenting cells, 190
 Memory cells, 204–205
 LCMV specific, 206
 Memory phase
 of CD4⁺ T cells, 214
 of CD8⁺ T cells, 202–206
 Metal ion binding (MIB) helicase, 397
 Metalloproteinases, 106
Metapenaeus ensis, 388

- MHC. *See* Major histocompatibility complex
- MIB helicase. *See* Metal ion binding helicase
- Middle surface protein, 8
structure and function of, 30–31
- Mitochondrial viruses, 455–457
C. parasitica, 457
- Mitogen-activated protein (MAP), 265
kinase cascade, 446
- MLV. *See* Murine leukemia virus
- Modoc virus (MODV), 267
- Monoclonal antibodies (mAb), 375, 391
- Monotypes, 365
- Mouse models, 222
CD8⁺ memory T cell maintenance
in, 203
- MPA, 260–261
- Murine gamma-herpesvirus
T cell mediated control in, 219–220
- Murine leukemia virus (MLV), 97
- Murray Valley encephalitis virus
(MVEV), 250
- Mus musculus domesticus*
HCV models, 88
- MVEV. *See* Murray Valley encephalitis virus
- MxA protein
expression of, 142, 144
- Myocarditis, 222
- Myoviridae, 287
- N**
- Narnaviridae
of *C. parasitica*, 455–457
- NC-EIA. *See* Nitrocellulose enzyme immunoassay
- Neem leaves, 265–266
- Nelp
formation, 132
- Neurospora crassa*, 445
- NH₄CL, 42
- Nitrocellulose enzyme immunoassay
(NC-EIA), 406–407
- NK cells, 261
- N-nonyl-DNJ (NN-DNJ), 264
- Nodaviridae, 366
- Nonantigen specific responses, 183
- Non-primate orthohepadnaviruses, 5–6
- Nontranslated regions (NTR), 74
in RNA replication, 113–114
structure of, 100, 112–113
- Northern blot analysis, 402
of CHV1, 444
of TSV, 371
- NS proteins, 252
- NS1, 270
- NS2
membrane topology of, 128–129
- NS2 region, 76
- NS2-3 proteinase
Escherichia coli expressed in, 107
proteolytic processing of, 104, 106
- NS2A, 253
- NS2B, 253
- NS3, 252, 270
activation of, 109
definition of, 108
enzymatic activity in, 109
IFN regulatory factor-3 and, 145
membrane topology of, 129
mutations, 135
NS4A interaction with, 131
serine protease domain of, 263
zinc binding site in, 109–110
- NS3 helicase
activity, 118
in RNA replication, 116–119
in virus replication, 119
X-ray crystal structure of, 118
- NS3 region, 76
- NS3/4A proteinase complex
proteolytic processing of, 108–111
- NS4A, 253
IFN regulatory factor-3 and, 145
NS3 interaction with, 131
NS3 proteinase activated by, 109
- NS4B, 253
in HCV RNA replication, 124–126
K1846T substitution in, 135
membrane topology of, 129
protein, 77
- NS5, 263
- NS5A
amphiphysin II and, 125–126
binding of, 145
gene substitutions in, 135
membrane topology of, 129–130

- NS5A protein, 77, 108
 in HCV RNA replication, 124–126
- NS5B
 β -hairpin loop in, 122, 124
 binding of, 121
 low-affinity GPT-specific binding site
 in, 123
 X-ray crystal structure of, 122,
 135–136
- NS5B RdRp
 membrane topology of, 130
 in RNA replication, 119–124
- N-terminal
 capsid proteins at, 374
 of CHV4, 450
 of cleavage products, 110
 core proteins at, 78
 ectodomain, 80
 of gp5, 323–325, 340
 of gp9, 315
 of gp11, 317
 of P proteins, 21
 in pigmentation suppression, 439
 structural proteins in, 76
- N-terminal myristoylation signal
 (Meg-Gly), 30
- NTR. *See* Nontranslated regions
- Nucleic acids
 long-range interactions of, 29–30
- Nucleocapsids, 19
 YHV, 389
- Nucleoside triphosphatase (NTPase), 252
 activity of, 116
 APT and, 117
 binding, 120

O

- O. novo-ulmi*, 461
- Okavirus*, 393
- Oligodeoxylate synthetases (OAS), 144
- OMP. *See* Orotidine monophosphatase
- One-step growth kinetics, 39
- Open reading frames (ORFs)
 C, 8, 10
 of CHV1, 442–444
 of CHV2, 448
 of CHV3, 449–450, 459
 of CHV4, 459

- of DHBV, 8, 10
 of GAV, 396, 398
 HCV, 101
 N-terminal of, 369, 374
 P, 8, 10
 S, 8, 10
 sequence alignment of, 402
 of TSV, 368
 UTRs and, 247
 X, 10
 of YHV, 392, 398–399, 401
- Ophiostoma*, 456
- OR1/2, 210
- ORFs. *See* Open reading frames
- Orotidine monophosphatase (OMP)
 decarboxylase, 261
- Orthohepadnaviruses
 non-primate, 5–6
 primate, 3–5
- Oscillation Browning process
 LTFs in, 340
- Oxide anion, 257

P

- P. aztecus*, 360, 388, 405
- P. chinensis*, 361
- P. duorarum*, 360, 388, 405
- P. esculentus*, 388
- P. japonicus*, 361, 388, 405
- P. merguensis*, 388
- P. monodon*, 361, 388, 403, 405
 electron micrographs of, 389
 GAV in, 406
 YHD in, 383, 387
- P ORF, 8, 10
- P protein, 11, 19
 activation of, in DHBV, 25–26
 encoding of, 8
 enzymatic activities of, 23–29
 genome maturation of, 27–29
 Hsp90 in *in vitro* activation
 of, 26–27
 replication initiation of, 23–27
 structure of, 21–23
 TP domain of, 24, 27–28
- P. schmitti*, 360
- P. setiferus*, 360, 388, 405
 WSSV in, 387

- P. stylirostris*, 360, 378
TSV in, 375
- P. troglodytes*
HCV in, 87
- P. vannamei*, 355, 359, 378, 405
farmed, 357
hypothesized TSV disease cycle
in, 362
infected, 357, 358
TSV acute phase in, 361–364
TSV disease cycle in, 361
TSV transitional phase in, 364
TSV transmission in, 359, 360
WSSV in, 387
- p7
ion channels formed by, 76
membrane topology of, 128
P1 position of, 103
- P22 phage, 308
- p29, 437–440
expression of, 439
potyviral HC-Pro and, 438
- p40
basic nature of, 441–442
- p69
C-terminal of, 441–442
- Palivizumab, 189
- Pararetroviruses, 7
- Pathogenesis
of DENV, 243–244
- PBMCs. *See* Peripheral blood
mononuclear cells
- PCBP-2. *See* Poly(rC)-binding protein
- PCD. *See* Programmed cell death
- PCR, 113
- PDA media, 439
- PDB media, 439
- PDVI. *See* Pediatric Dengue
Vaccine Initiative
- Pediatric Dengue Vaccine Initiative
(PDVI), 271
- Peplotion, 269
- Peptidoglycan layers, 291
- Peripheral blood mononuclear cells
(PBMCs), 90
- PERK. *See* PKR-like ER kinase
- Pestivirus*, 73
- pgRNA, 10–11
reverse transcription of, in
hepadnaviruses, 19
- Photomicrographs
of TSV phases, 363
- Phytoplankton, 356–357
- Picornaviridae, 366, 368
cells infected with, 374–375
phylogenetic tree of, 372
RdRp genes of, 370
TSV and, 371–375
- PKR, 262
in HCV replication, 142–143
PKR-like ER kinase (PERK), 140
- Poly(rC)-binding protein
(PCBP-2), 102
- Polyethylene glycol (PEG)
interferon alpha conjugated
by, 74
- Polyoxometalates, 257
- Polyproteins, 75
- Polypyrimidine tract binding system
(PTB), 101
- Post-transcriptional gene silencing
(PTGS), 440
- Post-transcriptional regulatory elements
(PRE), 10–11
- Potyviral HC-Pro
p29 and, 438
- Potyviruses, 458
- PRE. *See* Post-transcriptional
regulatory elements
- Precore proteins
C ORG and, 20
HBV, 20–21
- Primary duck hepatocytes
age/dose-dependence of infection
outcome of, 43–44
culture conditions for, 37–38
DHBV infection of, 37–38
experimental *in vivo* infection
of, 43–46
kinetics of infection of, 38–40
- Primate orthohepadnaviruses
as HBV models, 3–5
- prM proteins, 270
- Programmed cell death (PCD), 199
apoptosis like, 200
necrosis like, 200
- Protease, 369
- Proteolytic processing
of DENV, 251–253
- PSIV, 372, 374

PTB. *See* Polypyrimidine tract binding system
 Pyrazofurin, 261

Q

Quasi-optical filtration
 of bacteriophage T4, 299

R

RC DNA, 13
 RC. *See* Replication complex
 RdRp. *See* RNA-dependent RNA polymerases
 Receptor binding domains
 zinc ions in, 311
 Receptor-binding domain
 of bacteriophage T4, 310
 Regulatory proteins, 10
Reoviruses, 453–455
 properties of, 454
 Repeat segments
 of T4 tail fiber, 307
 Replication complex (RC), 253
 HCV, 126–127
 Replication initiation
 of P protein, 23–27
 Replicative form (RF), 253
 Replicative intermediate (RI), 253
 Replicon system
 of HCV, 91–92
 Huh-7, 138
 structure of, 92
 Respiratory syncytial virus (RSV), 189
 Retroviridae, 97
 Reverse transcriptase
 enzymatic activities of, 23–29
 structure of, 21–23
 Reverse transcriptase polymerase chain reaction (RT-PCR), 72, 88
 ORF1b gene targeted by, 393
 primers for detection with, 384, 385
 for TSV diagnosis, 382–383
 for YHV diagnosis, 407–410
 RF. *See* Replicative form
 Rhesus monkeys
 DENV in, 266–267
 RhPV, 374

RI. *See* Replicative intermediate
 Ribavirin, 259, 262, 266
 in HCV, 146–147
 RNA helicase, 252
 RNA oligonucleotides, 28
 RNA replication
 of DENV, 251–253
 HCV, 115–116
 mutations and, 135
 NS3 helicase in, 116–119
 NS5B RdRp in, 119–124
 RNA synthesis
 in DENV, 247
 RNA-dependent RNA polymerases (RdRp), 240, 262–263, 368
 amino acid sequence of, 370
 metal ion binding helicase, 397
 NS5B, 119–124
 replication of, 244
 in vitro activity of, 122–123
 RNAs
 viral, 10–11
Rosellinia necatrix, 454
 RSV. *See* Respiratory syncytial virus
 RT-PCR. *See* Reverse transcriptase polymerase chain reaction

S

S monomers, 35
 S ORF, 8, 10
 hydrophobic regions of, 31–32
 TM1 of, 33
 S protein
 in HBV spherical SVPs, 34
 structure and function of, 30–32
 S-adenosyl-L-homocysteine hydrolase, 445
 S-adenosyl-L-methionine synthetase, 445
 SARS, 182
 Satellite RNAs
 of hypoviruses, 451–453
 SBV, 372
 SCID mice. *See* Severe combined immunodeficient mice
Sclerotina, 461
 Semliki Forest virus replicons, 132
 Serine protease domain
 gp21 and, 295
 of NS3, 263

- Severe combined immunodeficient (SCID) mice
 DENV in, 266–267
 HCV in, 88
- Short tail fibers (STF)
 assembly of, 316
 dissociation of, 340
 gp10 and, 337–339
 structure of, 329–331
 of T4, 305, 309
 x-ray structure of, 306–308
- Signal peptide peptidase (SPP), 103
- Signaling pathways
 CHV1 affecting, 444–447
- Sindbis virus (SinV), 87
- SinV. *See* Sindbis virus
- siRNAs. *See* Small interfering RNAs
- Small interfering RNAs (siRNAs)
 in HCV treatment, 147–148
- Small murine model
 for DENV infection, 267
- Small surface protein
 encoding of, 8
- Sodium metaperiodate oxidization, 391
- Somatic hypermutation, 192
- Sporulation
 of *C. parasitica*, 433
- SPP. *See* Signal peptide peptidase
- Staphylococcus aureus*, 299
- Star-shaped baseplate
 structure of, 337–339
- Stem-loop I, 112, 113
- STF. *See* Short tail fibers
- STF-connecting proteins, 305
- Structural proteins
 defining, 78
 HCV, 94
 proteolytic processing of, 103–104
- Subviral particles
 structure and assembly of, 33–35
- Sulfated polysaccharides, 257
- SVPs
 of HBV, 34–35
- T**
- T cell receptors (TcR), 193
 CD4⁺ response maturity,
 220–221
- direct/bystander antiviral functions,
 218–220
- MHC interaction with, 208
- T cells, 190
 antigen triggering of, 208–209
 antiviral, 192–194, 206
 B cells and, 216
 biologic roles of, 194
 CD4⁺ contraction phase of, 213–214
 CD4⁺ expansion phase of, 213
 CD4⁺ memory phase of, 214
 CD4⁺ subsets, 214–216
 CD8⁺ contraction phase of, 198–202
 CD8⁺ expansion phase of, 195–198
 CD8⁺ memory phase of, 202–206
 CD8⁺ responses, 216–218
 cytolytic capability of, 206–207
 death, 201–202
 distribution of, 198
 HBV replication blocked by, 4–5
 IFN-production and, 211
 IFN- γ production of, 209–210
 mature functions of, 207
 viral epitope response of, 196
- T helper cells, 214–215
- T lymphocytes
 CD4⁺, 211–213
 in immune response, 194–195
- T4Ppase
 activation of, 295
 phage-coded, 299
- T7 promoters
 bacteriophage, 91
- Tail-tube baseplate structure
 of bacteriophage T4, 328–329
- TaqMan probe, 382–383
- Task Force on Clinical trials of Dengue
 Vaccines, 271
- Taura syndrome virus (TSV)
 acute phase of, 361–364, 380
 amplification plots/dissociation curves
 of, 386
 bioassay of, 379
 chronic, 364–365, 380
 clinical signs of, 356–358
 C-terminal of, 368
 disease cycle of, 361–366
 economic impact of, 410
 endemic, 360
 genetic diversity of, 375–378

- Taura syndrome virus (TSV) (*continued*)
 genome organization of, 367–371
 histological methods for diagnosis
 of, 379–382
 history of, 354–356
 immunodot blot analysis of, 378
 immunological methods for diagnosis of,
 379–382
 northern blot analysis of, 371
 ORF2 capsid proteins, 369
 photomicrographs of phases of, 363
 physical properties of, 366–367
 picornaviruses and, 371–375
 primers used for detection of,
 384, 385
 RT-PCR for, 382–383
 transitional phase of, 364
 transmission electron micrographs
 of, 366
 transmission of, 358–361
 Western blot analysis of, 378
- TBEV. *See* Tick-borne encephalitis virus
- TcR. *See* T cell receptors
- Terminal nucleotidyl transferases
 (TNTases)
 activity of, 121
- Tetavalent live attenuated vaccines,
 268–269
- Tick-borne encephalitis virus (TBEV),
 250, 251
- Tilt, 355, 356
- T-lymphocytes, 183
- TM2
 in post-translational translocation of
 HBV, 33
- TNF- α . *See* Tumor necrosis
 factor alpha
- TNTases. *See* Terminal nucleotidyl
 transferases
- TP domain
 of P proteins, 24, 27–28
- Transfection
 of *Cryphonectria parasitica*, 434
- Transgenic mice
 HBV, 4–5, 47
- Translation
 of DENV, 251–253
- Transmembrane domains, 35
 of E1/E2 proteins, 82–83
 of vesicular stomatitis virus, 82
- Transmembrane topologies
 of L protein, 32–33
- Transmissible hypovirulence, 428
- Transmission electron micrographs
 of TSV particles, 366
 of YHV virion, 390, 407
- Trimera mouse
 HCV in, 88, 89
- TrV, 372
- Trypsin, 306–308
- TSV. *See* Taura syndrome virus
- TT-PCR, 375
- Tumor necrosis factor alpha (TNF- α), 47,
 206, 215
 T cell initiated production of, 211
- ## U
- Ultracentrifugation
 of gp8, 317
- Untranslated regions (241)
 ORFs and, 247
- Urbanization, 182
- Uridines, 264
- ## V
- Vaccination
 DENV, 268–272
 DHBV as model for, 52–53
- Vaccinia virus, 270
- Vegetative incompatibility, 426
- Vero, 248, 249, 256
- Vesicular stomatitis (VSV)
 transmembrane domain of, 82
- Viral binding
 inhibitors of, 254–259
- Viral infection
 overview of, 182–183
- Viral proteins
 membrane topologies of,
 127–132
- Viral transcript pools, 15
- Virions
 of bacteriophage T4, 288
 DENV, 246–247
 GAV, 390
 production of, 33

- structure and assembly of, 33–35
- YHV, 390, 391
- Virulence tests
 - for *C. parasitica*, 433
- Virus life cycle
 - DENV, 241
- Virus particles
 - HCV structure, 83–86
- VLP, 96–97
- VP1, 369
 - amino acid sequence, 377
 - coding sequence, 375
- VP2, 369
 - amino acid sequence, 377
 - amino acid sequence of, 373
 - coding sequence, 375
- VP3, 369
 - amino acid sequence of, 373
- VSV. *See* Vesicular stomatitis

W

- West Nile virus (WNV), 263
- Western blot analysis
 - of HCV, 90
 - of TSV, 378
- White spot syndrome virus (WSSV), 354
 - symptoms of, 354
- WHV
 - spread of, 5–6
- WMHBV. *See* Woolly monkey HBV
- WNV. *See* West Nile virus
- Woolly monkey HBV (WMHBV), 3–5
- World Health Organization, 246, 271
- WSSV. *See* White spot syndrome virus

X

- X ORF, 10
- Xanthosine monophosphate (XMP), 259
- Xenotransplants, 88–89
- X-ray crystallography, 17
 - of bacteriophage T4, 290, 297
 - of fibrin, 309
 - of gp9, 314–315
 - of NS3 helicase, 118
 - of NS3 zinc binding domain, 110
 - of NS5B, 122, 135
 - of TBEV E protein, 83

- X-ray structure
 - of fibrin E, 309
 - of gp8, 317
 - of gp11, 318
 - of STFs, 306–308
- X-tail sequences, 113–114

Y

- Yellow fever virus (YFV), 250
 - GAV and, 403–404
 - ribosomal frameshifts in, 396
- Yellowhead virus (YHV), 354
 - amplification of, 408
 - amplification plots and dissociation curves of, 409
 - economic impact of, 410
 - 5' terminal sequences of, 395
 - genome organization of, 393–403
 - histopathology of, 404–406
 - history of, 383–384
 - IGR of, 395
 - immunodetection of, 406–407
 - membrane topology of, 400
 - natural occurrence of, 387
 - nature of, 392
 - nucleocapsid of, 389
 - ORF of, 392–393
 - ORF sequence alignment of, 402
 - ORF1b sequence of, 398
 - ORF3 gene of, 398–399, 401
 - in *P. monodon*, 383, 387
 - phylogenetic tree of, 399
 - physical properties of, 389–393
 - primers used for detection of, 384, 385
 - RT-PCR for diagnosis of, 407–410
 - ssRNA genomes of, 393
 - structural genes of, 394
 - structural proteins of, 392
 - target tissues of, 405
 - transmission of, 388–389
 - virion of, 390, 391
- YFV. *See* Yellow fever virus
- YHV. *See* Yellowhead virus

Z

- Zinc ions, 306–308
 - at receptor binding domains, 311

This Page Intentionally Left Blank